FINAL TECHNICAL REPORT

Project Title: Offshore Gulf of Mexico Partnership for Carbon Storage Resources and Technology Development, "GoMCarb"

May 28, 2026

WORK PERFORMED UNDER AGREEMENT

DE-FE0031558

SUBMITTED BY

The University of Texas at Austin
Jackson School of Geosciences
Bureau of Economic Geology
10100 Burnet Rd., Bldg. 130
Austin, Texas, 78758-4445

PI: Dr. Susan Hovorka

PH: 512-471-4863

susan.hovorka@beg.utexas.edu

Co-PI: Dr. Tip Meckel

PH: 512-471-4306
tip.meckel@beg.utexas.edu

Prepared by

Co-PI: Ramon Trevino

PH: 512 471-3362

ramon.trevino@beg.utexas.edu

SUBMITTED TO

U.S. Department of Energy

National Energy Technology Laboratory

Kyle Smith– Federal Project Manager

Executive Summary

In the past decade, US CCS research about use of the subsurface beneath state and federal offshore waters has increased. A leader among US CCS research has been the Offshore Gulf of Mexico Partnership for Carbon Storage Resources and Technology Development (GoMCarb), funded under DOE/NETL Cooperative Agreement DE-FE0031558 and led by the Bureau of Economic Geology at The University of Texas at Austin, ran from April 1, 2018 through March 31, 2026. The Partnership's goal was to advance the geologic, engineering, monitoring, and outreach foundations needed for industrial-scale carbon capture and storage (CCS) in the federal and state waters of the northwestern Gulf of Mexico (aka "Gulf of America"), a region that combines extensive proven reservoirs and confining zones, two single landowners across federal and state waters, respectively, and proximity to one of North America's densest concentrations of point-source industrial emissions.. The period of performance was extended beyond the original March 2023 end date to accommodate marine field-work delays caused by the COVID-19 pandemic.

The GoMCarb Partnership included 15 different groups across industry, government and academia and addressed six major tasks: 1) Project Management; 2) Offshore Storage-Resource Assessment; 3) Risk Assessment, Simulation and Modeling; 4) Monitoring, Verification, and Assessment; 5) Infrastructure, Operations and Permitting; and 6) Knowledge Dissemination. GoMCarb focused on highly prospective areas offshore Texas and Louisiana state waters plus western Louisiana federal waters. A sister partnership studied offshore Louisiana federal waters and offshore Alabama, Mississippi, and Florida.

GoMCarb supported several important changes in the CCS landscape. The General Land Office of Texas opened areas for leasing in state waters, which resulted in commercial activities. Three CarbonSafe projects were also selected to conduct site-specific studies in marine settings. Per Congressional mandate, since 2021 the Bureau of Ocean Energy Management (BOEM) and the Bureau of Safety and Environmental Enforcement (BSEE) have been actively establishing frameworks to permit sub-seabed carbon dioxide sequestration beneath federal waters.

Storage Resource Assessment. Regional characterization across the offshore Texas–Louisiana shelf identified Pliocene and Miocene sand-prone intervals—bounded above by the supercritical CO_2 depth (~800 m) and below by hard overpressure—as the primary storage window. A basin-scale pressure-based assessment yielded approximately 85 Gt of total CO_2 storage resource across the federal OCS study area, with an average pore occupancy of ~0.8%. Detailed sub-area work in Chandeleur Sound (LA), Cameron Parish (LA), High Island (TX), and the mid-Texas coast quantified site-scale capacity for seven Upper Miocene reservoirs (~306 Mt realistic closed-boundary capacity), screened fault-bounded compartments for industrial-scale viability, and mapped the regional Anahuac and *Amphistegina* B confining zones—both of which thicken basinward and provide widespread, high-quality confinement. Offshore CO_2-EOR potential in mature Texas and Louisiana oil fields was estimated at ~169 Mt of associated CO_2 storage paired with ~49 MMBbl of incremental oil recovery.

Risk Assessment, Simulation and Modeling. The GoMCarb team adapted petroleum-exploration tools (Common Risk Segment mapping, fault seal analysis) to CCS site screening; quantified the geomechanical effects of water depth on confining-system capacity; modeled across-fault CO_2 migration under varying boundary conditions (estimated to range from ~1.6% to ~26% of injected mass over 40 years); simulated injection and post-injection plume evolution at the High Island 24-L analog; and demonstrated through dry-hole analysis that the large majority of legacy hydrocarbon failures along the coastal Texas–Louisiana border reflect missing trap or charge rather than petroleum seal failure, thus supporting the regional viability of CCS. Blowout modeling by LBNL indicated a downwind exclusion radius of approximately 400 m for credible shallow-water release scenarios.

Monitoring, Verification, and Assessment (MVA). Although, GoMCarb was unable to conduct a high-resolution 3D (HR3D / P-cable) marine seismic survey (i.e., because of a change in political/policy priorities), it did advance

seabed and water-column geochemical analytical frameworks, distributed acoustic sensing, and pipeline MVA techniques tailored to warm, shallow Gulf conditions, and GoMCarb produced a prioritized roadmap for offshore MVA technology deployment.

Infrastructure, Operations, and Permitting. Engineering studies by Aker Solutions developed subsea injection-template concepts; risk assessment addressed CO_2 release during truck-and-barge transfer; and scenario optimization examined multimodal pipeline-and-marine transport linking the Houston, Beaumont–Port Arthur, and Corpus Christi industrial clusters to offshore storage in the Corsair Trough and various other geographic areas.

Knowledge Dissemination. Stakeholder-engagement research and outreach informed offshore-CCS communication strategy, and Partnership findings supported the Texas General Land Office's 2021–2024 carbon-storage leasing program.

Key contributions of the Partnership include:

- **A new concept and framework for storage capacity.** A central scientific contribution from the Partnership is the *pressure space* framework (Bump & Hovorka, 2024), which redefines CCS capacity as the integrated product of accessible pore volume and allowable pressure increase. The concept, "pressure space," is the fundamental subsurface commodity for CCS. Pressure space reconciles inconsistencies between static and dynamic capacity estimates and offers a tractable basis for valuing, leasing, and de-conflicting storage resources at basin scale. The concept unifies static and dynamic capacity estimation, captures the depth-dependence of storage efficiency, and offers a practical basis for valuing and allocating subsurface storage rights.
- **Confining-system and structural characterization.** The first regional isopach mapping of the upper Oligocene Anahuac and lower Miocene *Amphistegina* B confining units across ~350 miles of the Texas coast, combined with 3D seismic interpretation, showed that practical industrial-scale (>25 Mt) capacity is materially constrained by fault-compartment size—only the largest compartments qualify at typical reservoir thicknesses.
- **Geomechanics from onshore to deep water.** First-principles analyses quantified how pressure space, supercritical-CO_2 depth, and fracture pressure vary with water depth, directly addressing concerns about the competence of offshore sediments as confining systems.
- **MVA technology development.** A prioritized portfolio of offshore monitoring approaches was advanced, including geochemical monitoring of seabed sediments and the seawater column, ultra-high-resolution 3D (UHR3D) marine seismic, distributed acoustic sensing, and pipeline monitoring.
- **Infrastructure, transport, and operations.** A transect-based methodology was developed for evaluating re-use of existing GoM oil-and-gas infrastructure (pipelines, platforms, wells), supported by subsea-template feasibility work and CO_2 transfer-operation risk assessment.
- **Stakeholder engagement and risk communication.** Mental-model research across local community, NGO, industry, and government audiences revealed sharply differing perceptions of CCS benefits and risks and produced evidence-based guidance for communication that moves beyond climate framing alone.

GoMCarb produced more than a two-dozen peer-reviewed publications and an extensive body of regional seismic, well-log, and geomechanical data based products that establish a technical foundation for commercial offshore CCS development in the U.S. Gulf of Mexico. Collectively, GoMCarb advanced the offshore Gulf of Mexico Basin from a conceptual storage province to a quantitatively characterized portfolio of play fairways, prospects, monitoring strategies, and operational pathways—providing a technical foundation for forthcoming commercial-scale offshore CCS deployment.

(The foregoing executive summary was partially generated using AI (artificial intelligence) to support summarizing this project final report.)

1. Task 1 – Project Management, Planning, and Reporting

The Partnership commenced on April 1, 2018 and ended on March 31, 2026. The time period spanned the Covid-19 pandemic, which resulted in the need to extend the period of performance beyond the initial end date of March 31, 2023. The pandemic delayed the planned acquisition of a high-resolution 3D seismic (HR3D) marine dataset in the Gulf of Mexico, which could not be conducted during the pandemic due to health concerns for onboard spread of Covid-19. See subtask 4.1.3 for details about the HR3D survey (aka "UHR3D" survey).

2. Task 2 – Offshore Storage Resource Assessment

Pressure Space: The Key Subsurface Commodity for Geologic Carbon Sequestration

The following discussion was a significant advance in the understanding of CCS capacity and resulted from research partially supported by GoMCarb. The peer-reviewed concept paper, A. P. Bump and Hovorka (2024) was the ultimate result and the following is a summary, thereof. See A. P. Bump and Hovorka (2024) for the list of references cited here.

In the development of Carbon Capture and Storage to date, there has been considerable focus on the subsurface pore space occupied by CO_2. This interest shows up in assessments of available pore volume, studies of CO_2 migration and regulatory requirements to track the plume (Halland et al., 2013; US EPA, 2013; Bentham et al., 2014; Cowton et al., 2016; ISO/TC 265, 2017). In particular, a great deal of work has been invested in quantification of reservoir pore volume as a means to estimate storage capacity (Blondes et al., 2013; Goodman et al., 2016; US DOE-NETL, 2017). The attention is understandable. Quantification of the resource is fundamental to understanding its value. These capacity estimates are analogous to familiar volumetric assessments of oil and gas accumulations, and they are reinforced by seismic imaging of plume growth and regulatory focus on the injected fluid. They are popular for frontier and basin-scale evaluation of storage resources, where building more sophisticated reservoir models is simply too costly in time and data.

Considerable effort has been invested in defining storage efficiency numbers for these static capacity estimates, but the application is often murky (Figure 2.1). Unlike oil and gas accumulating at pressure equilibrium on a geologic time scale and gradually saturating a reservoir from the top down, the sweep efficiency of CO_2 injected at industrial rates is highly uneven. Variations in pressure and reservoir permeability cause it to spread highly unevenly (Hovorka et al., 2013; Cowton et al., 2016; Krishnamurthy et al., 2017). Should storage efficiency be calculated as a fraction of the total reservoir volume? Only the connected reservoir volume? Reservoir volume within a lease block? Or reservoir volume contacted by CO_2, and how should anomalously-pressured reservoirs be treated? Pressure depletion is widely acknowledged to enhance storage capacity while pressure elevation reduces it. Static capacity is widely used but often viewed as a first-pass number that will ultimately be supplanted by a more accurate but time-consuming dynamic capacity estimate.

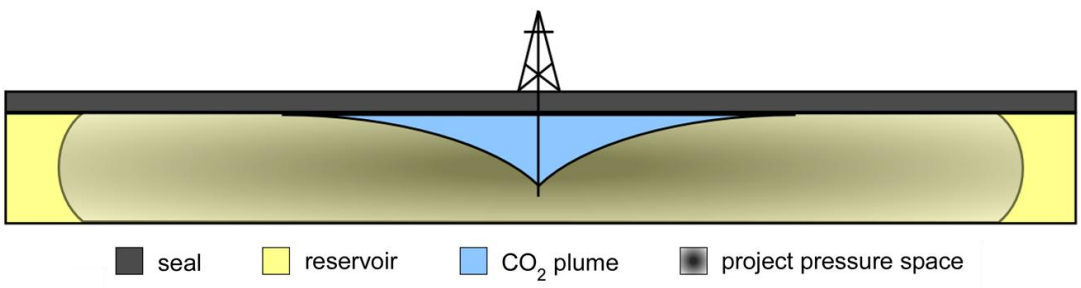

Figure 2.1: Illustration of a typical injection project showing the relative sizes of CO_2 plume and pressure plume.

At the root of the problem is the fact that the subsurface pore space into which CO_2 is injected is not empty prior to injection. Rather it is filled with high-salinity brines and in some cases hydrocarbons. Injecting additional fluids requires either 1) increasing the reservoir volume by elevating the land surface; 2) displacing the pre-existing fluids; or 3) raising the injection zone fluid pressure and compressing the rock. Elevation of the land surface is observed in some cases but the magnitude is generally very small and the pore volume gained is minimal (Karegar et al., 2015; Bohloli et al., 2018). Similarly, displacement of pre-existing fluids is inevitable near the injector but likely to be limited in the far-field reservoir. Regulatory requirements to protect freshwater aquifers naturally steer operators toward reservoirs with robust confining systems that preclude displacement of brines to the surface. The potential for lateral fluid displacement is governed by the permeability architecture of the reservoir, but even in the best case, no reservoir is infinite. Depositional systems have limited extents and faults often subdivide them into smaller compartments. Without access to the ground surface, pore fluids cannot be displaced indefinitely. The net result is that injection capacity relies fundamentally on compression of the rock and/or the pre-existing pore fluids. Pressure build-up is inescapable and the magnitude of acceptable pressure increase is a fundamental determinant of storage capacity (Figure 2.1).

Some stakeholders have recognized the importance of pressure build-up. The US EPA, for example, defines a pressure-based Area of Review within which all legacy penetrations must be reviewed and assured. Similarly, pressure interference between injection wells is a commonly accepted consequence of large-scale injection and some regulators have expressed quiet concern over CCS project spacing and the potential for interference between projects. Regulation also commonly limits CO_2 injection pressure to avoid creating or propagating fractures in the injection zone. At the same time however, pressure build-up is related to pore volume. The bigger the connected pore volume, the smaller the pressure build-up for a given injection volume.

Both pore volume and the magnitude of allowable pressure increases are important. To date they have generally been considered separately by regulators, landowners and explorers of storage resources. A unified concept could reduce the debates about storage efficiency and enable effective determination and valuation of storage capacity. The purpose of this work is to propose such a unified concept. We name the concept *pressure space,* and it is simply the product of accessible pore volume times allowable pressure increase. If either quantity varies with geography or depth, then pressure space is the 3D integral of pore volume and allowable pressure increase as functions of x, y, and z.

Pressure space has the units of energy, reflecting the fact that elevating reservoir pressure is a form of energy storage. Figure 2.2 illustrates the concept in one dimension. The left panel shows porosity as a function of depth, using the sand compaction function of Chen (Chen et al., 2020). The middle panel shows a typical set of pressure curves with two predictions of fracture (aka “frac”) pressure that are chosen to bracket the range of likely possibilities (Zhang, 2019). Assuming an initially hydrostatically pressured reservoir, the allowable pressure increase is taken as the difference between hydrostatic and the minimum estimate of frac pressure (shown by the arrows). Note that both allowable pressure increase and porosity vary with depth. The final panel (right side) shows the product of the first two; that is, it shows pressure space per square meter as a function of depth.

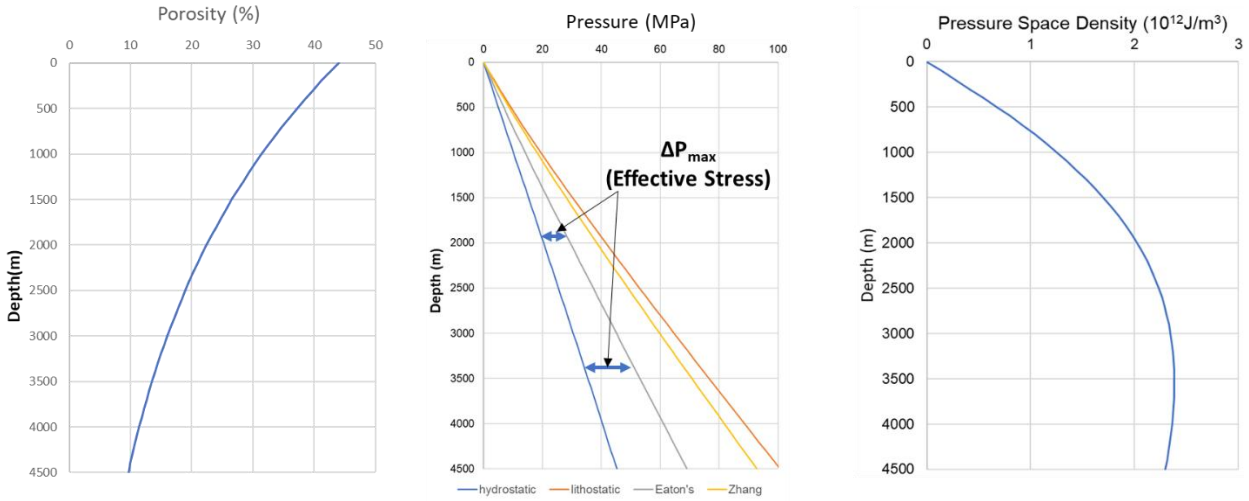

Figure 2.2: Graphs illustrating the calculation of pressure space per square meter for an idealized 1-dimensional example. See text for discussion.

Figure 2.3 applies the concept to data from the Gulf of Mexico Oligocene (Kreitler et al., 1988). As before, the left-hand panel shows porosity as a function of depth while the middle panel shows pressure versus depth. Note that initial reservoir pressure is hydrostatic at shallow depths but transitions to frac pressure at 3000-3500m depth, creating a floor to the available injection zone. That is reflected in the right-hand panel showing the curve of pressure space per square meter with respect to depth.

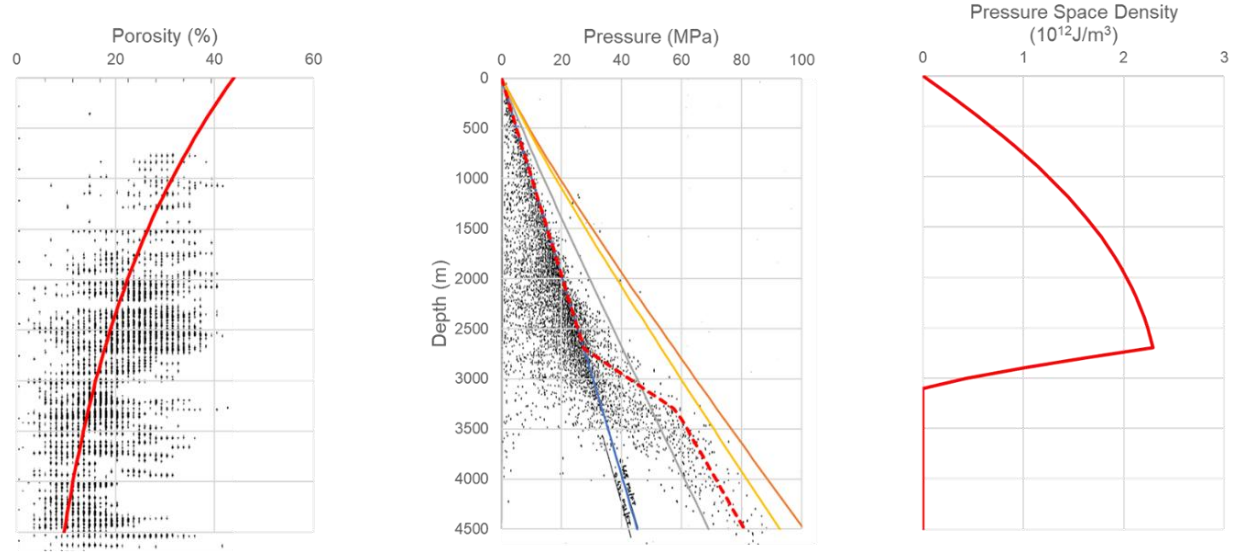

Figure 2.3: Graphs illustrating the calculation of pressure space per square meter for the Gulf Coast Oligocene section. Data from Kreilter (1988). See text for discussion.

Among other things, this analysis highlights the fact that not all pore space is equal in storage terms. Depth matters. The deeper the injection, the greater the allowable pressure increase (effective stress, by another name) and therefore the greater the storage capacity for a given pore volume. That trend plays against porosity, which generally decreases with depth, due to compaction and diagenesis. The net result is shown by the curves of pressure space, which show a maximum around 3-3.5km depth. Ultimately, the complete loss of either effective stress or porosity creates a floor to the storage window. Effective stress commonly disappears with the transition to overpressure, observed in many if not most of the world's sedimentary basins (e.g., Burke et al., 2012). Porosity may be lost to gradually increasing cementation and compaction or abruptly at the contact with basement or other

non-reservoir units.

Ultimately, what matters is not pressure space per se, but its equivalent in storage capacity. Figure 2.4 shows a first pass at translating pressure space to storage capacity, calibrated using EASiTool (Ganjdanesh and Hosseini, 2017, 2018). As the preceding discussion should make clear, both accessible pore volume and allowable pressure increase have first-order effects on storage capacity. The graph explicitly recognizes that interdependence and makes capacity estimation easy.

Definition of pressure space as the key commodity for geologic CO_2 sequestration capacity offers a number of attractive improvements on current practice. First, it can use the same widely available inputs as static capacity but accounts for the importance of pressure and gives an answer that is closer to realizable dynamic capacity. Second, because it is simple and reasonably accurate, it can be applied at the multi-project to basin-scale to get an accurate idea of the storage resource volume and show the regional variations. As such it could be useful to both operators looking for optimal sites and to landowners considering supply and demand as the basis for storage resource valuation. Third, and perhaps most significantly, it suggests a new way of allocating storage resources. Rather than leasing pore space, it suggests selling pressure space. It would be relatively easy to calculate the pressure space available in a given reservoir and trivial to calculate the pressure space requirements for a given injection project. Rather than worry about defining plume edges and trying to avoid interference between projects, a regulator/landowner could simply quantify the pressure space available beneath a given tract and sell it in fractions to different operators.

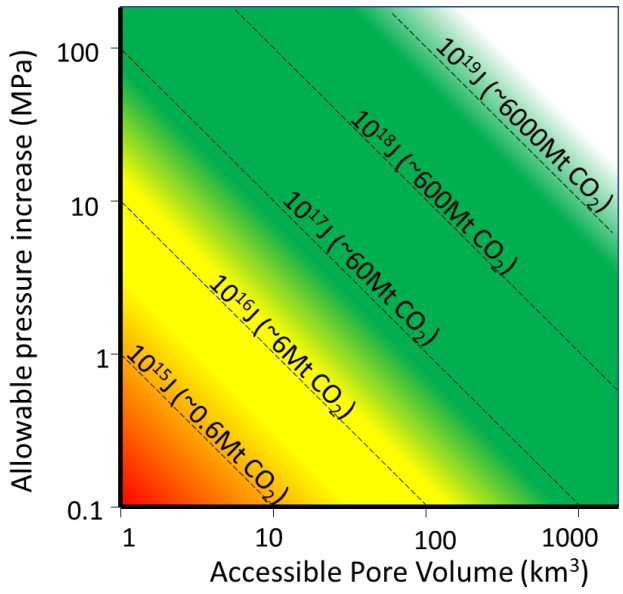

Figure 2.4: Graph showing the relationships between allowable pressure increase (effective stress), accessible pore volume, pressure space and CO2 storage capacity. Background colors reflect suitability for industrial-scale storage projects on the scale of 10s of megatons.

2.1 Subtask: Database Development

The Partnership greatly benefited from preceding DOE-funded studies of offshore Texas and Louisiana (i.e., DE-FE0001941, FE0026083, FE0029487 and FE0028193). In addition to advances in geological understanding, which the Partnership inherited from the legacy studies, the previous studies generated well and seismic databases. Nonetheless, digitization of additional well logs continued throughout most of the Partnership's period of performance because GoMCarb covered a much larger area of study than the previous studies. In general, raster well logs were digitized in-house by undergraduate research assistants. The files were then loaded to a the Petra™

project database with well curve raster images and digitized well log curves. They did this by loading raster images from available sources (e.g., Lexco OWL7) and digitizing log curves from the images, thus, generating digital LAS (Log ASCII Standard) curves. Primarily, SP (spontaneous potential) curves were digitized because they were used to define log facies and correlate wells. However, other important well-log curves were also digitized when available (e.g., acoustic, density and neutron curves). In addition to in-house digitization, some logs were digitized by companies. The total number of wells with LAS curves as of the end of the project was more than 2,900. The Petra well interpretation software was available to the Partnership's Bureau of Economic Geology (BEG) team via IHS Petra's university grant program, for which we are very grateful.

In addition, regional 2D seismic lines and regionally extensive the primary 3D seismic datasets (Figure 2.37) in Texas and Louisiana state waters were leased by some of the previous DOE studies, and GoMCarb leased additional ones. Another advantage to the Partnership was the coincidental public availability of extensive, historical regional 3D seismic datasets in Federal waters (OCS) (Figure 2.37), which continued to be released to the public as their, respective, proprietary periods expired (i.e., 25 years after they were acquired). As the 3D surveys became publicly available, they were downloaded and added to the Partnership's seismic database. The seismic datasets (volumes) were interpreted using Haliburton's Landmark and Schlumberger's Petrel platforms. The software from both platforms was available to the Partnership's Bureau of Economic Geology (BEG) team via the Haliburton's and Schlumberger's university grant programs, for which we are very grateful.

2.1.1 Subtask - Geographic Focus Area A - Lake Jackson, Lake Charles, and Lafayette (OCS) districts

CO_2 Storage Potential in the Federal Offshore, Gulf of Mexico Shelf

The federal waters region of the Gulf of Mexico (Offshore Continental Shelf – OCS) (Figure 2.5) is attractive due to several factors: proven reservoirs and confining zones, a single landowner, fewer and newer legacy wells relative to onshore wells, and potentially less opposition from local communities. Thus, the purpose of this study is to explore the potential of CO_2 storage sites in the OCS.

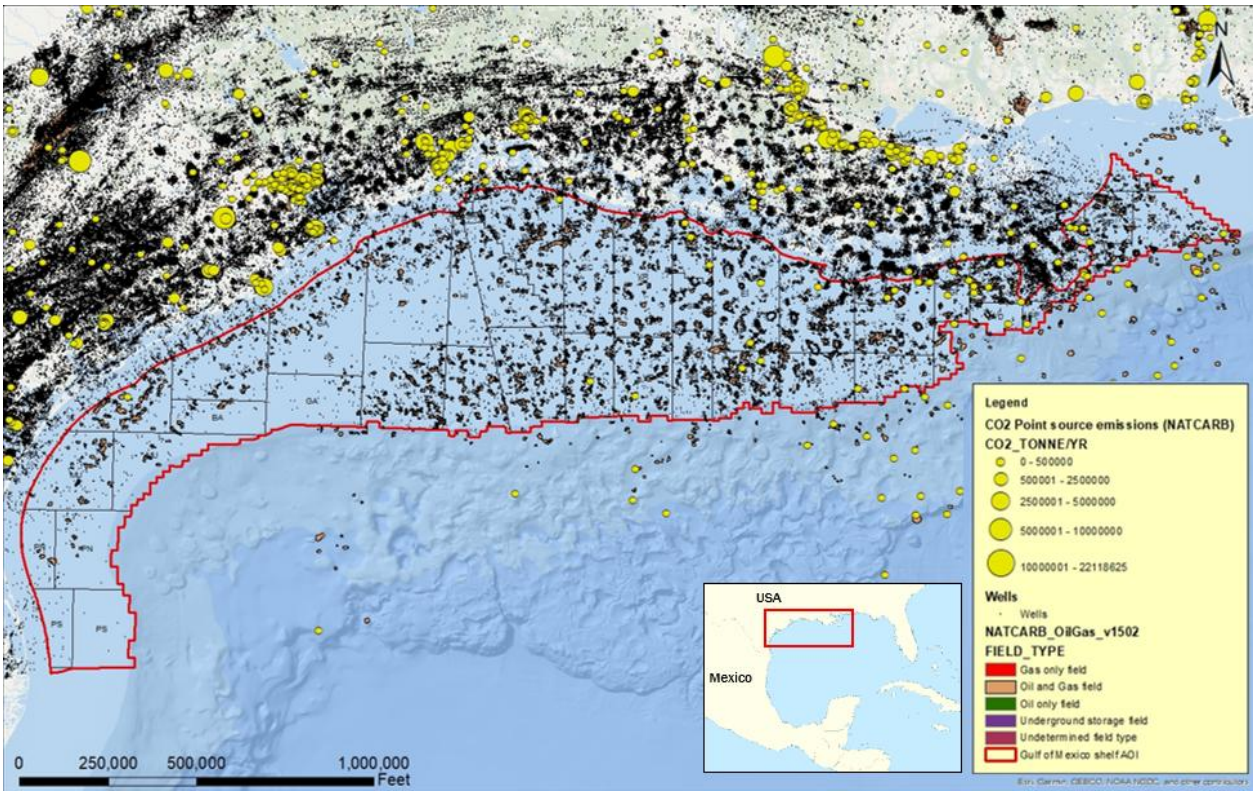

Figure 2.5 – Map showing the study area within the red polygon. The map shows legacy wells (black dots), hydrocarbon fields (orange polygon), and sources of CO_2 emission (yellow dots).

Data used for the study includes 25 2D dip-oriented regional seismic lines across the shelf and approximately 700 wells with raster and LAS wireline logs, and well reports. The data sources were IHS Enerdeq, Enverus PRISM, and the Bureau of Ocean Energy Management (BOEM) 2019 Sand and Paleontology database.

Results indicate significant CO_2 storage potential in the Pliocene interval of the northern and northwest Gulf of Mexico shelf, characterized by basinward prograding stratigraphy and a mix of sand and mud layers (Figure 2.6). The thickness of the CO_2 storage window highlights several regions offshore Louisiana and south Texas as prime storage locations. Net reservoir thickness suggests widespread reservoir presence with porosity ranges between 25 - 30% across the study area. Injectable sands are prevalent and achieving million ton per annum (Mtpa)-scale injectivity is feasible, though it may require perforating multiple sands.

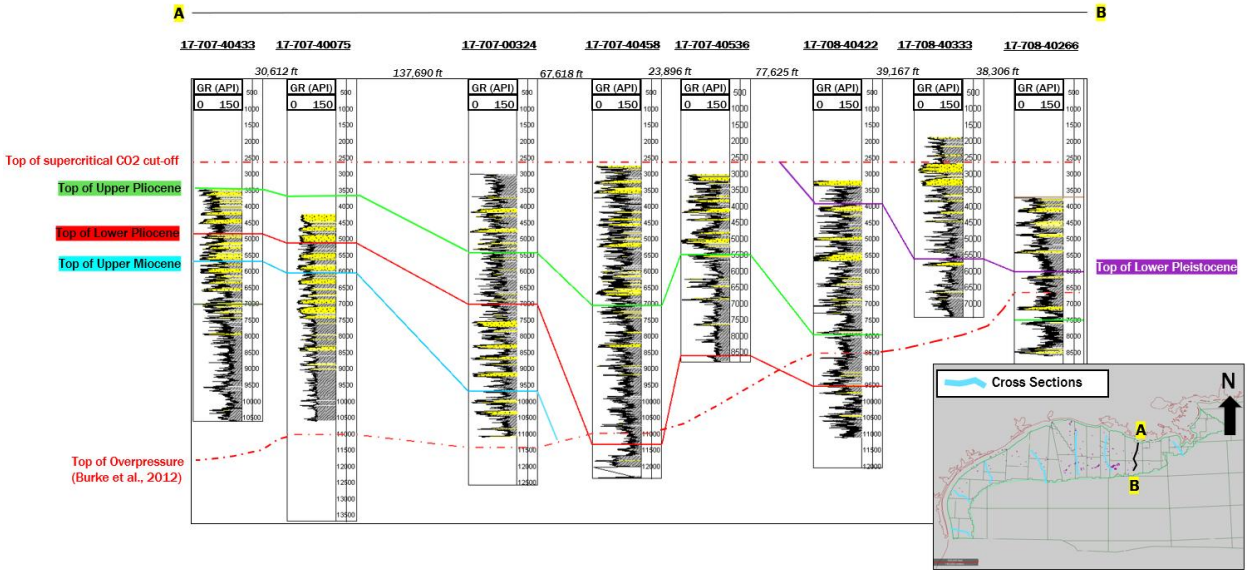

Figure 2.6 - Example of a geological cross-section from offshore Louisiana where A on the left is North, and B on the right is south. This section shows the CO_2 storage window, defined by the top of CO_2 supercritical phase at 800 m below sea level (horizontal red dashed line) and the top of the overpressure (irregular red dashed line). The top of overpressure is defined as hard pressure at 0.7 psi/ft.

The results indicate that the total pressure-based storage capacity/resource is about 85 Gt (gigatons) across the study area and average storage efficiency or pore occupancy is 0.8% (Figure 2.7).

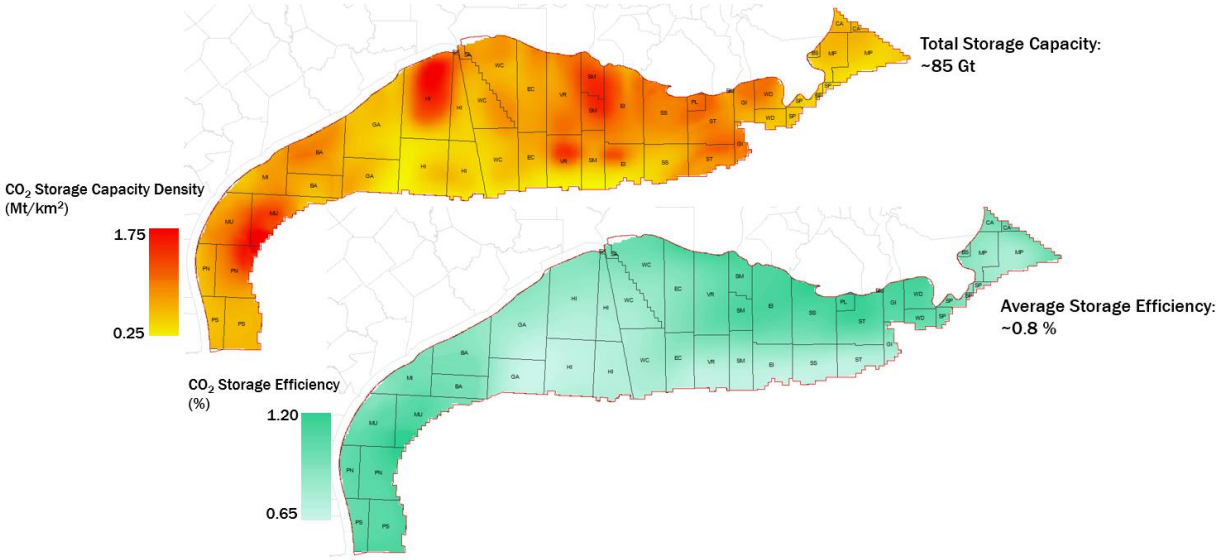

Figure 2.7 - Isocapacity map (top) where the total CO_2 storage resources sum to a potential capacity of 85 Gt with high storage capacity shown in red, reaching almost 1.20 Mt/km2. The CO_2 storage efficiency map (bottom) where the average pore occupancy of 0.8%.

Major containment risks identified include 1) legacy well penetrations to the CO_2 storage window 2) faults as potential leakage pathways and 3) shallow salt beneath the CO_2 storage window. Shallow salt may impact overlying formations due to salt-detachment faulting, potentially leading to the formation of roll-over anticlines or steep angles near fault blocks, which may result in high CO_2 columns and cause leakage risks from the high buoyancy pressure (Figure 2.8).

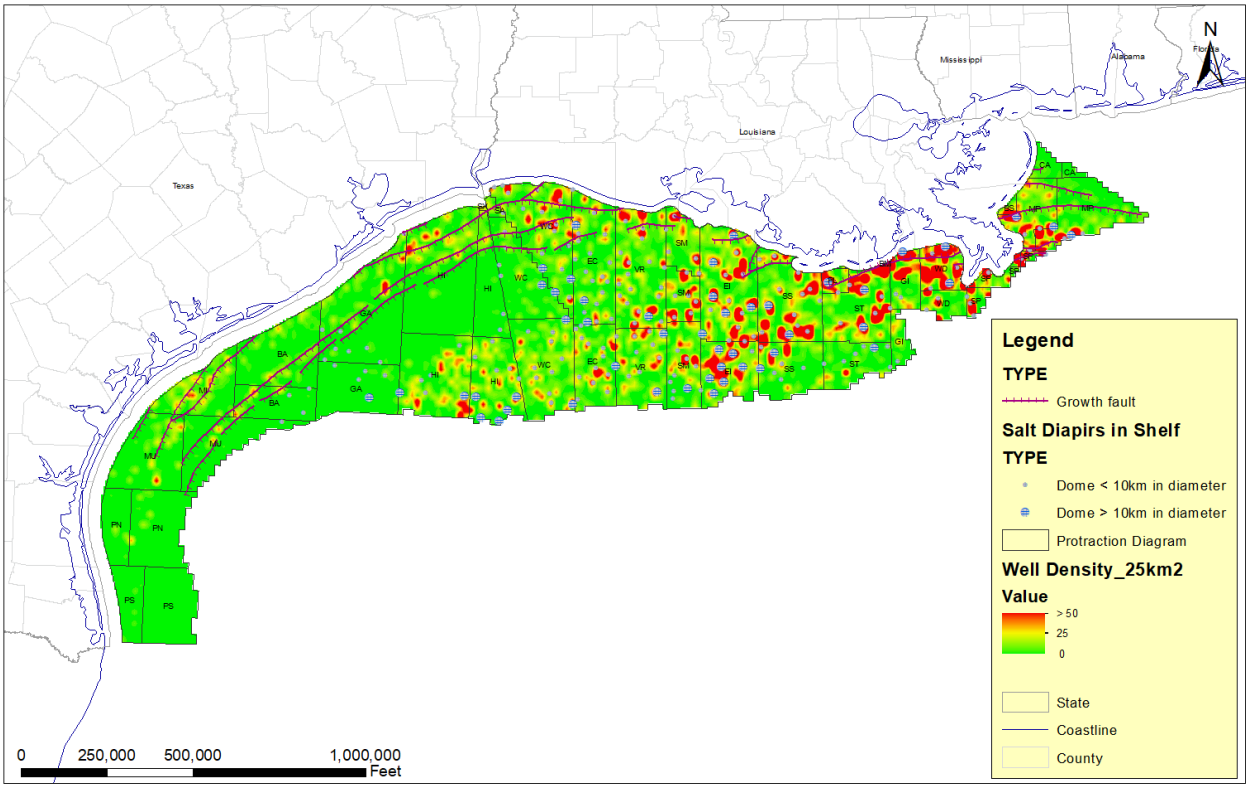

Figure 2.8 - Map showing well density per 5x5 km grid in the Gulf of Mexico shelf. Low density per block is

shown as green, medium density in yellow, and high density in red, with red areas indicating more than 50 wells per 25 km². Map also shows spatial distribution of regional growth fault zones (dark purple line) and salt domes (grey circles). The size of the circles corresponds to the diameter of the salt dome.

Upon examining well density across the shelf, this study identified a total of 72,129 wells. The minimum number of wells per block is 0, while the maximum is 798, located offshore Louisiana. The average number of wells per block is 12, with a median of 1. In the offshore Texas region close to the coast, well counts mostly range from 5 to 30 per block. Conversely, beyond the Corsair Trough fault, the well density decreases significantly, ranging from 0 to 3 wells per block. The area with the highest well density is located offshore Louisiana, where the wells per block vary between 15 and 50. Additionally, some areas exhibit extremely high well density, surpassing 50 wells per block.

In the offshore Texas region, regional growth faults are more prominent compared to the presence of salt bodies. The faulted areas comprise Miocene-age fault zones that have been recognized as key trapping mechanisms for hydrocarbon fields in this region. However, changes in pressure could destabilize these faults, potentially creating a pathway for CO_2 leakage.

Conversely, the offshore Louisiana region features more salt diapirs intersecting shallower intervals. The salt diapirs within the study area have a diameter of generally less than 10 km, but in some parts of the region such as Eugene Island and some parts in West Cameron, the salt diapirs' diameters can extend as wide as 10 km. In areas where salt is close to the surface, the potential for salt weld distortion arises, leading to variations from gently to steeply dipping beds.

Based on regional basin-scale screening analysis, which involves considering trade-offs between proximity to emissions, storage resource, injectivity, and containment risk, two styles or types of potential geological carbon storage sites have been identified: offshore Houston and offshore New Orleans. Offshore Houston offers a larger exploration area with fewer legacy wells, while offshore New Orleans offers higher storage capacity but amid a dense concentration of legacy wells (Figure 2.9). The screening analysis was included in the January – March quarter of year 2024 quarterly report. For details, see that report.

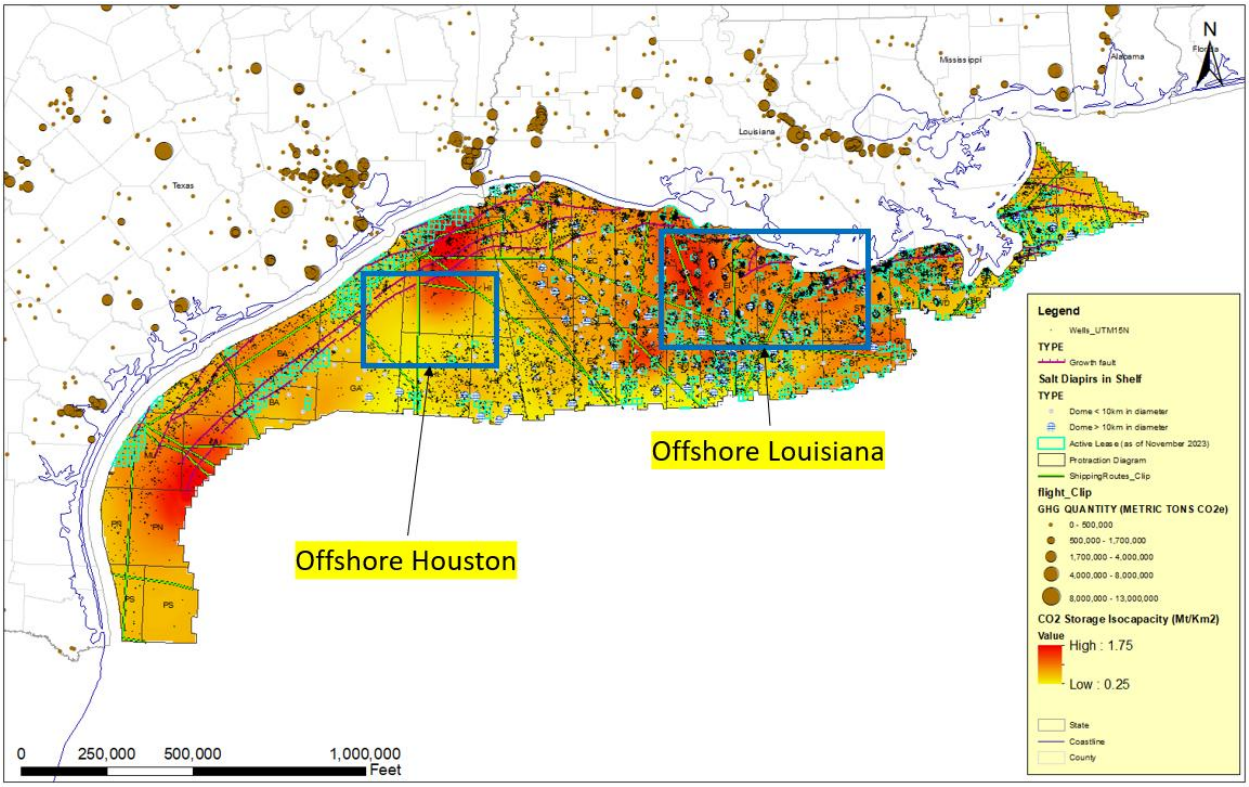

Figure 2.9 - Examples of potential prospect-scale sites are offshore Houston and offshore New Orleans. Offshore Houston exhibits large geographic areas for CO_2 storage site exploration, while offshore New Orleans offers higher storage capacity.

In the offshore Houston region, there are two potential storage site regions identified as project areas. The first area is situated near the NE-SW Corsair fault zone and remains in proximity to a cluster of legacy wells. The second area is positioned outside the Corsair fault zone, closer to synclinal areas, and lacks fault presence. The latter region presents more promising prospects because of minimal legacy wells and the potential for a larger reservoir area. Conversely, the zone adjacent to the NE-SW Corsair fault zone is potentially constrained by narrow growth faults in the northern and southern parts, leading to a reduced reservoir area.

2.1.1.1 Subtask - Western Louisiana, Lafayette and Lake Charles Districts

Three-dimensional (3D) seismic depth volume, FF3D Cameron, was interpreted to extend our understanding of the subsurface of the near offshore Louisiana waters, Cameron Parish. (Figure 2.10).

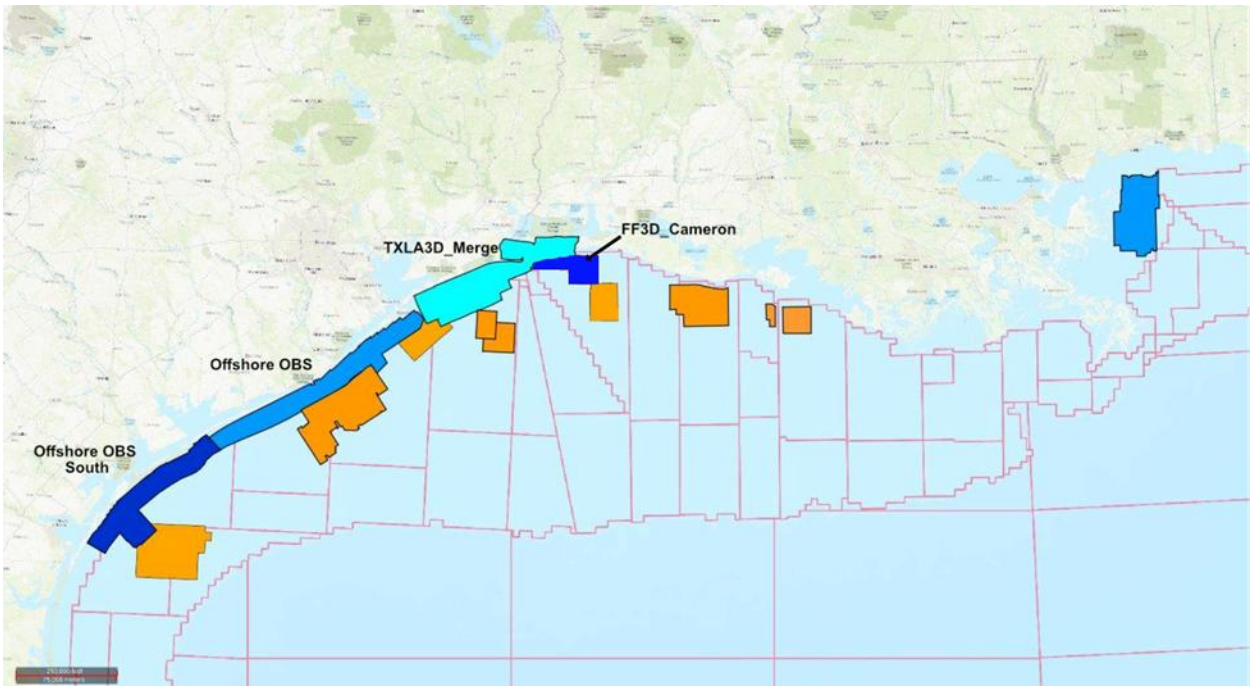

Figure 2.10 - Base map of GoMCarb 3D seismic volumes with leased datasets in different shades of blue. From left to right: Offshore OBS South 3D (cobalt blue), Offshore OBS 3D (cerulean blue), TXLA Merge (turquoise blue), FF3D_Cameron (Navy Blue), and Chandeleur Sound 3D (cerulean blue), and publicly available NAMSS 3D seismic data sets (orange).

Seven horizons interpreted in previous regional analyses were depth converted and used to correlate between two overlapping 3D surveys, TXLA_Merge and FF3D_Cameron (Figure 2.11). The depth conversion used a migration velocity volume generated during the TXLA_Merge data processing process to convert the two-way time horizons to TVD Depth. Figure 2.12 shows a map with annotated cross-section location extracted from the FF3D_Cameron seismic data. Figure 2.13 shows the un-interpreted north-south seismic dip line. Figure 2.14 has interpretations with SP logs, faults, picks, and associated horizons.

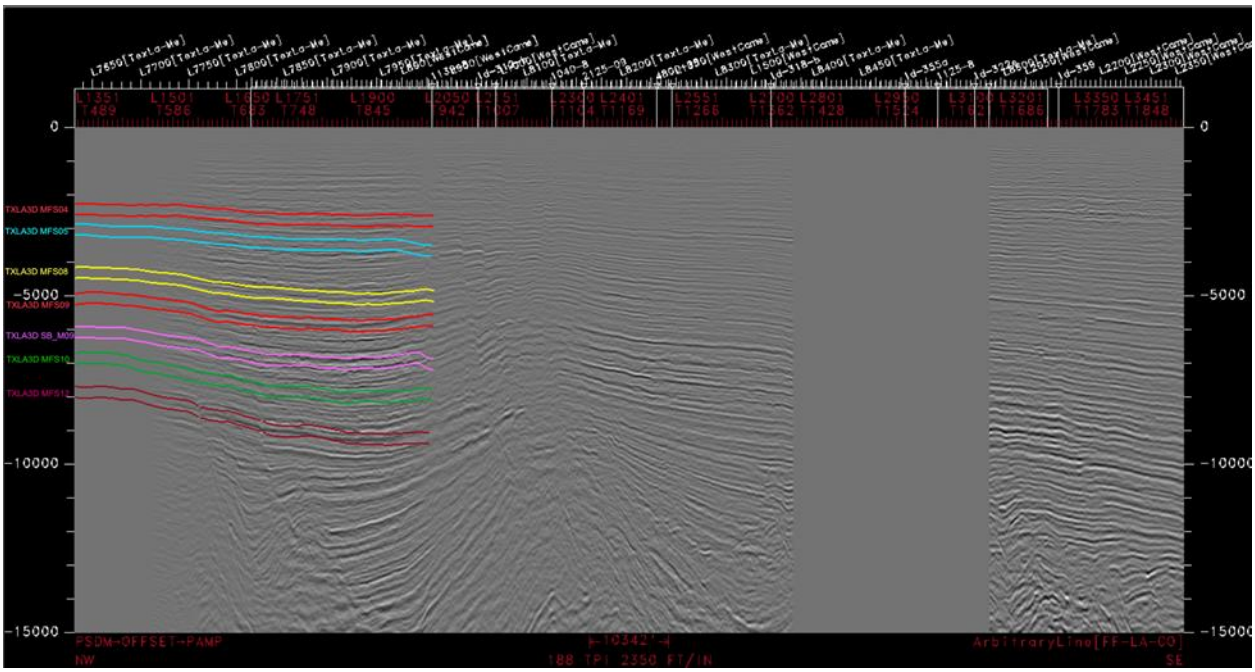

Figure 2.11 - Seismic section showing seven key horizons mapped from previous regional analysis were extended into the overlapping FF3D_Cameron seismic survey. (Proprietary seismic data figure redacted.)

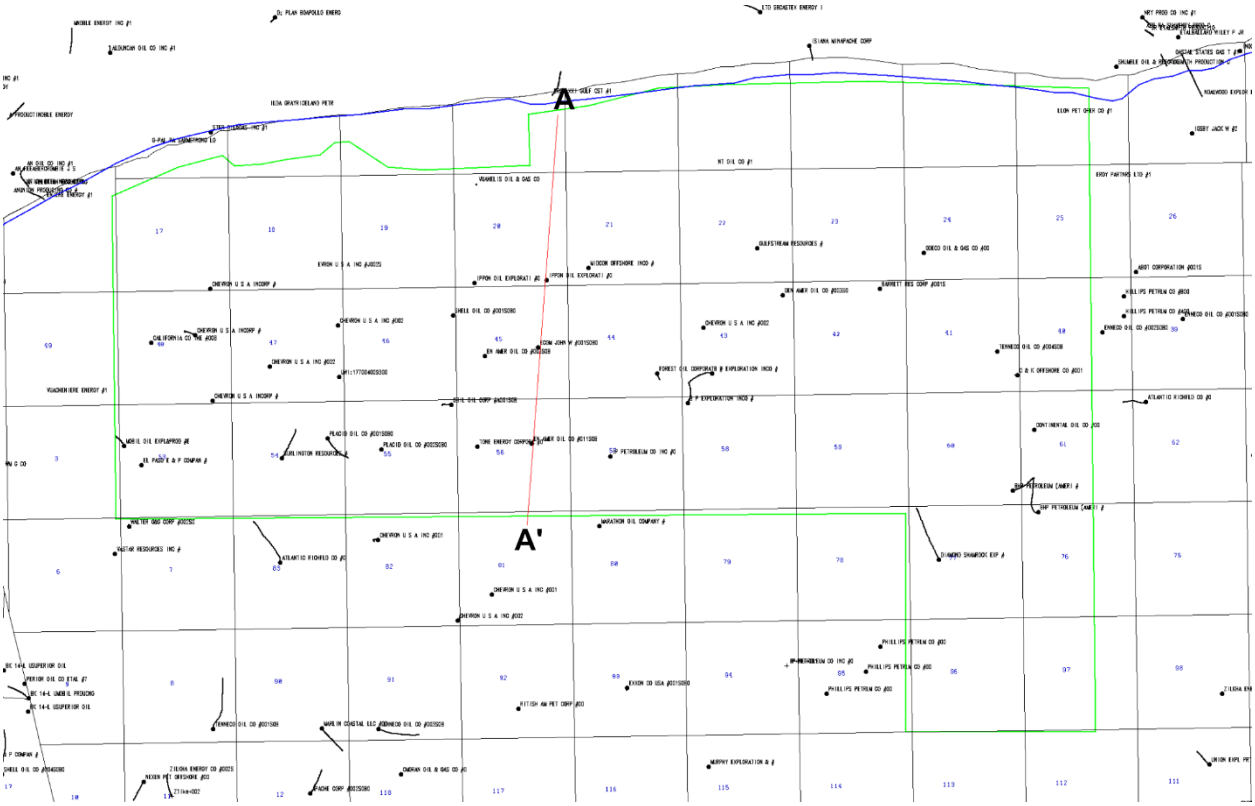

Figure 2.12 - Base map of the FF3D_Cameron study area with cross-section A-A' annotated.

Figure 2.13 - An un-interpreted seismic cross-section A-A'. (Proprietary seismic data figure redacted.)

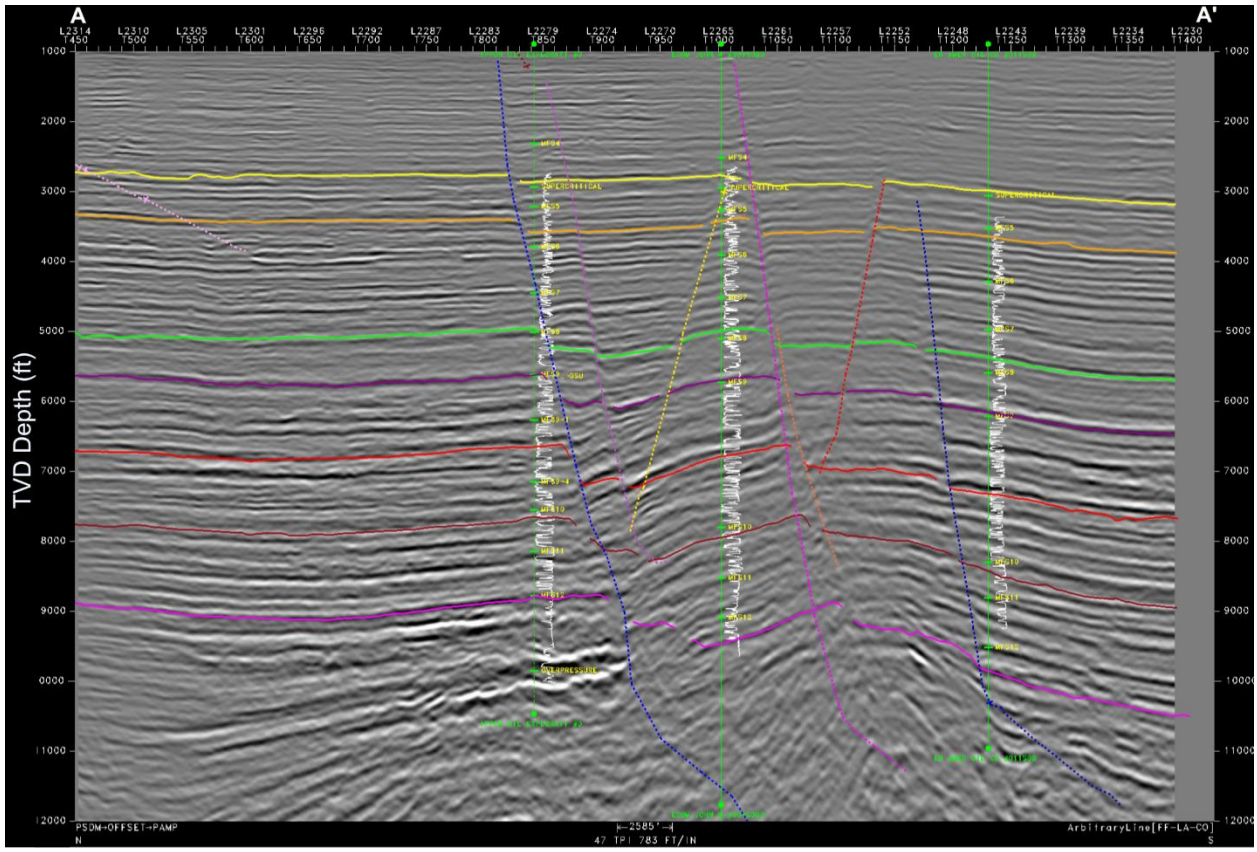

Figure 2.14 - An interpreted seismic cross-section A-A'.

Structural maps (Figure 2.15) are used to identify areas that might be structurally conducive (high areas with closure/trapping features) for carbon capture and storage (CCS). RMS amplitude maps (Figure 2.16) can identify mudstone-dominated rocks, typically manifested as low amplitude zones/areas in seismic. In addition, the RMS amplitudes are sensitive to sandstone-bearing depositional systems, usually manifested as high amplitudes, within the reservoir-bearing successions and help define the spatial distribution of genetically related depositional successions. (Proprietary seismic data figure redacted.)

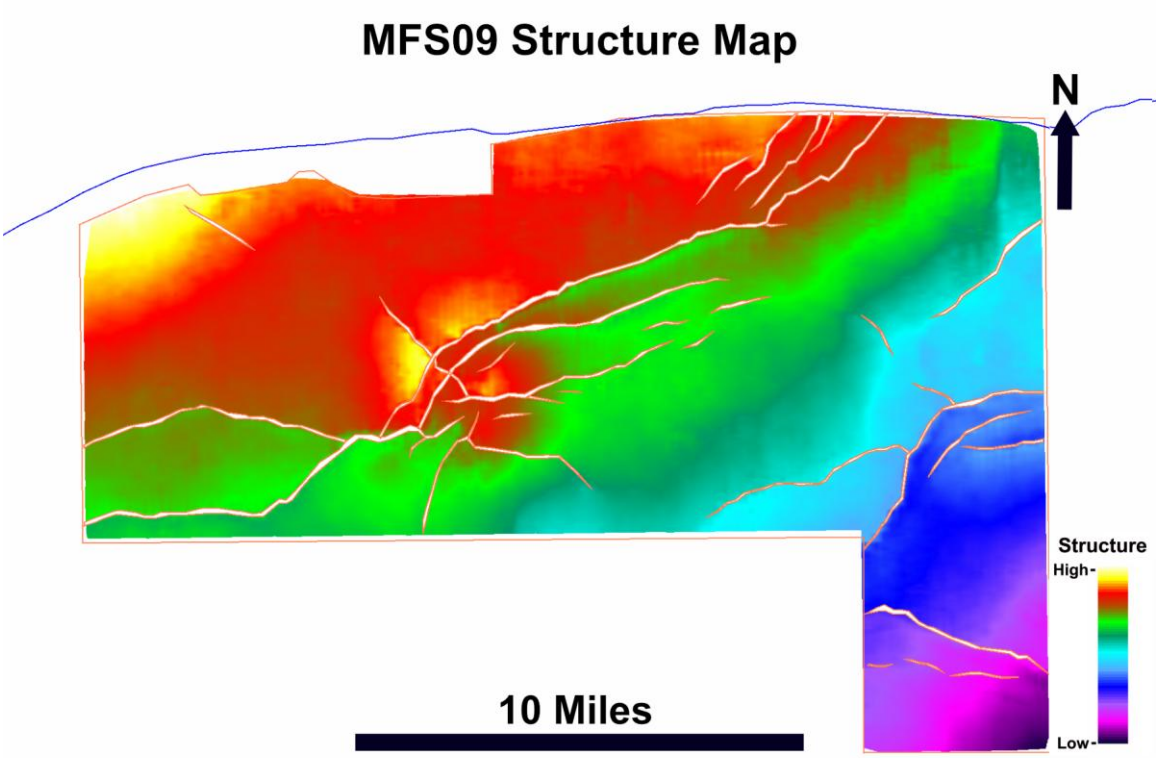

Figure 2.15 - Surface MFS09 structure map in the FF3D_Cameron seismic survey. There are 34 interpreted fault planes (polygons) that contact this horizon.

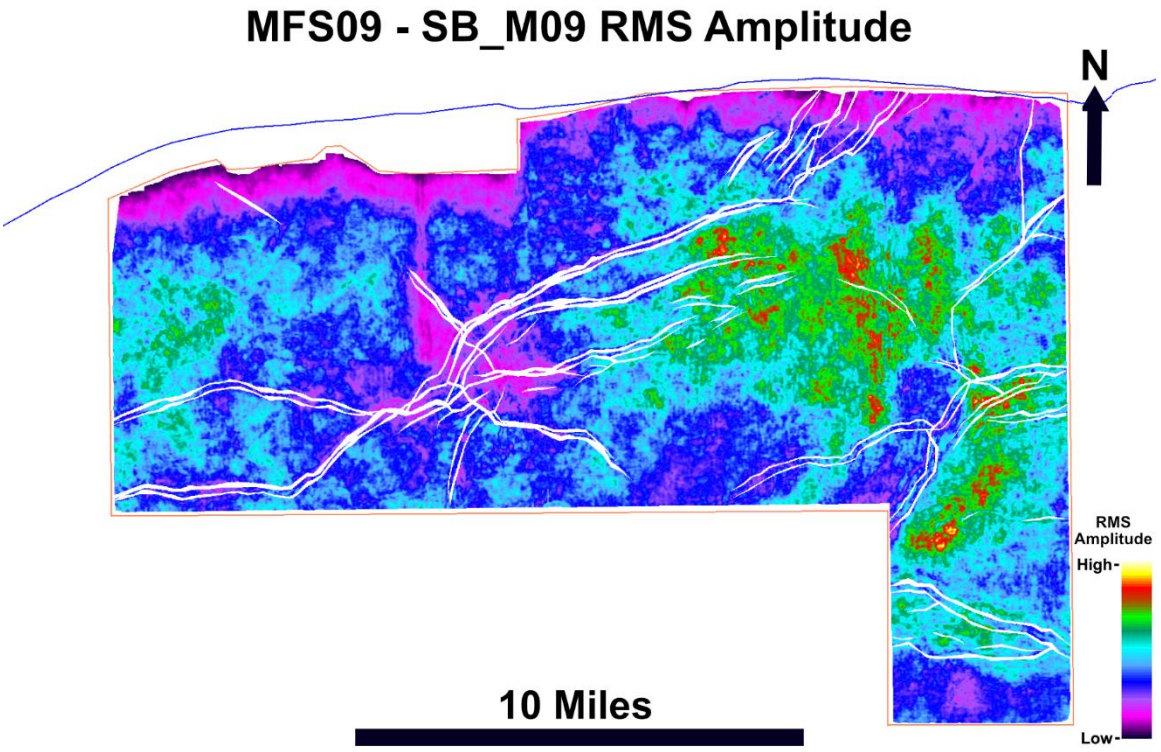

Figure 2.16 - RMS amplitude map extracted from the interval between MFS09 and SB_M09 in the FF3D_Cameron seismic survey. High-amplitude signatures (yellow to red) record largely sand rich facies.

The MFS09 surface (top of the prime geological storage interval) was used to identify the largest 50 structural closures in the FF3D_Cameron study area. The associated "fetch areas" represented in Figure 2.17 defines zones that could contain migrating fluids by capillary trapping and/or dissolution throughout the migration path (Figure 2.18 and Figure 2.19). Figure 2.20 shows known culture (pipelines, oil & gas fields, etc.) and the closure/fetch pairs within the study area. By combining the seismic structural interpretation, seismic attribute analysis, well logs, historical production, and closure/fetch analytical quantitative information, we can begin ranking potential CCS sequestration sites.

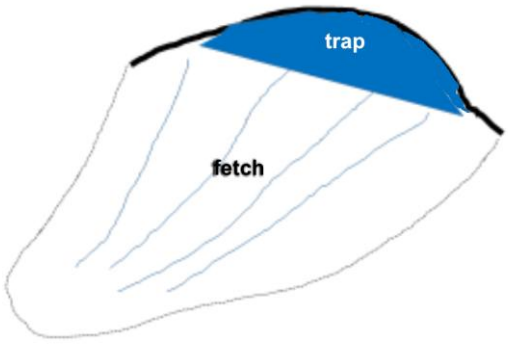

Figure 2.17- Depiction of trap and fetch.

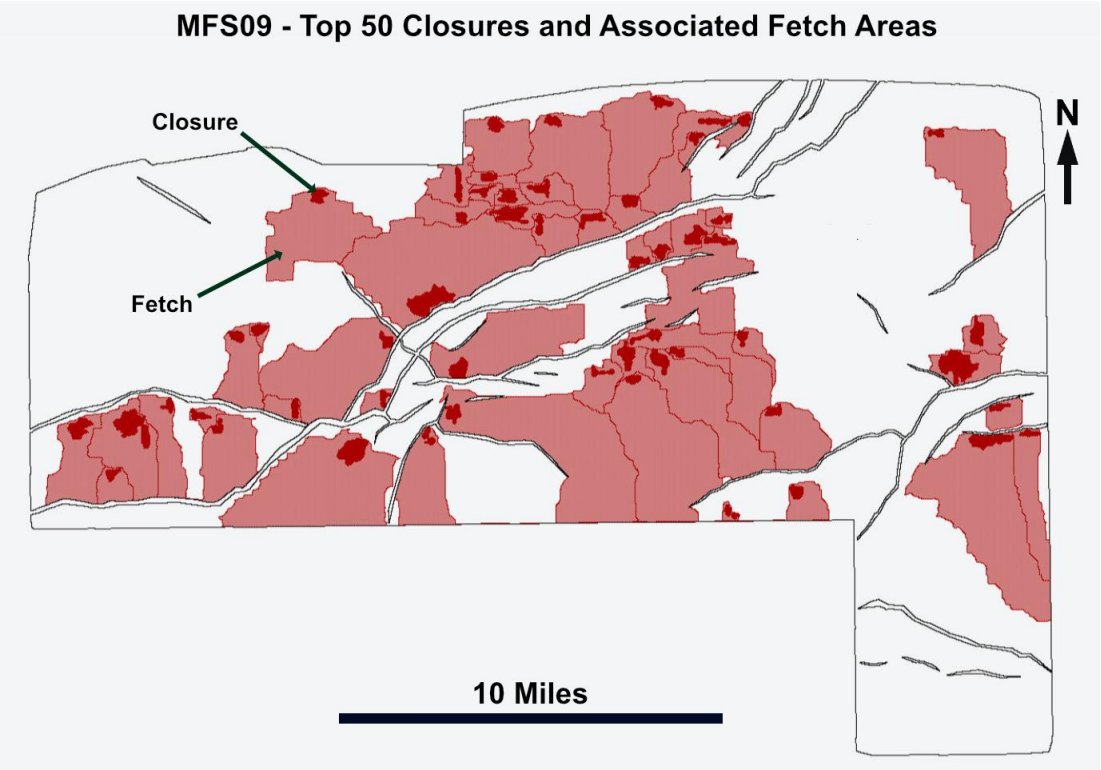

Figure 2.18 - FF3D_Cameron survey showing the top 50 closures (dark red) mapped on the MFS09 horizon with their associated fetch areas (light red).

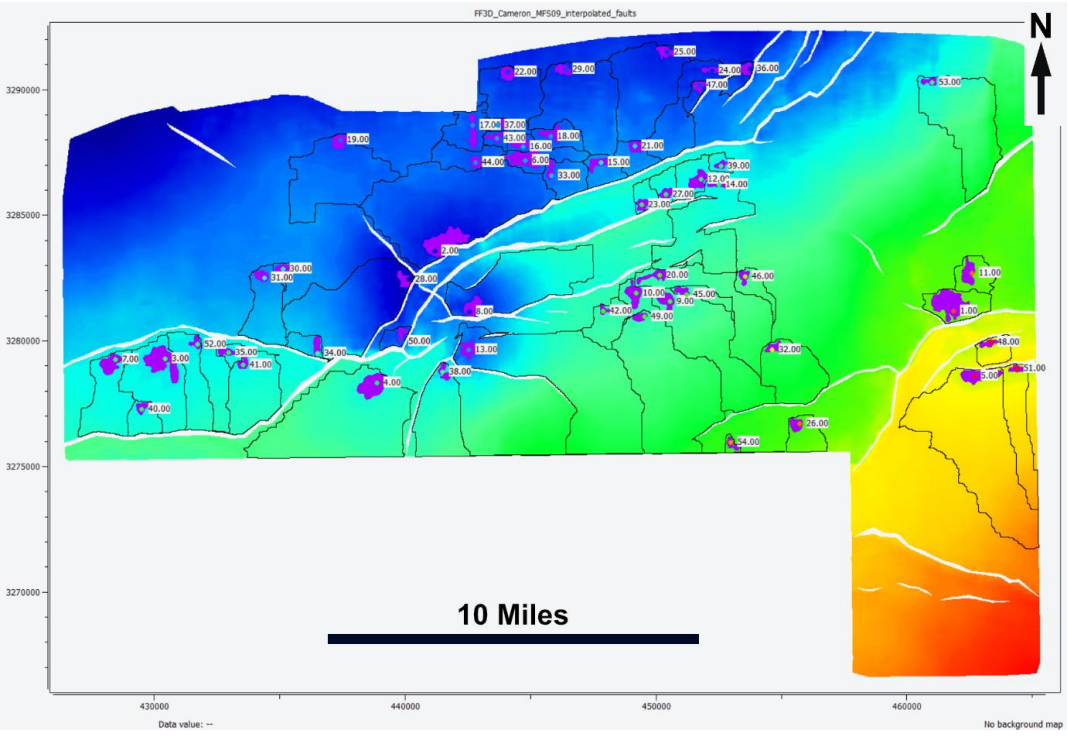

Figure 2.19 - FF3D_Cameron survey showing the top 50 closures and fetch areas overlain with the MFS09 horizon with their associated ID numbers.

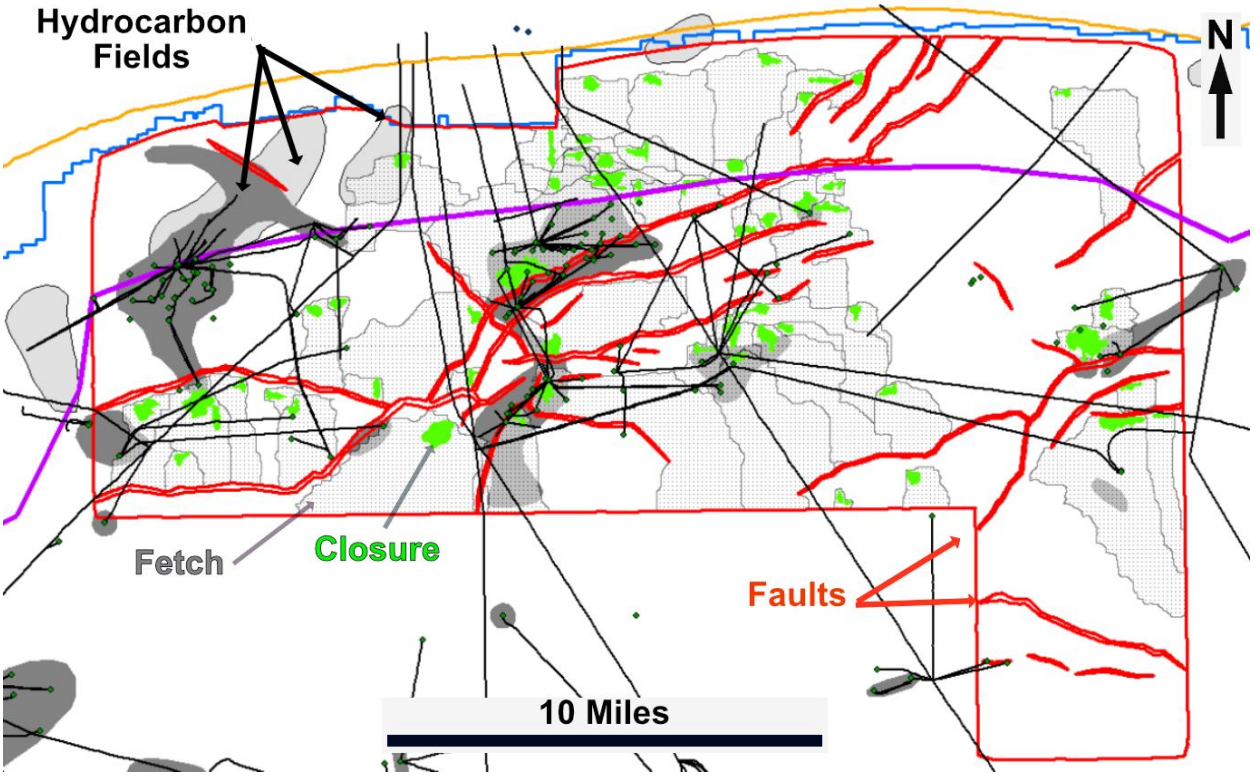

Figure 2.20 - FF3D_Cameron survey showing within the survey outlines the top 50 structural closures (green) mapped on the MFS09 horizon with their associated fetch areas (stippled gray) overlain with fault polygons (thick red lines), hydrocarbon fields (gray polygons), and pipelines (thin black lines).

2.1.1.2 Subtask - Mid-Texas coast offshore Houston to Corpus Christi

In addition to the following work for, two theses within this subtask were supported by GoMCarb:

Franey, John, 2021, High Order Stratigraphic Framework of Intraslope Growth Faulted Subbasins Offshore Matagorda Bay, Texas; master's thesis – The University of Texas at Austin; http://dx.doi.org/10.26153/tsw/41918 .

Hull, Harry Lejeune, 2021, Characterizing Reservoir Quality for Geologic Storage of CO_2 - A Case Study from the Lower Miocene Shore Zone at Matagorda Bay, Texas; master's thesis – The University of Texas at Austin; http://dx.doi.org/10.26153/tsw/21487 .

Major Confining Zones Regional Analysis

Regional Mapping of the *Amphistegina* B and Anahuac Confining Zones

The upper Oligocene Anahuac and lower Miocene *Amphistegina* B ("Amph. B") units serve as regional confining zones in the offshore and near-onshore regions of the Texas Gulf coast. Both units occur within successions of interbedded abundant sandstone and shale and represent periods of relatively low sedimentation rates during widespread shoreline transgression. Many of the sandstones compose reservoirs for hydrocarbons and, when depleted, could serve as reservoirs for injected CO_2. Analysis of wireline well-log signature, regional distribution, and thickness variation of the Anahuac and *Amphistegina* B units as confining zones is essential for evaluating the potential for CO_2 storage in stratigraphically adjacent non-hydrocarbon-bearing sandstone reservoir facies. No regional-scale isopach map of the Anahuac or *Amphistegina* B units was identified in the scientific literature, perhaps because of uncertainty of stratigraphic boundaries. Therefore, GoMCarb has undertaken the regional isopach mapping of the two units in an area of the near-onshore and adjacent state offshore waters of coastal Texas

that extend approximately 350 miles from the Rio Grande in the southwest to Galveston Bay in the northeast. Figure 2.21 is a map of the Texas coast including wells with available well-logs and the location of original regional-dip-oriented cross sections 1-1' through 3-3' in the study area.

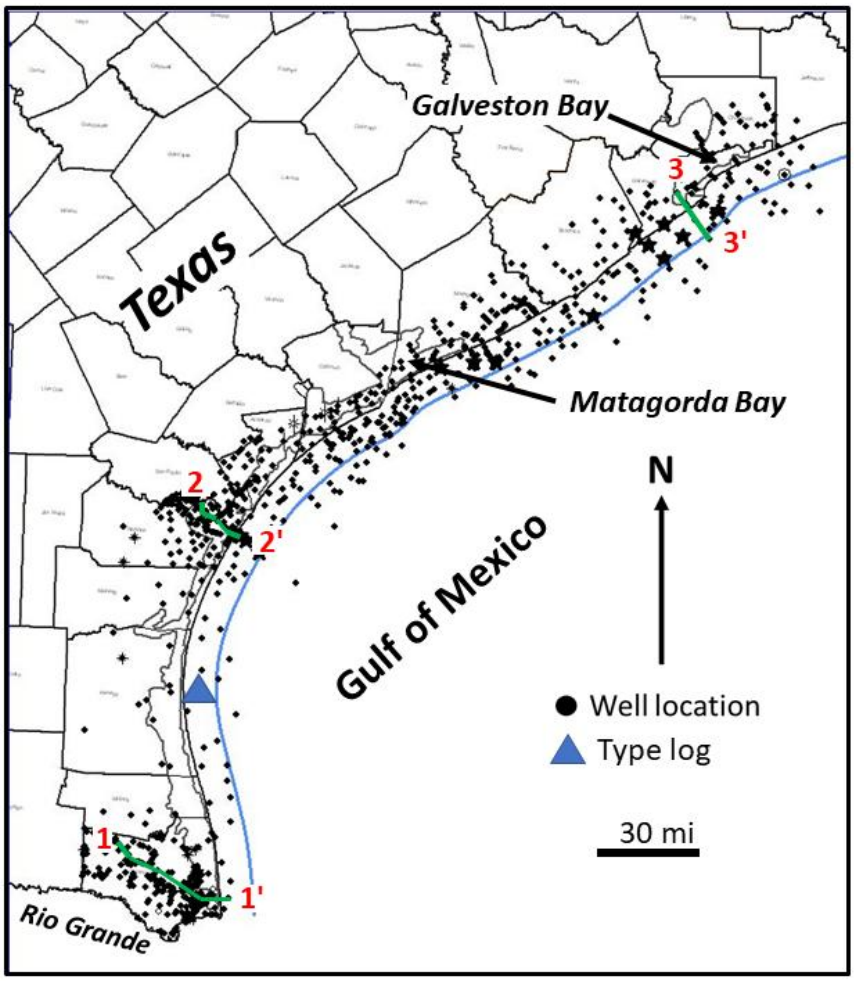

Figure 2.21 - Map of available well-log distribution and location of regional-dip-oriented cross sections 1-1' through 3-3' in the coastal Texas study area extending from the lower Rio Grande Valley to Galveston Bay.

Type Section and Lithology

The dominant lithology of the upper Oligocene to lower Miocene section is interbedded sandstone and shale in successions of a few hundred feet to a few thousand feet thick (Figure 2.22). Thick (500-1000 ft) upward-coarsening and blocky to blocky-serrate sandstone wireline-log facies separated by thinner (100-500 ft) upward-fining intervals predominate throughout the lower Miocene successions. Many faults, including regional growth faults that are more abundant in the offshore area, truncate sections of the study succession and complicate the process of well-to-well correlation. Another limitation in correlation is well-log depth. Many wells, especially those in state offshore waters (Figure 2.21) are not deep enough to record the base of the Anahuac unit (Figure 2.23 - Figure 2.25).

Correlations were primarily based on well log signatures and did not fully benefit from biostratigraphic data; although a few wells with some biostratigraphic data did serve to confirm regional correlations of the *Amphistegina*

B unit. In general, however, correlation of the confining units was undertaken lithostratigraphically even though we recognize that such correlations cross time lines. The goal of the effort was to map the gross thickness of the two confining units under the assumption that they comprise mostly fine-grained facies that can serve to impede and/or retain fluid flow and increase pressure resulting from CO_2 injection.

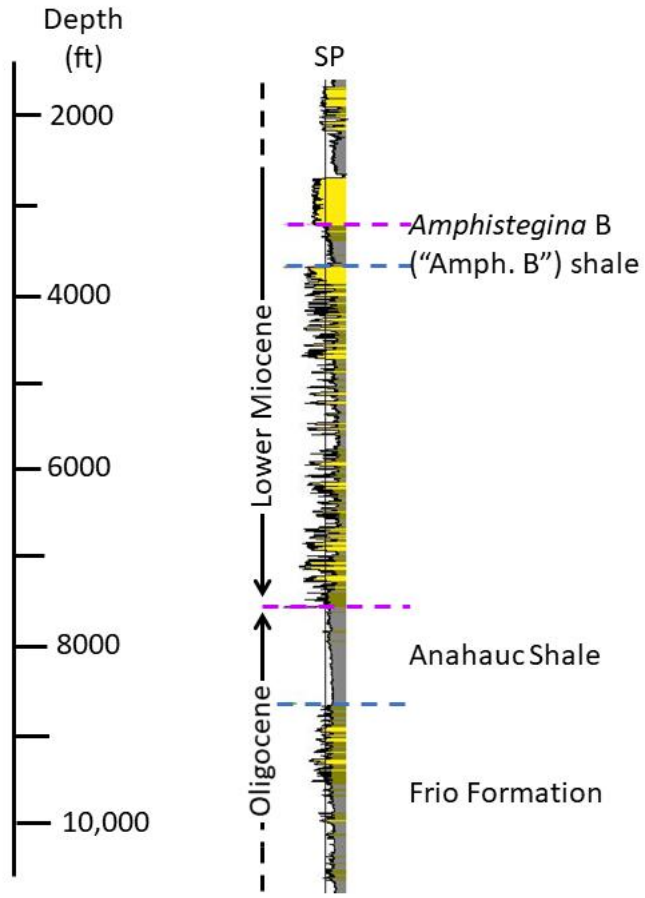

Figure 2.22 - Regional type log of the upper Oligocene and lower Miocene succession of the Texas Gulf Coast (CNG Producing Co. No. 1, SL76512 – offshore Texas State waters of Kenedy, County). Both the Anahuac and *Amphistegina* B units (aka "shale") thicken eastward into the basin. The Oligocene Frio Formation and lower Miocene age section are major hydrocarbon-bearing units. Type log location shown in Figure 2.21.

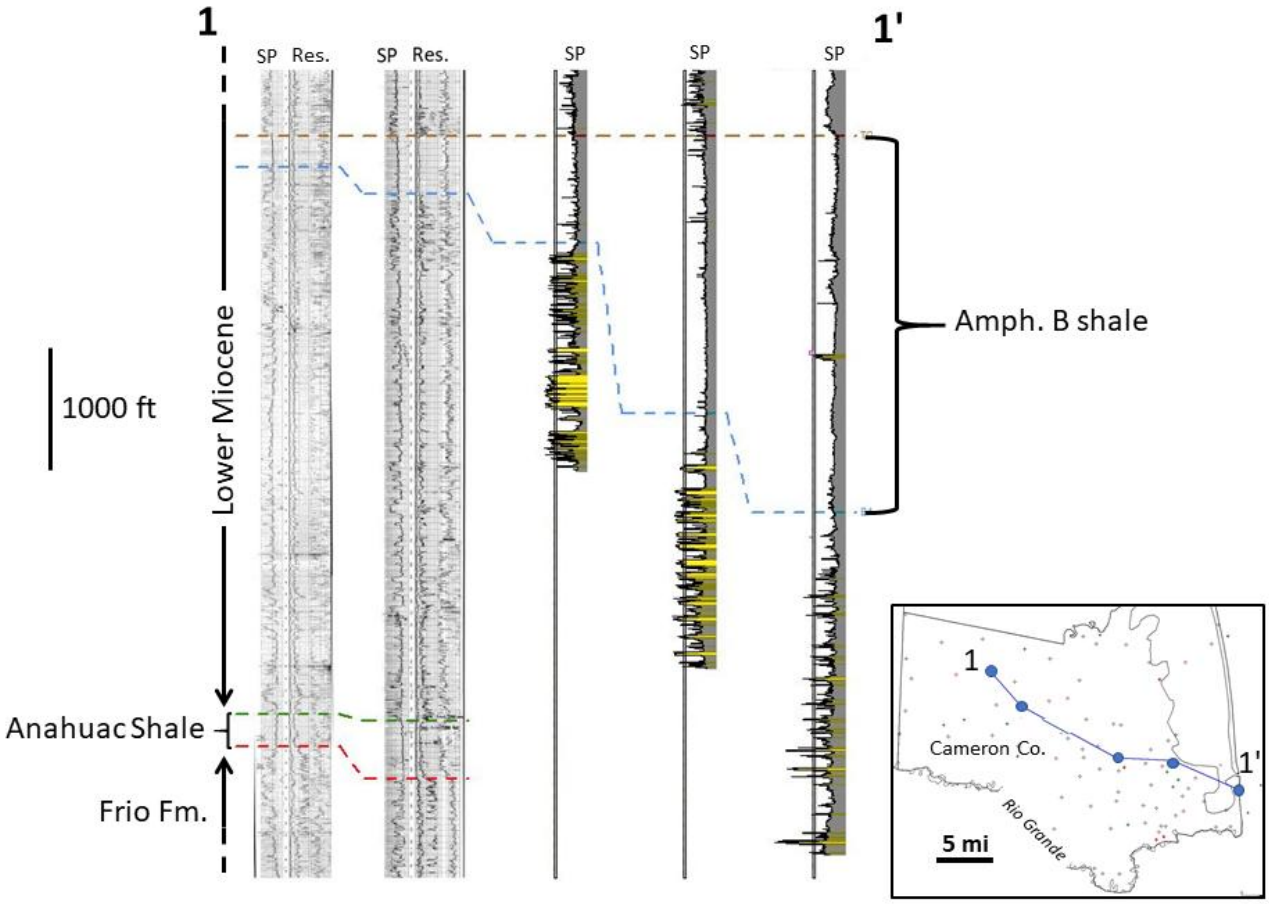

Figure 2.23 - Stratigraphic cross section 1-1'. Datum is the top of the *Amphistegina* B unit.

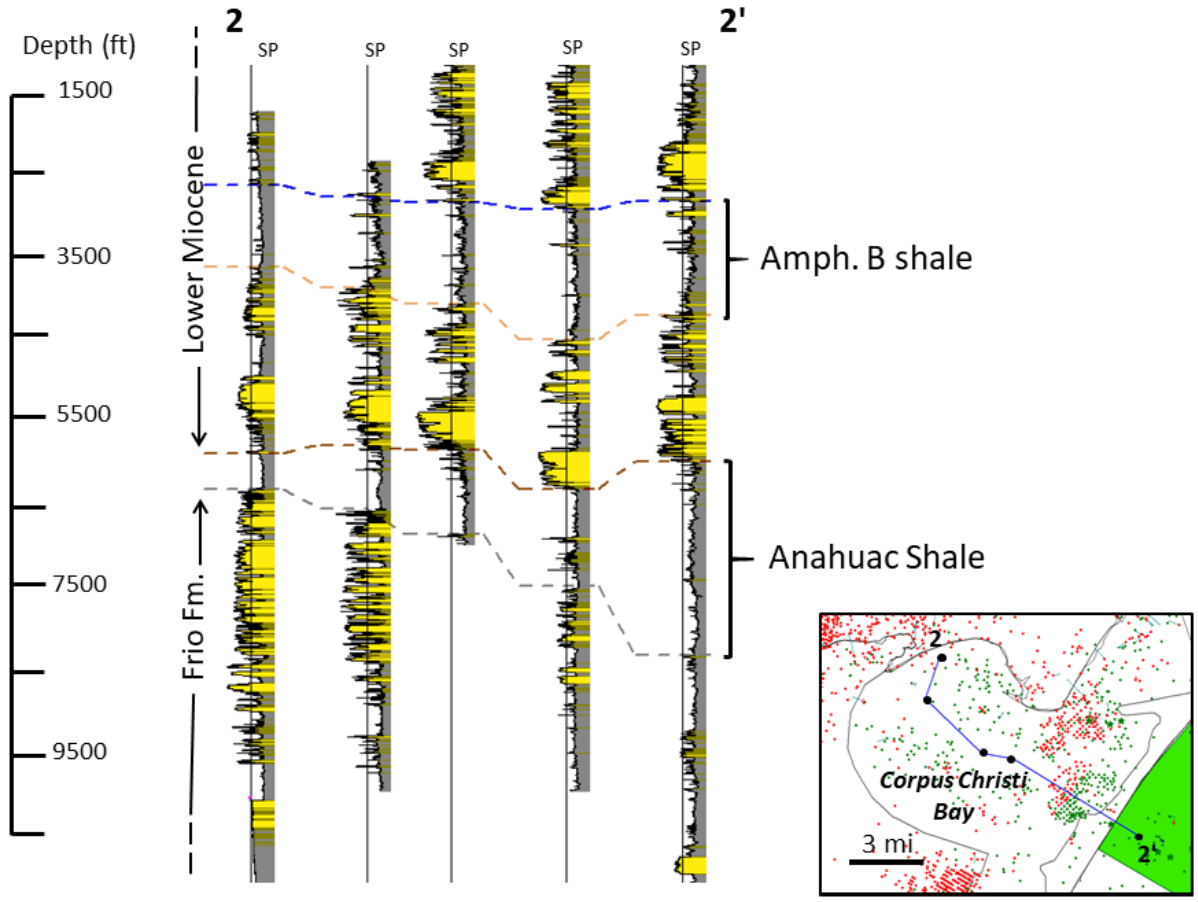

Figure 2.24 - Structural cross section 2-2'. Cross section also located in Figure 2.22.

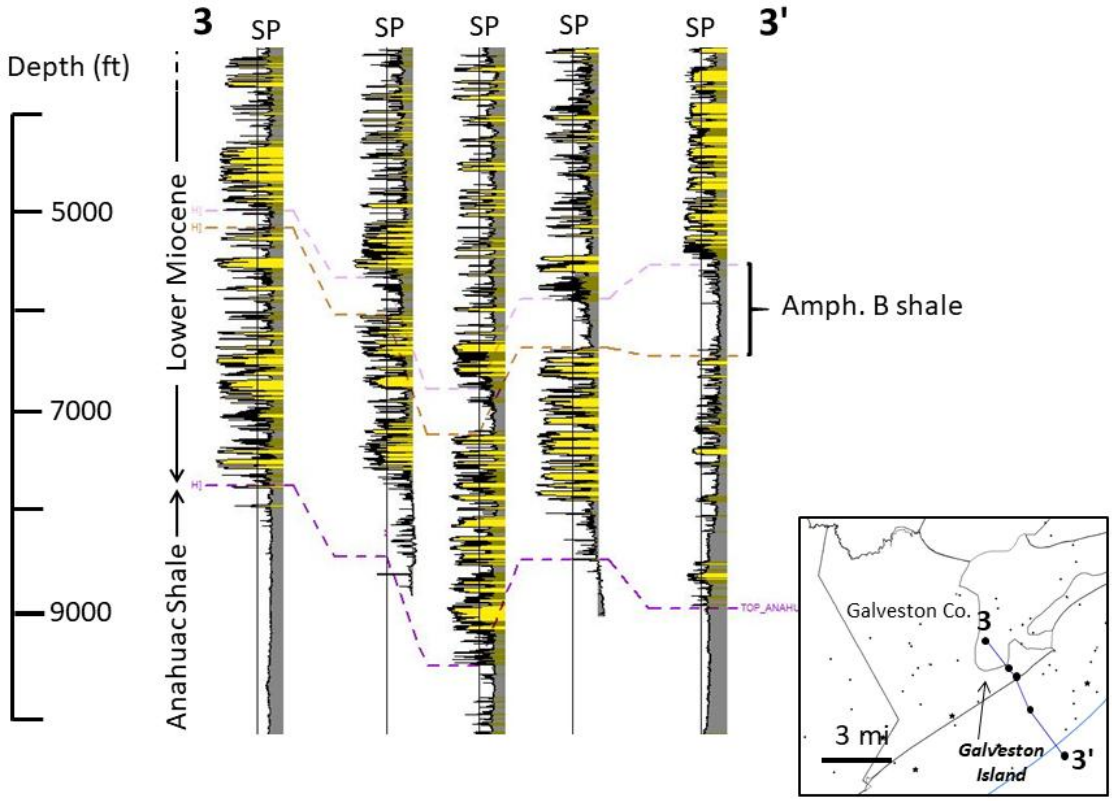

Figure 2.25 - Structural cross section 3-3'. Cross section also located in Figure 2.21.

Regional Stratigraphy

Initially, the regional correlation exercise encompassed the entire Texas coast and included only the three cross sections discussed above. Subsequently, it concentrated on the southern portion of the coast (Figure 2.26) as this area had received less attention from the nascent CCS industry at the time of the study. Except for cross section 1-1', the numbering scheme for the original three cross sections changed to that shown in Figure 2.26.

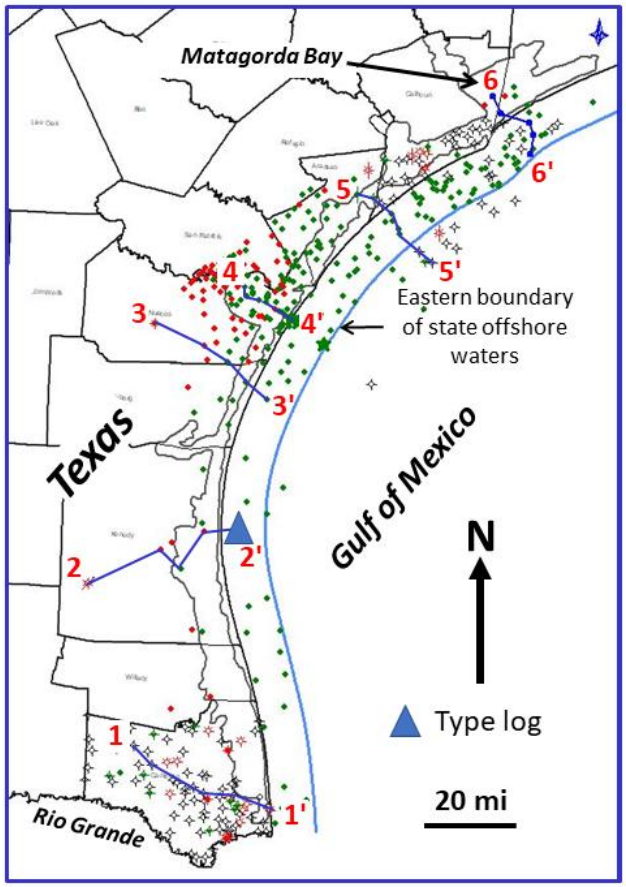

Figure 2.26 - Map of available well-log distribution and location of regional-dip-oriented cross along the southern Texas coastal region.

Anahuac Unit

In the updip, western part of the study area, lithostratigraphic boundaries of the Anahuac unit are generally sharp. In the down-dip, eastern half of the study area, lithostratigraphic boundaries of the Anahuac unit are generally gradational, occurring as retrogradational, upward-thinning and upward-fining thin (<20 ft) sandstone beds at the basal boundary and as progradational, upward-thickening and upward-fining sandstone beds at the upper boundary (Figure 2.23 - Figure 2.24).

Amphistegina B Unit

As with the Anahuac successions, lithostratigraphic boundaries of the *Amphistegina* B unit are generally sharp in the updip, western part of the study area and gradational in the downdip, eastern part of the area (Figure 2.23-5).

Thickness of the Anahuac and *Amphistegina* B Units

Anahuac Unit

The Anahuac Unit markedly thickens basinward (Figure 2.23, Figure 2.24). It ranges from about 250 ft in the western, onshore areas to greater than 3,500 ft in the eastern extent of correlations. Structurally, the Anahuac Unit is generally gently eastward-dipping (Figure 2.24, Figure 2.25), except across major growth faults that are salient features of the eastern half of the study area (Figure 2.27, Figure 2.28). The unit appears to thicken more abruptly in the southern and northern thirds of the study area; although this observation may be influenced by the lower degree of well control in the central portion of the study area (Figure 2.27).

Amphistegina B Unit

The *Amphistegina* B unit also generally thickens basinward in the southern part of the map area, generally thins in the central part, and thickens in the northern part (Figure 2.23 - Figure 2.25). Thickness of the unit varies from a minimum of about 170 ft in western Kenedy County to greater than 3,100 ft in easternmost Cameron County across an inferred growth-fault zone (Figure 2.23).

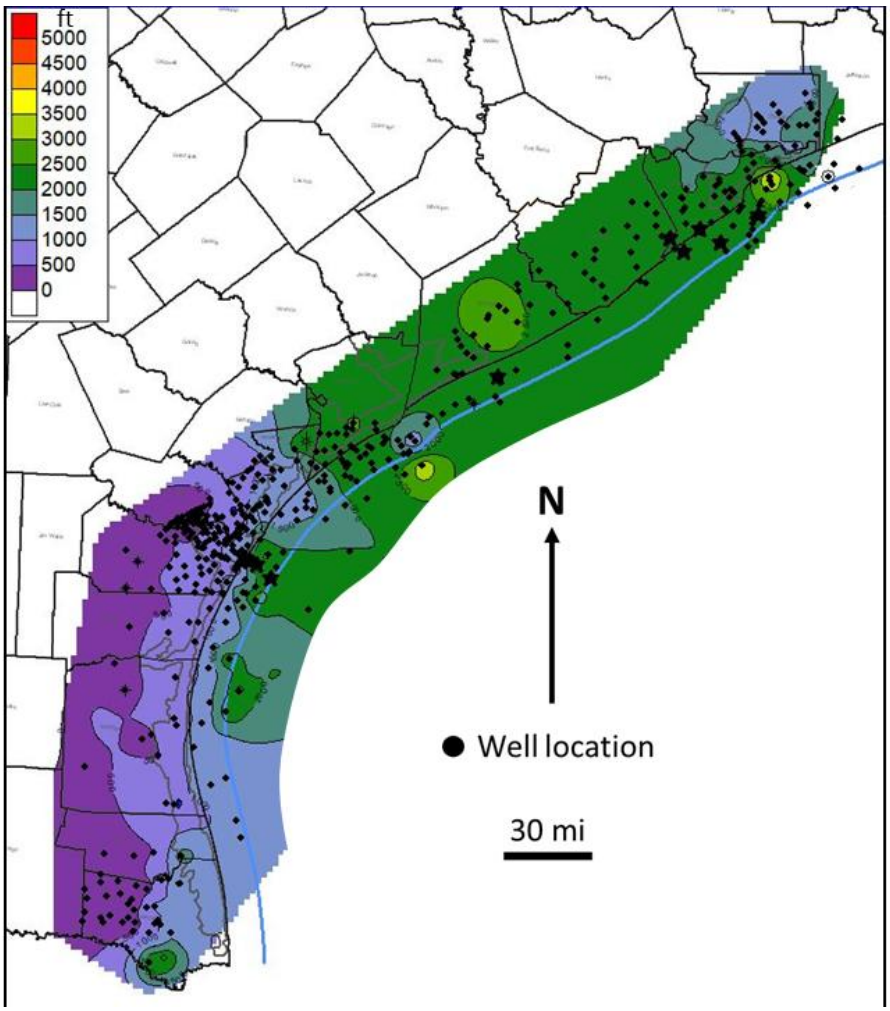

Figure 2.27 - Isopach map of the Anahuac Unit illustrating the marked thickening of the unit toward the east (Figure 2.23, Figure 2.24). Local, abrupt thickening of the section in the far southern, central, and northern parts of the map record the presence of basinward-dipping growth faults that cannot be precisely defined using only well-log data.

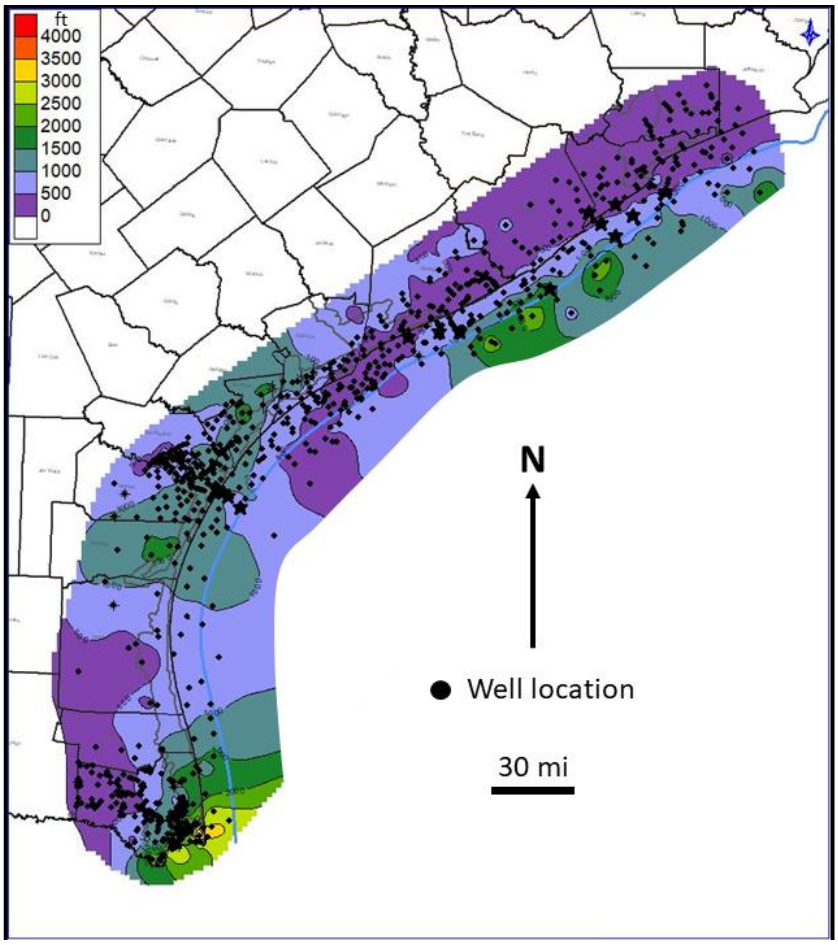

Figure 2.28 - Isopach map of the *Amphistegina* B illustrating basinward thickening of the unit in the southern half of the map area, the general basinward thinning of the unit in the central part of the map area, and thickening in the northern part. Area of inferred, pronounced growth-fault thickening is evident in the southernmost part of the area.

Amphistegina B Unit

Unlike the Anahuac, the *Amphistegina* B unit thickens basinward in the southern half of the map area (Figure 2.29-Figure 2.32), but it generally thins basinward in the northern half of the map area (Figure 2.33, Figure 2.34, Figure 2.35). Thickness of the unit varies from a minimum of about 170 ft in western Kenedy County (Figure 2.30) to greater than 3,100 ft in easternmost Cameron County (Figure 2.29) across an inferred growth-fault zone (Figure 2.36).

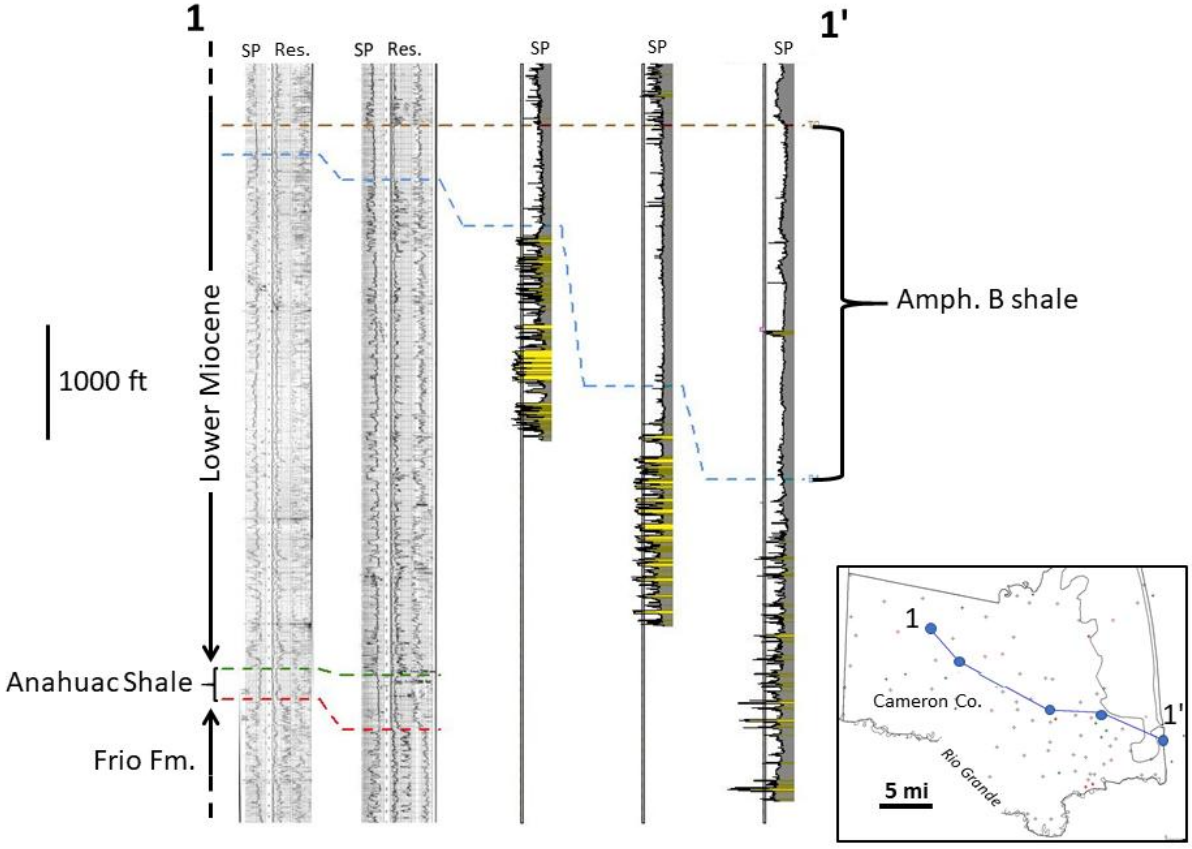

Figure 2.29 - Stratigraphic cross section 1-1'. Datum is the top of the *Amphistegina* B unit. See also cross section located in Figure 2.26.

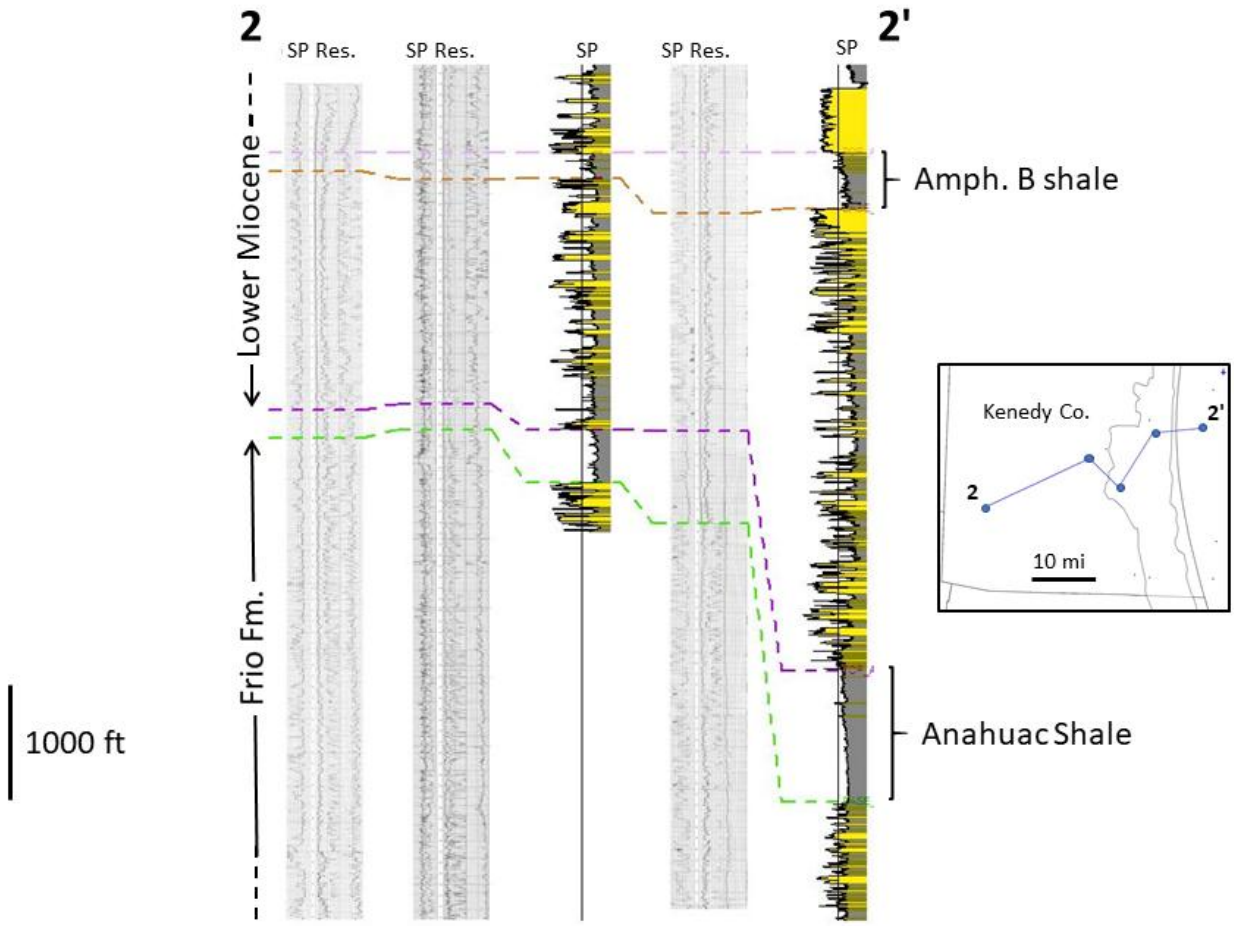

Figure 2.30 - Stratigraphic cross section 2-2'. Datum is the top of the *Amphistegina* B unit. See also line of section located in Figure 2.26.

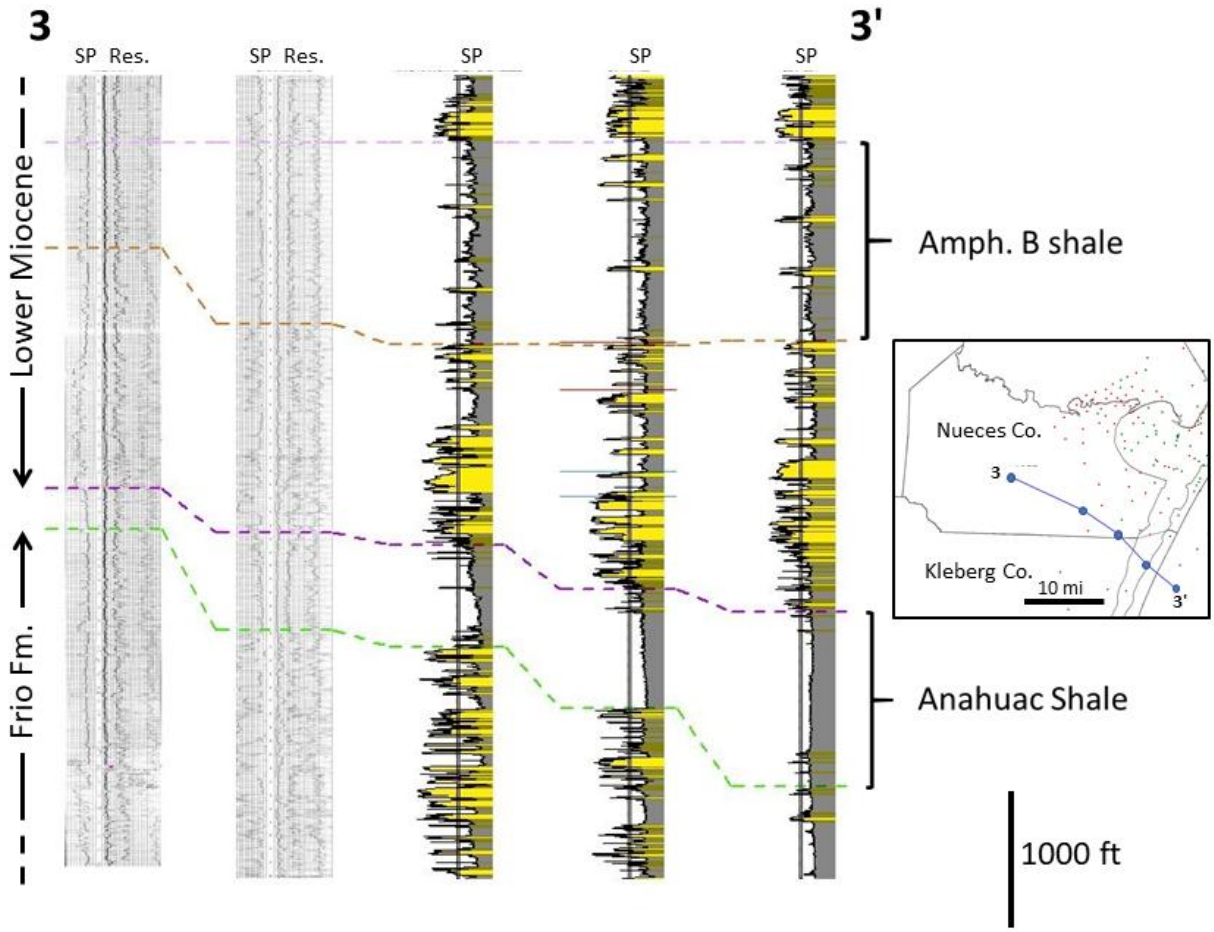

Figure 2.31 - Stratigraphic cross section 3-3'. Datum is the top of the *Amphistegina* B unit. See also line of section located in Figure 2.26.

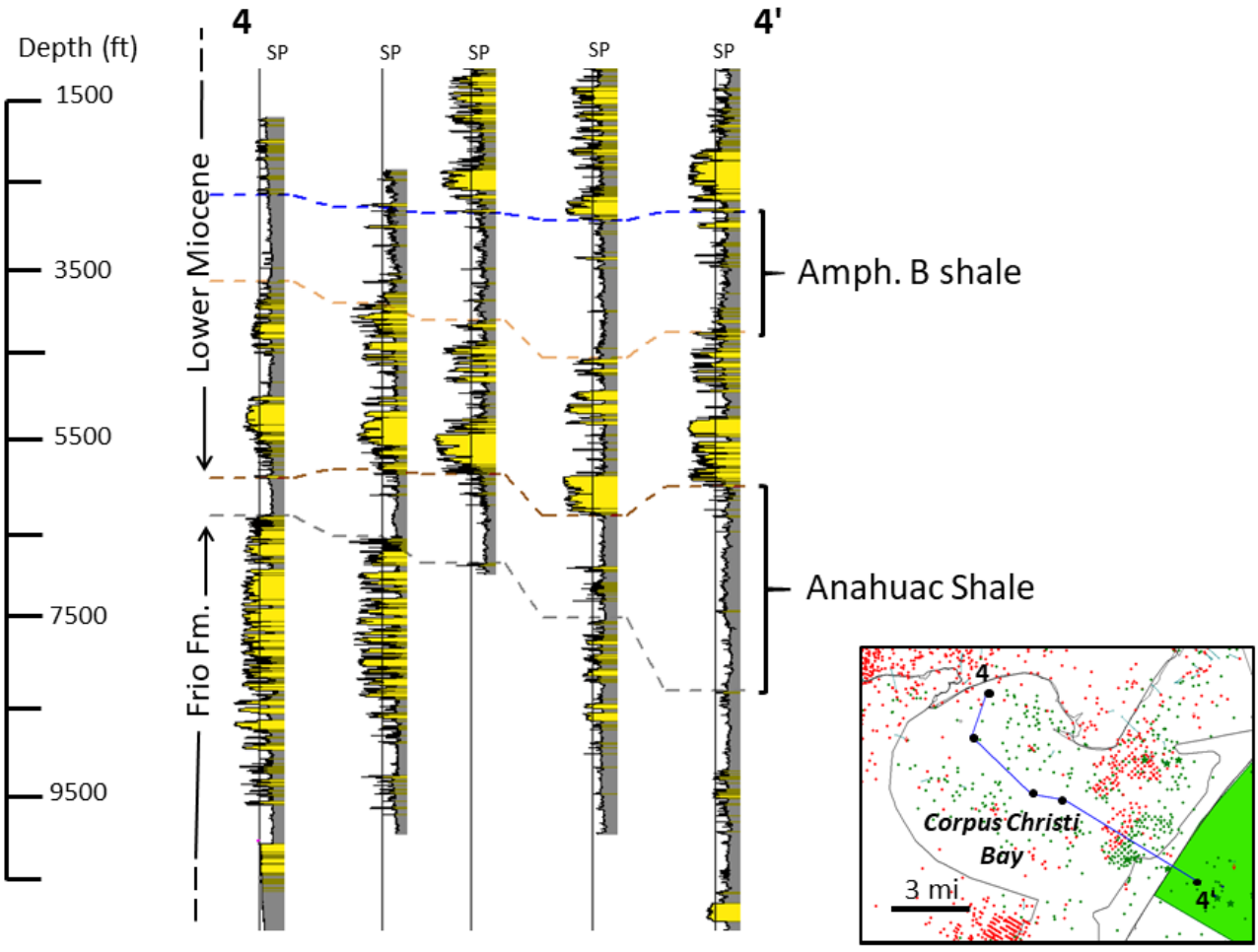

Figure 2.32 - Structural cross section 4-4'. See also line of section located in Figure 2.26.

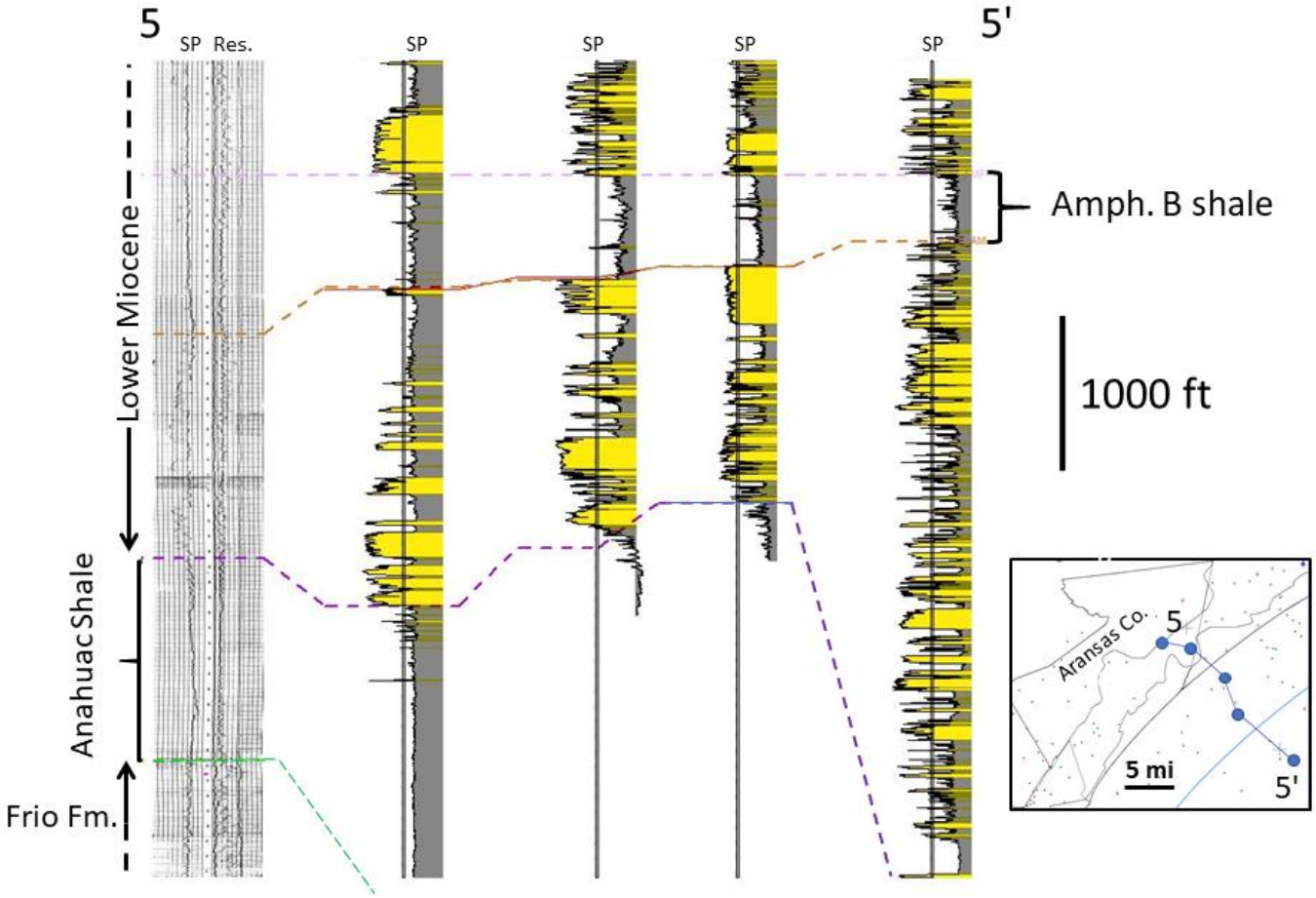

Figure 2.33 - Stratigraphic cross section 5-5'. Datum is the top of the *Amphistegina* B unit. Depth to base of Anahuac Unit exceeds that of the well in most of the wells. See also line of section located in Figure 2.26.

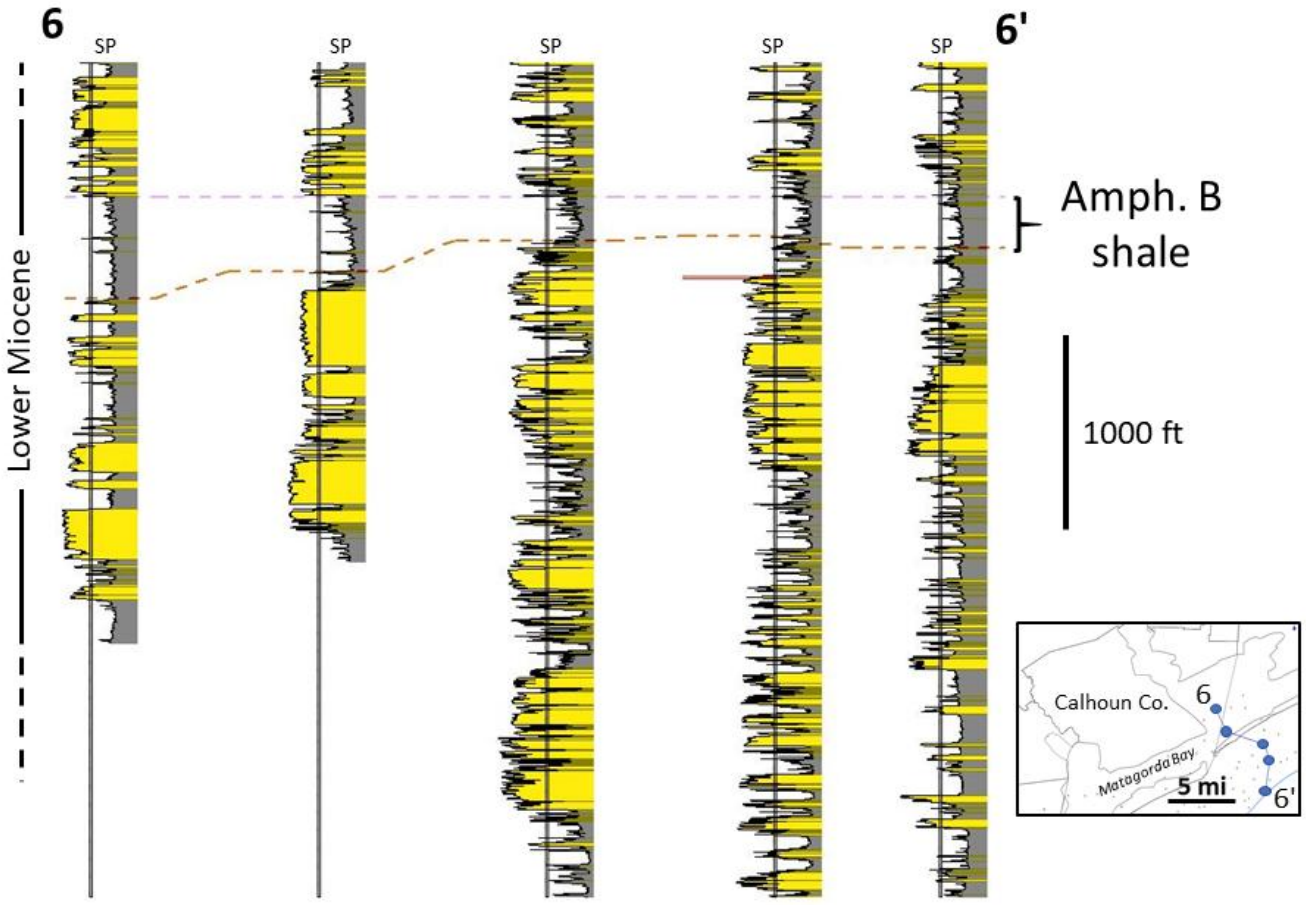

Figure 2.34 - Stratigraphic cross section 6-6'. Datum is the top of the *Amphistegina* B unit. Depth to base of Anahuac Unit exceeds that of all of the wells in the cross section. See also line of section located in Figure 2.26.

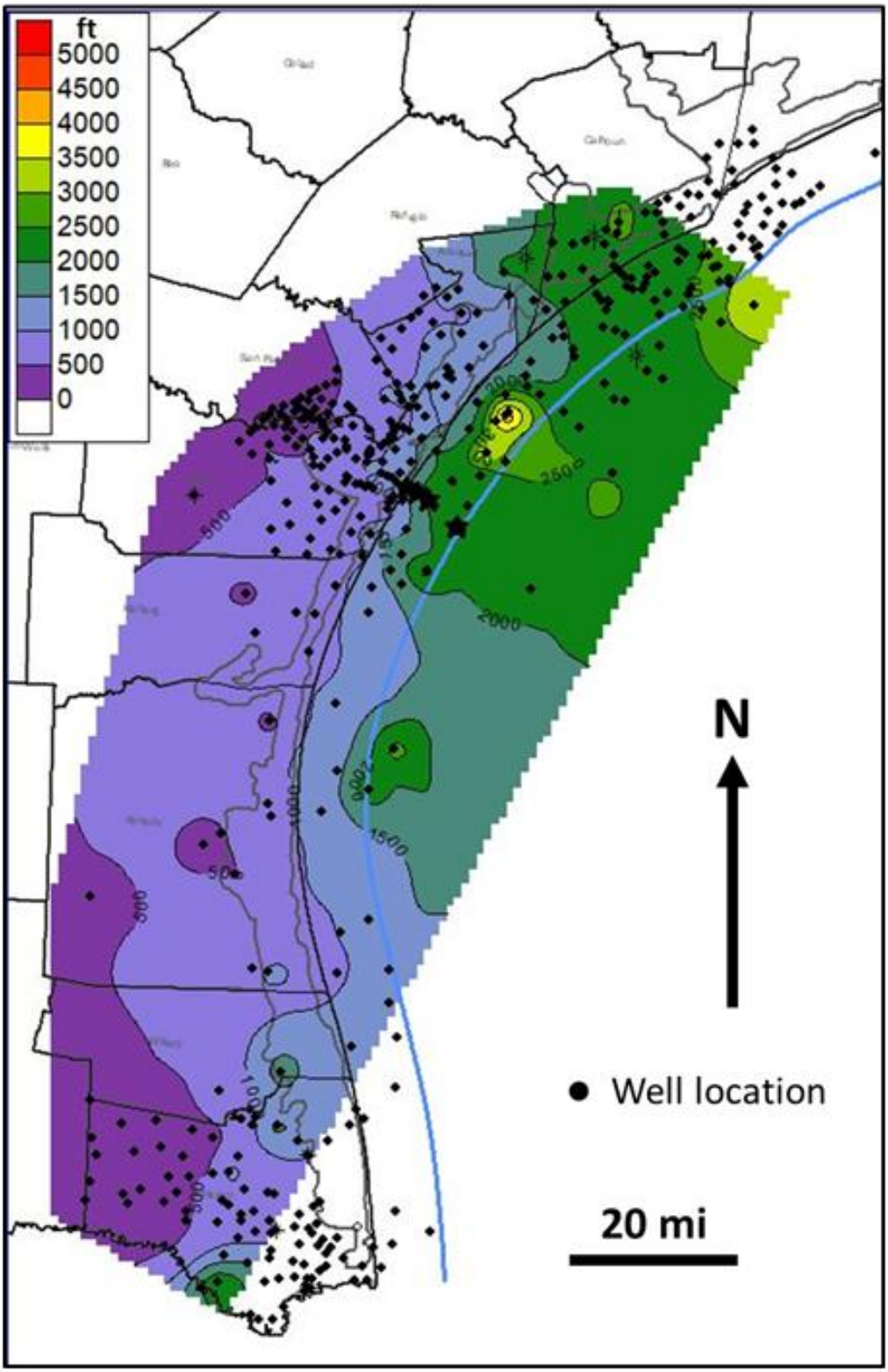

Figure 2.35 - Isopach map of the Anahuac Unit illustrating the marked thickening of the unit toward the east (Figure 2.29, Figure 2.30, Figure 2.31). Local, abrupt thickening of the section in the far southern, central, and northern parts of the map record the presence of basinward-dipping growth faults that cannot be precisely defined using only well-log data.

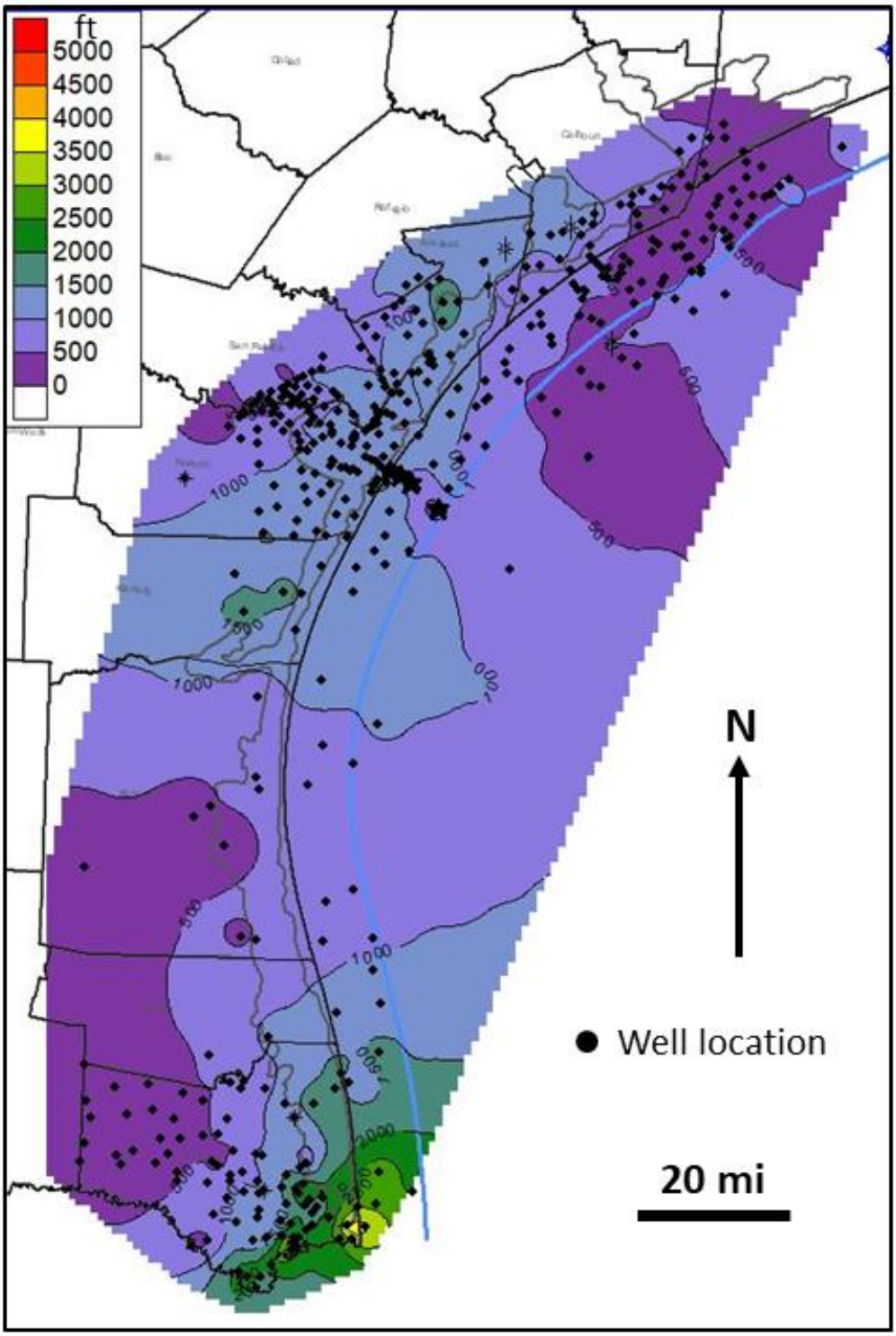

Figure 2.36 - Isopach map of the *Amphistegina* B unit illustrating basinward thickening of the unit in the southern half of the map area and the general basinward thinning of the unit in the northern half of the map area. Area of inferred, pronounced growth-fault thickening is evident in the southernmost part of the area.

Potential for CO_2 Storage

The Anahuac and *Amphistegina* B units are continuous and widespread across the coastal areas of Texas and maintain thicknesses greater than 200 ft (regionally much thicker) over the same region. These units are commonly faulted in the eastern part of the coastal plain and offshore, but they occur in fault blocks that are aerially large enough to effectively form confining zones for hydrocarbon traps, as evidenced by the large number of oil and gas fields in the region. In the western part of the study area, the units are relatively unfaulted and form extensive potential confining zones for CO_2 injection. Therefore, the potential for the Anahuac and *Amphistegina* B units to confining zone sandstone reservoir compartments of the Frio and lower Miocene successions for CO_2 storage is high. However, detailed seismic analysis would need to be conducted to fully assess the regional geologic structures.

Regional 3D Seismic Interpretations

In addition to the well-based mapping of the Anahuac and Amphistegina B units regional 3D seismic datasets downloaded from the USGS NAMSS website provided the Partnership the ability to analyze regional geologic trends (Figure 2.37). (See also subtask 2.1.4.) Following is a discussion of interpretations of some of those regional datasets, GalBrazos and Calibre High Island 3D.

Thirty-seven and 82 major fault planes were, respectively, interpreted in the Calibre High Island 3D and GalBrazos 3D surveys. The results were subsequently integrated into the GoMCarb Partnership's regional characterization efforts.

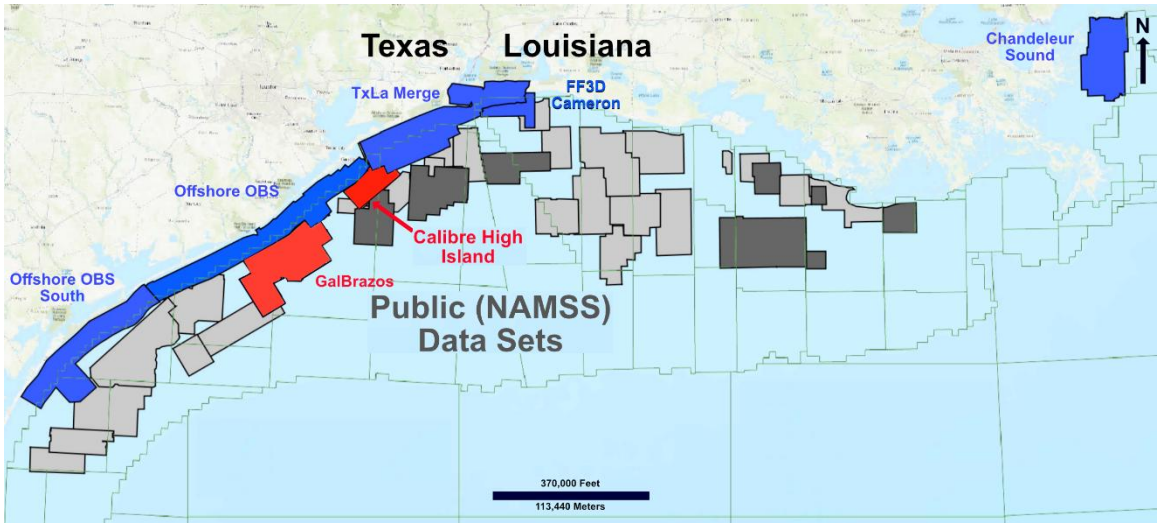

Figure 2.37 - Base map of GoMCarb 3D surveys. Blue surveys were leased and are mostly in state waters. The gray and red surveys are publicly available NAMSS 3D seismic data sets in federal waters. The red surveys were interpreted during the reporting quarter.

Initial steps in the interpretation workflow involved generating a semblance seismic attribute volume in order to robustly interpret faulting throughout the 3D seismic dataset. The semblance attribute compares waveform similarities between adjacent seismic traces and calculates the amount of difference within a specific analysis window (e.g., 40 ms). In the case of the GalBrazos and Calibre High Island, semblance values ranged between +100 and -100. Semblance values near +100 highlight areas with little lateral variations in stratigraphy or structure, typical of zones with significant rock homogeneity (e.g., mudrocks aka shales). In contrast, low (negative) values may indicate significant lateral changes in rock type (pore-fluid content, facies, fault planes, etc.). One advantage of the semblance attribute is that it can image discontinuities within the data volume without being biased by any previous interpretations. We systematically interpreted/correlated the major faults throughout the Calibre High Island 3D seismic survey. Consequently, 37 major fault planes were identified. Figure 2.38 is an example of the uninterpreted semblance attribute for a time slice taken at 800 ms. The lighter colors (negative) depict areas with

significant differences between adjacent seismic traces, indicating faulting or significant lateral stratigraphic changes (ex: salt domes, riverbanks, crevasse splays, dipping beds, etc.). Figure 2.39 shows colored faults that have been interpreted, assigned a specific name, and then triangulated. A total of 37 major fault planes were interpreted. The faults, along with any interpreted horizons, can then be used to establish a robust baseline structural framework for subsequent subsurface modeling efforts.

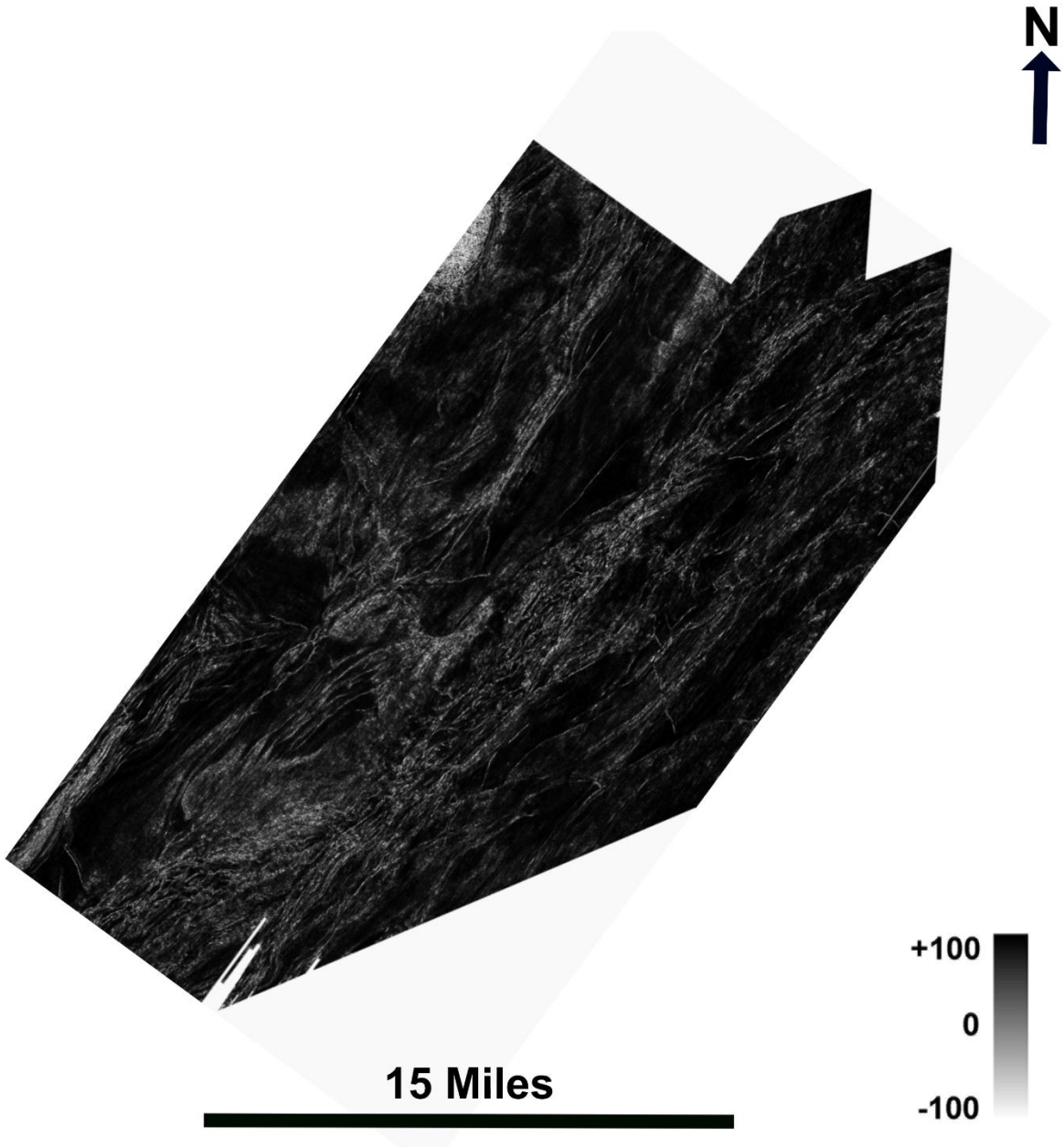

Figure 2.38 - An uninterpreted horizontal slice taken at 2000 ms from the Calibre High Island 3D semblance attribute data volume.

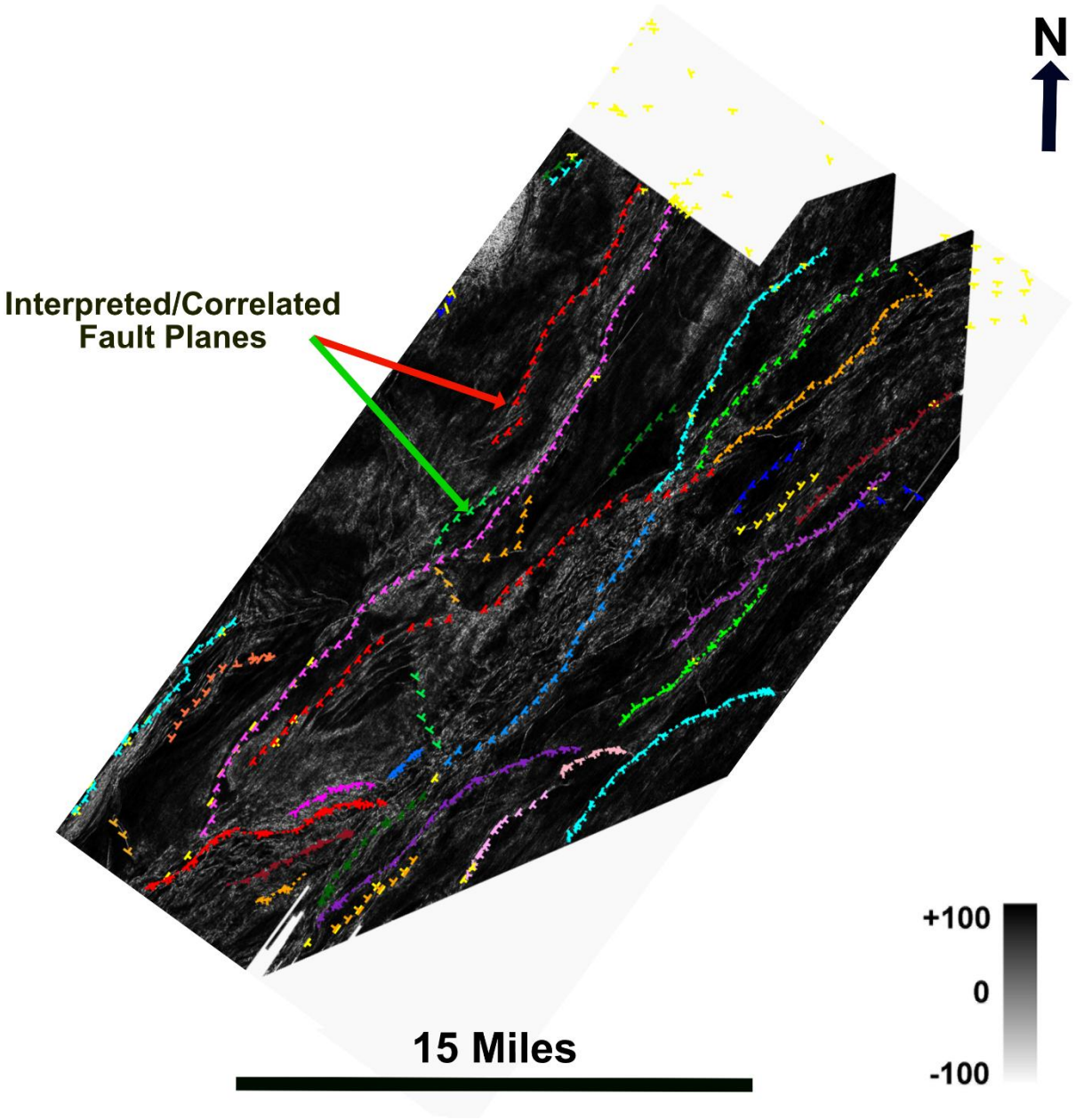

Figure 2.39 - An interpreted horizontal slice taken at 2000 ms from the Calibre High Island 3D semblance attribute data volume. Colored icons have been interpreted, assigned an unique name, and triangulated.

The offshore structure in the GOM offshore waters is characterized by gently dipping horizons in state waters until edge of the shelf; then, the structures begin to increase dip basinward. The structures of the Calibre High Island survey are shown in Figure 2.40 and Figure 2.41.

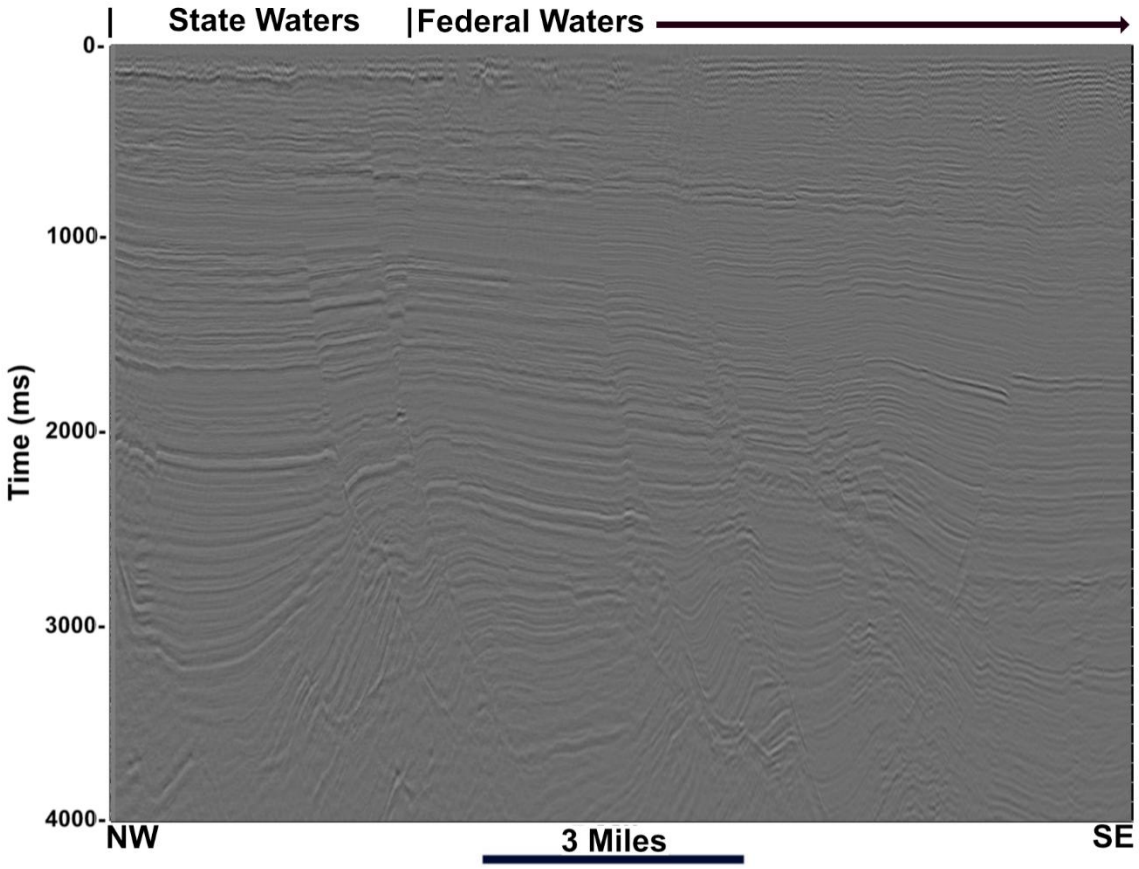

Figure 2.40 - An uninterpreted dip-line from Calibre High Island 3D seismic amplitude volume.

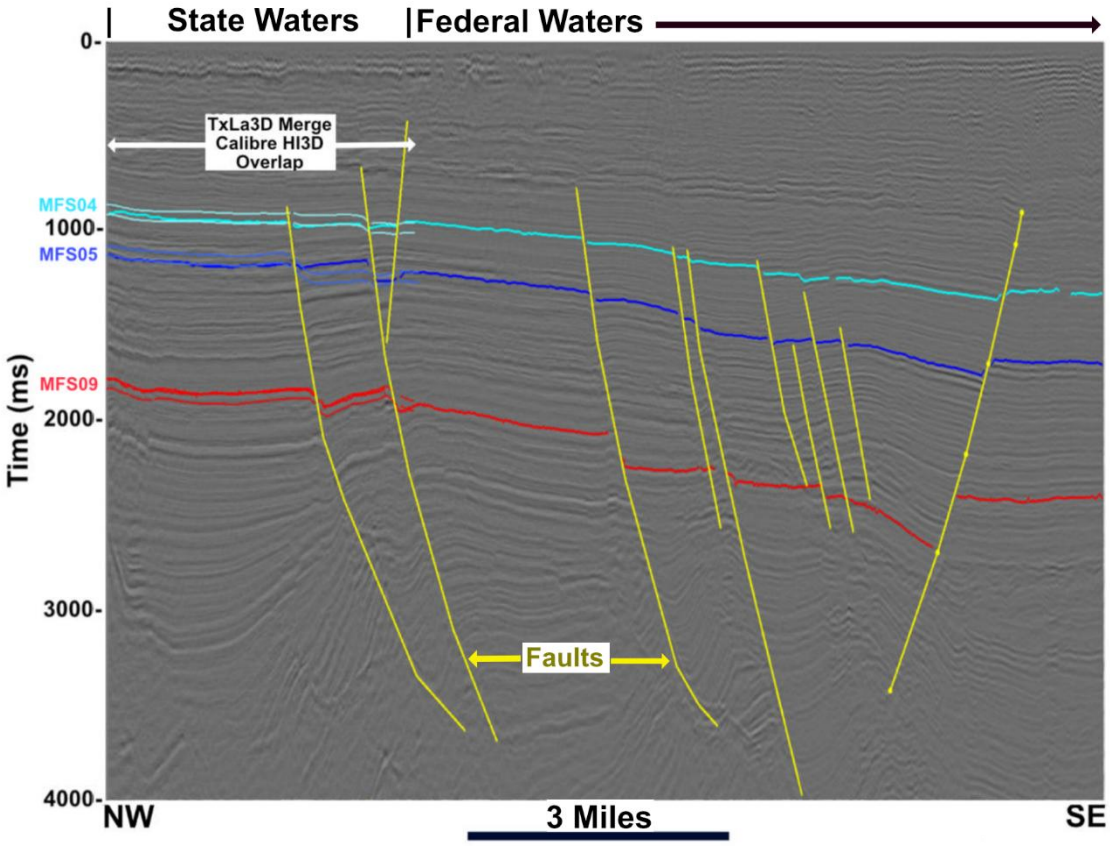

Figure 2.41 - An interpreted dip-line from Calibre High Island 3D seismic amplitude volume. Colored bands on the left are horizons (MFS04, MFS05, and MFS09) previously interpreted in the overlapping TxLa Merge 3D survey.

The MFS04 horizon (Figure 2.42) has been mapped over 1,690 mi^2, the MFS05 horizon (Figure 2.43) has been mapped over 4,465 mi^2, and the MFS09 horizons (Figure 2.44 and Figure 2.45) has been mapped over 4,860 mi^2, respectively.

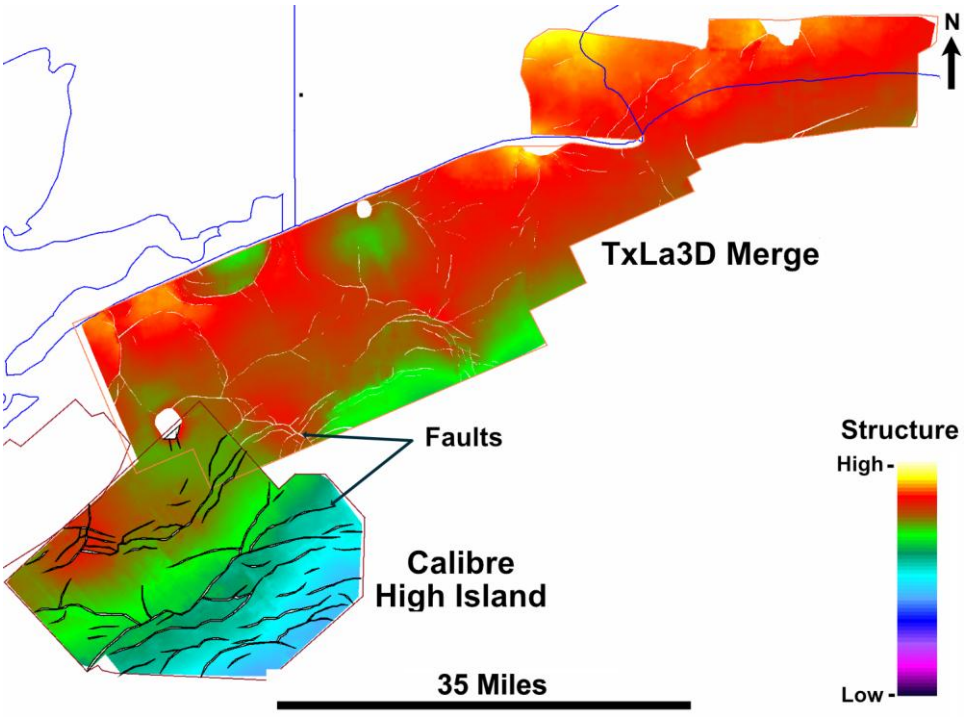

Figure 2.42 - Integrated TxLa Merge 3D and Calibre High Island 3D structure map for the MFS04 horizon.

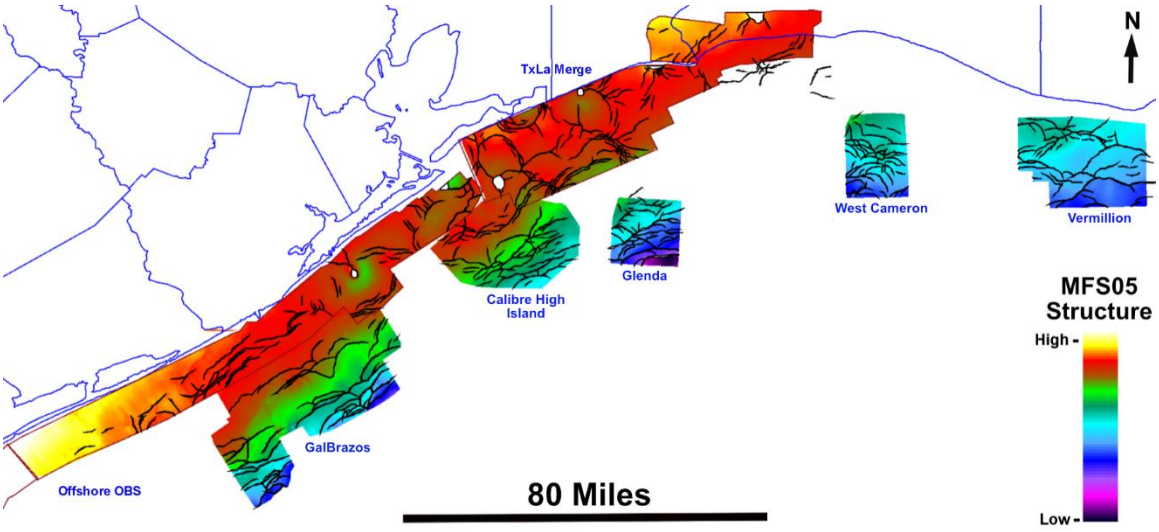

Figure 2.43 - Integrated Regional structure map for the MFS05 horizon. We interpreted 495 fault polygons for the regional MFS05 horizon.

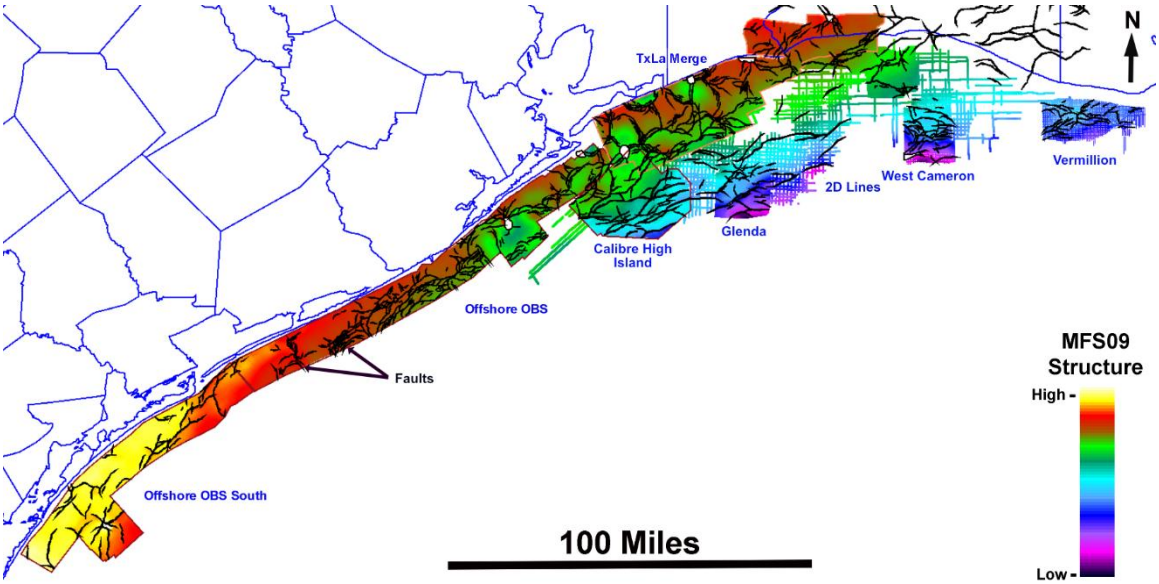

Figure 2.44 - Integrated regional structure map for the MFS09 horizon. We interpreted 925 fault polygons for the regional MFS09 horizon.

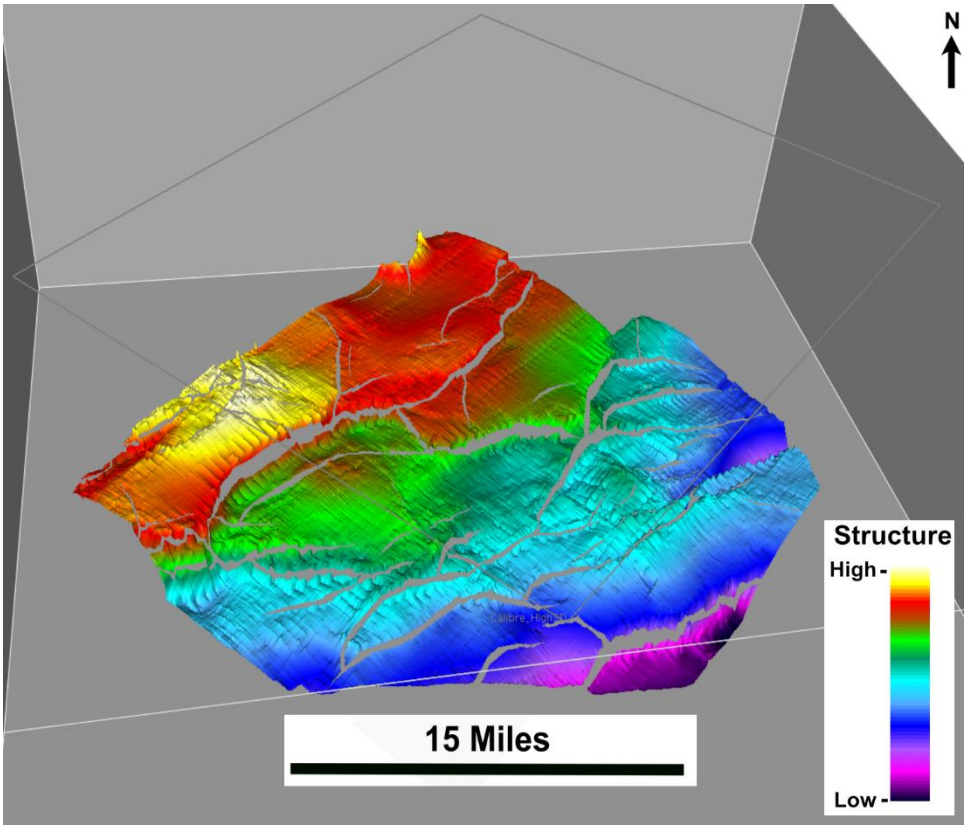

Figure 2.45 - A 3D perspective of the Calibre High Island 3D interpreted MFS09 horizon. See also Figure 2.44, and note that it uses a different color scale.

The regional MFS09 horizon was also extended into the GalBrazos 3D survey. However, the steeply dipping structure, extensive faulting, and poor seismic data quality make it difficult to interpret a robust surface (Figure 2.46). In addition, any horizons in distal Federal Waters deepen toward the over-pressured zones below 3000 ms (milliseconds), making such interpretations not optimal for suitable CCS sites.

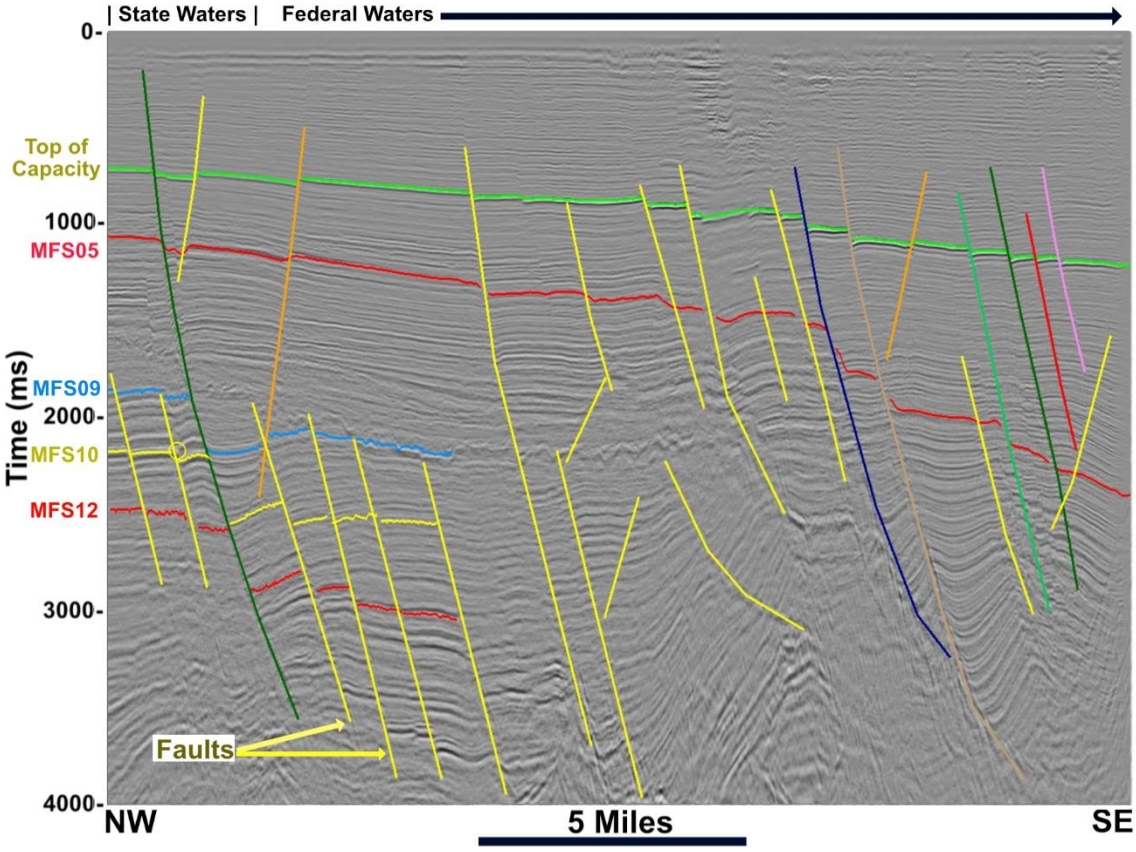

Figure 2.46 - Dip line from the GalBrazos seismic survey. Horizons MFS09, MFS10, and MFS12 quickly dip basinward.

Fault Compartmentalization Limits CO_2 Storage Capacity: Prescreening Offshore Middle Texas Coast

Pressure buildup during CO_2 injection is a significant limitation of storage capacity, controlled by multiple factors, including injection rate, permeability, and accessible pore volume of the reservoir. Therefore, pressure compartmentalization is a real constraint, defining the boundary of closed reservoir systems. Saline reservoirs in the Gulf of Mexico (GOM) have been a focus of research and can potentially be a locus for national carbon sequestration efforts (Meckel et al., 2021). However, the GOM geologic section is heavily faulted due to salt movement in the basin. The faults can comprise effective barriers to fluid movement at industrial injection rates, limiting the potential storage size and, thus, capacity in the GOM. Consequently, previous estimates of GOM storage capacity based solely on pore volume may have been overestimated (Teletzke et al., 2020). A reassessment of the GOM saline reservoir as CO_2 storage incorporating pressure space concepts is necessary.

In this study, we are interested in the distribution of the fault compartment sizes in the GOM and their capacities serving as potential CO_2 storage: 1. What fraction is too small (not economic)? 2. What is the capacity of the biggest? 3. How much of the area is useful? We conduct seismic interpretations on three 3D volumes (Brazos, Matagorda, and Mustang Island) in the offshore middle Texas coast federal waters (a.k.a., OCS – offshore continental shelf) to prescreen the area for potential CO_2 storage (Figure 2.47). The results provide a realistic view of CO_2 storage resources, improving our concepts in CCS project planning and business decisions that could be employed in other locations in the GOM.

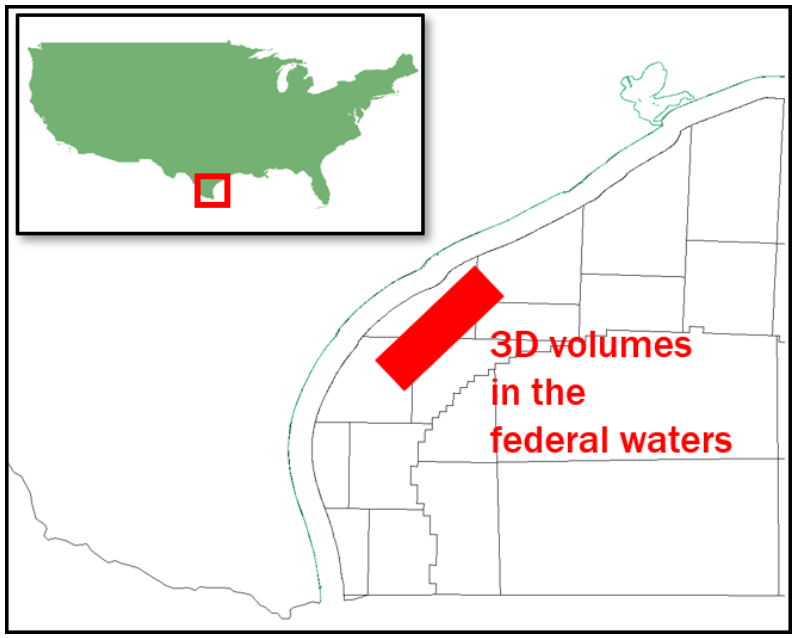

Figure 2.47 - Location map of the three 3D seismic volumes in the federal waters offshore Corpus Christi.

Results

The targeted sand-prone interval is situated within the storage window below the top of supercritical depth and above the top of regional overpressure, overlain by a thick, mudrock-prone confining interval (Figure 2.48). The targeted interval dips basinward but is still above the top of overpressure at the basinward (downdip) position. A series of complex fault systems fragment the targeted interval with a few large faults dissecting the surface. Abundant deep-rooted faults occur at a greater depth (Figure 2.48).

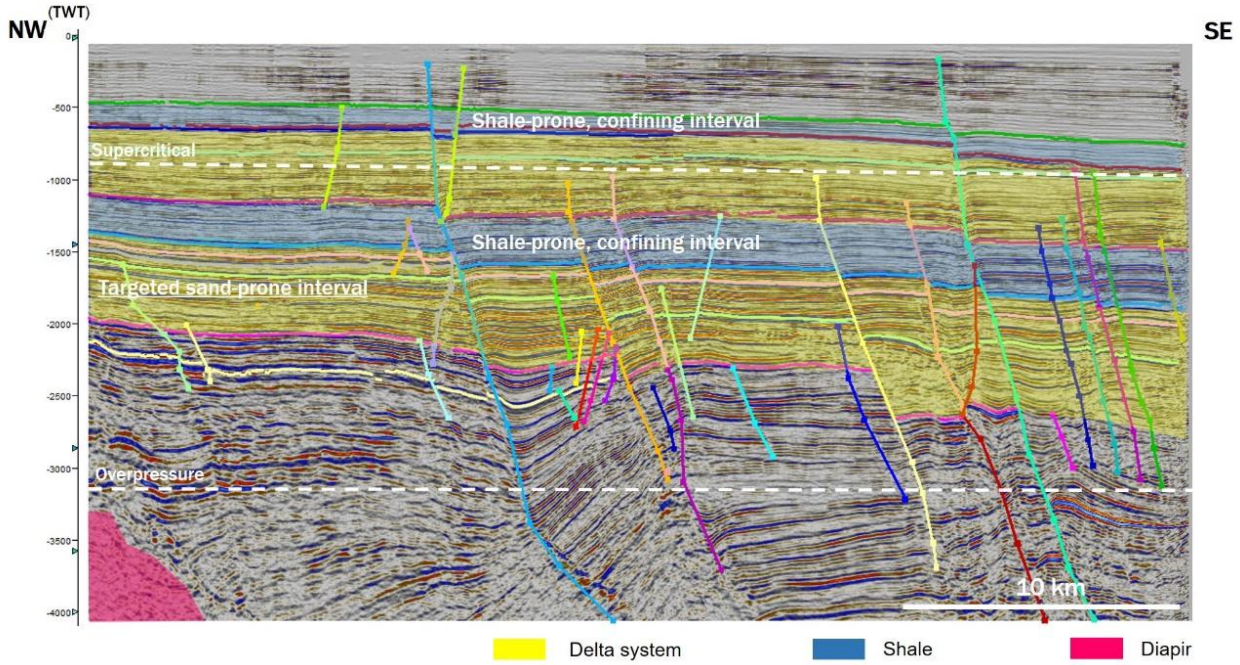

Figure 2.48 - Cross-section showing the complicated structural components related to salt diapir development in the study area. NW: landwards. SE: basinward.

Figure 2.49 is a map view of an interpreted seismic surface near the top of the targeted interval that shows major fault trends dividing the area. The faults are oriented along strike, creating the fault compartments "stepping down" basinward. The area becomes more fragmented basinward due to smaller but complex fault systems. Note that some sizable compartments are present although the area is overall heavily faulted.

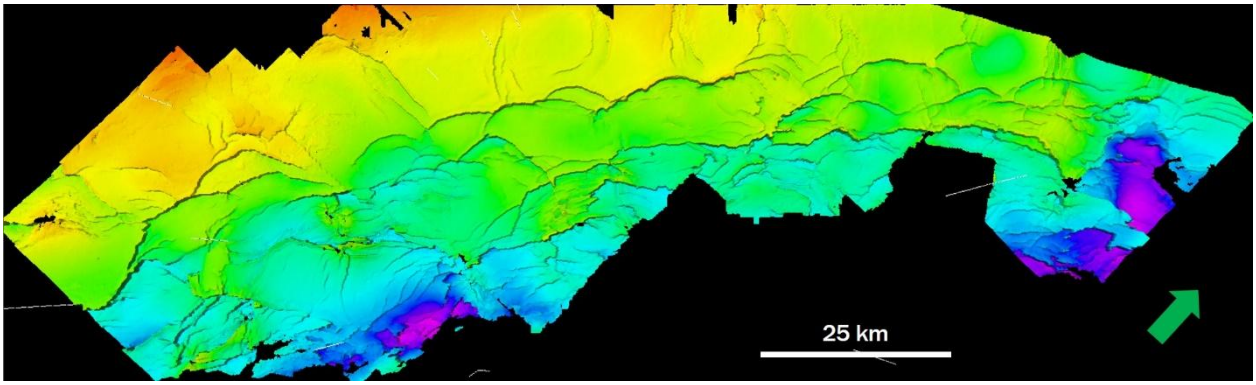

Figure 2.49 - Time-structure map at ~1400 ms showing fault compartments in the offshore Corpus Christi. (Data owned or controlled by SEI. Interpretation is that of the University of Texas at Austin.)

We manually mapped and outlined sizeable compartments in the area (Figure 2.50). The compartments cover 60% of the area and are oriented with the major regional fault trends, while the other 40% of the area was too fragmented and was not mapped in detail. The median size of the compartments is ~ 25 km^2, and the P90 is > 100 km^2 (the four big compartments) (Figure 2.51A). CO_2 static storage capacities of these compartments are calculated with EASiTool, given 100 m thick net reservoir with 25% porosity, 200 mD permeability, injected at ~2 km depth. The median capacity of these compartments is ~ 8MT (megatons), and the P 90 is > 20 MT (four big compartments).

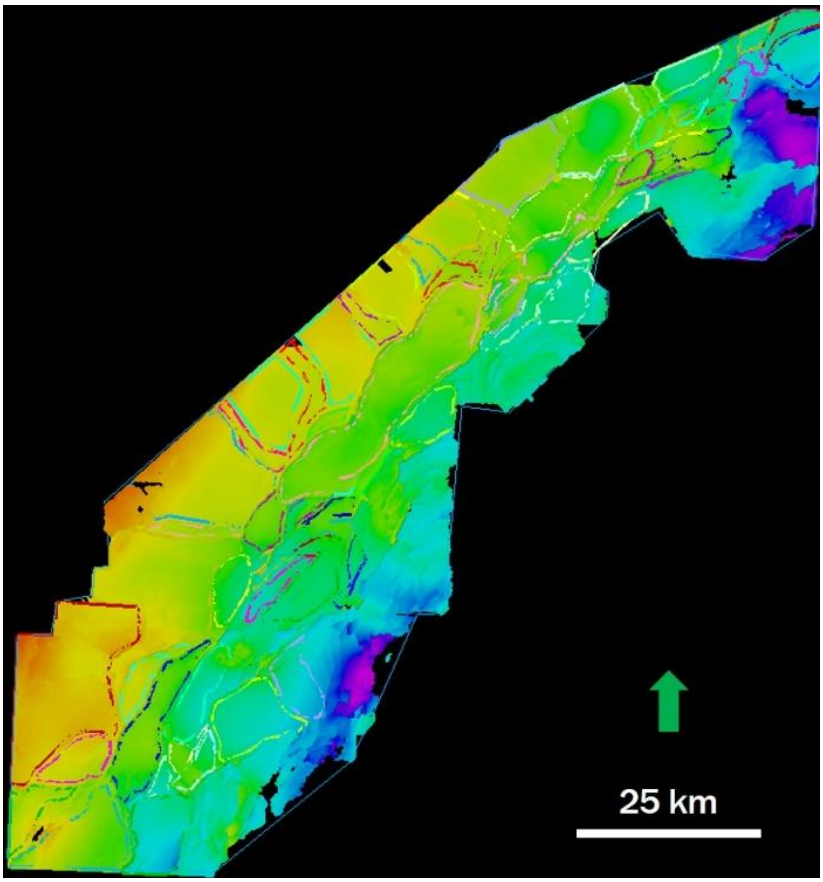

Figure 2.50 - Mapped compartments in the area.

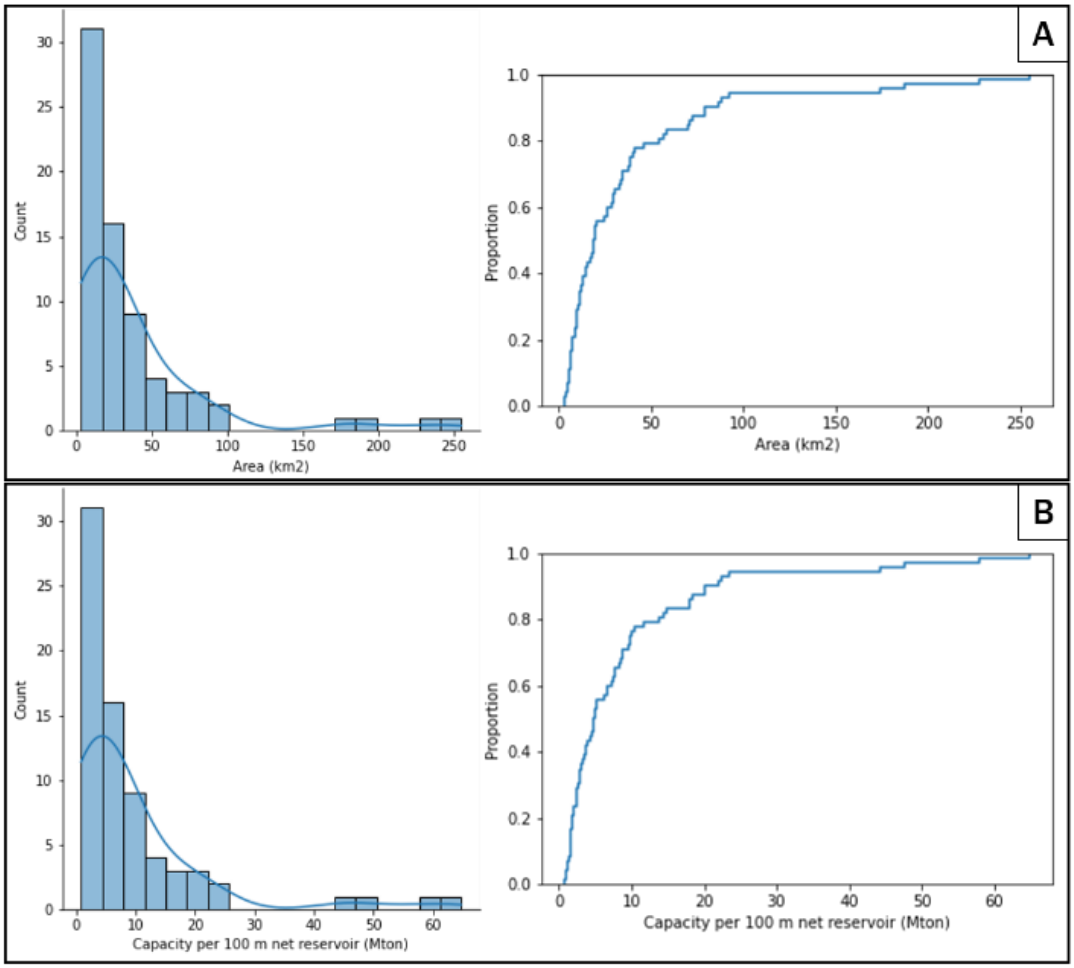

Figure 2.51 - **A.** Histogram and CDF (cumulative distribution function) plot of the size of the compartments. **B.** Histogram and CDF plot of the capacity of the compartments in MT (given 25% porosity, 200 mD permeability, 100 m thick net reservoir, injected at ~ 2 km depth).

Despite the highly debated economic prospect of a carbon sequestration project, we adopt the criteria of a standard industrial-scale project that requires storage containing> 25 Mton capacity to determine the practicality of the fault compartment as potential CO_2 storage. Under a 100 m net reservoir scenario, only the four big compartments qualify as industrial-scale CO_2 storage (Figure 2.52). More compartments become useful if given a 200 m net reservoir: ~ 20% of the compartments are practical. Furthermore, ~ 40% of the compartments are practical if given a 400 m net reservoir (Figure 2.52). Through performing this scenario analysis, we gain a better view of the worth of the area at the early stage of the assessment process, allowing us to allocate resource and budget adequately for the next phase of the project and make business decisions.

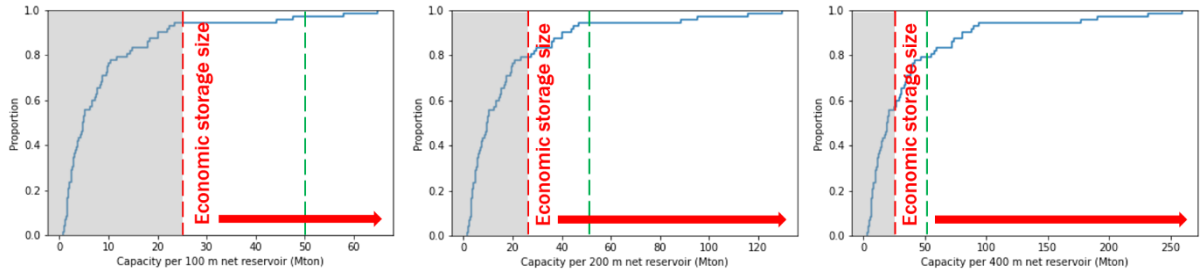

Figure 2.52 - CDF plots of storage capacities with 100, 200, and 400 m net reservoirs, respectively (given reservoir

quality of 25% porosity, 200 mD permeability, injected at ~ 2 km depth).

Future work

After using the structural component and accessible pressure space concept as the first-order, high-level screening criteria, qualified compartments and areas are spotlighted to promote the next steps of the projects: to characterize the reservoir distribution in the area of our interests integrating with well-logs data and precise static geomodels.

References Cited

Meckel, T.A., Bump, A.P., Hovorka, S.D., Trevino, R.H., 2021. Carbon capture, utilization, and storage hub development on the Gulf Coast. Greenhouse Gases: Science and Technology, 11(4), 619-632.

Teletzke, G., Palmer, J., Drueppel, E., Sullivan, M. B., Hood, K., Dasari, G., Shipman, G., 2020. Evaluation of practicable subsurface CO2 storage capacity and potential CO2 transportation networks, onshore North America. In 14th Greenhouse Gas Control Technologies Conference Melbourne (pp. 21-26).

2.1.1.3 Subtask - Buoyant storage capacity

In the January-March quarter of 2020, the USGS focused on assessing one unit in the Gulf of Mexico, the middle and lower Lower Miocene strata of the Gulf of Mexico shelf. For this effort, the reservoirs that produce from this unit were grouped, and their hydrocarbon production was determined. The undiscovered hydrocarbons from the unit were gathered from the BOEM assessment (BOEM, 2017). The major work was building a probabilistic model for assessing buoyant storage. The hydrocarbon production and undiscovered volumes are given in oil, gas, and natural gas liquid amounts. The volumes were measured at surficial conditions and had to be adjusted to subsurface volumes. To determine the subsurface volumes, formation volume factors from the USGS values of the onshore portion of this same assessment unit (U.S. Geological Survey Geologic Carbon Dioxide Storage Resources Assessment Team, 2013) were used to convert the surficial volumes. This conversion was handled probabilistically using distributions of the formation volume factors, and the known and undiscovered hydrocarbon volumes, and potential maximum pore volumes within traps. The volumes were then used to create a total available pore volume distribution for the assessment unit. The total buoyant pore volume distribution, combined with the buoyant storage efficiency distribution from the USGS assessment (Blondes, et al., 2013) and a CO_2 density distribution based on the pressure and temperature of hydrocarbon reservoirs in the assessment unit, were used to probabilistically estimate the total mass of CO_2 that could be stored buoyantly within the assessment unit. The results of the model were presented at the joint GoMCARB and SECARB-Offshore virtual meeting held on March 26 and 27th of 2020.

Table 2.1 and

Table 2.2 show probabilistic estimates of the maximum pore volumes of buoyant CO_2 storage resource for the Lower Miocene in the assessment area (i.e., using the known produced and undiscovered petroleum in the assessment area).

Table 2.1 - Maximum buoyant pore volumes of buoyant CO_2 storage resource for the lower Miocene in this assessment area in gigatons (Gt).

Mean	P95	P50	P5
1.11	0.39	0.77	2.89

Table 2.2 - Maximum buoyant pore volumes of buoyant CO_2 storage resource for the lower Miocene in this assessment area in gigatons (Gt) if the most likely value of natural gas is increased from 20 TCF to 50 TCF, while keeping all the other inputs the same

Mean	P95	P50	P5
1.24	0.46	1.04	2.69

2.1.1.4 Subtask - Fluid inclusion stratigraphy

As a result of ongoing discussions with subject matter experts, Dr. Christopher and Dr. Michael Smith (Advanced Hydrocarbon Stratigraphy, Inc.), fluid inclusion data from two wells (Appendix A and Appendix B) were analyzed by Michael Smith, who invented the fluid inclusion stratigraphy method while working at Amoco Research in the 1980s. His quoted summary follows.

> "Helium: Both wells show scattered Helium with no discernible pattern
>
> CO_2: Both wells show higher CO_2 shallower. This is more strongly developed in the 22 well than the 23 well. After water, CO_2 is the most common fluid in fluid inclusions. The amount of CO_2 from fluid inclusions on crushing is primarily related to the size of fluid inclusions. For the same fluid a 10-micron diameter fluid inclusion holds 1000 times the volume of CO_2 and volatiles as one 1-micron fluid inclusion. So, the variation of FI CO_2 may simply reflect a change in size, and possibly abundance, of the fluid inclusions. Large Fluid Inclusion size often correlates with large grain size, so it is possible that the shallower sediments in both of these wells have increased grain size compared to the deeper samples. Also, the amount of CO2 can be a reflection on the origins of the quartz grain hosts. Some quartz grains from deeper crustal rocks have nearly 100% liquid CO_2 fluid inclusions. So that is another possibility that there is the original quartz grain source of the shallower sediments may contain appreciable amounts of CO_2-rich fluid inclusions. It is unlikely that the higher CO_2 in the shallow sediments Fluid Inclusions represents higher CO_2 contents in shallow subsurface fluids in as much as young shallow unconsolidated sediments in the GOM usually have not undergone sufficient diagenesis to have abundant or large Fluid Inclusions from their present location. At least this has been my experience.
>
> Methane: Again, I don't see convincing evidence of regional seals based on the methane from fluid inclusions. The 970022 well shows 2 strong Methane packages near the base of the well. Two less well-developed Methane packages are also observed near the base of the 970023 well. It is important to understand that there is usually not a direct correlation between Fluid Inclusion anomalies versus present day fluid distribution. The most important factor in the formation of FIS anomalies is the formation of large fluid inclusions. This requires just the right sedimentological and diagenetic conditions. Such conditions are often more important in highlighting water legs and seals than the pay zone itself.
>
> Paraffins, Alkylated Naphthenes, and Aromatics: These compounds are mainly liquid hydrocarbon indicators; however, paraffins can have high abundances in wet gas. In the 97022 well the Paraffins show anomalies coincident with the 2 deep methane anomalies around 11,400' and 9800'. A third paraffin anomaly occurs around 8000', coincident with a small Methane anomaly. The alkylated naphthenes show anomalies of various strength at all three of the same zones, and the aromatics pick out the upper 8000' zone and the lowest zone around 11,400'. These zones are formed by a complex combination of petroleum migration, sedimentological provenance, and diagenesis. In my opinion these spatially restricted anomalies do not provide evidence of any regional seals. Although, combined with other geological and geophysical information may be a help to oil and gas exploration and production.
>
> In the 970023 well the paraffin curve reveals few systematic trends, possibly the lower part of the paraffin curve has some potential similarities to the methane distribution in the same depth range. Interestingly the alkylated naphthenes and the aromatics show 2 distinct deep anomalies, surprisingly similar in shape to the 2 methane anomalies in 970022, including a small spike that occurs in both wells. Perhaps these are the same sands? Impossible to know with this limited data set. However, this pattern in both wells shows the importance of the rock and diagenetic control over fluid inclusion abundances. The 2 alkylated naphthene and aromatic anomalies in 970023 are striking in the lack of an appreciable corresponding paraffin anomaly. This suggests the oil in these 2 zones is heavily biodegraded as the bugs eat out the paraffins

first. If this is the case it would suggest that there is now, or was in the past, connection of this depth to the surface to allow Oxygen and micro-organisms access to this oil for biodegradation.

I think that is about all I can offer you from this data. I invented FIS at Amoco Research in the 1980's. It is fascinating stuff, but it is ruled by the nature of the rock and diagenesis. Anomalies observed are all formed in the past. Might be recent past or might be the more distant past. But it is the past."

2.1.2 Subtask - Geologic Characterization of Chandeleur Sound, LA

Analysis of Chandeleur Sound geology was divided among two researchers based on two distinct geologic sections. The Upper Miocene, was interpreted as a large fluvial-dominated depositional system. Whereas, the Middle Miocene section was dominated by the Chandeleur submarine canyon and its associated depositional systems. Both sections, Upper and Middle Miocene, was finalized with estimations of static and dynamic capacity. Each is discussed below.

Stratal Slicing was performed on the Chandeleur Sound 3D seismic survey. Methods such as RMS Amplitude and Sum Negative Amplitude indicated that the southern shelf of Upper Miocene tends to have sand-prone, high amplitude reflections. Figure 2.53 shows the stratal slices using of an RMS Amplitude attribute seismic volume; the bright areas indicate high-amplitude reservoirs possibly feasible for CO_2 storage.

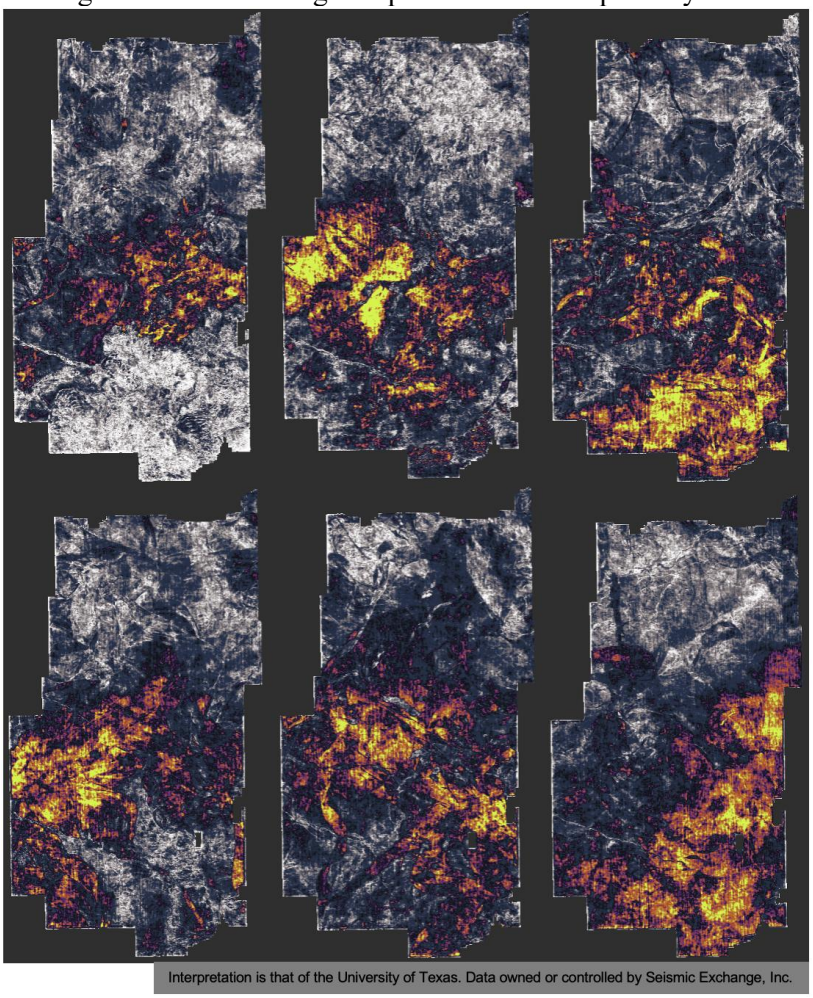

Figure 2.53 - RMS Amplitude stratal slices within Upper Miocene. Top left to bottom right: Lower Upper Miocene to Upper Upper Miocene. Bright areas indicate sand-prone reservoirs

The spectral decomposition attribute showed the detailed morphology within the seismic survey and revealed some

channel systems where sand is likely to be deposited. One major channel system above the top of Upper Miocene horizon, interpreted as related to the paleo Tennessee River delta displays a bright reflection.

Low amplitude reflections occur in the northern Upper Miocene and Middle Miocene shelf, especially in a mass transport complex within Middle Miocene Canyon (Figure 2.55). Ideal storage intervals observed in the seismic data include high-amplitude areas in the southern Upper Miocene shelf (Figure 2.53), and sand-prone lobate geometries (Figure 2.54) which are interpreted as a major channel system near the top of Upper Miocene. The entire storage interval can is shown in Figure 2.56. The areas with high-amplitude strata shown in attribute maps are estimated to range in size from 280 to 480 square kilometers.

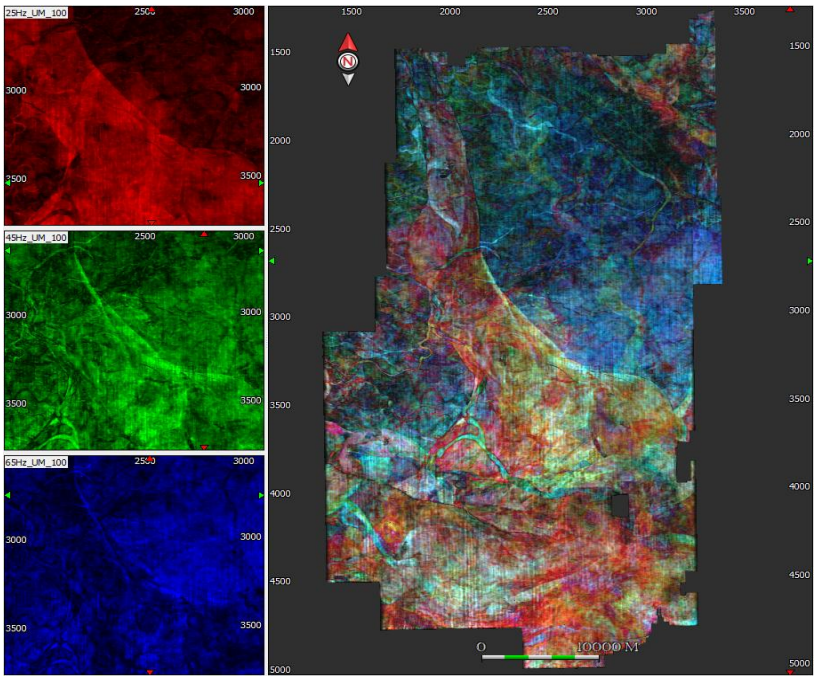

Figure 2.54 - Massive channel system from stratal slices near top of Upper Miocene, highlighted using spectral decomposition attribute.

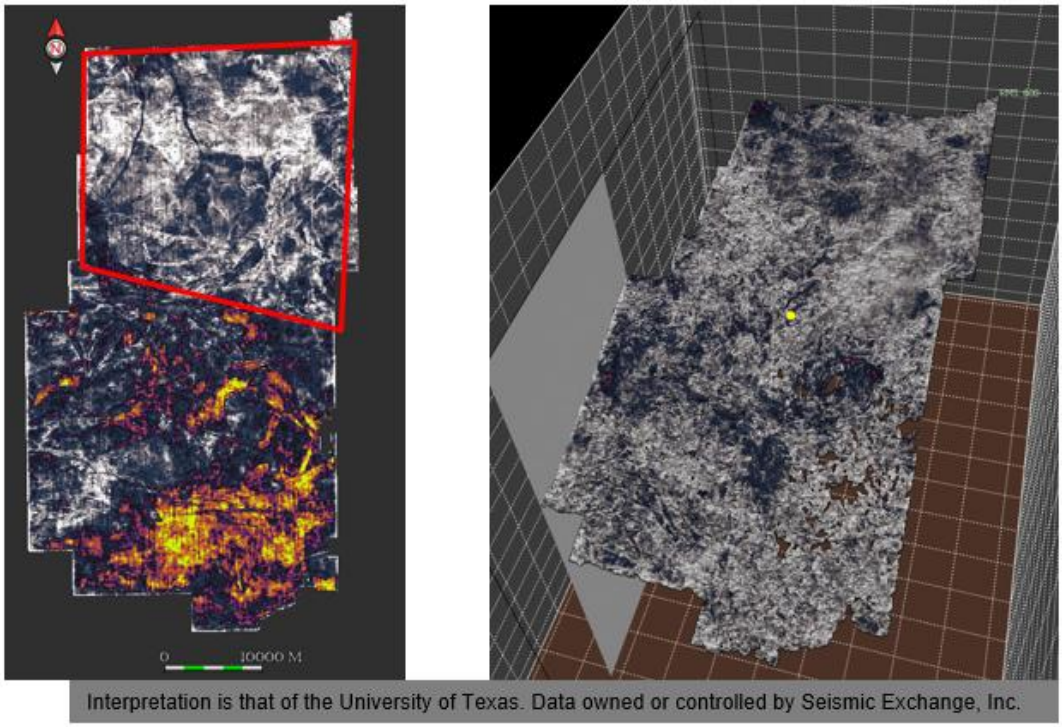

Figure 2.55 - Stratal slices in RMS Amplitude attribute. Low amplitude areas occur on the Middle Miocene shelf (right) and within Chandeleur Canyon, as well as the northern shelf of Upper Miocene (left, within the red polygon).

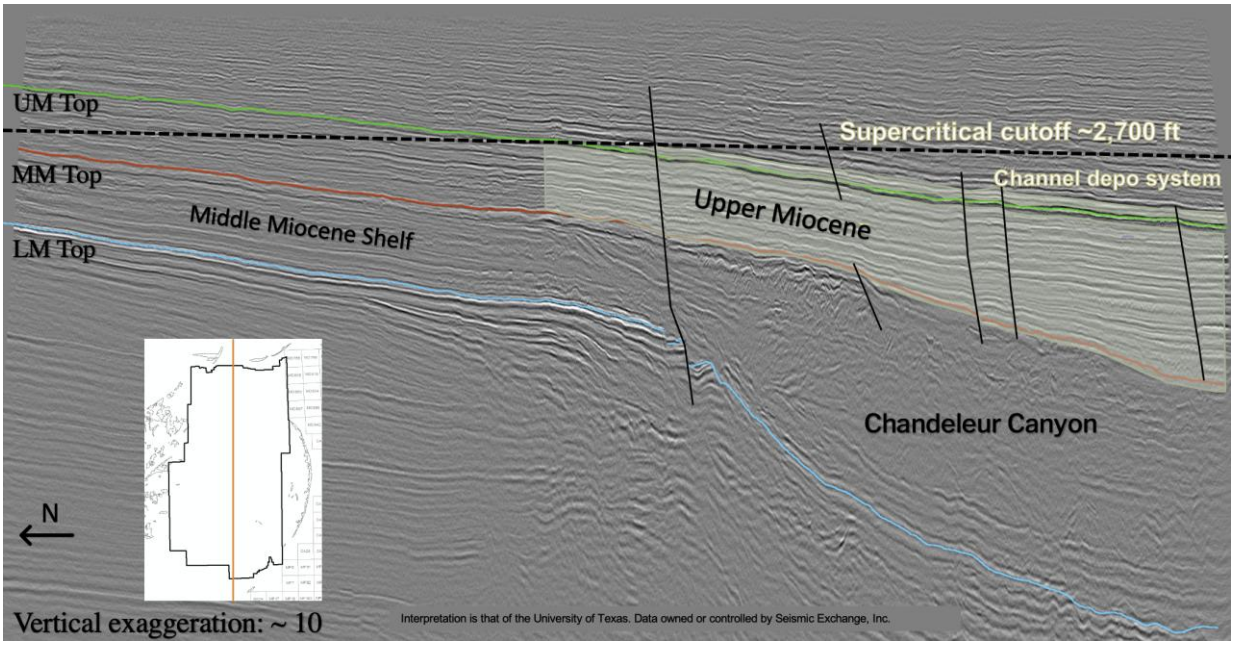

Figure 2.56 - Seismic cross section showing ideal storage intervals defined after stratal slicing (light green) on seismic cross section. Data owned or controlled by SEI Inc. Interpretation by University of Texas at Austin.

Petrophysical well log analyses provided more detailed information and interpretation of ideal storage intervals. The distribution of wells drilled within the Chandeleur Sound seismic survey is shown in Figure 2.57. Three wells

were selected for analysis (Figure 2.57.). Effective porosity was used as a measurement of the actual connected pore spaces that contribute to fluid flow in the reservoirs, which can be expressed numerically as:

$$PHIe = PHIa - PHIsh \times Vsh$$

$$PHIa = \frac{NPHIcorr + DPHI}{2}$$

$$NPHIcorr = NPHI - (Vsh \times NPHIsh)$$

Where:

$PHIe$ = effective porosity

$NPHIcorr$ = Neutron curve porosity corrected by shale volume

Vsh = shale volume

$NPHIsh$ = Neutron porosity in shale

$PHIa$ = average porosity

$PHIsh$ = porosity in shale

A dip-oriented well log correlation cross section (Figure 2.58), indicates that sand bodies tend to thin to the south (basinward). The net sand map of the entire Upper Miocene interval estimates that most sand occurs in the central to southwest Chandeleur Sound study area (Figure 2.58). Seven continuous sand bodies were identified as reservoir candidates and were informally named S1, S2, S3, S4, S5, S6, and S7 with S1 is at the bottom of the ideal interval and S7, the massive channel system, at the top.

Petrophysical calculations indicate that the effective porosity for the seven reservoirs ranges from 23% to 31%. Based on the porosity values, permeability was calculated using an unpublished transformation (Bhattacharya, personal communication), which can be expressed as:

$$K = 0.0005e^{0.4424x}$$

Where:

K = Permeability in mD (millidarcies)

x = Porosity %

Permeability values ranged from 11 to 452 millidarcies (Table 2.3). See Table 2.3 for other detailed reservoir properties. Due to the limited number of wells in the northern portion of the seismic survey, the geology of that area remains poorly constrained. The proposed trapping mechanism for CO_2 would be residual trapping. Bump, et al.(2023) propose that a composite confining system can retain large amounts of carbon dioxide without the specific requirement of a confining zone (aka seal or caprock). In addition, shale units above each sand unit can impede vertical CO_2 migration.

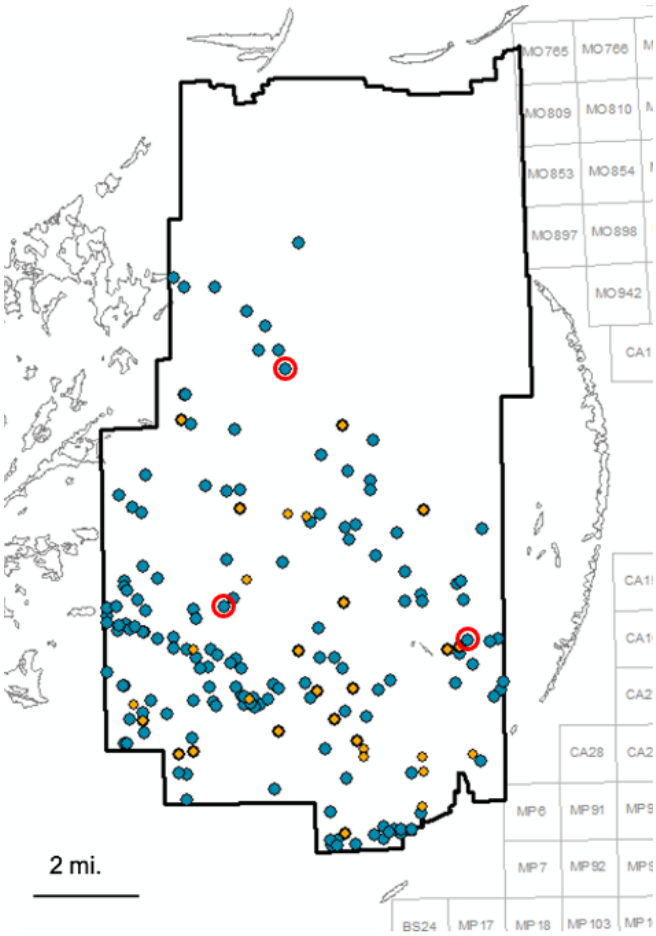

Figure 2.57 - Well distribution within Chandeleur Sound seismic survey. Wells in yellow indicate wells with biostratigraphic markers. Wells in red circles are the three wells selected for petrophysical analysis.

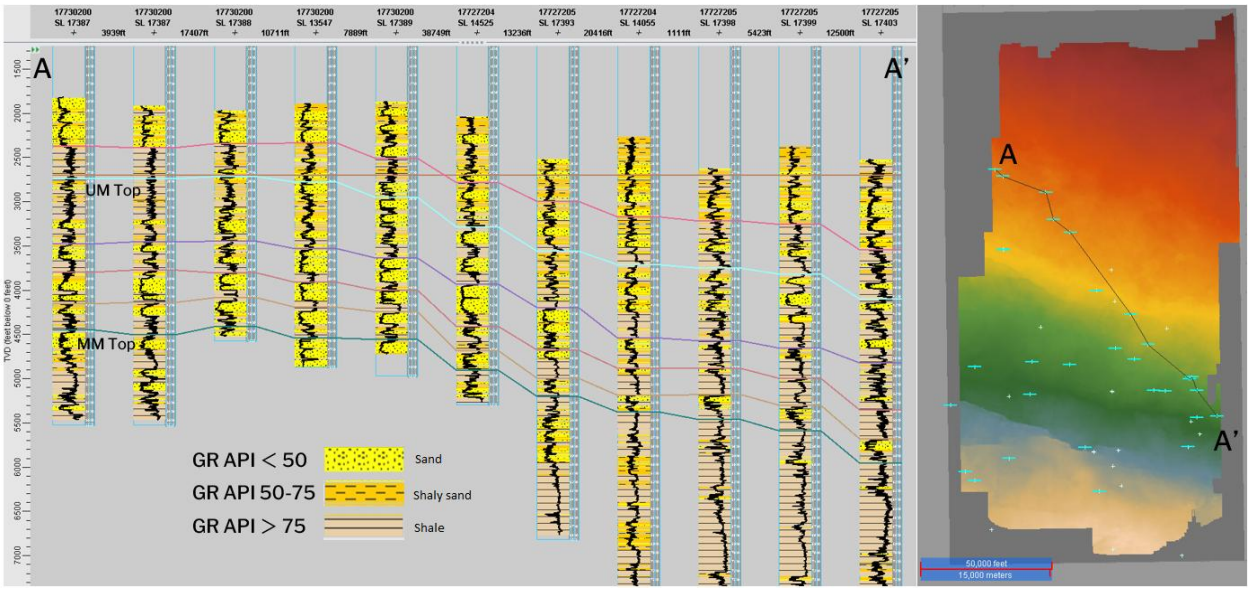

Figure 2.58 - Structural correlation from A to A' using Gamma Ray curves. The lithology strips show the general lithology of each well, where the cut-off value for clean sand is 50. Brown straight line is the supercritical cut-off

(2,700 ft). Light blue line indicates the top of Upper Miocene while the dark green line indicates the top of Middle Miocene.

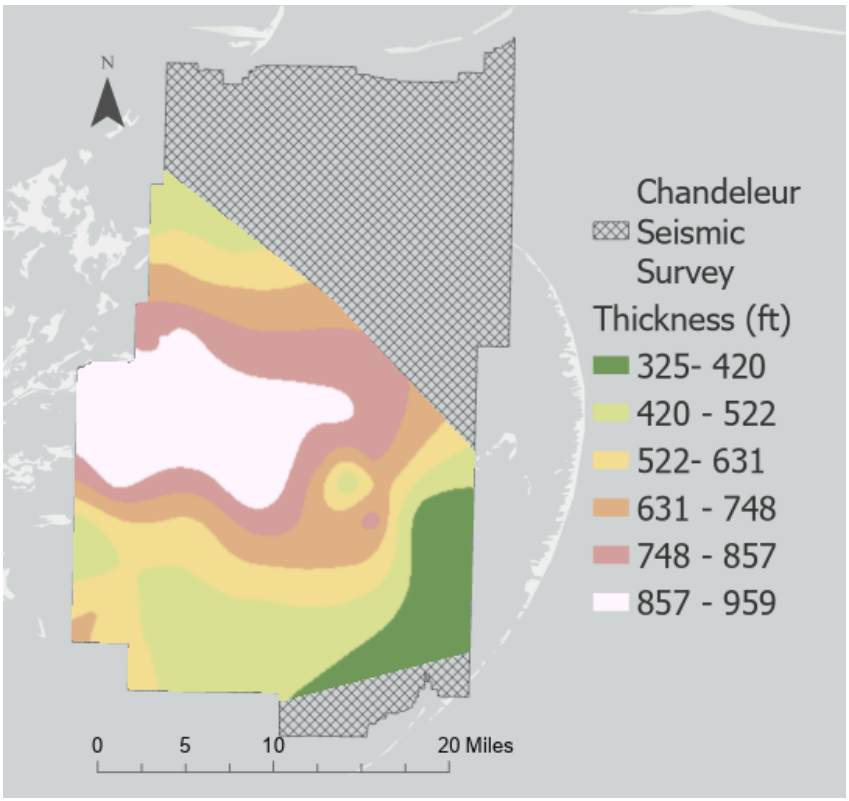

Figure 2.59 - Net sand map for the Upper Miocene (hatched indicates the areas without well control).

		S1	S2	S3	S4	S5	S6	S7
Porosity	Mean	0.27	0.23	0.25	0.26	0.29	0.31	0.31
	Max	0.33	0.29	0.31	0.32	0.35	0.37	0.37
	Min	0.21	0.17	0.19	0.20	0.23	0.25	0.25
Permeability - GoM MM (mD)	Mean	77.01	11.32	36.84	49.48	216.19	362.24	451.92
	Max	1094.77	160.97	523.72	703.38	3073.48	5149.72	6424.65
	Min	5.42	0.80	2.59	3.48	15.21	25.48	31.79
Depth (m)	Mean	1694.48	1574.25	1473.84	1359.75	1242.23	1188.36	1099.29
	Max	1984.25	1805.18	1693.16	1632.20	1562.10	1392.94	1260.35
	Min	1379.22	1289.30	1199.39	1069.85	995.17	931.16	835.15
Thickness (m)	Mean	42.16	53.34	49.02	64.01	61.72	47.55	47.85
	Max	57.91	60.20	60.58	82.30	90.30	79.25	55.63
	Min	30.48	48.77	30.48	44.58	38.86	32.77	36.58
Temperature (°C)	Mean	57.36	54.36	51.85	48.99	46.06	44.71	42.48
	Max	64.61	60.13	57.33	55.81	54.05	49.82	46.51
	Min	49.48	47.23	44.98	41.75	39.88	38.28	35.88
Pressure (Mpa)	Mean	17.79	16.53	15.48	14.28	13.04	12.48	11.54
	Max	20.83	18.95	17.78	17.14	16.40	14.63	13.23

	Min	14.48	13.54	12.59	11.23	10.45	9.78	8.77
Max Injection Pressure (Mpa)	Mean	28.81	26.76	25.06	23.12	21.12	20.20	18.69
	Max	33.73	30.69	28.78	27.75	26.56	23.68	21.43
	Min	23.45	21.92	20.39	18.19	16.92	15.83	14.20
Reservoir Area (km^2)	Reservoir Area	278.59	283.51	301.02	261.81	477.52	450.55	405.78

Table 2.3. Reservoir characteristics of reservoirs S1 to S7.

Static and dynamic storage capacity analyses were conducted using the CO_2 storage capacity for the entire interval (i.e., S1, S2, S3, S4, S5, S6, S7). The static volumetric method of Goodman et al. (2011) was utilized for static capacity estimation:

$$G_{co_2} = Ah_n\varphi_e(1 - S_{wi})B\rho_{co2std}E_{oil/gas}$$

Where:

V_{net} = Total volume = A_t* h_{net} (m^3)

φ_{tot} = Total porosity

ρ = CO_2 density (kg/m^3)

E_{net} = Net storage efficiency factor in a saline aquifer, 2% was used in this research.

Table 2.4 shows the parameters and estimated capacity for each reservoir unit using the Goodman et al. (2011) method.

Name	Density (kg/m^3)	Total Porosity	Thickness (m)	Area (km^2)	Estimated Capacity (Mt)
S1	703	33.46%	42.16	278.59	55.26
S2	700	33.28%	53.34	283.51	70.46
S3	696	34.87%	49.02	301.02	71.63
S4	691	34.37%	64.01	261.81	79.60
S5	685	34.68%	61.72	477.52	152.15
S6	681	35.39%	47.55	450.55	103.26
S7	673	36.54%	47.85	405.78	95.50

Table 2.4 - Storage capacity for each reservoir using static volumetric method.

CO_2 storage capacity was also calculated using the EASiTool (Ganjdanesh & Hosseini, 2017) with the parameters shown in Table 2.3. The boundary condition is the main variable affecting the capacity. We used both 'open' and 'closed' boundary conditions and compared the results as a sensitivity analysis. According to the tool developers,

the boundary condition applies to the basin. If a basin has closed boundary, EASiTool will assume that the pressure front and plume cannot go beyond the basin boundary. For open-boundary conditions, the basin boundaries do not affect the limits of the aquifer, which is infinite acting. Table 2.5 shows the results for storage capacity using dynamic EASiTool method.

	CAPACITY (MILLION METRIC TONS)	
	Open Boundary	**Closed Boundary**
S1	198.60	43.97
S2	62.71	41.14
S3	113.50	41.00
S4	157.00	50.77
S5	463.40	51.53
S6	492.10	40.27
S7	512.40	37.33
TOTAL	1999.71	306.01

Table 2.5 - Summary of dynamic storage capacity and for seven reservoirs.

Comparing the results from both methods shows that the dynamic method with open-boundary conditions yields the highest storage capacity values; while closed-boundary condition gives the lowest values. Realistically, the reservoirs are more likely to be closed boundary. From the stratal slices, the edge of a sand body could be seen as boundary, because the reservoir presence and quality are decreasing beyond the bright, high-amplitude areas. The heterogeneity within the sand bodies could also act as an impediment, preventing the CO_2 plume from extending infinitely. In conclusion, 306.01 Mt is the most realistic.

Prospective Carbon Storage Interval Within Chandeleur Canyon and Storage Capacity Estimates

The primary criticisms against CCS storage potential within Chandeleur Canyon have been 1) lack of sandy intervals and 2) lack of continuous sands, if any, due to the heterogeneous nature of canyon infill. However, the Chandeleur Canyon composes approximately 40-50% of the entire prospective interval within the Chandeleur Canyon 3D Seismic Survey Area (SA), and we would be remiss not to follow through on a full evaluation of CCS potential there. To further address the concerns and fully evaluate the canyon for CCS prospectivity, gamma ray logs within the Canyon were gathered, and sand, silt, and shale volumes were calculated by API values as follows: GR API <50 = Sand; GR API 51-75 = Silt; GR API >75 = Shale. The well control across and through the canyon is neither extensive nor comprehensive; but based on the data that we have the GR logs show that the vast majority of the canyon fill is shale infrequently punctuated by thin silts and sands (Figure 2.60).

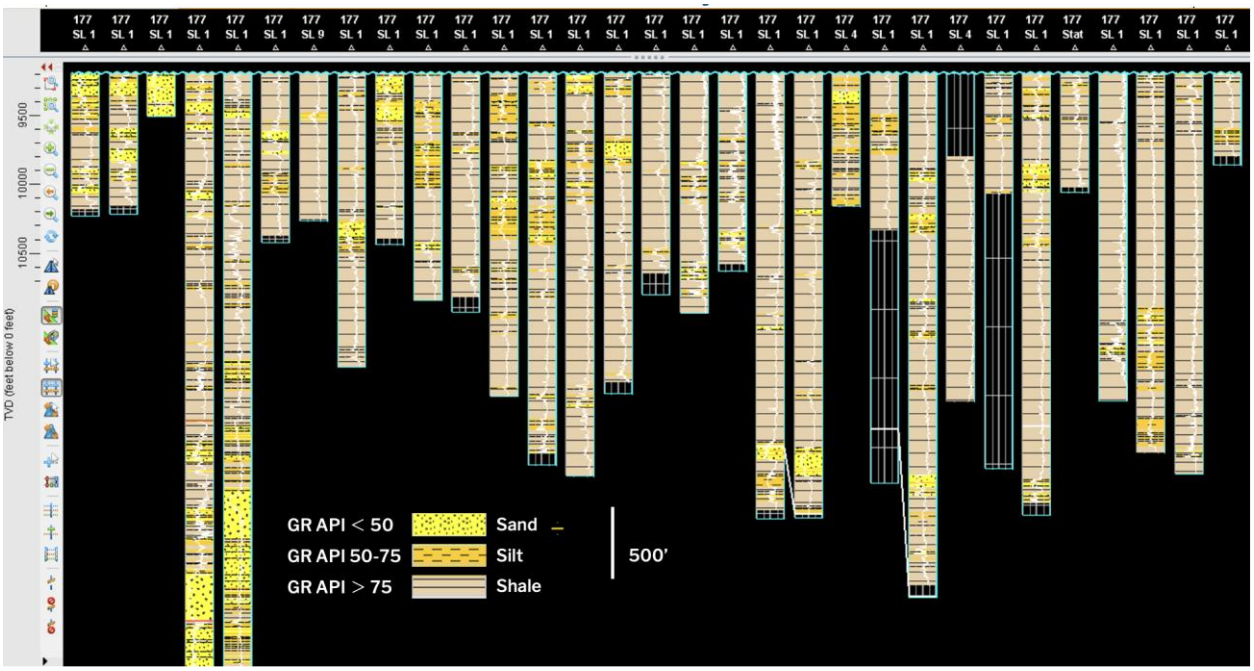

Figure 2.60 - Cross section showing all wells with gamma ray (GR) logs through Chandeleur Canyon. Logs have been flattened on the top MM stratigraphic boundary (wavy cyan line), which also denotes the top of the canyon. Sand, silt, and shale have been identified according to GR API values: <50 = sand (yellow with black spots), 51-75 = Silt (orange with black dashes), and >75 = shale (tan with black stripes).

Five wells in a NW/SE-trending cross section show a promising laterally-continuous sand interval capping the canyon at the top MM boundary (Figure 2.61). This sandy interval ranges in thickness from approximately 160 to 300 feet thick including some very thin intermittent layers of silt and shale. The trajectory of these wells goes through the incised canyon that enters the NW quadrant of the survey area to just beyond the continental shelf break in the SE quadrant. The trajectory of the wells follows the path apparently carved by the flow through the incised canyon, that accessed the Tennessee River Delta during the Middle Miocene, into the greater Chandeleur Canyon. This sand interval is mappable on seismic cross section (Figure 2.62).

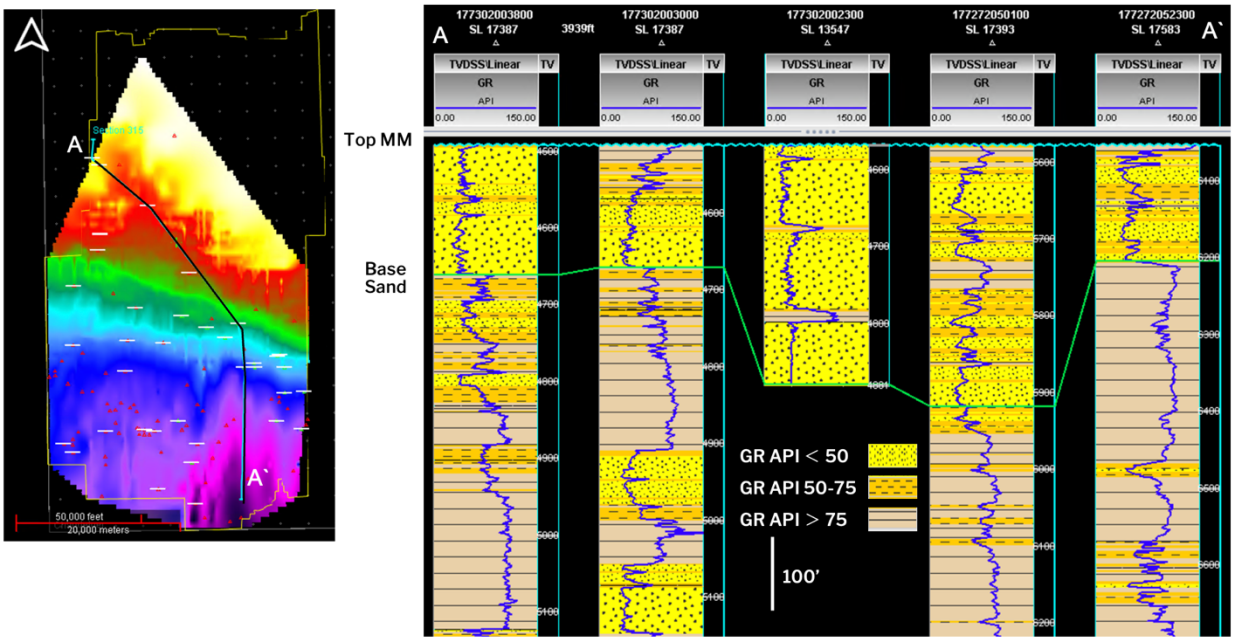

Figure 2.61 - (Left) Plan view of the mapped and gridded canyon base; warm colors are shallower, cool colors are deeper. A-A' connects the wells that are shown in cross section on the right. The sandy interval that caps the canyon (i.e., the "canyon sand") is bound by the top Middle Miocene stratigraphic boundary (wavy cyan line) and the bright green line. Sand is interpreted by Gamma Ray measurements of <50 API.

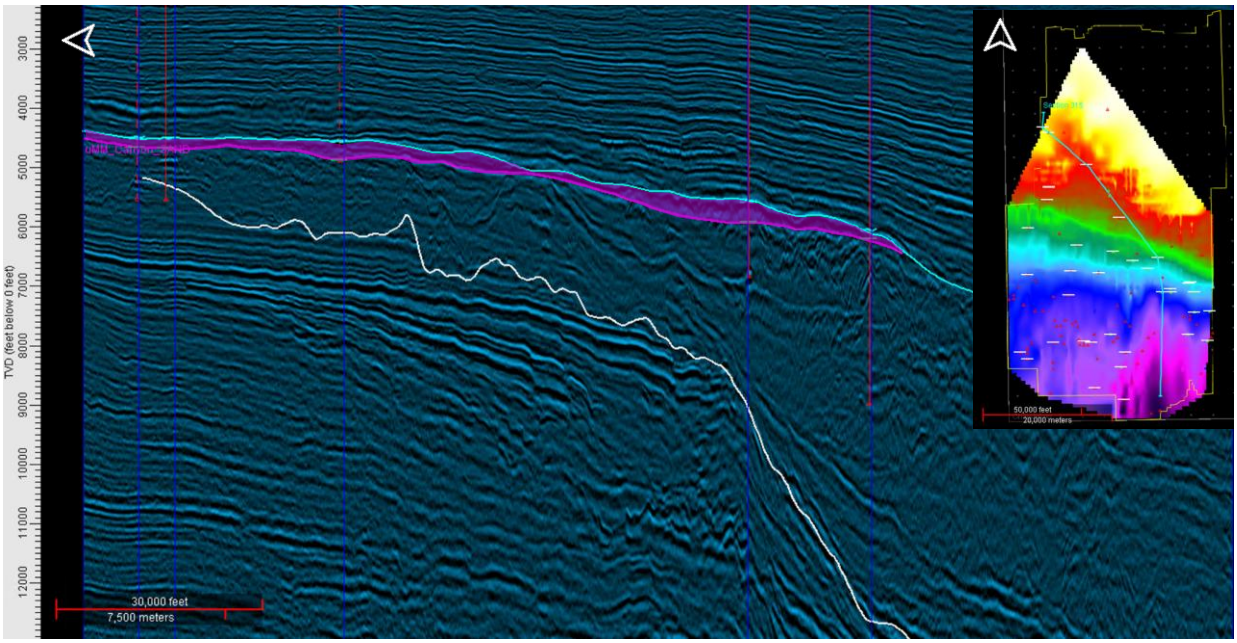

Figure 2.62 - Seismic cross section highlighting the canyon sand (purple) based on the 5 wells that construct A-A' (inset, upper right). (Data owned or controlled by SEI. Interpretation is that of the University of Texas at Austin.)

Initial reservoir property values and estimates of storage capacity on this sand, nicknamed the "canyon sand", are listed in Table 2.6. Storage capacity estimates were calculated using EASiTool, a software developed within the GCCC for this particular purpose. Since the estimation standards have changed over time, both "dynamic closed boundary" and "static boundary" estimates were calculated. For the canyon sand, these estimates are quite close. However, the storage estimates, particularly for the canyon sand, are likely underestimates. Some caveats to the calculations include lack of well control, which leads to underestimates of reservoir values, such as total area and thickness, and ultimately of storage estimates. In conclusion, CCS viability within Chandeleur Canyon is relatively small, but it is not completely unviable as previously thought.

Reservoir Properties (mean values) of the Canyon Sand	
Depth (m)	1694.48
Pressure (MPa)	17.79
Temperature (°C)	57.36
Porosity	27%
Permeability (mD)	77.01
Thickness (m)	42.16
Area (km^2)	278.59
Estimated Storage Capacity of the Canyon Sand (million metric tons)	
Dynamic Closed Boundary	43.97
Static Boundary	55.26

Table 2.6 - Petrophysical reservoir properties and estimated storage capacity of the canyon sand. Note: these

estimates are likely to be low due to lack of well control.

2.1.3 Subtask - Geologic Characterization of High Island, TX

Introduction

Legacy hydrocarbon wells offer valuable data for Carbon Capture and Storage (CCS), including stratigraphic characterization, detailed logs of potential reservoirs and confining zones, and historic fluid flow performance. However, those same wells also carry labels of success or failure that may influence the perception of risk for future efforts, including CCS. The problem is particularly relevant for CCS in prolific hydrocarbon basins. Successful hydrocarbon wells prove a working reservoir and seal, but failed wells inevitably raise questions as to why they failed and the implications for CCS. It is relatively easy to check for reservoir presence but much harder to verify confining zone because hydrocarbon exploration success depends not only on the hydrocarbon seal quality at the well location but also its lateral continuity and capillary entry pressure at its weakest point. CCS is not simply petroleum geoscience with a different fluid and flow direction, but like hydrocarbons, success requires containment. In particular, the need for ongoing assurance of containment under increasing pressure puts new focus on seal (or in CCS terminology, "confining zone" or "confining system) performance and the risks posed by existing breaches (e.g., faults, salt diapirs and particularly legacy wells).

The US Gulf Coast offers a timely example and a natural place to explore ways to de-risk containment. The industrial clusters around Corpus Christi, Houston, Port Arthur, Lake Charles and the Mississippi River chemical corridor are home to some of the densest clusters of point-source CO_2 emissions in the US (EPA, 2020). Historic oil and gas production proves the quality of local reservoirs in the Lower and Middle Miocene section and suggests that they would make good repositories for CO_2. Hydrocarbon discoveries also prove the capacity of the associated hydrocarbon seals. In the case of the Lower Miocene, that seal is the *Amphistegina B* shale unit, the result of a major marine transgression with a pinch-out up-dip of the study area (Figure 2.63) (Olariu et al., 2019). Detailed mapping of the coastal Texas-Louisiana border region shows an abundance of structural highs in the Lower Miocene (DeAngelo et al., 2019). The structural highs have the potential to trap buoyant fluids, including both hydrocarbons and CO_2. They are thus attractive as possible storage sites. Most of the traps have been explored for oil and gas but only some have been found to contain hydrocarbons (Figure 2.64) (Seni et al., 1997; Kreitler et al.). The exploration "dry holes" raise a question, however—why did those prospects fail? Some failure mechanisms, such as lack of a hydrocarbon source rock, would be inconsequential for CCS. Others, such as lack of a trap or a specific reservoir interval might be perfectly acceptable for storage projects with the flexibility to target migration-assisted trapping and/or other reservoir intervals. However, there are some failure mechanisms that could present fatal flaws for CCS as well as for petroleum exploration. Lack of a top confining zone falls in that category and the possibility of a problem with the confining zone casts doubt on the viability of these sites for carbon storage.

The work presented here is an analysis of the hydrocarbon exploration dry holes in the coastal Texas-Louisiana border region. Our first aim is to understand why they failed and what that implies for future CCS on the Gulf Coast. Our broader goal is to demonstrate a workflow to help de-risk CO_2 containment in other basins with exploration dry holes. After a century and a half of hydrocarbon exploration, most basins have been tested, and some have proven successful. Dry holes are a common feature in the world's sedimentary basins. Understanding them, de-risking seal (confining zone) and demonstrating robust containment will be critical for CCS to grow to the scale needed.

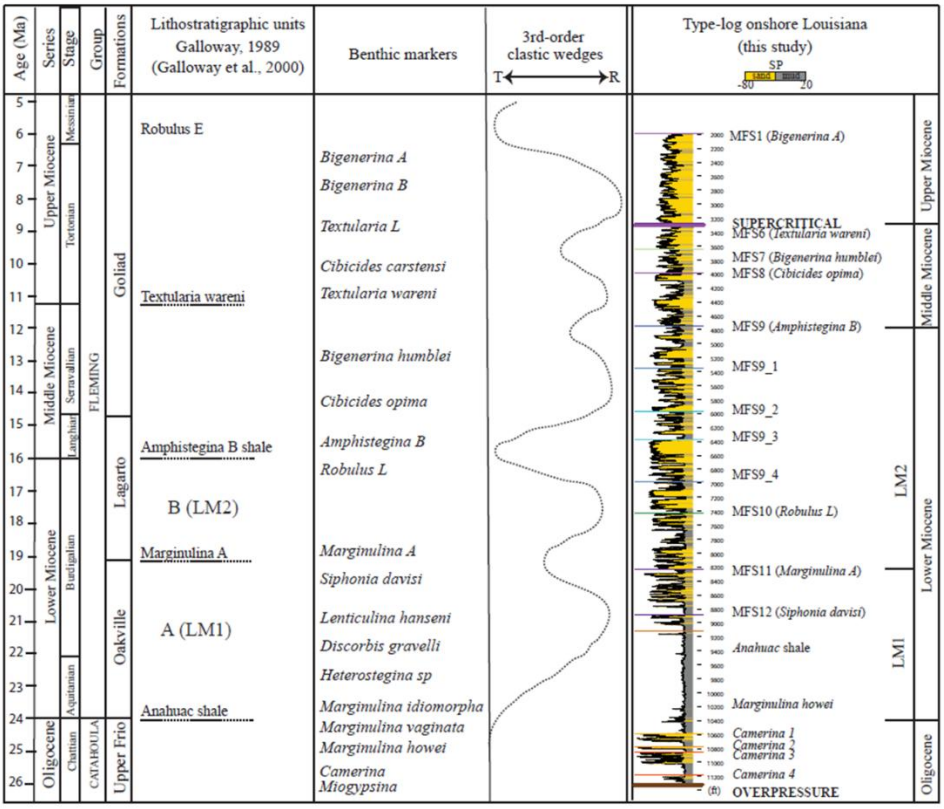

Figure 2.63: Miocene stratigraphy, offshore southeast Texas (from Olariu et al, 2019). Note the *Amphistegina* B shale which is a significant marine transgressive shale and a proven regional seal (confining zone) with a pinch-out up-dip of the study area.

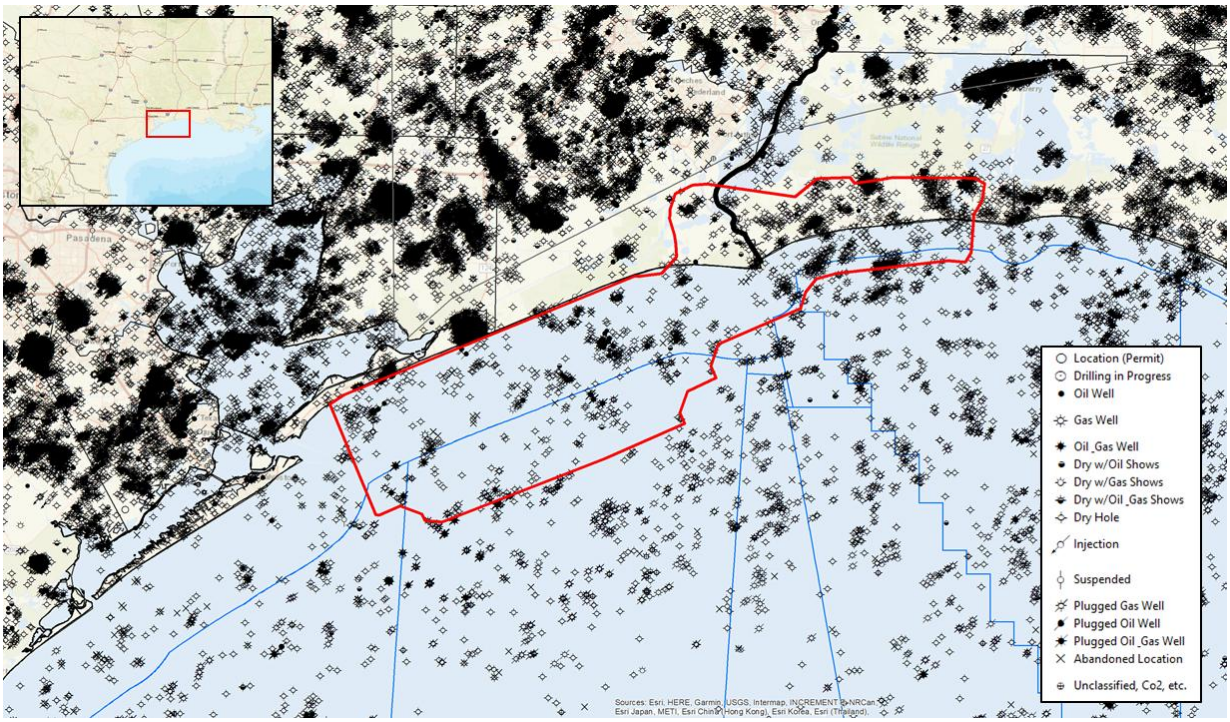

Figure 2.64: Map of all existing hydrocarbon wells near the Texas-Louisiana border, showing the distribution of producing wells and dry holes. The location is shown on the inset map and the focus area for this study is shown by the red polygon on the main map. Well data courtesy of IHS (IHS Markit Inc., 2020).

Petroleum and CCS

Petroleum exploration depends on the combination of six individual play elements, all of which must work in order to create an economically recoverable accumulation (Figure 2.65). From the bottom of the system to the top, these elements are:

1. Source Presence: An organic-rich source rock with sufficient hydrocarbon generation potential to charge the overlying migration paths and reservoirs.
2. Charge Access: Effectively a path to get hydrocarbons into a given prospect. In detail, charge access has three components: A) Thermal maturity of the source rock; B) A viable migration path from source to trap; and C) Reservoir and trap present in time to receive the charge. In concept, fluid movement in the subsurface is driven by the interplay of pressure gradients and permeability architecture. Buoyant fluids such as hydrocarbons thus tend to move vertically through low-permeability rocks until they encounter a higher permeability zone. They then follow that zone ("carrier bed" if it is stratigraphically defined) up-dip until they encounter a trap, at which point they build column height until they either spill from the trap or they develop sufficient buoyancy pressure to force their way vertically into the overlying unit and the process repeats.
3. Reservoir Presence: A reservoir interval with sufficient porosity, thickness and lateral extent to hold the hydrocarbon accumulation
4. Reservoir Quality: A reservoir with sufficient permeability and connected pore space to flow hydrocarbons at economic rates and volumes.
5. Trap: a concave-downward reservoir geometry that stops the upward migration of buoyant fluids.
6. Seal Capacity: A unit immediately overlying the reservoir, with sufficiently high capillary entry pressure to retain the buoyant column of trapped fluids.

Note (Figure 2.65) that hydrocarbons migrate expelled from the source rock migrate quasi-vertically through the mudstones (grey on Figure 2.65) until they hit a permeable carrier bed (yellow). They follow the carrier into a trap where accumulation builds column height to the point that the trapped hydrocarbons either spill laterally or overcome the capillary entry pressure of the overlying mudstones and begin to migrate vertically through it. In Figure 2.65, the shallow traps on the edges are not charged because migrating hydrocarbons are focused elsewhere by the deeper carrier bed.

Partial failure of any of these elements would result in hydrocarbon "shows" (traces) or a sub-economic accumulation. Complete failure of one or more elements would result in a dry hole. Depending on the reason for failure, there might not even be shows.

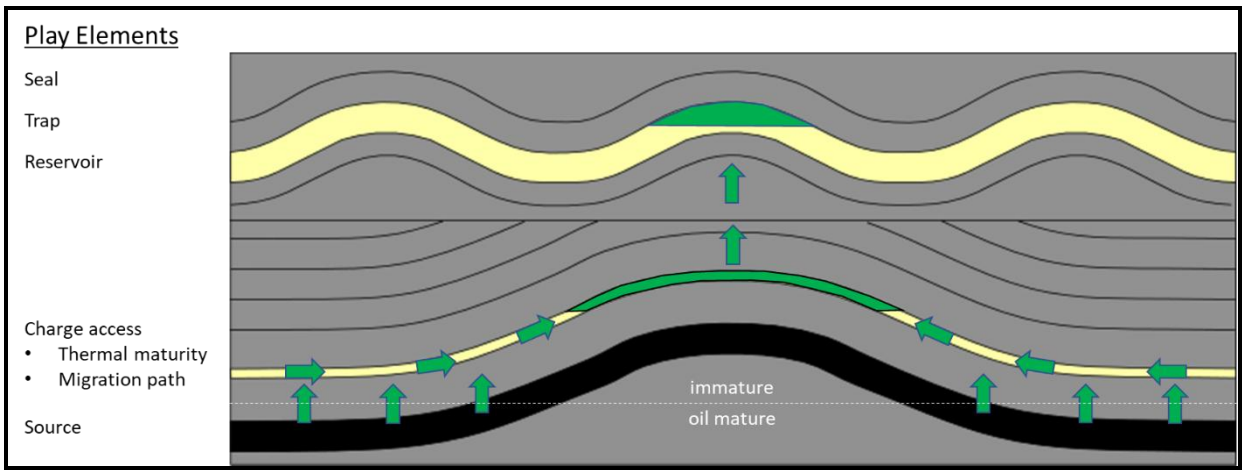

Figure 2.65: Cartoon figure showing the play elements of the petroleum system. To create a producible hydrocarbon accumulation, the required elements are 1) a thermally-mature organic-rich source rock; 2) a hydrocarbon-wet migration path from source rock to reservoir (green arrows); 3) a reservoir with economically sufficient porosity and permeability; 4) a buoyant trap, (i.e. a concave-downward geometry enclosing sufficient volume); and 5) a seal with sufficiently high capillary entry pressure to retain an economic hydrocarbon column.

CCS relies on some of the same play elements as hydrocarbons, but the requirements are different. Source and charge access (at least in the petroleum sense) are irrelevant, but a good reservoir for CCS needs high porosity, permeability, thickness and areal extent. Individual reservoir parameters may vary, but the cumulative result must have the injectivity to accept the expected injectate stream, and the connected pore volume to dissipate injection pressure for a decade or more. That is, it must offer capacity to store CO_2 injectate for the lifespan of the project. If anything, the economics of CCS suggest that in general, reservoirs may need to be better for CCS than for hydrocarbons in order to keep the well costs within acceptable limits (van der Meer and Yavuz, 2009; Hoffman et al., 2015).

Trap and confining zone or confining system (Bump et al., 2023) are required for CCS, but the spectrum of acceptable variation is wide. Without the need for recovery, CCS need not rely on large buoyant traps alone. Residual trapping (pore throat trapping), dissolution and small or even tiny buoyant traps can all usefully arrest CO_2 (Bourg et al., 2015; Ulfah, 2021). If column heights are small, then even low-quality seals would be sufficient. On the other hand, large column heights, as produced by injection into buoyant traps, require high-quality geologic seals for CO_2, just as they do for hydrocarbons. Retention of injected CO_2 is critical to building public trust, maintaining regulatory permission and ensuring financial viability. With much of the current interest in CCS focusing on buoyant traps, confining zone capacity is a concern.

Geology of the Coastal Texas-Louisiana Border Region

The Gulf of Mexico (aka “Gulf of America”) Basin has been a prograding passive margin basin with depositional systems building progressively into the basin since its opening during the Triassic. Historic hydrocarbon production has proven reservoirs and seals at every stratigraphic level from the Jurassic to the Pliocene and world-class source rocks in the Jurassic, Cretaceous and Paleogene sections (Galloway, 2009; Snedden and Galloway, 2019). The subset of the geology available for CCS is defined by pore fluid pressure--roughly 800m below top of the water column down to the top of geologic overpressure (Figure 2.66). The top of the storage window is defined by the minimum pressure needed to keep CCS in a super-critical state, thereby maximizing storage efficiency by minimizing required reservoir pore volumes. The base of the window is defined by the loss of needed pressure headroom between reservoir pressure and frac pressure.

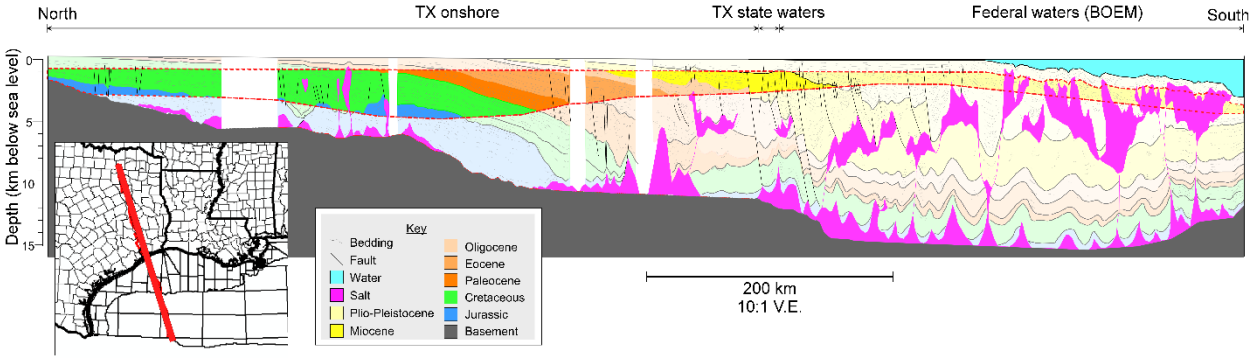

Figure 2.66: Cross-section of the US Gulf of Mexico ("America) Basin showing the geologic storage window for CO_2 (band of saturated colors near the top of the section; Bump et al., 2021). The focus for this study is the area labeled "Texas state waters."

Within the storage window, the geology of the study area consists of Miocene paralic deposits—deltaic and shore zone systems with interbedded sands and mudstones and often complex geometries (Galloway, 1989; Snedden and Galloway, 2019; Olariu et al., 2019). The main seal is the *Amphistegina* B (MFS-9 of this study), which caps the Lower Miocene (Figure 2.63). It is a well-described transgressive marine shale, present all along the Texas and Louisiana coasts. Over the study area, it is greater than 100m thick, thinning northward toward an onshore pinch-out. Mercury injection capillary entry pressure tests indicate that the *Amphistegina* B is capable of retaining hydrocarbon columns of several 10s-100s of meters, depending on burial depth. Observed column heights are generally toward the low end of that range, perhaps limited by low-relief structures and/or poor-quality fault seals (Trevino and Meckel, 2017). In short, MFS-9 appears to be a good regional seal (confining zone or system) that should work for both hydrocarbons and CCS.

Figure 2.67 shows a depth map on the MFS-9 surface along with all wells targeting Miocene reservoirs. It is a highly deformed surface, due to the underlying presence of mobile salt. Inspection of the map shows a large number of buoyant traps. Some are 4-way dip closures; more commonly, they are 3-way closures against faults. Producing wells tend to cluster on the highs; although, there is one group toward the southeastern end of the map that is located well down-dip of any structural high, perhaps stratigraphically trapped. Dry holes (red dots in Figure 2.67) are scattered across the study area and are roughly equal in number to the producing wells. These are the data points we will focus on. Our aim is to understand the reasons for hydrocarbon failure and the implications for CCS.

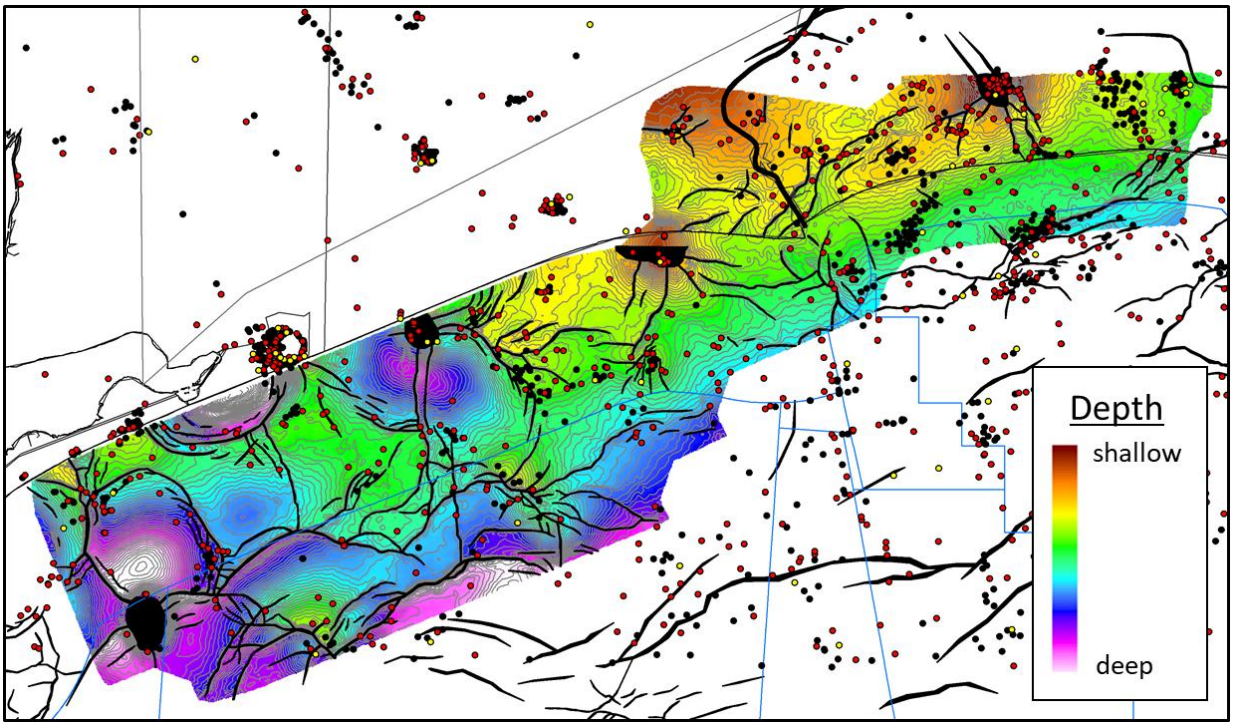

Figure 2.67: Depth structure map of MFS-9 (Amphistegina-B) with 50m contours showing the distribution of traps (DeAngelo et al., 2019). Faults are shown by the thin black polygons. Wells targeting Miocene reservoirs are denoted by the dots. Black dots are producing wells, red are dry holes and yellow are dry holes with hydrocarbon "shows." Well data courtesy of IHS.

Dry Hole Analysis

Our approach to dry hole analysis attempts to balance accuracy and specificity with pragmatic, map-scale filters. It is based on a combination of seismic mapping and GIS analysis of wells, beginning with the shallow play elements and becoming progressively deeper. Ultimately, our aim is to see how many of the dry holes we can explain as failures of trap, reservoir or charge access; that is, by mechanisms other than top seal failure.

We begin by looking at the distribution of dry holes with respect to traps. As a first pass, we assume that all faults seal, and we use the structure contours on the MFS-9 depth map to identify and define valid traps (Figure 2.67). Our definition of trap is thus a conservative one, based purely on geometry, without regard to seal. Even by this definition, approximately 50 of the dry holes are clearly outside of any valid trap (Figure 2.68). Likely many were drilled without benefit of 3D seismic and some may have been drilled without even 2D seismic. In any case, lack of a trap is a clear failure mechanism for hydrocarbon wells.

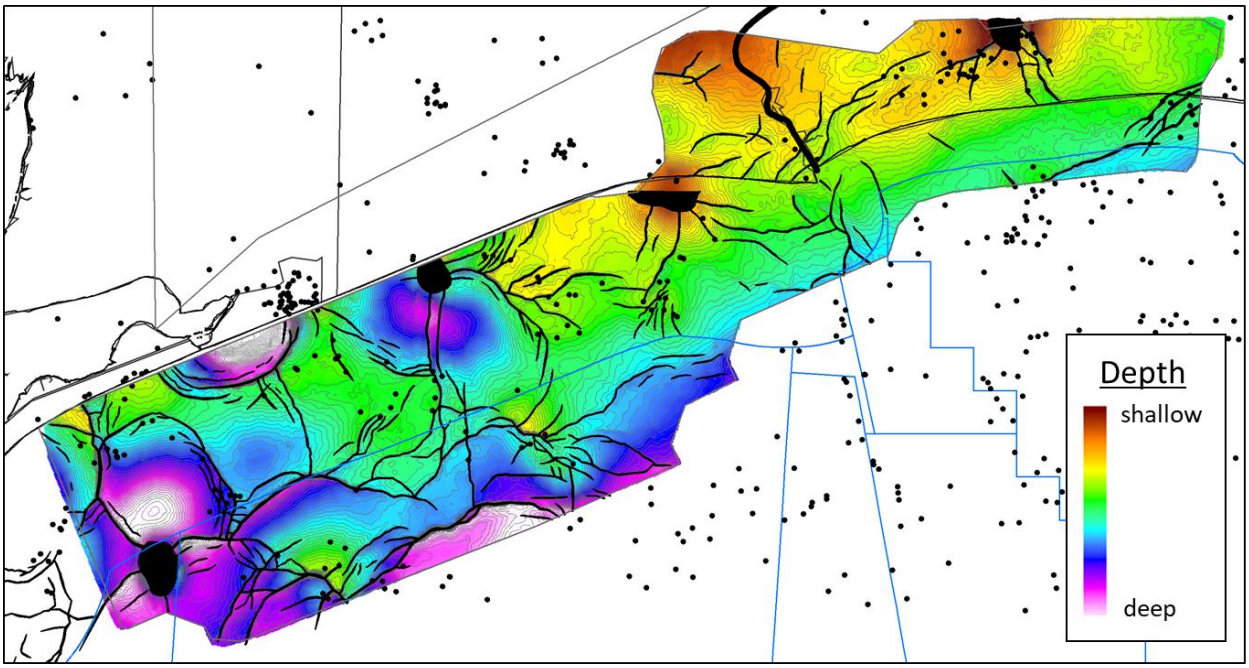

Figure 2.68: Depth structure map of MFS-9 (*Amphistegina*-B) with contours (50m interval) showing the distribution of traps. Black dots show dry holes that targeted Miocene reservoirs but failed to drill a valid structural trap.

In terms of depth, the next logical play element would be reservoir. However, the study area is sand-rich and in our experience, every well encounters potential reservoir sands. Without knowing the details of individual well plans, it is impossible to say whether they encountered the exact target sand intended. We therefore choose to temporarily bypass questions of reservoir and look at charge access instead. Specifically, we look at charge focus.

The shallowest potentially mature source rocks in the study area are roughly Eocene in age (Galloway, 2009; Swanson et al., 2013). To access Miocene reservoirs, expelled hydrocarbons must migrate across at least the Oligocene section, if not more. Seismic imaging clearly shows that the Oligocene-level structure is strongly discordant with the Miocene (Figure 2.69). In concept, hydrocarbons migrate generally upward from the source rock where they are generated, driven by the interplay of pressure gradients and permeability architecture. In a mixed clastic system with abundant sands, migrating hydrocarbons are likely to migrate up-dip along strata of permeable sands. Where they encounter pinch-outs or structural traps, the hydrocarbons will accumulate, building column height until they either spill or overcome the capillary entry pressure of the overlying muds and migrate vertically until they find the next sand. Oligocene age highs are thus expected to form the entry points for charge into the overlying Miocene section.

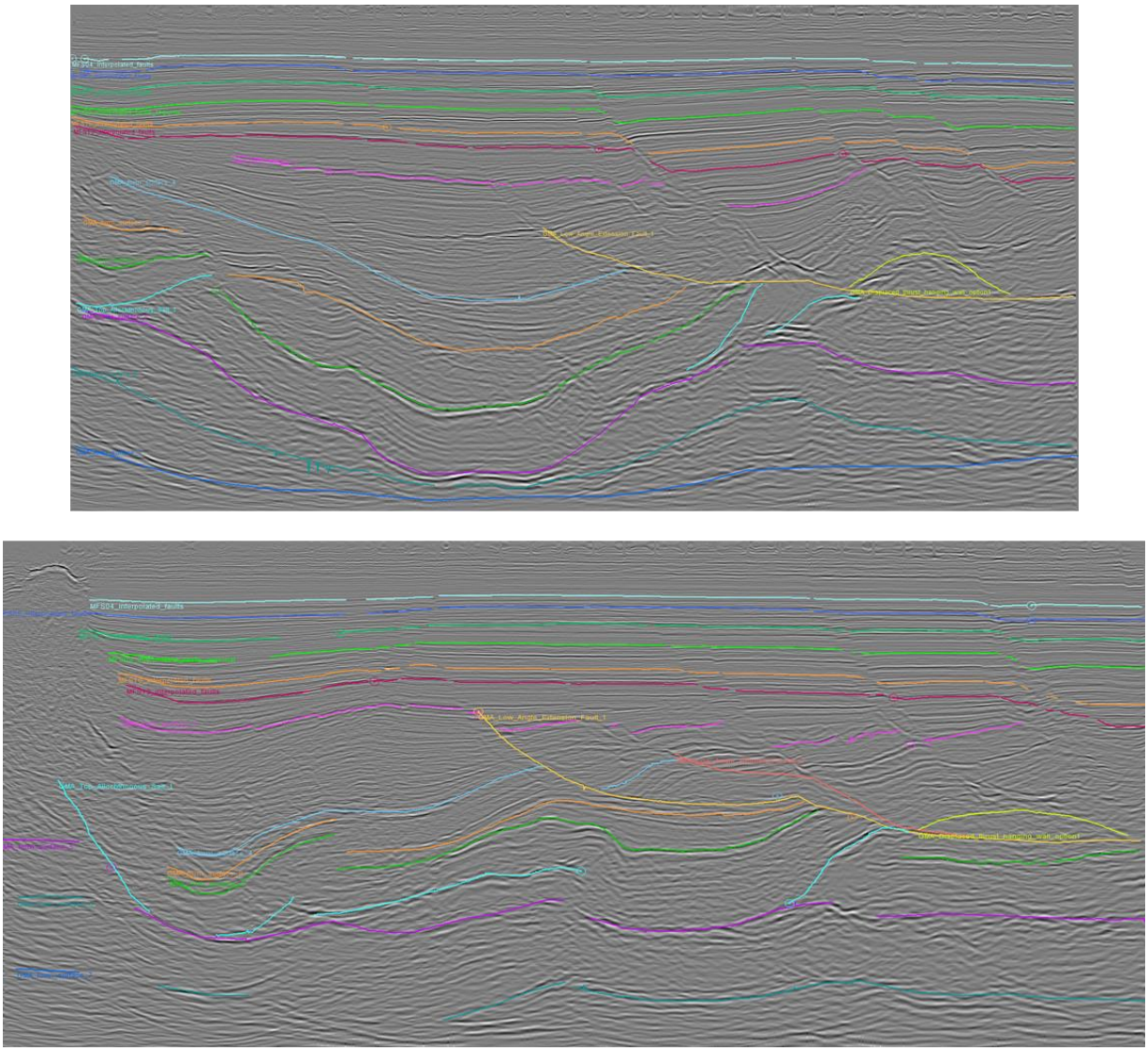

Figure 2.69: Examples of NNW-SSE (dip-oriented) seismic lines showing the structure of the study area. Note the discordance between the shallow, sub-horizontal Miocene horizons and the heavily deformed deeper horizons (pink and lower). These deeper horizons are interpreted to be Oligocene and older, and the horizons' structural highs create strong focal points for migrating hydrocarbons, similar to the cartoon in Figure 2.65. (Data owned or controlled by SEI. Interpretation is that of the University of Texas at Austin.)

Inspection of the Oligocene structure map (Figure 2.70) shows a number of highs and lows. Plotting the Miocene dry holes that were not explained by lack of a valid trap shows that several of those clusters overlie Oligocene synclines. Many of those wells almost certainly never received a charge (solid red ellipses in Figure 2.70), which would easily explain those failures. Comparing the Miocene and Oligocene structure maps more closely (Figure 2.70 and Figure 2.71) shows that some of the remaining Miocene dry holes are close to Oligocene focal points, without being directly above them. In these cases, we look at Miocene structure to judge migration direction from the point where hydrocarbons exit the Oligocene section. The dashed red ellipses in Figure 2.70 and Figure 2.71 identify clusters of wells that may have received a charge, despite not quite overlying Oligocene focal points. These clusters warrant a closer look.

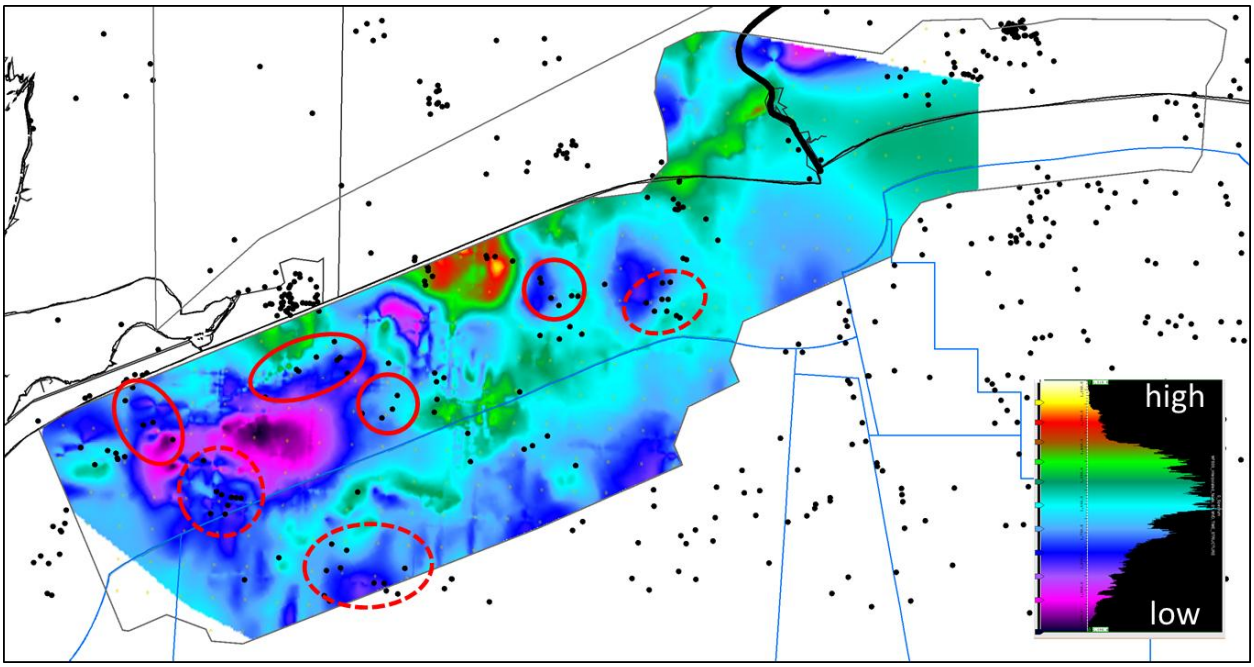

Figure 2.70: Oligocene depth structure map. Local highs create focal points for migrating hydrocarbons. Black dots show dry holes that targeted valid Miocene traps (i.e., failures not explained by lack of trap). Solid red ellipses show clusters of wells that clearly lack Oligocene-level charge focus and likely failed for that reason. Dashed ellipses show clusters of wells that are close to a focal point

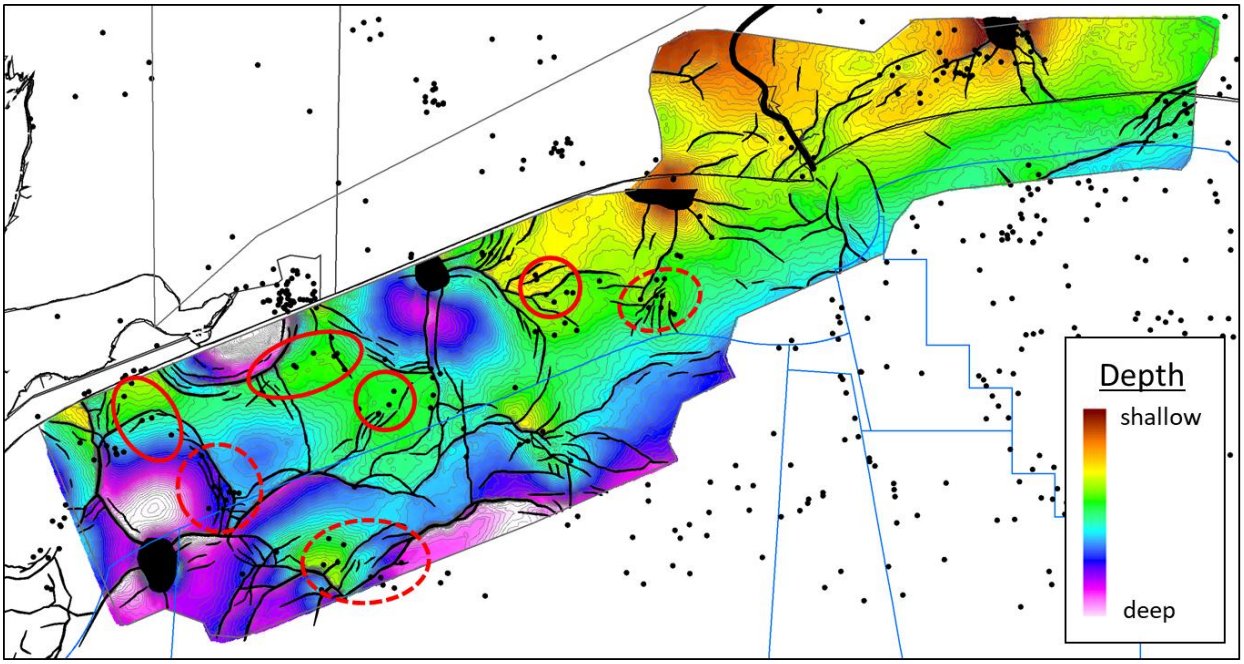

Figure 2.71: Miocene MFS-9 depth structure map with dry holes (black dots) that drilled a valid trap. Solid red ellipses show clusters of wells that clearly lack a deeper (Oligocene-level) charge focus and likely failed for that reason. Dashed ellipses show clusters of wells for which the deeper charge focus is moderately offset in a down-dip direction, such that hydrocarbons migrating vertically from Oligocene highs might reasonably be expected to hit Miocene carrier beds and migrated laterally into the Miocene highs.

Figure 2.72 shows a zoom on each of three clusters, looking not only at the dry holes (black dots in Figure 2.72)

but also at the producing wells (green dots). All three clusters have a mix of producing wells and dry holes, clearly showing that there is a valid trap, a reservoir and indicating that charge was received. Clearly the dry holes must have a different explanation. In the first example (left panel of Figure 2.72), we note that the producing wells are all up-dip of the dry holes that are in the same fault compartment. Although, that could be due to reservoir distribution, a more likely explanation is limited seal capacity and consequently a small hydrocarbon column. Integrity of the trap in question depends on both fault seals and the top seal and either could limit the column height. However, fault seals tend to be poorer quality than top seals, due to the mixing with reservoir materials in the fault gouge and the disruption of depositional fabrics. We have no proof but we hypothesize that the limitation here is the fault seal.

The remaining two clusters of wells (center and left panels in Figure 2.72) both show producing wells intermingled with dry holes. The explanation of limited seal capacity and short hydrocarbon column cannot explain that distribution. Indeed, it suggests that all the play elements are working, but the distribution of one of them is patchy. The most plausible explanation is a channelized reservoir, with narrow, sinuous sand bodies holding the recoverable hydrocarbons. Some wells access the sand bodies and some wells miss them. In any case, the observed failures do not appear to implicate the top seal.

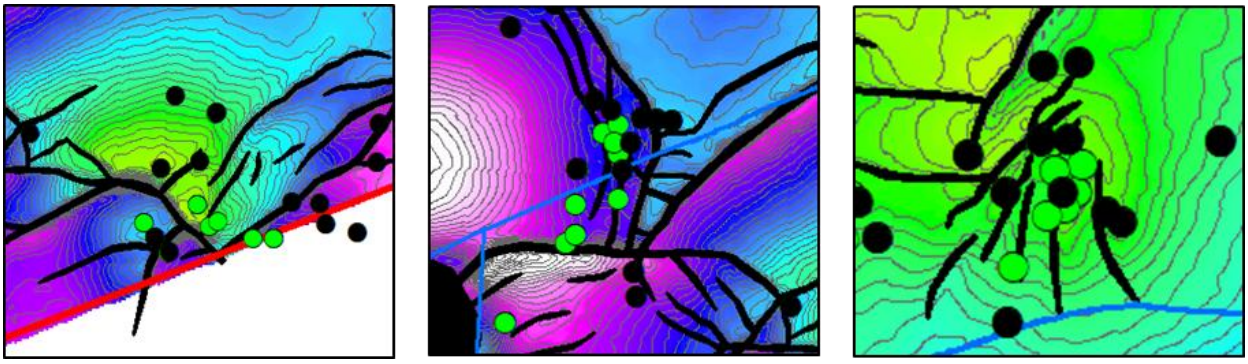

Figure 2.72: Miocene MFS-9 depth structure maps with examples of mixed producing wells (green dots) and dry holes (black dots). The mix suggests that both trap and charge are working; the dry holes must have another explanation. In the example on the left, the producers are all at the crest of the trap, with the dry holes down-dip, suggesting a short hydrocarbon column height, probably a result of limited fault seal capacity. The center and right examples show producing wells intermingled with dry holes, which cannot be explained by trap, charge or seal. Most likely, these result from channelized reservoirs with limited areal extent.

Conclusions

The focus area for this study has been heavily drilled, but ~50% of the wells have been dry, a worryingly high fraction for prospective CCS project developers. Understandably, that provokes concern, particularly in terms of seal capacity but perhaps also in terms of predictive capability. Both are fair concerns that need to be addressed for CCS to move forward, both in this area, in the wider Gulf of Mexico, and also in any basin in the world with failed exploration wells.

Here we can show that the large majority of dry holes failed for either lack of a valid trap or for lack of charge focus. Of the remaining wells, only one set appears to indicate limited seal capacity. Even those wells are juxtaposed with up-dip producers, clearly indicating that the seals work, albeit perhaps with limited capacity. In that case, the dry holes may actually help to constrain and quantify seal performance. In all other cases within the study area, the dry holes are simply not relevant to seal capacity. Consideration of seal integrity for CCS thus reverts to the regional characterization and local observations of producing fields (i.e., successfully retained hydrocarbons.) In summary, the *Amphistegina* B seal in the focus area should work for carbon sequestration.

References

Bourg, I.C., Beckingham, L.E., and DePaolo, D.J., 2015, The Nanoscale Basis of CO_2 Trapping for Geologic Storage: Environmental Science & Technology, v. 49, p. 10265–10284, doi:10.1021/acs.est.5b03003.

Bump, A.P., Hovorka, S.D., and Meckel, T.A., 2021, Common risk segment mapping: Streamlining exploration for carbon storage sites, with application to coastal Texas and Louisiana: International Journal of Greenhouse Gas Control, v. 111, p. 103457, doi:10.1016/j.ijggc.2021.103457.

A. P. Bump, S. Bakhshian, H. Ni, S. D. Hovorka, M. I. Olariu, D. Dunlap, et al.
International Journal of Greenhouse Gas Control 2023 Vol. 126 Pages 103908
DOI: https://doi.org/10.1016/j.ijggc.2023.103908

DeAngelo, M.V., Fifariz, R., Meckel, T., and Treviño, R.H., 2019, A seismic-based CO2-sequestration regional assessment of the Miocene section, northern Gulf of Mexico, Texas and Louisiana: International Journal of Greenhouse Gas Control, v. 81, p. 29–37, doi:10.1016/j.ijggc.2018.12.009.

EPA, 2020, EPA Facility Level GHG Emissions Data: EPA Facility level information on greenhouse gases tool (FLIGHT), http://ghgdata.epa.gov/ghgp/main.do (accessed December 2020).
Galloway, W.E., 1989, Depositional framework and hydrocarbon resources of the early Miocene (Fleming) episode, northwest Gulf Coast Basin: Marine Geology, v. 90, p. 19–29, doi:10.1016/0025-3227(89)90110-2.

Galloway, W.E., 2009, Gulf of Mexico: GEO ExPro, v. 6,
http://www.geoexpro.com/articles/2009/03/gulf-of-mexico (accessed April 2020).
Hoffman, N., Carman, G., Bagheri, M., and Goebel, T., 2015, Site Characterisation for Carbon Sequestration in the Nearshore Gippsland Basin, *in* International Conference and Exhibition, Melbourne, Australia 13-16 September 2015, Melbourne, Australia, Society of Exploration Geophysicists and American Association of Petroleum Geologists, p. 265–265, doi:10.1190/ice2015-2209980.

IHS Markit Inc., 2020, IHS Enerdeq: Enerdeq Browser, https://my.ihs.com/Energy/Products (accessed October 2020).

Kreitler, C.W., Collins, E.W., Fogg, G.E., Jackson, M., and Seni, S.J. Hydrogeologic Characterization of the Saline Aquifers, East Texas Basin--Implications to Nuclear-Waste Storage, in East Texas Salt Domes: , p. 182.

van der Meer, L.G.H., and Yavuz, F., 2009, CO2 storage capacity calculations for the Dutch subsurface: Energy Procedia, v. 1, p. 2615–2622, doi:10.1016/j.egypro.2009.02.028.
Olariu, M.I., DeAngelo, M., Dunlap, D., and Treviño, R.H., 2019, High frequency (4th order) sequence stratigraphy of Early Miocene deltaic shorelines, offshore Texas and Louisiana: Marine and Petroleum Geology, v. 110, p. 575–586, doi:10.1016/j.marpetgeo.2019.07.040.
Seni, S.J., Hentz, T.F., Kaiser, W.R., and Wermund, E.G.J. (Eds.), 1997, Atlas of Northern Gulf of Mexico Gas and Oil Reservoirs, Volume 1: Miocene and Older Reservoirs: Austin, TX, Bureau of Economic Geology, The University of Texas at Austin, 199 p.

Snedden, J.W., and Galloway, W.E., 2019, The Gulf of Mexico Sedimentary Basin: Depositional Evolution and Petroleum Applications: Cambridge University Press, doi:10.1017/9781108292795.

Swanson, S.W., Karlsen, A.W., and Valentine, B.J., 2013, Geologic Assessment of Undiscovered Oil and Gas Resources--Oligocene Frio and Anahuac Formations, United States Gulf of Mexico Coastal Plain and State Waters: USGS Open-File Report Open-File Report 2013–1257.

Trevino, R.H., and Meckel, T.A., 2017, Geological CO2 Sequestration Atlas for Miocene Strata Offshore Texas State Waters: Bureau of Economic Geology, The University of Texas at Austin Report of Investigation 0082–3309, 73 p.

Ulfah, M., 2021, Plume Migration and Pressure Evolution Analyses for Recommendations in Offshore CO2 Storage Acreage Leasing Policy [MS]: University of Texas at Austin, 146 p.

2.1.4 Subtask - NAMSS 3D seismic data sets from Federal waters

Throughout the duration of the GoMCarb Partnership, regional seismic datasets available for study increased thanks to downloading of newly available to the public 3D seismic from the USGS NAMSS (National Archive of Marine Seismic Surveys) site (Figure 2.73). Seismic datasets in federal waters were required to be made public 25 years after they were acquired, and the Partnership's period of performance coincided with the 25th anniversaries of many historical 3D seismic surveys. Regional seismic datasets closer to the coast were systematically interpreted throughout the project.

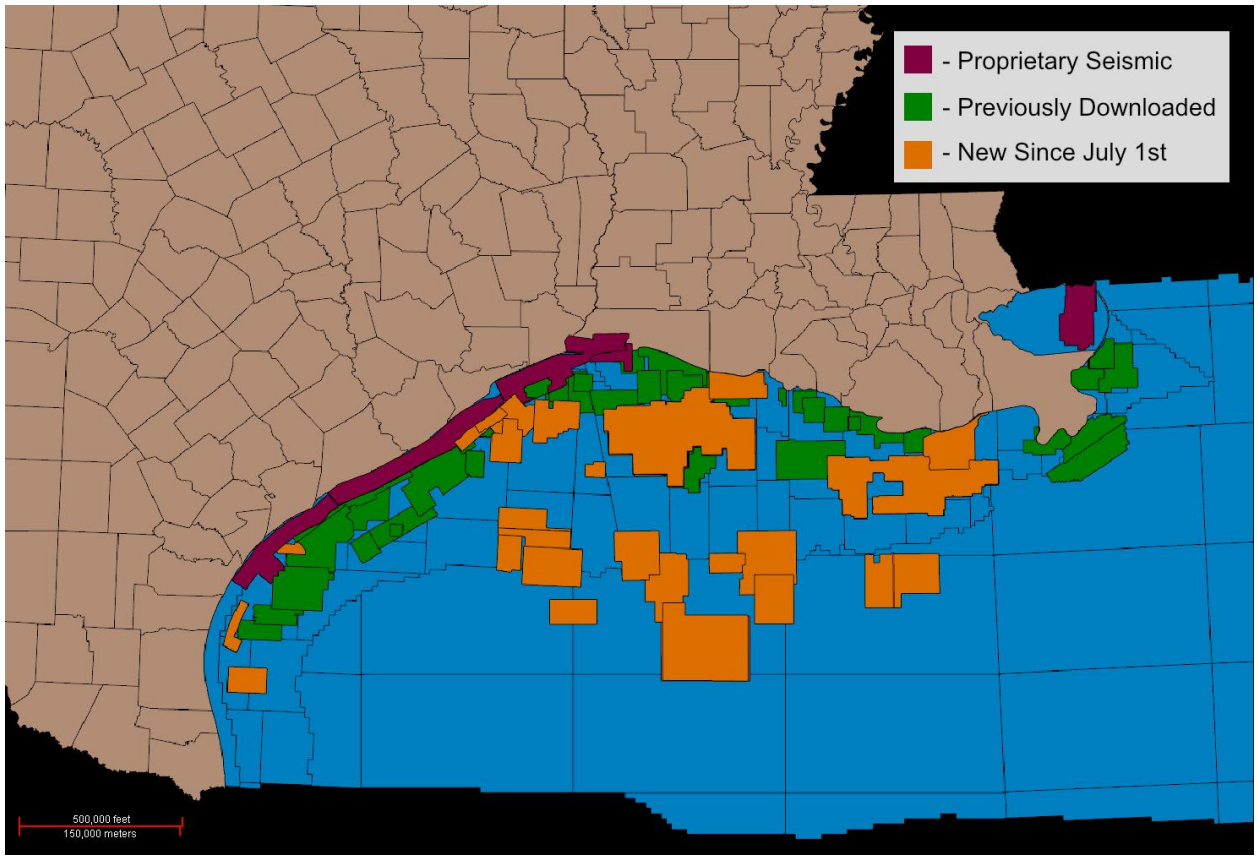

Figure 2.73 – Map of Partnership's regional 3D seismic database The orange-colored polygons, which indicate the dimensions of publicly available 3D seismic datasets, which were downloaded from NAMSS since July 1, 2022. The green-colored polygons show publicly available 3D seismic datasets downloaded before July 1, 2022.

2.2 Subtask: Data Gap Assessment

The following (Table 2.7) was submitted in the Deliverable 2.2a report in fulfillment of Subtask 2.2 and is included here for the reader's convenience.

Table 2.7 - List of data gaps, acquisition strategies and plans to address data gaps

Data Gaps	Acquisition Strategy	Plans to address gaps
Seeps- occurrence and geochemistry	Inquire at Global Offshore Seepage Database (GOSD), discussion with Ian MacDonald https://www.cgg.com/en/What-We-Do/Multi-Client-Data/Geological/Seep-Explorer	Discussion with experts, database interrogation, and site characterization
Occurrence and geochemical signatures of submarine groundwater discharge.		https://www.twdb.texas.gov/groundwater/aquifer/majors/gulf-coast.asp
Freshwater inflows to Texas bays and estuaries.	Texas Water Development Board Datasonde collects water temperature, conductivity, water level, and salinity data of freshwater inputs	https://www.twdb.texas.gov/surfacewater/bays/coastal_hydrology/index.asp
Groundwater discharge into shelf	Riverine input; estuaries and submarine groundwater discharge; air-sea exchange; exchange at the ocean boundary; primary production; and respiration.	https://pubs.er.usgs.gov/publication/70194664
Shallow sediment pore water/dissolved gas geochemistry	Shallow sediment coring and geochemical assessment	Large data base, personal communication with TDI-Brooks, Int. and site characterization
Mineralogy and redox chemistry of shallow sediments	discussion with TDI Brooks	site characterization coring

Geochemical and isotopic composition of seawater		site characterization sampling
Shallow sediment pore water to water column CO2 fluxes	benthic chambers	site characterization sampling
Shallow sediment pore water/dissolved gas geochemistry	Shallow sediment coring and geochemical assessment	Large data base, personal communication with TDI-Brooks, Int.
Incomplete wireline well-log coverage	purchase currently unavailable raster images of well logs from IHS, Inc. ($19/raster)	In-house digitizing of selected well log raster images;
Unavailable 3D seismic velocity data for converting from time to depth	Identify and lease velocity processing volumes (if funds available).	
Reservoir properties (relative permeability, maximum residual gas saturation, capillary pressure, anisotropy ratio and rock compressibility). Lack of rock cores from Miocene sandstone reservoir units.	No commercial sources identified to-date. Continue searching core databases. Mine reservoir data reports and from Class 1 disposal permits.	Options: 1) Further search literature. 2) Use Oligocene reservoirs (sub-optimal). In future, propose a project to drill, core and conduct high quality hydraulic tests, preferably with a gas phase to obtain good quality inputs for fluid flow modeling
Data identifying pressure seals vs. capillary seals or baffles (top seal prediction)	Map facies (seismic and log characteristics of confining system units (aka seals); collect hydrocarbon column heights and distributions.	Collect cores and open hole logs to calibrate the petrophysical interpretation of permeability and capillary entry pressure. (Part of a possible future study.)

Data for fault seal prediction	Geomechanical modeling to assess the limits of additional pressure in a weakly consolidated section dissected by faults is under way at LLNL. Information about the distribution of hydrocarbon accumulations are being assessed to extract information about fault sealing capacity.	Mapping faults from 3D seismic and net to gross thickness of the reservoir units.
Plume stabilization prediction in “fetch” areas	Field testing is a critical need to validate plume stabilization assessments, and fit-to-purpose measurements are needed.	Improved conceptualization of trapping process via pore scale and meter scale modeling and by improved upscaling concepts
Boundary condition definition	Field testing	
Monitoring optimization	Planning to deploy GCCC's high resolution 3D seismic (HR3D) system, which is ideal for overburden monitoring. Design of environmental monitoring for Gulf of Mexico conditions (warm and shallow marine) is underway.	GoMCarb partners by design are tapping into the best practices in development for offshore projects in the Norwegian and UK segments of the North Sea and in the Tomakomai project in Japan.
Infrastructure cost gaps	Two GoMCarb partners are focusing efforts on infrastructure costs and the value of reuse.	

Procedures for remediating existing offshore wells that have not been properly plugged and abandoned are needed		In the current scope of work, the possible activity is to make others aware of this need.
CO2 blowouts have never been handled offshore	GoMCarb LBNL study provided an excellent starting point and needed analytical tools.	With future funding, field testing (for example at LSU well facility) under controlled blowout conditions to prove up well control effectiveness with CO2 and mixtures.
Policy gaps Federal waters - CCS permitting process and non-coal CO2 authorization for Federal waters	Provide data and exchange information with BOEM.	Increased BOEM activity, which might happen during GoMCarb active period.

Geotechnical gaps

Reservoir properties for Miocene reservoirs

Gap: Many wells penetrate the Miocene and produce from this interval; however little core has been collected from sandstone reservoir units. A database for quantitative inversion of log based porosity to permeability and the important multi-phase flow endpoint saturations are not available. Maximum residual gas saturation, capillary pressure, anisotropy ratio and rock compressibility data are lacking. In proximal settings Miocene composition is somewhat more carbonate -rich than Oligocene rocks, so interval-specific data are needed to increase confidence in fluid flow modeling

Plans to address gap: Core databases have been searched with only small success. We are mining data from reservoir data reports and from Class 1 disposal permits to collect what is possible. No funds are available in the current phase of GoMCarb for coring a well.

Remaining need: Propose in a future project to drill, core and conduct high quality hydraulic tests, preferably with a gas phase to obtain good quality inputs for fluid flow modeling

Top seal prediction, within zone pressure or CO2 seals

Gap: The Miocene geologic section offshore has excellent storage capacity because it is sand-rich. However, the thickness, lateral continuity, and clay-content of the numerous within-Miocene inter-channel and marine transgressive units vary. It is in many cases not clear which zones are pressure seals and which are capillary seals or baffles. These data are needed for capacity and area of review calculations.

Plans to address gap: Current work mapping facies and seismic and log-based characteristics of Miocene lays the groundwork for classification of top-of-storage-complex and within-Miocene confining system performance. Information about the column height and distribution of hydrocarbon accumulations is being assessed to extract information about top seal. In many settings the hydrocarbon distribution can confirm the performance of a fine-grained layer; however, absence of hydrocarbon accumulation is a non-unique interpretation.

Remaining need: Collection of cores and open hole logs to calibrate the petrophysical interpretation of Miocene units with respect to permeability and capillary entry pressure is needed. For this gap, we also propose in a future project to drill, core and conduct high quality hydraulic tests

Fault seal prediction

Gap: the Miocene offshore has excellent storage capacity because of high net sand to gross thickness. This same sand-rich property that favors good injectivity however makes identification of fault seal more challenging. If fault seal is questionable, the amount of CO2 injected in each site is limited to volumes that do not contact the fault. In converse outcome, leaky fault seals on the margins of injection volumes can allow larger volume injection at higher rate because boundary conditions are open.

Plans to address gap: Current work mapping faults from 3-D seismic volumes and net to gross thickness of the Miocene lays the groundwork for classic fault analysis and sets up for innovative work on fault seal. Information about the distribution of hydrocarbon accumulations are being assessed to extract information about fault sealing capacity. In addition, standard techniques to assess the sealing properties created by fault offset and shale gouge on faults are being applied to the study areas. State-of-the art geomechanical modeling to assess the best approach assessment of the limits of additional pressure in a weakly consolidated section dissected by faults is under way at LLNL.

Remaining need: Field assessment techniques are needed for two linked purposes: 1) to assess the validity of existing assumptions made during characterization and 2) to develop and test monitoring tools to assess fault performance during injection. Faults may be in the far field, however fault performance may be important to long commercial injection periods as well as to attaining certainty of permanence prior to closure. Further modeling with realistically complex faults followed by field testing is needed.

Plume stabilization prediction in "fetch".

Gap: Much of the subsurface capacity in the Gulf of Mexico is in synclines or regionally dipping strata not in structural closures. CO_2 migrates though these rocks, and as it migrates it is incrementally and permanently trapped by capillary forces and by dissolution. To assess these effects, models need to properly cope with the conditions that occur far-from-injection point physics where injection pressure is not a major driving force and fluid movement is slow. Similar conditions occur post injection over the entire plume area, this must be assessed to understand plume stabilization. Most models have been validated by comparison to observed fluid flow in short-term, near-injection well settings. Adding confidence to models' long-term and far-field predictions (i.e., far from injection wells) remains a need for CCS globally and for the Gulf Coast in particular.

Plans to address gap: improved conceptualization of trapping process via pore scale and meter scale modeling and by improved upscaling concepts are major efforts in GoMCarb research. This activity is based on use of combined numerical modeling and physical measurements of cores and constructed meter-sale heterogeneous sand packs (physical models). Flow velocities and scales are designed to be relevant to the long term and far field stabilization issues and address the needed physics.

Remaining need: Field testing is a critical need to validate plume stabilization assessments, and fit-to-purpose measurements are needed. It is critical to know prior to project start that over the long-term, the plume will stabilize and not migrate into unprepared areas. This requires experiments in the field to test the correctness of the models, and by careful design can be accomplished at a small scale and short experimental durations. For example, the scale of the Frio test might be sufficient.

Boundary condition definition

Gap: Capacity is strongly dependent on the pressure performance of the reservoir in the far field. A reservoir with a strong "water drive" can accept CO2 faster and also likely in large volumes than a hydrologically confined reservoir. However, conventional tools to define the far field hydraulic conditions are not well defined. Large faults and facies changes can be relatively straightforward to define; the performance of smaller faults and sand body discontinuity is not easy to quantify based

on current data.

Plans to address gap: Analysis of production history using decline curves was undertaken; however, data quality limited the data's utility.

Remaining need: Field testing can improve assessment of boundary condition assessment. In a transmissive unit, a long recovery time can probe the far field and improve conceptualization of this parameter as linked to geologic assessment.

Monitoring optimization

Gap: the options and optimum for monitoring offshore is quite different, in addition, the risk profile is different. This is true in injection zone, overburden, and sea floor- water column monitoring.

Plans to address gap: GoMCarb partners by design are tapping into the best practices in development for offshore projects in the Norwegian and UK segments of the North Sea and in the Tomakomai project in Japan. In addition, we are deploying the high-resolution seismic area (P-cable) which is ideal for overburden monitoring. Design of environmental monitoring for Gulf of Mexico conditions (warm and shallow marine water) is underway,

Remaining need: Field testing in Gulf of Mexico conditions is needed.

Infrastructure cost gaps

Gap: optimization of new build infrastructure and the realistic cost for this construction remains a gap. Items that need cost information include pipelines across the sensitive zones at the shoreline, subsea shallow water pipeline, drilling platforms, operational platform or sub-sea wellheads, and installed monitoring equipment such as seabed cables and any fixed arrays to probe reservoir and seabed environments for conformance or leakage signals. New data are needed primarily because some of the most attractive major GoM targets are in State waters less than 3-10.3 miles offshore, and little new data are available in this setting. New drilling in the Gulf of Mexico in past few decades has focused on targets in deep water, and the cost and risk profiles for this deep-water work compared to CO2 storage in shallow water settings are quite different. At what cost is reuse of existing infrastructure a positive for projects? Northern Lights CCS project in Norway has recommended that they found existing infrastructure a strong positive in that setting. However, the GoM is shallower and in general the infrastructure is older.

Plans to address gap: Two GoMCarb partners are focusing efforts on infrastructure costs and the value of reuse

Remaining need: To obtain reliable modern cost for the shallow-water GoM, progressing to the FEED study with funded engineering design work is needed.

Infrastructure need remediating old wells

Gap: procedures for remediating existing offshore wells that have not been properly plugged and abandoned are needed. Onshore the process of excavating a casing and install a well head to re-enter and remediate a well is well known, although it can be costly if problems are encountered. However, similar processes are not available for an offshore well that no longer has a well-head but needs to be re-entered, inspected, and may need to be re-used or re-plugged.

Plans to address gap: This need is one of the issues that has been raised by the GoMCarb Advisors. In the current scope of work, the possible activity is to make others aware of this need

Remaining need: additional funding targeted to well engineering process.

Well blow out management

Gap: CO2 blowouts have never been handled offshore

Plans to address gap: LBNL study provided an excellent starting point and needed analytical tools

Remaining need: Additional modeling, including mixed fluid response under different P-V-T conditions. Field testing (for example at LSU well facility) under controlled blowout conditions to prove up well control effectiveness with CO2 and mixtures. Preparation of a commonly accessible best practice manual for control and remediation after CO_2 blowout (both offshore and onshore) is needed to support the many groups entering this business while lowering risk for all.

2.2.1 Subtask - Data gap assessments will focus on regionally relevant analog settings

Subsurface CO_2 storage is complex, with many relevant factors to consider and different datasets to integrate. Evaluation must identify the pressure window available for storage and incorporate the details of reservoir, confining system, faults, legacy wells, USDW (underground sources of drinking water), existing hydrocarbon fields, and structural and stratigraphic boundaries. In addition, all of those parameters vary geographically. Seeing the big picture is a major challenge but critical to identifying, understanding and communicating opportunities, constraints and knowledge gaps.

This work addressed that challenge through construction of a series of long, basin-spanning cross-sections that incorporated seismic data (courtesy of ION Geophysical), well logs, biostratigraphic picks, groundwater data, hydrocarbon exploration and production, published literature and new interpretation. In short, we integrated all available data to create the most complete illustration possible.

Figure 2.74 is a section running from just east of Dallas through Houston and out to the Gulf of Mexico abyssal plain. It highlights some of the notable differences between onshore and offshore, including:

- The variation in the geology available for storage, from Jurassic through Middle Miocene age units onshore vs. Lower Miocene through Pleistocene offshore, all due to progradational deposition
- The variable base of the pressure-defined storage window, which is deepest in the East Texas basin onshore and thinnest at the continental shelf edge, largely as a function of the time since deposition and the ability of sediments to dewater and pressure-equilibrate
- The variable top of the pressure-defined storage window, which is at ~800m below the top of the water table or seabed, whichever is deeper
- The variation in structural styles, from widely spaced normal faults and salt diapirs onshore to shallow salt and complex mini basins in the deepwater
- A vastly lower density of legacy wells and producing hydrocarbon fields offshore
- Much less well data available offshore, but newer wells and newer and more complete seismic data (note the data gaps onshore)
- The almost universal absence of USDW offshore

It is worth noting that the cross section in Figure 2.74 also illustrates the continuity of geologic systems from onshore to offshore. In subsurface terms, the modern shoreline is a transitory and largely irrelevant marker. With the exception of USDW, the geologic systems take no note of the modern shoreline. The differences from one side of the beach to the other are largely human. In fact, the geologic units become progressively muddier (more seal dominated) to the south but the decreasing data density and increasing geologic variability make it difficult to portray accurately.

Figure 2.75 is a section running from the outskirts of San Antonio, past Corpus Christi and out to the deep water. It incorporates similar data to Figure 2.74 and shows differences from onshore to offshore similar to those in Figure 2.74, but it also highlights some of the significant differences between East Texas and South Texas. In particular,

the highest rates of sediment deposition occurred in the Paleocene through Eocene in South Texas, versus Oligocene and Miocene in East Texas. As such, the pressure window and the distribution of reservoirs available for CO2 storage look a bit different. Additionally, the Eagle Ford and Yegua/Wilcox reservoirs are heavily drilled, creating a greater density of legacy wells than seen on the East Texas line.

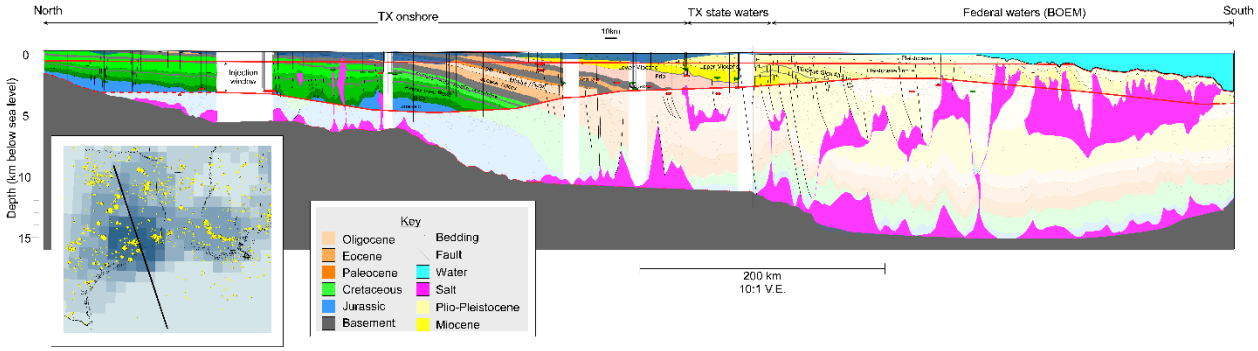

Figure 2.74: Cross-section extending from ~Dallas though Houston to the abyssal plain. Section is shown at 10:1 vertical exaggeration. The pressure-defined storage window for CO_2 is shown by the red outline and the saturated color fills. Producing hydrocarbon fields are shown by red and green ovals (gas and oil, respectively) at the reservoir level. USDW are shown by the shallow dark blue swaths onshore. Proven regional confining systems are shown by the grey bands. (Note that there are far more offshore than shown here). Legacy wells are shown by the vertical black lines. Note also the variations described in the text.

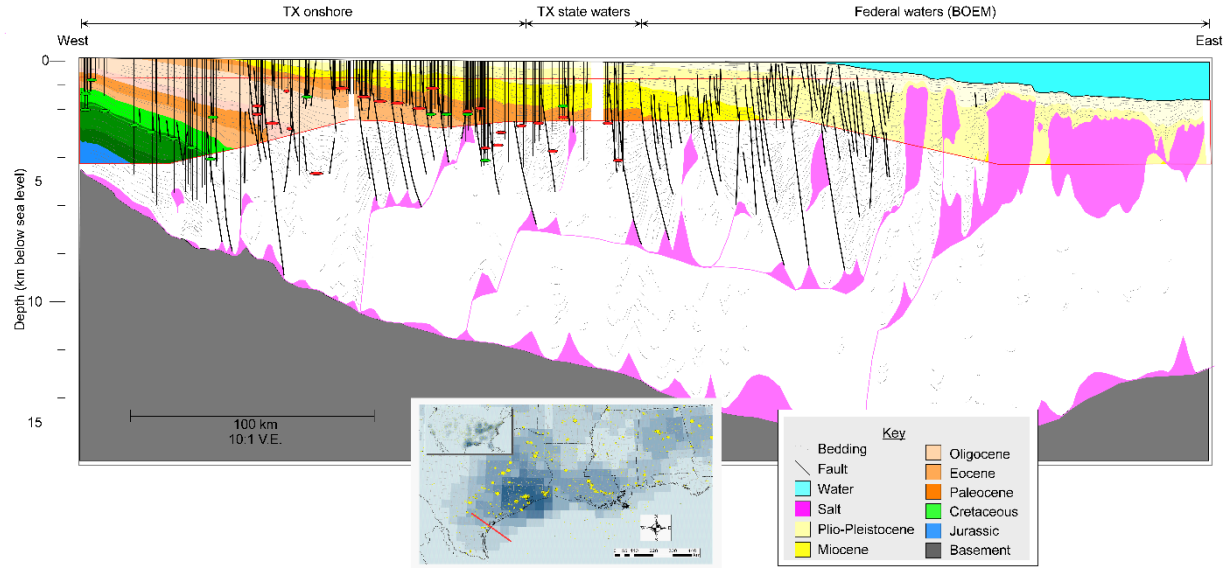

Figure 2.75: Cross-section running from ~San Antonio though Corpus Christi to the deep water. Section is shown at 10:1 vertical exaggeration. The pressure-defined storage window for CO_2 is shown by the red outline and the color fills. Producing hydrocarbon fields are shown by red and green ovals (gas and oil, respectively) at the reservoir level. USDW, regional confining systems and deeper geology are yet to be interpreted. Legacy wells are shown by the vertical black lines. Note also the variations described in the text. The apparent difference in size compared to Figure 2.74 is a function of what fits on the page—this section is half the length of Figure 2.74.

2.3 ***Subtask: Offshore and reservoir storage Enhanced Oil Recovery (EOR) Potential***

2.3.1 Subtask: Hydrocarbon fields: High Island, TX & Lake Charles / Lafayette districts, LA

The work for this subtask was also reported in deliverable report 2.3a.

This report summarizes the work conducted under subtask 2.3.1, to assess storage potential of offshore hydrocarbon reservoirs. The subtask focuses specifically on hydrocarbon fields selected in State waters in Texas (High Island area of Lake Jackson district), Louisiana (Lake Charles and Lafayette districts), and Houma (Figure 2.76).

Sources considered include those in Texas and western Louisiana. Western Louisiana sources are those occurring west of a line drawn connecting Houma and Alexandria, generally west of the Atchafalaya River along Highway 90 and the Interstate 10 corridor from Lafayette westward through Lake Charles to the Texas border at Orange, TX. More specifically, sources evaluated occur in the following parishes: Saint Mary, Saint Martin, Iberia, Lafayette, Acadia, Vermilion, Jefferson Davis, Calcasieu, Cameron, Saint Landry, Evangeline, Allen, Beauregard, Rapides, Vernon, and Avoyelles. In the offshore regions, this partnership studied both State and Federal waters. It considered the entire State waters of Texas and Louisiana. In Eastern Louisiana State Waters, the project utilized a 3D seismic dataset in the area west of the Chandeleur Islands in Chandeleur Sound. In the Federal offshore continental shelf region (OCS), this partnership studied the following districts: Lake Jackson, Lake Charles, Lafayette and for saline storage, Houma.

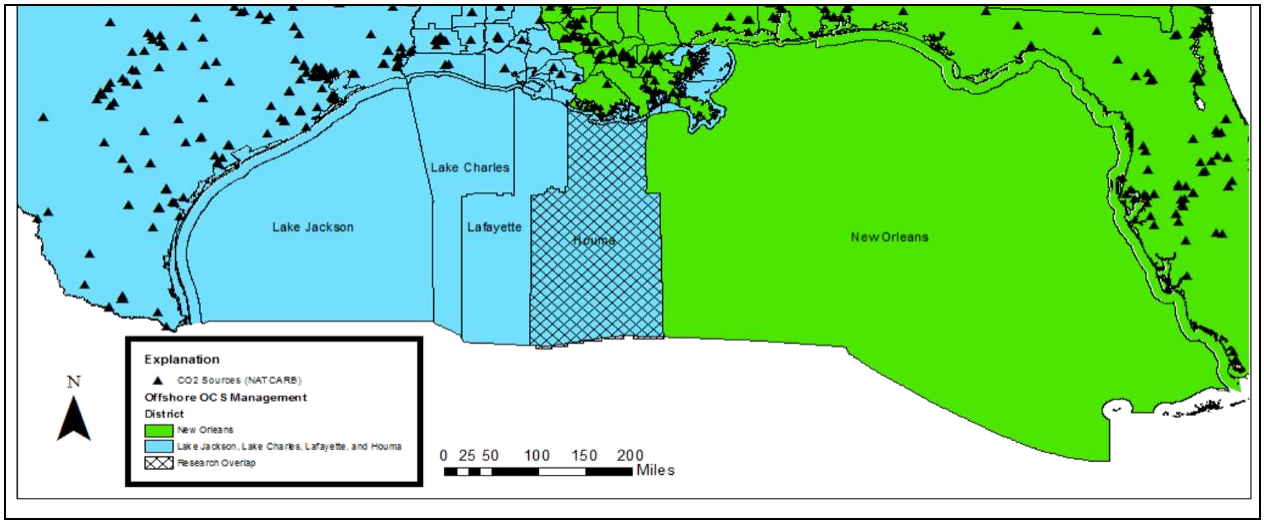

Figure 2.76 - The primary geographic region of emphasis for the GoMCarb partnership. The figure indicates both the onshore region for source consideration and the primary offshore geography for evaluating CO2 storage and related topics.

Feasibility of CO_2-EOR in offshore Oil Fields and Methodology for Miscible EOR

A database built for "Offshore CO2 Storage Resource Assessment of the Northern Gulf of Mexico (Texas-Louisiana)" (DE-FE0026083) was completed with EOR relevant data and used for the current (DE-FE0031558) EOR study. A quick-look screening methodology published by Nuñez-López et al., (2008) was used as part of the geotechnical approach to identify options for CO_2-EOR in the study area. The methodology focuses on determining whether the enhanced oil recovery process (the displacement of oil with CO_2) in oil reservoirs of significant size (cumulative production > one million barrels of oil) would achieve miscibility. Miscible displacements are preferred over immiscible displacements as ultimate incremental oil recovery decreases significantly at pressures below Minimum Miscibility Pressure, MMP (Figure 2.77). Holm and Josendal, 1980, define the MMP as the pressure that causes 80% oil recovery at CO_2 breakthrough and 94% recovery at a gas-to-oil ratio of 40,000 standard cubic feet per stock tank barrel (SCF/STB). For miscibility to

occur, the process should develop at or above MMP, which is a function of reservoir temperature, the molecular weight (Mw) of the C5+ components of the reservoir oil, and the purity of the injected CO_2.

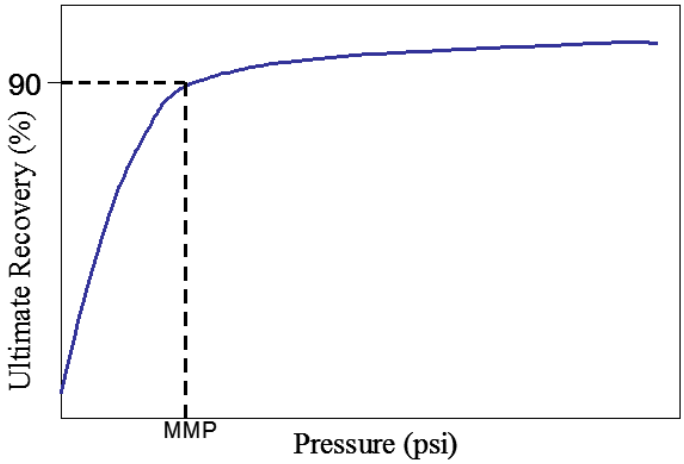

Figure 2.77 - Optimal recovery achieved at Minimum Miscibility Pressure (Lake, 1989)

MMP Estimation

Empirical correlations by Holm and Josendal (1982), Mungan (1981, and Lasater (1958) were used to estimate the MMP (Equation 2.1) and the Mw (Equation 2.2) under reservoir conditions:

Equation	Outcome	Source
$MMP = -329.558 + (7.727 \times M_w \times 1.005^T) - (4.377 \times M_w)$ Equation 2.1 Where: MMP: Minimum miscibility Pressure [psi] M_w: molecular weight of C5+ T : Temperature [F°]	MMP: minimum miscibility pressure. [psi]	(Holm and Josendal, 1980) (Mungan, 1981)
$M_w = \left(\frac{7864.9}{\gamma}\right)^{\frac{1}{1.0386}}$ Equation 2.2 Where: M_w: molecular weight of C5+ γ : API oil gravity	Mw: molecular weight of crude oil.	(Lasater, 1958)

For reservoirs missing API gravity data, necessary for the MMP estimation, a depth greater than 6,000 ft. was assigned as a miscibility criterion.

Methane content effect on MMP

In nearly all the correlations in the literature, the methane content of the oil is assumed to not affect the MMP significantly. However, we know from operational experience on the Gulf Coast that in reservoirs where the operating pressure is near the MMP, methane content has an effect on the development of partial miscibility throughout the flood. For reservoirs estimated to perform at near miscible conditions, this effect is considered in the study as a 5% of original oil in place (OOIP) deduction in estimated incremental oil recovery.

Incremental oil recovery estimation

In a report by Advanced Resources International (ARI) titled "Basin Oriented Strategies for CO_2 Enhanced Oil Recovery: Offshore Louisiana" it is assumed that 56% of the OOIP remains unproduced, and that 34% of the original gas in place (OGIP) also remains untapped. This is consistent with relevant data related to reservoirs for which we did have this information. In this study, we assumed that 55% of the OOIP remained in the reservoirs.

In the same report, ARI assumed that CO_2-EOR would produce an additional 20% of OOIP. Given the lack of EOR experience offshore and the recent experience in analogous onshore reservoirs in proximity to the study area, a 20% of OOIP is also assumed in this study. An exception was made for reservoirs with an estimated near miscible displacement and high methane production, for which an incremental recovery of 15% of OOIP was assumed.

CO_2 Storage Capacity Estimation

A quick-look CO_2 storage potential (capacity) is obtained by analyzing the cumulative production of an oil field. Here, it is assumed that the pore volume represented by oil and gas production is available in the reservoir for CO_2 storage. Gas production in these offshore reservoirs is significant and has an impact on carbon storage capacity. Incremental EOR production is added to cumulative fluid production to account for the additional delta pressure during EOR production. Stock-tank oil volumes are converted back to reservoir volumes, and resultant pore volumes are converted to the amount of CO_2 that could be put into that volume at initial reservoir conditions Equation 2.3).

$$CO2QLSC \text{ (metric tons)} = 0.05259 * N_p * B_{oi} / B_{CO2}$$

Equation 2.3

Results

The total original oil in place (OOIP) in the area of study was estimated at ~247MMBbl, with ~238MMBbl located offshore Louisiana (Table 2.8). Petroleum fields in the Louisiana offshore area have produced more oil than counterparts in Texas offshore waters. The Texas fields are much more gas-prone. A significant percentage of these two resources is located offshore Louisiana (Table 2.9). Figure 2.78 provides a visual comparison between the Texas and Louisiana oil resource and EOR potential. The total incremental oil recovery through miscible and near-miscible CO_2-EOR in the area of study was estimated at ~49MMBbl, and the storage capacity at ~169 million metric tons.

Table 2.8: Total Cumulative Oil Production, OOIP

	Cumulative Oil Production (Bbl)	OOIP (Bbl)
TOTAL	111,137,999	246,973,331

LA	107,005,227	237,789,393
TEXAS	4,132,772	9,183,938

Table 2.9: Total CO_2-EOR potential and carbon storage capacity in area of study

	CO_2 Storage Capacity (Million Metric Tons)	Estimated EOR Potential (MBbl)
Total	169.0	49,361
LA	133.0	47,524
TEXAS	36.0	1,837

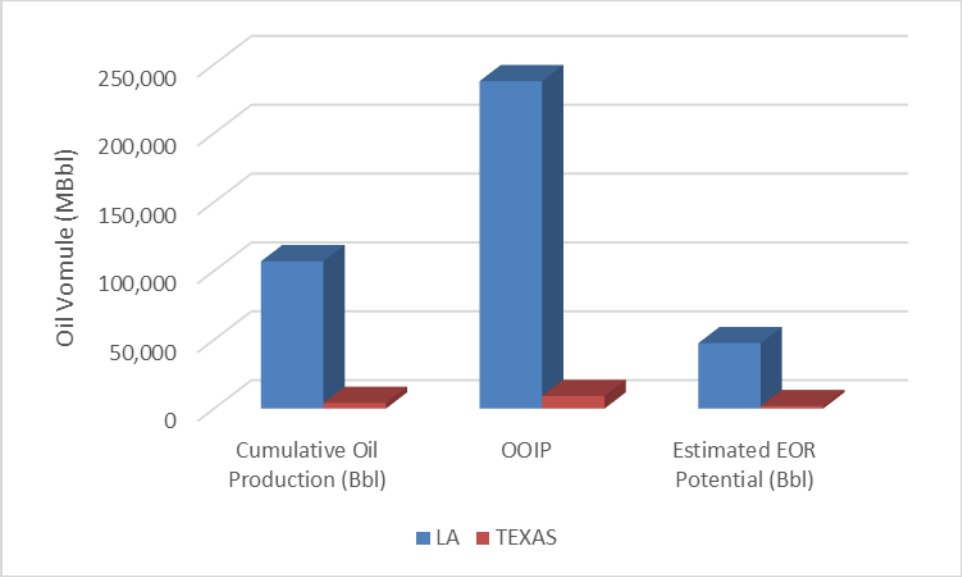

Figure 2.78 - Estimated total cumulative oil production, OOIP and EOR potential in offshore Texas and Louisiana.

The top twenty oil reservoirs, for which miscible CO_2-EOR is technically feasible, are ranked in terms of estimated incremental EOR recovery (EOR potential) from largest to smallest in Table 2.10. West Cameron 66, in the Lower Miocene 4 production zone, was ranked best with an estimated CO_2 EOR potential of almost 23 MMBbl and associated storage of 8.5 million metric tons. Even though EOR potential is assumed to be proportional to cumulative oil production, storage capacity is not proportional to EOR potential. This is because cumulative gas production is also utilized in the estimation of storage capacity.

Seventeen out of the top twenty oil reservoirs are located offshore Louisiana in West Cameron and East Cameron leases. The best ranked offshore Texas reservoir (Caplen) was ranked 16th, with an estimated EOR potential of 120 MBls, followed by High Island Block 14-L which was ranked 19th. Figure 2.79 shows the geographic location of the West Cameron and East Cameron leases where most of the top EOR reservoirs are located.

The 10 best-ranked offshore Texas reservoirs are included in Table 2.11. High Island 160, reservoir C, offers the largest storage capacity of the 10, attributed to large volumes of gas production from the zone.

Table 2.10: Top 20 reservoirs with miscible EOR potential in the study area

Production Zone	Field	Reservoir	Depth (ft)	Estimated EOR Potential (Bbl)	Volume Replacement Storage without EOR (Million Metric Tons)	Volume Replacement Storage with EOR (Million Metric Tons)
Middle Miocene 4	West Cameron 66 (Louisiana)	IT	7,996	22,855,664	5.93	8.54
Middle Miocene 4	West Cameron 66 (Louisiana)	JA	8,048	9,793,428	2.65	3.79
Lower Miocene 4	East Cameron 14 (Louisiana)	DB-1	11,663	1,464,196	4.20	4.37
Lower Miocene 4	West Cameron 71 (Louisiana)	46	11,044	1,096,731	12.93	13.04
Lower Miocene 2	West Cameron 45 (Louisiana)	F6	10,241	1,095,150	15.38	15.50
Lower Miocene 4	West Cameron 45 (Louisiana)	DISB1	8,681	1,094,901	1.61	1.73
Lower Miocene 4	East Cameron 14 (Louisiana)	DB-2	12,158	1,068,825	4.19	4.32
Middle Miocene 4	West Cameron 71 (Louisiana)	3034	9,262	766,824	1.74	1.82
Middle Miocene 4	West Cameron 71 (Louisiana)	44	10,793	752,936	8.86	8.94
Lower Miocene 4	West Cameron 71 (Louisiana)	47	11,125	746,181	0.62	0.70
Lower Miocene 4	West Cameron 45 (Louisiana)	DISB2	8,637	701,366	1.20	1.28
Lower Miocene 4	West Cameron 71 (Louisiana)	51	11,542	683,375	7.56	7.63
Middle Miocene 4	Hog Bayou Offshore (Louisiana)	AMPHISTEGINA	8,100	618,543	--------	--------
Middle Miocene 4	West Cameron 71 (Louisiana)	39	10,267	405,547	4.08	4.12
Lower Miocene 4	West Cameron 66 (Louisiana)	LJ	10,327	328,732	7.80	7.83
Lower Miocene 2	Caplen (Texas)	FB-5, 10	7,552	319,556	0.08	0.11
Lower Miocene 4	West Cameron 45 (Louisiana)	DISB5	8,967	285,469	0.50	0.53
Lower Miocene 2	West Cameron 45 (Louisiana)	E8/E9/F9	9,900	275,284	2.15	2.18
Middle Miocene 4	High Island 14-L (Texas)	6700*	7,045	249,778	0.12	0.15
Lower Miocene 2	West Cameron 45 (Louisiana)	E9/F4	9,900	213,853	2.91	2.94

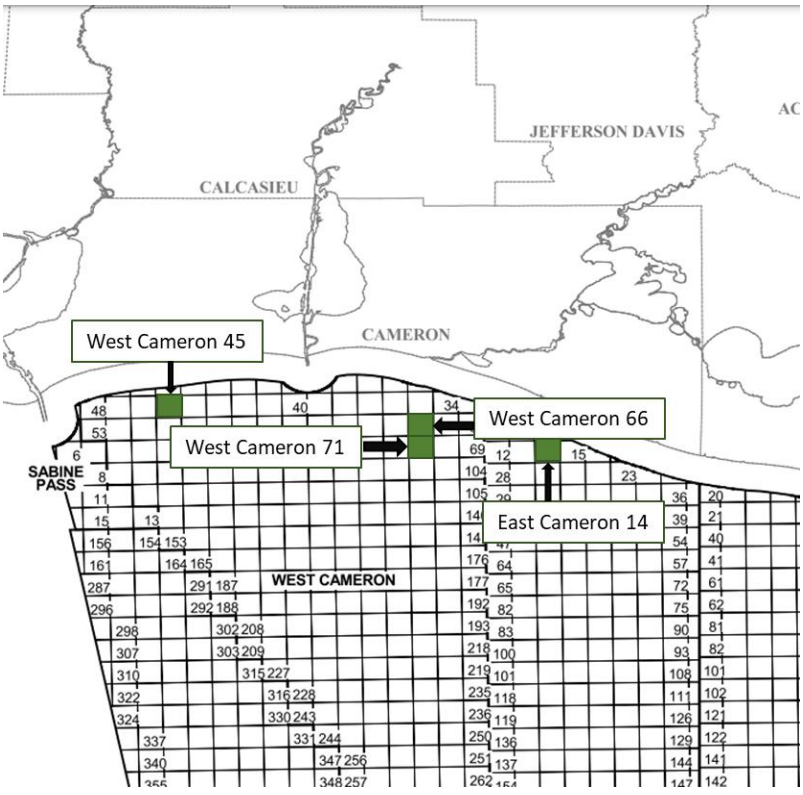

Figure 2.79 - Location of offshore leases containing most of the top EOR reservoir candidates in the study area.

Table 2.11: Top 10 reservoirs with miscible EOR potential in offshore Texas

Production Zone	Field	Reservoir	Depth (ft)	Estimated EOR Potential (Bbl)	Volume Replacement Storage with EOR (Million Metric Tons)
Lower Miocene 2	Caplen (Texas)	FB-5, 10	7,552	319,556	0.11
Middle Miocene 4	High Island 14-L (Texas)	6700*	7,045	249,778	0.15
Lower Miocene 1	High Island 14-L (Texas)	10000*	10,241	172,000	7.94
Middle Miocene 4	High Island 160 (Texas)	C	8,372	131,662	8.63
Lower Miocene 4	High Island 52 (Texas)	M50	9,118	129,738	4.11
Lower Miocene 2	High Island 179 (Texas)	60	11,075	102,318	0.99
Middle Miocene 9	Caplen (Texas)	MIOCENE 4430	4,427	82,222	0.02
Lower Miocene 4	High Island 179 (Texas)	N SD	9,271	73,790	2.04
Middle Miocene 4	High Island 160 (Texas)	B	8,349	72,470	5.37
Middle Miocene 4	High Island 19-S (Texas)	36-B SD.	5,635	56,889	0.02

References

ARI, Basin Oriented Strategies for CO_2 Enhanced Oil Recovery: Offshore Louisiana, Report, 2005.

Holm, L. W., and Josendal, V. A: "Discussion of determination and prediction of CO_2 minimum miscibility pressure", Journal of Petroleum Technology, May 1980, p. 870–871.

Lake, L.W.: "Enhanced Oil Recovery", Prentice Hall, 1989, 550 p.

Lasater, J. A.: "Bubble point pressure correlation", Trans., AIME, 1958, p. 379

Mungan, N.: "Carbon dioxide flooding fundamentals", Journal of Canadian Petroleum Technology, January–March 1981, p. 87.

Nuñez-López, Vanessa, Wood, D. H., Ambrose, W. A., and Hovorka, S. D. (2008). Quick-look assessments to identify optimal CO2 EOR storage sites. Environmental Geology, v. 54, p. 1695-1706. DOI 10.1007/s00254-007-0944-y

2.3.2 Subtask - Initial scoping study of EOR potential in selected reservoirs in Federal waters, beginning in the High Island area of the Lake Jackson District

An analog field in federal waters was studied as a potential example for infrastructure re-use and enhanced oil recovery; although, the latter would probably not be economically feasible. The field was discovered in the early 1980s by a major oil company. It has produced both gas and oil (cumulative ~55 mmbbl oil & water and ~325 Bcf gas). On a fluid replacement basis, we can get ~ 30Mt CO_2 storage capacity. However, there are some complexities: the field has had 6 operators, 20 surface well locations and 61 bottom hole locations (all, or most of the wells sidetracked and/or recompleted, often multiple times) and has produced from 19 reservoirs. Some reservoirs are at or close to abandonment; others are anticipated to have significant remaining production life.

The field is a small fault-bounded compartment with a narrow connection to an aquifer at the Miocene level. The younger section (Pliocene age?) is less affected by faulting. The main reservoirs are Middle Miocene age, with an upside potential for storage in the Pliocene section. The general depositional systems for the Middle Miocene correspond to deltas prograding on the shelf and possibly reaching the shelf margin. Figure 2.80 shows a type log of the Middle Miocene and Pliocene sections in the field. Sand bodies are likely delta-front with thin channelized sands showing moderate connectivity. Net thicknesses of individual reservoirs range from 17 to 62 feet, and porosities from 22 to 28 %.

The field has produced a total of ~25 mmbbl of oil, ~325 Bcf of gas and 30 mmbbl water from 19 separate reservoir intervals. Most of the oil and water production comes from a single reservoir in the upper part of the Middle Miocene. Gas production is widely distributed but three intervals (individual reservoirs) stand out as

particularly prolific producers with each of them having produced over 40 Bcf (billion cubic feet) of gas.

Analysis of depth-normalized reservoir pressures shows that all of the producing reservoirs were close to hydrostatic pressure at the time of discovery, and most have declined significantly with production (Figure 2.81). The three main gas reservoirs show steady declines in both production rate and reservoir pressure as a function of time, indicating little aquifer support. The oil reservoir is an exception to this pattern since the pressure initially declined from hydrostatic, but it has been constant since about 1998 despite continuing to produce large volumes of both oil and water, indicating good aquifer support here.

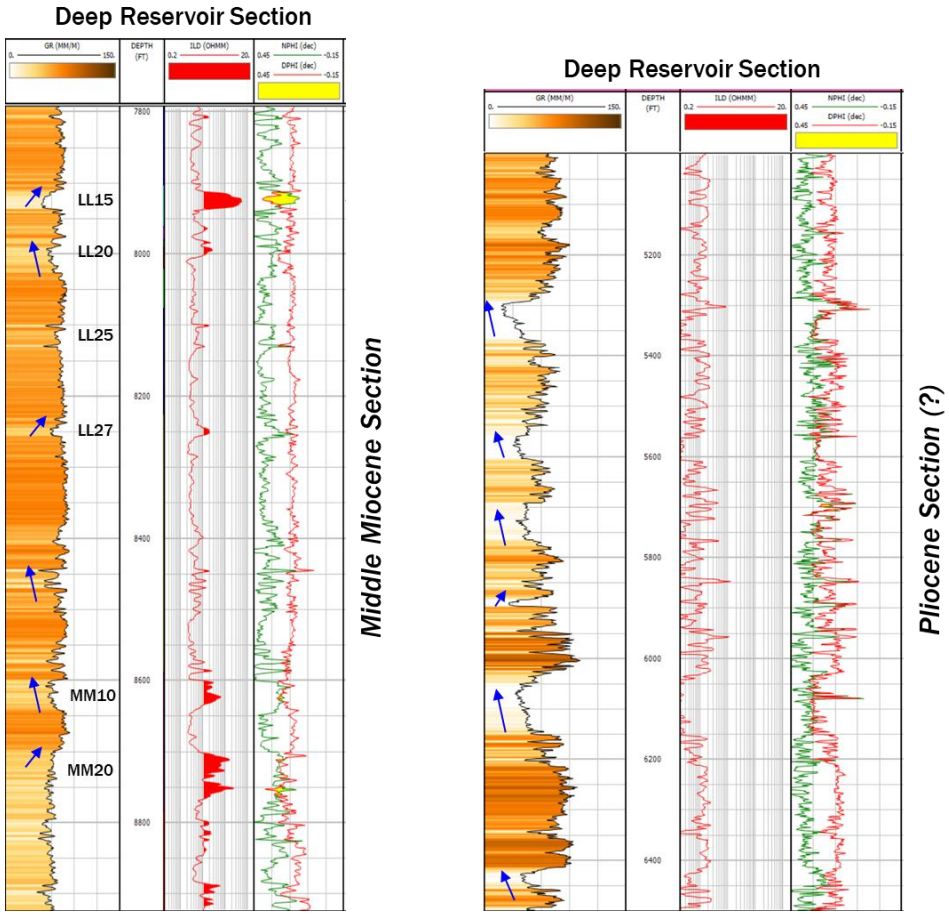

Figure 2.80 – Overview of the deep reservoir and shallow reservoir sections showing stacking patterns based on GR (gamma ray). Fining upward units could be channel bodies; whereas, coarsening up sections could be delta-front sandstones.

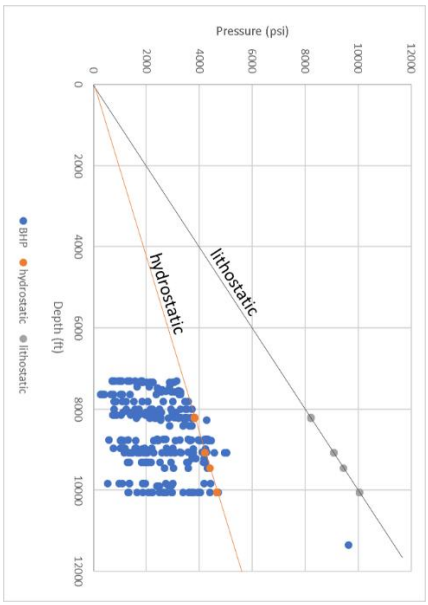

Figure 2.81 – All reported reservoir pressures over the life of the field plotted as a function of depth (TVDSS). Pressures in the producing reservoirs show a range from slightly over hydrostatic to much under hydrostatic.

Carbon Storage Potential:

Depleted hydrocarbon reservoirs are highly prospective for CO_2 storage. Their properties and flow behavior are generally well understood, and production data allows history matching of reservoir models. Where present, pressure depletion creates additional storage capacity. In addition, the overlying confining systems have proven capable of retaining buoyant fluids over geologic time.

For CO_2 capacity we first considered fluid replacement calculation which equates produced hydrocarbon volumes with injectable CO_2 volumes (both at reservoir conditions). The four main reservoirs that have produced large amounts of oil & gas were analyzed with 3 cases: Fifty percent is a reasonable minimum replacement ratio. Seventy-five percent is an average expectation, and 100% is the highest possible without exceeding virgin pressure or producing water. Total storage capacity for the four reservoirs is approximately 15 Mt, assuming injection up to virgin pressure without simultaneous water production.

Another assessment of CO_2 storage utilizes EASiTool, a rate-based, analytical storage capacity estimator, which offers a useful way to get a quick look at pressure build-up and ultimate injection capacity as well as to explore the upside capacity associated with higher pressures and water extraction. Calculations with EasiTool indicate capacity of ~4Mt per reservoir (Figure 2.82). Note that the software cannot completely honor the pressure space available; so, the actual capacity may be higher (5-6 Mt per reservoir?). Adding water extraction would allow further pressure management.

Alternatives to increase capacity would include the shallow (Pliocene age?) sand section. Capacity could increase ~20 Mt, but there are uncertainties on a reliable confining system and well remediation costs. In addition, the wells' cement in the shallow geologic section is uncertain. Another alternative to increase ~20Mt capacity would be to inject in the water leg (aquifer), but this would require new leases and a long step-out from the existing platform. As for commercial injectivity we need good permeability and thickness. The analog depleted field average ~100mD (millidarcies) permeability and 10m (meter) thickness for a typical reservoir sand. Consequently, the field does not meet the criteria for good injectivity in a vertical well. Reservoir injectivity could improve by drilling deviated or horizontal wells or adding multi-zone completions.

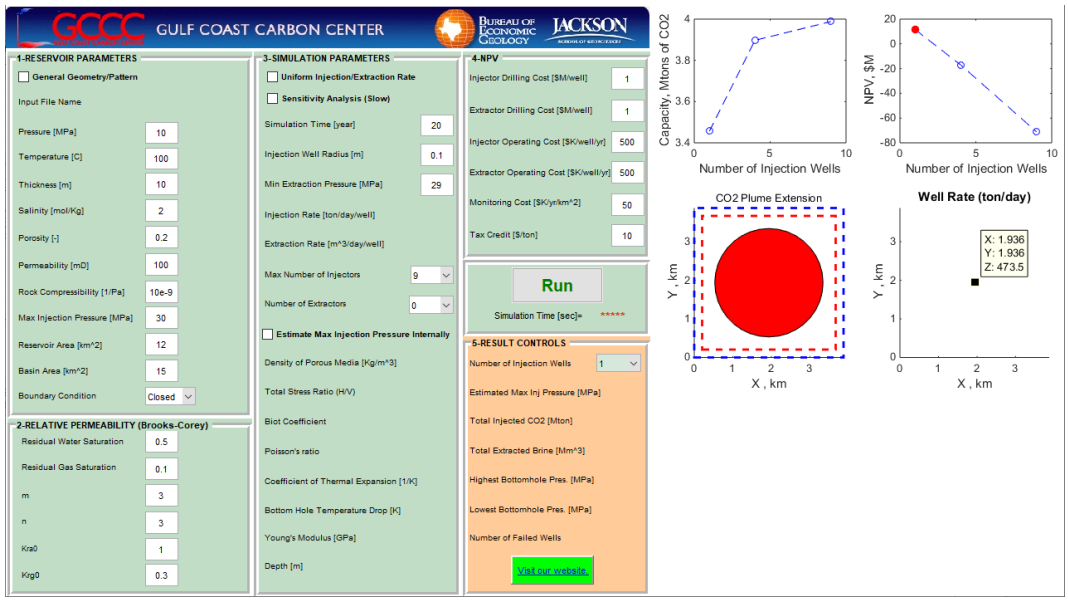

Figure 2.82 – EasiTool model run for a single depleted reservoir 10m thick, starting at 50% hydrostatic and ending at ~85% frac pressure. Capacity is estimated at 4Mt.

3. Task 3 – Risk Assessment, Simulation and Modeling

3.1 Subtask: Risk Assessment and Mitigation Strategies

3.1.1 Subtask - Assess adaptation of existing tools to offshore settings

Optimization of storage resource is a key parameter in siting and financing storage hubs. We invert petroleum exploration approaches at a geologic play level to assess subsurface risks to long-term storage, as a mechanism to lower cost and increased security. Basin-scale screening, play definition and prospect description are core tasks of petroleum exploration however and there is a well-defined suite of tools to deal with the problem. The work described here adapts and applies one of those tools to the identification of CCS sites. We focus on the U.S. Gulf of Mexico (aka "Gulf of America") as it is a well-understood petroleum basin and the Gulf Coast is a hub of CO2 emissions (Figure 3.1).

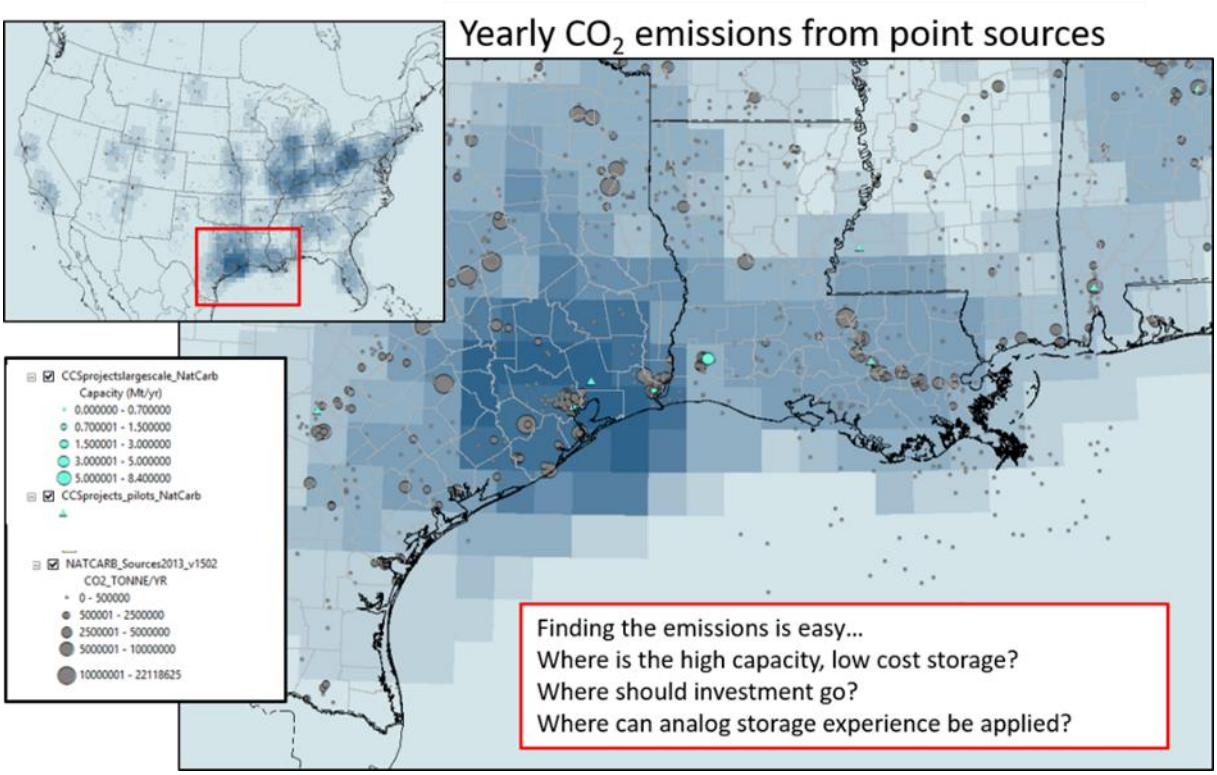

Figure 3.1 - Yearly point-source CO2 emissions (data: NATCARB, 2019). Individual sources are shown as grey circles (sized by emissions volume). The background colors show the total emissions within a 1.5degree radius (darker shades for greater emissions volumes).

This is essentially a three-part approach. First, we use regional cross-sections to identify and describe potential storage plays. Second, we map the intersection of potential reservoir strata with the subsurface pressure window for CO_2 storage. Third, we create maps of layered subsurface elements to describe the suitability of potential sites, based on the areal quality variation of available reservoirs and seals, the locations of potential traps and CO_2 sources, and the distribution of surface constraints such as land usage, available infrastructure and accessibility.

With respect to the Gulf of Mexico CO_2 source locations, current land use, site access and the density of existing well penetrations all favor offshore storage. Accordingly, we have focused our efforts on the coastal waters of Texas and Louisiana, constructing a series of exploration-inspired cross-sections and maps that serve both to help adapt the tools of exploration for CCS and to identify and high-grade potential storage sites in coastal waters.

The depth window for CO_2 injection is defined by subsurface temperature and fluid pressure. Specifically, it lies between the minimum depth for supercritical CO_2, which lies at roughly 1km depth and the top of hard over-pressure, which varies between 1.5 and 4km depth, based on extensive drilling data. Within this window, stratal ages vary from Early Cretaceous at the northern (onshore) basin edge to Plio-Pleistocene in the south (offshore), reflecting the long-term progradation of depositional systems toward the basin (Figure 3.2 and Figure 3.3). For each of these stratigraphic intervals, play fairways are defined by a regional seal and its underlying reservoirs.

As shown in Figure 3.4, geologic data, including well logs, seismic, outcrop descriptions and rock composition (upper right) are used to create maps of depositional environments and litho-facies (lower left). The maps are then turned into CRS maps for the key elements of the play (middle), including reservoir presence (porosity), reservoir quality (permeability) and seal capacity. We then turn these maps into traffic light-colored risk maps describing the likelihood of finding the key play elements, specifically reservoir presence (pore space), reservoir quality (permeability) and seal capacity (pressure retention potential). We then clip these maps to the geographic limits of the upper Oligocene within the CO_2 storage window (Figure 3.2 and Figure 3.3) and add them together to create a composite risk map that describes the chance of finding high-quality, low-cost storage in Oligocene reservoirs. In

petroleum terms, this is a play fairway map and it is important to note that *red is simply higher risk*, **not** a "no go" area. Upper Oligocene storage is available in all colored areas of the map. What varies is the capacity of storage and the effort/cost required to identify and characterize it.

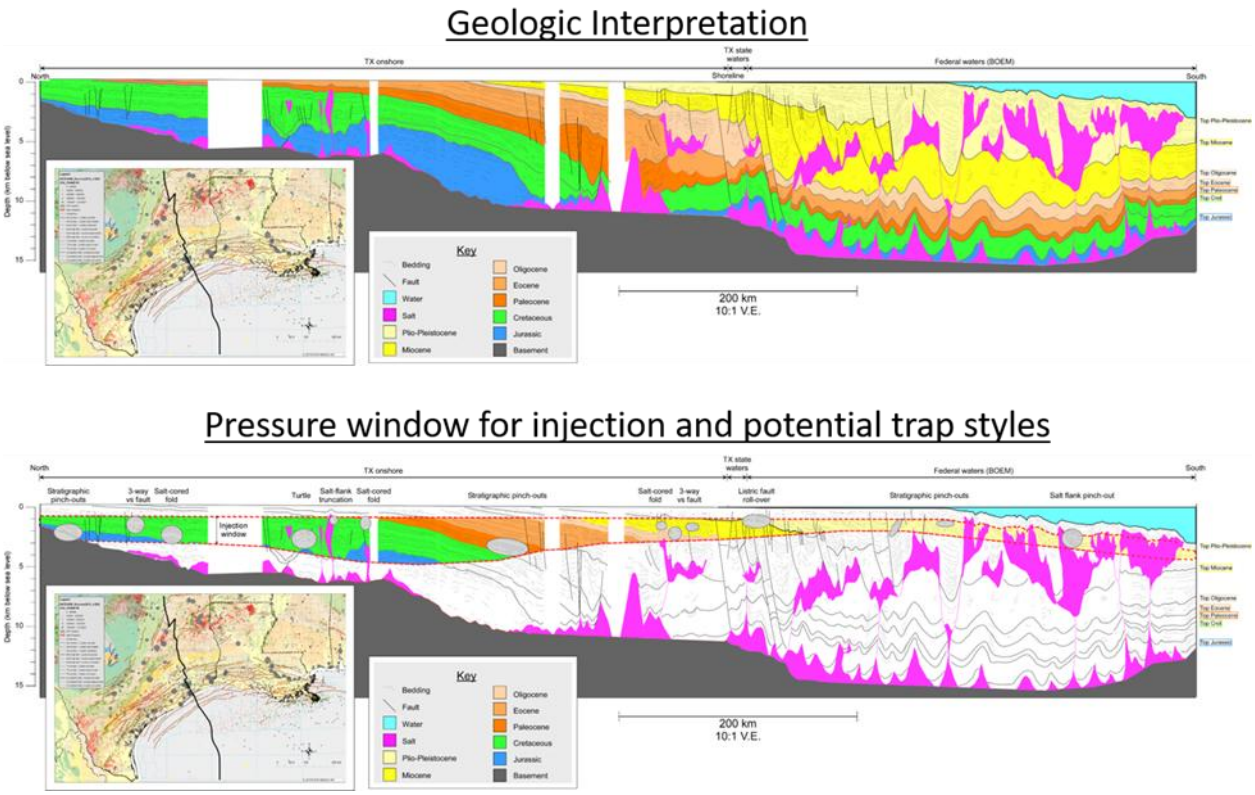

Figure 3.2 - Geologic cross-sections interpreted from seismic, well and outcrop data. Location is shown by the black line on the inset map and runs roughly from Dallas, through Houston and into the deep-water Gulf of Mexico. The top section shows stratal ages and structure. The bottom section shows the geology clipped to the pressure window for CO2 storage and identifies trap styles and their locations (grey ovals).

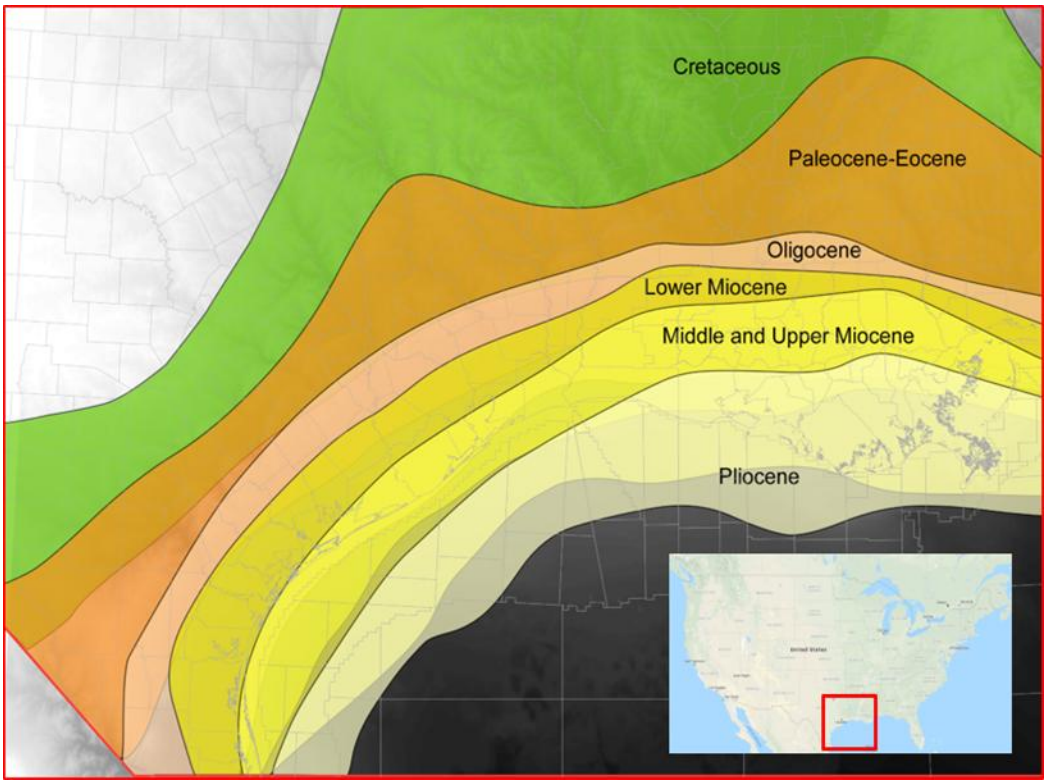

Figure 3.3 - Map-view of stratal footrpints within the pressure window for CO_2 storage. Map is based on seismic mapping of stratal ages and published maps of the top of geo-pressure.

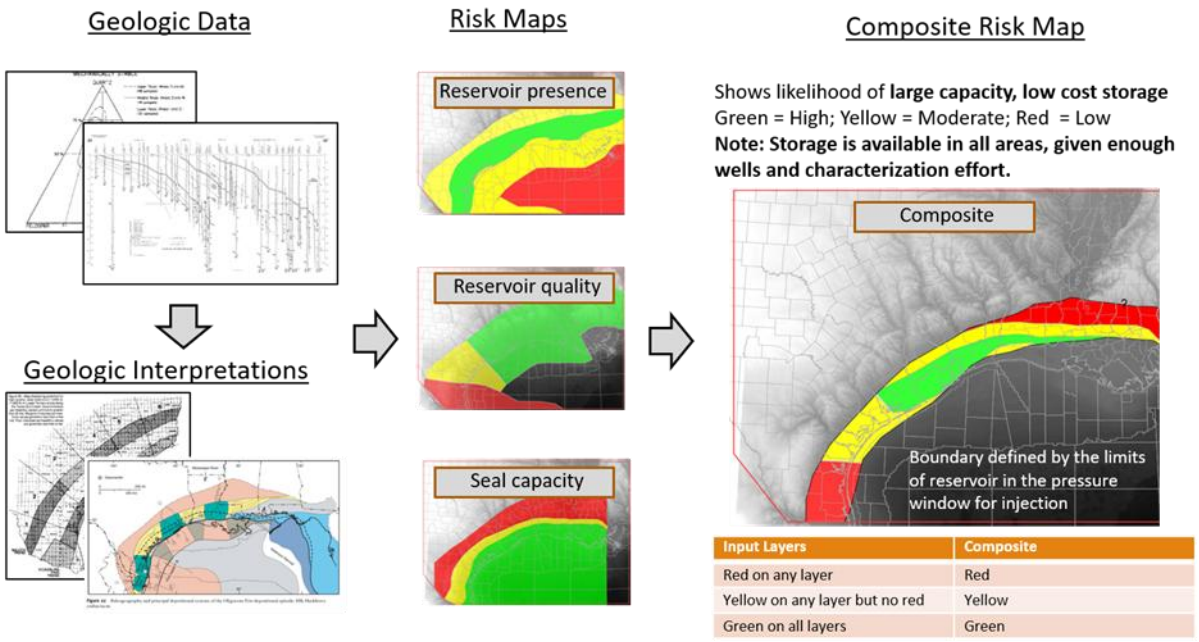

Figure 3.4 - Summary of Common risk Segment (CRS) mapping tool. The maps are added together according to the rules shown to create a composite risk map (right), showing the geographic chance of finding large, low-cost

storage volumes. The map is clipped to the area of the formation within the pressure window for CO_2 storage (Figure 3.3). The example shown is for the Oligocene Frio reservoir and Anahuac seal.

Focusing on the coastal region (i.e. the Oligo-Miocene), we have constructed a series of maps for the upper Oligocene reservoir and seal system (Figure 3.4), describing the distribution of lithofacies and depositional environments for both reservoir and seal. The objective of this work is to allow efficient screening for storage sites, ensure that the focus on specific opportunities is well placed and create a framework for the intelligent application of analogs. More broadly, it creates a framework for strategic investment in storage hubs and infrastructure.

3.1.2 Subtask - Extend geomechanical assessment to additional areas of the basin

The offshore Gulf of Mexico Basin offers attractive opportunities for carbon storage, but there are also concerns about confining system capacity and the security of storage. The region is attractive because it offers large areas with a single landowner and few competing uses close to dense clusters of emissions. The subsurface geology is largely similar to the onshore with a wide variety of proven reservoirs and confining systems. However, we have encountered concerns, perhaps informed by common experiences with sand at a modern beach, that offshore sediments are 'mushy' and therefore incapable of reliably retaining CO_2. This work aims to address that concern by quantifying the geomechanical trade-offs and risks associated with varying water depth, from onshore to deep water. For further discussion, see also A. P. Bump and Hovorka (2024).

We do this by making a series of calculations from first principles, based on calculating compaction, density, stresses, and fracture strengths for clastic sediments under varying water depth. The calculations take account of varying water salinity, temperature gradients and sand/shale mixes. At present, they are limited to clastics (i.e., no carbonates) and to normal-faulting stress regimes, including passive margins such as the GoM. The details reported here are chosen with reference to the Gulf of Mexico, but the same approach could be applied to any passive margin basin by making different choices of temperature, depth of USDW and depth to overpressure.

Figure 3.5 shows a comparison of strength vs depth for onshore versus the near offshore geologic sections. The plots show:

- the hydrostatic pressure gradient in blue (total weight of the water column for any given depth)
- the lithostatic pressure gradient in orange (total weight of the rock column for any given depth, corrected for compaction)
- two calculations for fracture strength, using different algorithms. Eaton's method is shown by the gray line and Zhang's is shown in the yellow
- the pressure space (ΔP) available for CO_2 injection at representative depths, defined as the difference between hydrostatic (initial) pressure and the lowest estimation of fracture pressure (Eaton's)

The two plots are very similar, with similar rock strengths at a given depth. The small differences in strength arise from differences in hydrostatic and lithostatic pressure. The presence of 700m of fresh water onshore creates a slightly lighter water column compared to entirely saline pore fluids offshore. Similarly, the loss of 10m from the rock column offshore creates a slightly lower lithostatic pressure. Together, these two factors result in a 0.2MPa decrease in the pressure space available for injection offshore. The depths for USDW and overpressure are representative but highly variable. Both would need to be verified and adjusted for any actual comparison of sites.

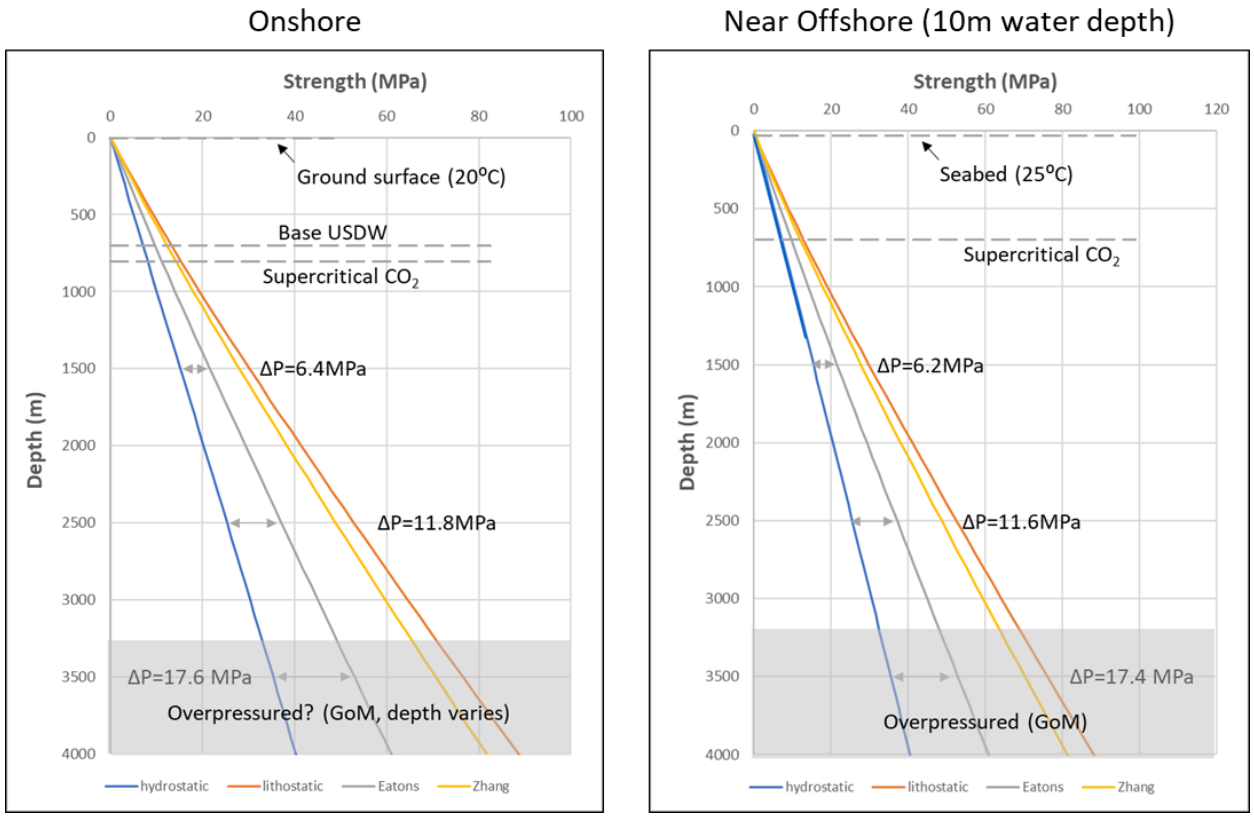

Figure 3.5 – Pressure vs depth plots for onshore and near offshore (10m of water). See text for discussion. Note the depths to base USDW, top of super-critical CO2, top of overpressure and the ΔP values at differing depths. "Eatons" refers to Eaton's Method (Eaton, 1969), which is a conservative estimate of fracture pressure. "Zhang" refers to Zhang's method for calculating fracture pressure, which gives an optimistic (high) value (Zhang, 2019).

Figure 3.6 explores the effect of increasing water depth, with a comparison of 100m water depth (shelf edge) versus 1000m (deep water). Neither of these is likely to be economically or otherwise attractive anytime soon in the Gulf of Mexico, but they are useful for illustrating the effects of water depth. There are several effects worth noting:

- The temperature profile in the water column (hydrothermal gradient) is very different to the profile in rock (geothermal gradient). The mean annual sea surface temperature in the GoM is 25C and decreases rapidly with depth. The mean annual seabed temperature is 21C at 100m water depth and only 4C at 1000m of water depth but then increases rapidly with depth below seabed (30C/km). The net effect is that for a constant salinity, water density increases with depth to the seabed and then decreases with further depth.
- Lithostatic pressure begins to build only at the seabed. The curves are almost identical between the two plots, but the different starting depths mean that there is far less pressure space for injection at a given depth in deep water than there is at the shelf edge; (note that for the same reason, there is slightly less pressure space at a given depth on the shelf edge than in shallow water or onshore).
- The depth to overpressure (bottom of the CO_2 storage window) is a function of time since reservoir deposition (time to dewater). The shelf edge features high rates of very young deposition, and therefore much shallower overpressure than the deep water, which has much slower depositional rates. The depth window for storage is therefore much more limited at the shelf edge than in deep water.

There is thus a sharp decrease in confining system capacity at a given depth below sea level with increasing water depth that is entirely a function of the reduced rock column. At a given depth below ground surface (or seabed offshore), the confining system capacity is very similar—compare 6.4MPa at 1.5km below ground surface onshore

with 6.4MPa at 1.5km below seabed in deep water.

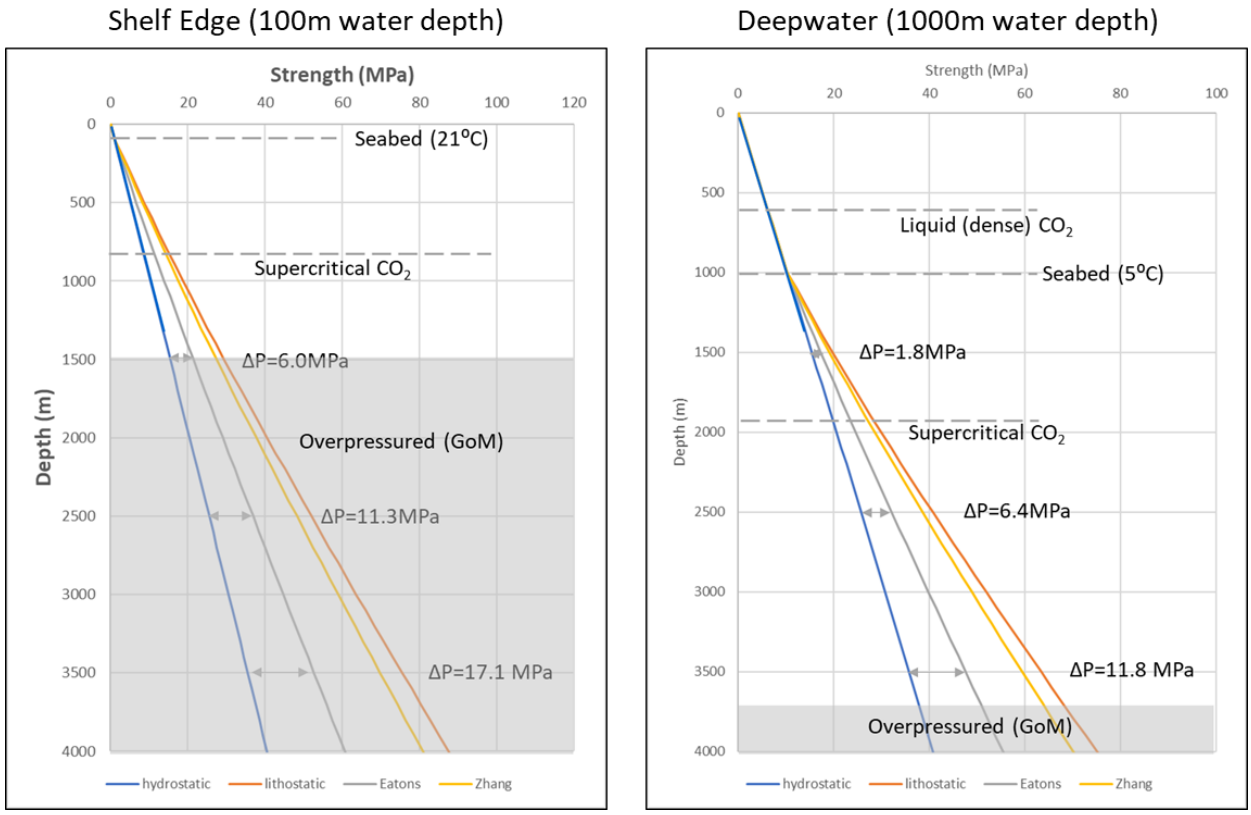

Figure 3.6 - Pressure vs depth plots for shelf edge (100m water depth) and deep water (1000m of water). See text for discussion. Note the depths to base USDW, top of super-critical CO2, top of overpressure and the ΔP values at differing depths.

Figure 3.7 shows a phase diagram for CO_2 with the temperature pressure profiles of different well locations superimposed. For the Gulf of Mexico, the mean annual temperatures onshore and in shallow water are largely similar so there is little difference in the depth to dense-phase CO_2 for those locations. Deep water is remarkably different, however. The temperature-pressure profile of the ocean is very different to that of the sedimentary section, and it means that in deep water, we get dense-phase CO_2 as a liquid long before it becomes a supercritical fluid. The lower temperatures also result in much denser CO_2 at a given depth below seabed than in shallower water. This could mean greater storage efficiency.

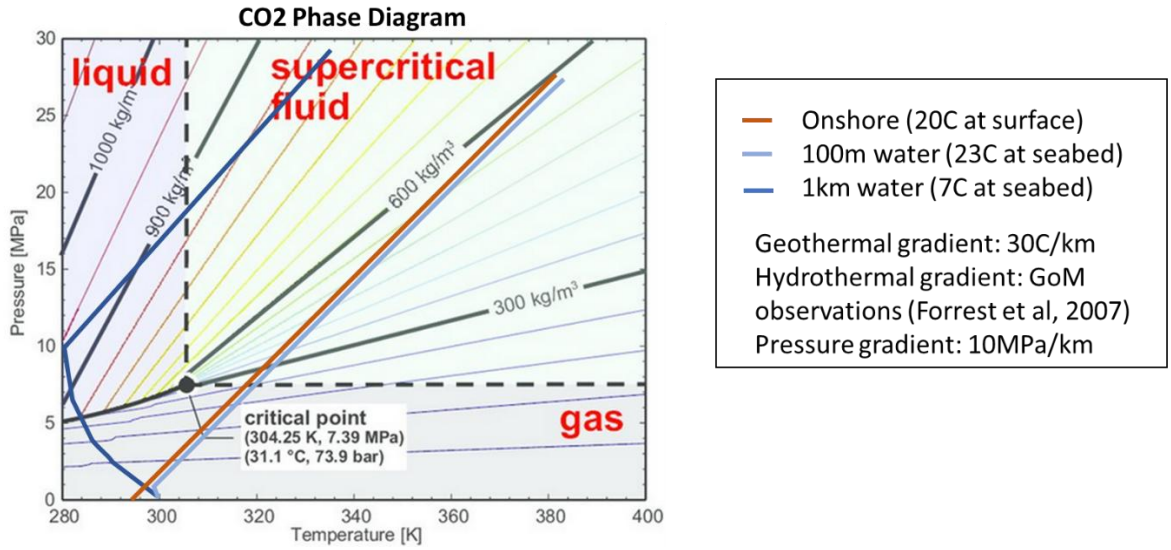

Figure 3.7 - CO_2 phase diagram showing the pressure-temperature profiles of wells in varying water depth. Note the difference between 1km of water and less than 100m.

References Cited

Brace, W. F., and D. L. Kohlstedt. "Limits on Lithospheric Stress Imposed by Laboratory Experiments." *Journal of Geophysical Research: Solid Earth* 85, no. B11 (November 10, 1980): 6248–52. https://doi.org/10.1029/JB085iB11p06248.

A. P. Bump and S. D. Hovorka, 2024, Pressure space: The key subsurface commodity for CCS; International Journal of Greenhouse Gas Control: Vol. 136, Pages 16; Accession Number: WOS:001287329400001; DOI: 10.1016/j.ijggc.2024.104174.

B. Burke, Lauri A, Scott A Kinney, Russell F Dubiel, and Janet K Pitman. "REGIONAL MAP OF THE 0.70 PSI/FT PRESSURE GRADIENT AND DEVELOPMENT OF THE REGIONAL GEOPRESSURE-GRADIENT MODEL FOR THE ONSHORE AND OFFSHORE GULF OF MEXICO BASIN, U.S.A." *Gulf Coast Association of Geological Societies Journal* 1 (2012): 97–106.

Eaton, Ben A. "Fracture Gradient Prediction and Its Application in Oilfield Operations." *Journal of Petroleum Technology* 21, no. 10 (October 1, 1969): 1353–60. https://doi.org/10.2118/2163-PA.

Finkbeiner, Thomas, Mark Zoback, Peter B Flemings, and Beth B Stump. "Stress, Pore Pressure, and Dynamically Constrained Hydrocarbon Columns in the South Eugene Island 330 Field, Northern Gulf of Mexico." *AAPG Bulletin* 85 (2001). https://doi.org/10.1306/8626CA55-173B-11D7-8645000102C1865D.

3.1.3 Subtask - Dissolution and bubbling in water column

LBNL modeled the atmospheric dispersion of CO_2 emitted from the sea surface due to a large-scale well blowout on the sea floor and quantified the results in terms of a downwind dispersion length (DDL) which can be thought of as the radius of a safety exclusion zone (Figure 3.8). The modeling results suggest that for a large-scale blowout in shallow water, the exclusion zone will be approximately 400 m in radius for moderate-weak winds speeds.

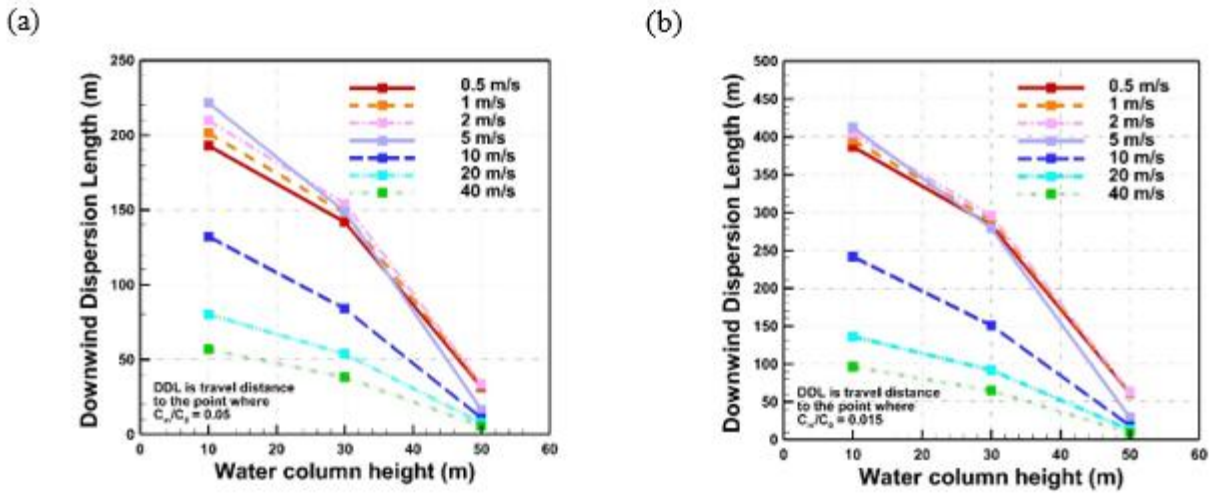

Figure 3.8 – Downwind dispersion length (DDL) for the subsea CO_2 blowout scenarios for different water column heights and wind speeds for two different critical concentrations: (a) C_m/C_0 = 0.05; (b) C_m/C_0 = 0.015 (note the different y-axis scales).

3.1.4 Subtask - Numerical modeling of heterogeneous reservoirs

LBNL obtained from BEG the GoM HI-24L model and analyzed the model data to understand the geological model. LBNL was developing a multi-continua model to deal with natural heterogeneity and its effects on CO2 migration and trapping. This model accurately represents the site-specific multiscale heterogeneity and will be executed to capture the dynamic migration and trapping of injected CO2 in next quarter. This modeling effort will complement the modeling efforts using single continuum with heterogeneity by Seyyed A. Hosseini at BEG.

LBNL started to develop the multi-continuum model for the HI (High Island)4L geological model.

LBNL tested the multi-continuum approach for modeling multiphase CO_2-brine flow in idealized heterogeneous storage formations.

A study by GCCC graduate research assistant, Melianna Ulfah, inputs extensive geological and petrophysical data into a reservoir simulation to model the CO_2 migration and analyze the plume and pressure distribution and evolution. Ulfah built a reservoir model, based on 3-D seismic interpretation of Middle Miocene strata, offshore Galveston, Texas and utilizes well logs to characterize key intervals. The modeling investigates how far the CO_2 plume migrates under two scenarios: 1) injecting CO_2 at the base of the structural closure (base scenario) and 2) injecting CO_2 at the base of the salt withdrawal basin (syncline scenario). The simulation shows that, for the same amount of CO_2, injecting the CO_2 into the syncline requires more leased acreage vs. injecting CO_2 at the base of the structural closure because of more migration. The other reason why the syncline scenario requires more acreage is because the geological layer around the injection point is more heterogeneous than the base scenario, thus the CO_2 tends to migrate laterally. On the positive side, this mechanism also limits the vertical migration of CO_2, thus making the syncline mechanism less prone to the risk of CO_2 escape into shallower geological strata. Moreover, the simulation also indicates that with the syncline scenario, the time needed for the reservoir to reach stabilized pressure after the end of injection is faster. Another result of the simulation is that adding more wells into the study area would not significantly increase the storage capacity because each well suffers injectivity loss due to increasing reservoir pressure. See Appendix C for figures.

3.2 ***Subtask: Geologic Modeling***

Compositional Poromechanics Simulations of High Island 24L

Based on a geologic model of the High Island Block 24L (HI 24L) site in Texas State Waters (i.e., the HI 24L depleted gas field), the Lawrence Livermore National Laboratory (LLNL) team working with colleagues from Total at Stanford University built an unstructured mesh honoring the faulted geometry for the site. They populated it with geostatistical properties honoring active seismic and well log data and ran preliminary compositional simulations to confirm the model worked well. They also worked to constrain fault transmissibility properties to appropriately represent sealing and non-sealing sections of the faults, using a shale gauge ratio approach and fault offset data. The team also started developing an elastoplastic model to analyze the potential for ductile deformation at the HI 24L analogue site.

The goal of the study was to assess appropriate deformation monitoring techniques that would have sufficient sensitivity to measure the seabed uplift induced by fluid injection into a depleted hydrocarbon field (i.e., HI 24L). Before deploying such measuring instruments in an offshore environment, it was essential that we first simulate the coupled solid deformation-fluid flow phenomena as realistically as possible to gain some insight into the precision of instruments needed for such field study. To this end, the LLNL-led team, created a finite element-finite volume model that incorporated a spatially heterogeneous permeability distribution expected at this site (Figure 3.9).

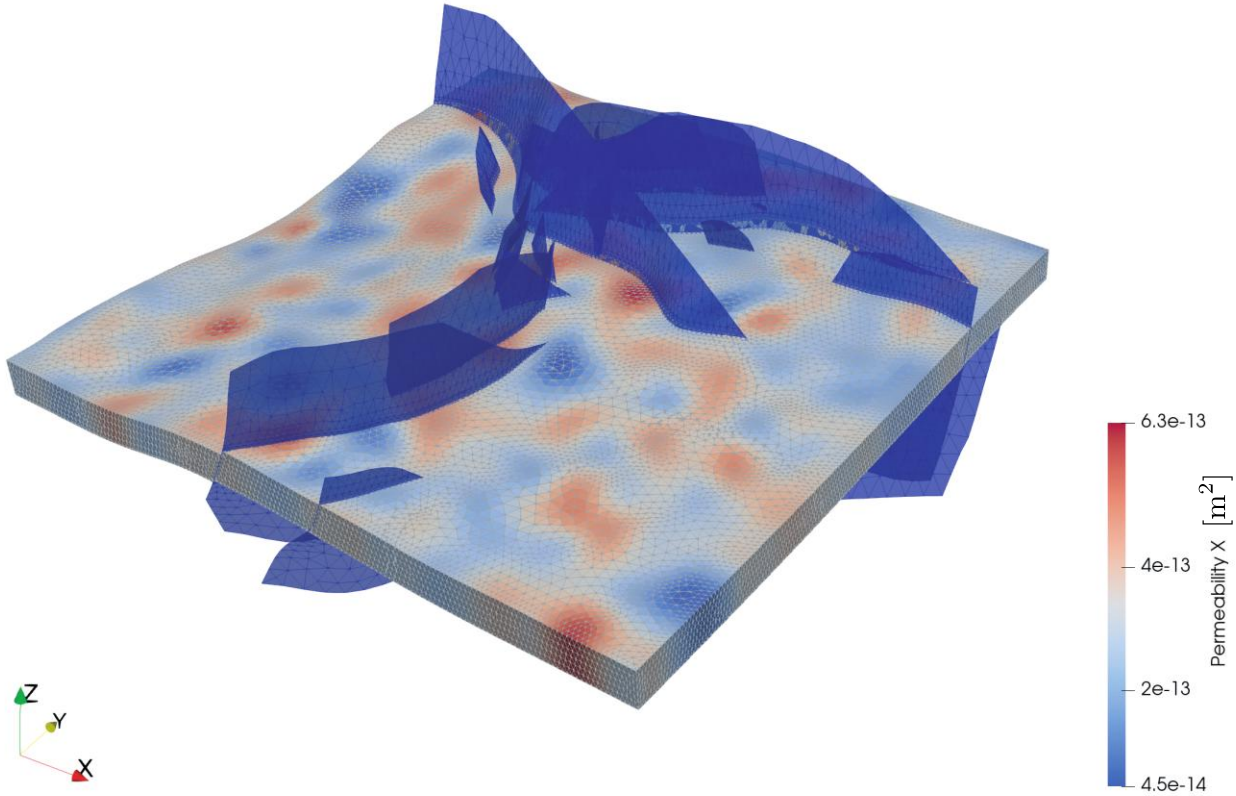

Figure 3.9 - Horizontal permeability distribution in the reservoir, statistically generated. The faults cutting the domain are illustrated in blue.

The LLNL team conducted a sensitivity analysis on the geomechanical parameters and investigated the influence of fault sealing on fluid flow. Results of the simulations suggested that the reservoir had remarkable injectivity, allowing for a large amount of fluid to be injected without a substantial increase in pore pressure. The computed

seabed deformations were equally small and could be monitored with distributed fiber optic cables and ocean bottom pressure recorders. The absolute accuracy of ocean bottom pressure recorders for the site is approximately 1 mm and most of the simulations from the sensitivity analysis indicated a maximum seabed floor uplift of more than 5 mm. The results also showed how fault sealing substantially changed the fluid flow and consequently the deformation pattern. Sealing led to a concentration of excess pore pressure and vertical displacement in the vicinity of the injector well that was not crossed by a fault (Figure 3.10).

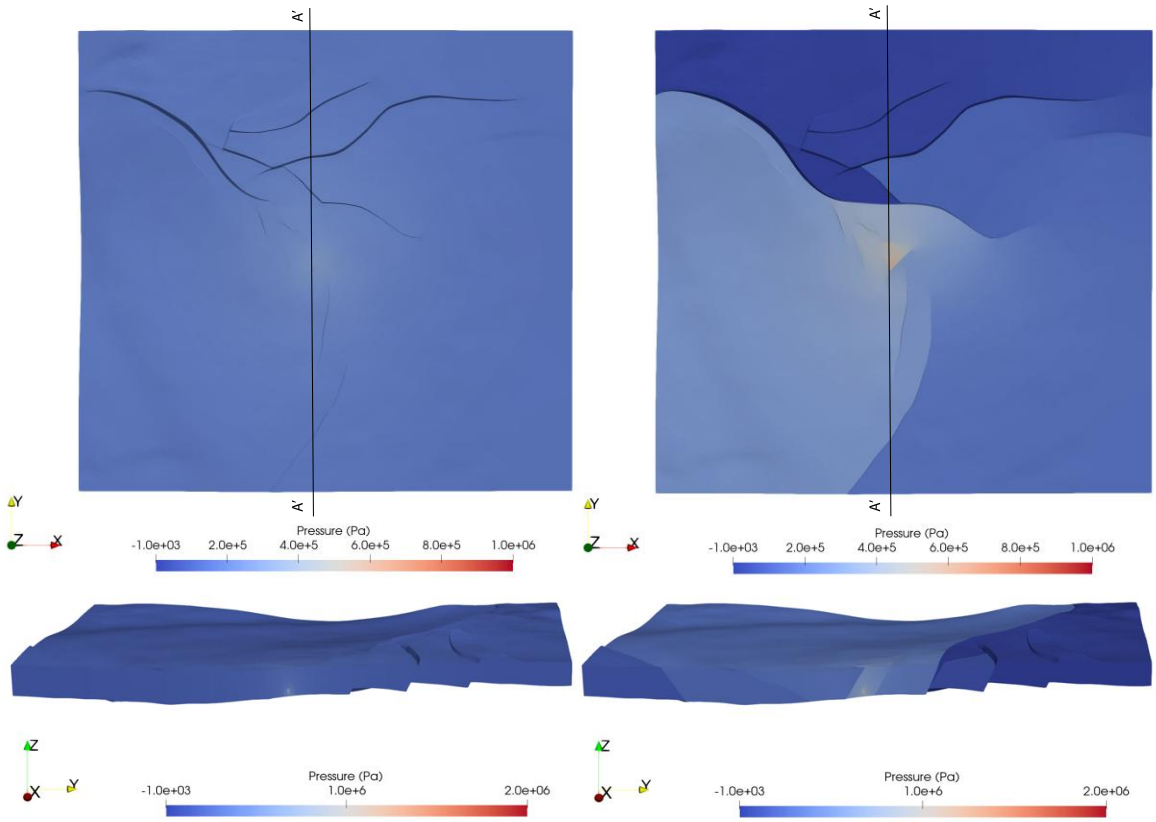

Figure 3.10 - Simulation results for the base case scenario. Excess pore pressure after 3 years of injection at a rate of 1 Mt/yr for two cases: permeable faults (left) and impermeable faults (right) for top and lateral views of the reservoir.

This assessment provided a comprehensive understanding of the reservoir and confining system units' behavior. It enabled us to draw practical conclusions on cost-effective monitoring systems, which was essential to better plan such a complex venture. However, many topics may be further explored to increase the reliability of the predictions. In particular, future work should focus on better geostatistical constraints on permeability and porosity, more detailed analysis of well log data to have a better estimate of anisotropic elastic properties, studies on the influence of finite-volume discretization chosen, and extension to true compositional flow simulation. Some of the research results were incorporated into T. Camargo et al. (2022).

Micromodels

Predicting the effectiveness of a storage project and retention of injected carbon dioxide underground is heavily reliant on leveraging predictive fluid dynamics models of the migration of subsurface CO_2. Due to the heterogeneity of reservoir units, the multiphase nature of the system, and capillarity limiting buoyancy, microscale features can significantly influence CO_2 transport through storage formations. These heterogeneities can exist as multiphase capillary pressure barriers of contrasting sand grain size distributions, and therefore pore geometries,

which impact CO_2 flow paths and residual and dissolution trapping mechanisms.

The effect and impact of microscale heterogeneities are the focus of the Partnership's research on micromodels and the microfluidics laboratory. Regions of large grain and pore sizes can be interbedded with distinct laminations of smaller sizes caused by stratigraphic variations. These laminations can be of the millimeter scale with features of the micrometer scale. Geometries representing the transitions between the bulk matrix grain structures and those of their interbedded laminations are generated using representative statistics and custom software. Small volumes of these heterogeneities are created and flow tested. Fine-grained laminations act as capillary barriers requiring additional pressure to be traversed. This causes changes in the direction of CO_2 flow as well as retention of CO_2 as it migrates through the heterogeneous regions.

The research conducted on real-rock micromodels (microfluidics) yielded useful results, which laid the groundwork for finishing the validation and comparisons. A two-dimensional framing of this problem was used to utilize high-precision microfabrication techniques in tandem with computational mathematical models to elucidate information on the relationships between these geometric non-uniformities and multiphase transport properties.

Capillary barrier behavior is known to occur, but we demonstrate some of the effects of the couplings that can inform CO_2 migration in several sets of multiphase fluid mechanics simulations using lattice Boltzmann methods (LBMs) and computational fluid dynamics (CFD). In CO_2 injection tests through the computationally generated porous media, the maximum pressure needed to breakthrough to the outlet of the flow domain correlates with the grain size of the fine region as seen in Figure 3.11. In such a way, we can approximate capillary pressures that represent the modeled rock volumes.

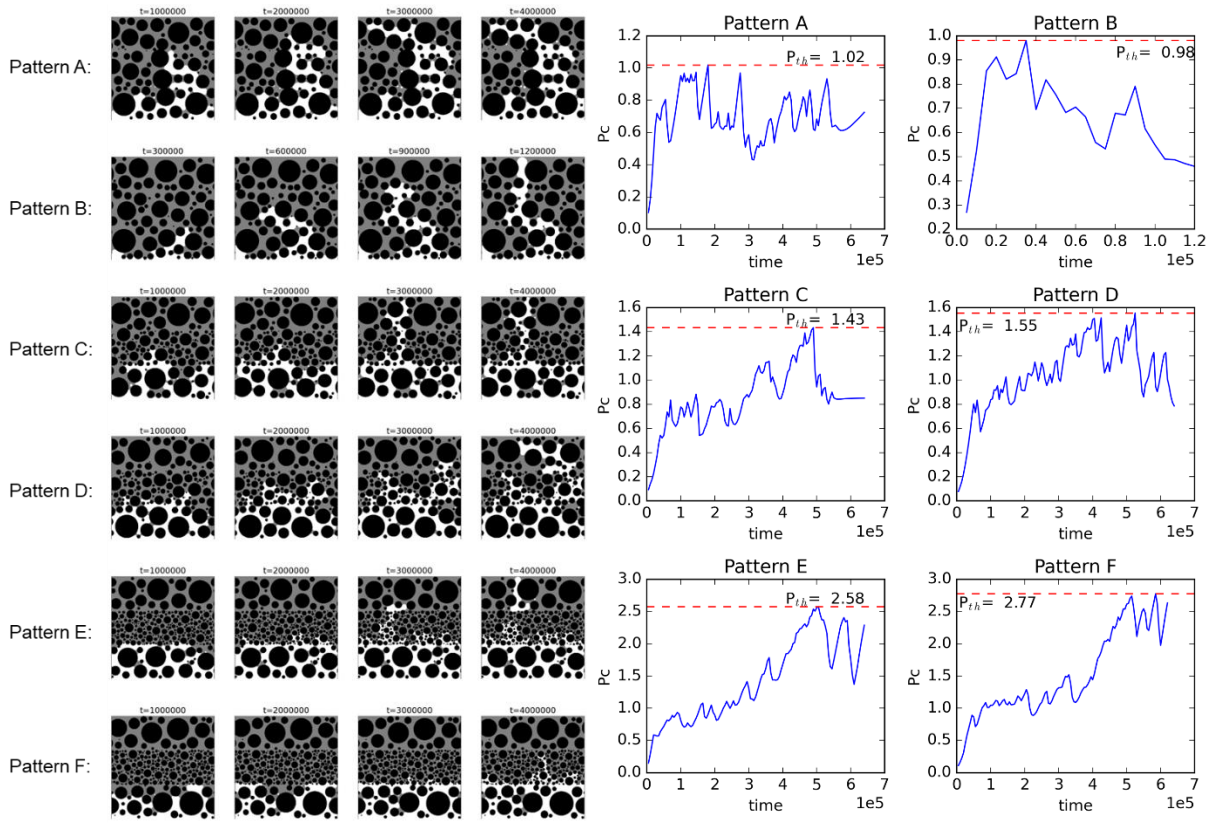

Figure 3.11 - LBM flow tests on different patterns of various coupled grain size distributions within a layered orientation. The left shows spatial distribution of the phases (white - CO_2, gray - water, black - solid) over time. The right shows the pressure of the CO_2 phase over time with the maximum pressure (capillary breakthrough

pressure) highlighted.

While the fine-grained regions restrict flow, we present evidence (such as in Figure 3.12) that it is a coupled effect of both regions as the coarse-grained regions act to dissipate pressure leading up to the critical pore-throats. The pressure needed to overcome pressure dissipation along with the capillary pressure bottlenecks would make for the best representation of an effective capillary breakthrough pressure of the system.

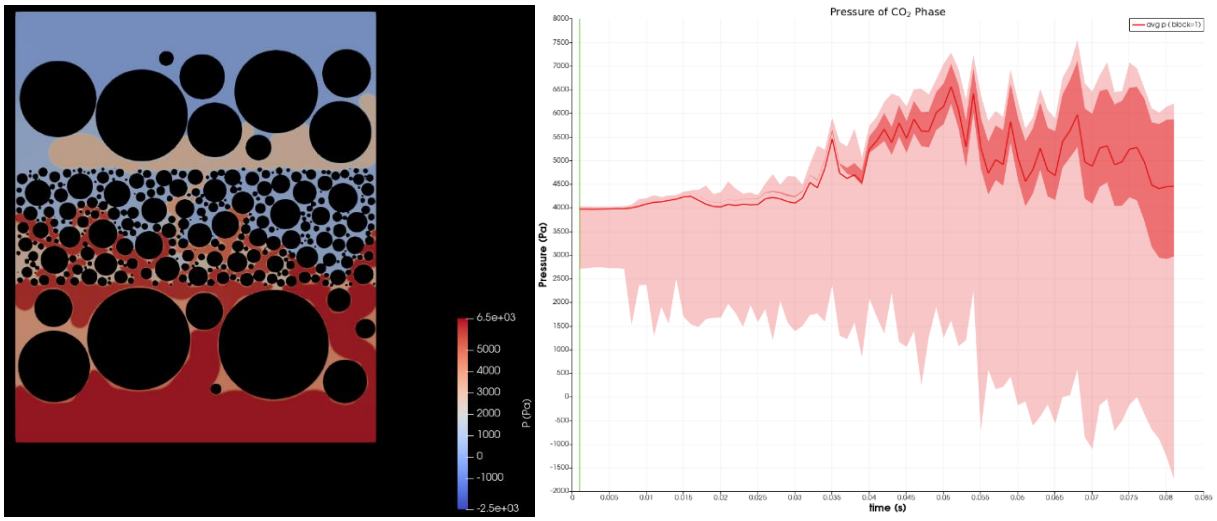

Figure 3.12 - Pressure dissipation of a CO_2 flow test using OpenFOAM's interFoam solver. The right side shows the pressure dissipation from the inlet (bottom) to the outlet (top) at one timestep. The plot on the right shows the CO_2 average pressure that peaks as the interface passes through pore throats and the ranges show how much pressure variation exists in the CO_2 which is correlated to pressure dissipation.

This breakthrough capillary pressure is often overcome by the buoyancy of the CO_2 in a sequestration reservoir leading to larger local column heights (and higher CO_2 phase saturations) in coarse regions underlying laminations. The properties of both the coarse and fine region inform this pressure and therefore inform the capillarity heterogeneity trapping saturations.

These methods and results illustrate the initial steps in developing approximations of capillary pressure for rocks with these sorts of fine laminations when effective capillary pressure of rock volumes is more accurately approximated. These findings also show the feasibility of such an approximation.

The correlation between the pattern statistics with the maximum capillary pressure experienced during drainage exhibits that an approximation for the metrics can be found given grain size distribution and structural information. With the foundational work provided here, an initial approximation equation can be formulated. Further refinement is possible with more characterization of the pore morphology, layering geometries and orientations, extrapolations to three dimensions, and comparisons to a corresponding theoretical geometric intuition. The lab's microfluidic experiments were conducted to tune and compare with these models; however, more experimental work would also improve the accuracy of these approximations.

To frame the practicality of a more accurate capillary pressure approximation, the sensitivity of projects or estimations of project performance to capillary pressure and anisotropy was tested using reservoir scale simulation. The existence and scale of capillary pressure were shown to have significant impacts on CO_2 plume extent. A simple anisotropic permeability ratio was also implemented as an alternative method for incorporating these effects and did likewise produce significant variation among CO_2 plume migration. These results show the importance of the inclusion and accuracy of capillary pressure within a geologic model. When the risk and uncertainty of carbon

sequestration models are reduced, the storage project becomes more predictable, insurable, safer, and effective in reaching carbon mitigation goals.

Modeling Faults

An important component of geologic models is understanding whether specific subsurface faults act as migration pathways or migration barriers (i.e., confining systems). Faults are prominent subsurface structures in the Gulf of Mexico (GoM) Basin, and the discontinuities they create in reservoirs affect the flow of fluids such as supercritical CO_2. Because the permeability and porosity of a fault is typically smaller relative to the host rock in siliciclastic basins, faults tend to behave as CO_2 flow barriers that aid in containment (i.e., lateral confining systems defining a fault trap where millions of tons of CO_2 can be injected and trapped for thousands of years due to capillary effects). In some cases, faults can have a transmissibility that leads to CO_2 migration either along or across the fault plane. In this study, we considered across-fault migration of CO_2 (Figure 3.13B). Petroleum fault seal analysis predicts which areas of a fault surface would act as a seal and which areas would be transmissive to hydrocarbons. While this analysis suffices to reveal whether accumulations drain over geologic timescales, CCS operates on human timescales. Thus, quantification of the rate of a potential migration is an essential component in CCS that remains relatively unexplored. We offer a scoping tool to estimate across-fault migration rates.

Estimating across-fault migration rates allows for predicting the portion of the CO_2 plume that crosses to the adjacent structural block. The size in turn determines if the migration is detectable with seismic monitoring and when the migration may first be detected. Migration of CO_2 into the adjacent block when the fault was expected to be sealing can cause a problem when it endangers other resources (e.g., hydrocarbons, USDWs) and assets (e.g., unleased area, producing/legacy wells) present across the fault or the potential for leakage. CO_2 that migrates across the fault into an area that was not prepared and permitted may require the return of carbon credits. In this study, the out-of-storage complex migration rate determines the timing and magnitude of additional costs that are used to obtain the net present value (NPV) of the storage project. If the migration rate is slow-enough the costs can be non-existent or negligible.

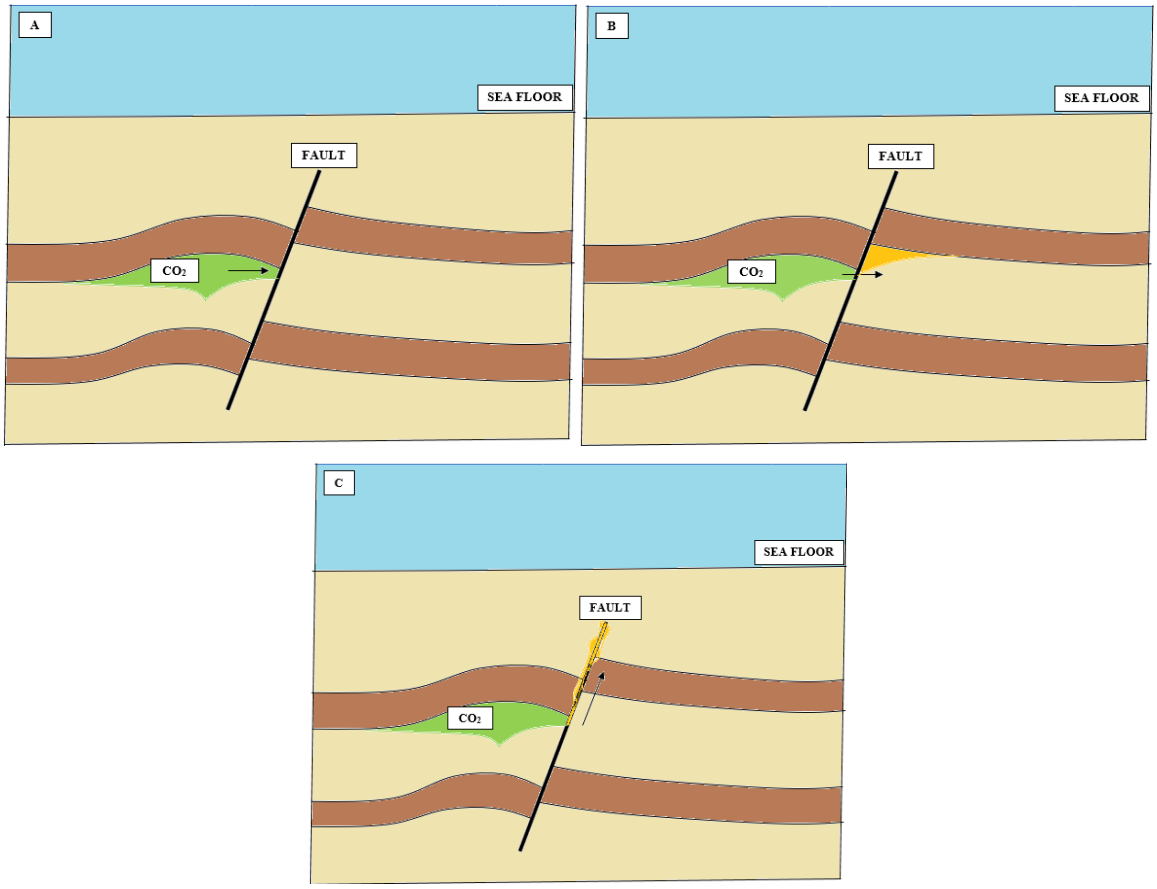

Figure 3.13 - Possible outcomes when CO2 reaches a fault. Black arrow represents CO_2 plume (green) flow; orange patches represent fault-related migration of CO_2. A) Ideal fault trap: the fault is a barrier to CO_2 in all dimensions and keeps the CO_2 within the target reservoir, B) Across-fault migration: The fault is not an ideal seal in the horizontal axis and allows CO_2 to move across the fault from the injection block to the adjacent block, C) Up-fault migration: the fault is not an ideal seal in the vertical axis and allows CO_2 to flow upwards along its plane and approach the surface. Both B) and C) are cases of partial fault trapping.

To estimate across-fault migration rates, we first used fault seal analysis to identify the areas on the fault with the highest transmission potential. This analysis relies on the identification of a) fault juxtaposition seals (Figure 3.14), and b) fault membrane seals as determined by the following fault gouge algorithm developed by Yielding et al., (1997):

$$SGR = \frac{\sum_{i=1}^{n} Vcl_i \times \Delta z_i}{D} \qquad (1)$$

Where, SGR is the shale gouge ratio, a ratio that serves as a proxy for clay content and fault permeability. Within an interval of interest, Vcl_i is the volume of clay in each of the layers, Δz_i is the height of each of the layers, and D is the absolute displacement of the layers.

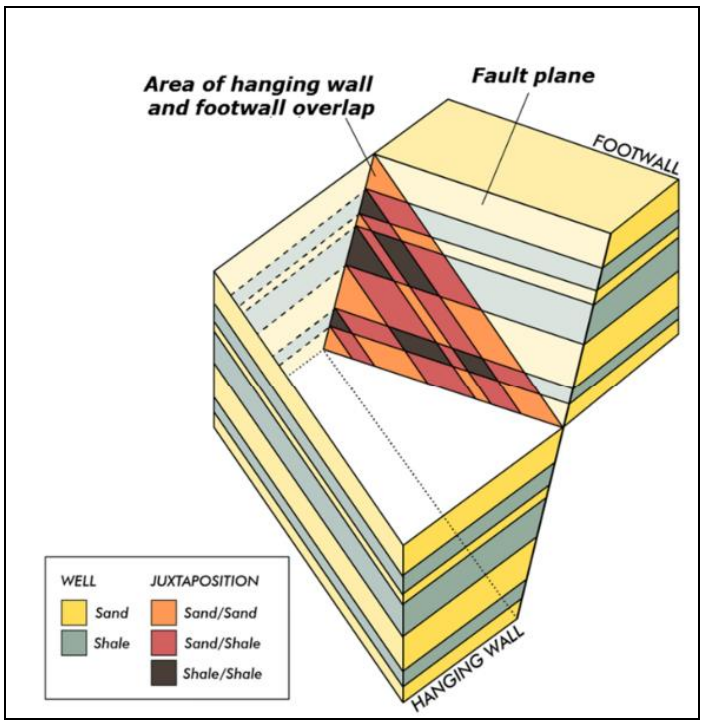

Figure 3.14 - Juxtaposition triangle. Foot-wall (top right) and hanging-wall (bottom left) blocks offset by normal fault plane, creating different juxtaposition types (key at the bottom left). It is typical to assume the orange areas allow fluids to migrate across and the rest do not. From Knipe, 1997.

Across-fault migration can occur in areas on the fault plane where footwall sands are juxtaposed with hanging-wall sands (i.e., orange areas in Figure 3.14). Among those areas, the ones with the highest transmission potential are the ones with the lowest SGR values. We applied Darcy's law to areas of a fault plane where cross-migration is most likely to estimate migration rates using the following equation:

$$Q_{i,j} = \frac{\widetilde{FCk} \times a_i \times \Delta P_j}{\mu \times \widetilde{FCt}} \qquad (2)$$

Where $Q_{i,j}$ is the total discharge (with dimensions [V/T]) through the identified areas of highest transmission potential. Additionally, $j = 1, 2, \ldots, n$; and $i = 1, 2, \ldots, z$ (where z is the total number of identified areas); FCk is fault core permeability; a is the size of the area; ΔP is the pressure differential across the fault that drives fluid flow which, in hydrostatically-pressured formations, is equal to injection-induced pressure buildup; μ is the dynamic viscosity of supercritical CO_2; and FCt is the fault core thickness. Any calculation of fault core attributes (e.g., permeability and thickness) is inherently uncertain due to the structural complexity and heterogeneity in a fault core. Uncertainty distributions for these parameters serve as input for Monte Carlo simulations of migration rates. Empirical relationships between fault-rock permeability and SGR from Manzocchi et al. (1999) and Sperrevick et al. (2002) are used to obtain the parameters in Equation 2. De Simone and Krevor's (2021) analytical equations of pressure buildup in open and closed boundary condition systems and Ouyang's (2011) empirical correlations between CO_2 viscosity and reservoir temperature-pressure conditions were used. We measured cross fault areas on 3D models. Finally, we used Torabi et al.'s (2019) scaling relationships between a fault's thickness and displacement. From the estimated yearly migration rates during the injection phase of a storage project we calculated cumulative transmitted masses at the end of injection.

We applied the procedure described to a fault-bounded CCS prospect located offshore in the northern GoM shelf 20 km south off Jefferson County, TX. 3D seismic data from the TexLa 3D merge survey was used to build a 3D

structural framework of the fault-trap (Figure 3.15). We identified the cap rock, injection zone (Figure 3.16), and the lateral trapping elements in the reservoir, the green and blue faults —F1 and F2— in Figure 3.16. Then after performing fault seal analysis on these two faults (Figure 3.17), we calculated migration rates across their areas of highest transmission potential (Figure 3.18 & Figure 3.19). The problem was set up with 40 years of injection at a rate of 0.7 $MtCO_2$ per year into the faulted reservoir with average depth of 1,900 meters and typical petrophysical and mechanical properties for GoM sandstones. To bracket the range of across-fault migration rates, we considered three boundary condition scenarios that affect pore water pressure-buildup: a) open, b) closed, and c) semi-closed; and three injector-to-fault distance scenarios: a) 100 m, b) 1 km, and c) 2 km.

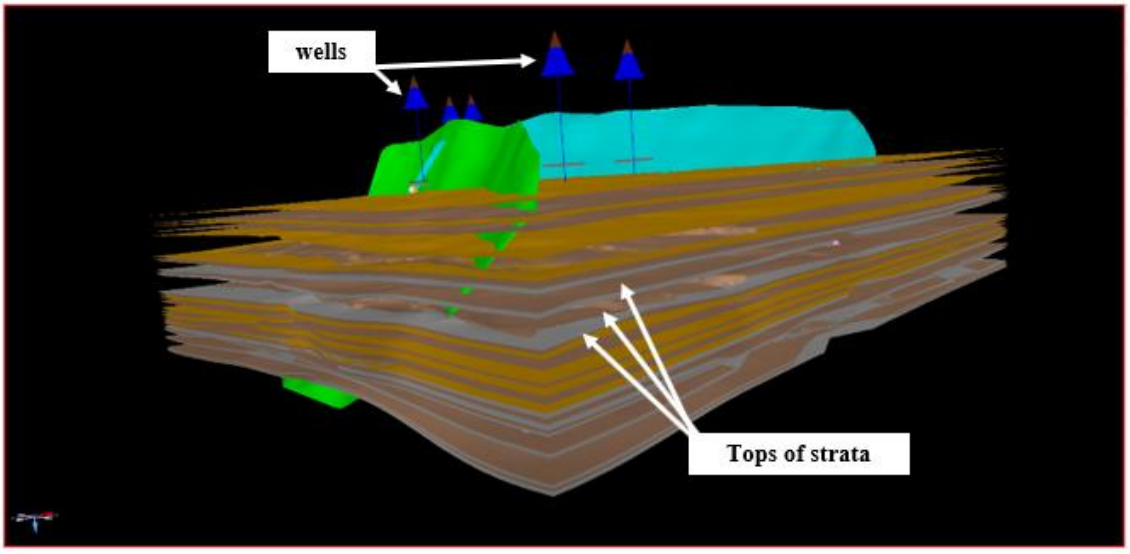

Figure 3.15 - Layered geologic 3D model of GoM example. Model shows primary and marker horizons with assigned reservoir quality (brown, orange, and gray) and three fault surfaces (green, blue, and pink). The wells used for lithological and shale content interpretation are shown as blue cones.

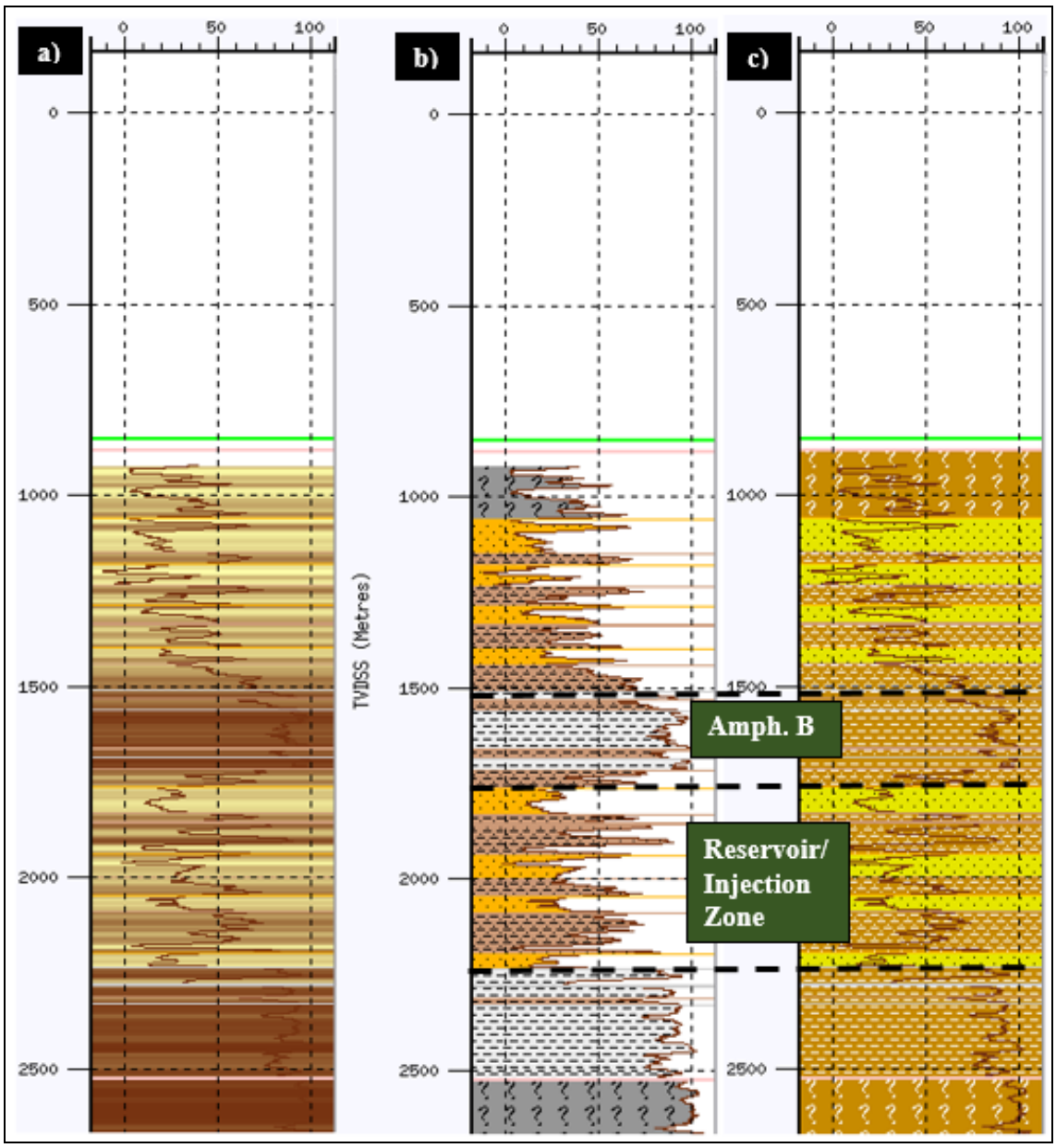

Figure 3.16 - Generalized stratigraphic column of a GoM faulted storage site continued, depicting a) clay volume (darker brown is more clay %), b) lithotype (orange for sandstone, brown for shaly sandstone, light gray for shale, and dark gray for "undefined"), and c) reservoir type (yellow is good reservoir quality). Stratigraphy shown based on gamma ray curves for one of the wells: a) and c) are filled across curve, and b) is filled to curve.

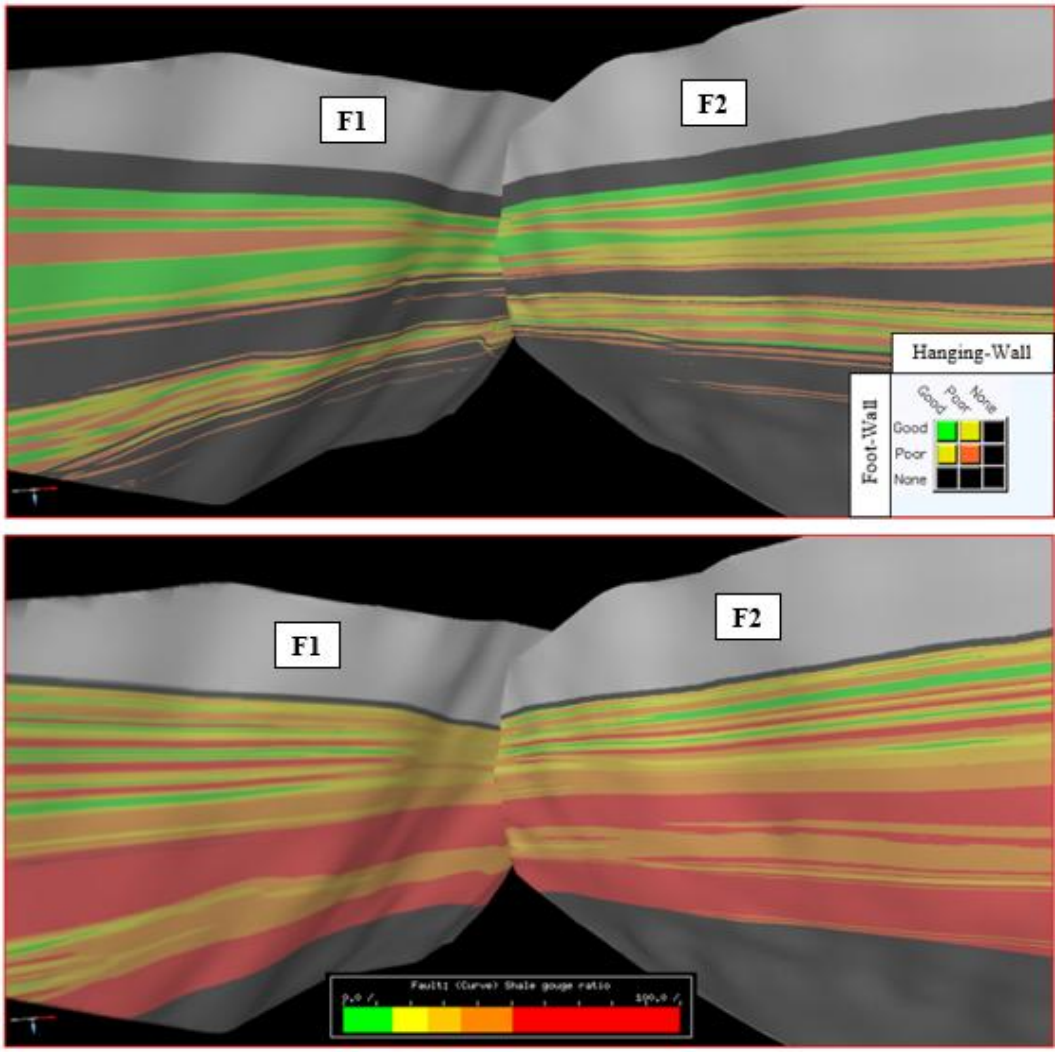

Figure 3.17 - Juxtaposition (top) and SGR (bottom) fault maps. Juxtapositions and SGR distributions are displayed for the entire fault surface. Good-good juxtapositions are shown in green (key at the bottom right of top image). Warmer colors in the SGR fault map reflect higher clay content in the fault core.

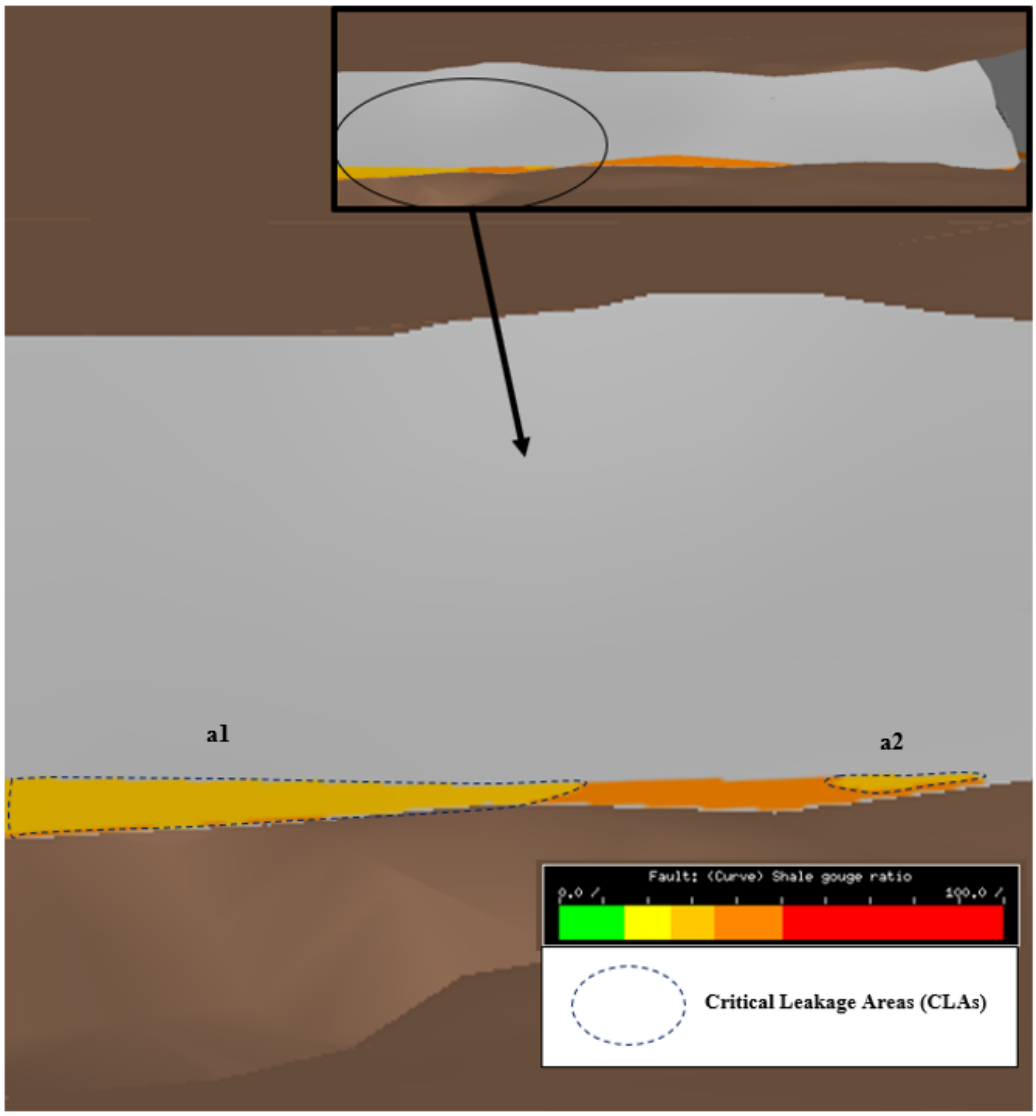

Figure 3.18 - Critical leakage areas (blue dashed outlines) on fault F1 (areas of highest transmission potential based on juxtaposition and SGR). Close-up taken from F1 potential leakage window shown at the top right. SGR scale displayed at the bottom for reference. The light orange (> 25% SGR) superposed on good-good reservoir (other juxtaposition types are displayed in gray) represents the areas of highest transmission potential. Brown surfaces are top and bottom of reservoir zone.

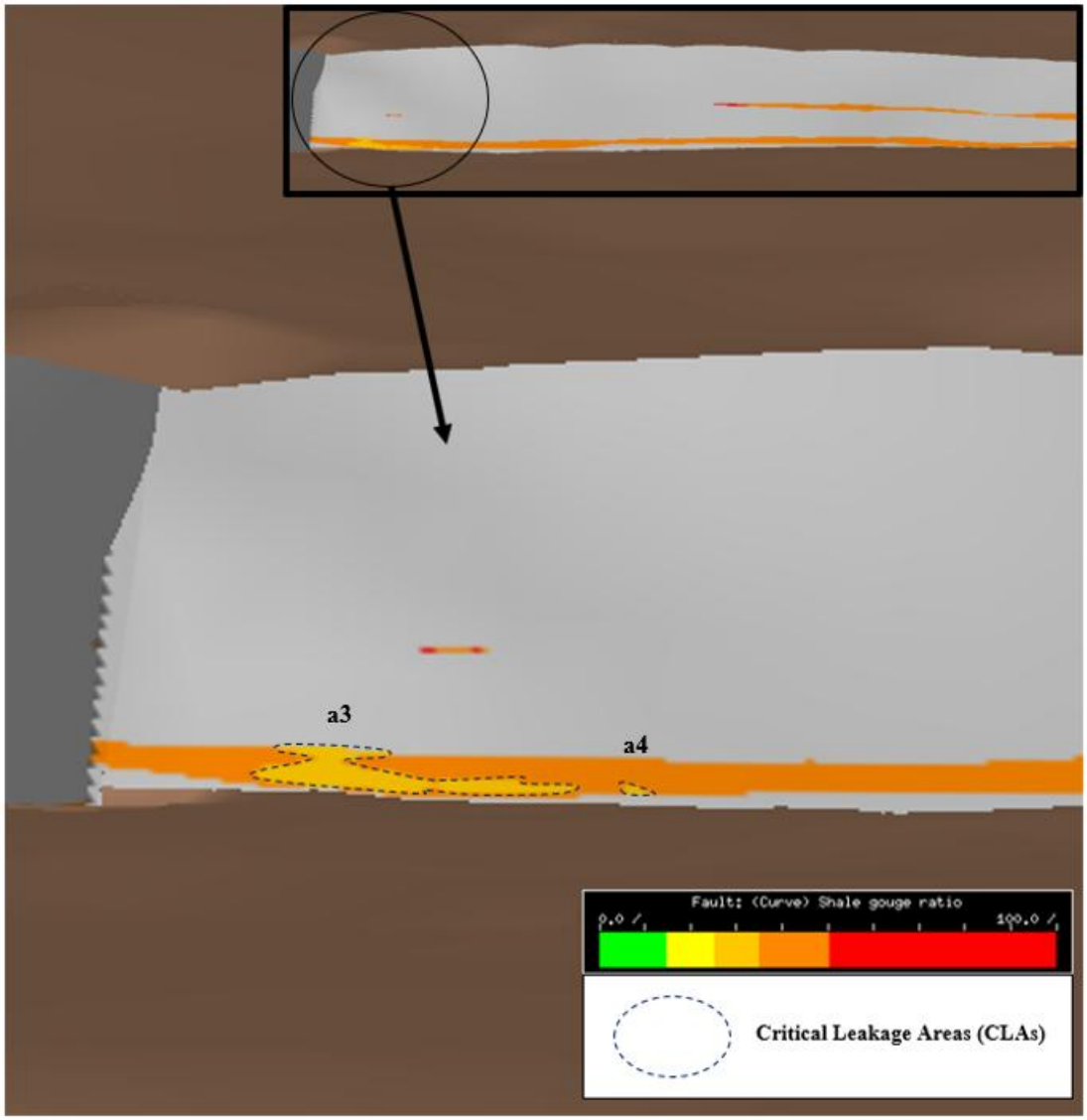

Figure 3.19 - Critical leakage areas (blue dashed outlines) on fault F2 (areas of highest transmission potential based on juxtaposition and SGR). Close-up taken from F2 potential leakage window shown at the top right. SGR scale displayed at the bottom for reference. The light orange (> 25% SGR) superposed on good-good reservoir (other juxtaposition types are displayed in gray) represents the areas of highest transmission potential. Brown surfaces are top and bottom of reservoir zone.

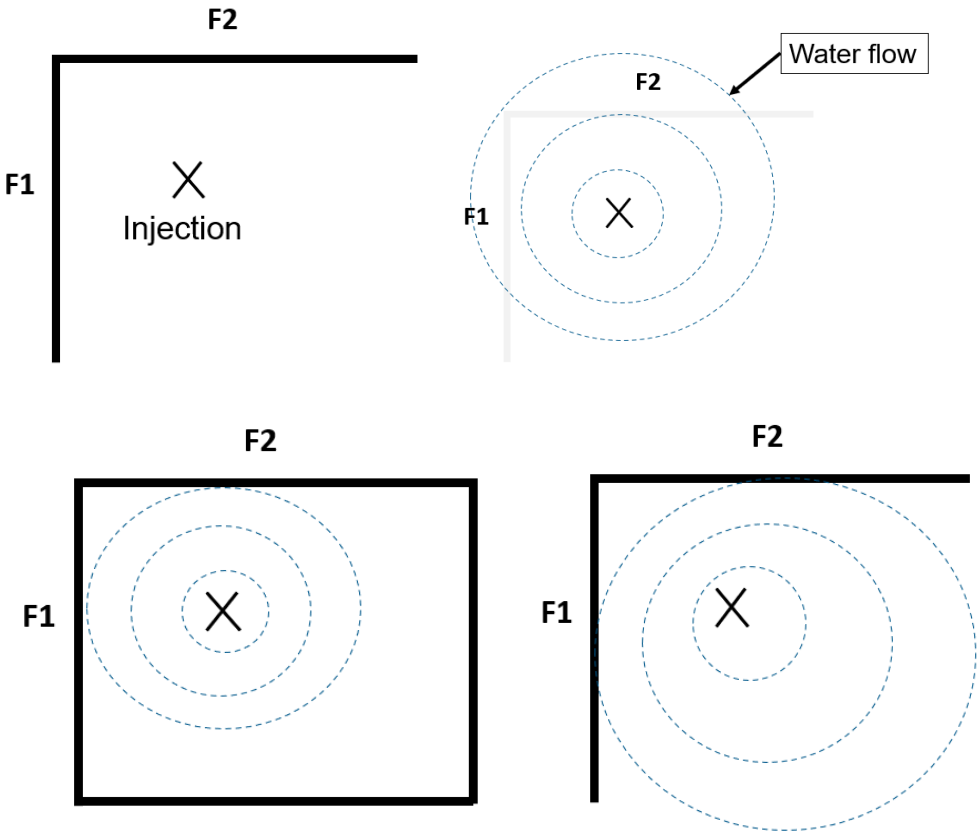

Figure 3.20 - Boundary condition illustrations for pressure buildup. Top left: simplified map-view of fault-bounded reservoir showing F1 and F2 and the injection point. Top right: F1 and F2 grayed out to represent the ability of water to flow past them as if the aquifer was infinite-acting. Bottom left: F1 and F2 block water flow and 2 more closed boundaries added to create a reservoir with a radius of 2,250 m. Bottom right: F1 and F2 block water flow and the two remaining boundaries are open for water flow and pressure dissipation.

Both the open (Figure 3.21) and semi-closed (Figure 3.22) boundary systems exhibit an asymptotic growth in migration rates where rates increase faster the first 5 to 10 years of injection and then gradually slower the remaining 35 to 30 years, respectively. Conversely, the closed system rates (Figure 3.23) exhibit a steep linear increase over the injection period, leading to rates that are, on average, 54 and 16 times greater than the open and semi-closed boundary systems, respectively. In addition, migration rates through fault F1 were found to be 6 to 9 times greater than those through fault F2 chiefly due to F1 having an area of highest transmission potential that was 5 times greater in size. Furthermore, Table 3.1 demonstrates that injection wells placed closer to the fault produce an earlier onset of migration and faster rates due to a higher pressure-gradient that transfers quicker across the fault. Table 3.1 also shows that boundary conditions have a much greater impact on migration rates.

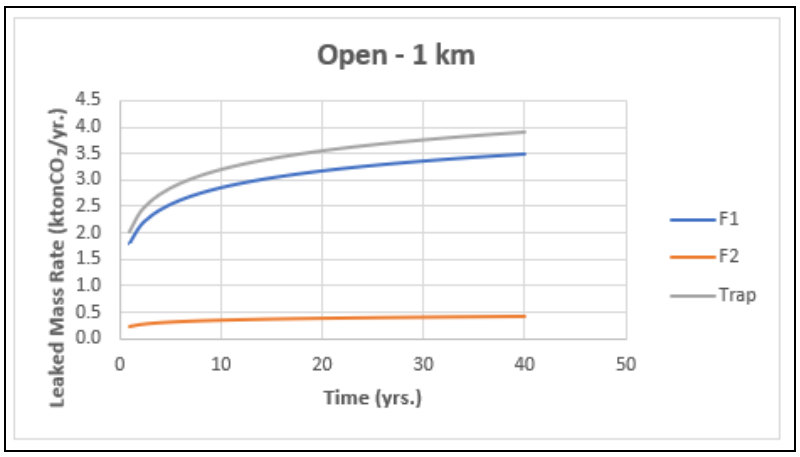

Figure 3.21 - Migration rate time series for CO2 injection into GoM faulted storage reservoir in the open boundary case. Leak rate (ktCO2/year) on y-axis and time (years) on x-axis. Curves shown for leakage rate across F1, F2, and entire trap. Note asymptotic growth and gap between orange and blue lines.

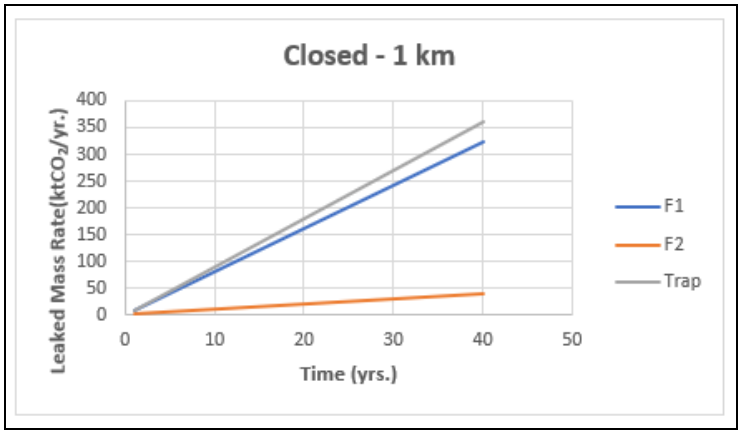

Figure 3.22 - Migration rate time series for CO2 injection into GoM faulted storage reservoir in the closed case. Leak rate (ktCO2/year) on y-axis and time (years) on x-axis. Curves shown for leakage rate across F1, F2, and entire trap. Note linear growth and gap between orange and blue lines.

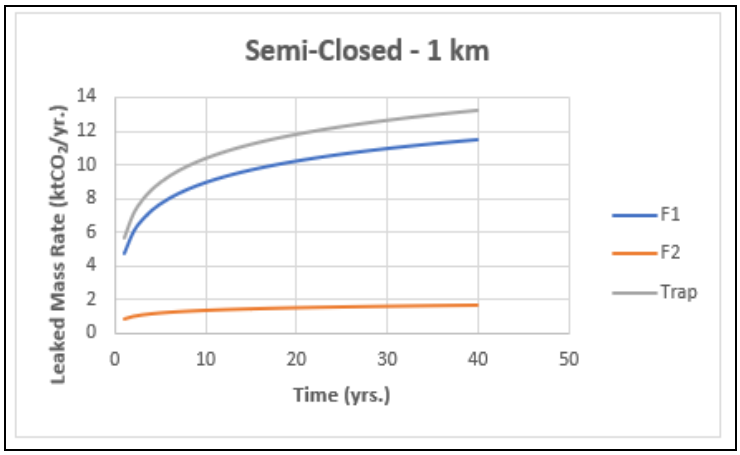

Figure 3.23 - Migration rate time series for CO2 injection into GoM faulted storage reservoir in the semi-closed case. Leak rate (ktCO2/year) on y-axis and time (years) on x-axis. Curves shown for leakage rate across F1, F2,

and entire trap. Note asymptotic growth and gap between orange and blue lines.

Table 3.1 - Average yearly across-fault migration rates in $ktCO_2$/year.

Boundary Conditions	*Well Placement Distance from fault (m)*		
	100	***1,000***	***2,000***
Open	4.25	3.43	2.72
Closed	186.05	185.22	184.51
Semi-Closed	13.15	11.23	9.54

Converting the rates to end-injection cumulative masses of CO_2 transmitted across the faults, we found transmission between 137.19 and 7,408.93 ktCO2 for open and closed boundary conditions respectively (or between 0.49% and 26.46% of the injected total). It is likely more realistic to assume that the reservoir's boundaries are semi-closed. In this case, 5,000 Monte Carlo simulations output between 372.03 and 570.24 ktCO2 (1.61% average of injected total) of CO_2 transmission after 40 years with 90% confidence. The results show that pressure buildup determines the magnitude of across-fault pressure gradient, and the size of the areas of highest transmission potential are the key drivers of migration rates in the studied GoM faulted site. In the GoM and analogous storage sites with abundant shales interbedded in the reservoir zone, the fault core permeabilities will favor slow migration. Similarly, for fault displacements like those seen in the studied GoM site—65 to 240 m—the fault core is likely to be thick enough (i.e., close to 1 or 2 meters thick rather than at the millimeter scale) to favor slow migration. In any case, this work encourages appropriate distribution modeling of fault core attributes, as they were found to exhibit 3 and 1 orders of magnitude of variation respectively.

Estimated migration rates are input into discounted cashflow analysis to compute the NPV of the injection phase of a CCS project under different migration rate scenarios. Revenue of the injection project was based on sold carbon credits per ton of CO_2 permanently sequestered in the target formation. The cost of across-fault migration was split into a) a liability cost (i.e., additional investment incurred to comply with regulations, remediation, acreage purchase, settlements, or other monetary penalties), and b) returned carbon credits. In this study CAPEX and OPEX were calculated for only the injection phase of an offshore project. Assuming the 3D seismic detection threshold of fault-transmitted plumes to be 10 $ktCO_2$, the NPV was obtained for different across-fault migration scenarios. Among them, an expected scenario where no across-fault migration is ever detected (Figure 3.24), a scenario where across-fault migration occurs at the rates estimated for the case of semi-closed boundaries and 1 km well-to-fault distance (Figure 3.25), and a scenario where migration occurs at probability-weighted rates (Figure 3.26). Under these conditions, the NPV of an injection project into the GoM trap varied from $52.32M to $63.02M depending on migration rates. Figure 3.24, Figure 3.25 and Figure 3.26 suggest that migration rates can be used to predict when the migration will be detected as well as in which year the liability cost of migration will be paid, and how many carbon credits can be expected to be returned. The result indicates that migration rates are key in scoping for financially viable projects.

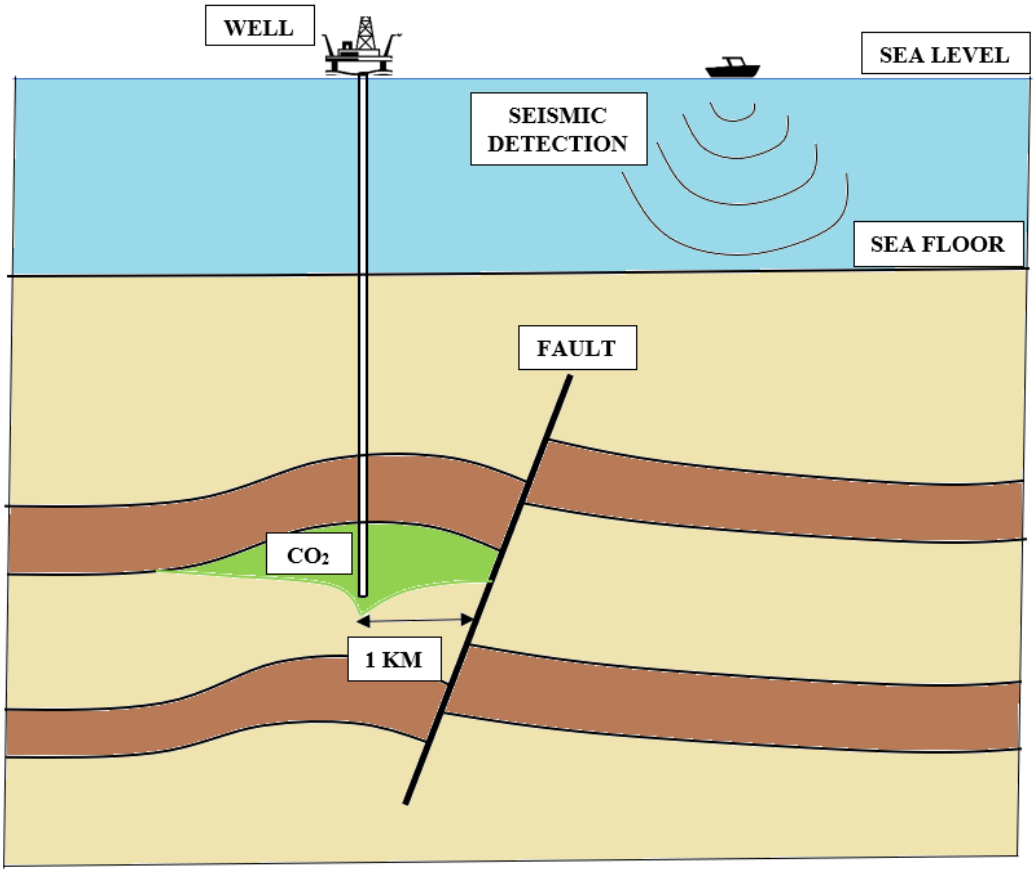

Figure 3.24 - *Schematic for valuation of injection project into the GoM faulted storage site for CASE 1 – No leakage occurs.

Years of forgone carbon credits: 0

Year of detection and financial liability investment: N/A (no detection)

NPV: $63.02M

Internal rate of return: 13.61%

* Boat and oil rig art from http://www.clipartbest.com/clipart-LiK5nKeXT and http://clipart-library.com/clipart/oil-rig-clipart 10.htm

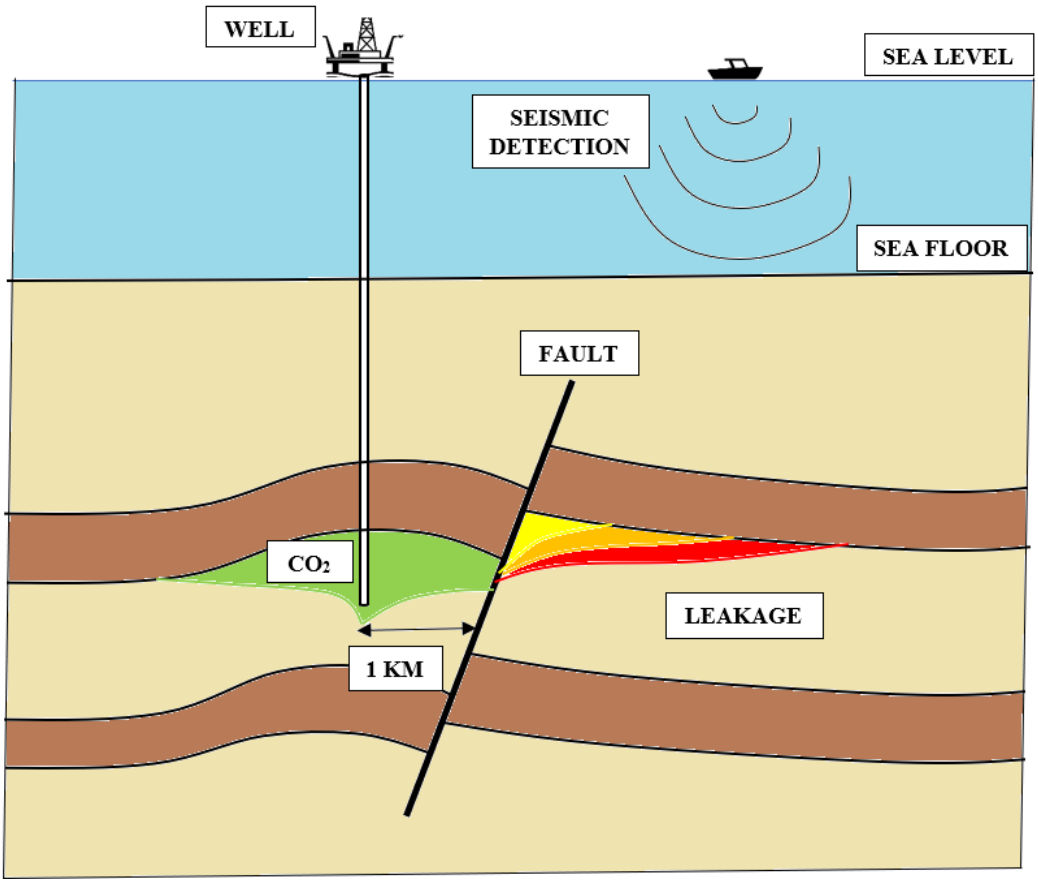

Figure 3.25 - *Schematic for valuation of injection project into the GoM faulted storage site for CASE 2 – Leakage occurs at estimated rates.

Years of foregone carbon credits: 3 years costing a total of $0.73M in liability

Year 1 = yellow plume: 5.6 ktCO2 leaked… undetectable

Year 2 = orange plume growth: 12.7 ktCO2 leaked… detectable but no seismic shot in year 2

Year 3 = red plume growth: 20.5 ktCO2 leaked… detectable and seismic shot in year 3

Year of detection and financial liability investment: leak is detected and remediated in year 3 costing $5.87M. No further leakage and liability cost starting in year 4.

NPV: $52.32M

Internal rate of return: 12.25%

* Boat and oil rig art from http://www.clipartbest.com/clipart-LiK5nKeXT and http://clipart-library.com/clipart/oil-rig-clipart_10.htm

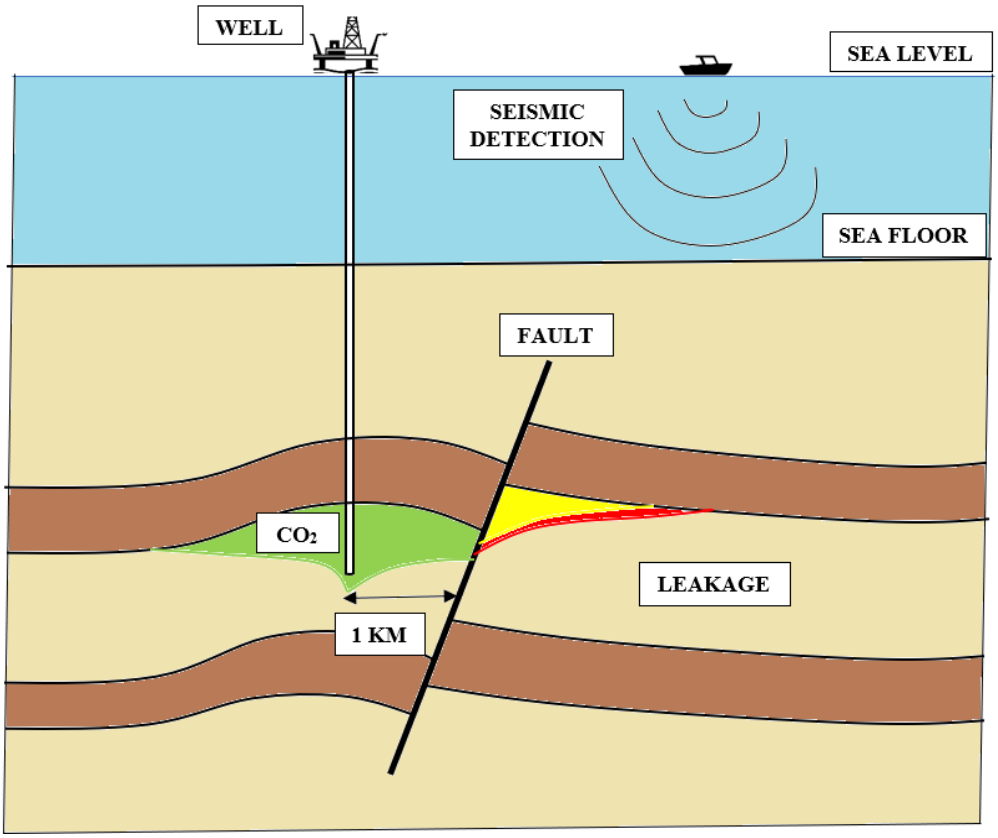

Figure 3.26 - Schematic for valuation of injection project into the GoM faulted storage site for CASE 3 – Leakage occurs at probability-based rates (certainty-equivalent case).*

*Note: Here, leakage rates are probability-weighted averages of a 0 tCO_2/year rate and the estimated leakage rate. I have assigned a probability of 90% for no leakage and 10% for the estimated leakage rates.

Years of foregone carbon credits: 12 years costing a total of $0.35M in liability

Years 1 through 11 = yellow plume: 9.8 $ktCO_2$ leaked… undetectable

Year 12 = red plume growth: 10.8 $ktCO_2$ leaked… detectable and seismic shot in year 12

Year of detection and financial liability investment: leak is detected and remediated in year 12 costing $5.87M. No further leakage and liability cost starting in year 13.

NPV: $54.63M

Internal rate of return: 12.76%

* Boat and oil rig art from http://www.clipartbest.com/clipart-LiK5nKeXT and http://clipart-library.com/clipart/oil-rig-clipart_10.htm

Following are some of the implications for CCS projects and limitations of this research:

- The financial profitability of a CCS project can be calibrated with knowledge of potential across-fault migration rates and migration related costs.
- While injection-induced pressure buildup and cross-sectional area of flux seemed to be the determining factors for migration rates, they can be estimated.
- Fault core attributes had a smaller impact on migration rates in this study, but their values varied considerably due to the complex nature and deformation of faults and also depending on the interpretation of seismic and log data. Improvements from this study would be to calibrate the log curves with physical

core data.

- Seismic and log data must be accurately interpreted, and a stochastic process is recommended to decrease uncertainty. Otherwise, inaccurate fault core permeability and thickness values as well as inaccurate sizes of the areas of highest transmission potential are possible.
- Reservoir pressure during injection impacts cross-fault leakage. Across-fault migration can be significantly reduced in reservoirs with an open boundary. Injection wells placed far from the faults reduce cross-fault leakage.
- Post-injection leakage was not considered in this study. While post-injection leakage is a possibility, its rate is reduced because of driving pressure dissipation once injection stops.
- In order to obtain a conservative estimate of migration rates and to simplify the problem to consider only Darcy flow, we only considered single-phase flow of supercritical CO_2 across the fault. In a saline aquifer, flow can be two-phase so more research can be done to refine the algorithm proposed in this work.

The fractions of CO_2 found to be transmitted across the fault are likely smaller in reality than in these models due to immobilization of CO_2 through trapping mechanisms like dissolution and capillarity, the asynchronous arrival of the pressure front and the CO_2 saturation front at the fault plane, geochemical processes in the fault, and the interruption of migration over time.

3.2.1 Subtask - Reservoir modeling

We investigated different scenarios of CO_2 injection and post-injection in the High Island 24-L (HI 24L) Field as a potential CCS prospect. We employed compositional reservoir simulation in the HI 24-L geologic model to provide better estimates of CO_2 plume evolution.

In a base case scenario, we perforated the injection wells in the sand layers close to the bottom of the reservoir and injected CO_2 for a total amount of 50Mt. In this case, the injection points were away from the faults and perforated in the bottom layers of the formation. We monitored the behavior of CO_2 plume during the 30 years of injection along with its post-injection for 100 years. To investigate the role of fault a zone on the CO_2 storage capacity and the possibility of storing CO_2 without relying on full sealing capacity of the faults, another scenario was run in which the well perforations were shifted to the sand layers close to the reservoir top. We inspected how the well perforation affected the occurrence of flow across the fault zone. The model showed that the 50 million Mt of CO_2 could be easily stored in HI 24L Field.

We were also interested in investigating the effect of capillary trapping, which is a key mechanism for security and permanence of CO_2 plumes within a defined geologic boundary. To this end, we ran another scenario incorporating the effect of capillary forces on the plume stabilization and amount of stored CO2. Results showed that capillary forces had a huge role in distributing equally the CO_2 plume in different rock types, improving the probability of safely storing larger volumes of CO_2.

We initially considered 3 different scenarios. 1) A 30-year injection of CO_2 into the HI 24-L geologic model through five wells perforated in the bottom layers of reservoir, followed by 100-year post-injection. In this case the effect of capillary trapping was ignored. 2) A 30-year injection of CO_2 into the HI 24-L geologic model through five wells perforated in the top layers of reservoir, followed by 100-year post-injection. In this case the effect of capillary trapping was ignored. 3) A 30-year injection of CO_2 into the HI 24-L geologic model through five wells perforated in the bottom layers of reservoir, followed by 100-year post-injection. In this case the effect of capillary trapping was applied to the simulations.

In the following, we explain the details of these three different scenarios.

Scenario 1:

We used the static model of the HI 24L Field to perform the multiphase flow simulations. Figure 3.27 shows the

geologic model and its corresponding permeability field.

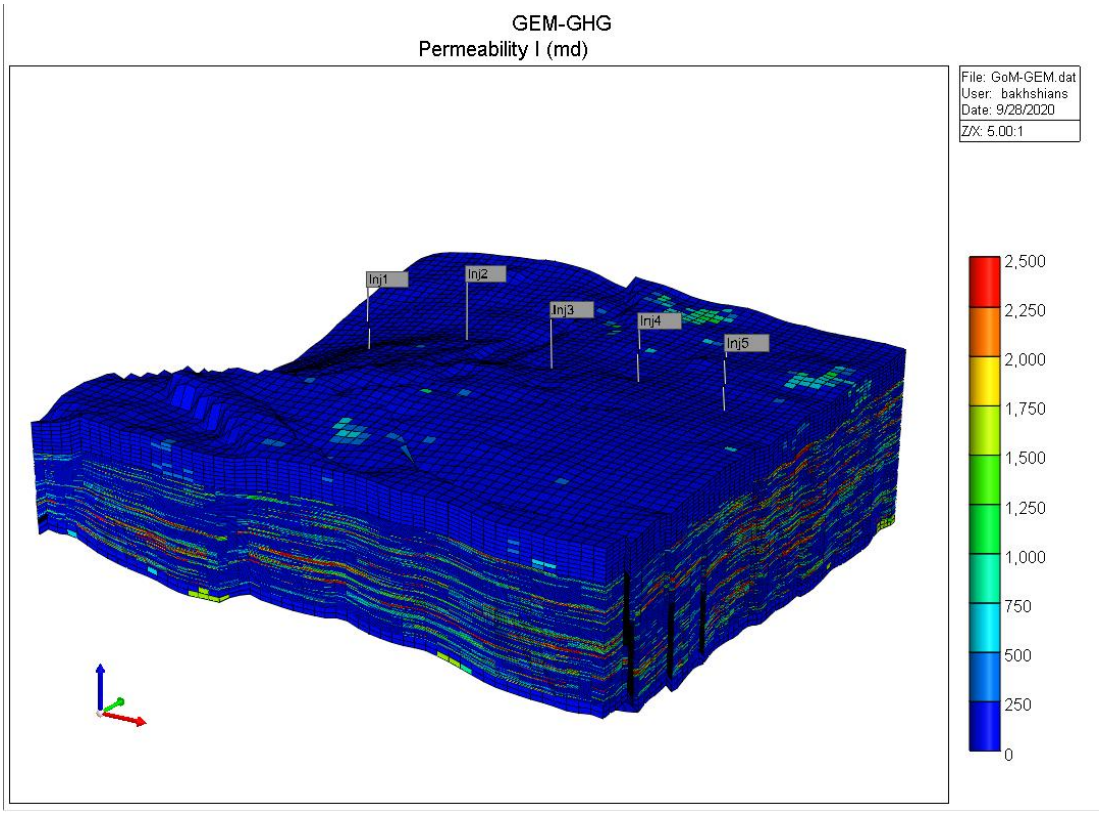

Figure 3.27 - Permeability field in the geologic model. Injection is performed through 5 wells.

The simulations were in CMG-GEM reservoir simulation software (Computer Modelling Group Ltd.). We assumed a continuous CO_2 injection with a constant rate of 16×10^6 scf/day, injecting a total of 50 million tons over the 30-year period. The injection simulation used five injection wells (Figure 3.27). For the base case scenario, the injection wells were perforated along the sand layers close to the bottom of the reservoir. Due to the density contrast between CO_2 and brine, the CO_2 plume tends to migrate upward in the reservoir. The perforation of wells in the lower portion of the reservoir allows the ability to explore how far the CO_2 plume migrated upward and how quickly it reached the fault zone, which is basically concentrated in the upper layers of the geologic model.

In the base case, we ignored the effect of capillary pressure on the dynamics of CO_2 plume migration. We investigated the effect of this parameter in the third case scenario.

Figure 3.28 represents the relative permeability curves used in the simulations.

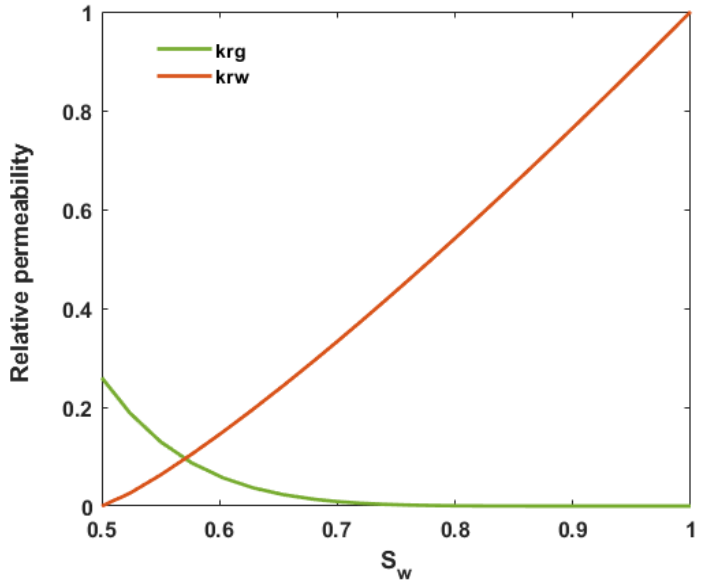

Figure 3.28 - Relative permeability curves used in the simulations.

Figure 3.29 displays how the CO_2 plume is extended at the end of injection period (year 2030) and after 100 years of post-injection (year 2130).

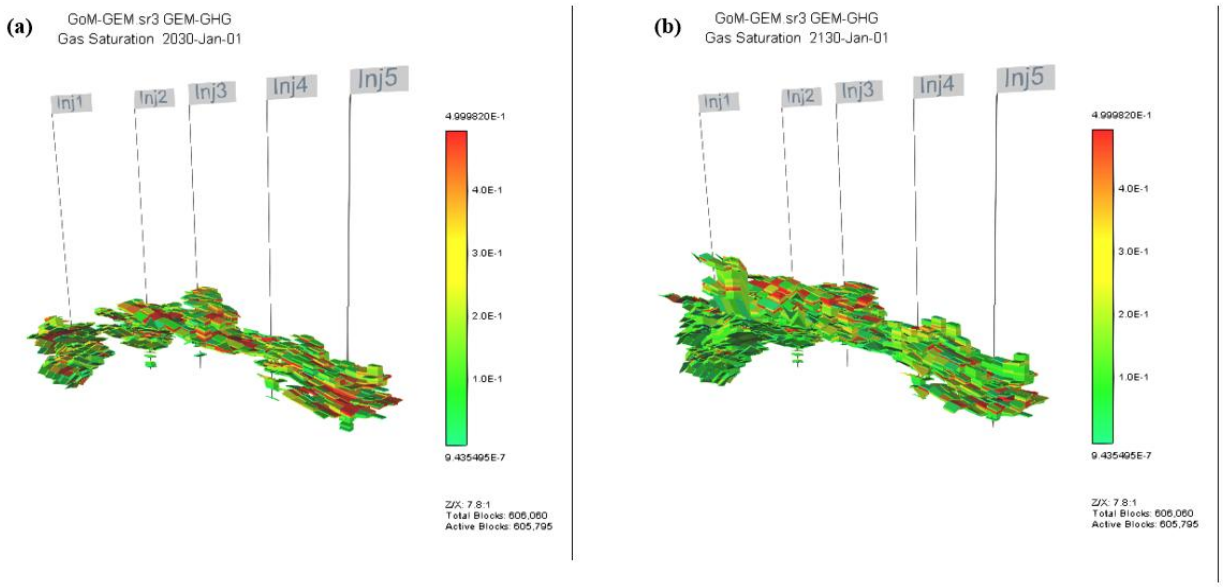

Figure 3.29 - CO_2 saturation distribution at the end of the injection (a) and post-injection (b) period. Capillarity is not considered in this case. Wells are perforated close to the bottom layers of the reservoir. The shape of the plume is representative of the upward migration of CO_2 due to the density contrast.

We have also shown CO_2 saturation profile at different cross-sections along the x and y directions at the end of post-injection period (year 2130) in Figure 3.30 and Figure 3.31.

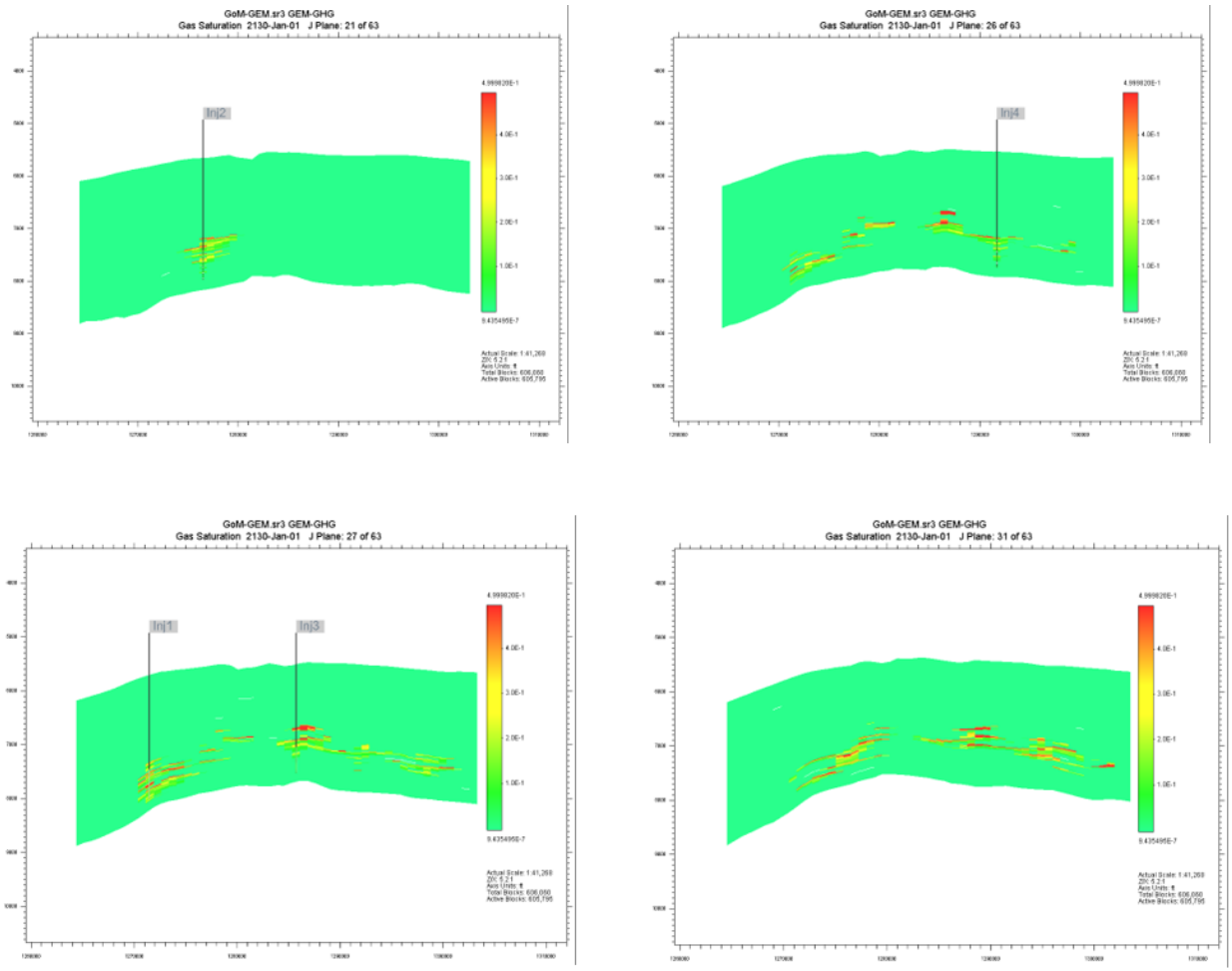

Figure 3.30 – CO_2 saturation profile in different 2D cross-sections along the y direction.

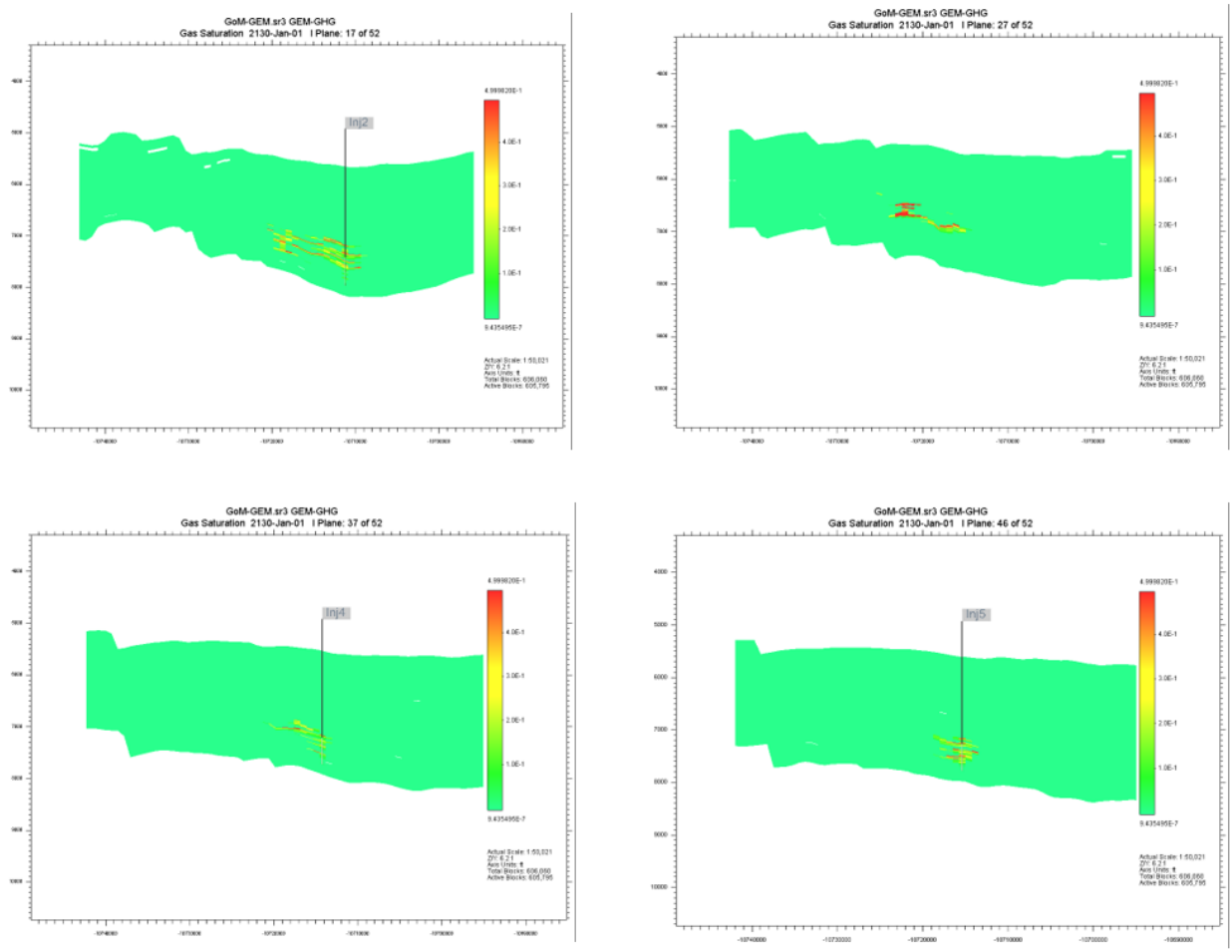

Figure 3.31 - CO_2 saturation profile in different 2D cross-sections along the x direction.

Figure 3.32 shows the variation of CO_2 average saturation along the reservoir depth at the end of injection and post-injection stage. It should be noted that since all grid cells, including gas-filled and empty cells, are considered in calculating the average saturation of each layer, the resulting average saturation profile displays very small values. Note that the saturation profile has moved to the lower depth at the end of post-injection period (2130), indicating the upward movement of the CO_2 plume. Moreover, the saturation distribution becomes wider at the end of post-injection compared with the distribution at the end of injection.

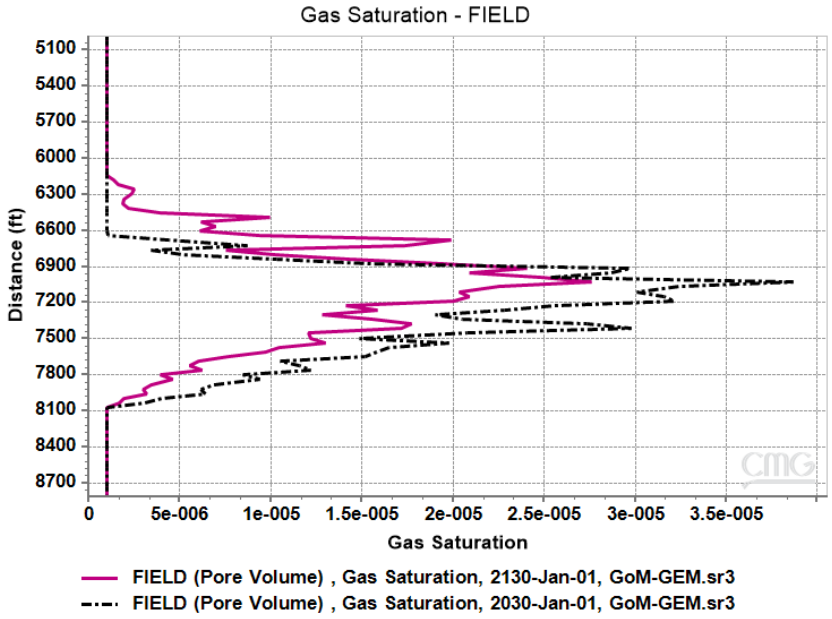

Figure 3.32 - CO_2 average saturation along the reservoir depth at the end of injection and post-injection stage.

To explore the plume stabilization during the post-injection stage, we calculated the variation of CO_2 saturation during the last 10 years of post-injection period (2120-2130). Figure 3.33 represents how the average saturation of CO_2 plume varies in a 10-year time period within the last 10 years of post-injection (Figure 3.34). We observe that the average saturation varies up to around 17% in this timeframe.

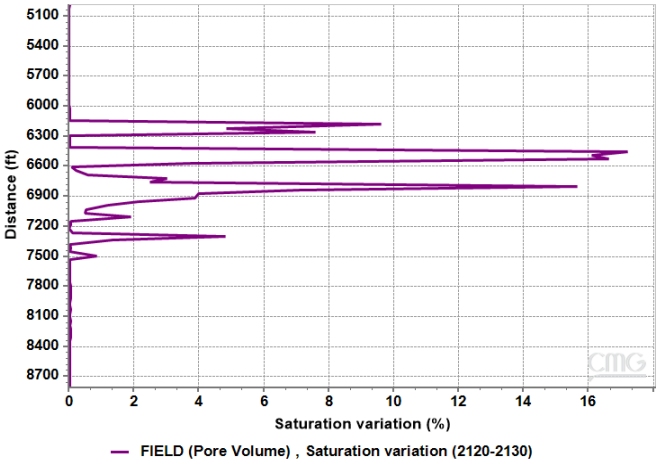

Figure 3.33 - Variation of average CO_2 saturation along the reservoir depth.

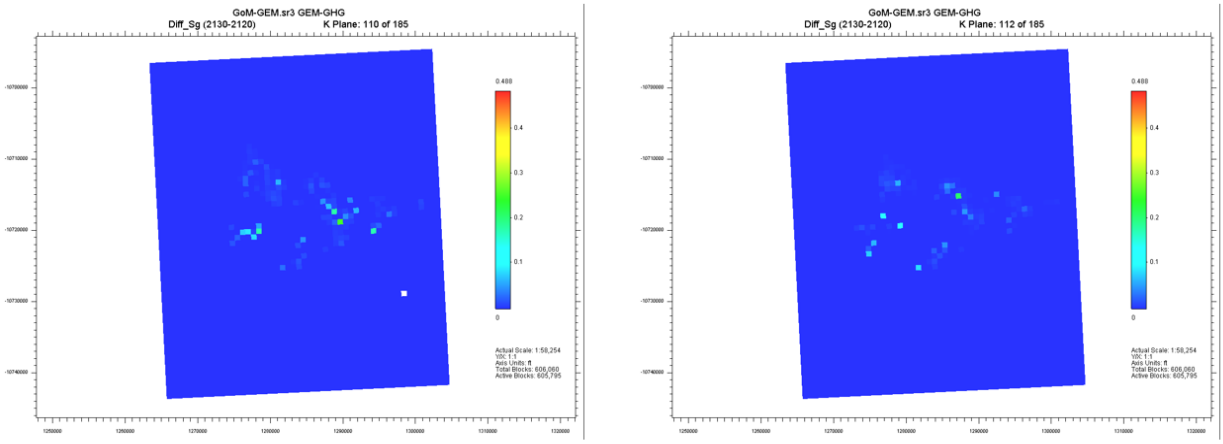

Figure 3.34 - Variation of CO2 saturation profile within the last 10 years of post-injection (2120-2130) in two different 2D cross-sections along the reservoir depth.

Scenario 2:

In this scenario, we alter the perforation of the wells to the upper sand layers, close to the reservoir top to inspect how the well perforation can affect the occurrence of flow across the fault zone.

The plume shape and its saturation profiles are displayed in Figure 3.35, Figure 3.36, and

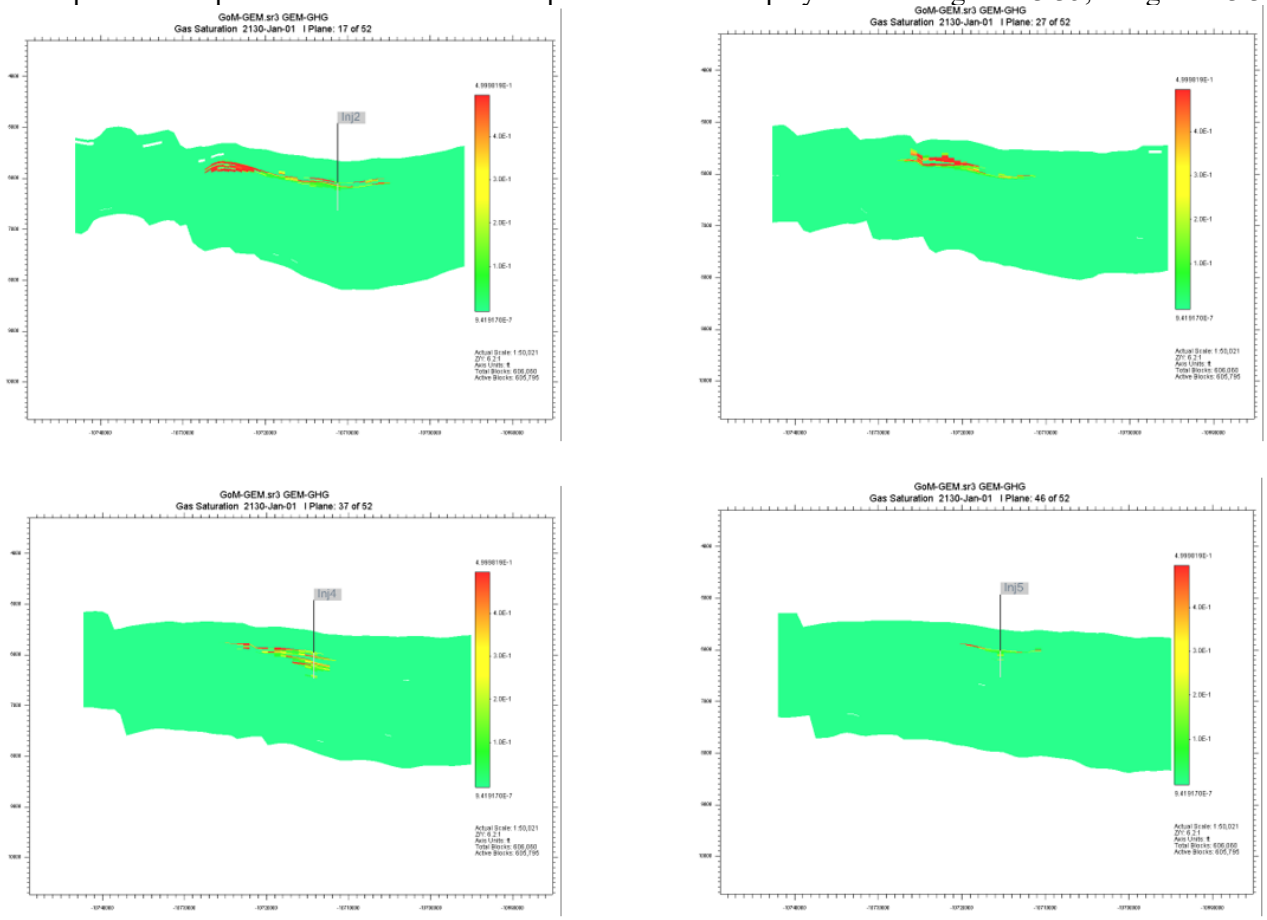

Figure 3.37.

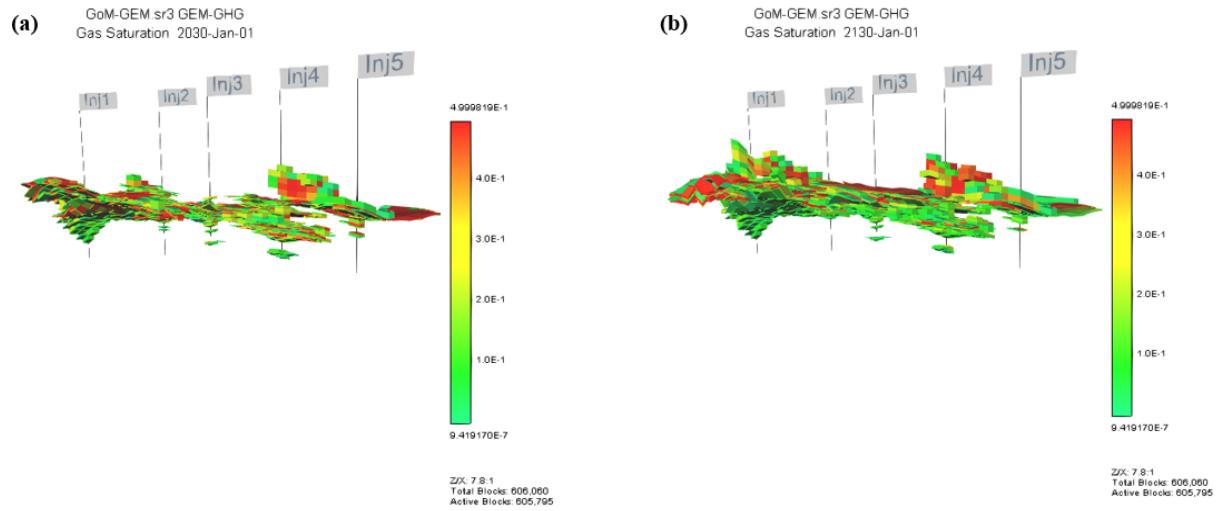

Figure 3.35 - CO_2 saturation distribution at the end of injection (a) and post-injection (b) period. Capillarity is not considered in this case. Wells are perforated in top layers of the reservoir.

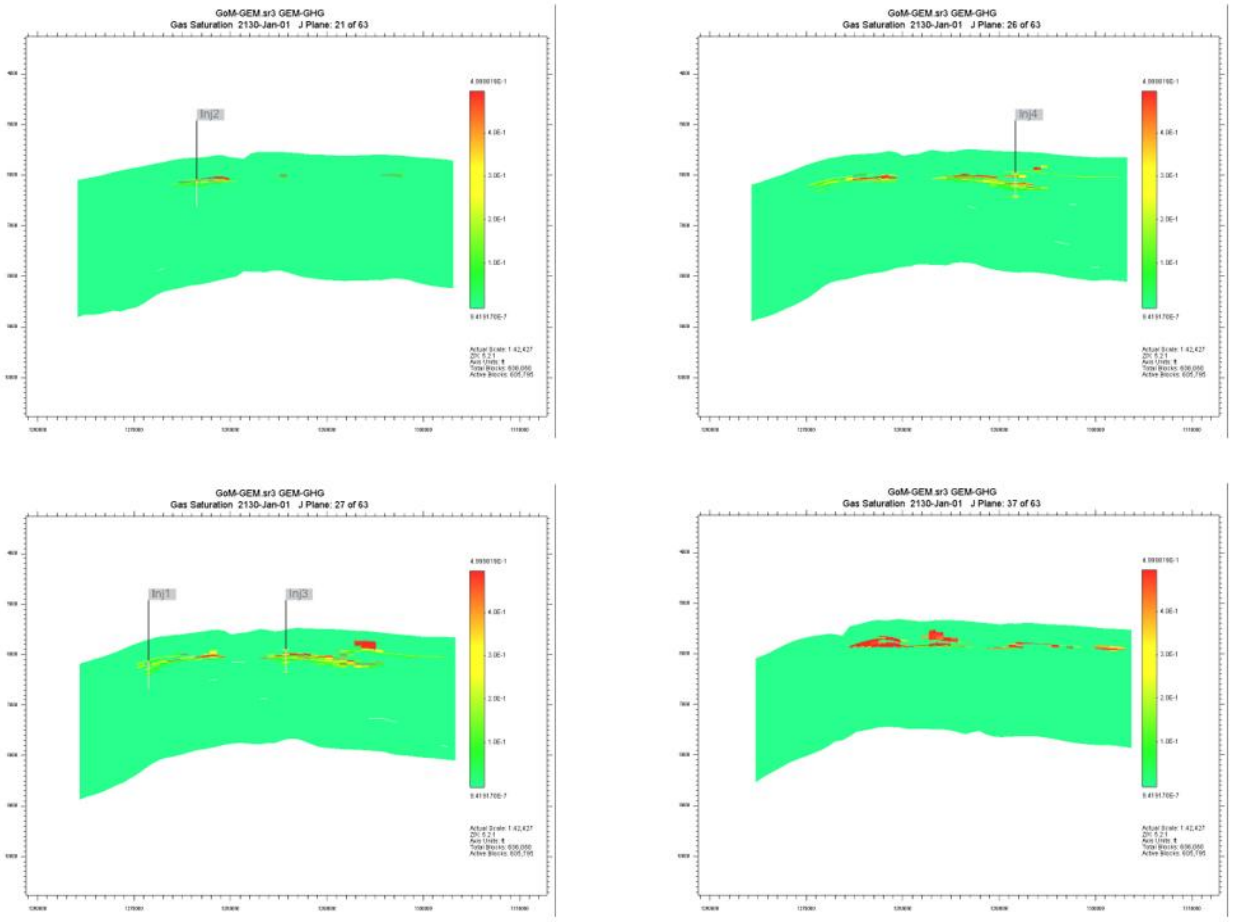

Figure 3.36 - CO_2 saturation profile in different 2D cross-sections along the y direction.

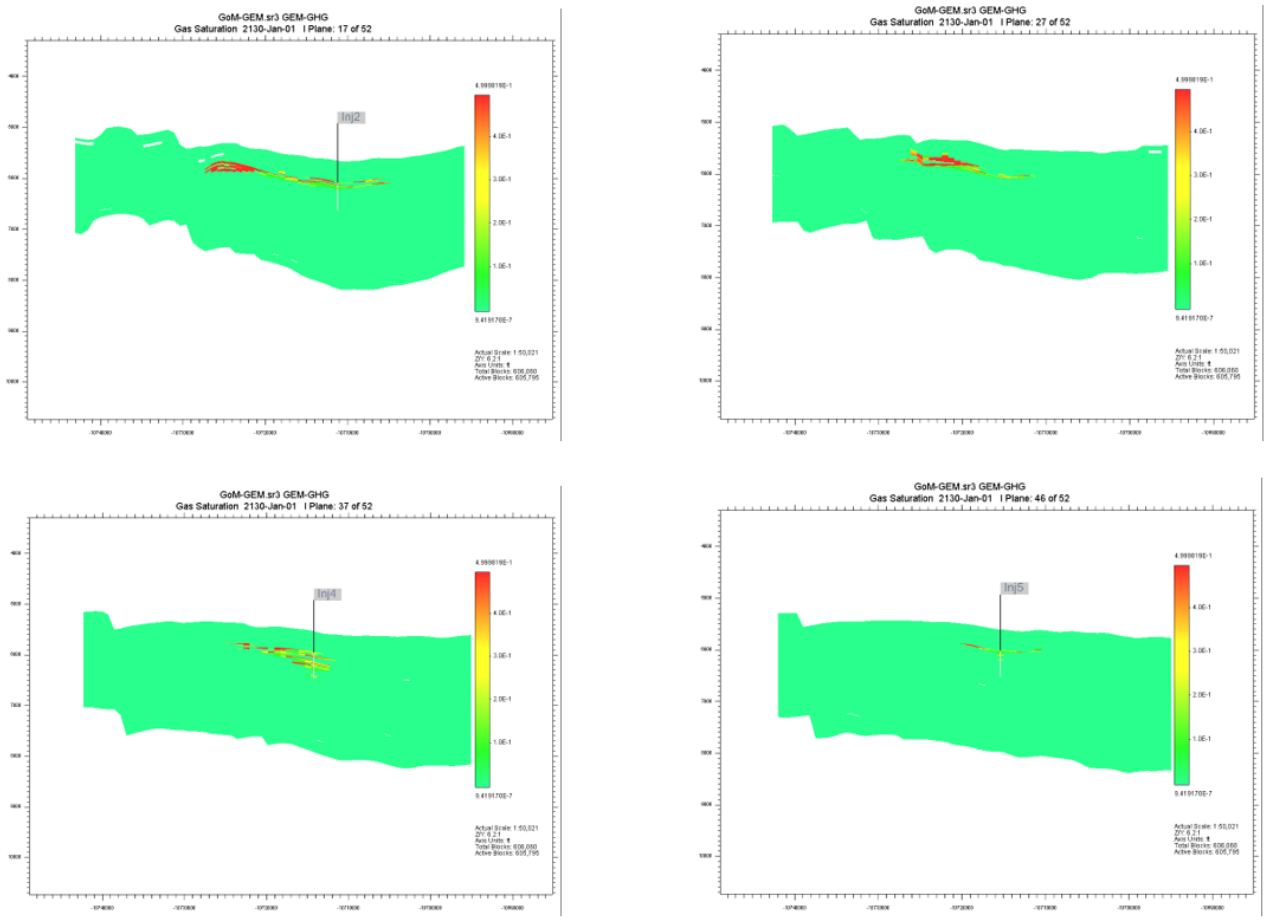

Figure 3.37 - CO_2 saturation profile in different 2D cross-sections along the x direction.

According to the plume distribution, the CO_2 mostly accumulated under the top sealing layer, as its migration is governed by buoyancy. Figure 3.38 also confirms this fact, as the width of the saturation distribution is narrow, indicating the accumulation of CO_2 plume in the top layers under the confining layer.

Moreover, by placing the well perforation close to the confining layer, the plume mostly distributes laterally. Comparing Figure 3.31 with Figure 3.37 shows that in the second scenario, the CO_2 plume tends to migrate laterally as it is bounded by the sealing layer from the top, hindering its upward migration. This can lead to the occurrence of flow across the fault zone, which is concentrated close to the top layers.

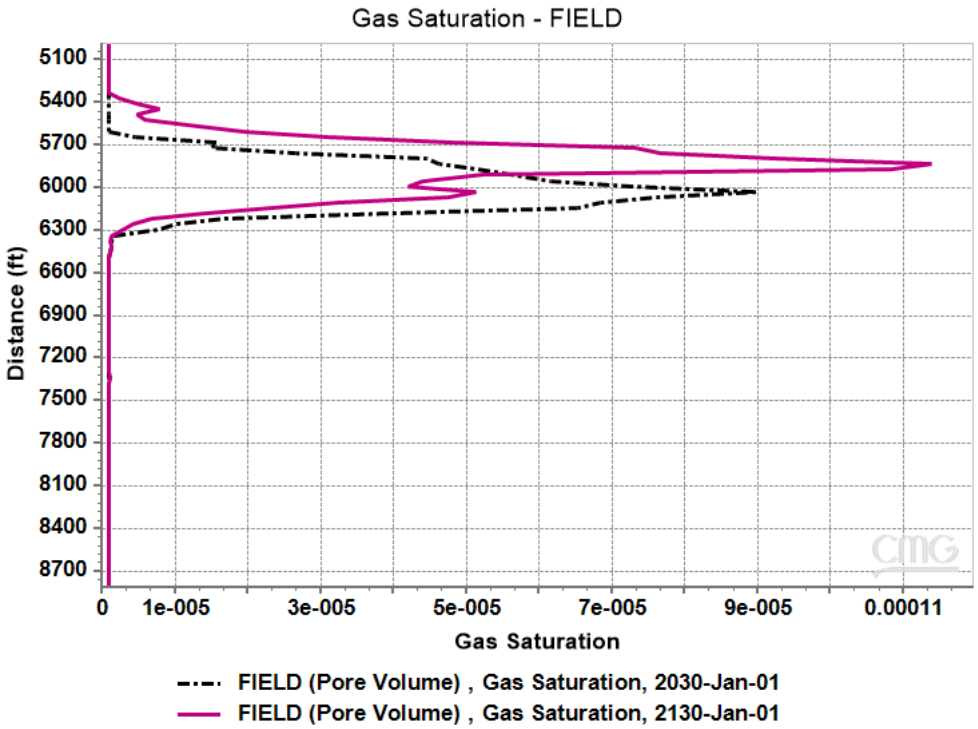

Figure 3.38 - CO_2 average saturation along the reservoir depth at the end of injection and post-injection stage.

Scenario 3:

In this scenario, we incorporated the effect of capillarity into the simulations. All other simulation conditions and well perforations remained the same as scenario 1.

Comparing Figure 3.29 with Figure 3.39 indicates that with capillary trapping, CO_2 plume distribution is more uniform than that of scenario 1, which ignores the effect of capillarity. Figure 3.42 also indicates this fact as it shows a smoother curve for the distribution of the average saturation compared with the one for scenario 1 (Figure 3.32).

We also observed a gradual change in the shape of the plume between the end of injection (2030) and the end of the post-injection (2130) period (Figure 3.39). This is confirmed by Figure 3.42, which displays a small variation in the distribution of CO_2 average saturation within the 100-year post-injection. So, it can be concluded that capillary trapping plays an important role in the CO_2 plume stabilization. The small variation of CO_2 saturation within the last 10 years of post-injection also implies a stabilized state for the CO_2 plume (Figure 3.43 and Figure 3.44). Figure 3.43 shows that the maximum variation of 0.33 % for the CO_2 saturation within the last 10 years of post-injection, indicating plume stabilization. In comparison with scenario 1 in which capillarity was ignored and saturation varied up to 17%, the average saturation in scenario 3 varied negligibly, confirming the pivotal role of capillary trapping in plume stabilization.

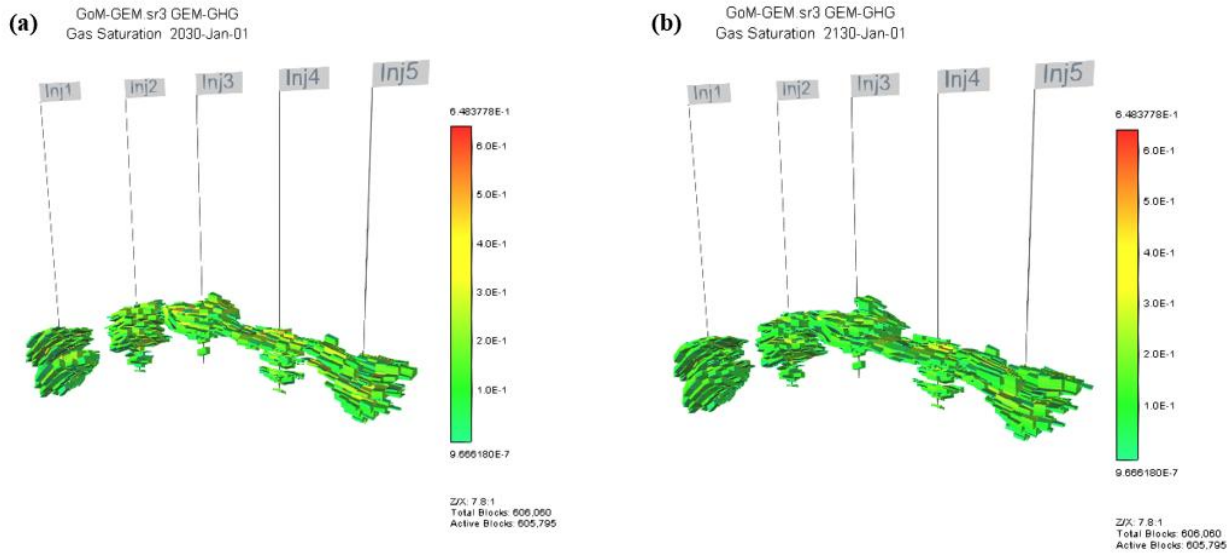

Figure 3.39 - CO_2 saturation distribution at the end of injection (a) and post-injection (b) period. Wells are perforated close to the bottom layers of the reservoir. Capillary trapping is considered in this case.

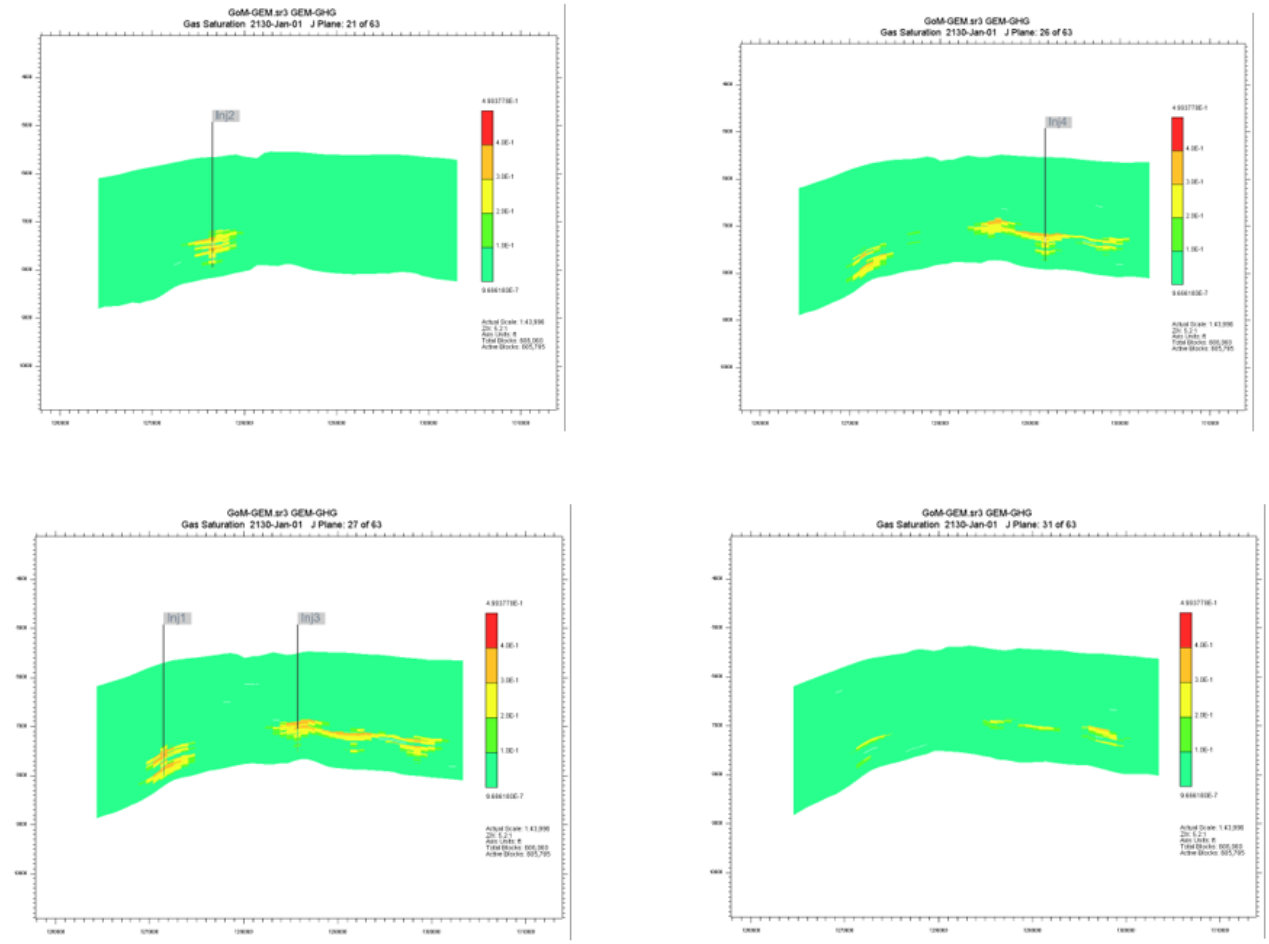

Figure 3.40 - CO_2 saturation profile in 2D cross-sections along the y direction.

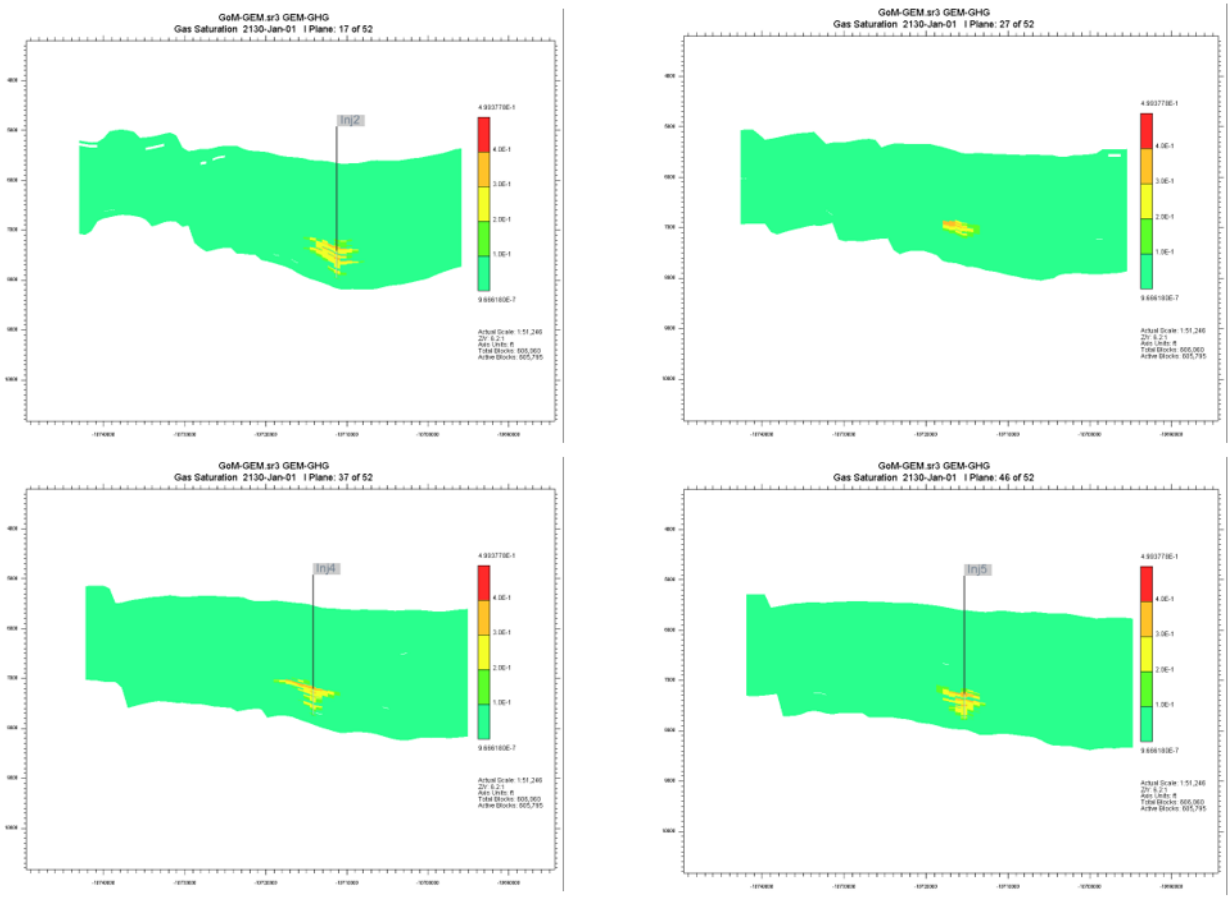

Figure 3.41 - CO_2 saturation profile in different 2D cross-sections along the x direction.

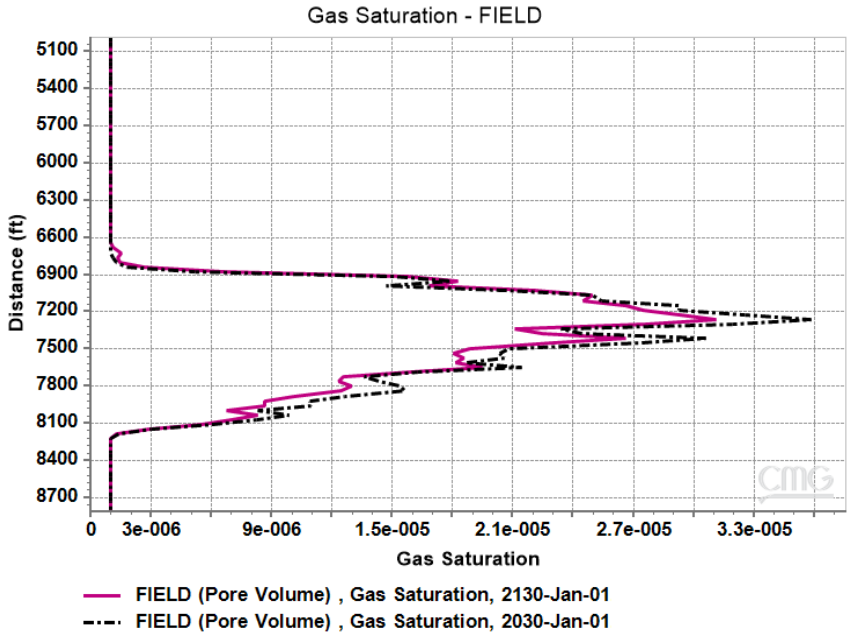

Figure 3.42 - CO_2 average saturation along the reservoir depth at the end of injection and post-injection stage.

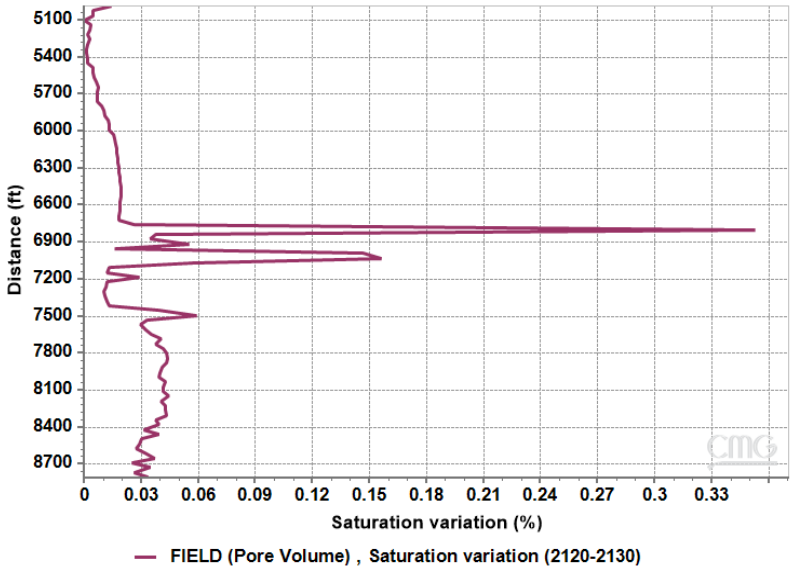

Figure 3.43 Variation of average CO2 saturation along the reservoir depth.

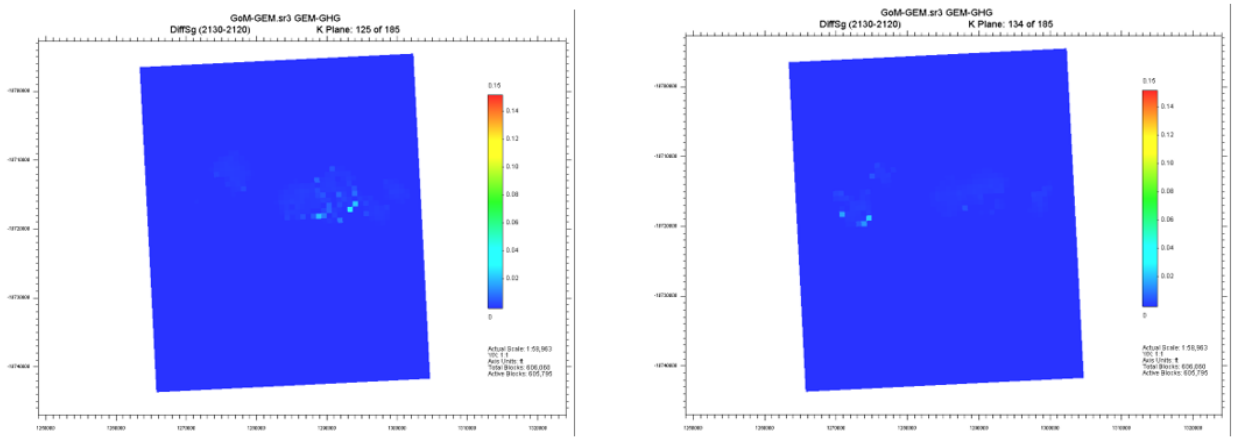

Figure 3.44 - Variation of CO2 saturation profile within the last 10 years of post-injection (2120-2130) in two different 2D cross-sections along the reservoir depth.

Scenario 4:

In scenario 4, we considered the geologic model to be semi-isotropic ($\frac{K_v}{K_h} = 0.5$), meaning that we alleviate the degree of heterogeneity in the formation. All other parameters including the location of well perforations are the same as those in scenario 1. Snapshots of the CO_2 plume and its trapped portion at the end of injection and post-injection periods are shown in Figure 3.45. We observed that an isotropic medium facilitated the upward movement of the plume, since vertical permeability imposes less restriction on the vertical movement of the CO_2 plume. Compared with scenario 1, we did not observe a significant variation in the bottom hole pressure of injection wells during the injection period, while the ultimate pressure observed in the post-injection period is the same as scenario 1 (Figure 3.46). Another point to highlight here is that running simulations with higher Kv/Kh ratio takes much longer time. This is mostly because gravity forces are now dominant and numerical convergence rates are very slow. For scenario #4, after several days of running simulation stopped at year 2048 and this is the results we are providing here as end of post injection period.

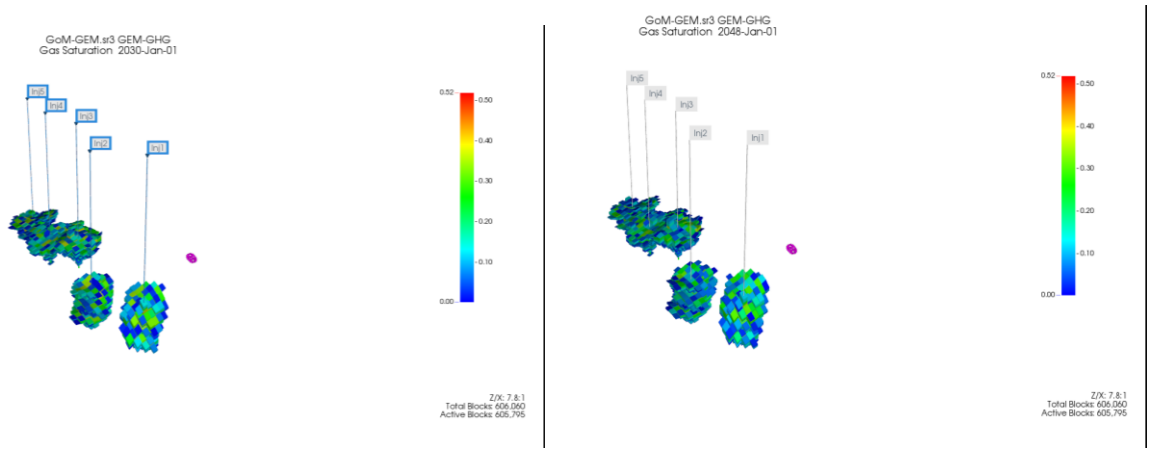

Figure 3.45 - CO_2 plume at the end of injection (left) and post-injection (right) periods for scenario 4.

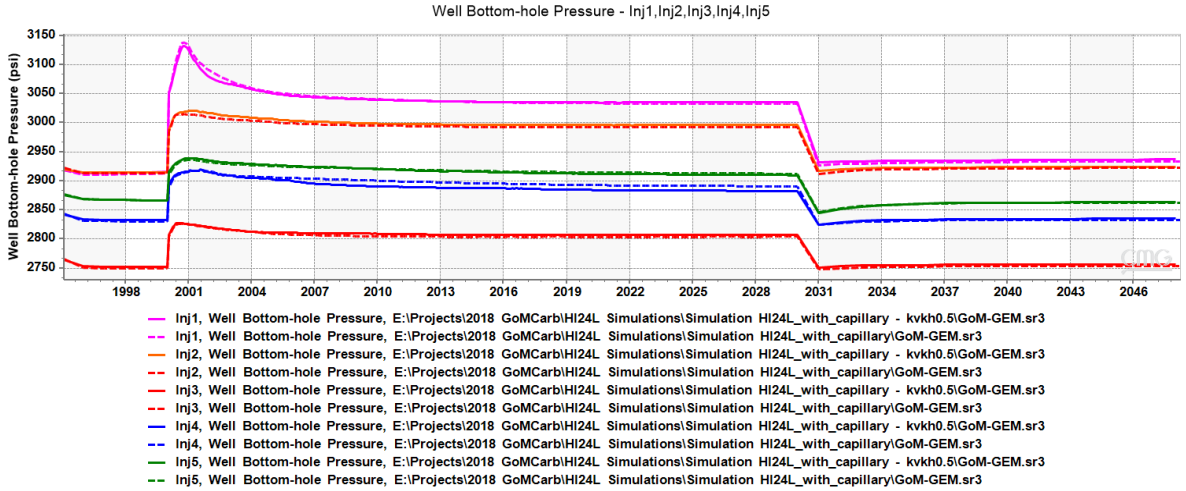

Figure 3.46 - Comparison chart of BHP values in scenario #1 vs. scenario #4 for all 5 injection wells.

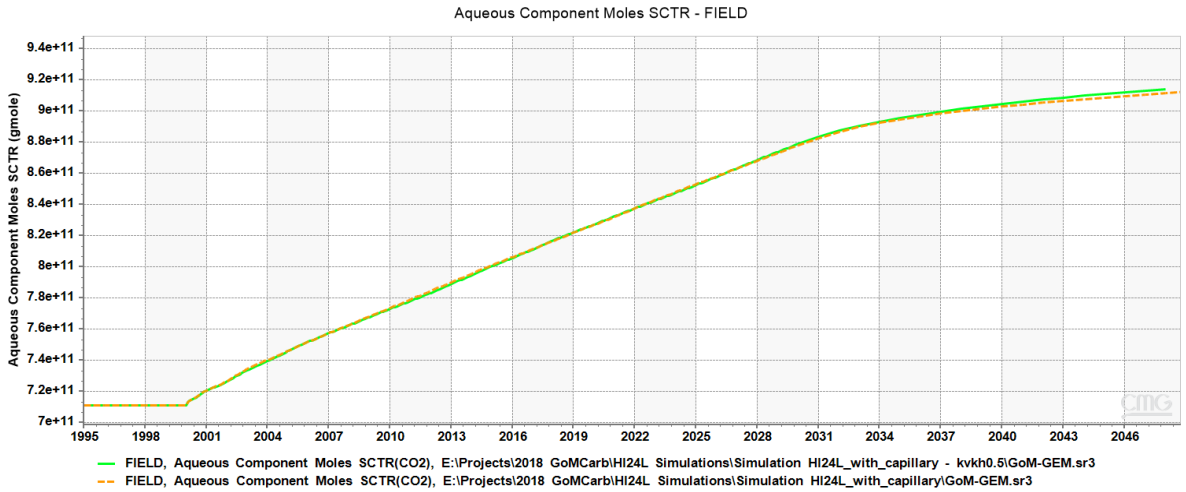

Time evolution of CO_2 dissolved into the brine for scenarios 1 and 4. Higher kv/kh ratio has slightly increased the amount of CO2 dissolution into the brine.

Scenario 5:

In this scenario, the effect of hysteresis is neglected, meaning that CO_2 cannot be residually trapped in the formation. All other parameters are the same as in scenario 1. According to the shape of the CO_2 plume shown in Figure 3.47 and its comparison with that in scenario 1, we observe that the CO_2 plume is further extended in the absence of hysteresis, since no portion of plume can become residually trapped. No significant variation is observed in the reservoir pressure compared with scenario 1 (Figure 3.48). In these simulations we were able to run the model for all period of post injection until year 2132.

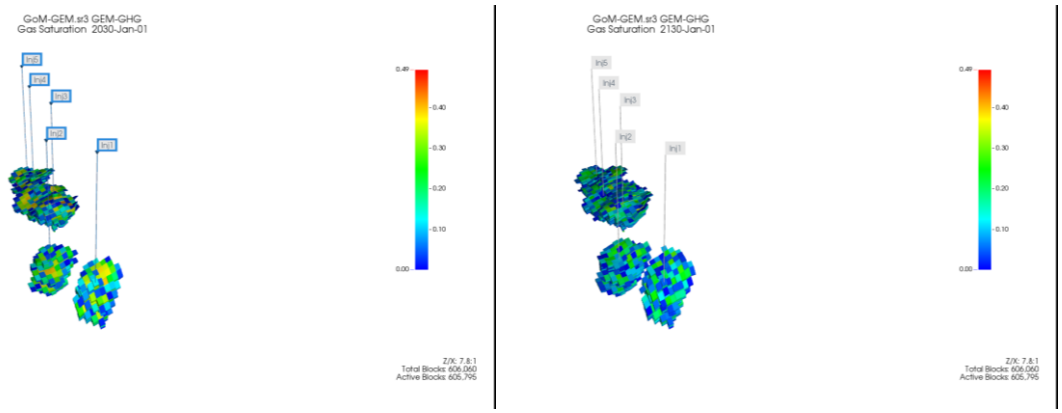

Figure 5.

Figure 3.47 - CO_2 plume at the end of injection (left) and post-injection (b) periods for scenario 5.

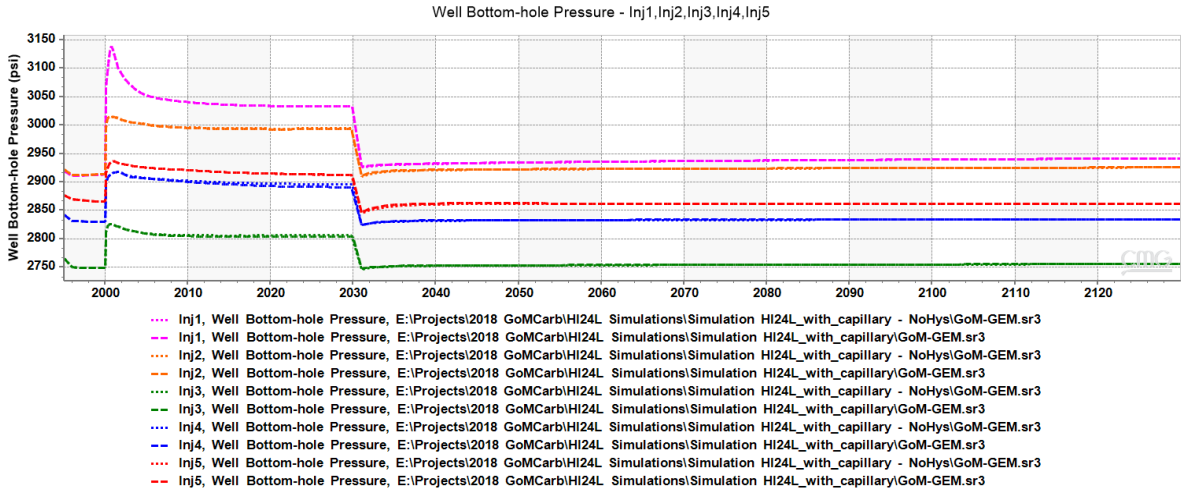

Figure 3.48 - Comparison of BHP values in scenario #1 vs. scenario #5 for all 5 injection wells.

One major observation for all the scenarios is that even after injecting 50 million tonnes of CO_2 into the Miocene age reservoir, the CO_2 plume did not reach the faulted area shown in Figure 3.27. Even when we consider worse case scenarios where vertical permeabilities are exaggerated or hysteresis effects are completely ignored, and even though the plume grows larger, the CO_2, nonetheless, remains within the intended area and zone. These are positive results.

3.2.2 Subtask - Sub-basinal scale modeling

A static geologic model of the TexLa Merge 3D dataset's coverage area was generated. The framework of the

model, built in Petrel, is based on detailed stratigraphic and structural seismic interpretations. The model consists of six surfaces and 147 faults. Figure 3.49 shows the location and the extent of the model. Stratigraphic zones including MFS 04, MFS 05, MFS 07, MFS 08, MFS 09, MFS 10. Figure 3.50 shows a dip well log cross section of the Miocene stratigraphy in the Texas Gulf of Mexico. Stratigraphic zones, including the upper, middle, and lower Miocene, were subdivided into layers with an average cell thickness of 5 ft and an average lateral cell size of 100m × 100m, resulting in the creation the 3D model for the TexLa Merge area.

The best way to integrate reservoir properties (e.g., lithology and porosity) into the model was to use properties derived from seismic data. To do this a pre-stack seismic inversion was performed. Previous work on NETL study FE0026083 obtained reservoir properties from the TexLa Merge seismic dataset. GoMCarb work expanded the previous work to populate the static geologic model with reservoir properties.

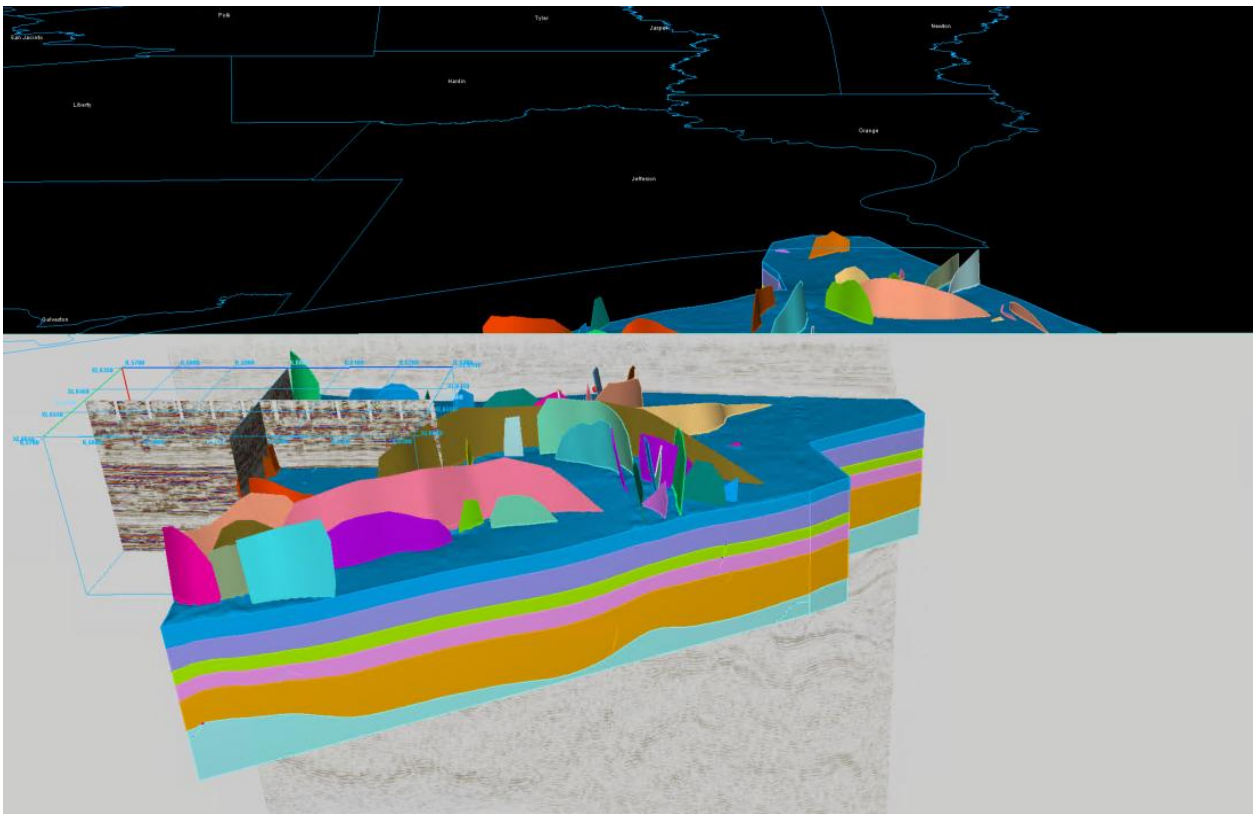

Figure 3.49 - 3D strike view of the TexLa model as of the end of the reporting quarter. Note that there are six stratigraphic zones and the 147 faults.

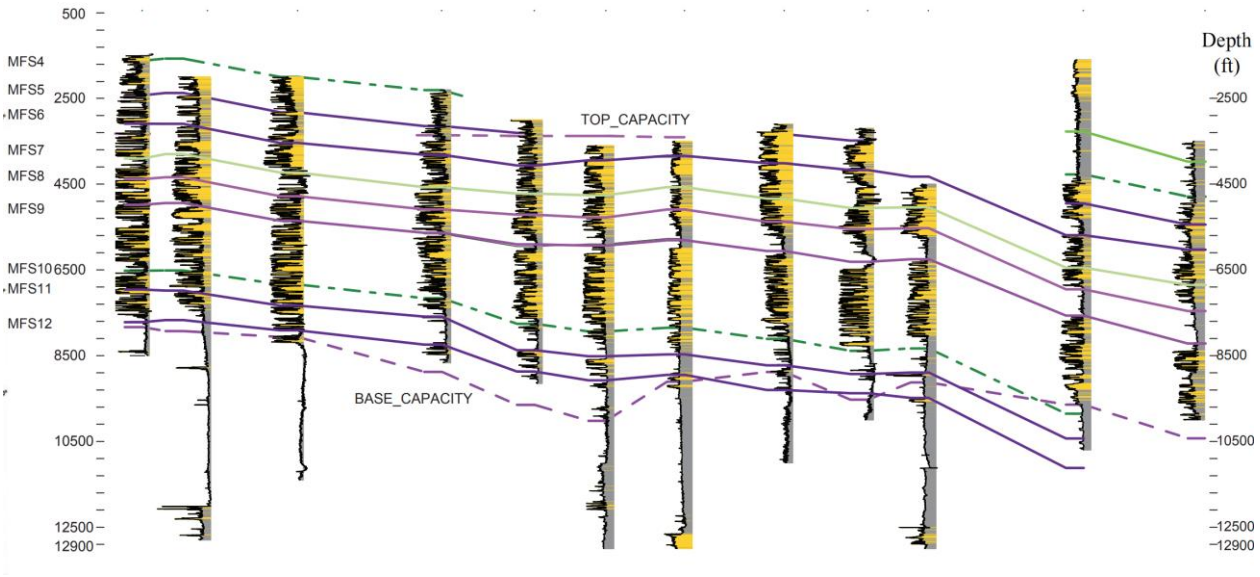

Figure 3.50 - Dip well log cross section showing the stratigraphy and horizons used in the TexLa model.

Because well-data are very dispersed in the study area, the best way to populate the model is to use reservoir properties derived from the much more extensive TexLa Merge seismic dataset. This provides a better estimation of properties in areas away from wells. Lithology and porosity from seismic data were derived from rock physics models and pre-stack seismic inversion. Using elastic properties (e.g., Vp/Vs ratio and P-Impedance) it is possible to differentiate between rock facies, specifically between shales and sand. Using rock physics models that were calibrated with well data it is possible to understand the relationships between rock properties. Using these relationships, we can estimate the porosity in the area of study for the two facies in the geologic model. The steps for generating the porosity and facies models are as follows:

(1) Selection of a rock physics model. In this case the soft sand model (Dvorkin & Nur, 1996) was selected, because of the assumed, poorly indurated nature of the Lower Miocene sandstones.

(2) Classify and discriminate between facies, specifically classify between shales and sand. This classification was done combining Vp/Vs and P-Impedance.

(3) Then, using the P-impedance and porosity relationship we can derive porosity from the P-impedance volume obtained from inverting the dataset seismic.

Figure 3.51 shows the two facies obtained from the seismic data. Sand facies is shown in blue. The sands correlate well data. Figure 3.52 shows the porosity obtained from the rock physics models, which indicate that the Lower Miocene sandstones of the area have porosities greater than 20%.

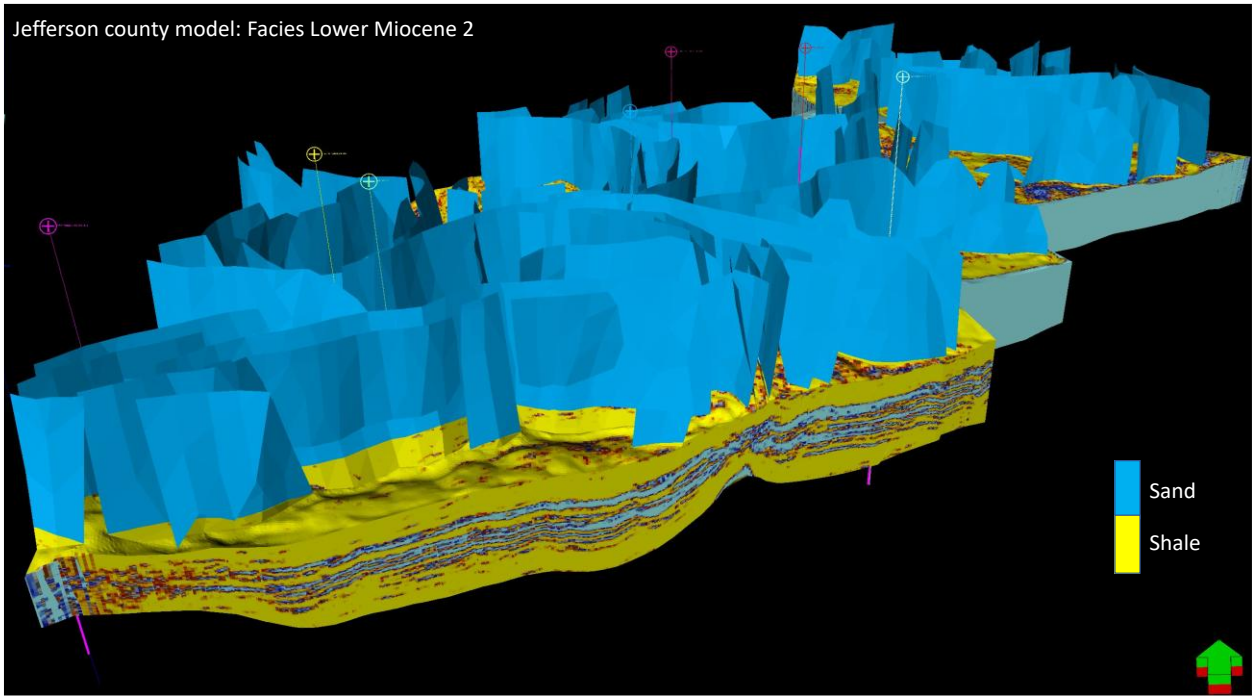

Figure 3.51 - 3D view of the TexLa model, showing facies interpretations derived from seismic data.

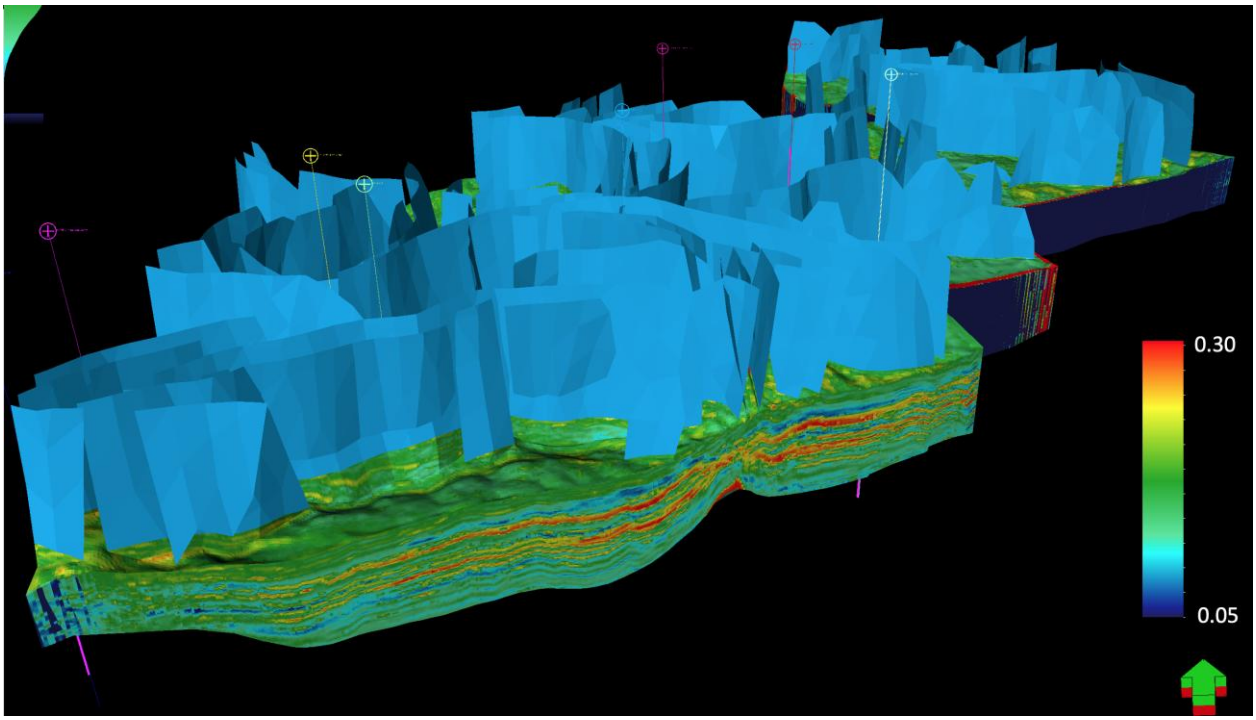

Figure 3.52 - 3D view of the TexLa model, showing porosity estimated with seismic data.

TEXLA Sector Model:

To understand how CO_2 will behave in the subsurface, we extracted a sector model from a regional geological model based on interpretations of the TexLa Merge 3D seismic dataset to simulate CO_2 injection. This sector model is located offshore the Texas Gulf of Mexico in a deep saline aquifer. Figure 3.53 shows the sector model

grid. In the model, we have specified four geological arbitrarily selected layers of different thickness and permeability. The first layer has an average permeability of 100 mD (millidarcies), the second layer 400mD, the third layer 50 mD and the fourth layer 350 mD.

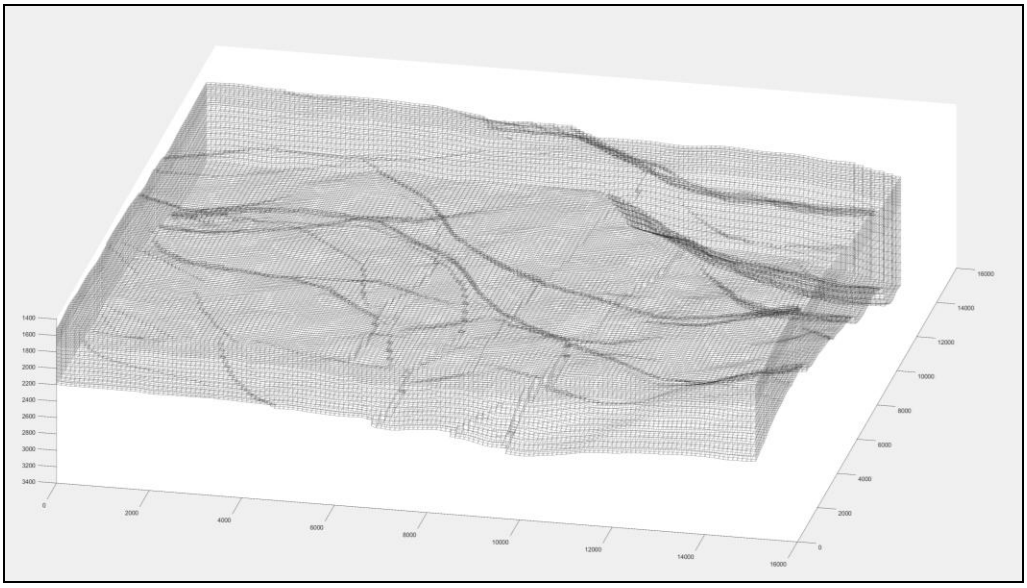

Figure 3.53 - Grid of the sector model extracted from the regional TexLa geological model.

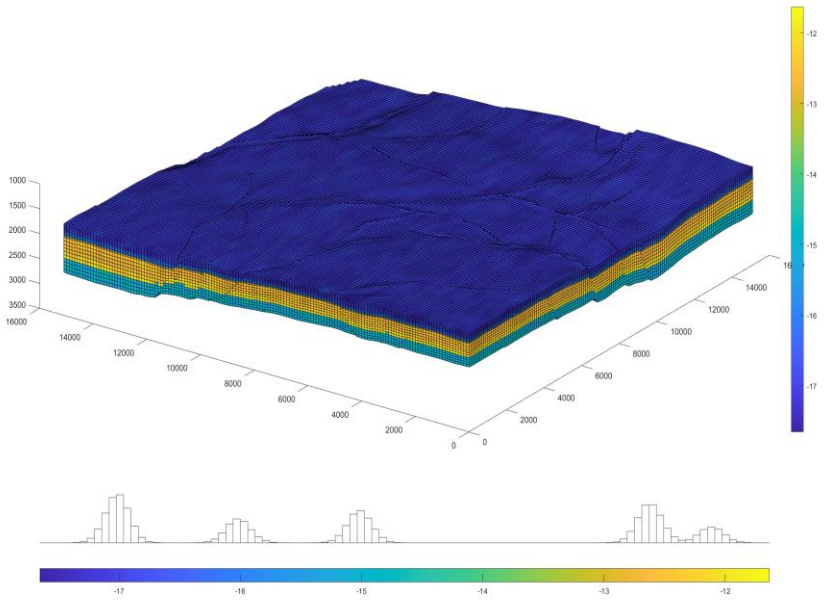

Figure 3.54 - Sector model showing permeability four layers.

CO_2 Modeling:

We subsequently simulated an injection scenario where CO_2 is injected for 100 years, followed by 1000 years of migration. The intended reservoir is the Lower Miocene 2, which is a candidate site for large-scale CO_2 storage. The initial water pressure for the simulations is assumed to be determined by hydrostatic equilibrium with open boundaries. The simulation was performed using Matlab Reservoir Simulation Toolbox. **Error! Reference source**

not found. shows CO_2 saturation distributions after 100 years of injection.

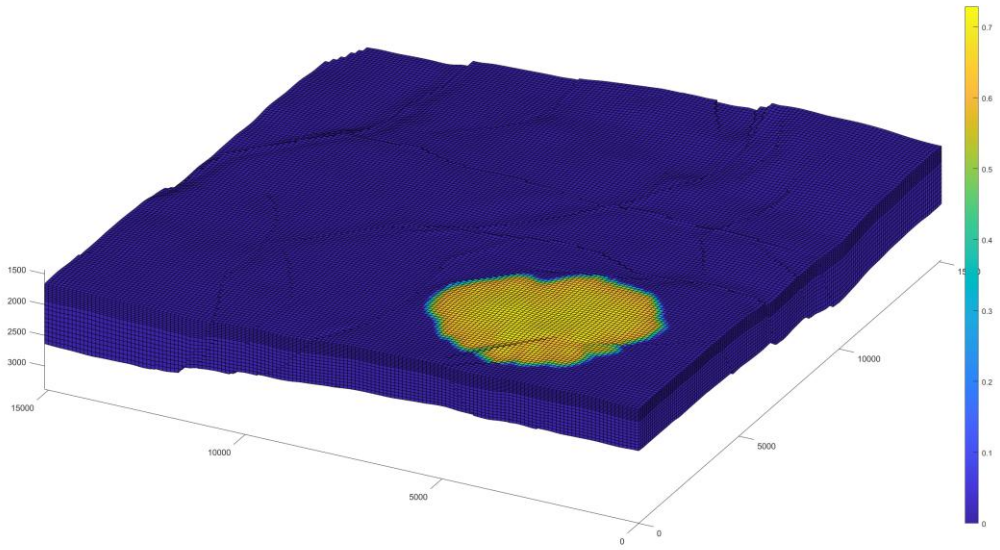

Figure 3.55 - Distribution of CO2 saturation after 100 years of injection.

Error! Reference source not found.shows a cross section of the CO_2 saturation around the injection site. CO_2 migration is highly dependent on the model's permeability. In this example the CO_2 breaks through the layers in the model because of the high permeability used in the model.

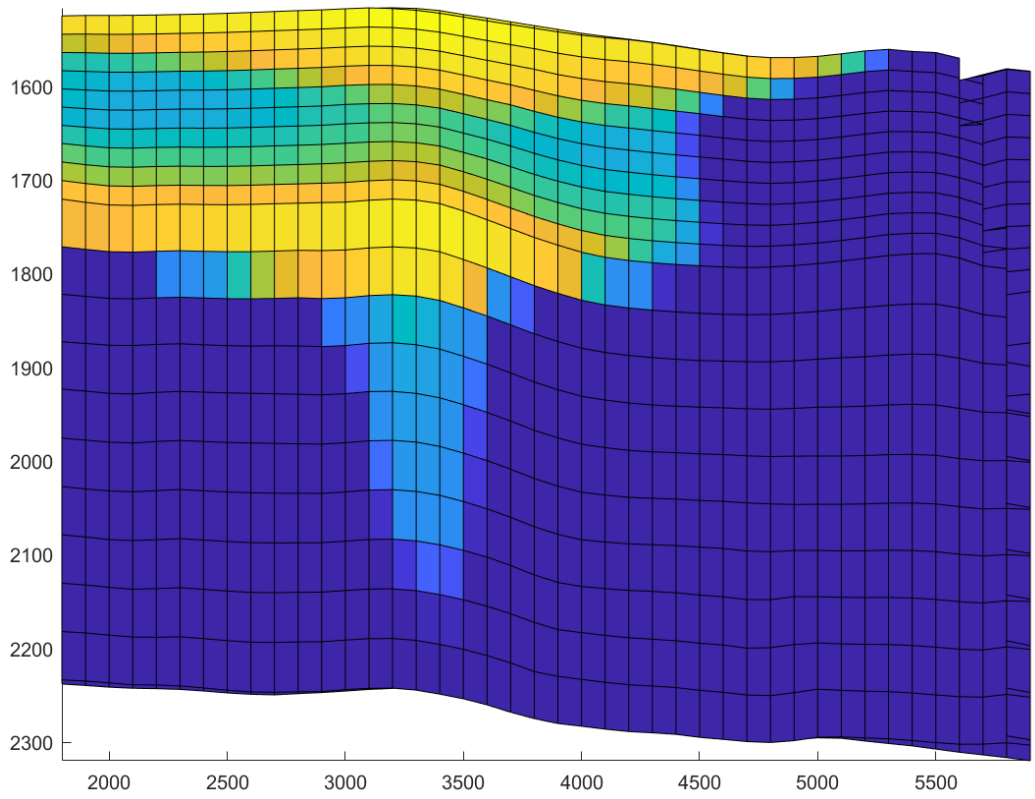

Figure 3.56 - Cross-section of CO2 saturation near the injection well.

3.2.3 Subtask - History matching experiment via modeling

CO_2 saturation prediction with ML (machine learning): Dr. Hailun Ni collaborated on a machine learning (ML) project building a CO_2 saturation prediction model for heterogeneous domains based on their types and degrees of heterogeneity. In order to investigate how grain size and bedform structure affect CO_2 buoyant flow saturation, we ran 118,000 modified invasion percolation simulations on Permedia™, including 59 bedform structures, 40 grain size contrast cases, and 50 stochastic variations. From the simulation results, we found that grain size contrast has a first order impact on the domain drainage CO_2 saturation, while bedform structure only has a second order impact. We also successfully mentored an undergraduate summer student. With the student's help, we were able to develop a multi-feature ML model to predict CO_2 buoyant flow saturation at percolation for heterogeneous domains. The resulting model has a R^2 value of 0.95 on the test dataset, which is quite accurate. Having such a predictive upscaling model is highly desirable for quickly and accurately simulating CO_2 retention amount during the plume's migration to the trap in heterogeneous reservoirs. This work was published in Ni et al. (2023).

Lab-scale ultrasonic sensing: A lab-scale ultrasonic sensing collaborative study was undertaken with Dr. Nicola Tisato's (Figure 3.57). In the field, seismic surveys are commonly conducted to explore local geology. In our one-of-a-kind, lab-scale ultrasonic experimental setup, we applied the same principles to investigate how small-scale heterogeneity affects CO_2 migration and trapping in a tank. We mounted two ultrasonic sensors on motors on a rail and acquired acoustic data by varying the sensor locations while shooting and receiving acoustic signals of the tank. The tank was packed with heterogeneous glass beads and either air or heptane was injected to mimic CO_2

plume buoyant migration through the domain.

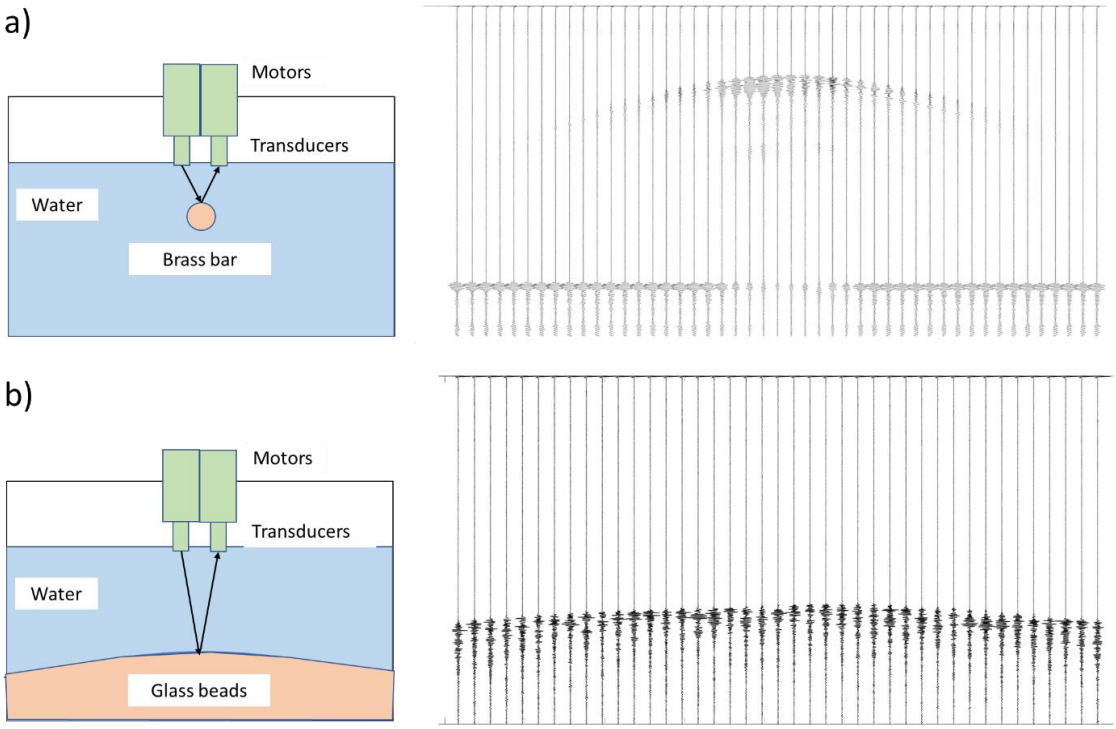

Figure 3.57 – Illustration of the ultrasonic system setup (left) and the corresponding acquired 2D zero-offset images (right) for a submerged brass bar (a) and water-filled glass beads (b).

Baffled containment systems: A set of experiments characterizing CO_2 buoyant migration through baffled systems was conducted. Pre-experiment simulation results showed that in baffled containment systems at the tank scale, both grain size contrast and baffle length are important factors affecting CO_2 buoyant flow saturation. We also conducted experiments on the fining upward sequence that is characteristic of such baffled systems. Shown in Figure 3.58 are the experimental results for three beadpack experiments with varying baffle lengths, shapes, and gradation. Experimental results showed that as the length of baffles increased, both the saturation and the height of the nonwetting phase column increased underneath the baffles. Curvature in the baffle shape further increased the amount of CO_2 trapped, while the effect of gradation was not significant.

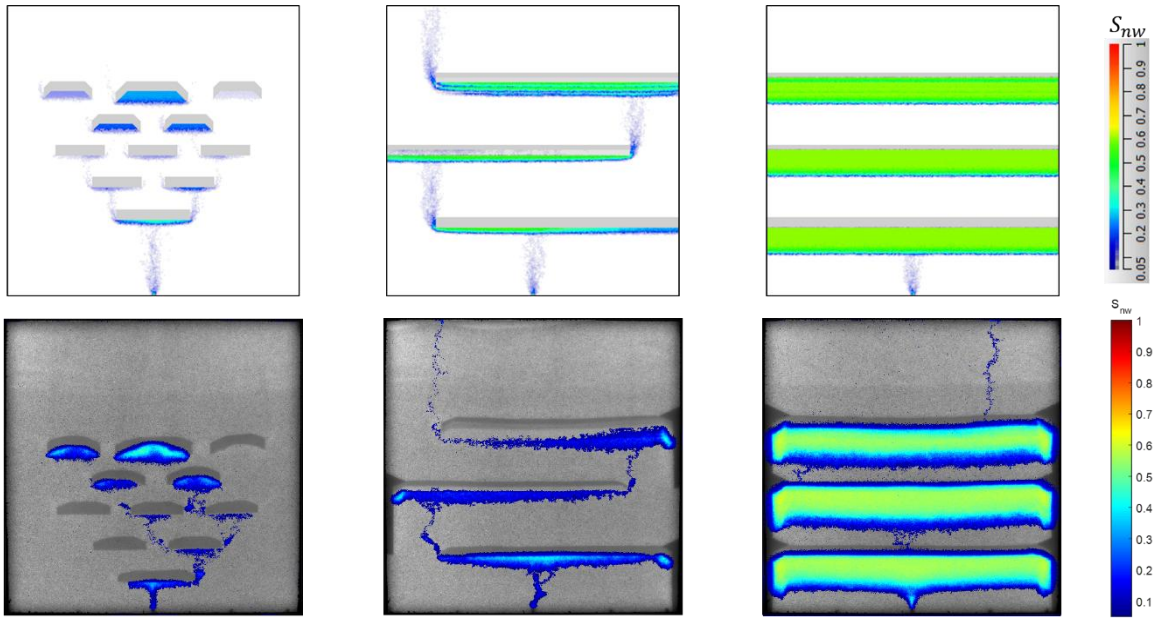

Figure 3.58 - Simulated (upper row) and experimental (lower row) nonwetting phase saturation fields of the beadpack experiments with baffles with different length, shape, and fining upward gradation. The simulator used is a modified invasion percolation simulator.

During geologic carbon storage, the flow regime is strongly capillary- and buoyancy-dominated as the CO_2 plume migrates away from the injection well and during the post-injection redistribution period. Small-scale geological heterogeneities in the targeted storage formations can affect CO_2 saturation and cause a substantial increase in trapped CO_2 during this flow regime. These heterogeneities can retain a significant amount of CO_2 because of capillary heterogeneity trapping, also known as local capillary trapping. Sand tank laboratory experiments have shown that the value of this parameter can vary greatly depending on the type (i.e., geometry) and degree (i.e., grain size contrast) of heterogeneity. This work aims first to investigate the impact of small-scale heterogeneities on trapping performance using sand tank experiments and then examine how heterogeneity-induced trapping affects field-scale simulation results.

Various realistic ripple deposits with varying grain size contrast and wettability were produced using an automated glass bead packing system in a meter-scale slab chamber to study the impact of small-scale heterogeneities trapping performance. A surrogate fluid pair was used to mimic the properties of in-situ brine and supercritical CO_2. Using a light transmission system, we measure the infiltration patterns, capillary heterogeneity trapping, and overall trapping performance. The experimental results showed variations in trapped saturation and capillary heterogeneity trapping exhibited when the ripple bedform architecture was altered (10% to 20% increment) (Figure 3.59). Similar growth in trapping performance is observed when grain size contrast increases. Additionally, wettability changes (water-to-oil-wet) increased nonwetting saturation and capillary heterogeneity trapping up to 5% and 10% to 20%, respectively (Figure 3.60).

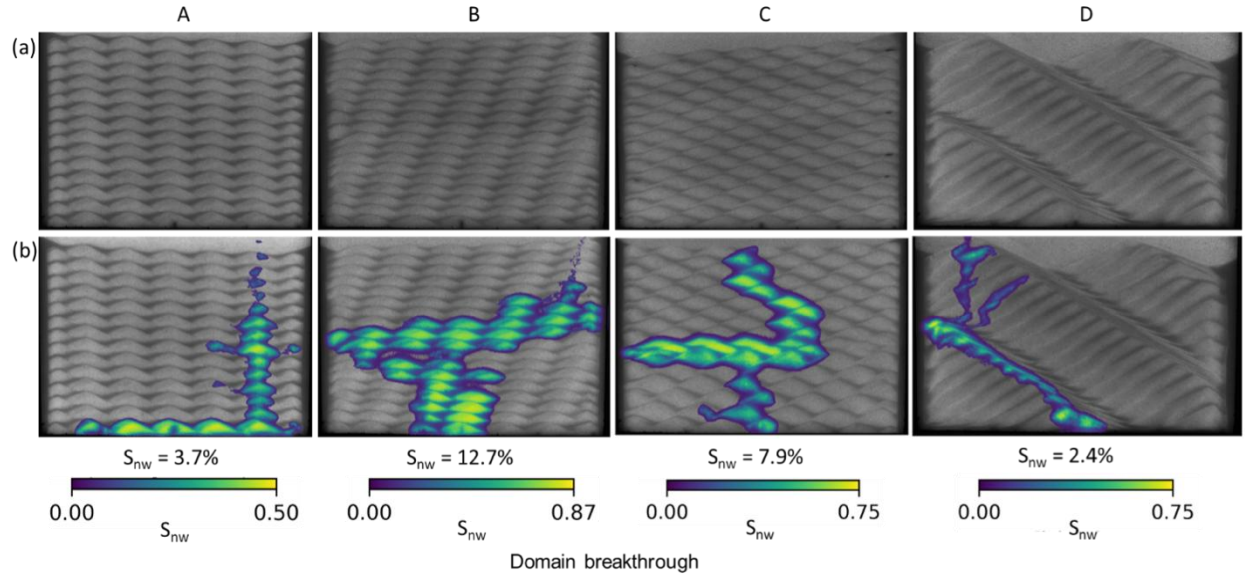

Figure 3.59- (a) Ripple domain patterns with slight changes in the ripple crest phase. A: in-phase, B: slightly out-of-phase, C: out-of-phase, and D: large out-of-phase. (b) Breakthrough nonwetting phase saturation field and domain average saturation values for all patterns. The color bar shows pixel-wise nonwetting saturation.

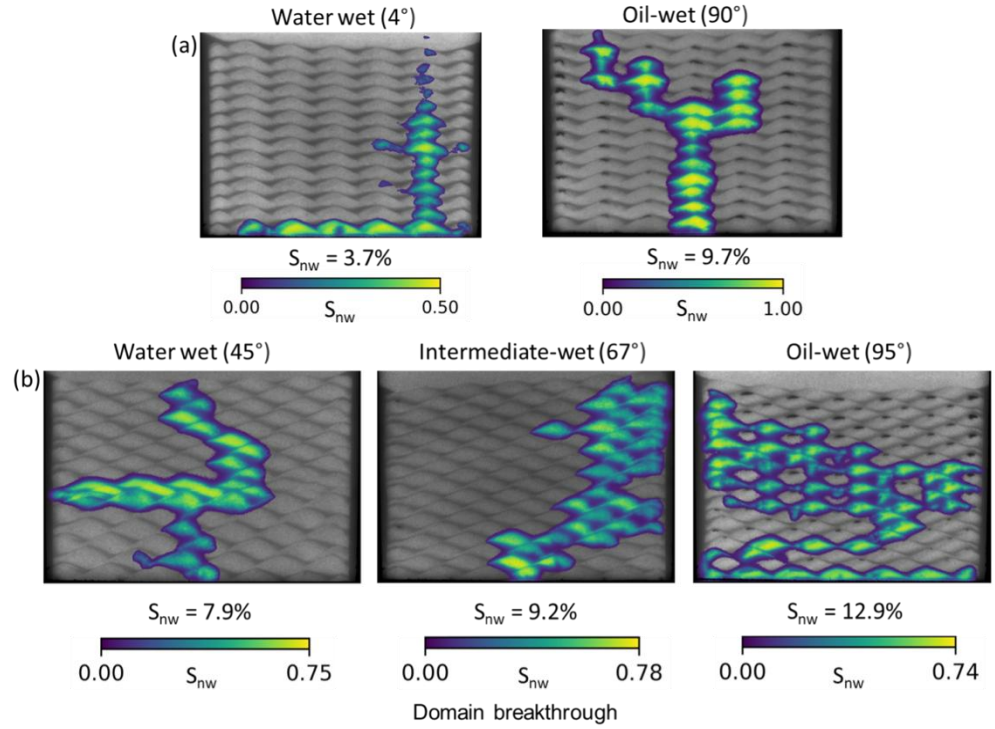

Figure 3.60 - Heptane (representing supercritical CO_2) saturation field and domain average saturation values at breakthrough for in-phase (a) and out-of-phase (b) ripples with varying wettability. The color bar shows pixel-wise nonwetting saturation.

It is crucial to upscale the effect of small-scale heterogeneities adequately; otherwise, it can lead to inaccurate field-scale CO_2 storage simulations. Capillary heterogeneity trapping buoyancy-driven flow can be captured through a parameter known as the critical CO_2 saturation. This parameter, representing the first nonzero value on the CO_2

drainage relative permeability curve, can inform field-scale numerical simulations (Figure 3.61).

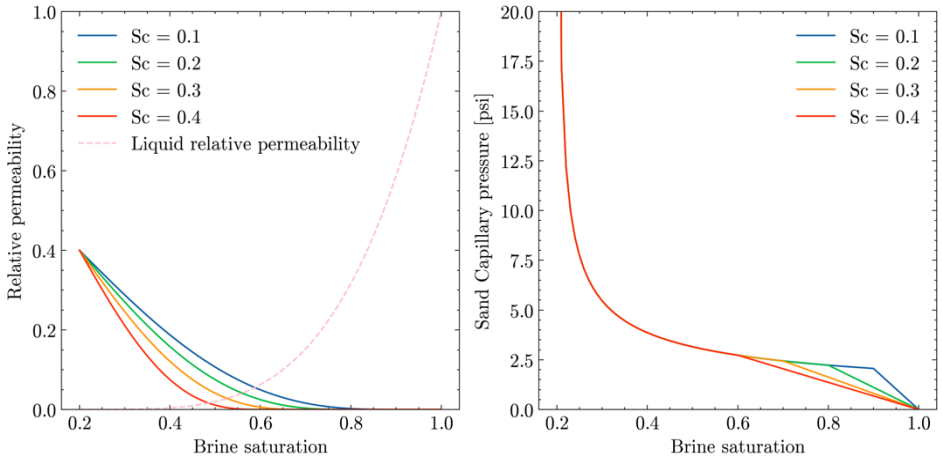

Figure 3.61 - Relative permeability and capillary pressure curves modified by the critical CO_2 saturation.

We conducted numerical full-physics simulations to investigate the influence of critical CO_2 saturation on plume dynamics distribution and trapping mechanisms. Three sets of 2D field-scale simulations were run in a synthetic composite confining system with varying critical CO_2 saturations from 0.1 to 0.4. The first set was implemented without hysteresis and dissolution effects to capture only the impact of critical saturation on residual trapping. The second set included dissolution to understand the role of critical saturation in solubility trapping. Lastly, simulations involving hysteresis and dissolution were performed to study the influence of different trapping mechanisms on CO_2 retention and plume migration.

The simulation showed that the plume size and lateral extent decreased as critical saturation increased, keeping the plume confined within the pore space domain boundaries (Figure 3.62). Moreover, movable gas decreased over time as critical saturation increased. As expected, hysteresis boosted CO_2 residual trapping due to imbibition. However, the impact of imbibition trapping diminished with increasing critical saturation since a more significant proportion of CO_2 had already been trapped during the drainage process thanks to the effect of capillary heterogeneity trapping. Additionally, the VG capillary pressure model contributed more to residual and solubility trapping than the MBC model. These results indicate that the shape of the capillary pressure curve near the critical saturation plays a significant role in trapping mechanisms. Regardless of the capillary pressure model, an increase in critical saturation causes the CO_2 plume dynamics distribution and trapping performance to converge (Figure 3.63).

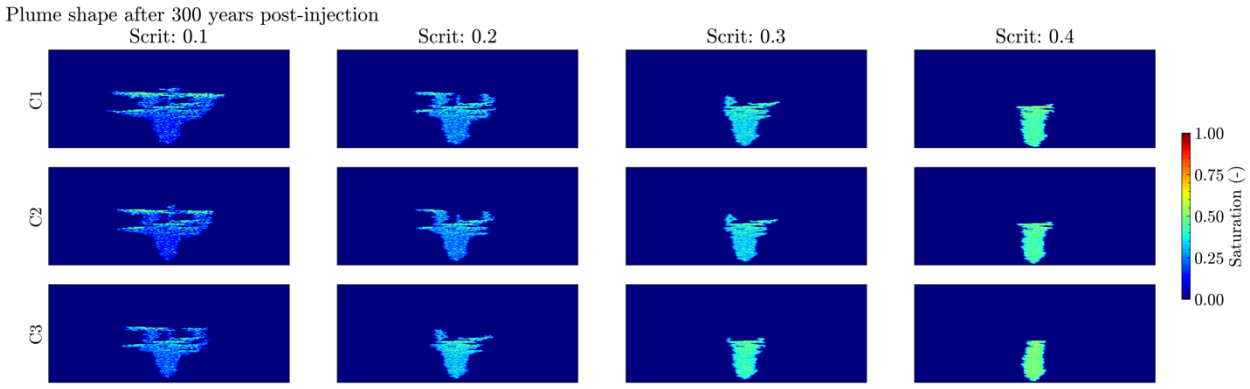

Figure 3.62 - CO_2 plume shape and saturation 300 years after injection with increasing critical CO_2 saturation. C1 to C3 represent multiple selected scenarios. The color bar shows the grid block CO_2 saturation.

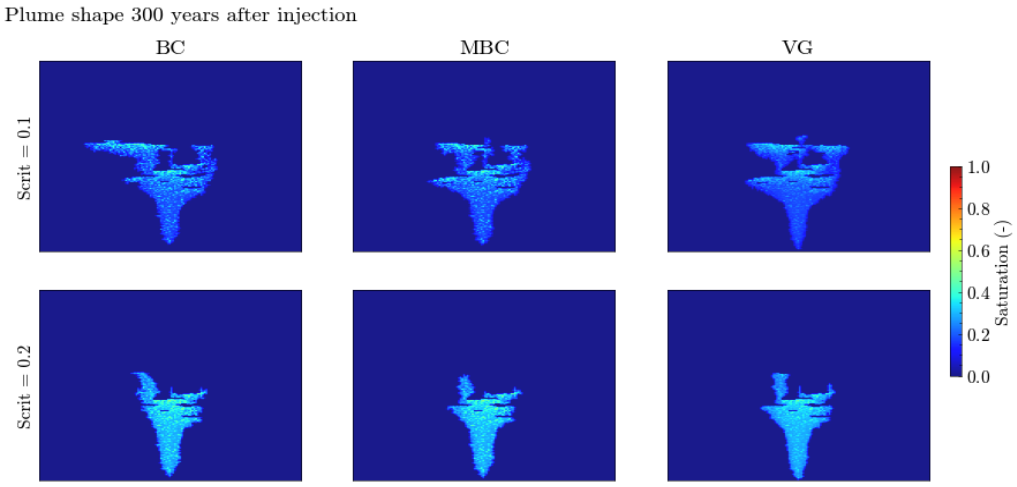

Figure 3.63 - The spatial distribution of the CO_2 plume after 300 years post-injection using multiple capillary pressure models. S_{crit} increases from 0.1 to 0.2. The color bar represents the CO_2 saturation within each grid block.

Critical CO_2 saturation significantly affects the field-scale simulations' plume size, lateral extent, and trapping mechanisms. Therefore, these results provide insightful information about the behavior of CO_2 migration and trapping in heterogeneous geologic formations.

3.2.4 Subtask - Economic modeling

In response to a request from the GoMCarb Partnership, NETL shared their economic modeling package in March 2025. Unfortunately, there was a source code problem in the model that only NETL could fix. The Partnership alerted NETL about the issue, and NETL acknowledged the problem. As the end of the Partnership's period of performance, NETL had been unable to comply with requests to fix the issue.

4. Task 4.0 – Monitoring, Verification, and Assessment (MVA)

4.1 Subtask 4.1: MVA Technologies and Methodologies

4.1.1 Subtask - Geochemical Monitoring of Seabed Sediments

Drs. Romanak and Knap (TX A&M GERG) researched and discussed the methods and measurements required for a purposeful release of CO2. Dr. Knap reviewed also the ANLEC R&D reports and also discussed them with Dr. Romanak

Drs. Romanak (BEG, GCCC) and Knap (Texas A&M, GERG - Geochemical and Environmental Research Group) discussed and reviewed ANLEC R&D reports. ANLEC is an Australian national research initiative supporting Carbon Capture and Storage (CCS) deployment in Australia. ANLEC funded studies in marine monitoring in the Gippsland basin, which subsequently published and can inform our approach in the GoM. They include methods to deploy shallow-focused subsea CCS technologies, Optimizing sensor configurations on fixed and mobile platforms for improved signal retrieval design study of a cabled marine monitoring system and biological Investigation.

More details were in the ANLEC eReport, Issue 29, July 2022 as follows:

Monitoring CCS in the near-shore is different - Methods to deploy shallow-focused subsea CCS technologies

ANLEC R&D funded a major study to inform the development of assurance monitoring approaches for subsea CCS operations in near-shore coastal regions. Over the course of the project the CSIRO team completed 22 voyages in the Gippsland CCS study area, gathering data to characterise the area and test the suitability of equipment (moorings and sensors) for CCS monitoring. This report synthesises the learnings of several research tasks to address key technical assurance monitoring challenges such as:

- The "signal-to-noise" problem: distinguishing CO2 release signatures from similar naturally occurring variability to reduce false alarm rates in future baseline monitoring design,
- Characterising impact: determining the level of CO2 release that would be associated with environmental impact at a range of scales,
- Attributing impact: distinguishing changes resulting from other drivers and pressures in multiple-use zones (e.g. climate change) from the activities of CCS.

Reporting from this work is available as follows:

Integrated Executive Summary on network designs for shallow focussed CCS site marine MMV

This provides an overarching executive summary to the whole project consisting of 7 separate research studies.

The detailed reports from the 7 different studies are provided in the links below

Optimising sensor configurations on fixed and mobile platforms for improved signal retrieval

Key outcomes from the experimental investigation of optimal sensor configurations include:

- The validation, in-field, of sensors integrated on several platforms;
- Conclusion of initial testing of the sensor configurations on the Unmanned Surface Vehicle (USV), moorings and landers;
- The development of operational configurations and procedures for the USV;
- Limited demonstration of near-real time (NRT) data stream processing for data from the sensors due to issues with acoustic performance (with alterations to be implemented prior to the May 2019 field deployment of equipment); and
- The development of initial recommendations for optimisation of the MM&V network design.

Near Real Time and Delayed Mode data QC protocols

The report documents the near-real-time (NRT) and delayed mode (DM) data quality control protocols, metadata structures and archive file formats for data generated by the fixed and mobile platforms deployed into the near shore area during 2018.

Modelling

The work addresses CO_2 plume signal analysis and optimised sensor network configuration within a 3D hydrodynamic model of Bass Strait. Two numerical ocean models were deployed for offshore Gippsland. The models provide unique insight into the morphology of a hypothetical CO_2 release and how it differs from the naturally varying background and allow the detection and impact length scales of any artificial release to be estimated providing critical information for monitoring design.

Biological Investigation

The study focuses on investigation of natural variability in biological indicators of environmental impact. The approach taken has been to first gather biological data on the Gippsland area via a number of targeted field surveys. This data has enabled an understanding of the patterns of diversity and abundance of subtidal benthic sediment infauna, meiofauna and flora present in the area. This data was then considered in the context of international literature on biological impacts of CO_2 to assess whether any biota present in the Gippsland region may prove to be useful parameters for CCS monitoring purposes.

Fixed Platforms

The report highlights application of fixed sensor network designs for CCS site marine measurement, monitoring and verification. The work demonstrates instrumental and operational constraints of fixed MM&V platform deployment into the coastal Gippsland marine environment are now well understood. The surface moorings and seabed landers tested during this project have been proven to be capable of sustained observations of the order of 6 to 9 months without intervention. The on-board sensor systems provided high quality datasets which have enabled characterisation of the oceanographically complex, high energy coastal Gippsland environment. The in-water measurements taken during the deployments have also begun to characterise the tidal, diurnal and seasonal variation at the Gippsland study site. These data have been critical calibration data for the 3D biogeochemical models developed for the project.

Mobile Platforms

The work reports on considerations for integration of mobile platforms with a fixed sensor design network. It investigates how the spatio-temporal variance structure of a marine CCS site may be characterised and monitored using mobile monitoring platforms. Within the marine technology domain, it is widely acknowledged that autonomy will underpin the future of ocean operations. Unmanned surface and autonomous underwater vehicles (USVs and AUVs) are rapidly evolving in their performance, sophistication, and accessibility.

The work demonstrates that mobile platforms are an essential part of a MM&V crewed vessels and unmanned surface vessels play a valuable and differentiated MM&V role.

Design study of a cabled marine monitoring system

This work delivers a design study for integrating the sensor technologies into a cabled observatory concept. It was designed to provide a CCS proponent with several options that will permit robust and cost-effective Marine M&V plans to be developed. It reports on engineering constraints, data processing requirements and a suite of sensors and platforms that might be employed during the planning process.

Several cabled observatory configuration scenarios, from sparsely to highly instrumented, were developed and discussed to compare and contrast different deployment configurations and replications of the core 3 - platform system. In addition, three potential construction and maintenance vessel options were examined and a cost developed.

4.1.2 Subtask - Geochemical Monitoring of Seawater Column

The following was part of a manuscript in preparation in federal quarter four of 2021.

The USA has a long history of research and development in CCS which began in 2003 with the Frio Brine Pilot injection [1]. With onshore monitoring approaches and technologies robustly tested, proven and developed, the US is now moving towards characterizing and developing its offshore resources, specifically in the Gulf of Mexico and

along the Atlantic Coast. In addition to providing increased national storage capacity, offshore storage sites have advantages in those concerns over the protection of underground sources of drinking water, the need to secure leases from multiple landowners, and the lack of population and corresponding need for public engagement are reduced [2]. Challenges of moving offshore are generally operational and economic, because access to offshore infrastructure for build out and upkeep decreases with increasing water depth. In cases where the offshore hosts prolific oil and gas activities such as in the GoM, pre-existing infrastructure could be repurposed for CO2 transport and injection, however this infrastructure also includes historic oil and gas wells which could become pathways for leakage from the reservoir to the seabed [3, 4]. Thus, characterization and monitoring activities can utilize lessons learned from onshore projects and other offshore global projects, but they must be tailored to the specific environmental conditions of the offshore environment in which they will be applied.

We first consider the large-scale processes occurring in the GoM. This type of assessment provides; 1) an overview of the large-scale factors that should be considered when assessing potential CO2 leakage, and 2) an understanding of how monitoring approaches at other subseabed storage projects (e.g., as in Tomakomai Bay, Japan or the North Sea) might be applicable to the GoM. These assessments are needed because CO2 gas is a highly reactive component of the bio-geochemical carbon cycle in the marine environment. It can exist in the seawater column and in marine sediments as either a geochemical product or a reactant, either consumed or produced by a myriad of biotic and abiotic transformations. To develop leakage detection and attribution approaches for CO2 geologic storage beneath the seabed in the GoM, the most important carbon cycling processes must be geochemically constrained. Such constraints will lead to methods for distinguishing CO2 leakage from naturally-occurring CO_2 in the ocean and ocean sediments. We begin by outlining the macro systems of the GoM and will continue to determine those local processes that could be important for developing leakage location and attribution approaches for the CO2 storage beneath the GoM.

Overall, continental margins represent some of the largest areas of carbon cycling in the ocean, but these systems are difficult to characterize, and the data needed for in-depth assessment are sparse, especially in the GoM [5]. To address the need for quantifying carbon flux in the GoM, and to identify gaps in the data required for such calculations, the Ocean Carbon and Biogeochemistry (OCB) Program and the North American Carbon Program (NACP) collaborated to improve understanding of the large-scale dynamics affecting carbon fluxes. One such collaborative effort was the Gulf of Mexico Coastal Synthesis workshop where working groups were established to analyze each type of carbon flux in detail. Whereas the workshop focused on quantifying net carbon fluxes due to each input, the insights on the processes presented have relevance for developing leakage detection methods in for CO2 geological storage in the GoM [5].

The main sources and sinks of carbon in the near coastal shelf marine environment that were deemed important include river input, estuarine fluxes, submarine groundwater discharge, air-sea fluxes, primary production, respiration and net community production (NCP), and exchange at the ocean boundary. The report outlines 5 regions within the GoM based on the different inputs, biogeochemical characteristics and processes. These regions and their dominant drivers are:

- West Florida Shelf (WFS) - influenced by upwelling, river discharge, and groundwater influx
- Louisiana Shelf (LA) - river dominated, receiving major discharge from the Mississippi---Atchafalaya River system creating variable seasons of significant hypoxia.
- Texas Shelf (TX) - dominated by upwelling and by eddies shed from the Loop Current
- Mexican Shelf (MX) - influenced by upwelling and by groundwater and river (Usumacinta---Grijalva) discharge
- Open Gulf – deep semi-enclosed oligotrophic basin with an energetic circulation strongly connected to the Caribbean Sea and Atlantic Ocean.

The Louisiana shelf and Texas shelf regions are concurrent with the study sites for the GoMCARB GoM project (outlined in black) as seen in Figure 4.1.

Figure 4.1 - Map of regions of the GoM separated based on the dominant physio-chemical drivers. The GoMCARB study area roughly correlates with the Texas and Louisiana shelf regions. Map is modified from Benway and Coble, 2014.

TX-shelf Loop current

The Loop Current is a dominant control on the circulation within the GoM and forms when warm water travels up from the Caribbean, past the Yucatan Peninsula, and into the Gulf of Mexico (Figure 4.2). The loop current then travels eastward and south along the Florida coast, exiting the GoM at the straits of Florida. The strength of the Loop Current is highly variable on weekly, monthly and annual time scales. At times it barely enters the GoM and at other times it penetrates almost as far as the Louisiana coast [6]. When the loop is elongated, it is unstable and can form large-scale clockwise-spinning eddies that travel westward and down the western gulf as far as the Texas coast. These eddies are also affected by winds and fresh water runoff at the coast that mixes with ocean water. The Loop Current and related eddies support a wealth of sea life such as pelagic fish moving into the Gulf of Mexico from the Caribbean Sea and also drives mass distribution of primary producers such as phytoplankton [7]. Thus, the loop current and its associated eddies can have an impact on overall carbon cycling within TX-shelf areas of the GoM.

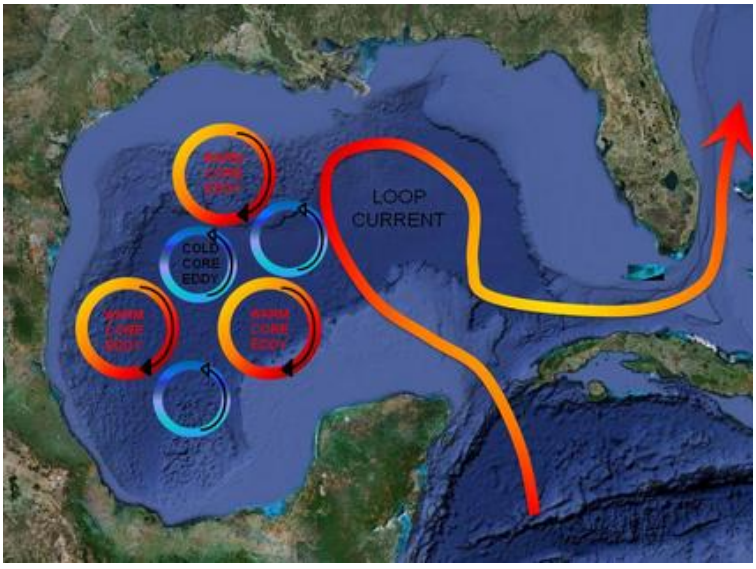

Figure 4.2 - The Loop Current in the GoM and associated eddies. Map from https://texaspelagics.com/gom-

info/gom-loop/ accessed 10/8/2021

La-shelf Hypoxia and the Sediment/Seawater column interface

A large area of the continental shelf off Louisiana is seasonally hypoxic (< 2mg O2/L) west of the Mississippi River plume where the freshwater plume enters the GoM. This hypoxia is caused by high concentrations of nitrate in agricultural runoff [8, 9], excess suspended and dissolved organic matter [10], vertical water column stratification [11, 12], and the seasonal reversal of coastal currents [13]. The size of the area can be predicted from annual Mississippi River runoff in the Spring [14, 15]. During uncommonly 'wet' years, it has been known to stretch into Texas waters [13].

The sediment uptake of oxygen (SCOC) and the release of CO2 (DIC), as well as the regeneration of inorganic nutrients, have been investigated in the hypoxic area using benthic chambers [12, 16-21]. These benthic chamber incubations in hypoxic conditions illustrate that the ratio of DIC to SCOC can be high (> 1.0) when oxygen uptake rate is limited by low oxygen concentrations [11, 22].

The Mechanisms Causing Hypoxia (MCH) project conducted 14, 24-hour anchor-station time series during which a comprehensive suite of observations was made in the water column, including oxygen flux. Four of the locations have been analyzed in substantial detail. They reveal the rate at which oxygen is produced during the day and consumed, by respiration, during the night. DIC should be the reverse of oxygen (i.e., taken up during the day and released at night). However, DIC was not measured. A model of the day-night sequence of oxygen assumes a 1 to 1 stoichiometric relationship between oxygen and DIC and predicts that the water column DIC production is greater than the DIC regeneration from the sediment, in agreement with Lehrter et al. 2012 [19]. Quantifying loss of oxygen (respiration) in the water column is difficult [23, 24]. This approach and the resulting model need to be repeated and the model validated with 24-hour anchor stations in Texas water that is not associated with seasonal hypoxic conditions.

Benthic Chambers

Incubation chambers have a considerable history for measuring the flux of dissolved gases across the sediment water interface [25]. Oxygen decline in the chamber is used to estimate sediment community oxygen consumption, or respiration. Inorganic nutrient regeneration can be added as an estimate of 'benthic-pelagic coupling' [26] [20]. Dissolved inorganic carbon (DIC) can be included, as it has been in studies of the hypoxic area off Louisiana [17, 27]. The benthic chamber flux measurements were extended into the deep sea using autonomous landers [28, 29] or deep submergence research vessels [30]. Gradients of solutes in the sediments can be used to estimate fluxes, but these can underestimate the turnover of organic matter (regeneration of DIC) because considerable metabolism occurs on the surface of the sediment [31]. Pore water in cores could be used to estimate solute movement that might be coming from deep stored CO_2, however. Primary production (taking up DIC and producing oxygen) by diatoms living on the sediment surface can be estimated by using paired clear and opaque chambers. An issue with these 'batch' incubations is that the system within the enclosure 'crashes' as oxygen declines to limiting levels, although some possible approaches allow refreshing the chamber with oxygen using an oxygen-permeable 'gill' (Morse [17] et al. 1999). The characteristics of the numerous designs of benthic chambers now in use world-wide have been compared in an exhaustive set of laboratory study [32, 33].

The DIC sediment flux measurements in the northern GoM using benthic chambers is limited to Galveston Bay, the Texas continental shelf and the seasonally hypoxic area off. The flux of DIC out of the sediment is slightly higher than the oxygen flux into the sediment, according to the latter data. More data are needed to confirm the background stoichiometry and thus separate natural production of CO2 by respiration from escape of geologically sequestered CO2 at depth in the sediment. Benthic chambers will be a useful, available tool in assessing CO2 exchanges at the sediment water interface.

References

1. Hovorka, S., Frio brine pilot: The first US sequestration test. Southwest Hydrology, 2009. 8(5): p. 26-31.

2. CSLF, Technical Barriers and R&D Opportunities for Offshore, Sub-Seabed Geologic Storage of Carbon Dioxide. 2015, Report Prepared for the Carbon Sequestration Leadership Forum (CSLF) Technical Group. p. 128.

3. Nazarian, B. and P. Ringrose. Risk Associated with Legacy Wells in CCS and CO2 EOR Projects; a Simulation Study. in 79th EAGE Conference and Exhibition 2017. 2017. European Association of Geoscientists & Engineers.

4. Pawar, R.J., et al., Recent advances in risk assessment and risk management of geologic CO 2 storage. International Journal of Greenhouse Gas Control, 2015. 40: p. 292-311.

5. Benway, H.M., and Coble, P. G. (Editors), Report of The U.S. Gulf of Mexico Carbon Cycle Synthesis Workshop, 2013. 2014. p. 64.

6. Brokaw, R.J., B. Subrahmanyam, and S.L. Morey, Loop current and eddy-driven salinity variability in the Gulf of Mexico. Geophysical Research Letters, 2019. 46(11): p. 5978-5986.

7. Damien, P., et al., Do Loop Current eddies stimulate productivity in the Gulf of Mexico? Biogeosciences, 2021. 18(14): p. 4281-4303.

8. Rabalais, N.N., R.E. Turner, and D. Scavia, Beyond Science into Policy: Gulf of Mexico Hypoxia and the Mississippi River: Nutrient policy development for the Mississippi River watershed reflects the accumulated scientific evidence that the increase in nitrogen loading is the primary factor in the worsening of hypoxia in the northern Gulf of Mexico. BioScience, 2002. 52(2): p. 129-142.

9. Rabalais, N.N., et al., Hypoxia in the northern Gulf of Mexico: Does the science support the plan to reduce, mitigate, and control hypoxia? Estuaries and Coasts, 2007. 30(5): p. 753-772.

10. Bianchi, T.S., et al., The science of hypoxia in the Northern Gulf of Mexico: a review. Science of the Total Environment, 2010. 408(7): p. 1471-1484.

11. Rowe, G.T., Seasonal hypoxia in the bottom water off the Mississippi River delta. Journal of Environmental Quality, 2001. 30(2): p. 281-290.

12. Rowe, G. and P. Chapman, Hypoxia in the northern Gulf of Mexico: some nagging questions. Gulf Mex Sci, 2002. 20: p. 153-60.

13. Jarvis, B.M., et al., Modeling spatiotemporal patterns of ecosystem metabolism and organic carbon dynamics affecting hypoxia on the Louisiana Continental Shelf. Journal of Geophysical Research: Oceans, 2020. 125(4): p. e2019JC015630.

14. Turner, R., N. Rabalais, and D. Justić, Predicting summer hypoxia in the northern Gulf of Mexico: Redux. Marine Pollution Bulletin, 2012. 64(2): p. 319-324.

15. Turner, R., N. Rabalais, and D. Justic, Predicting summer hypoxia in the northern Gulf of Mexico: Riverine N, P, and Si loading. Marine pollution bulletin, 2006. 52(2): p. 139-148.

16. Miller-Way, T., et al., Sediment oxygen consumption and benthic nutrient fluxes on the Louisiana continental shelf: a methodological comparison. Estuaries, 1994. 17(4): p. 809-815.

17. Morse, J.W., G. Boland, and G.T. Rowe, Agilled'benthic chamber for extended measurement of sediment-water fluxes. Marine chemistry, 1999. 66(3-4): p. 225-230.

18. Berelson, W.M., et al., Benthic fluxes from hypoxia-influenced Gulf of Mexico sediments: Impact on bottom water acidification. Marine Chemistry, 2019. 209: p. 94-106.

19. Lehrter, J.C., et al., Sediment-water fluxes of dissolved inorganic carbon, O 2, nutrients, and N 2 from the hypoxic region of the Louisiana continental shelf. Biogeochemistry, 2012. 109(1): p. 233-252.

20. Nunnally, C.C., et al., Benthic–pelagic coupling in the Gulf of Mexico hypoxic area: Sedimentary

enhancement of hypoxic conditions and near bottom primary production. Continental Shelf Research, 2014. 85: p. 143-152.

21. Nunnally, C.C., et al., Sedimentary oxygen consumption and nutrient regeneration in the northern Gulf of Mexico hypoxic zone. Journal of Coastal Research, 2013(63 (10063)): p. 84-96.

22. Hetland, R.D. and S.F. DiMarco, How does the character of oxygen demand control the structure of hypoxia on the Texas–Louisiana continental shelf? Journal of Marine Systems, 2008. 70(1-2): p. 49-62.

23. Dortch, Q., et al., Respiration rates and hypoxia on the Louisiana shelf. Estuaries, 1994. 17(4): p. 862-872.

24. Guo, X., et al., M., Jiang, L.-Q. and Culp, R.: CO2 dynamics and community metabolism in the Mississippi River plume. Limnol. Oceanogr, 2012. 57: p. 1-17.

25. Teal, J.M. and J. Kanwisher, GAS EXCHANGE IN A GEORGIA SALT MARSH 1. Limnology and Oceanography, 1961. 6(4): p. 388-399.

26. Rowe, G.T., et al., Benthic nutrient regeneration and its coupling to primary productivity in coastal waters. Nature, 1975. 255(5505): p. 215-217.

27. Rowe, G.T., et al., Sediment community metabolism associated with continental shelf hypoxia, northern Gulf of Mexico. Estuaries, 2002. 25(6): p. 1097-1106.

28. Smith Jr, K.L., et al., A free vehicle for measuring benthic community metabolism 1. Limnology and Oceanography, 1976. 21(1): p. 164-170.

29. Rowe, G.T., et al., Sediment community oxygen consumption in the deep Gulf of Mexico. Deep Sea Research Part II: Topical Studies in Oceanography, 2008. 55(24-26): p. 2686-2691.

30. Smith, K. and J. Teal, Deep-sea benthic community respiration: an in situ study at 1850 meters. Science, 1973. 179(4070): p. 282-283.

31. Rowe, G.T. and A.P. McNichol, Carbon cycling in coastal sediments: estimating remineralization in Buzzards Bay, Massachusetts. Geochimica et Cosmochimica Acta;(United States), 1991. 55(10).

32. Tengberg, A., et al., Intercalibration of benthic flux chambers: II. Hydrodynamic characterization and flux comparisons of 14 different designs. Marine Chemistry, 2005. 94(1-4): p. 147-173.

33. Tengberg, A., et al., Benthic chamber and profiling landers in oceanography—a review of design, technical solutions and functioning. Progress in Oceanography, 1995. 35(3): p. 253-294.

4.1.3 Subtask - UHR3D Seismic

In federal quarter 2 of 2022 on NETL project DE-FE0028193, it was determined that future federally-funded high-resolution 3D surveys would require a finding of no significant impact (FONSI) after preparation and submission of an environmental assessment (EA) to the NETL NEPA office, which would determine whether or not a FONSI was warranted. If so, the survey could proceed. The same process was required for the GoMCarb Partnership before a GoMCarb UHR3D seismic survey would be possible. The EA process for GoMCarb began in federal quarter 2 of 2024 and resulted in a FONSI issued on January 23, 2026. Similarly, the EA process included application to the National Marine Fisheries Service (NMFS) for an incidental harassment authorization (IHA) of protected species. The original IHA was issued on January 12, 2025. However, because the FONSI was not issued until late January 2026, the original IHA had already expired on January 13, 2026. In anticipation of this issue, the GoMCarb PIs submitted a request for reissuance of the IHA to NMFS on October 8, 2025.

As of January 29, 2026, which was the go/no-go date for the scheduled early February survey cruise, the required reissuance of the IHA (incidental harassment authorization) issued by NMFS was still pending. Consequently, the survey was postponed. Nonetheless, the UT (University of Texas at Austin) management team was able to

negotiate with subrecipient TDI-Brooks Intl., Inc. for an open-ended commitment to have a ship available throughout February and until mid-March. Therefore, the UT team continued to communicate with NMFS regarding the need to receive a re-issued IHA. UT was informed that there was no technical reason that the IHA had not been re-issued. In fact, the technical review had ended and been forwarded with a positive recommendation for NMFS management approval.

As of mid-February, the UT co-PIs had to set a deadline of February 20 for a go/no-go decision for the HR3D survey (i.e., because of survey crew availability and logistical reasons). Meanwhile, the co-PIs informed the NETL Project Manager about the situation, and he communicated the issue to his management up to and including DOE headquarters (HQ). The co-PIs were informed that DOE HQ was in communication with the NOAA (National Oceanic and Atmospheric Administration) Policy group regarding the IHA issue. In addition, the co-PIs had informed ExxonMobil, the state waters leaseholder of the blocks to be surveyed by the HR3D, and ExxonMobil informed NMFS that they supported the survey and requested that the IHA be re-issued.

Despite all the internal and external support for the survey, the IHA was not re-issued by NMFS. Apparently, the re-issuance request was refused for policy/political reasons and not for technical reasons. NMFS communicated the following: "After consultation with DOE, we will *not* be issuing the permit at this time... DOE is communicating with the applicant regarding potential revisions to the project, so no further action is needed on our part until we hear otherwise from the lead agency." Consequently, the survey had to be canceled, and with only one month left in the period of performance, there were no revisions to the project. This result is significant for future federally supported HR3D surveys.

4.1.4 Subtask - Distributed Acoustic Sensors

During Q1 FY2023 the team at Rice University continued our efforts examining passive seafloor DAS for reservoir leakage monitoring. As discussed in our Q4 2022 report, we have been working on passive acoustic monitoring of seafloor gas leaks using DAS. During prior quarters, we developed and improved our marine testing tank to include fiber instrumentation at both the water column/sediment boundary as well as buried within sediment to probe the expected response for different installation conditions. During Q1 FY2023 we also upgraded our system to generate CO_2 gas plumes (vs N_2) as well as to allow for finer control of gas emission rates via a more precise mass flow regulator.

With improved flow control, we started to investigate acoustic signal variation during CO_2 bubble emission as a function of leakage rates. We showed that the noise from the simulated seafloor bubble plume had measurable spectral peaks, likely characteristic of the bubble size at the sediment interface. During Q1 FY2023, we conducted several experiments where we examined RMS acoustic noise levels within the water column as a function of leakage rate. Figure 4.3 shows the results from two sets of experiments investigating RMS acoustic energy in the water column as a function of gas flow rates varied between 100 mL/min to 1 L/min; for reference, 100 mL/min is sufficiently slow that bubbles are only intermittently generated. The green dots indicate data acquired with the prior manual flow controller while the blue dots show the improved mass flow controller. In this case, RMS acoustic energy values were derived from the hydrophone datasets due to challenges with appropriate triggering of the DAS acquisition system. As can be seen, RMS acoustic noise increases linearly with flow rate assuming a fixed measurement distance. Higher RMS variability was observed at higher flow rates; these differences may be related to sediment disturbance. Small pock marks were observed at the sediment interface above the gas emission port. Similar features have been observed during seafloor studies of active methane seeps.

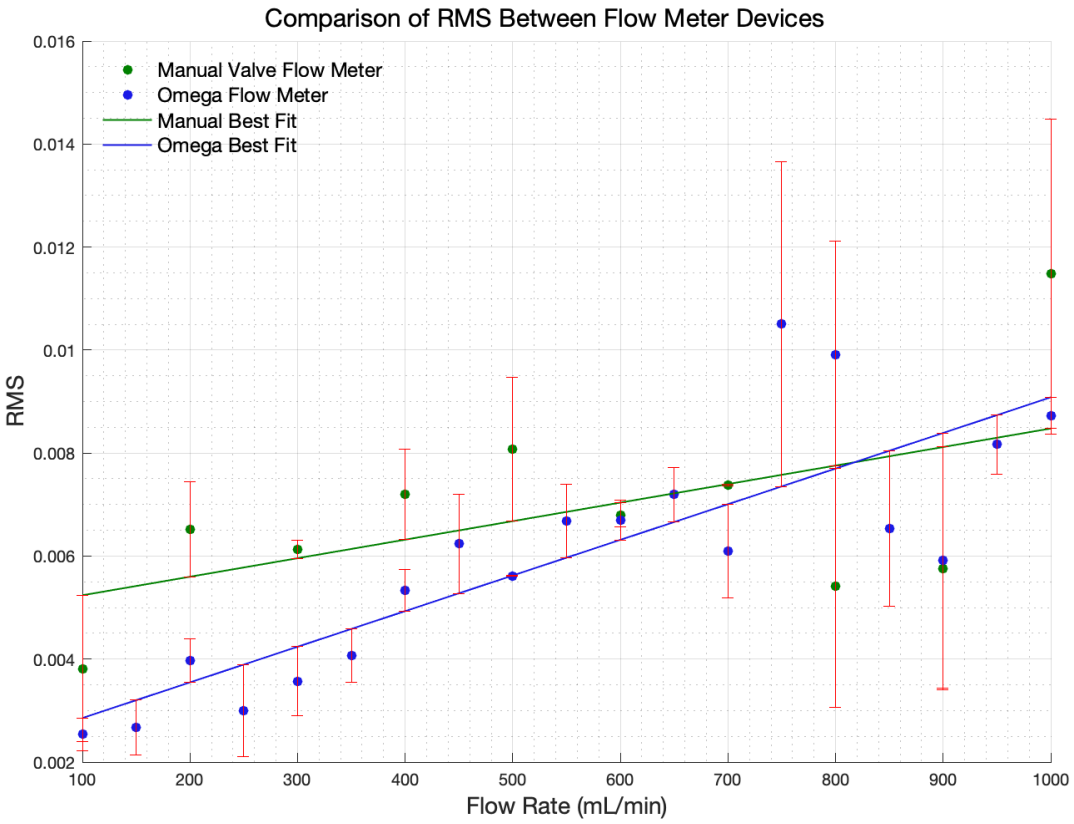

Figure 4.3 – RMS signal amplitude generated by simulated gas leakage as a function of volumetric flow rate at the sediment interface. Data show for both the first generation ("manual") and improved mass flow controllers.

Another activity was software development to allow simplified triggering, recording, and processing of DAS data in similar experiments. While the initial results shown above were acquired with a triggered hydrophone, we are now capable of performing such measurements with the DAS cable discussed previously. A key question we hope to address is the differences between the acoustic signatures measured in the water column and the strain signal measured by DAS coupled to seafloor sediment. The latter would provide insight as to whether seafloor DAS will be an effective tool for measuring the passive signals generated by CO_2 leakage into the water column. Based on the results of these experiments, we are planning a small field gas release experiment in May/June 2023 to evaluate this approach in a shallow water environment.

The Rice team's research established that, in a laboratory environment, passive aquatic DAS measurements can be used to measure gas flux and potentially bubble size from leakage, even at relatively low flow rates. However, they have not yet established the lateral distance at which such detection can be accomplished as well as the performance of such systems in more realistic environments with higher noise levels. In order to better constrain the uncertainties, they conducted a small field experiment and have been analyzing the acquired data. Note that the fieldwork portion of the research was not financially supported by GoMCarb or any federal funding source.

To assist in answering some of our outstanding questions concerning detectability, we executed a micro-pilot field-scale monitoring experiment at Lake Conroe, Texas. The deployment utilized a DAS fiber placed above the lakebed, paired with a custom-built low-frequency acoustic source designed to minimize disturbance to marine life. The experiment compared passive recordings of bubble noise with active monitoring strategies to assess DAS's performance in the noisy near-shore environment. **Error! Reference source not found.** shows the location of the test site (a), the conceptual fiber layout (b), and the final mapped fiber trajectory (c).

Figure 4.4 - The location of our DAS bubble detection micro-pilot experiment. (a) pilot location at Lake Conroe, TX, (b) notional fiber network design, (c) mapped cable geometry.

The primary goal of our micro-pilot study was to determine whether DAS can detect bubble acoustics or whether they are masked by ambient noise (wind-induced and anthropogenic) in the natural environment at varying flow rates. This micro-pilot builds on the earlier laboratory experiments, which demonstrated a linear relationship between the RMS amplitude of bubble acoustic signals and flow rates (Figure 4.3). In addition to passive monitoring of gas injection, active monitoring with a controlled resonant seismic source were conducted. The DAS fiber, a PE-jacketed tactical cable with 4 x SM fibers, was deployed in a U-shaped geometry along a pier, extending 150 meters offshore for a total length of ~300 meters, at water depths ranging from 2 to 4.5 meters, as shown in Figure 4.4. Shallow burial of the fiber at two locations near the pier was attempted, but time constraints with the temporary field location limited the effectiveness of this method which could be significantly improved with a permanent field site. Gas was introduced into the lakebed sediment using a short insertion pipe and gas flux was controlled using a mass flow regulator at rates from 100 ml/min to 2 L/min. A controlled seismic source was mounted on the dock to allow timelapse imaging in the water column as well as passive listening for bubble noise. Figure 4.5a shows the dock deployment geometry and Figure 4.5b shows CO_2 bubbles rising from the lake floor "leakage" point.

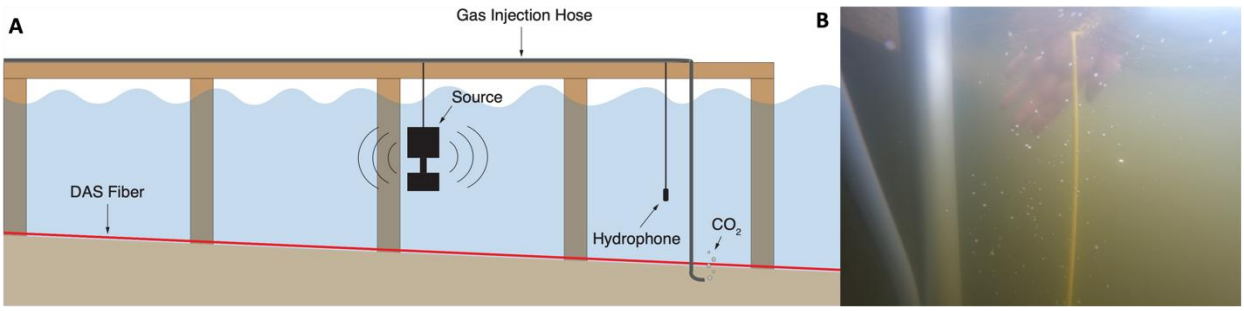

Figure 4.5 - Schematic of dock showing experimental source, CO2 leak point, and DAS fiber. Panel (b) shows CO2 rising in the water column.

In active source DAS monitoring of lakebed sediments, bubbles were expected to attenuate seismic signals in both the water column and at the sediment interface due to the low Q of gassy materials. Initial findings suggest that bubble signals at the highest flow rates remain unresolved in passive monitoring although our analysis is on-going. This was a prediction made prior to the experiment, believed to be likely due to masking by near-shore ambient noise. However, cross-correlation analysis of the low-frequency source data revealed minimal attenuation of the source signal at the injection point (Figure 4.6). Furthermore, our experimental low-frequency source did not generate sufficiently high amplitudes to effectively record high S/N at distant offsets. Our signal processing workflow is still in development, and further refinement is required before concluding the effectiveness of DAS for detecting gas leakage in shallow, noisy, offshore environments. There are several noises of uncertain origin that are still being filtered from the dataset, and we expect improved results in future quarters.

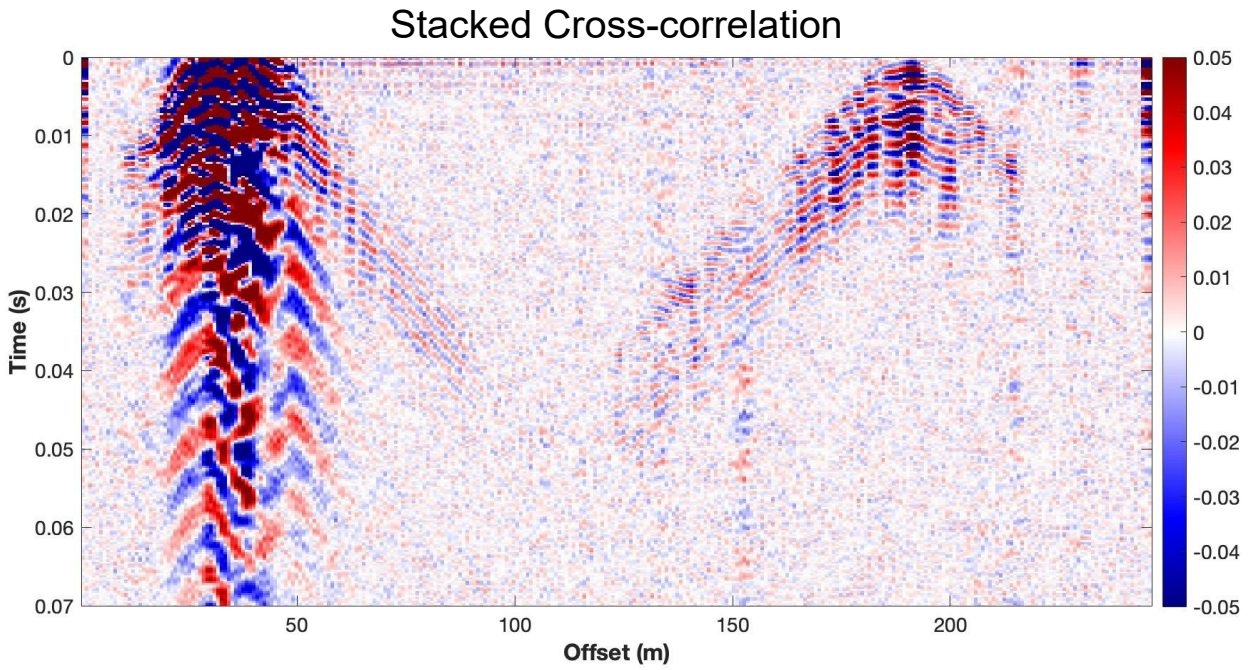

Figure 4.6 - Stacked cross-correlation recorded during 1000 and 2000 mL/min injections.

4.1.5 Subtask - Pipeline MVA

The 3-D modeling of hypothetical High Island 10L CO_2 leaks into the Gulf of Mexico were simulated with ANSYS Fluent. The boundary conditions were investigated based on experimental (literature) CO_2 property data, literature gas leak models, and Aspen Plus simulations. The boundary conditions then will be implemented in the upcoming CFD simulations. CO_2 dissolution kinetics, mass transfer coefficient is estimated using Hughmark correlation is used in this work. Seawater temperature and salinity is used for estimating Dissociation and Henrys Law constant.

1. Mathematical Model for Bubble Plume

The Ansys Fluent software was utilized to perform the simulation. Ansys Fluent is computational fluid dynamics software that can be used to model a variety of fluid flow problems. It provides different models options to simulate different flow regimes. For the simulation of this work, the Eulerian, Turbulence, Mass Transfer, Drag and Lift Force, and Chemical Reaction were selected.

1.1 Eulerian Model

The Eulerian Model simulates the interaction between a gas and liquid. Figure 4.7 describes the continuity and momentum equations used.

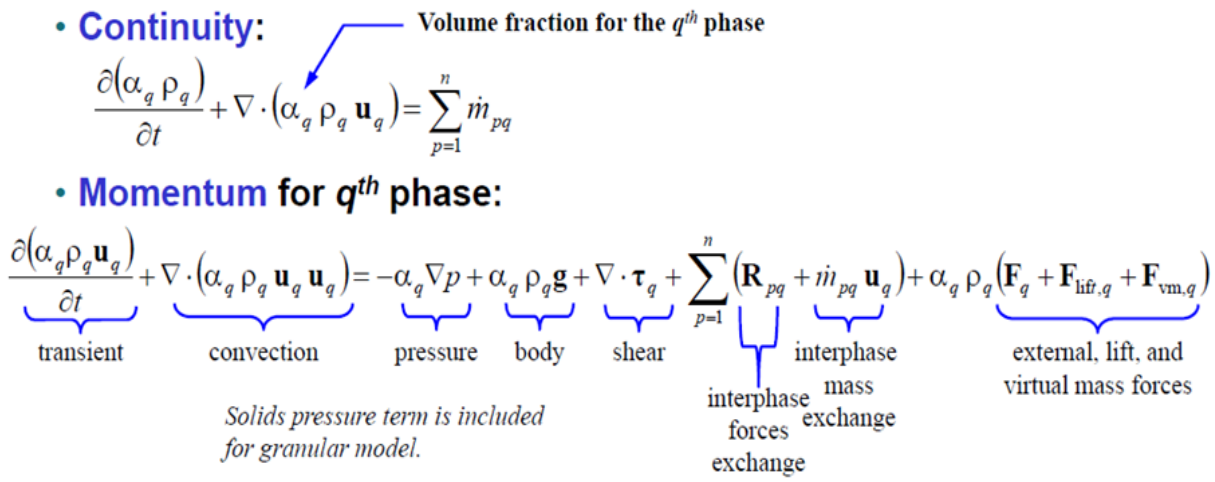

Figure 4.7 - Continuity and Momentum Equations, Ansys (2010)

Where the volume fraction can be expressed as:

$$\alpha = \frac{Volume\ of\ Phase\ in\ Cell}{Volume\ of\ Cell} \qquad \text{Eqn 4.1.5.1}$$

1.2 Turbulence Model

The turbulent model used is the standard k- ε. It uses the transport equations based on the turbulence kinetic energy (k) and its dissipation rate (ε). Eqn 4.1.5.2 and 4.1.5.3 describe the transport equations used in the turbulent model standard k- ε.

$$\frac{\partial(\rho k)}{\partial t} + \text{div}\,(\rho k \vec{u}) = \text{div}\left(\frac{\mu_t}{\sigma_k}\text{grad}\ k\right) + 2\mu_t S_{ij} \cdot S_{ij} - \rho\varepsilon \qquad \text{Eqn 4.1.5.2}$$

$$\frac{\partial(\rho \varepsilon)}{\partial t} + \text{div}\,(\rho \varepsilon \vec{u}) = \text{div}\left(\frac{\mu_t}{\sigma_s}\text{grad}\ \varepsilon\right) + C_{1s}\frac{\varepsilon}{k}2\mu_t S_{lj} \cdot S_{ij} - C_{2\varepsilon}\rho\frac{\varepsilon^2}{k} \qquad \text{Eqn 4.1.5.3}$$

Where G_k represents the generation of turbulence kinetic energy due to the mean velocity gradients, G_b is the generation of turbulence kinetic energy due to buoyancy, Y_M represents the contribution of the fluctuating dilatation in compressible turbulence to the overall dissipation rate, $C_{1\varepsilon}$, $C_{2\varepsilon}$ and $C_{3\varepsilon}$ are constants. k and ε are the turbulent Prandtl numbers for σ_k and σ_ε respectively. S_k and S_ε are user-defined source terms.

Table 4.1 - Default values of model constant $C_{1\varepsilon}$, $C_{2\varepsilon}$, C_μ, σ_k and σ_ε.

Model Constants	$C_{1\varepsilon}$	$C_{2\varepsilon}$	C_μ	σ_k	σ_ε
Default Value	1.44	1.92	0.09	1.0	1.3

1.3 Mass Transfer Model

The Two Resistance Model (Figure 4.8) was utilized to simulate the mass transfer.

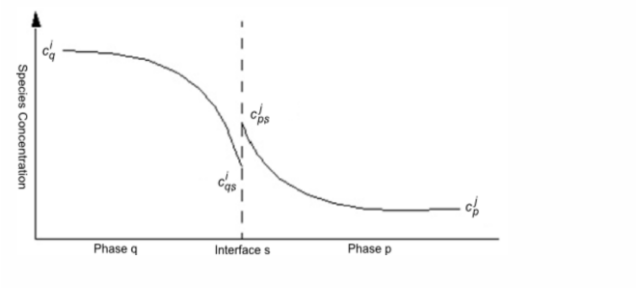

Figure 4.8 - Mass Transfer Two Resistance, Ansys (2020)

The mass transfer rate equation can be expressed as:

$$\dot{m}_q = K_L A\left(C_{q,s} - C_q\right) \quad \text{Eqn 4.1.5.4}$$

where $\dot{m}_q$ is the mass transfer rate (kg/s), K_L is the overall mass transfer coefficient (m/s), A is the interfacial area (m^2), $C_{q,s}$ is the mass concentration at the interface and C_q is the mass concentration at the seawater phase (kg/m^3). K_L can be expressed as:

$$\frac{1}{K_L} = \frac{1}{k_L} + \frac{1}{k_G H_c} \quad \text{Eqn 4.1.5.5}$$

where, k_L is the mass transfer coefficient of the liquid phase (m/s), k_G is the mass transfer coefficient of the gas phase (m/s) and H_c is Henry's law constant. For gases that are not very soluble in water like CO_2, the mass transfer is controlled by liquid the mass transfer coefficient. The overall mass transfer can be expressed as:

$$\frac{1}{K_L} = \frac{1}{k_L} \quad \text{Eqn 4.1.5.6}$$

In this study the mass transfer rate per volume was evaluated. The mass transfer rate per volume can be expressed as:

$$\frac{\dot{m}_q}{V} = K_L a\left(C_{q,s} - C_q\right) \quad \text{Eqn 4.1.5.7}$$

where $\dot{m}_q/V$ is the mass transfer rate per volume ($kg/s\ m^3$) and a is the interfacial area per volume (m^2/m^3).

The Hughmark correlation, equations 8 to 11 is used to estimate the mass transfer coefficient. The Hughmark correlation can be expressed as:

$$k_p = \frac{ShD}{L} \quad \text{Eqn 4.1.5.8}$$

$$Sc = \frac{\mu}{\rho D} \quad \text{Eqn 4.1.5.9}$$

$$Re = \frac{\rho|V_q - V_p|d}{\mu} \quad \text{Eqn 4.1.5.10}$$

$$Sh = 2 + 0.95 Re^{\frac{1}{2}} Sc^{\frac{1}{3}} \quad \text{Eqn 4.1.5.11}$$

Where kd is the mass transfer coefficient, Sh the Sherwood number, Sc the Schmidt number, Re the Reynolds

number, L, and d the CO_2 bubble diameter, μ_{water} dynamic viscosity, ρ_{water} the density and $|V_{water}-V_{CO2}|$ the magnitude relative velocities of the phases. The correlation is a function of the CO_2 diameter and the velocities of seawater and CO_2.

1.4 Drag and Lift Force

The drag force is simulated by the Grace model. It is used for gas and liquid flows when bubbles have different shapes. The lift force is simulated by the Tomiyama model. It is used for deformable bubbles.

1.5 Chemical Reaction Model for Carbonate System

CO_2 participates in several reactions when it comes into contact with aqueous solutions. One of these is the dissolution of the gaseous CO_2:

$$CO_{2\,(g)} \rightleftharpoons CO_{2\,(aq)} \qquad \text{Eqn 4.1.5.12}$$

When carbon dioxide (CO_2) is absorbed by seawater, chemical reactions occur that reduce seawater pH, carbonate ion concentration, and saturation states of biologically important calcium carbonate minerals.

In the ocean, carbon dioxide exists in three different inorganic forms: as free carbon dioxide, aqueous Carbon dioxide, as bicarbonate and as carbonate ion. A fourth form is carbonic acid; the concentration of carbonic acid is, however, much smaller than that of aqueous Carbon dioxide ($\sim< 0.3\%$).

When CO_2 dissolves in seawater it forms carbonic acid (H_2CO_3) (Eqn 4.1.5.14). Carbonic acid rapidly dissociates to produce bicarbonate ions (HCO_3^-) (Eqn 15). In turn, bicarbonate ions can also dissociate into carbonate ions (CO_3^{2-}) (Eqn 4.1.5.16). Both reactions (Eqn 4.1.5.15 & 4.1.5.16) also produce protons (H^+) and therefore lower the pH of the seawater.

Hydration and dehydration of CO_2 in aqueous bicarbonate–carbonate solutions occur by the following reaction mechanisms in parallel.

Reaction mechanism I – Acidic

$$CO_2 + H_2O \rightleftharpoons H_2CO_3 \rightleftharpoons H^+ + HCO_3^- \rightleftharpoons 2H^+ + CO_3^{2-} \qquad \text{Eqn 4.1.5.13}$$

$$CO_2 + H_2O \rightleftharpoons H_2CO_3 \qquad \text{Eqn 4.1.5.14}$$

$$H_2CO_3 \rightleftharpoons H^+ + HCO_3^- \qquad \text{Eqn 4.1.5.15}$$

$$HCO_3^- \rightleftharpoons H^+ + CO_3^{2-} \qquad \text{Eqn 4.1.5.16}$$

By combining the reaction rate constants, the reactions (Eqn 4.1.5.14), and (Eqn 4.1.5.15) can be summarized as

$$CO_2 + H_2O \rightleftharpoons HCO_3^- + H^+ \qquad \text{Eqn 4.1.5.17}$$

$$HCO_3^- \rightleftharpoons CO_3^{2-} + H^+ \qquad \text{Eqn 4.1.5.18}$$

Using CO_2 instead of carbonic acid and aqueous carbon dioxide (Eqn 4.1.5.12) and equilibria (Eqn 4.1.5.13) can be simplified as:

$$CO_2 + H_2O \rightleftharpoons H^+ + HCO_3^- \rightleftharpoons 2H^+ + CO_3^{2-} \qquad \text{Eqn 4.1.5.19}$$

The sum of the dissolved forms CO_2, HCO_3^-, and CO_3^{2-}, is called total dissolved inorganic carbon, which we will denote by $T_{(DIC)}$

$$T_{(DIC)} = [CO_2] + [HCO_3^-] + [CO_3^{2-}] \qquad \text{Eqn 4.1.5.20}$$

The water itself dissociates to form H+ and OH− ions:

$$H2O \rightleftharpoons H^+ + OH^- \qquad \text{Eqn 4.1.5.21}$$

Reaction mechanism II – Alkaline

$CO_2 + OH^- \rightleftharpoons HCO_3^-$ Eqn 4.1.5.22

$HCO_3^- + OH^- \rightleftharpoons CO_3^{2-} + H_2O$ Eqn 4.1.5.23

The overall reaction which occurs when CO_2 is desorbed from an aqueous bicarbonate– carbonate solution is.

$2HCO_3^- \rightleftharpoons CO_2 + CO_3^{2-} + H_2O$ Eqn 4.1.5.24

When a substantial amount of OH− ions is present, the alkaline mechanism predominates, and reaction (6) is completely shifted to the right. Thus, the overall reaction, which is assumed to occur when CO2 is released from a strong alkaline aqueous solution, can be expressed as follows:

$CO_3^{2-} + H_2O \rightleftharpoons CO_2 + 2OH^-$ Eqn 4.1.5.25

The pH was calculated with the concentration of H^+. The initial pH was set to 8.2. Eqn 4.1.5.26 was used to calculate the pH.

$$pH = -\log 10[H+]$$ Eqn 4.1.5.26

The reaction rates applied for the study are as follows.

$R_{CO2} = - k_{1f}[CO_{2(aq)}] + k_{1r}[HCO_3^-][H^+] - k_{2f}[CO_{2(aq)}][OH^-] + k_{2r}[HCO_3^-]$ Eqn 4.1.5.27

$R_{H+} = k_1[CO_{2(aq)}] – k_{1r}[HCO_3^-][H^+]$ Eqn 4.1.5.28

$R_{HCO3-} = k_1[CO_{2(aq)}] - k_{1r}[HCO_3^-][H^+] + k_{2f}[CO_{2(aq)}][OH^-] - k_{2r}[HCO_3^-]$ Eqn 4.1.5.29

$R_{OH-} = -k_{2f}[CO_{2(aq)}][OH^-] + k_{2r}[HCO_3^-]$ Eqn 4.1.5.30

The pH, temperature, salinity and pCO_2 values are used for the estimation of initial concentration of species in seawater using the methodology mentioned in Table 4.2 and are defined in the simulation (as initial mass fraction).

Table 4.2 - Initial Concentration Estimation

Remarks		
Concentration of Hydrogen ions	$[H^+] = 10^{-pH^{SW}}$	Eqn 4.1.5.31
Concentration of Bicarbonate ions	$[HCO_3^-] = \frac{TA[H^+]+[H^+]^2-K_W^{SW}}{[H^+]+2K_2^{SW}}$	Eqn 4.1.5.32
Concentration of Carbonate ions	$[CO_3^{2-}] = \frac{K_2^{SW}[HCO_3^-]}{[H^+]}$	Eqn 4.1.5.33
Concentration of Dissolved Carbon dioxide	$[CO_2] = \frac{[HCO_3^-][H^+]}{K_1^{SW}}$	Eqn 4.1.5.34
Concentration of Hydroxide ions	$[OH^-] = \frac{K_W^{SW}}{[H^+]}$	Eqn 4.1.5.35
Total alkalinity of carbonate system	$TA = 0.0001185 * Cl$	Eqn 4.1.5.36
	$Cl = \frac{S}{1.80655}$	Eqn 4.1.5.37

K_w^{SW} is on the basis mol/kg seawater, T is in K and S is in g/kg. The equilibrium constant of water in seawater K_w^{SW} was measured for temperatures up to 35°C and salinities up to 44 g/kg	$\log K_w^{SW} = -\left(\frac{3441}{T} + 2.241 - 0.09415 S^{0.5}\right)$ Eqn 4.1.5.38
K_2^{SW} is on the basis mol/kg seawater, T is in K and S is in g/kg	$\ln K_2^{SW} = -0.84226 - \frac{3741.1288}{T} - 1.437139 \ln T + \left(-0.128417 - \frac{24.41239}{T}\right) S^{0.5} + 0.1195308 S - 0.00912840 S^{1.5}$ Eqn 39
K_1^{SW} is on the basis mol/kg seawater, T is in K and S is in g/kg	$\ln K_1^{SW} = 2.18867 - \frac{2275.036}{T} - 1.468591 \ln T + \left(-0.138681 - \frac{9.33291}{T}\right) S^{0.5} + 0.0726483 S - 0.00574938 S^{1.5}$ Eqn 40
Because the main constituent of seawater is NaCl (73% of the ionic strength of seawater), the ion specific parameters of Na^+ and Cl^- are the only considered parameters.	$\log\left(\frac{H_{G,W}}{H_{G,Sw}}\right) = hI$ Eqn 4.1.5.41 $h = h_+ + h_- + h_G$ Eqn 4.1.5.42 $h_+ = 0.091$ L/mol $h_- = 0.021$ L/mol $h_g = -5*10^{-3} - 5.3*10^{-4}$ $\log H_{CO_2,W} = 108.3865 + 0.01985076 \cdot T - \frac{6919.53}{T} - 40.45154 \cdot \log T + \frac{669365}{T^2}$ Eqn 43

2. Simulation setup

2.1 Meshing and Patching

In Ansys Fluent meshing comprises of triangular or quadrilateral cells (or a combination of the two) in 2D. The choice of which mesh type is dependent on the application, setup time, computational time, and numerical diffusion. To capture accurately the vertical rising and horizontal migration distance at a lower computational cost, structured Hexcore meshing is used as shown in Figure 4.9(a).

To define an interface between air and water column(seawater) in the simulation setup, volume of fluid (VOF) method is used. VOF is a free-surface modelling technique that tracks and locates the free surface (or fluid–fluid interface). It belongs to the class of Eulerian methods which are characterized by a mesh that is either stationary or is moving in a certain prescribed manner to accommodate the evolving shape of the interface. VOF allows the software to track the shape and position of the interface, but its algorithm does not solve flow problem standalone, therefore Navier–Stokes equations describing the motion of the flow must be solved separately. Here, water is defined as the primary phase mainly for convenience in setting up the problem, and air as secondary phase. While

defining the initial solution, patching was done as shown in Figure 4.9(b). It is more convenient to patch a water volume fraction of 1 there than to patch an air volume fraction of 1 in the domain.

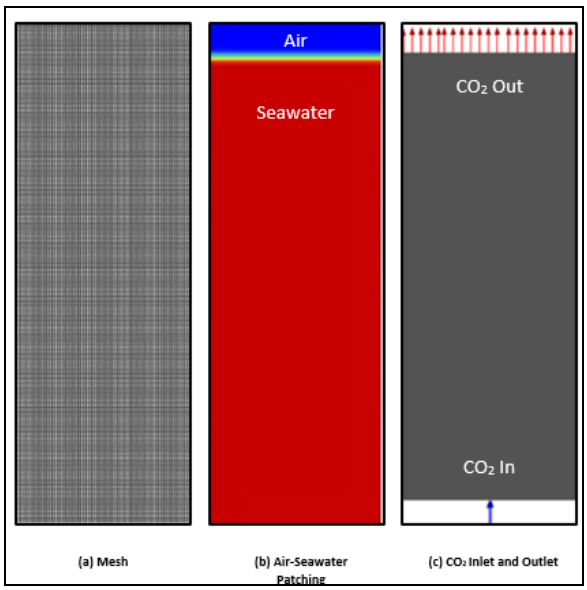

Figure 4.9 (a) - Meshing used for simulation (Hexcore), (b) Air and Seawater patching and (c) Carbon dioxide Inlet and Outlet

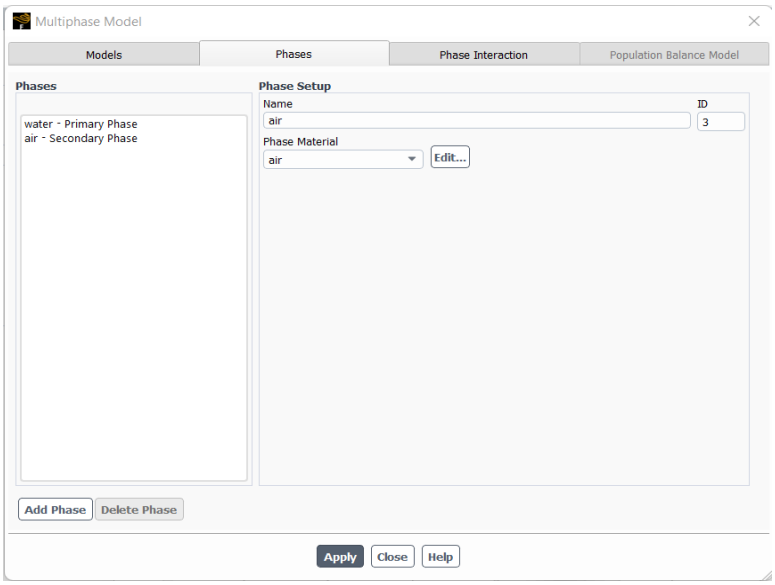

Figure 4.10 - Phase setup for patching

2.2 Boundary and Initial Conditions

The boundary conditions as shown in Table 4.3 are the following ones: Mass Flow inlet boundary condition was defined at the bottom side to allow Carbon dioxide to enter the domain. The velocity of current was set as 0.15 m/s. Besides, initial turbulence parameters such as turbulent kinetic energy, k, and turbulent dissipation rate, ε, were also defined at this boundary. It is crucial to specify these parameters at the inlet boundaries for simulation of the turbulence flows due to their influences on the development of the fluctuation turbulence field (Tauseef et al.,

2011). Seawater pH was set to 8.2 and temperature of 22.8 C.

The Eulerian multiphase model was selected with two phases, Seawater phase (water-CO_2) and CO_2 phase. The seawater phase consists of $H_2O_{(l)}$, $H_2CO_{3(l)}$, $HCO_3^-{}_{(l)}$, $CO_3^{-2}{}_{(l)}$, $CO_{2(l)}$ and $H^+{}_{(l)}$ and $OH^-{}_{(l)}$. While the CO_2 phase consists of only pure $CO_{2\ (gas)}$. The initial mass concentration of seawater phase was estimated using Table 4.2 based on the temperature, salinity, pH and $pCO_{2(initial)}$ values of seawater and entered in the simulation as initial condition.

Table 4.3 - Boundary Conditions (Olsen et al. 2017)

		Units	**50m depth**
CO_2 Properties			
Pressure of CO_2 at leakage orifice		Mpa	4
Temperature at orifice		C	13
CO_2 density at orifice		Kg m^{-3}	106.4
Diameter of orifice		m	0.0508 (2 in)
Area of orifice		m2	0.002027
CO_2 leakage flowrate		Kg s^{-1}	35.52
Mass flux-based velocity		M s^{-1}	162.3
CO_2 surface tension		N m^{-1}	0.05
CO_2 bubble size		mm	0.5
Seawater Properties			
Seawater temperature		C	22.8
Ambient Salinity		ppt or g kg^{-1}	34.5
Seawater Density		Kg m^{-3}	1025
Seawater Ambient Current		ms^{-1}	0.15
Seawater pH			8.2

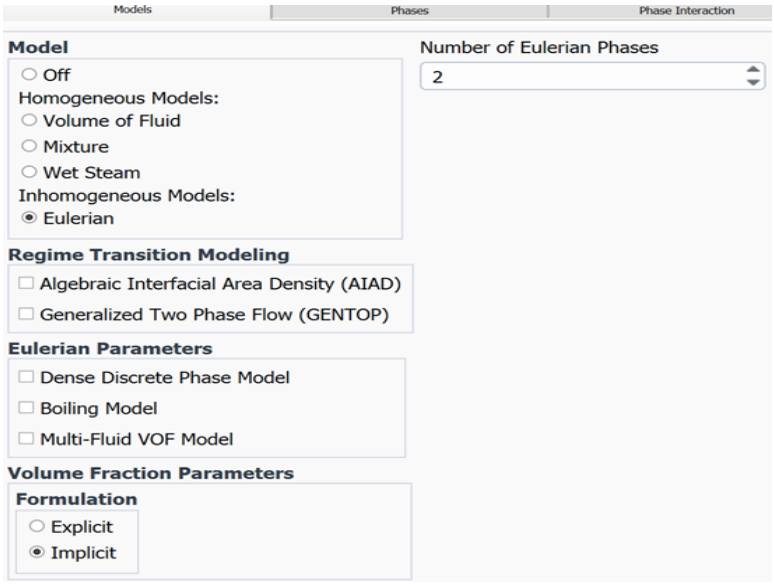

Figure 4.11 - Eulerian Multiphase Model setup (Seawater phase and CO_2 phase).

2.3 Reaction Model Setup

The reaction rate constants and equations are added to the simulation to model the reaction of Carbon dioxide with Seawater. The Reaction Dialog Box in Ansys Fluent allows to define the reactions that comprise a mixture, here Water-CO2 mix. The Mixture tab shows the species defined in the system, the stoichiometric coefficient, and the rate constant (Table 4.4) for the reactant species defined in the Stoich. Coefficient and Rate Exponent Tab's respectively.

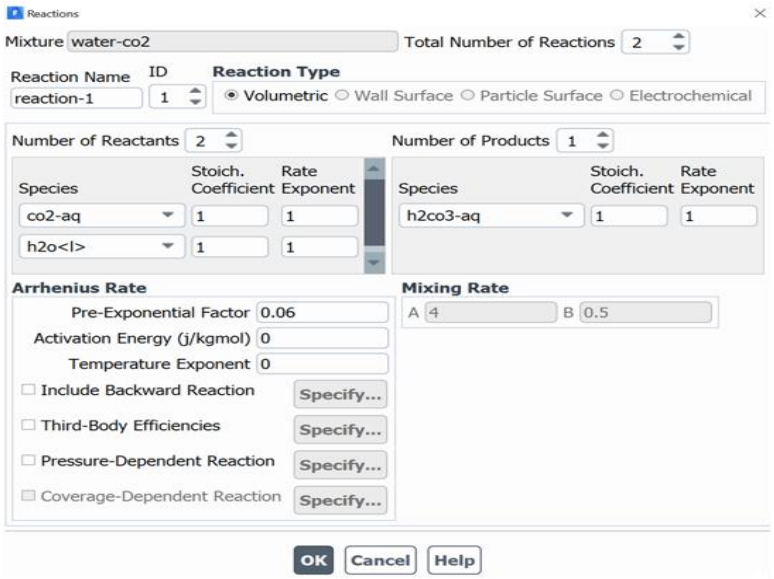

Figure 4.12 - Reaction Dialog Box

Table 4.4 - Reaction Rates for Acidic Mechanism

Reaction	$k_{forward}$	$k_{reverse}$	$k_{equilibrium}$
$H_2O + CO_{2(aq)} \leftrightarrow H_2CO_3$	6×10^{-2} s^{-1}	2×10 s^{-1}	3×10^{-3}
$H_2CO_3 \leftrightarrow H^+ + HCO_3^-$	1×10^{7} s^{-1}	5×10^{10} M^{-1} s^{-1}	2×10^{-4} M
$HCO_3^- \leftrightarrow H^+ + CO_3^{-2}$	3 s^{-1}	5×10^{10} M^{-1} s^{-1}	6×10^{-11} M
$H_2CO_3 \leftrightarrow 2H^+ + CO_3^{-2}$	3×10^{7} s^{-2}	2.50×10^{21} M^{-2} s^{-2}	1.20×10^{-14} M^2

3. Results and Discussion

3.1 QICS Validation

The CFD model was verified by an experiment called QICS (Quantifying and Monitoring Possible Ecological Effects of Geological Carbon Storage) (2015). The velocity of the CO_2 bubbles was measured after they were injected at the ocean floor. The rate of CO_2 injection at the seabed in this CFD simulation was 2.89×10^{-3} kg/s.

At the marker in the simulation, the average bubble velocity is between 24 and 36 cm/s (Figure 4.13 a). The bubble velocities measured in the QICS experiment are consistent with these findings, 20 to 45 cm/s for bubble diameter range of 0.2 to 1.2 cm. (Figure 4.13 b).

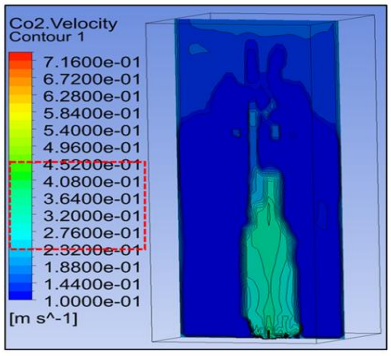

(a) QICS Simulation

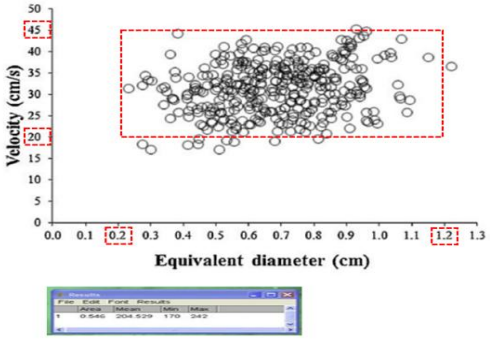

(b) QICS Experiment (Sellami et al, 2015)

Figure 4.13 - QICS Results

3.2 Hydrodynamics & Kinetics of Plume

To investigate the hydrodynamics and kinetics of CO_2 release in seawater, the model was run for 9 seconds after the leak began. It was observed that the bubble plume reaches the top of 50m water column rapidly. When gas rises through the water column, it transitions from jet to buoyant plume. Due to the high solubility of Carbon dioxide in seawater, the bubbles immediately disintegrate, and Carbon dioxide is absorbed in seawater. As buoyant plume rises, the velocity drops and the bubble dissolves faster in seawater.

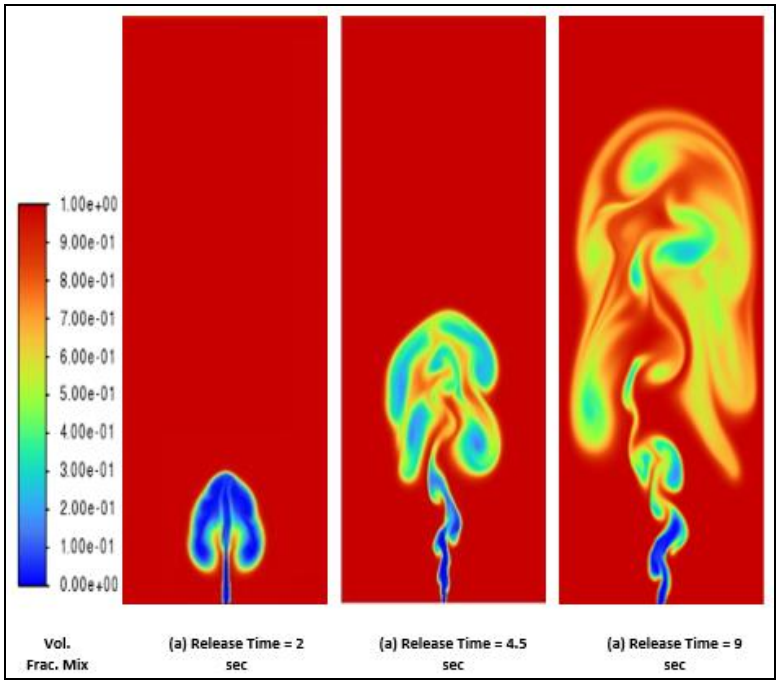

Figure 4.14 - Volume fraction of Water-CO_2 mix at release time 2, 4.5 and 9 seconds.

From Figure 4.14 there is a slight deflection from the centerline of Carbon dioxide plume, the plume extends 16 m laterally and reaches height of 48 m at 9 seconds after the leak started. The transition length for plume to buoyant plume is around 3m. There is a significant loss in pressure as the plume ascends, Figure 4.15 (d) & 10(d). An indication of reduction of bubble velocity and dissolution of CO_2, since the volume fraction of CO_2 also decreases.

In the H_2CO_3 contour (Figure 4.15 & Figure 4.16), we can see that reaction takes place quickly as the spread of H_2CO_3 is much less as compared to the other species. Also, the mass fraction of H_2CO_3 reaches a max value at the hot spots generated. It can be seen from Figure 4.16(b) that, after 9 seconds of CO_2 release the CO_3^{2-} produced from the reaction between H_2O & CO_2 is trapped inside bubble areas and dissolved in seawater the mass concentration contour shows the area with the most concentration of CO_3^{2-} is the bubble in the lower left. The highest mass concentration value for CO_3^{2-} is 1.8×10^{-4} kg/m^3. and the average value is 8.54×10^{-5} kg/m^3. The seawater pH was reduced from 8.2 to 7.2 after 9 seconds of release respectively at the hotspots; a more significant decrease will be observed after a longer release duration. The presence of the carbonate ion in seawater acts as a buffer, reacting with the hydrogen ions. The lowest pH is observed at around 25m from the seafloor due to the higher concentration of $CO_{2\,(aq)}$.

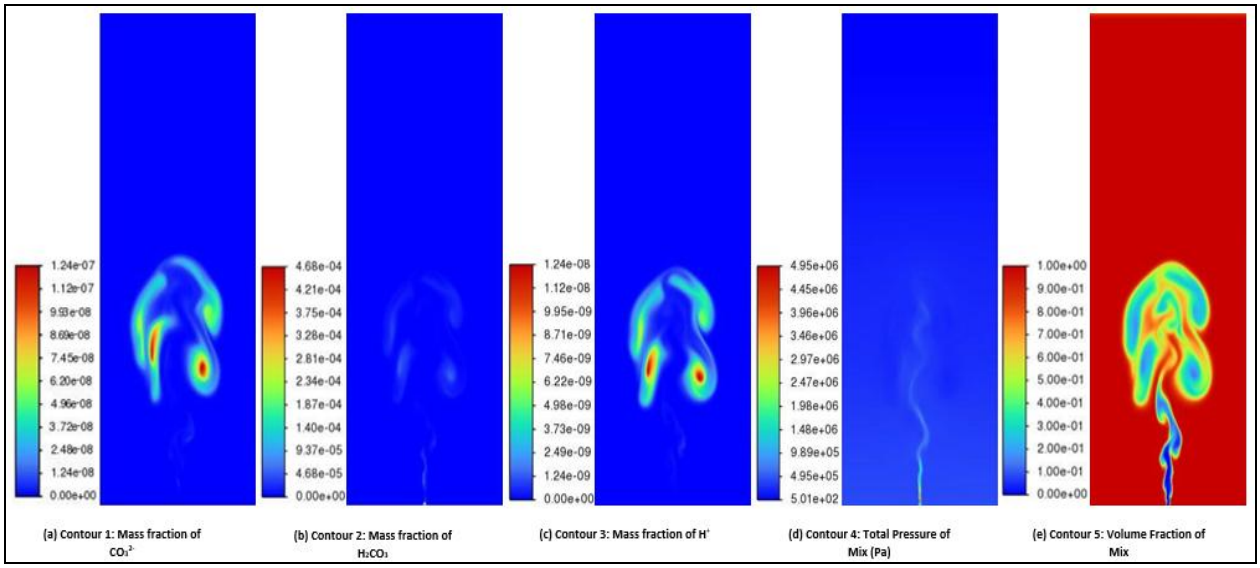

Figure 4.15 - Hydrodynamics and kinetics of plume at release time = 4.5 seconds

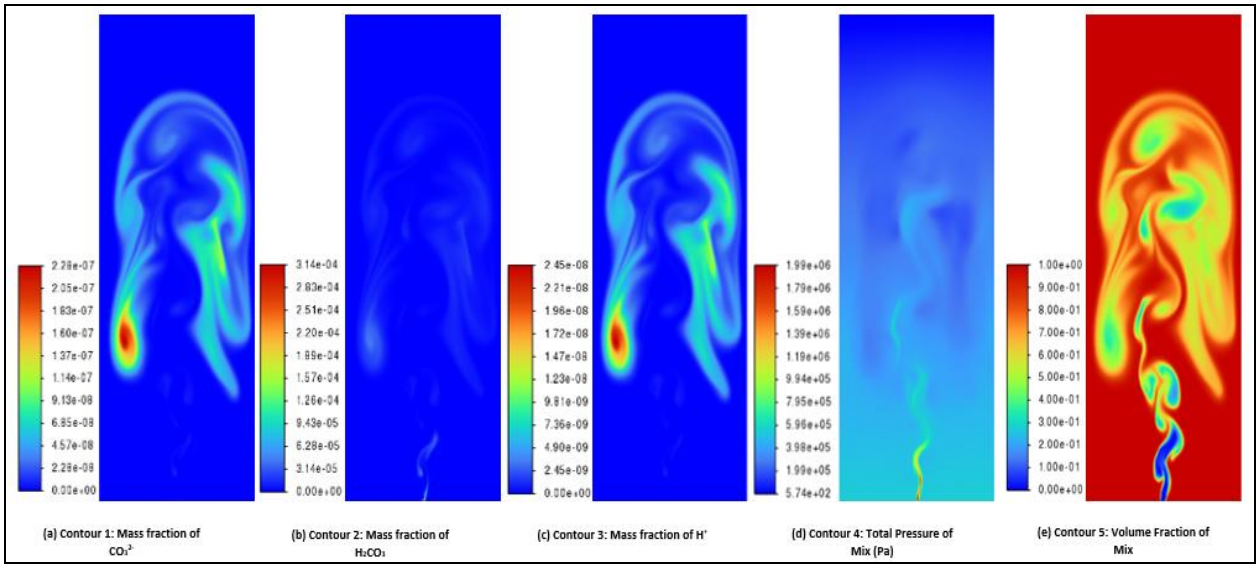

Figure 4.16 - Hydrodynamics and kinetics of plume at release time = 9 seconds

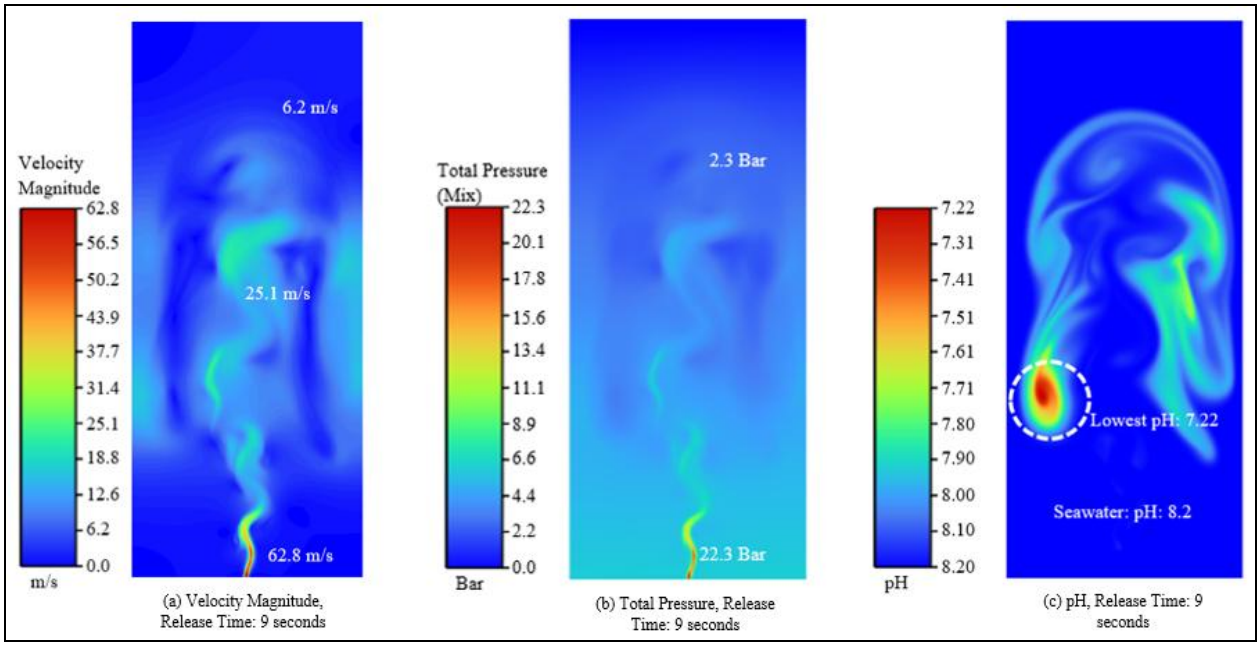

Figure 4.17 - Velocity, Total pressure, and pH change of bubble plume at release time of 9 seconds

4. Conclusion

In this study, a computational fluid dynamics approach using Ansys Fluent software was used to evaluate the consequences of Carbon dioxide dissolution in seawater.

We have carried out a modeling study of a simple generalized without using User Defined Function's (UDF) for a hypothetical blowout of an offshore CO_2 well in shallow water. Although validation of the results presented here will have to await experiments or field observations of equivalent major blowout systems, based on the simulations carried out in this study, we offer the following conclusions:

- The water column will absorb the CO_2 released in about 50 m of height. Major blowouts in shallow water (e.g., 10 m or less) will not absorb the released Carbon dioxide as the gas flows as jet and it need to travel a certain height to transition into a buoyant plume when Carbon dioxide will react with seawater and will get absorbed. The surface emission and reaction of Carbon dioxide is strongly controlled by the water column height.
- The length scale for the transition from jet to buoyant plume of CO_2 leaking out of the orifice into ambient seawater is approximately 3m at depths of 50 m. There is a significant change in pH at around 25m of column height since most of the reaction takes place there.

5. References

Oldenburg, Curtis M., and Lehua Pan. "Major CO2 Blowouts from Offshore Wells are Strongly Attenuated in Water Deeper than 50 m." *Greenhouse Gases: Science and Technology* 10, no. 1 (2020): 15-31.

Olsen, Jan Erik, Dorien Dunnebier, Emlyn Davies, Paal Skjetne, and John Morud. "Mass transfer between bubbles and seawater." *Chemical Engineering Science* 161 (2017): 308-315

Ramirez Garcia, Omar. “Geologic characterization and modeling for quantifying CO_2 storage capacity of the High Island 10-L field in Texas state waters, offshore Gulf of Mexico.” PhD diss., 2019.

Sellami, Nazmi, Marius Dewar, Henrik Stahl, and Baixin Chen. “Dynamics of rising CO2 bubble plumes in the QICS field experiment: Part 1–The experiment.” *International Journal of Greenhouse Gas Control* 38 (2015): 44-51.

Ansys, I. “ANSYS Fluent Theory Guide; Ansys.” *Inc.: Canonsburg, PA, USA* (2020).

4.2 Subtask: Plans for Testing of MVA Technologies

The deliverable D4.2a report addressed this subtask.

4.2.1 Subtask - A priority list for MVA technologies

Following is an excerpt from Deliverable report D4.2a (2022), which fulfills this subtask:

Active-source seismic imaging

Field-testing non-active source seismic techniques

An on-going challenge for marine monitoring of geologic carbon storage is development of approaches which provide improved temporal resolution for tracking CO_2 movement in the deep subsurface, near seafloor, and water column environments. In addition to tracking movement of CO_2, techniques are needed to attribute the source of gases and to easily identify CO_2 leakage from other marine gases which are spatially and temporally variable in the Gulf of Mexico (GoM). The near-seafloor environment is a particular challenge in the GoM where natural leaky petroleum systems are abundant and can exhibit time-varying gas flux and where seasonal hypoxia is a significant environmental factor. These scenarios are characteristic of the GoM and do not exist to such a degree in other previously studied offshore storage environments. Therefore, site specific field testing of techniques to overcome these challenges are needed to provide robust monitoring systems for the future large-scale CO_2 storage that is expected to develop in the GoM.

Geophysical constraints on both the existence and geometry of gas leakage below/near the seafloor as well as the time history of such fluxes is important to aid in attribution. While modern streamer-based marine seismic acquisitions can provide excellent structural imaging of gas plumes in such environments, cost typically limits the number of surveys that can be repeated during monitoring efforts. Thus, an integrated and flexible monitoring system that can be adopted to the changing conditions in the GoM is needed.

Passive seismic imaging

Deployment of permanent seafloor monitoring networks can provide an additional degree of data availability. To take full advantage of these networks for higher time resolution imaging, either persistent seismic sources and/or ambient noise must be utilized to provide data over short epochs. In this vein, several interesting results have been generated during the initial geophysical MVA efforts in GoMCARB including demonstration of seafloor distributed acoustic sensing (DAS) as a potential passive seismic imaging tool (Lindsey et al. 2019, Cheng et al. 2021) as well as early development of a persistent low-power marine source for near-seafloor monitoring.

Despite initial successes, there is a significant need for follow-on studies at larger scales and in more realistic offshore environments. Marine ambient noise conditions vary dramatically as a function of water depth and distance from shore, hence evaluation above potential reservoirs is crucial if passive imaging using fiber optic

sensing is an MVA goal. Likewise, the development of robust cabled monitoring systems incorporating fiber optics and conventional sensors remains a significant engineering challenge. A particular opportunity is to explore integrated fiber optic sensors of varied modality (DAS, DTS) including seafloor chemistry (distributed chemical sensing or DCS) for gas flux characterization at the subsurface interface. Lastly, exploration of persistent low-power seismic sources is crucial to balance need for timely monitoring with protection of marine ecosystems.

Attribution in sediments and seawater

Experience gained developing, testing and applying monitoring technologies to onshore geological CO_2 storage sites during the past years of research within the US DOE regional carbon sequestration partnership program has taught us the importance of anomaly attribution (Dixon & Romanak, 2015; K. Romanak & Dixon, 2022). For example, we have learned that there are many factors that can create environmental CO_2 anomalies, one of which is climate change itself. CO_2 concentrations are increasing in soils, aquifers, and seawater due to increasing temperatures and increasing anthropogenic CO_2 in the atmosphere. Ecosystems are rapidly changing and shifting; thus, the presence of a high CO_2 concentration over a storage site does not automatically mean that the site is leaking. The source of the anomalous CO_2 must be attributed either to the project or to something that is not project-related. This is the importance of anomaly source attribution.

We now see that using baseline CO_2 measurements for environmental source attribution is an outdated notion. With natural CO_2 concentrations rising due to climate change, using baselines as an attribution method will repeatedly cause false positives for leakage. Already this has happened at the Tomakomai project in Hokkaido Japan after only one month of injection when a measurement of CO_2 concentration in seawater above the site exceeded the threshold that had been set using one year of baseline measurements.

To address this problem a process-based soil gas approach was developed and is now becoming a standard method for attribution worldwide (Jenkins, 2020; Jenkins et al., 2015; K. D. Romanak et al., 2012). This method compares ratios of coexisting gases to the stoichiometry of system processes to understand the processes creating the gas signatures. This method was successful at determining that the Kerr leakage claim was false. This method has now been adapted by international colleagues for use in marine monitoring (Omar et al., 2021; Sun et al., 2020; Uchimoto et al., 2018; Uchimoto et al., 2021). In short, this method has revolutionized our ability to decipher the difference between a leak signal and natural variability, especially since carbon isotopes are also not a definitive method due to the overlap of isotopic compositions between natural CO_2 and anthropogenic CO_2.

We know that a process-based approach can work in the North Sea, as shown by research carried out by the STEMM-CCS controlled release (Sands et al., 2021), but already there is indication that the processes in the GoM are quite different than in the North Sea. A large area of the continental shelf in the Gulf of Mexico is seasonally hypoxic (< 2mg O2/L) west of the Mississippi River plume where the freshwater plume enters the GoM. The area of hypoxia is caused by high concentrations of nitrate in agricultural runoff (Rabalais et al., 2007; Rabalais et al., 2002), excess suspended and dissolved organic matter (Bianchi et al., 2010), vertical water column stratification (G. Rowe & Chapman, 2002; G. T. Rowe, 2001), and the seasonal reversal of coastal currents (Jarvis et al., 2020).

The sediment uptake of oxygen (SCOC) and the release of CO_2 (DIC), as well as the regeneration of inorganic nutrients, have been investigated in the hypoxic area using benthic chambers (Berelson et al., 2019; Lehrter et al., 2012; Miller-Way et al., 1994; Morse et al., 1999; Nunnally et al., 2014; Nunnally et al., 2013; G. Rowe & Chapman, 2002). These benthic chamber incubations in hypoxic conditions illustrate that the ratio of DIC to SCOC can be high (> 1.0) when oxygen uptake rate is limited by low oxygen concentrations (Hetland & DiMarco, 2008; G. T. Rowe, 2001). Thus, there is already a disconnection between the stoichiometry that we would expect and that which we observe. Many questions arise: 1) can stochiometric methods be used in the GoM for anomaly attribution? 2) what is causing the difference in expected stoichiometry and can we correct for it? 4) How will the stratification created by hypoxia be affected by a leak? 5) what is the sensitivity needed by leakage monitoring technologies under hypoxic conditions?

More data are needed to confirm the background stoichiometry and thus separate natural production of CO_2 by

respiration from escape of geologically sequestered CO_2 at depth in the sediment. Benthic chambers are a useful, could clarify the differences in leak detection technologies during normal and hypoxic conditions. In addition to using the benthic chambers to look at stoichiometry of fluxes from the sediments, we will also monitor water column chemistry to determine if we can detect changes in the water column or if the signal of leaked CO_2 is overcome by the abundant CO_2 inherent during hypoxic conditions. How can we attribute a leakage signal during these conditions? What is the fate of CO_2 during these conditions, and what would be the consequence of CO_2 leakage on the pycnocline? A controlled release experiment would help answer these questions.

4.2.1.1 Subtask - High-resolution 3D seismic (HR3D)

On December, 16, 2022, the two Partnership co-PIs and the NETL PM attended an online meeting with an NETL compliance officer and two representatives from LGL, Ltd., an environmental consulting firm hired to prepare and submit an environmental assessment (EA) for an HR3D survey for DE-FE0028193. Part of the topic of discussion was whether or not the EA for FE0028193 could be leveraged for the EA (or potentially two EAs) that would, likewise, be required before the GoMCarb HR3D surveys could receive FONSIs (findings of no significant impact) from the NETL NEPA compliance office. It was determined in 2022 that FONSIs rather than categorial exclusions (CXs) would be required before the GoMCarb Partnership's two pending surveys could occur. Ultimately, it was decided that the GoMCarb and FE0028193 EAs should be separate in order to avoid questions about co-mingling funding from the two NETL projects.

See also subtask 4.1.3 for a complete explanation of the results of the efforts to acquire an HR3D seismic dataset.

4.2.1.2 Subtask -Geochemical monitoring in the Seawater Column

The GERG team at Texas A&M University worked with Dr. Romanak (UT GCCC) to determine the details of a controlled release at a site in coastal/offshore Texas. The controlled release was to be carried out at the High Island lease block 24L using either an existing but abandoned well platform or a marine barge tethered to such a platform. GERG consulted the Texas General Land Office (TGLO) to identify the most useful platform. The release was planned to occur seasonally and reflect the greatly different environmental conditions due to "normal" and hypoxic conditions under various temperature regimes. Cabled CO_2 and O_2 sensors were to be installed in large benthic chambers over the release area and real-time sampling would reflect the CO_2 concentrations. GERG engineers worked on the methods to achieve a successful outcome. GERG relied on some of the early intentional release literature (Sands et al. 2021).

Unfortunately, as planning for the activity progressed, it became clear that the scope, logistics, and permitting requirements associated with the proposed offshore controlled release could not be supported within the budget and schedule constraints of the GoMCarb study. In particular, securing the necessary infrastructure, permits, and operational coordination required for a meaningful field deployment within the available timeframe proved unfeasible. As a result, the controlled release testing was not carried out under the project.

Reference Cited

Sands, C., Connely, D, and Blackford, J. Introduction to the STEMM-CCS special issue. International Journal of Greenhouse gas control. 113, [2021] 103553.

4.3 Subtask: Testing MVA technologies

From the beginning of the Partnership, the main MVA technology planned to be tested by the Partnership was

high-resolution 3D (HR3D) seismic. As reported in other portions of this report acquisition of the HR3D seismic dataset encountered many challenges. The Covid-19 pandemic significantly delayed acquisition of an HR3D seismic survey as did the need to generate an environmental assessment and receive a FONSI (finding of no significant impact) from NETL NEPA compliance. (See also subtasks 4.1.3 and 4.2.1.1.) Consequently, no test of the HR3D seismic technology's MVA capability was tested by the Partnership, per se. However, a separately funded NETL study was able to test the technology's MVA capabilities within the GoMCarb geographic area and during GoMCarb's period of performance. The other study was FE0028193 "Field Validation of MVA Technology for Offshore CCS: Novel Ultra-High-Resolution 3D Marine Seismic Technology (P-Cable)," which acquired a repeat HR3D seismic dataset in March 2024 (i.e., during GoMCarb's period of performance). The HR3D dataset was acquired offshore San Luis Pass, Texas over portions of the same area as a 2013 HR3D seismic dataset (i.e., for DE-FE0001941, "Gulf of Mexico Miocene CO_2 Site Characterization Mega Transect").

As reported in the final report of FE0028193, the HR3D dataset verified that "HR3D can be used in a time-lapse 4D monitoring mode for applications similar to CCS monitoring. The positioning methods and experience gained illustrated that the" seismic "positions in these data acquisitions can be very precise and repeatable over time, allowing for temporal analysis of" geologic and fluid "features of interest."

5. Task – Infrastructure, Operations and Permitting

5.1 Subtask: CO_2 Transport and Delivery

5.1.1 Subtask - Transport to near-shore sites (High Island area)

The GoMCarb region of interest (nominally offshore Texas and Louisiana) is identified in Figure 5.1. In addition to the broad region of focus defined on this map, UT BEG has geologic datasets in specific locations in the near-offshore region of Texas and Louisiana. Evaluation of the data indicated favorable geology, particularly in the region offshore of Beaumont-Port Arthur in Texas (i.e., Jefferson County). In addition, this region has many large CO_2 emission sources that could serve as part of project development. In fact, since the initiation of the GoMCarb Partnership, the Texas General Land Office (GLO) offered and awarded a lease[1] for CO_2 storage in offshore Jefferson County. At the outset of the Partnership, the focus for offshore CO_2 storage in the Gulf of Mexico was near-shore. Furthermore, where specific locations or sites would facilitate analyses, UT BEG identified two specific lease blocks in Texas state waters[2] where geology was well-characterized and could potentially support CO_2 storage to serve as "analog" sites: High Island Block 10L (HI-10L) and High Island Block 24L (HI-24L), as shown in the inset of Figure 5.1.

[1] https://www.ogj.com/energy-transition/article/14241617/talos-signs-texas-carbon-capture-site-lease

[2] Jurisdiction of offshore oil and gas leases (and presumably CO_2 storage) is split between states and the Federal government. In Texas, state waters extend 9 nautical miles from the coast at every point along the shoreline. Beyond this point, the region is considered "Federal waters". In Louisiana, the state-federal boundary is 3 nautical miles offshore.

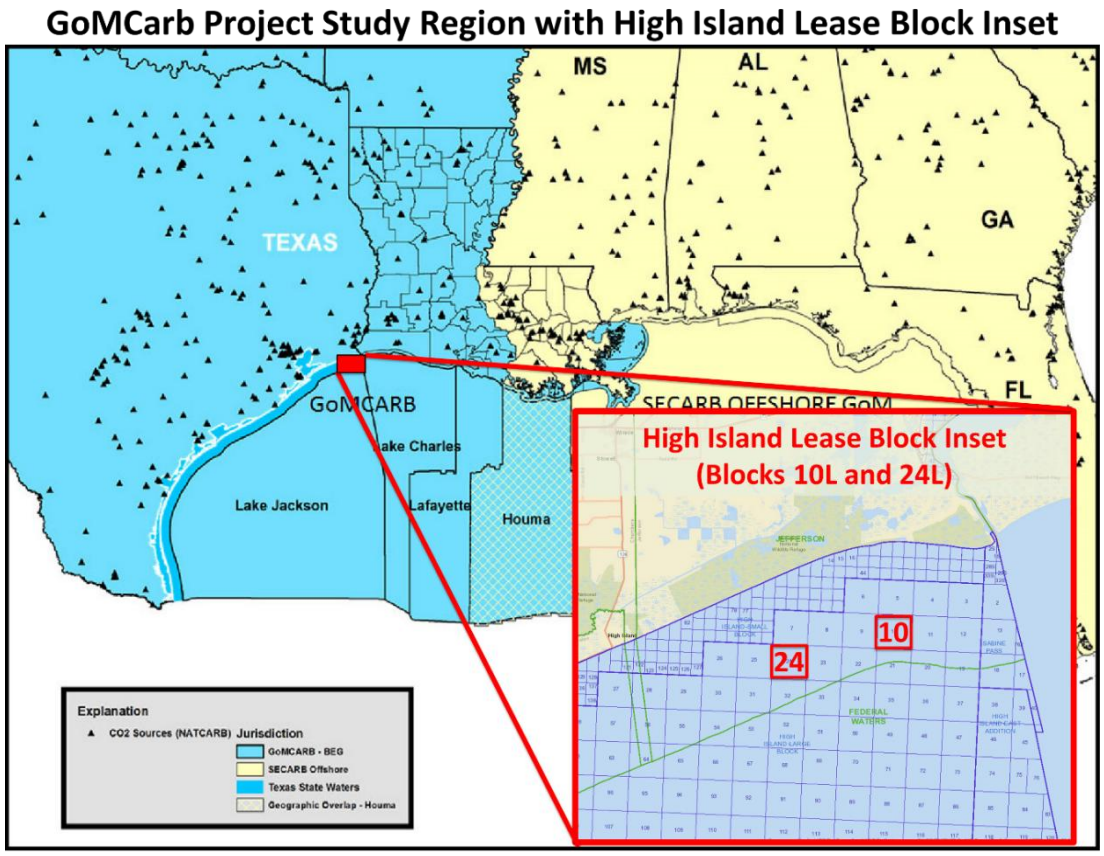

Figure 5.1 - Map of Northern Gulf of Mexico with Regional Research Partnerships (GoMCarb = blue, SECARB = yellow). High Island Lease Block Inset added by Trimeric. Reproduced and modified from https://www.beg.utexas.edu/gccc/research/gomcarb.

Existing Oil and Gas Infrastructure Evaluation Background

Within the general project context outlined above, Trimeric was tasked with evaluating the potential to re-use existing oil and gas infrastructure in the Gulf of Mexico. Trimeric[3] has performed a review of existing infrastructure (pipelines, wells, platforms) at varying levels of detail with a focus on the near offshore region for the reasons outlined in the general background above. The previous infrastructure review has been documented in several places (infrastructure re-use memorandums, presentations, quarterly reports, and other internal reports). The primary goals of the initial review of near-shore existing oil and gas infrastructure included the following:

1) Identify data sources, quality/type of data available, and gaps in data for each major infrastructure group (wells, pipelines, platforms) in both state and federal waters offshore of Texas and Louisiana.
2) Develop screening criteria to narrow datasets for oil and gas infrastructure based on potential suitability for re-use.
3) Develop "workflows" that define the major steps required to assess a specific asset for re-use, comment on the potential cost/regulatory requirements/data needs for each step in the workflow, and highlight key decision points in the workflow (i.e., places to abandon the re-use assessment).
4) "Test" and refine the screening approach and workflows via case studies of specific assets.

While the initial analysis yielded insights on each asset class and identified key questions or potential limitations

[3] With several tasks being led by external consultant, Darrell Davis

for re-use, the focus on the near offshore region limits the potential to apply the findings in a general manner across the GoMCarb region. For example, initial analyses of platform data in federal waters highlighted key trends in regional variation of platform characteristics. The type and age of the platforms varies with water depth (following trends in oil and gas exploration in the GoM). Therefore, Trimeric and UT BEG decided to seek a more general approach to infrastructure evaluation across the GoMCarb region without attempting to evaluate all infrastructure datasets in the GoM (not practically feasible or likely to yield useful conclusions).

Introduction to Transect Study of Existing Infrastructure

UT BEG proposed using geologic transects in the GoM to identify specific regions of focus across the GoMCarb region. A transect is a line spanning geographic regions which represents points where geologic analyses have been performed, and/or data are available to interpret the subsurface geology. By "following" a transect to guide infrastructure evaluation, it ensures that the infrastructure analysis can be coupled with an assessment of underlying geology to determine feasibility of long-term geologic storage of CO_2 (as opposed to selecting regions for infrastructure evaluation irrespective of the data available to assess the quality of the underlying geology for CO_2 storage). UT BEG provided the following map (Figure 5.2) to identify specific transects (to guide infrastructure evaluation, moving from the near offshore to deeper waters and across the GoMCarb region. Three transects (blue arrows in Figure 5.2 identify transects of interest) were chosen by UT BEG as the basis for the infrastructure evaluation: 1) Corpus Christi Transect (westernmost transect originating from Texas coastline near Corpus Christi; 2) Galveston Transect (central/middle transect on the map originating from the Texas coastline near Galveston; 3) Louisiana Transect (easternmost transect originating from the Louisiana coastline).

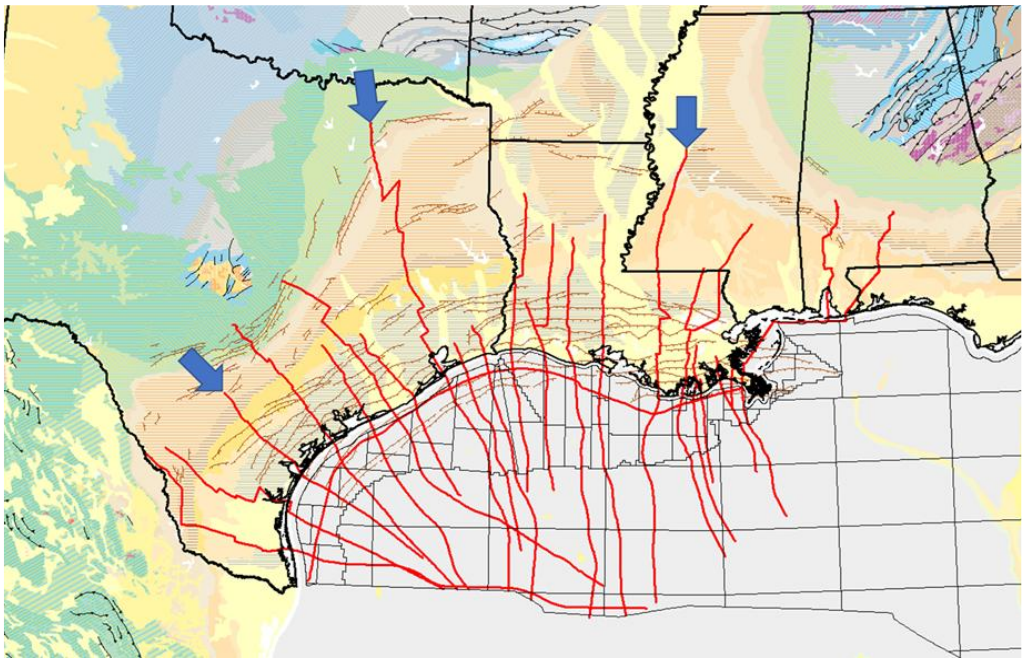

Figure 5.2 - Transect map provided by UT BEG (transects = red lines), including three proposed transects to guide infrastructure evaluation (blue arrows)

Trimeric's approach to using the transects to develop additional infrastructure evaluation includes the following major steps:

- Infrastructure Data Gathering and Mapping: Using the transects as anchors, Trimeric will gather data (e.g., via mapping) regarding the quantity and type of existing oil and gas infrastructure along each transect. While the transect appears as a discrete line, Trimeric will use judgement to determine what defines a reasonable region in the "vicinity" of the transect to gather infrastructure data. A region that is too broad

undermines the concept of the transect and may lead to prohibitively large datasets. A region that is too narrow risks being unrepresentative of the regional infrastructure trends.

    - This process may require review of both state and federal databases for infrastructure data, though the primary focus is federal infrastructure.

- Development/application of screening criteria to focus datasets: In previous infrastructure evaluations performed by Trimeric, screening criteria were developed and applied (in particular for pipelines) to focus on assets with the highest likelihood of re-use in CO_2 capture. For the transect analysis, a similar approach (perhaps using some of the same screening criteria) for each region may be applied, depending on the amount of data available and potential value of screening. Given the natural "screening" effect of selecting specific geographies (i.e., transects) and the intended goal of performing a broader, more representative analysis of infrastructure, the screening criteria may be less restrictive (or fewer criteria will be applied) than the previous phase, with the goal of removing obvious outliers.
- Identify and Summarize Trends in Infrastructure Availability and Characteristics: Based on the data gathered and remaining after any preliminary screening, Trimeric will attempt to identify trends in quantity and characteristics of existing oil and gas infrastructure both within an individual transect and between different transects. The evaluation of these trends may yield high-level conclusions about where infrastructure re-use might be more favorable (e.g., where newer infrastructure exists), where re-use might be more valuable (e.g., regions with multiple viable existing pipelines), or regions where infrastructure might represent a higher risk for CO_2 storage (high density of existing wells).
- Develop a proposed approach and potential costs of performing more detailed assessments of existing infrastructure at a level sufficient to facilitate project/investment decisions: Using the trends identified in the preceding step to focus on areas with high re-use potential and/or value, Trimeric will develop a proposed approach to evaluate the infrastructure and assets in each identified region for re-use. The approach in this case refers to the activities that would be required for project development and/or investment as opposed to the high-level evaluations performed as part of the GoMCarb study. For example, the proposed approach might be analogous to a Pre-FEED or FEED study for project development. This represents an extension of the generalized workflow concept developed in the preliminary infrastructure evaluation to define a more specific scope of work that could be performed by engineering firms with expertise in the specific offshore infrastructure of interest. In addition to developing a "scope of work", Trimeric will estimate the expected costs to perform the proposed scope of work. This may include soliciting input from offshore development industry experts and firms that would be suited to execute the scope of work.
    - Note that the goal of this activity is not to perform the re-use assessment itself or perform any technical or economic analyses for re-use. It is to identify the needs and requirements (including costs) to perform the more detailed evaluations required to make decisions on the re-use of specific assets. This represents a logical extension/next step from the GoMCarb Partnership focus and scope.

The following discussion focuses on well-data analysis and review for the Galveston transect. Trimeric gathered information about platforms and pipelines as well (leveraging work done previously through the course of the GoMCarb project), but these infrastructure types are not reviewed in detail here.

Overview of Data Sources

This section provides an overview of the data sources Trimeric used to gather information on existing infrastructure in Federal and State waters along transects identified for this study. Trimeric has summarized key terminology, structure of datasets, and other practical aspects of data gathering from sources to facilitate an understanding of the type of data collected and the interpretation of the data for this study. This section is not intended to be an exhaustive review of the data sources themselves or serve as a "how to" guide for accessing data from the sources.

Texas State Waters

Trimeric relied on the Texas Railroad Commission (RRC) GIS Viewer tool (publicly available) and subscription databases available to UT BEG (OWL, Petra, and possibly others) to gather and analyze data for Texas State Waters. Section 3 of Trimeric's memorandum to UT BEG, "Existing Well Re-Use Assessment for CO_2 Injection for GoMCarb, rev0", dated 25 March 2022 (Appendix D), describes the data obtained from these sources and will not be repeated here.

Federal Waters

Trimeric relied on the following sources for infrastructure data in Federal waters:

Bureau of Ocean Energy Management (BOEM): The BOEM website[4] provides access to map shapefiles (viewable in Google Earth software) that defined **Federal leasing areas, platforms, and pipelines**.

Bureau of Safety and Environmental Enforcement (BSEE): The BSEE website[5] includes raw data and information about **wells in Federal waters** via the "Borehole Online Query". Trimeric exported these data for statistical evaluation. The BSEE website also includes a "Disc Media Store[6]" which is a database of well reports available for purchase. Trimeric used the Disc Media Store to catalog the type and prevalence of reports available for wells in Federal waters.

MarineCadastre Data Registry Website[7]: This website provides **shapefiles for wells**, but mapping the wells in Google Earth was impractical due to the total number of wells in the Gulf of Mexico.

ArcGIS Mapping Tool: The Federal websites include several mapping tools to view infrastructure data. Trimeric used the ArcGIS website[8] to map oil and gas wells in the Gulf of Mexico. Trimeric overlayed the "Galveston" transect identified in Figure 5.2 and adjacent/overlapping Federal lease areas on top of the ArcGIS map of wells to provide a quick visual representation of well locations and density along the transect (discussed later in Figure 5.5). Trimeric will develop similar maps for the other transects in the study.

Subscription Databases: Subscription databases are another source of data on infrastructure in federal waters. Trimeric has not accessed these databases thus far in the analysis of the federal wells, but they may be consulted moving forward. The subscription databases are built from the data available from BSEE/BOEM, but they are more user-friendly for performing data queries.

Explanation of Well Data from BSEE

The data evaluation for wells generally requires more interpretation and understanding of specific nomenclature and definitions than the other infrastructure groups (pipelines, platforms). In general, Trimeric refers the reader to the BSEE website[9] for a list of data fields and associated definitions. However, to facilitate evaluation and interpretation of well data from the BSEE website, Trimeric has summarized key information regarding select data fields available in the BSEE database and has provided guidance for interpretation of the data. This guidance was

[4] https://www.data.boem.gov/Main/Mapping.aspx

[5] https://www.data.bsee.gov/Well/Borehole/Default.aspx

[6] https://www.data.bsee.gov/Other/DiscMediaStore/WellData.aspx

[7] https://marinecadastre.gov/data/ This website is a collaboration between BOEM and the National Oceanic and Atmospheric Administration (NOAA).

[8] https://www.arcgis.com/home/webmap/viewer.html?url=https://gis.boem.gov/arcgis/rest/services/BOEM_BSEE/MMC_Layers/MapServer/1&extent=-100,40&level=4

[9] https://www.data.bsee.gov/Well/Borehole/FieldDefinitions.aspx

developed from Trimeric's review of various BSEE documents[10] and consultation with Jeff Harris, a geologist at BSEE. The following key fields are summarized due to their relevance to Trimeric's evaluation:

- General Note: Wells may include one or more wellbores. A wellbore is a unique, oriented hole from the bottom of a drilled interval to the surface. If more than one path exists from a surface location to a bottom-hole point (s), then more than one wellbore exists. The terms wellbore and borehole may be used interchangeably in the context of this data analysis.
- API Number: Defined by BSEE as a unique well identification number consisting of (from left to right) a two digit state code (or pseudo for Offshore), a three digit county code (or pseudo for Offshore), a five digit unique well code, and if applicable, a two digit sidetrack code as defined in API Bulletin D12A. Trimeric relied on the API Number as the starting point for identifying/quantifying unique wells when performing a statistical evaluation of a region/area.
- All wellbores originating from a single surface location will share the same first 10 digits of the API number. Prior to 1996, a sidetrack or bypass wellbore did not require a unique API number. After 1996, these wellbores are tracked with "01", "02", "03", etc. in the 11th and 12th digits of the API number. Sidetracks and bypasses that were not given a unique API number in the past (before 1996) may be assigned a "70-series" code in the 11th and 12th digits of API number. Each individual wellbore has its own unique identifying number. Wellbores with the same surface location (well) will have the same API number until the 11th and 12th digits.
- Borehole Status Code: Defined by BSEE as indicating the conditions relating to a borehole (e.g., drilling active, drilling suspended, canceled, permanently abandoned). A full list of status codes is available via the BSEE website. Trimeric used this data to categorize wells as part of the statistical evaluation of different regions along a transect. Borehole Status Codes are reviewed in further detail later in this report.
- Spud Date: Defined by BSEE as the date that the drilling rig first begins boring into the earth's surface and used by Trimeric as a proxy for the age of a well.
- Well Name Suffix: Defined by BSEE as an extension to the well name that indicates the number of times that a new wellbore has been drilled.
    - In discussions with BSEE, the well name suffix may indicate if the wellbore is a sidetrack or bypass. A bypass is a remedial drilling effort in which a portion of a well is re-drilled around an obstruction. In general, the proposed bottom-hole location of the new borehole is within 500 feet of the proposed bottom-hole location of the previous borehole. A sidetrack is a drilling effort in which an additional hole is drilled by leaving a previously drilled hole at some depth below the surface and above the total depth. A whipstock or cement plug is set in the previously drilled hole, which is the starting point for the sidetracking operations. This section of the hole is directionally drilled to a new objective bottom-hole location, which is generally more than 500 feet from the previously proposed bottom-hole location.
    - Trimeric used the well name suffix to differentiate between bypasses and sidetracks; API number may indicate if there is a bypass or sidetrack but will not differentiate between the two.

Bottom Area Code: Defined by BSEE as the designated abbreviation assigned to Outer Continental Shelf (OCS) geographical units for identification purposes and for use on maps and in data bases as applied to the bottomhole location of a well and used by Trimeric to organize/structure data gathering and mapping of results.

---

[10]NOTICE TO LESSEES AND OPERATORS OF FEDERAL OIL AND GAS LEASES OUTER CONTINENTAL SHELF, GULF OF MEXICO OCS REGION: Well Naming and Numbering Standards. UNITED STATES DEPARTMENT OF THE INTERIOR MINERALS MANAGEMENT SERVICE GULF OF MEXICO OCS REGION. NTL No. 2009-G33. Nov 4, 2009.

The BSEE website includes many other data fields that may be important when reviewing a specific wells, such as Well Type Code which indicates the specific type of well that was drilled (e.g., exploratory, development) or various data fields providing information on the depth of wells. These fields include the raw datasets Trimeric downloaded and used as the basis for the statistical evaluation.

Trimeric's research and review of BSEE documents and consultation with Jeff Harris of BSEE also yielded the following relevant information for the evaluation of well data:

- The BSEE database may contain wells in state waters. This may happen if the well has a surface location in state waters, and a bottomhole location in federal waters, or vice versa. State leases in the federal database will start with an "S". **This information is important for data analysis to avoid double-counting wells between different sources (e.g., state data vs. Federal data).**
- According to Mr. Harris, there is no single marker used to identify orphaned wells in the BSEE wellbore data; this is in contrast to the Texas RRC dataset which does include an orphaned well status marker. The Texas RRC defines an orphaned well as inactive and non-compliant wells that have been inactive for at least 12 months. Trimeric has not found an analogous term used in the Federal databases.

There are several different well type codes in the BSEE database. According to Mr. Harris, D and E are most common – development and exploration. A well may be permitted as an exploratory well; if it is completed and becomes a production location, it will still have E as in its well type code – which is how it was initially permitted. Therefore, an exploratory well can produce hydrocarbons. "Discovery" well is another term for exploration wells that produce. The other well type codes are not as common and likely not relevant to this GoMCARB study.

Interpretation of Borehole Status Codes in BSEE Database

As noted in the preceding section, the Borehole Status Code represents a key data field that Trimeric used to categorize wells in Federal Waters. A list of Borehole Status Codes is provided below, with definitions provided where available/applicable. The definitions are based on definitions provided on the BSEE website, supplemented with context developed by Trimeric as part of further research regarding the status codes.

- Application for permit to drill (APD): application has been approved
- Cancelled (CNL): borehole is cancelled. The request to drill the borehole is cancelled after the APD or Sundry (any additional action done on a well; could be information in sundry about what they are hoping to do) has been approved.
- Drilling active (DRL)
- Drilling suspended (DSI)
- Completed (COM): completed well that is active and producing or inactive.
- Borehole sidetracked (ST): A previously drilled hole below surface but above the total depth, which is plugged at the starting point of a sidetrack. An API number with the status ST is not the sidetrack itself, but rather the borehole that has been sidetracked (or bypassed). The sidetrack is drilled to a new bottom-hole location and will have a status such as COM, TA, or PA. A sidetrack will have a well name that indicates it is a sidetrack.
- Temp abandoned (TA): A well can be temporarily abandoned.
    - In the Garden Banks area there are wells with status code date data that they have been temporarily abandoned since 2003.
- Perm abandoned (PA): Well has been plugged.

To illustrate the interpretation for the Borehole Status Codes, Trimeric selected an example for the BSEE database within the Garden Banks lease area, well API number 6080740280XX. Table 5.1 shows some of the key borehole data for the well. The example well has four associated boreholes with four unique API numbers. The well

numbering and naming help to tell a story for the well. The original well (API 60807402800, Well Name 002, Well Name Suffix ST00BP00) spudded in June of 2006 and was sidetracked a few months later. Sidetrack 01 (API 608074028001, Well Name 002, Well Name Suffix ST01BP00) was sidetracked again one month later (API 608074028002, Well Name 002, Well Name Suffix ST02BP00) and finally was bypassed to the completed well in January 2008 (API 608074028003, Well Name SS002, Well Name Suffix ST02BP01). Trimeric found production data for Bottom Lease Number G27632 starting in 2008 up to the present. Trimeric did not find a platform associated with the well.

Table 5.1 - Example Gulf of Mexico Well from BSEE Database (Federal Waters).

API Well Number	Well Name	Well Name Suffix	Bottom Lease Number	Bottom Block	Spud Date	BH Total MD (feet)	True Vertical Depth (feet)	TVD Subsea (feet)	KOP	Total Depth Date	Status Date	Type Code	Status Code	Surface Lease Number
608074028000	002	ST00BP00	G24479	302	6/30/2006	19606	19549	19475		8/31/2006	9/11/2006	E	ST	G24479
608074028001	002	ST01BP00	G24479	302	9/11/2006	20808	20683	20609	16905	10/3/2006	10/10/2006	E	ST	G24479
608074028002	002	ST02BP00	G24479	302	10/10/2006	13459	13455	13381	13060	10/13/2006	10/16/2006	E	ST	G24479
608074028003	SS002	ST02BP01	G27632	258	10/15/2006	22277	21000	20926	12980	11/27/2006	1/8/2008	E	COM	G24479

Please refer to https://www.data.bsee.gov/Well/Borehole/FieldDefinitions.aspx for data field definitions.

Galveston Transect Evaluation Results

Trimeric began the transects study with the middle transect of interest in Figure 5.2; this transect is designated as the Galveston Transect as it crosses the shoreline in Galveston, TX. The analysis of well infrastructure near the transect was broken into two segments: (1) wells in state waters, and (2) wells in federal waters.

Galveston Transect Analysis - Wells in State Waters

Trimeric used the Texas RRC GIS Viewer Map (https://gis.rrc.texas.gov/GISViewer/) to gather data within a 2-mile radius of the Galveston Transect in the state waters. The data gathered from the GISViewer included, but were not limited to, the following information: API number (although some wells listed did not have the full API number), well coordinates, and well status.

Some key information on the wells was not available in the RRC database. Amanda Merida and Iulia Olariu from UT BEG queried the Petra and OWL databases for the following information for the wells found within a 2-mile radius of the Galveston Transect in state waters:

- **Well completion dates**: Well completion dates were found for all but one of the completed wells in the study area
- **The unique identifier for the wells with 3-digit API numbers**: Several wells in the state waters of interest had incomplete API numbers; three wells were designated with 605 as an API number, and four wells were designated with 706 as an API number. UT used the GIS coordinates from the RRC data to match these wells to their full API numbers in the commercial databases. The coordinates were not exact matches between the two databases, but were very close to each other, as shown in Figure 5.3 and Figure 5.4.

A listing of the types of reports (plugging, cement logs, pressure tests, caliper logs) available in the subscription database: No caliper logs, cement logs, pressure test, or plugging reports were found in the databases that UT checked for the Galveston Transect state waters.

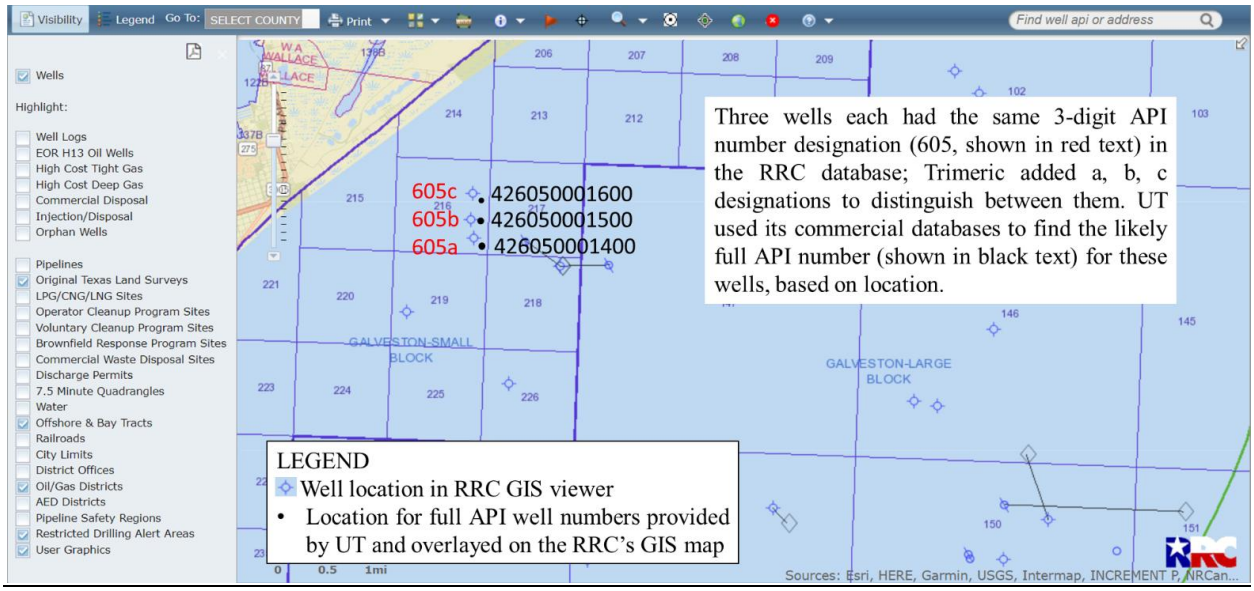

Figure 5.3 - Texas RRC 3-digit 605 API wells mapped with full API number well locations

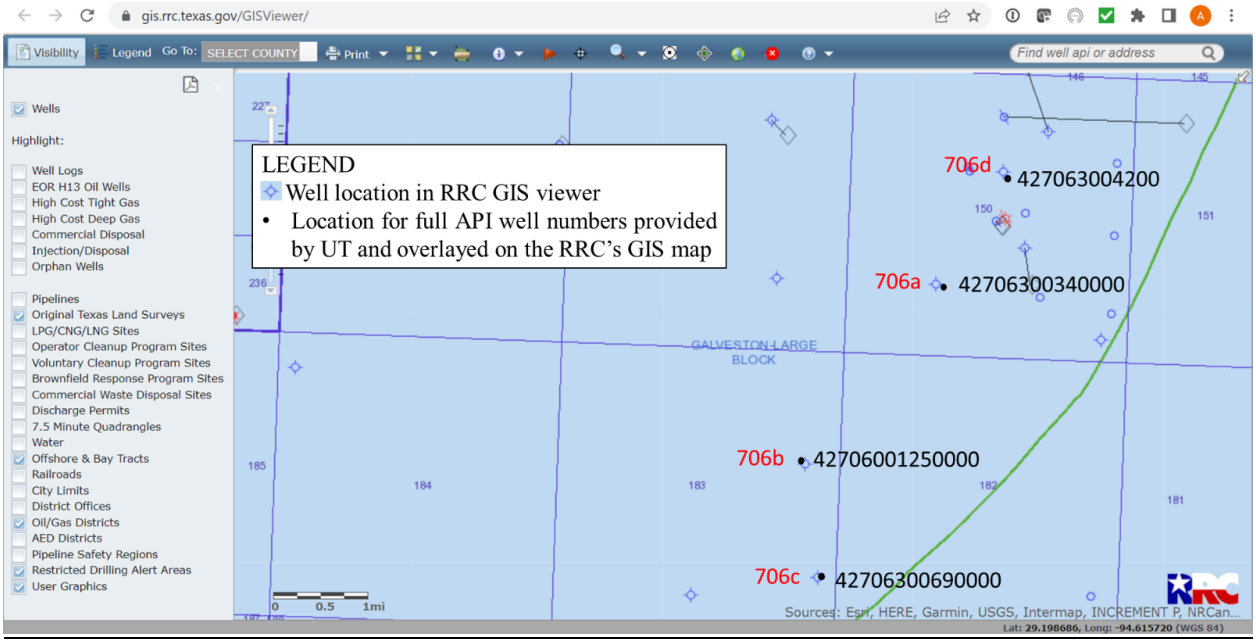

Figure 5.4 - Texas RRC 3-digit 706 API wells mapped with full API number well locations (green line is the border between state and federal waters).

As shown in Table 5.2, there were records for 21 API numbers in state waters within two miles of the Galveston transect; thirteen of these wellbores were plugged, while eight wellbores were never drilled. The records indicate there are no open wellbores within state waters near (i.e., within 2 miles of) the Galveston transect. Four of the 13 wells were completed prior to 1970, another four wells were completed in the 1970s, one well had an unknown completion date, and the remaining four wells were completed in 1980 or later.

Table 5.2 - Well data summary for State Waters within 2-mile radius of Galveston Transect

	# of Wells in State Waters near Galveston Transect
Number of UWIs/APIs	21
Wellbore status	
Plugged	13
Permitted/Cancelled	8
Unknown Status	0
Active: Producing	0
Inactive: Temp Abandoned	0
Inactive: Orphan	0
Well Completion Date	
< 1970	4
1970 – 1979	4
1980 – 1989	2
1990 – 1999	1
2000 – 2010	1
Unknown	1
# Wells w/ Reports Available in Subscription Database	
Plugging	0
Cement Logs	0
Pressure Tests	0
Caliper Logs	0

NOTE: Data represent query within 2 miles of the Galveston Transect.

Galveston Transect Analysis - Wells in Federal Waters

For a first pass, Trimeric collected borehole data for the entirety of the federal oil and gas areas through which the Galveston Transect passes (as shown in Figure 5.5):

- Galveston (GA)
- High Island (HI)
    - High Island includes four distinct areas: **High Island**, High Island East Addition, **High Island South Addition**, **High Island East Addition, South Extension**. Three of the High Island areas are depicted with the "HI" designation in the following figure.
- East Breaks (EB)

- Garden Banks (GB)
- Keathley Canyon (KC)

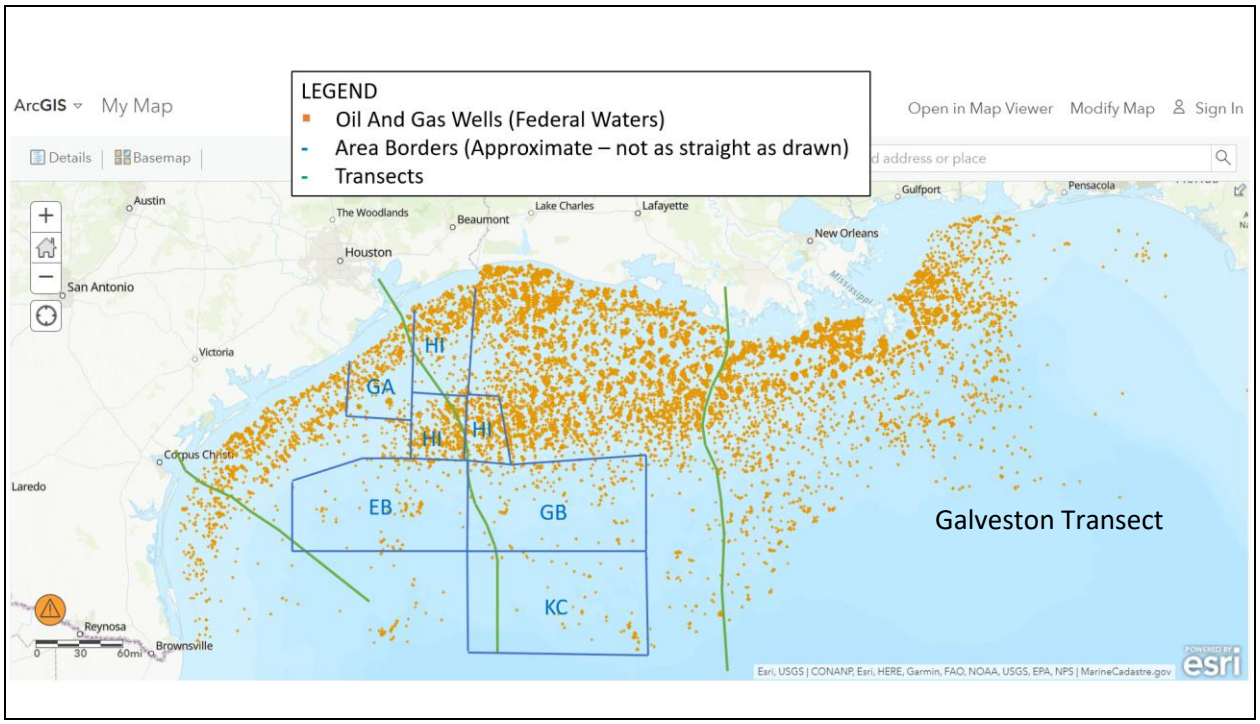

Figure 5.5 - Wells in federal waters mapped with three key transects and oil and gas areas through which the Galveston Transect passes.

In this first pass data gathering, the data were not filtered for a limited distance around the transect, as such a filtering approach was not readily achievable with the BSEE query tool. As Figure 5.5 shows, only a few wells are near the transect as it passes through Garden Banks (GB) and Keathley Canyon (KC), yet all of the wells from these oil and gas areas were included for this initial analysis.

Figure 5.1 shows the total number of spudded wells in each of the oil and gas areas. The High Island area has the greatest number of wells: 3,773 wells. Galveston Area, which is similarly near shore but is a smaller area, has 775 wells. Keathley Canyon, which is the farthest area from shore, has the fewest wells of the areas along the Galveston Transect: 122 wells. Note that Trimeric is currently working to develop analyses and metrics to provide a more descriptive statistic of well quantity and characteristics as a function of the position along the transect. While the online database tools favor data collection by oil and gas area, the statistics presented by area lack resolution for important trends (e.g., density of wells in specific geographic regions, trends in ages/depth of wells).

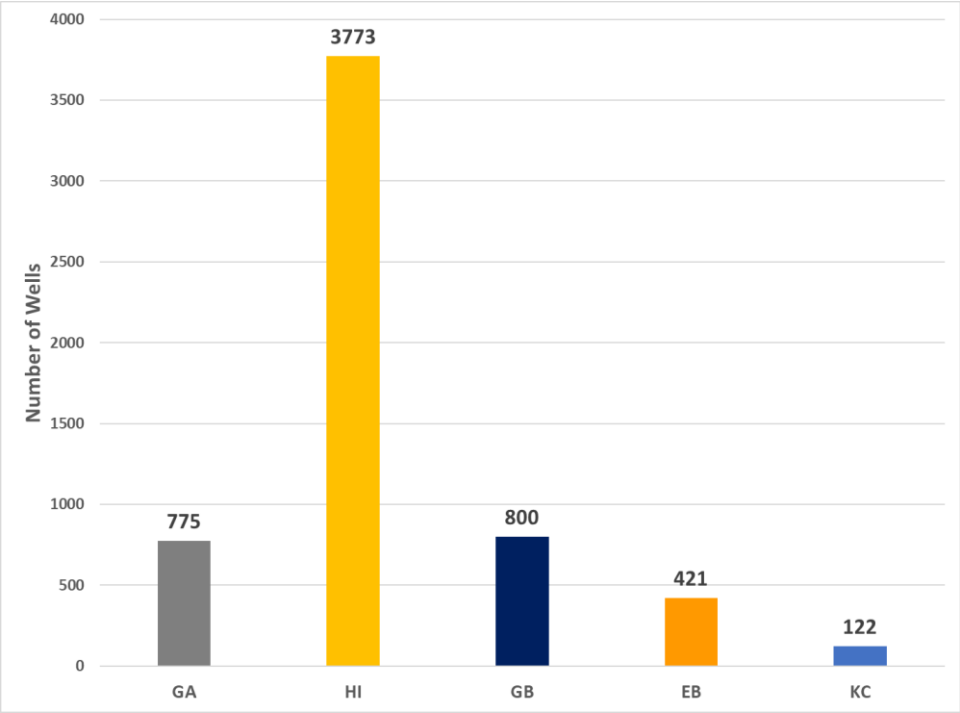

Figure 5.6 - Number of Spudded Wells in Each Area in Federal Waters.

The tables in Appendix E tally the spud date and wellbore status data, with one table per oil and gas area. Figure 5.5 and Figure 5.7 plot the entirety of the Galveston transect data by spud date and wellbore status, respectively.

The wells in the farthest offshore oil and gas areas (Garden Banks, Eastern Break, and Keathley Canyon) were all constructed after 1970; therefore, "modern" well construction methods (which went into widespread practice in 1970) were used for wells in these areas. The use of "modern" well construction methods should reduce the risk of well integrity problems as compared to pre-1970 wells.

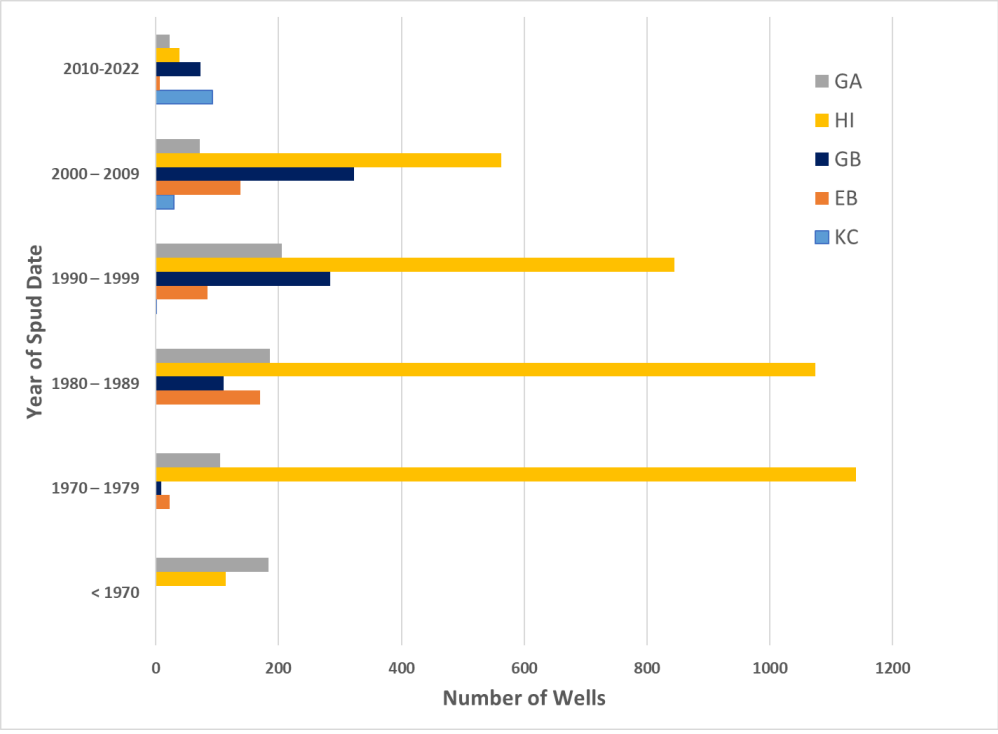

Figure 5.7 - Galveston Transect Well Data in Federal Waters, Sorted by Spud Date

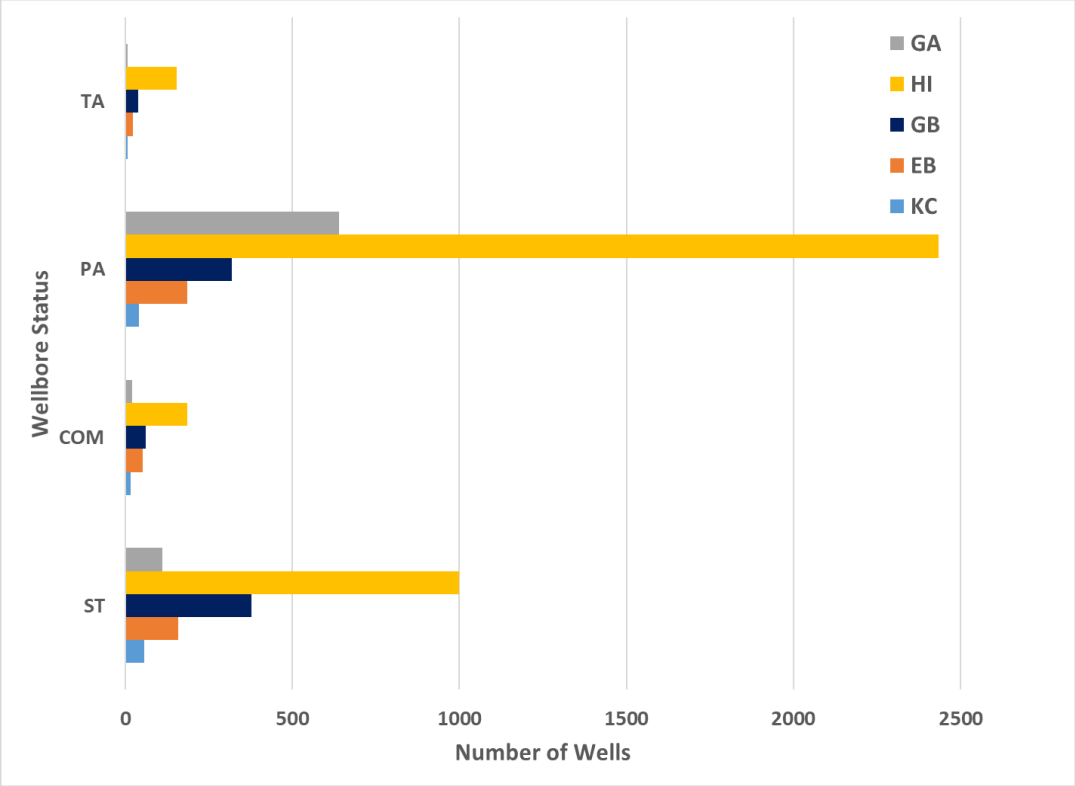

Figure 5.8 - Galveston Transect Well Data in Federal Waters, Sorted by Wellbore Status

5.1.2 Subtask - Evaluate feasibility of subsea template in GoM

Partner, Aker Solutions, generated detailed design options for subsea infrastructure for a shallow-water CO_2 injection well Appendix F. A major result from Aker's work was the following set of recommendations for future work:

Suggestions and recommendations for further work have been included in different sections of the report. The next natural step would be to perform more detailed studies to verify the feasibility of the proposed concepts and increase certainty while identifying optimization and simplification opportunities. The following additional activities are recommended in future study phases.

System Engineering, Process & Flow Assurance

• Update and develop design basis.

• Optimization of field layout and hardware selection based on location and distance between wells, plans for future expansion, maximum step-out distance, system sizing, etc.

• Define material compatibility analysis based on field specific injection fluid.

• Verify well operations to validate virtual metering and choke size for operations.

• Investigate alternatives for tree valve testing and chemical injection needs.

• Develop process safety philosophy.

Offshore Injection System

• Continue the evaluation of dry and wet trees considering field location and water depth.

• Define tree functional requirements and develop tree concepts.

• Design of foundation system according to actual soil condition data.

Control System

• Develop overall control and operating philosophy.

• Perform hydraulic, power and signal analyses to verify equipment sizing.

• Develop umbilical cross-section and evaluate umbilical-less system for dry tree alternatives.

• Define interfaces to remote control systems.

• Evaluate and select of a monitoring and leak detection strategy.

Cost and Schedule

• Produce updated cost and schedule estimates to increase execution certainty.

5.1.3 Subtask - Risk Assessment - CO_2 Release from Truck/Barge Transfer Operations

Context and Scope

Early-stage CCS projects along the Texas Gulf Coast may rely on refrigerated or low-temperature liquid CO_2 transported by truck and barge, particularly before high-volume trunk pipelines are permitted and constructed. In these systems, significant safety risks can arise at transfer interfaces, particularly during truck-to-barge and barge-to-shore loading and unloading operations at coastal terminals or river docks.

This preliminary risk assessment synthesizes existing technical literature, safety guidelines, and incident analyses to characterize the main hazards associated with CO_2 release during transfer operations and to identify the dominant failure modes, consequence mechanisms, and risk mitigation strategies relevant to Gulf Coast CCS deployment. The focus is on refrigerated liquid CO_2 handled in pressure vessels, transfer lines, and manifolds, recognizing that many safety principles parallel those used for other liquefied gases, but with CO_2-specific dispersion and toxicity characteristics.

Hazard Characteristics of CO_2 in Transfer Operations

CO_2 is often described as a simple asphyxiant, but contemporary toxicology and occupational safety literature indicate that it can act as both an asphyxiant and a toxicant at elevated concentrations (Permentier et al., 2017; EIGA, 2011). At ambient concentrations of about 400 ppm, it is not harmful. As concentrations rise, however, symptoms such as headache, dizziness, shortness of breath, and impaired judgment can occur. At higher concentrations, unconsciousness and death are possible (OSHA, 1996; Permentier et al., 2017; EIGA, 2011).

Because CO_2 is denser than air, releases tend to form ground-hugging clouds that can accumulate in low-lying areas, trenches, pits, and enclosed spaces (OSHA, 1996; HSE, 2024). Experimental work under the COOLTRANS

program and related dense-phase pipeline research shows that high-pressure or dense-phase releases can generate cold, dense plumes whose dispersion is strongly influenced by wind conditions, temperature, and terrain (Allason et al., 2012; Wen et al., 2013; Wareing et al., 2014). Although these studies focus on pipeline ruptures, their findings on near-field jet behavior and far-field dispersion are useful for understanding severe transfer accidents. In both cases, a cold, high-density cloud may move laterally and collect in depressions, potentially affecting workers on docks, tug crews, and nearby communities.

Occupational guidance from OSHA, the U.S. Department of Agriculture, and European industry groups also shows that CO_2 releases are especially hazardous in semi-enclosed or congested environments such as loading areas, pits, and other low-lying workspaces, where oxygen displacement and CO_2 buildup may not be immediately apparent (FSIS, 2013; OSHA, 1996; EIGA, 2011). This is directly relevant to truck and barge transfer points, which often include recessed manifolds, hose troughs, and partially sheltered work areas.

Relevant Lessons from CO_2 Transport Incidents

Although there is limited public documentation of major CO_2 releases specifically during truck or barge transfer, several related incident datasets provide insight into credible hazards.

- **Pipeline rupture at Satartia, Mississippi (2020).** A high-pressure CO_2 pipeline failure near Satartia generated a dense ground-hugging cloud that traveled along topographic lows, causing loss of consciousness, vehicle stall-outs, and a large emergency response (PHMSA, 2022; Ogle, 2025). Subsequent investigation highlighted how terrain and low-lying road cuts channeled and concentrated the plume. Although this was a transmission line failure rather than a transfer event, it demonstrates that CO_2 releases can have community-scale impacts when clouds move offsite.
- **Pipeline and CO_2 system incident analyses.** Statistical evaluations of CO_2 pipeline failures and risk assessments developed under projects such as CO_2PipeHaz and related research programs indicate that while the frequency of failures remains low compared to other pipeline systems, consequence modeling must account for dense phase behavior, prolonged discharge durations, and complex terrain (DNV, 2010; Gant, 2012; HSE, 2013; Johnsen et al., 2011).
- **Road tanker incidents involving cryogenic or pressurized liquid CO_2.** Safety bulletins from the European Industrial Gases Association describe incidents in which CO_2 road tanker drivers sustained severe cold burns or asphyxiation during unloading, typically linked to incorrect hose connections, valve maloperation, or unexpected liquid release (EIGA, 2020). These cases underscore the importance of connection integrity, isolation valves, and procedural controls in truck unloading scenarios analogous to truck-and-barge transfer.

Taken together, these incident records suggest that while catastrophic CO_2 release events are infrequent, the consequences of a major release in low-lying or congested terminal environments can be severe. For Gulf Coast CCS systems, this implies that risk management for truck and barge transfers should prioritize consequence limitation and exposure reduction rather than assuming rapid atmospheric dilution.

Credible Failure Modes During Transfer

Transfer operations introduce distinct failure modes beyond those present during steady-state transport:

1. **Hose or transfer-line failure.** Flexible hoses or articulated loading arms used between trucks, barges, and fixed manifolds are subject to mechanical damage, improper routing, and fatigue. A full-bore rupture during liquid transfer could release large quantities of CO_2 over a short period, forming a dense cloud along the dock surface (Wen et al., 2013).
2. **Connection and coupling failures.** Misaligned or improperly secured couplings can leak at high rates under pressure. Quick-connect couplings may partially disconnect if not fully engaged, particularly under vibration or pressure surges (EIGA, 2020).
3. **Valve maloperation or stuck valves.** Incorrect sequencing, such as opening the wrong valve or closing

isolation valves too quickly, can lead to overpressure or unintended discharge through relief valves. Evidence from CO_2 and gas conditioning systems shows that partial obstruction, freezing, or plugging can impair valve function (Kerr & Myers, 2021).

4. **Overfilling and overpressure.** If tank level monitoring is inadequate, overfilling can trigger relief device activation or cause liquid discharge from vent lines. For refrigerated CO_2, temperature changes during transfer can also contribute to pressure swings.
5. **Vehicle or vessel movement.** For truck-to-barge transfers, accidental vehicle movement or barge surge can impose high mechanical loads on hoses and arms, potentially causing failure at the weakest point.
6. **External impact.** Collisions from forklifts, service vehicles, or other equipment operating in the terminal can damage transfer systems, particularly where bollards or protective barriers are absent.

Each failure mode can produce either slow seepage releases, such as small flange leaks or valve leaks, or rapid, large releases, such as hose rupture or emergency-release coupling failure. Risk, therefore, depends on both the frequency of each failure mode and the consequences of a release, including the amount of CO_2 discharged, the direction of plume movement, and who may be exposed.

Dispersion, Exposure, and Consequence Mechanisms

Modeling studies of dense phase CO_2, including work from the COOLTRANS program and the HSE CO_2PipeHaz project, show that ground-level concentrations can remain elevated over considerable distances when releases occur close to the ground and under low wind conditions, particularly in complex terrain or built environments (Allason et al., 2012; Gant, 2012; HSE, 2013). For marine terminals, this creates heightened concern where physical features can trap or channel dense gas. Situations of particular concern include:

- docks or transfer areas adjacent to berms, bulkheads, or retaining walls that may confine cold gas;
- nearby facilities that contain below-grade rooms, trenches, or pits;
- tugs, barges, or other small craft positioned at lower elevations relative to jetty structures; and
- adjacent access points such as roads or walkways that lie at or below deck elevation.

Health impact literature indicates that exposure to CO_2 at concentrations of approximately 7 to 10 percent can lead to rapid unconsciousness, and higher concentrations may produce collapse or loss of consciousness within a very short time (Permentier et al., 2017; OSHA, 1996; HSE, 2024). For truck and barge transfer operations, this means that workers near a major release may have very little time to escape unless warning systems or gas detection are already in place.

Relative to long-distance pipeline transport, transfer operations at dedicated terminals often benefit from several mitigating characteristics. These include shorter potential release distances, generally limited to the transfer envelope; a clear line of sight between operators and equipment; the ability to deploy active monitoring or emergency shutdown systems at the berth; and controlled access that reduces the likelihood of large public exposure events when exclusion zones are enforced.

As a result, the dominant risk profile for truck and barge transfer tends to involve high local severity with limited geographic extent rather than long-distance plume transport across the landscape. However, the Satartia pipeline incident demonstrated that terrain and built-environment features can significantly influence plume movement and exposure when they channel CO_2 clouds toward populated areas (PHMSA, 2022; Ogle, 2025).

Mitigation Measures and Risk-Reduction Strategies

Existing CO_2 and gas industry guidance, together with recommended practices for CO_2 pipelines, identify several layers of risk reduction that apply to truck and barge transfer operations (DNV, 2010; HSE, 2013; EIGA, 2020). These measures can be broadly grouped into engineering controls, operational procedures, and emergency preparedness.

Engineering controls

- Robust hose and loading arm design, with pressure ratings above maximum operating conditions, materials suitable for low temperature CO_2 service, and appropriate bend radius limits to prevent mechanical damage (EIGA, 2020).
- Emergency shutdown systems with quick closing valves at both the truck or vessel connection and the shore manifold, with interlocks that depressurize lines before disconnection (DNV, 2010).
- Emergency release couplings designed to separate in a controlled manner under excessive tension, minimizing uncontrolled hose movement and reducing the potential release volume during an emergency (EIGA, 2020).
- Fixed and portable CO_2 detection near manifolds, hose troughs, and other low points, with alarms linked to emergency shutdown systems and clear alarm logic (OSHA, 1996; EIGA, 2011).
- Physical barriers and traffic control measures that protect hoses and manifolds from accidental vehicle impact.
- Vent stack design for controlled blowdown, with dispersion modeling used to position vents away from work areas and public access zones (DNV, 2010).

Operational and procedural controls

- Standardized loading and unloading procedures, including checklists for hose connection, valve sequencing, emergency shutdown testing, and completion verification (EIGA, 2020).
- Training and competency requirements for drivers, terminal operators, and deck crews handling CO_2 transfers, with emphasis on CO_2-specific hazards such as cold burns, the odorless and colorless asphyxiation hazard, and the rapid onset of symptoms (EIGA, 2020).
- Pre-transfer safety walks that verify hose routing, barricades, and the availability of emergency shutdown systems before initiating flow.
- Weather and wind awareness, including hold points during very low wind speeds or strong atmospheric inversion conditions when dispersion may be poorest (Allason et al., 2012).

Emergency preparedness

- Clearly identified muster points and escape routes located away from likely dispersion paths, with visible signage that allows workers to orient quickly during an alarm.
- Joint emergency drills involving terminal operators, barge crews, and local emergency responders that simulate CO_2 release scenarios and test communication and evacuation procedures (EIGA, 2020).
- Incident reporting and learning mechanisms that capture near misses, false alarms, and minor releases so that procedures and training can be refined over time.

For the Texas Gulf Coast, these measures would need to be integrated into existing marine terminal safety systems that already manage hazardous liquid cargoes. Compared with more flammable products, the principal hazard associated with CO_2 transfer arises from its colorless and odorless nature and its ability to cause rapid asphyxiation without the warning cues associated with fire or explosion (Permentier et al., 2017; EIGA, 2011). This reinforces the importance of robust gas detection, thorough operator training, and conservative exclusion zones during transfer operations.

References

Allason, D., Armstrong, K., Barnett, J., Cleaver, P., & Halford, A. (2012). *Experimental studies of the*

behaviour of pressurised releases of carbon dioxide. Hazards XXIII Conference Proceedings.

Det Norske Veritas. (2010). *DNV-RP-J202: Design and operation of CO_2 pipelines*. Det Norske Veritas.

European Industrial Gases Association. (2011). *Carbon dioxide physiological hazards: "Not just an asphyxiant!"* (Safety Information 24/11/E). EIGA.

European Industrial Gases Association. (2020). *Operation of carbon dioxide road tankers and equipment while loading and unloading* (Safety Information 28/20). EIGA.

Food Safety and Inspection Service. (2013). *Carbon dioxide health hazard information sheet*. U.S. Department of Agriculture.

Gant, S. (2012). *Framework for validation of pipeline release and dispersion models for the COOLTRANS research programme*. Third International Forum on Transportation of CO_2 by Pipeline.

Health and Safety Executive. (2013). *CO_2PipeHaz: Good practice guidelines for the safe design and operation of onshore CO_2 pipelines*. HSE.

Health and Safety Executive. (2024). *General hazards of carbon dioxide*. https://www.hse.gov.uk/carboncapture/carbondioxide.htm

Johnsen, K., Helle, K., Røneid, S., & Holt, H. (2011). DNV recommended practice: Design and operation of CO_2 pipelines. *Energy Procedia, 4*, 3032–3039.

Kerr, T. A., & Myers, D. B. (2021). *Avoid pressure relief valve plugging in gas conditioning applications*. Laurance Reid Gas Conditioning Conference.

Ogle, R., Schneider, J., Schulman, N., & Cox, B. (2025). Risk-based facility siting of CO_2 pipelines. *Process Safety Progress, 44*(3), 606–614.

Occupational Safety and Health Administration. (1996). *Potential carbon dioxide (CO_2) asphyxiation hazard when filling stationary low pressure CO_2 supply systems* (Hazard Information Bulletin, June 5, 1996). U.S. Department of Labor.

Permentier, K., Vercammen, S., Soetaert, S., & Schellemans, C. (2017). Carbon dioxide poisoning: A literature review of an often forgotten cause of intoxication in the emergency department. *International Journal of Emergency Medicine, 10*, 14.

Pipeline and Hazardous Materials Safety Administration. (2022). *Failure investigation report: Denbury Gulf Coast Pipelines, LLC—Pipeline rupture/Natural force damage*. U.S. Department of Transportation.

Wareing, C. J., Fairweather, M., Falle, S. A. E. G., & Woolley, R. M. (2014). Validation of a model of gas and dense-phase CO_2 jet releases for application to carbon capture and storage pipeline failure. *International Journal of Greenhouse Gas Control, 20*, 254–271.

Wen, J., Heidari, A., Xu, B., & Jie, H. (2013). Dispersion of carbon dioxide from vertical vent and horizontal releases—A numerical study. *Proceedings of the Institution of Mechanical Engineers, Part E: Journal of Process Mechanical Engineering, 227*(2), 125–139.

5.1.4 Subtask - Site Leasing

Arguably the most significant external change in the Partnership's study area was the initiation by the Texas General Land Office (GLO) of large tracts of submerged Texas state lands in Texas state waters. For example, Figure 5.9 shows the tracts, which the GLO offered for lease in mid-2024, and the first lease was awarded by GLO to Talos Energy, Inc. and its partner, Carbonvert, Inc. in the summer of 2021.

To a significant degree, DOE NETL's support of GoMCarb and preceding offshore Gulf of Mexico (GoM) carbon

sequestration (CS) studies provided GLO valuable information in establishing GLO's CS leasing program. Important preceding NETL studies include 1) the Gulf of Mexico Miocene CO_2 Site Characterization Mega Transect (FE0001941); 2) the CarbonSAFE Phase 1 Integrated Carbon Capture and Storage Pre-Feasibility in the Northwest Gulf of Mexico (FE0029487); and 3) the Offshore CO_2 Storage Resource Assessment of the Northern Gulf of Mexico (Texas-Louisiana) (FE0026083)

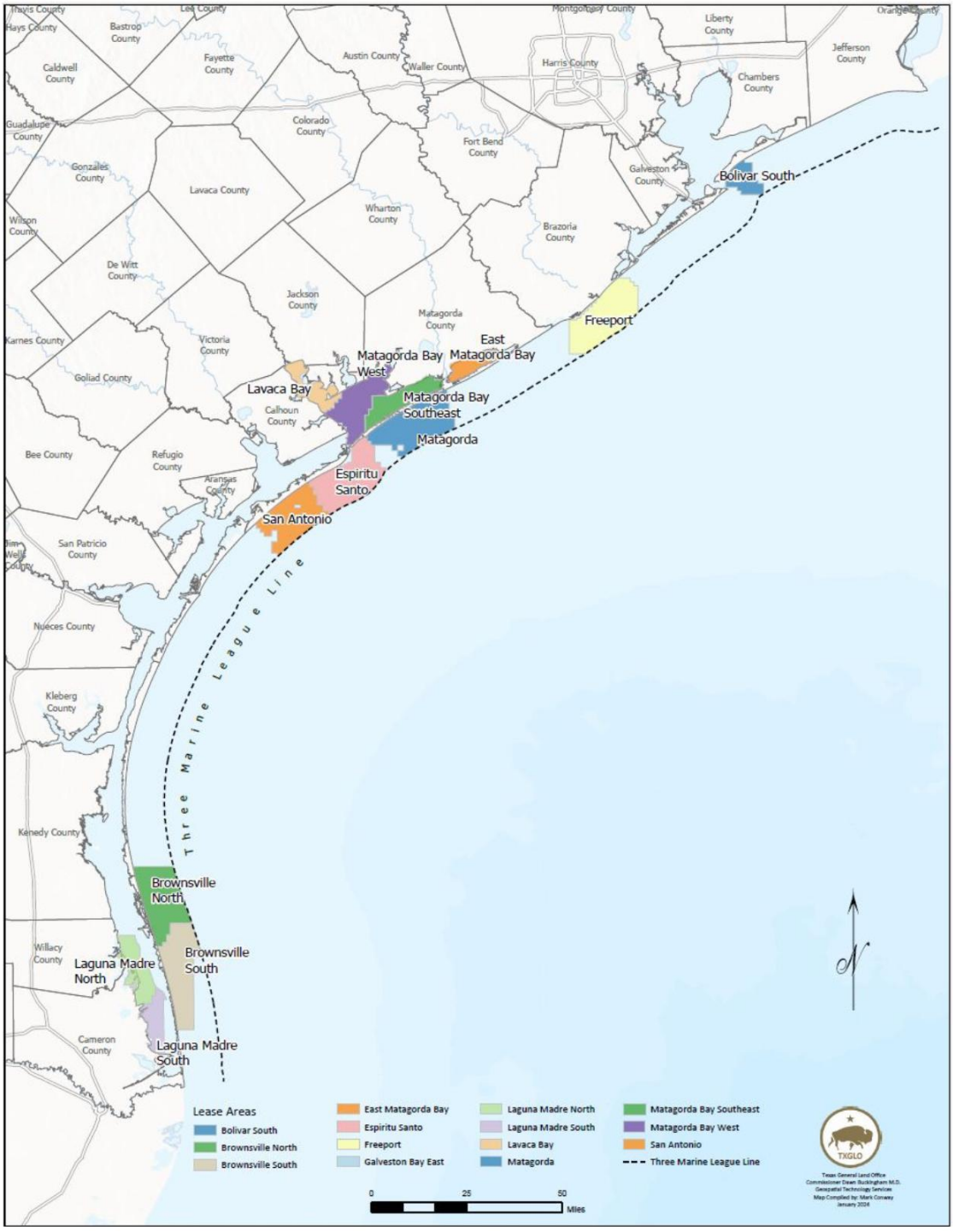

Figure 5.9 – Map showing the submerged lands leasing tracts offered for bid by the Texas General Land Office

(GLO) in the GLO's June 6, 2024 RFP.

5.2 Subtask: Scenario Optimization

Ionic liquids (IL) containing phosphonium cations paired with aprotic heterocyclic anions (AHAs) have shown to be effective in absorbing CO_2, particularly for post combustion processes with significant water concentration. In particular the ionic liquid, triethyl(octyl)phosphine 2-cyanopyrrolide ([P2228][2-CNPyr]), was found to be an ideal candidate to be blended with aqueous monoethanolamine (MEA) as the resulting hybrid solvent showed a significant reduction in the viscosity (compared to neat [P2228][2-CNPyr]) and exhibited a significantly lower the enthalpy of CO_2 desorption (compared to aqueous MEA). These characteristics suggest that phosphonium based ILs are a greener alternative to MEA. However, the current synthesis pathways for this IL contains phosphine and phosgene intermediate compounds. Therefore, this work suggests an alternate synthesis route without phosphine and phosgene intermediates. Using Lifecycle Assessment (LCA) tools, this study found that this novel synthesis route could produce the IL (and its corresponding hybrid solvent) with lower overall environmental impacts compared to aqueous monoethanolamine (MEA).

Conclusions

The work explored the environmental impacts of an alternative route for the synthesis of phosphonium-based AHA-ILs, which are seen as potential replacements to MEA as they exhibit higher CO_2 absorption capacity as well as lower CO_2 regeneration energy requirements. While studies have considered these ILs to be greener alternatives to MEA, most of the life cycle studies published in literature suggested that the current production route used to prepare phosphonium-based ionic liquids had higher environmental impacts compared to MEA due to toxic materials (i.e., phosgene and phosphine) used in their synthesis. Hence, an alternative route has been suggested in this work, and the environmental impacts were determined according to the TRACI 2.1 methodology using GaBi LCA software. This study finds that exploring alternative phosgene-free routes to produce the phosphonium ion can make ILs environmentally friendlier as a CO_2 capture solvent than aqueous MEA. Hence, utilizing an MEA – IL–H_2O hybrid solvent would help improve the CO_2 capture ability with a relatively low environmental impact, making the solvent both economically and environmentally viable.

5.2.1 Subtask - Extend Scenario optimization to mid-Texas Coast

Carbon capture and storage (CCS) systems require the movement of CO_2 from emission sources to suitable storage locations, which are often geographically separated. On the Texas coastal plain, large industrial emission sources are concentrated along coastal corridors, while some promising geologic storage resources, including saline formations in the Corsair Trough (Figure 5.10), are located offshore.

Storing CO_2 offshore has several advantages vs. onshore storage sites. One advantage is that there is only one pore-, and for the most part, pressure-space owner (i.e., the state of Texas in Texas state waters and the federal government in federal OCS waters). Onshore there can be multiple landowners and pore space owners at a given storage site. Another advantage for an offshore site is the general lack of a USDW (underground source of drinking water). Whereas, onshore, protecting USDW is the primary objective in CO_2 storage regulations (i.e., UIC Class VI).

In the offshore setting, transport becomes a defining component of system feasibility rather than a secondary consideration. The choice of transport pathway influences not only cost but also permitting complexity, infrastructure timing, and the ability to scale systems as capture volumes increase. While pipeline transport has historically supported large-scale CO_2 movement, emerging CCS systems in coastal regions increasingly consider marine and hybrid transport configurations to address shoreline constraints and infrastructure limitations.

Here, we provide a preliminary assessment of source distribution, offshore storage opportunities, and transport

pathways in the Texas coastal region. The focus is on identifying feasible approaches for linking onshore emission sources to offshore storage in the Corsair Trough under realistic infrastructure and deployment conditions.

Distribution and Types of Sources in the Mid-Coast

Industrial CO_2 emissions along the Texas Gulf Coast are spatially concentrated within major energy and industrial corridors. The highest density of emitters is located in the Houston–Beaumont region, with additional clusters near Corpus Christi and smaller, more dispersed sources extending along the mid-coast. The sources are primarily associated with refining, petrochemical processing, and power generation, resulting in relatively high and consistent CO_2 output.

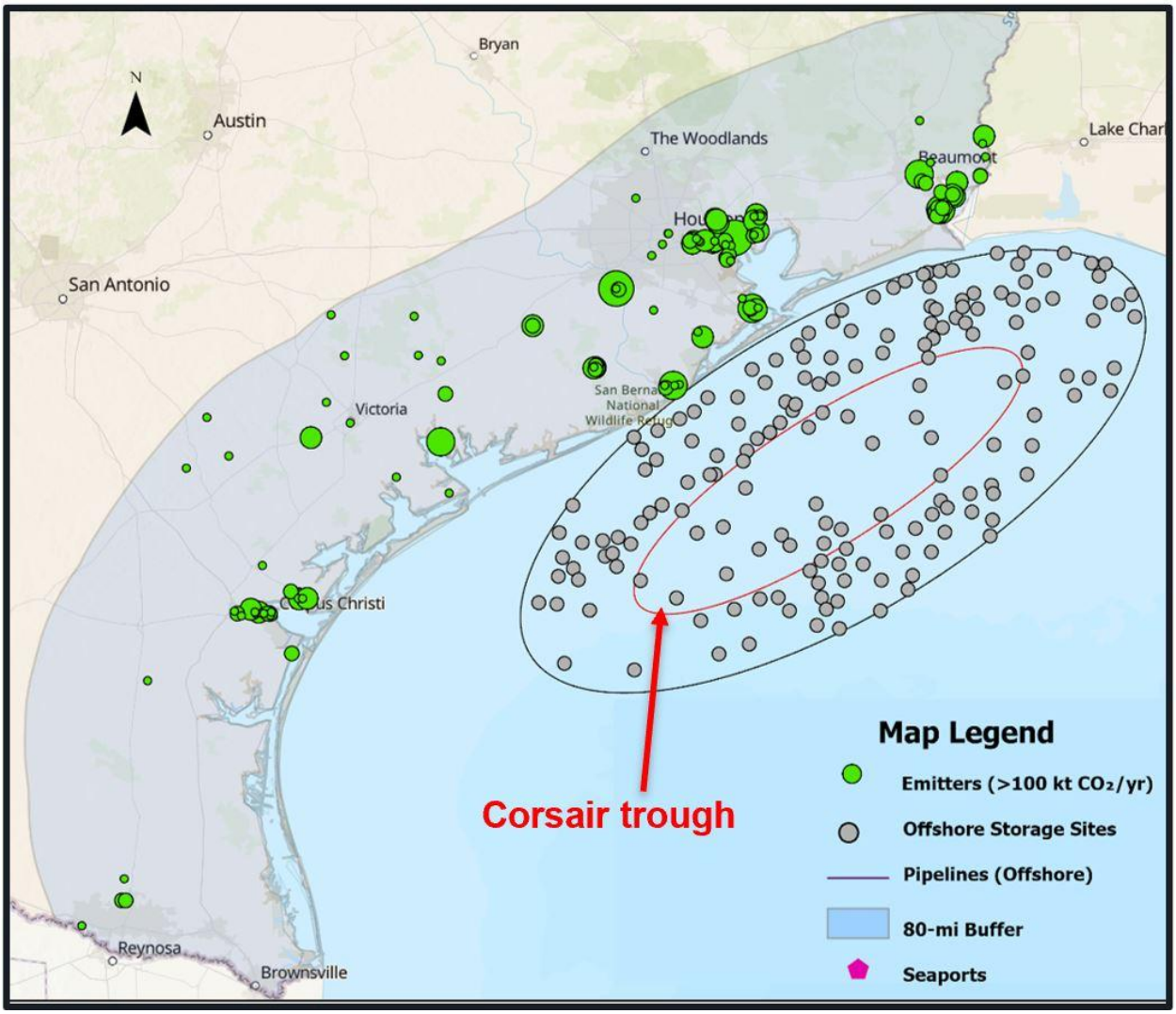

Figure 5.10 - Spatial distribution of CO_2 emission sources along the Texas coast and candidate offshore storage locations in the Corsair Trough. The figure highlights the geographic separation between major industrial emitters and offshore storage targets.

This distribution of CO_2 sources presents favorable conditions for source aggregation, which is an important consideration for transport system design. Clustering allows multiple emitters to share infrastructure, potentially improving the economics of both pipeline and marine transport systems. At the same time, the geographic spread of

sources, particularly outside of the main industrial hubs, introduces variability in transport distance and access to existing infrastructure.

A key challenge is the spatial separation between these emission sources and offshore storage resources. As shown in Figure 5.10, most emitters are located onshore, while candidate storage sites in the Corsair Trough are positioned offshore at varying distances from the coastline. This separation requires transport systems to span onshore, nearshore, and offshore segments, each with distinct technical and regulatory considerations.

Taken together, the distribution of sources suggests that no single transport pathway will be universally optimal. Instead, system design must account for both clustered and distributed emitters, as well as the need to connect these sources to offshore storage through a combination of infrastructure types.

Onshore to Offshore Transportation Options

Transport of CO_2 from onshore emission sources to offshore storage in the Corsair Trough requires the integration of multiple infrastructure segments, each operating under different physical, operational, and regulatory conditions. In practice, transport pathways must account for the transition from inland facilities to the coastline, followed by movement across nearshore and offshore environments. These segments introduce distinct constraints that influence both feasibility and system design.

In early-stage deployment or in cases where emitters are smaller or more geographically dispersed, truck and rail transport can serve as feeder systems that connect individual facilities to larger transport networks. These modes are typically used over shorter distances to move CO_2 to aggregation points where it can be transferred to higher-capacity systems such as pipelines or marine transport. While truck and rail introduce higher per-unit costs at scale, they provide flexibility in early deployment phases and enable the inclusion of sources that may not be directly connected to pipeline corridors or coastal infrastructure.

Pipeline transport remains the most established mode for large-scale CO_2 movement and is well suited for high-volume, continuous flow between fixed points. In regions where emission sources are clustered and routes can be established with minimal conflict, pipelines offer a reliable and cost-effective solution over long operating lifetimes. However, along the Gulf Coast, pipeline deployment is often constrained by permitting requirements, land access, and environmental considerations. Shoreline crossings in particular introduce additional engineering and regulatory complexity, as pipelines must traverse wetlands, coastal zones, or developed industrial areas before reaching offshore environments. Consequently, shoreline crossings can represent a disproportionate share of total project cost and timeline making them a key consideration in transport planning.

Marine transport, including both ship and barge-based systems, provides an alternative approach that avoids the need for continuous pipeline infrastructure across constrained zones. In these systems, CO_2 is typically conditioned and transported as a refrigerated liquid between port facilities and offshore injection sites. This allows transport pathways to be decoupled from fixed routes, enabling greater flexibility in connecting dispersed sources to storage locations. Marine transport is particularly relevant in coastal regions where access to ports and navigable waterways is already established, and where offshore storage sites are located at distances that would require complex or costly pipeline routing. However, this flexibility introduces additional system requirements. Marine transport depends on the availability of port infrastructure, intermediate storage, and loading and unloading systems capable of handling liquid CO_2. Operational constraints, including vessel capacity, turnaround time, and scheduling, also influence system performance. In inland and nearshore environments, marine vessel draft limitations and navigation constraints may restrict vessel size, particularly for barge-based systems operating along the Gulf Intracoastal Waterway. As a result, marine transport systems must be designed with attention to both infrastructure availability and operational logistics.

Given the tradeoffs, transport pathways in the mid-Texas coastal region are likely to involve hybrid configurations that combine pipeline and marine vessel segments (Figure 5.11). For example, pipelines may be used to aggregate CO_2 from clustered inland sources for delivery to coastal transfer points where it can be loaded onto barges or ships for transport to offshore storage. Such configurations allow system design to align transport modes with local

constraints, using pipelines where continuous high-volume flow is feasible and marine transport where flexibility or routing constraints dominate.

Alternatively, marine transport may be used to connect smaller or more distributed sources to centralized hubs, which serve as intermediate aggregation and transfer points within the transport network. At the hubs, CO_2 from multiple sources can be combined, temporarily stored, and conditioned for onward transport. The facilities enable transitions between transport modes, such as from truck or rail to pipeline, or from pipeline to ship or barge, and therefore play a critical role in enabling multimodal system configurations.

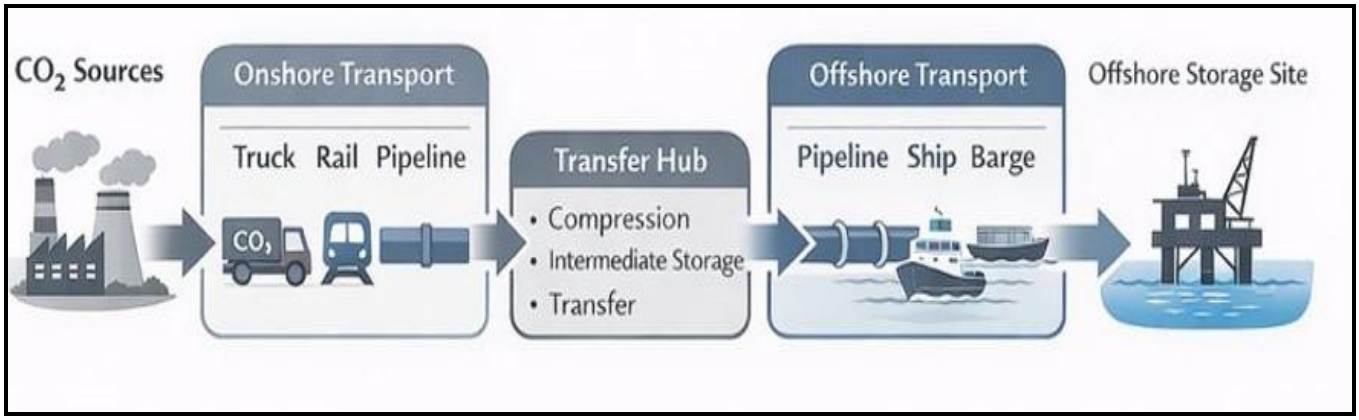

Figure 5.11 - Conceptual representation of a multimodal CO_2 transport system illustrating the integration of feeder systems, transfer hubs, and offshore transport modes in enabling transitions between transport modes.

The use of transfer hubs (Figure 5.11) also introduces additional system considerations. CO_2 may require conditioning or changes in pressure and temperature to meet the requirements of different transport modes, which can increase both infrastructure needs and operational costs. Nonetheless, hubs provide flexibility in system design by decoupling capture, transport, and storage, thus allowing infrastructure to be developed in phases as volumes increase. As a result, hubs often function as key decision points within the transport network where choices about mode selection, routing, and system configuration are made. While large-scale CO_2-specific hub infrastructure remains limited, analogous systems already exist in both CCS and broader industrial supply chains. Projects such as Northern Lights demonstrate centralized collection and transfer of CO_2 prior to offshore storage, while smaller-scale operations have historically used transfer points to move CO_2 between pipelines, trucks, and storage sites. More broadly, similar hub-based logistics are well established in hydrocarbon and chemical transport systems. Although, CO_2-specific hub design is still emerging, the underlying concept is grounded in existing industrial practice.

The selection of transport pathways, therefore, depends on a combination of factors, including transport distance, CO_2 volume, infrastructure availability, and permitting conditions. In early-stage deployment when volumes are uncertain and infrastructure is limited, marine and hybrid systems may offer advantages due to their scalability and lower upfront capital requirements. As systems mature and volumes increase, pipelines may become more favorable due to their efficiency at scale. Taken together, these considerations indicate that multimodal transport systems are not only feasible but necessary for connecting Gulf Coast emission sources to offshore storage under realistic deployment conditions.

References

Northern Lights Project. (n.d.). *Northern Lights CO_2 transport and storage infrastructure*. https://norlights.com

U.S. Environmental Protection Agency (EPA). (n.d.). *FLIGHT: Facility Level Information on Greenhouse Gases Tool*. https://ghgdata.epa.gov

5.2.2 Subtask - Analog Site Optimization

The following was reported in Deliverable 5.2a report:

Optimization assessment of offshore storage in the northwest Gulf of Mexico

Introduction

In subtask 5.2 we explored scenarios to optimize field operations, reservoir response, and operation costs for efficient storage and monitoring of CO_2. based on linking the source and transport options to storage resources. This summary reports integrates and highlights data identified in other GoMCarb tasks. The number of possible options for linking sources, pipeline routes, and storage options on the Gulf coast are very large, **and a key finding of this optimization report is that no one case is optimum for all situations**. In this report, we overview the components that define the options with a study area on the upper coast of Texas and southwest Louisiana. Components integrated are 1) evaluation of clusters of sources that can be amalgamated, 2) options for crossing the coastal zone, 3) offshore pipeline options for distribution of CO_2, and 4) consideration of the options for accessing and developing storage in the offshore, including issues of wells and platforms.

We observe that offshore storage becomes most valuable for storing large volumes of CO_2 for projects that are to be sustained for a long time. Factors favoring offshore storage for large volumes: a) single landowner is favorable for amalgamation of sufficient pore space for large projects, b) access from sources onshore to sinks offshore is higher overall cost than injecting very close to the sources; economies of scale created by amalgamation of sources is where offshore storage gains the highest value, c) excellent reservoir and confining system quality offshore favor very large quantity storage, d) the number of well penetrations is less than onshore, and the wells are newer, reducing risk of difficulty in establishing isolating completions of wells.

Amalgamation of Clusters of Sources

We assume that for mature offshore projects, amalgamation of CO_2 from multiple sources will be important. This follows the "cluster and hub" model which is becoming widely recognized as a cost-effective approach to maturing large volume storage, in for example, the Porthos project under development to serve the heavy industry area proximal to Rotterdam, Netherlands (Porthos website, accessed 2021). Some projects may consider one-source-to-one sink options, especially if a large source becomes a pioneer first-mover; however, this is not considered an optimum in this evaluation of full-scale options as explained below.

Relatively pure sources of CO_2 are present in the Gulf Coast region, for example from the manufacture of ethylene oxide, from purification of natural gas as needed prior to production of LNG (liquified natural gas), and from the manufacture of fertilizer. However, individually these high purity sources generally each produce less than 1 MMT per year. If these high purity sources are considered individually, it is likely that storage in available onshore storage complexes is most attractive. This is because onshore storage is abundant in this area, amalgamating and leasing sufficient acreage to host modest-size storage projects is likely to be successful, and pipeline transport for small volumes of CO_2 significantly increases the cost per unit volume. In addition, current funding mechanisms such as the 45Q tax credit are designed to support short term startups that can be accomplished quickly.

Whereas large volumes of CO_2 from combustion associated with both power generation and industrial processes need mitigation, industrial processes may be especially attractive because they are less feasible to offset with renewable energy sources. Combustion as a source of heat has higher efficiency and higher temperature ranges. In addition, use of fossil fuel sources is attractive because of efficiency of combining energy sources with requisite fossil feedstocks. Industrial processes include many elements of refining and petrochemical manufacture and increasing amounts of production of LNG. Energy use for LNG is for the trains that cool and liquify gas into shippable form. Substitution of electric power for combustion sources may not be either economically viable or suitable for existing process engineering; so decarbonization may be needed.

Interest and investment in decarbonized products is increasing, with discussion of manufacture of energy carriers such as hydrogen or ammonia. These products can be made from fossil fuel feedstocks from which the carbon is stripped during preparation, creating a large volume of pure CO_2 stream ready for storage. Location of such new

large volume capture facilities may consider proximity to storage as part of siting criteria. Using this consideration, location of future plant may be flexible.

Capture from fossil fuel fired power plants remains in the high-cost range (National Petroleum Council, 2019). However, breakthrough processes such of the Allam cycle (NetPower, accessed 2021) cost and feasibility may greatly improve incentivizing new build power plants, or incentives to capture from may increase such that capture from power plants is favored. In addition, the need for decarbonization mixed with other system requirements means that the future operation of power plants is difficult to predict.

Another uncertain source of CO_2 is from negative emissions technologies (NETs) that at large volumes are likely to require geologic storage. In particular, direct air capture (DAC) could be optimized to be placed proximal to large volume storage, favoring the Gulf Coast. However, humidity and storm severity issues would have to be overcome. Biofuel with capture could also be placed where storage is abundant.

Additionally, it is possible that CO_2 will be transported via pipeline to the Gulf Coast from regions that lack large volume or high-quality storage. Offshore storage may be attractive for the large volumes that would incentivize long-distance transport.

As volume of CO_2 is increased by capturing from large sources and amalgamating smaller ones, offshore storage is favored. Pure sources associated with industrial clusters allow these sources to be amalgamated and combined with less concentrated sources. Moderately high concentration CO_2 (in the range of 50%) is produced via most recently configured steam methane reforming (SMR) plants, which supply hydrogen for refining as well as other uses. Most SMR plants produce multiple millions of tons of CO_2 per year. However, a review of the operations of many of these plants (Tutton, 2018) shows that significant modification would be needed to the process engineering to permit capture. Space within the refining complex to install additional equipment for capture may also limit application. The Air Products hydrogen plant in Port Arthur has been successfully capturing and selling about 1 MMt/per year for use for EOR and storage at Hastings field; however, the Air Products capture project obtained federal financial support for significant retrofit of the facility for capture (Air Products, accessed 2021). Additional assessment of the value of CO_2 needed to overcome these barriers at current high concentration facilities is needed.

We consider that doing a strict evaluation of the distribution and amount of CO_2 that can be captured on the Gulf Coast is premature, because of the state of flux of carbon management activities. Optimization at this time includes consideration of a wide number of possible evolutions of sources as discussed below. We therefore do not follow the pathways used in previous work to use the existing sources as a strong guide on the distribution of future sources. However, it is possible that current heavy industry locations will continue to be the focus of future carbon-handling activities. Current clusters of large CO_2 emission sources within the study are in the Beaumont- Port-Arthur-Orange area, in the Houston ship channel area, and slightly south of there in the petrochemical complex of Texas City (large yellow circles, Figure 5.12).

For the optimization, we observe that the network of onshore pipeline rights-of-way (generalized locations shown in Figure 5.12) suggests that additional pipelines to transport large volumes of CO_2 around the region are possible. Supporting this assertion, in 2010 Denbury constructed a new 320-mile CO_2 pipeline, the Greenline from Donaldson, LA to Hastings Field South of Houston, TX (Denbury, accessed 2021). Therefore, specifying onshore locations for capture does not seem to be a key optimization parameter at this time.

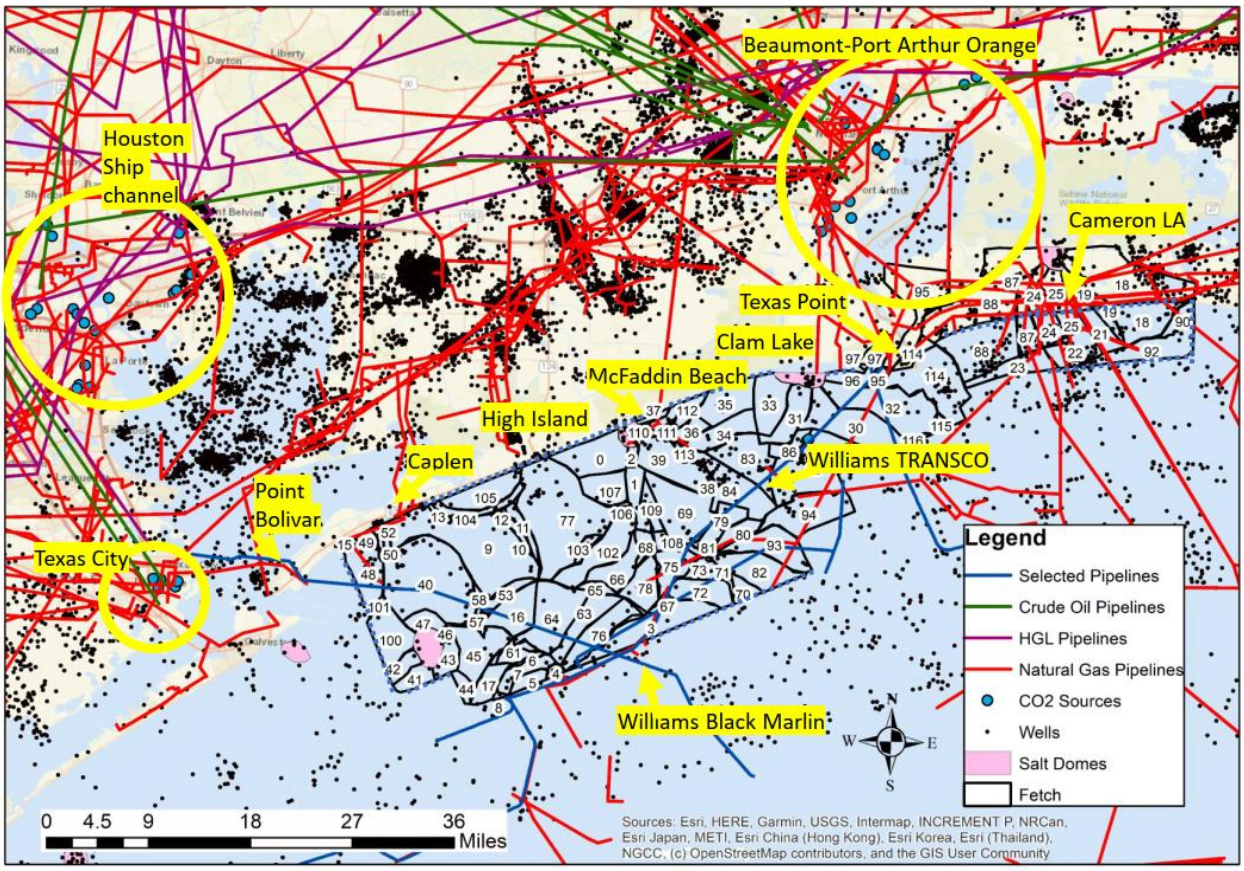

Figure 5.12 - Infrastructure related to storage in the study area. Large yellow circles indicate existing concentrations of CO2 sources. Generalized pipeline locations compiled and edited from the Department of Homeland Security, the Texas Road Commission (RRC), and the Bureau of Ocean Management (BOEM) and should be considered indicative not comprehensive. Possible pipeline shoreline crossing locations are noted in yellow; additional assessment via contacting owner and detailed examination of regulatory files is needed to validate and correct. Selected offshore pipelines discussed in the text are show in blue. The numbered polygons in the offshore study area are the fetch-trap boundaries described in the text. Well locations from IHS are shown as black dots. Offshore locations (in pink) of piercement salt domes at the approximate MFS9 map horizon are shown as they are not suitable for porous media storage.

Crossing the coastal zone

One of the consequential findings of GoMCarb research is that crossing the shoreline is a high-cost element of the transportation system cost. Initial finding is that shoreline crossing cost may be more than double the cost per mile compared to the offshore pipeline. In addition, the coastal zone is highly protected by environmental law and is used for tourism, creating possible barriers to permitting. The coastal area within the study is mostly operated as state park and wildlife preserves with sparse population and is composed of beach and small vegetated dunes areas fronting coastal marsh for most of the study area. At the southwest end of the study area, Bolivar Peninsula, which composes the southeast border of the East Bay arm of Galveston Bay, is the beginning of barrier island geomorphology. At the mouth of the Sabine River, a wave dominated progradational feature forms the chenier plain, which is low ridges separated by swales. Land use is the low-usage Texas Point National Wildlife Refuge.

Previous infrastructure in the coastal zone includes the intracoastal water way, which parallels this part of the coast about 2 miles inland. State highway 87 is part of the coastal infrastructure 500-to 100 ft inland from the beach in parts of the region; however, the middle portion of the highway was damaged and abandoned in 1987. Local business groups support reconstruction of the highway. Several north-south roads also approach the shoreline. All the roads have prominent water-filled bar ditches or fill dredge features. Mixed industrial/residential use areas exist

at Sabine Pass, TX and Cameron, LA. At High Island and the Bolivar Peninsula in the southwest end of the study, the land use is more residential.

We consider the existing pipeline rights of way with shoreline crossings to be resources that potentially could be re-used to increase project feasibility. Figure 5.12 and Table 5.3 provide generalized information about onshore pipelines' existing shoreline crossings. However, the operational status, ownership and feasibility of adding additional pipeline at these shoreline crossings has not been determined. We assume that adding additional CO_2 transportation pipelines would be easier that these points than a new crossing. The crossings then become "hubs" in the sense that pipelines are aggregated shoreward, using a unified large diameter pipeline system to make the shoreline crossing, and they can be distributed to multiple pipelines to different sinks seaward. This use of hub for a linkage point of a pipeline network is similar to the existing pipeline network of the Permian basin, which aggregates and distributes CO_2 via the pipeline network that links and monitors at the Denver City hub.

Table 5.3: Generalized possible shoreline crossing locations

State	Location name	Comment
Louisiana	Cameron	6 or more pipelines crossing the shoreline gathering from West Cameron offshore fields and associated with handling facilities for hydrocarbons
Texas	Texas Point	One pipeline on the point , connected to long regional pipeline
Texas	Clam Lake	Former* gathering system serving near shore fields
Texas	McFaddin Beach	Former* gathering system serving near shore fields, now abandoned
Texas	High Island	Not clear if this network for salt cavern storage continues offshore
Texas	Caplan	Local gathering point
Texas	Point Bolivar	Connection point to long offshore pipelines; continues across Galveston Bay toward the petrochemical complexes of Texas City.

* No longer in use

Pipeline options for distribution of CO_2 Offshore

Offshore pipelines are an important part of the cost and logistics of an offshore project. Although other offshore projects such as Northern Lights offshore Norway (Northern Lights accessed 2021) and Lula CO_2 mitigation (MIT, accessed 2021) in Santos Basin of offshore Brazil use ships for transporting CO_2 on part of its journey from source to sink, we postulate that CO_2 transport via ship will not be used on the Gulf Coast because 1) initial analysis shows that cost of preparing cooled CO_2 is high (Trimeric, written communication, 2019), 2) distances are relatively short and 3) existence of pipelines show that pipeline transportation is feasible.

Pipeline options include retrofit of existing pipelines for CO_2 transportation, reuse of existing pipeline locations for

new pipeline installation, and construction of new pipeline in new locations.

A detailed report (Trimeric, written communication, 2021) on the feasibility of reuse of pipelines was prepared by Trimeric and their contractor and is summarized as follows:

Natural gas and crude oil pipelines are possible candidates for re-purposing for CO_2 service. Gas transportation lines are exposed to water content in the gas and must be treated with corrosion inhibitors to prevent corrosion. Oil may provide a coating on the inside walls of the pipe, but paraffin and asphaltene buildup must be removed by "pigging" the line periodically. In our review we restricted our interest to > 8 inch lines in order to transport masses greater the 1MMt per year. Operating pressure may be a limit on viability of reuse, as CO_2 is shipped at higher pressure than hydrocarbons.

In Table 5.4 and shown in blue on Figure 5.12 we identify two, long, large-diameter pipelines which appear to have potential for reuse, Williams TRANSCO and Williams Black Marlin (Trimeric, written communication, 2021). These lines have not yet been abandoned; so, they may have avoided loss of corrosion inhibition. The Williams TRANSCO goes onshore near Clam Lake in the Port Arthur area and Williams Black Marlin goes onshore at Point Bolivar and then across Galveston Bay to the cluster at Texas City. Our search was not exhaustive, as we did not consider pipelines still in use that might be purchased. To advance toward qualifying a pipeline for reuse, additional negotiation with the owner and regulator would be needed, and an extensive workflow for assessment of the pipeline condition performed.

Table 5.4: Selected examples of pipelines for reuse.

Region/ Location	Line ID	Last Owner	In Service Date	Size	MAOP (psi)	Length (miles)	Water Depth (feet)	Status
Texas (High Island)	4073 4074 5381 4613 4590	Williams TRANSCO	12/13/1979 1/28/1980	12" 24"	1392 - 1440	84 (system length)	43-75	Proposed Abandonment (4613, 4590) & Active (4073, 4074, 5381)
Texas (Galveston)	7199 3489	Williams Black Marlin	12/1/1984	16"	1367	23.87	48-61	Proposed Abandonment

In general, the existence of pipelines in the offshore is considered as evidence that the ability to transport the CO_2 can be accomplished. The Denbury Greenline mentioned above crossed state waters of Galveston Bay showing that technology and permitting are available (Denbury, accessed 2021).

Storage in the offshore.

Previous work (for example, Meckel et al., 2012, Wallace, et al., 2014, Trevino and Meckel, 2019, and previous GoMcarb and TXLA contract reports) has shown that the entire offshore region has suitable injection zones and confining systems to accept CO_2. The injection window is within the Miocene strata above the top of overpressure and below the base of supercritical CO_2 set regionally at 1006 m, ~3300ft (Wallace, 2014). In this study we assessed only one of the intervals MFS9 to MFS10 where we had completed all data collection. There are many ways to assess suitability of storage volumes. In this effort, we use the natural geometry of the flow units in the injection window to divide the subsurface of the study area into fetch-trap polygons (numbered areas in figure 1, 2, and 3). The mapped polygons are shown and numbered in figure 1.

A trap is analogous to a hydrocarbon trap, a 4-way closed structure where buoyant fluid (oil, gas or CO_2) accumulates. Fetch is the area where buoyant fluids will migrate toward the trap. In this study we define traps generously. We assume faults with more than 100 ft of offset on the MFS9 horizon are generally sealing enough to retard lateral and vertical CO_2 migration. In addition, we assume that piercement salt domes (shown in pink on figure 1) seal the adjacent strata to vertical migration. Examination of hydrocarbon trapping shows that both sealing

and out-of-trap migration can occur in these settings. Detailed study of fault seal (e.g. Meckel et al, 2017) and salt-sediment contacts are needed additional steps to determine how much retardation of CO_2 is provided.

We consider a model of injection into the fetch, away from faults and typically away from wells. Using our current model assumptions (GoMCarb Milestone 5, 2020) large amounts of CO_2 can be injected into the fetch, and if the fetch is large enough, the CO_2 will be trapped by capillary and dissolution processes before it arrives at the trap. The boundaries of the fetch areas are set at 1) faults (again assumed generally retarding) and 2) changes in dip of the flow units that serve as flow divides. The prominent Miocene unit MFS 9 as interpreted from 3-D seismic was used to define the fetch and traps; if a different horizon was used the flow directions will change somewhat. We also used the thickness of only the lower Miocene below MFS9 - to MFS 10 because this mapping was complete and because MFS9 is a thick marine transgressive sequence that forms a single easily definable top confining system. Injection into shallower zones is possible; however, more characterization would be needed to define and qualify a top confining system that isolates buoyant CO_2 at elevated pressure.

The subsurface is continuous across the shoreline; however, the 3-D seismic data, on which the geologic interpretation largely depends, was collected by marine vessels and ends offshore from the shoreline in most of our study area. In Louisiana the seismic vendor has merged a land-based 3-D survey, and a similar (non-seismic based) process will eventually be conducted in Texas. However, in this assessment, the fetch areas (e.g., polygons 105, 0, 35 and 33 88, 24, 25, and 19) where the traps are onshore are simply truncated (indicated by dashed lines). In reality, CO_2 injection offshore may allow CO_2 migration and pressure increase onshore. Using these shoreline crossing polygons for injection will require working with both the offshore property owner, and the onshore state or federal or other owners. Compartments at the margins of the 3-D study are also truncated as shown in figure 1 with a dashed line

To evaluate how the system might be linked together, it is important to assess how much CO_2 can be injected into each polygon. For optimization, it is valuable for this to be rate-based, in that the ability of the subsurface to accept CO_2 at the rate provided and for an assumed 30-year project duration is limited by pressure build up. We use representative data from the dynamic capacity estimator, EASiTool, to conduct a first cut assessment. EASiTool can be set to assume that the polygon boundaries are hydrologically open or closed. In the Gulf of Mexico Basin, most polygons are semi-closed. If injection occurs into adjacent polygons, an assumption of closed boundaries is most applicable (Figure 5.13). Table 5.5 provides the inputs used in the EASiTool calculations, and S. Prentice, written communication provides a detailed methodology in a README file.

Table 5.5: Input assumptions for EASiTool capacity calculations.

Salinity: 2 mol/Kg
Rock Compressibility: 5e-10 1/Pa
Injection well radius: 0.1 m
Number of extractors: 0
All settings in NPV and Relative permeability
Min extraction pressure: 20 MPA (due to low pressures amongst values input)
Reservoir Area= Basin Area
Permeability: 300 mD
Number of Injectors: 100
Simulation time: 30 years

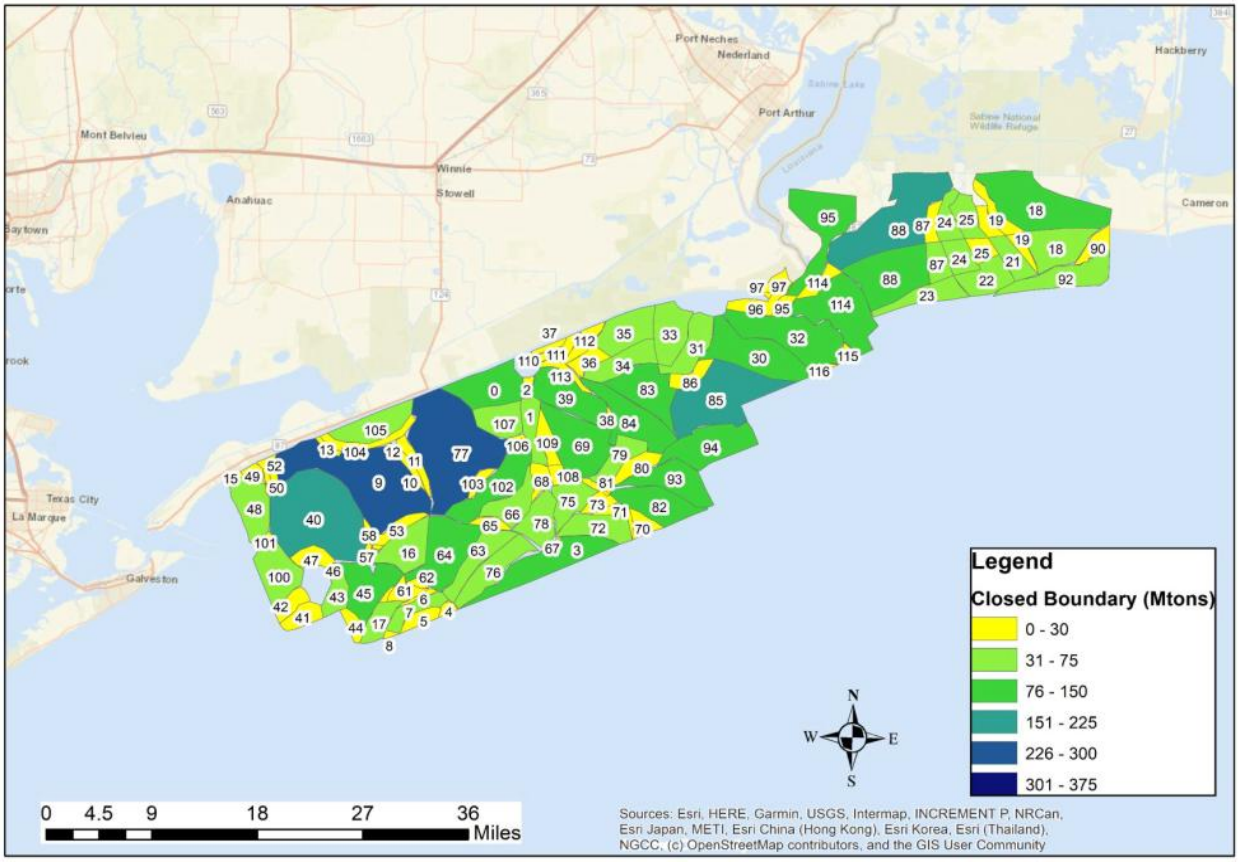

Figure 5.13 - A simple closed-boundary capacity assessment using EASITool for Miocene interval MFS9-10 based on available geologic data, data estimated or assumed in Table 5.5, and the mapped compartments. Note that only the mapped parts of polygons that are truncated at the shoreline or at the study area edge are assessed. S. Prentice (written communication) provides the detailed approximation methodology. We caution against using this too literally. Its principal use is to provide encouragement that much of the area (not only certain blocks) is suitable for large volume storage.

We see that in a quite conservative case, closed boundaries, and only the one zone of the Miocene receiving injection, the masses injectable per compartment (while considering pressure as the only limit) are quite high in most of the compartments. In smallest compartments (shown in yellow less than 30MMt in figure 2), injection into the specified zone is causing pressure build up and limiting capacity. These areas would likely be avoided for large volume injection. In the next category, injection might be limited to only a few wells receiving up to 75MMt over the 30-year lifespan, but capacity could be increased by accessing other Miocene zones. Larger compartments might accept 100's of millions of tons over 30 years. An all-open case (Figure 5.14) provides very high injection mass-limits. In aggregate this is unrealistic because compartments would pressure-interfere. However, it is provided to partially support a high maximum local injection rate and allow consideration of suitability of some locations to receive focused injection. Additional modeling with realistic sand body geometries and boundaries will likely reduce the maximum injection rate that can be sustained into one area (e.g. case study in Meckel, et al. 2012).

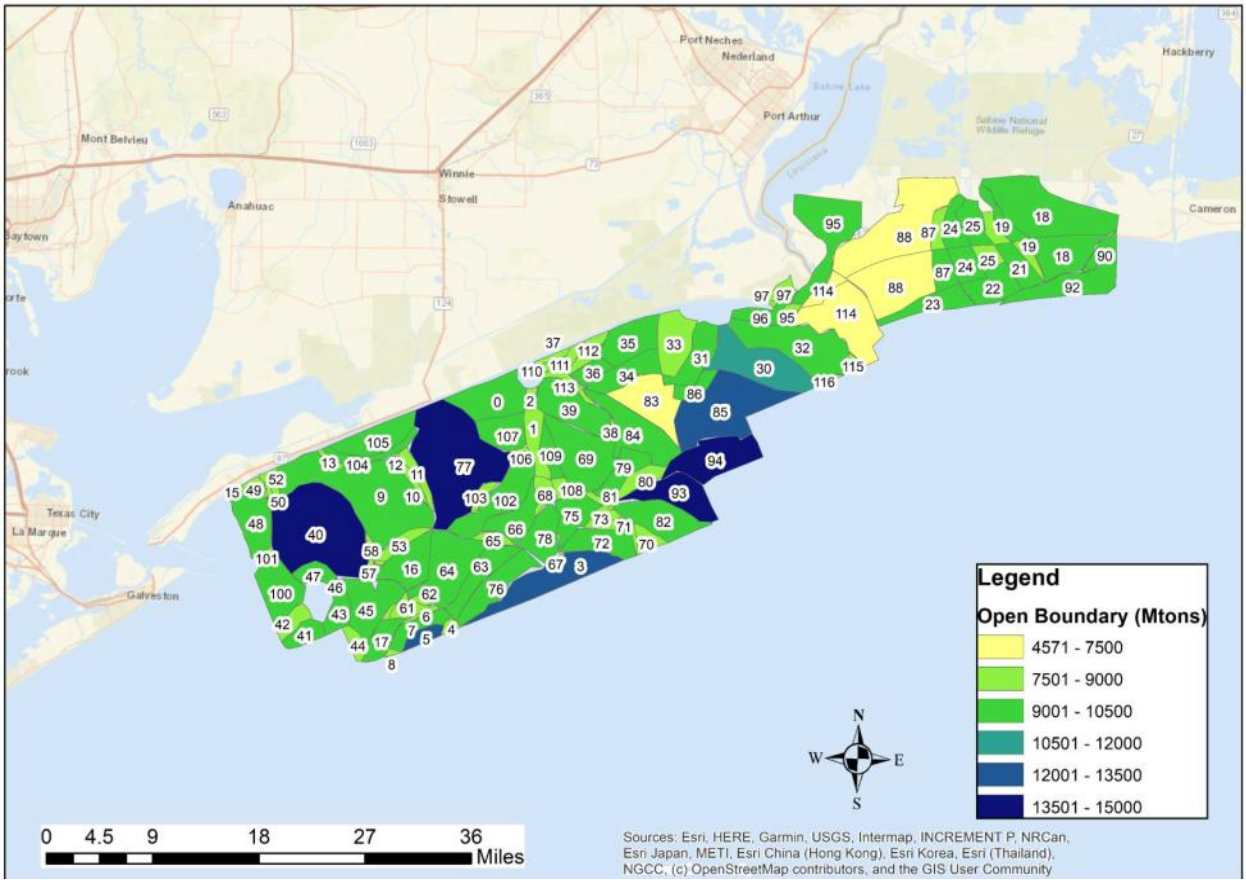

Figure 5.14 - Unrealistic maximum open-boundary capacity assessment for Miocene interval MFS9-10 based on available geologic data, data estimated or assumed in Table 5.5, and the mapped compartments. This map illustrates the significance of assessment of the area that allows pressure dissipation (good water drive). The viability of this assumption varies based on the type of compartment boundary and the extent to which adjacent compartments are used to maximum capacity.

For optimization, however, another factor in addition to the geology that will pragmatically limit the mass injected is plume and pressure limits imposed by the risk of existing wells. Wells are designed to isolate the production zone from shallower zones by placement of cement to close the rock-casing annulus across the production zone and lifting cement to the top of the reservoir confining system. However, two issues can cause this isolation to fail: 1) well age; older wells may have poor records so that completion cannot be documented, lack modern completion methods, or have been damaged; 2) if the well targeted a deeper interval for production, cement may not have been placed in the shallower zone intended for production. To consider these risks, we plot the age and depths of wells in Figure 5.15 and Figure 5.16. All polygons contain some wells, and most of the wells are more than 30 years old. Well density varies; therefore, optimization to avoid pressure or CO_2 plume intersection many well is possible, as is limiting the amount injected per zone to limit plume spread. Figure 5 shows the total depth of the wells, which is a coarse indicator of the likely completion interval and extent of cement. Many wells targeting intervals deeper than 9,000 feet (red, suggesting caution) are found in the study area; however, areas where most or all wells are likely targeting the Miocene and likely have cement also exist (green).

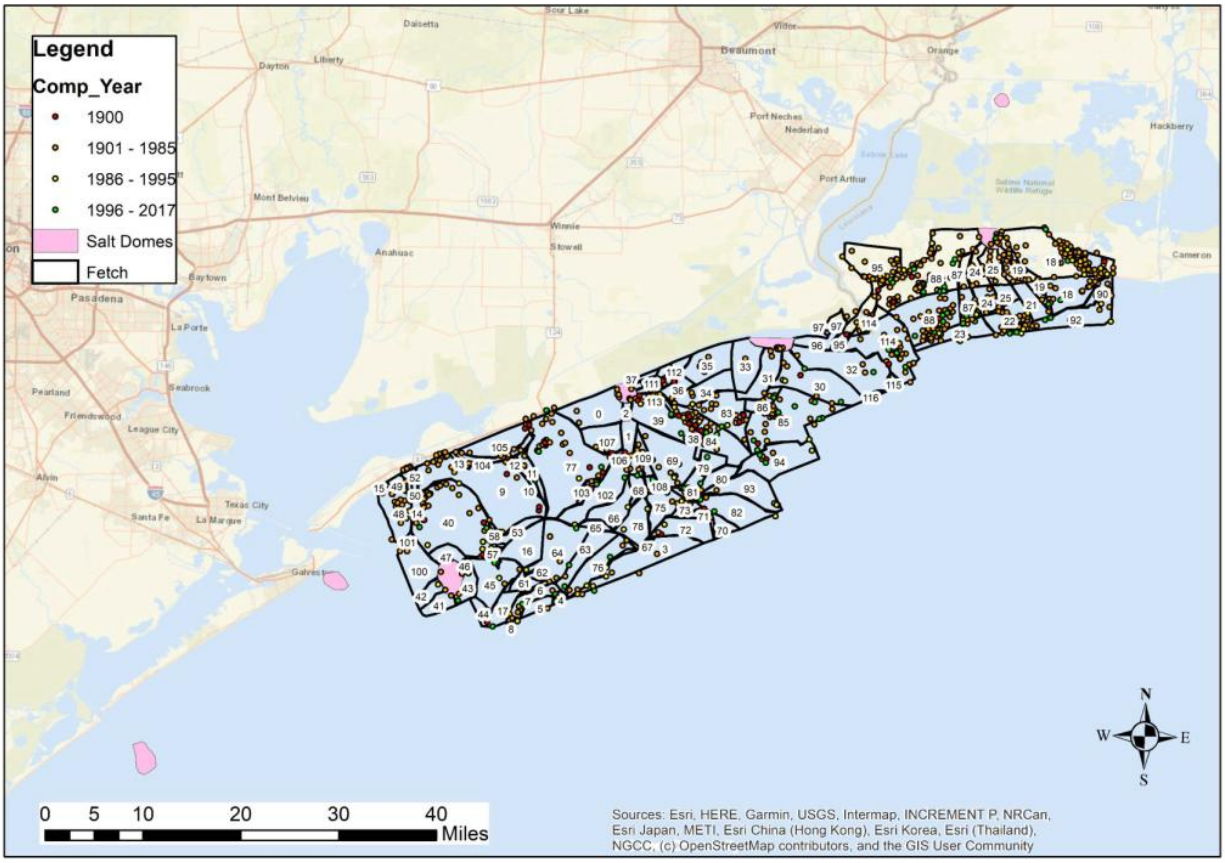

Figure 5.15 - Age of wells by well completion year in the study area from IHS database. Older wells (in red) are generally more problematic. Newer wells in green may be better targets for reuse of wells or platforms.

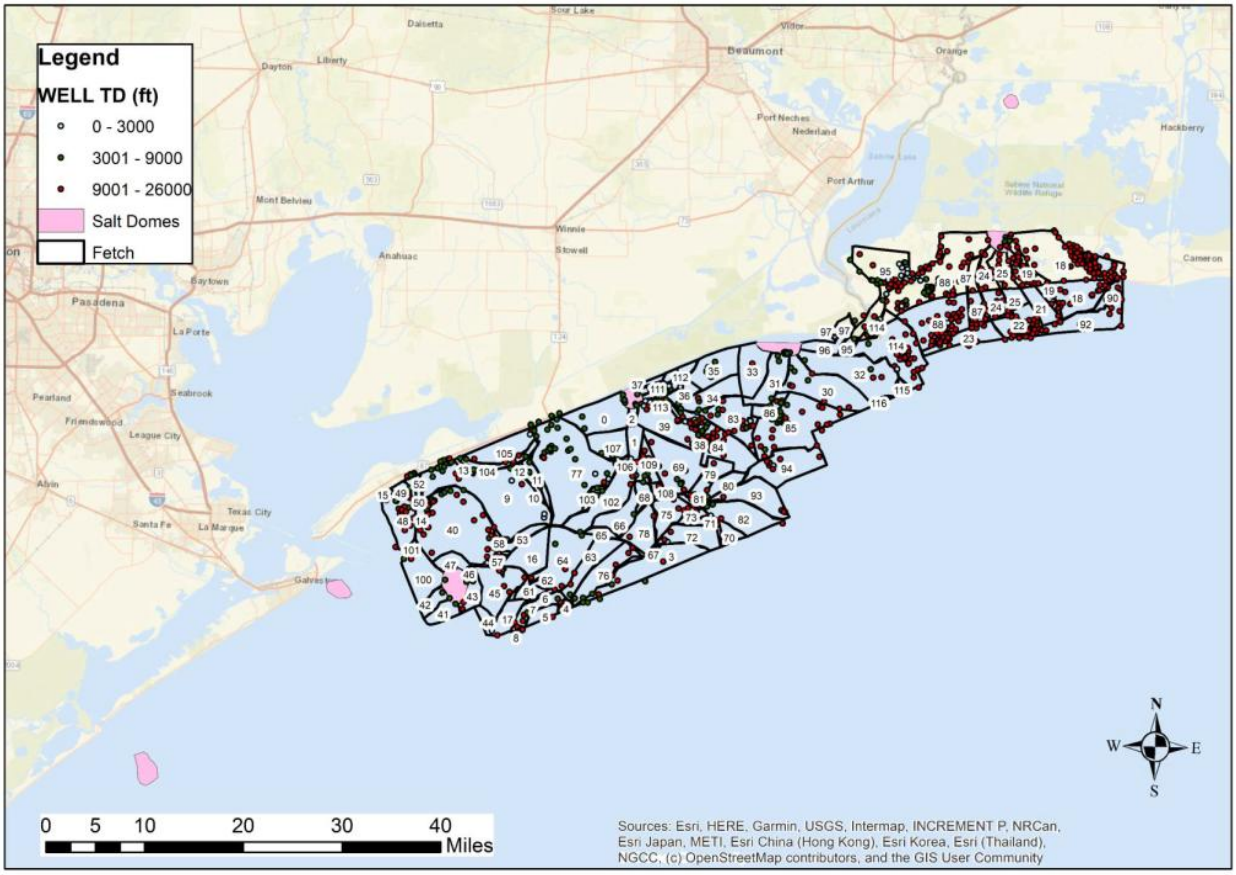

Figure 5.16 - Total depth of wells in feet in the study area from IHS database. Deep wells (in red) may be problematic because they may not have cement in the Miocene section. Shallower wells in green are likely to be targeting the Miocene and likely to have cement in the target interval. This is screening-level data only. Wells in the AOR of an injection need to be individually assessed.

Some data (Clark, et al, 2005) suggest that it is possible that cement is not required to close borehole aperture in poorly indurated sediments such as those in the Miocene section of the study area. The casing-sediment annulus is drilled to provide sufficient clearance to place the casing into the borehole and is managed during drilling by emplacement of viscous drilling mud engineered to hold the sediment in place. Zones with sand typically "wash out" during drilling, forming large diameter borehole sections. In a well-designed borehole the fine-grained layers will remain at designed borehole size. It is likely that in weeks to years following completion of the well, fine grained layers will creep and fill openings around the casing. Sand may also migrate to fill voids as drilling mud dewaters. However, additional work is needed to show that this so called "sloughed" infill of the annulus is reliable and can be accepted in a regulatory context in this setting. Tools for assessment of well completions are found in Wilson and McConnell (1993). In addition, because of the absence of fresh water, the AOR offshore is smaller than onshore.

Infrastructure for preparation and management of wells is another siting issue. Options under consideration include: Onshore to offshore drilling, re-use of existing platforms and wells, new platforms and new wells, subsea templates (no platforms). Trimeric and their consults and Aker Solutions have been working on cost and viability estimates for these types of infrastructure and more details have been and will in the future be provided in quarterly reports.

1) *Onshore to offshore drilling*

   Long laterals are seen in the well data in this area, and the technology of drilling long laterals has been rapidly improving. The advantage of the idea is that the well drilling site would be onshore, even if the injection location is offshore. The well itself would also have a lower cost onshore completion. Three possible limitations to this option are noted: a) the polygons near shore mostly continue onshore; therefore, the impact

of injection pressure (creating the Area of Review, AOR) on onshore fresh water resources would have to be assed; b) the permitting would have to involve multiple surface owners, who might be two state agencies or state or state and federal agencies, and 3) any ecosystem sensitivity of such as well location would have to be considered.

2) *Re-use of existing platforms and wells*
   Re-use is observed to have cost-savings in two ways – to avoid the cost of new build but also to avoid the substantial cost of decommissioning. One anecdotally provided estimate indicated that a re-purposed platform could save approximately 30% of the costs of an equivalent new platform. The main negatives are that safely standards have been improved since installation of most platforms and that cost to bring them to current requirements may be prohibitive. In particular, siting platforms may not meet the "100-year storm" design standards implemented in 1988. Photographs taken 2016-2017 of existing platform in Texas State waters can be reviewed in the GLO Oil Spill mapping viewer, which identifies the location of each platform. The newer wells in the database may be used to look for newer platform infrastructure. Surface casing of wells could be reused and laterals drilled to new locations, possibly accessing the fetch.
3) *New platforms and new wells*
   To inject the CO_2 as far from wells and possibly flawed traps requires access the fetch. Injection in the fetch may require placement of platforms and wells away from previous infrastructure, requiring new build. This would have a high cost, but fit-to-purpose design and a long lifespan might make new build worthwhile. Cost is depth-related; however, access-depth for various equipment may mean that shallowest settings are not necessarily lowest cost.
4) *Subsea templates (no platforms)*

   Aker Solutions is investigating these technologies for feasibility in shallow-water settings of the Gulf of Mexico. Subsea templates provide substantive savings as well as lower profile and less competition with surface use for both hydrocarbon production and CO_2 injection in deep water settings.

Synthesis

This study explores the options for linking the onshore sources via transport options to storage resources. No one optimum is identified because it appears that many pathways to success can be defined. Clusters of existing sources are noted at Port Arthur-Beaumont-Orange on the east end of the study area and at Texas City and the Houston Ship Channel on the western end. We speculate that the CO_2 source landscape will evolve and increase, and available large volumes of -CO_2 will be captured. However, the amount and distribution is uncertain, which should be considered in optimization. Onshore pipeline density signals that aggregation of sources is feasible.

Two coastal crossings are noted that may guide the CO_2 distribution network, serving as the hubs between systems of pipelines that aggregate CO_2 transport, if across the coast, and distribute it to multiple storage sites offshore. Pipelines that cross the coast south of Port Arthur link to an existing large diameter offshore pipeline system which is a possible target for reuse. Similarly, a pipeline coast crossing from Texas City across Point Bolivar provides access to much of the offshore via an existing long, large diameter pipeline. Even if the pipelines themselves are not suitable for reuse, re-occupancy of the costal crossing may be valuable. However other crossing and potential onshore-to-offshore drilling remain viable, and the assumption that reusing existing shoreline crossing is optimal requires substantive additional detailed discussions with pipeline owners and regulators and pipeline testing programs at sea. These needed activities will be incentivized by real capital investment intentions.

Assessment of the structurally defined fetch-trap geometries of the Miocene strata in the subsurface show that capacity is available across the region even using a very conservative stratigraphic down-selection to just part of the lower Miocene. Consideration of the entire section would yield capacities several times larger. As a result of this finding, site selection criteria may then focus on well density rather than storage availability. The risk of not being able to document effective zonal isolation at wells and cost to remediate is likely to be an important site selection criterion. For example, an attractive high-capacity area is noted offshore of southwest Louisiana (Figure 5.13). However, the well density and wells' total depth are noted in Figure 5.15 and Figure 5.16 to be high, targeting structures deeper than the Miocene interval. This means that cement may be installed to isolate only the deeper section and that no cement may have been emplaced to isolate Miocene zones from each other. Additional

evaluation to determine the hypothesis of natural isolation is needed. Additionally, in the Miocene strata of southwest Louisiana, the deeper portions of most polygons are on their, respective, offshore sides and dip toward offshore with subsurface continuation of shallower portions of the fetch onshore. This implies that as part of the feasibility assessment of storage options focused on CO_2 injection offshore in this area, project developers would need to consider migration of CO_2 plumes or elevated pressure onshore.

In the Texas coastal waters which are 10.3 miles wide, these complexities can be more readily avoided. Platform reuse options remain unclear; additional assessment requires investment in individual platform evaluation with budget in the multiple tens of thousands of dollars range.

References Cited

Air Products website, accessed March 2021, Carbon capture https://www.airproducts.com/company/innovation/carbon-capture#/

Clark, J.E., Bonura, D.K, Papadeas, P. W., and McGowen, R.R., 2005, Gulf Coast borehole closure test well near Orange Texas, Developments in Water Science, Volume 52, Pages 157-166, https://doi.org/10.1016/S0167-5648(05)52013-6..

Denbury, access March 2021, Operations, Gulf Coast Pipelines https://www.denbury.com/operations/gulf-coast-region/Pipelines/default.aspx

Hosseini, S.A, accessed March 2021, The EASiTool project, https://www.beg.utexas.edu/gccc/research/easitool

Meckel, T., Treviño, R. H., Carr, D. L., Nicholson, A. J., and Wallace, K., 2012, Offshore CCS in the northern Gulf of Mexico and the significance of regional structural compartmentalization: Energy Procedia, 11th International Conference on Greenhouse Gas Control Technologies, v.37, p. 4526-4532, http://doi.org/10.1016/j.egypro.2013.06.359

Meckel, T. A., Nicholson, A. J., and Treviño, R. H., 2017, Chapter 4: Capillary aspects of fault-seal capacity for CO2 storage, lower Miocene, Texas Gulf of Mexico, in Treviño, R. H., and Meckel, T. A., eds., Geological CO2 sequestration atlas for Miocene strata, offshore Texas state waters: Austin, Texas, The University of Texas at Austin, Bureau of Economic Geology, Report of Investigations, no. 283, p. 26-35, http://doi.org/10.23867/RI0283D.

MIT Carbon Capture and sequestration Technologies, accessed 2021, Lula Fact sheet, https://sequestration.mit.edu/tools/projects/lula.html

National Petroleum Council, 2019, Meeting the Dual Challenge, https://dualchallenge.npc.org/

NetPower, accessed March 2021, https://netpower.com/

Northern Lights, access March 2021, https://northernlightsccs.com/

Porthos website, accessed March 2021. CO_2 reduction through storage beneath the North Sea https://www.porthos CO_2.nl/en/

Trevino, R. T. and Meckel, T.A., , 2019, Geological CO_2 Sequestration Atlas of Miocene Strata, Offshore Texas State Waters, Bureau of Economic Geology RI0283, 74p, ISBN: 978-1-970007-12-

Tutton, P., 1918 Review of high concentration sources. Unpublished notes.

Warner, D.L. and McConnell, C.L., 1993, assessment of the environmental implications of abandoned oil and gas wells, Journal of Petroleum Technology

Wallace, K. J., Rhatigan, C. H., Treviño, R. H., and Meckel, T. A., 2017, Chapter 7: Estimating CO_2 storage capacity in a saline aquifer using 3D flow models, lower Miocene, Texas Gulf of Mexico, in Treviño, R. H., and Meckel, T. A.,

eds., Geological CO2 sequestration atlas of Miocene strata, offshore Texas state waters: Austin, Texas, The University of Texas at Austin, Bureau of Economic Geology, Report of Investigations, no. 283, p. 57-61, http://doi.org/10.23867/RI0283D.

5.3 Subtask: Communication

GoMCarb engaged many pertinent regulatory agencies in sustained and long-term discussions over the course of the Partnership. The agencies engaged included: 1) the Texas General Land Office (GLO), which overseas Texas state waters; 2) the Port of Corpus Christi Authority; 3) Louisiana Dept. of Natural Resources (LA) DNR; 4) the Bureau of Ocean Energy Management (BOEM); the Bureau of Safety and Environmental Enforcement (BSEE) 6) the Texas Railroad Commission (RRC) the state agency in charge of regulating oil and gas wells in the state of Texas; RRC has also applied for primacy for UIC Class VI wells in the state of Texas; 7) the Environmental Protection Agency (EPA); 8) the California Dept of Conservation/Air Resources Board; 9) TCEQ (Texas Commission on Environmental Quality); 10) the White House Council of Environmental Quality CCUS Permitting Task Force for Federal and non-Federal Lands; 11) the U.S. Geological Survey (USGS); and 12) the Port of Corpus Christi Authority (POCCA) (Figure 5.17). For details about the Partnership's interactions, with these agencies, see Deliverable 5.3a: Letter Report Summarizing Regulatory Communications.

Figure 5.17 - Scene from Dr. Tip Meckel's meeting with the Port of Corpus Christi Authority (June 16, 2021).

6. TASK 6.0 - Knowledge Dissemination

6.1 Subtask: Stakeholder Outreach

This subtask provided outreach and education mechanisms that raised awareness of potential subsea geologic CO_2 storage in the region and provided key local, state and national stakeholders with information about existing and future storage resources that may be valuable to further business development and environmental issues in the region. Outreach was conducted throughout the duration of the Partnership to scores of groups, organizations, companies, etc. Details can be found in the various quarterly reports.

6.1.1 Subtask: Develop strategies in environmental risk communication relevant to offshore CCS

The following is from the report, milestone M10: Outcomes of public acceptance studies. It is included here for the reader's convenience.

The body of this report is taken from a manuscript (Communicating Benefits and Risks about Carbon Capture and Storage (CCS): Understanding Stakeholder Mental Models to Inform Effective Messaging) based on research conducted for GoMCarb by Drs. Rachel Lim, Lucy Atkinson, Lee Ann Kahlor and Mr. Won-Ki Moon from the University of Texas at Austin's (UT) Stan Richards School of Advertising and Public Relations. Other collaborators included Dr. Hilary Olson from the UT Hildebrand Department of Petroleum and Geosystems Engineering and Ms. Emily Moskal from UT's Bureau of Economic Geology, Gulf Coast Carbon Center. Following is the discussion section from the manuscript, which the authors will submit the manuscript to the journal, Energy Policy.

> The findings show that key stakeholder groups vary in their attitudes about the environmental benefits of CCS technology and that these differences are informed by social factors, such as jobs, and by attitudes toward climate change. By using stakeholder theory, the study highlights the potential benefits and interests related to CCS technology, emphasizing how these perceptions differ meaningfully across groups.
>
> The findings reveal that not all stakeholders perceive environmental benefits from CCS technology. The potential for CCS to help mitigate the effects of climate change – the way CCS is most often framed by the media and by experts – held little sway with local community and government stakeholders. Local community stakeholders generally showed less interest in the environmental benefits, considering it to be the least important aspect. Instead, local stakeholders emphasized the health and economic opportunities of CCS. Indeed, stakeholders suggest that CCS may bring about better air quality, improve the community by creating jobs and open more opportunities to partner with industry. Similarly, local government stakeholders doubted whether CCS could have a significant environmental impact. They generally perceived the technology to be inefficient and showed concern about its negative impact on the local environment and community.
>
> NGO stakeholders, who generally viewed climate change as a priority, thought any potential environmental benefits were discounted by questions of scale and liability. They questioned whether CCS could be effective enough to mitigate CO2 emissions and whether the potential environmental risks, such as CO2 leakages or sinkholes, were worth the cost. They also voiced concerns about the unclear liabilities in times of crisis that could affect local residents' lives. Like industry stakeholders, they saw a role for the government in providing tax incentives to motivate large-scale CCS projects.
>
> Not surprisingly, compared with other stakeholder groups, industry experts showed the highest confidence in the effectiveness of the technology. However, this group was not without reservations. Their two primary concerns reflected similar concerns held by NGOs and focused on scale and liability. But unlike NGO stakeholders, industry stakeholders were less likely to prioritize climate change as a concern. Instead, public opinion about climate change served to motivate industry stakeholders to act. Interestingly, industry stakeholders see a clear role for federal government involvement in helping CCS to succeed.
>
> These findings underscore the importance of understanding the different mental models of stakeholder groups. While our four groups overlap in some areas, their mental models are distinct when it comes to perceptions of CCS technology and how – or even whether – it should be pursued. Stakeholder theory posits that successful organizational outcomes are likely when stakeholder values are aligned (Freeman, 1984; Freeman et al., 2007; 2012). This study demonstrated that each stakeholder sees different opportunities related to CCS technology as well as different risks. It is important to capture these different stakeholder values and interests and understand which aspects of the technology can offer what kinds of benefits to key stakeholders.
>
> The findings also offer important insights into best practices for communication messaging for

policymakers who are seeking public support for CCS policies. Rather than touting the potential climate change benefits of CCS, which the majority of messaging tends to focus on, more effective messaging might consider other benefits while keeping in mind the differing audiences for these messages. For example, messages directed to local stakeholders should focus on health and economic benefits. Similarly, ignoring perceived risks about CCS, which again is what most messaging does, is a disservice to the technology. Stakeholders are aware of associated risks but want to hear about how industry will address them. Rather than ignoring these perceived risks, CCS communication campaigns would do well to acknowledge them and deal with them head on. Developing messages that incorporate both benefits and risks would likely be perceived as more credible and meaningful to stakeholders than messages that gloss over risks and focus exclusively on climate change benefits that do not resonate with the audience. As researchers have emphasized, well-designed communication should enhance stakeholders' ability to understand the key issues, give them the opportunity to engage in the discussion, and motivate them to do so (Brunsting et al., 2011).

References

Aaltonen, K., 2011. Project stakeholder analysis as an environmental interpretation process. International Journal of Project Management, 29(2), 165-183.

Ashworth, P., Wade, S., Reiner, D., and Liang, X., 2015. Developments in public communications on CCS. International Journal of Greenhouse Gas Control, 40, 449-458.

Bhambhani, D., 2019. Everyone wants carbon capture and sequestration — Now how to make it a reality? Forbes. https://www.forbes.com/sites/dipkabhambhani/2019/11/21/washington-to-wall-street-hears-harmony-on-ccs-to-address-climate-change/

Bord, R. J., O'connor, R. E., and Fisher, A., 2000. In what sense does the public need to understand global climate change?. Public Understanding of Science, 9(3), 205-218.

Boyd, A.D., Hmielowski, J.D., and David, P., 2017. Public perceptions of carbon capture and storage in Canada: results of a national survey. International Journal of Greenhouse Gas Control 67, 1–9.

Bradbury, J., Ray, I., Peterson, T., Wade, S., Wong-Parodi, G., and Feldpausch, A., 2009. The role of social factors in shaping public perceptions of CCS: Results of multi-state focus group interviews in the US. Energy Procedia, 1(1), 4665-4672.

Brunsting, S., de Best-Waldhober, M., Feenstra, C. Y., and Mikunda, T., 2011. Stakeholder participation practices and onshore CCS: Lessons from the Dutch CCS Case Barendrecht. Energy Procedia, 4, 6376-6383.

de Bruin, W. B., and Bostrom, A., 2013. Assessing what to address in science communication. Proceedings of the National Academy of Sciences, 110, 14062-14068.

EIA, 2019. Carbon dioxide emissions by fuel. https://www.eia.gov/environment/

Freeman, R.E., 1984. Stakeholder management: framework and philosophy. Pitman, Mansfield, MA.

Freeman, R.E.,1994. The politics of stakeholder theory: Some future directions. Business Ethics Quarterly, 4(4), 409-421.

Freeman, R.E., 1995. Stakeholder thinking: the state of the art. In J. Nasi (ed.). Understanding Stakeholder Thinking (p. 35 - 46), Finnland: LSR-Publications.

Freeman, R. E., Harrison, J. S., and Wicks, A. C., 2007. Managing for stakeholders: Survival, reputation, and success. Yale University Press.

Freeman, R. E., Rusconi, G., Signori, S., and Strudler, A., 2012. Stakeholder theory (ies): Ethical ideas and managerial action. Journal of Business Ethics, 109(1), 1-2.

Gentner, D.,2002. Psychology of mental models. In Smelser, N.J. and Bates, P.B. (Eds.). International Encyclopedia of the Social and Behavioral Sciences (pp. 9683–9687), Amsterdam, Netherlands: Elsevier

Gilligan, C., Spencer, R., Weinberg, M. K., and Bertsch, T., 2003. On the Listening Guide: A voice-centered relational method. In P. M. Camic, J. E. Rhodes, and L. Yardley (Eds.), Qualitative research in psychology: Expanding perspectives in methodology and design (p. 157–172). DC: American Psychological Association.

Green, E.H., Skerlos, S.J., Winebrake, J.J., 2014. Increasing electric vehicle policy efficiency and effectiveness by reducing mainstream market bias. Energy Pol. 65, 562–566. https://doi.org/10.1016/j.enpol.2013.10.024.

Huijts, N.M., Midden, C.J., Meijnders, A.L., 2007. Social acceptance of carbon dioxide storage. Energy Pol. 35 (5), 2780–2789.

Itaoka, K., Saito, A., and Akai, M., 2004. Public acceptance of CO2 capture and storage technology: A survey of public opinion to explore influential factors' paper presented at the 7th International Conference on Greenhouse Gas Control Technologies.

Jepsen, A. L., and Eskerod, P., 2009. Stakeholder analysis in projects: Challenges in using current guidelines in the real world. International Journal of Project Management, 27(4), 335-343.

Kahneman, D., and Tversky, A., 1979. On the interpretation of intuitive probability: A reply to Jonathan Cohen. Cognition, 7(4), 409–411

Kainiemi, L., Eloneva, S., Toikka, A., Levänen, J., and Järvinen, M., 2015. Opportunities and obstacles for CO2 mineralization: CO2 mineralization specific frames in the interviews of Finnish carbon capture and storage (CCS) experts. Journal of Cleaner Production, 94, 352-358.

Kallbekken, S., Sælen, H., 2011. Public acceptance for environmental taxes: self-interest, environmental and distributional concerns. Energy Pol. 39 (5), 2966–2973. https:// doi.org/10.1016/j.enpol.2011.03.006.

Kraeusel, J., and Möst, D., 2012. Carbon Capture and Storage on its way to large-scale deployment: Social acceptance and willingness to pay in Germany. Energy Pol., 49, 642-651.

Leiserowitz, A., Maibach, E. W., Rosenthal, S., Kotcher, J., Bergquist, P., Ballew, M., ... and Gustafson, A., 2019. Climate change in the American mind: April 2019. Yale University and George Mason University. New Haven, CT: Yale Program on Climate Change Communication.

Leiserowitz, A., Maibach, E., Roser-Renouf, C., 2010. Climate Change in the American Mind: Americans' Global Warming Beliefs and Attitudes in January 2010. Yale University and George Mason University. New Haven, CT: Yale Program on Climate Change Communication.

Lindsey, R., 2020. Climate Change: Atmospheric Carbon Dioxide. https://www.climate.gov/news-features/understanding-climate/climate-change-atmospheric-carbon-dioxide

Lorenzoni, I., Nicholson-Cole, S., and Whitmarsh, L., 2007. Barriers perceived to engaging with climate change among the UK public and their policy implications. Global Environmental Change, 17(3-4), 445-459.

Lowe, T., Brown, K., Dessai, S., de França Doria, M., Haynes, K., and Vincent, K., 2006. Does tomorrow ever come? Disaster narrative and public perceptions of climate change. Public Understanding of Science, 15(4), 435-457.

Magness, V., 2008. Who are the stakeholders now? An empirical examination of the Mitchell, Agle, and Wood theory of stakeholder salience. Journal of Business Ethics, 83(2), 177-192.

McDonald, R. I., Chai, H. Y., and Newell, B. R., 2015. Personal experience and the 'psychological distance' of climate change: An integrative review. Journal of Environmental Psychology, 44, 109-118.

Meyer, D., Leventhal, H., and Gutmann, M., 1985. Common-sense models of illness: the example of hypertension. Health Psychology, 4(2), 115.

Merrill, R., Sintov, N., 2016. An affinity-to-commons model of public support for environmental energy policy.

Energy Pol. 99, 88–99. https://doi.org/10.1016/j. enpol.2016.09.048.

Mitchell, R. K., Agle, B. R., and Wood, D. J., 1997. Toward a theory of stakeholder identification and salience: Defining the principle of who and what really counts. Academy of Management Review, 22(4), 853-886.

Moon, W. K., Kahlor, L. A., and Olson, H. C., 2020. Understanding public support for carbon capture and storage policy: The roles of social capital, stakeholder perceptions, and perceived risk/benefit of technology. Energy Pol. 139, 111312.

Nersessian, N. J., 1992. In the Theoretician's Laboratory: Thought Experimenting as Mental Modeling. Proceedings of the Biennial Meeting of the Philosophy of Science Association, 1992(2), 291-301.

Olson-Hazboun, S.K., Howe, P.D., Leiserowitz, A., 2018. The influence of extractive activities on public support for renewable energy policy. Energy Pol. 123, 117–126. https://doi.org/10.1016/j.enpol.2018.08.044.

Oltra, C., Sala, R., and Boso, À., 2012. The influence of information on individuals' reactions to CCS technologies: results from experimental online survey research. Greenhouse Gases: Science and Technology, 2(3), 209-215.

Oltra, C., Sala, R., Solà, R., Di Masso, M., and Rowe, G., 2010. Lay perceptions of carbon capture and storage technology. International Journal of Greenhouse Gas Control, 4(4), 698-706.

Palmgren, C. R., Morgan, M. G., Bruine de Bruin, W., and Keith, D.W., 2004. Initial public perceptions of deep geological and oceanic disposal of carbon dioxide. Environmental Science and Technology, 38(24), 6441–6450.

Poortinga, W., Pidgeon, N.F., 2006. Exploring the structure of attitudes toward genetically modified food. Risk Analysis, 26 (6), 1–13.

Poortinga, W., Spence, A., Whitmarsh, L., Capstick, S., and Pidgeon, N. F., 2011. Uncertain climate: An investigation into public scepticism about anthropogenic climate change. Global Environmental Change, 21(3), 1015-1024.

Rahmstorf, S., 2004. The climate sceptics. Potsdam Institute for Climate Impact. Research. Retrieved from http://www.pik-potsdam.de/%7Estefan/Publications/Other/rahmstorf_climate_sceptics_2004.pdf

Ranängen, H., 2017. Stakeholder management theory meets CSR practice in Swedish mining. Mineral Economics, 30(1), 15-29.

Rossman, G. B., & Rallis, S. F., 2003. Major qualitative research genres. Learning in the field: An introduction to qualitative research, 89-110.

Seigo, S. L. O., Dohle, S., Diamond, L., and Siegrist, M., 2013. The effect of figures in CCS communication. International Journal of Greenhouse Gas Control, 16, 83-90.

Selma, L., Seigo, O., Dohle, S., and Siegrist, M., 2014. Public perception of carbon capture and storage (CCS): A review. Renewable and Sustainable Energy Reviews, 38, 848–863.

Shackley, S., Bray, D., and Bleda, M., 2004. Developing discourse coalitions to incorporate stakeholder perceptions and responses within the Tyndall Integrated Assessment. Tyndall Centre.

Spence, A., Poortinga, W., and Pidgeon, N., 2012. The psychological distance of climate change. Risk Analysis, 32(6), 957-972.

Stauffer, N., 2016. Moving away from fossil fuel energy? Not without aggressive policy action. http://energy.mit.edu/news/moving-away-fossil-fuel-energy-not-without-aggressive-policy-action/

Stoll-Kleemann, S., O'Riordan, T., and Jaeger, C.C., 2001. The psychology of denial concerning climate mitigation measures: evidence from Swiss focus groups. Global Environmental Change, 11(2), 107-117.

Stoutenborough, J.W., Sturgess, S.G., Vedlitz, A., 2013. Knowledge, risk, and policy support: public perceptions of nuclear power. Energy Pol. 62, 176–184. https://doi. org/10.1016/j.enpol.2013.06.098.

Stoutenborough, J.W., Bromley-Trujillo, R., Vedlitz, A., 2014. Public support for climate change policy:

consistency in the influence of values and attitudes over time and across specific policy alternatives. Review of Policy Research, 31(6), 555–583.

Tcvetkov, P., Cherepovitsyn, A., and Fedoseev, S., 2019. Public perception of carbon capture and storage: A state-of-the-art overview. Heliyon, 5(12).

Terwel, B. W., Harinck, F., Ellemers, N., and Daamen, D.D., 2011. Going beyond the properties of CO2 capture and storage (CCS) technology: How trust in stakeholders affects public acceptance of CCS. International Journal of Greenhouse Gas Control, 5(2), 181-188.

Tokushige, K., Akimoto, K., and Tomoda, T., 2007. Public perceptions on the acceptance of geological storage of carbon dioxide and information influencing the acceptance. International Journal of Greenhouse gas control, 1(1), 101-112.

Vosniadou, S., 2008. International Handbook of Research on Conceptual Change. New York, NY: Routledge.

Wallquist, L., Visschers, V.H., and Siegrist, M., 2010. Impact of knowledge and misconceptions on benefit and risk perception of CCS. Environmental Science and Technology, 44(17), 6557–6562.

Wallquist, L., Visschers, V.H., Dohle, S., Siegrist, M., 2012. The role of convictions and trust for public protest potential in the case of carbon dioxide capture and storage (CCS). Ecological Risk Assessment, 18(4), 919–932.

Wallquist, L., Visschers, V.H., Siegrist, M., 2010. Impact of knowledge and misconceptions on benefit and risk perception of CCS. Environmental Science and Technology, 44 (17), 6557–6562.

Weber, E.U., 2010. What shapes perceptions of climate change?. Wiley Interdisciplinary Reviews: Climate Change, 1(3), 332-342.

Whitmarsh, L., 2009. What's in a name? Commonalities and differences in public understanding of ''climate change'' and ''global warming''. Public Understanding of Science, 18, 401–420.

Whitmarsh, L., 2011. Scepticism and uncertainty about climate change: Dimensions, determinants and change over time. Global Environmental Change, 21(2), 690-700.

6.2 Subtask: Technical Outreach

This subtask disseminated the knowledge and lessons learned from previous and GoMCarb offshore storage efforts via scores of presentations (see quarterly reports) and dozens of publications (section 7, below) designed specifically for technical audiences, regulatory personnel or the general public. A specific component of this subtask was to continue and deepen engagement with source industries (e.g., at meetings and presentations in Port Arthur, Houston, Corpus Christi, etc.) to update them on progress in developing large volume storage resources. The Partnership also collaborated with CSLF and IEAGHG (e.g., the International Offshore Workshop) on a regular basis.

6.3 Subtask: Advisory Committee

This subtask included all activities related to organizing, presenting updates to and receiving advice from, domestic and international partners and advisors. The members of the advisory committee reviewed key project updates and attended annual meetings.

Following is a list of members of the GoMCarb Advisory Committee.

Advisors	Organization
Tim Dixon (Chair)	IEA GHG R&D Development program
Melissa Batum	BOEM
Thomas Berley	IEA
Niels Peter Christensen	Gassnova

Douglas Connelly	NOC (National Oceanography Centre)
Zhou Di	South China Sea Institute of Oceanology, Chinese Academy of Sciences
Robert Finley	Illinois Geological Survey (retired)
Ben Grove	Clean Air Task Force
Stuart Haszeldine	Scottish CCS Centre, University of Edinburgh
Bruce Hill	Clean Air Task Force
Nick Hoffman	CO2 GeoNET
Anastasia Ilgen	Sandia National Laboratories
Noel Kamrajh	South African National Energy Development Institute (SANEDI)
Jun Kita	Marine Ecology Research Institute
Jasmin Mota Nieto	Secretaría de Energía (SENER), México
Kari-Lise Rorvik	Gassnova
Jiro Tanaka	Japan CCS Co., Ltd.
Gary Teletzke	Exxon-Mobil
Owain Tucker	Shell
Christopher Walker	BP
Ziqiu Xue	RITE, University of Kyoto

The committee's final report was submitted on October 11, 2022 (deliverable report D6.3b) and is included here for the reader's convenience.

Overall impressions

The Advisory Committee (AC) observed that the GoMCarb work since last year was very extensive and detailed. It is high quality work and was well presented. The breadth of technical sessions was great. All in all, the project was perceived as successful.

The content of presentations and research focus is very heavy on reservoir scale modelling, and the project is trusting those models to do all the screening, but the presenters did not show much information on modelling uncertainties.

It is really encouraging to see the progress that's been made over the last couple of years, but the program is still not fully integrated to be successful at the program level, nor at the individual sub-project level. The presented projects appeared only somewhat loosely connected, particularly when it comes to public outreach and communication. So there is a need for more integration.

There is a need for more interaction between the groups. The team is missing an opportunity to have that sort of integration with the different institutions coming together to work on selected problems. This was reflected in the outreach report at the end. One Advisory Committee (AC) member really liked the specificity of the individual projects. While agreeing that some cross communication between aspects in individual presentations would be beneficial, but compared to SECARB, there's much more useful information for operators in the BEG work.

There are a lot of achievements by the team, for example, in the area of reservoir characterization. Also, there are a lot of current data and reservoir information, but there are challenges with understanding the role of legacy wells and the fault systems.

AC members learned new things, which is reflective of the research progress to date. There was new material. One particularly liked Tip's working out the rate of fluxes across the window that he got from combining simple Darcy's law with Allan position diagrams and then linking that to open and closed boundary systems. Many aspects were novel and new.

On an overall scale it was predominantly regional and the real learnings come in the details, like bringing in the wells. How do you deal with the wells for which you don't know their current status (i.e., suspended, properly or improperly plugged)? These sorts of things are day-to-day problems that influence development strategies. The infrastructure session was superficial, including the wells talk.

The MVA work was very nice on the marine environment side, but it needs to anchor itself into what should an MVA plan be looking like for this area? Pick an example site and say if I have this example, how would I bring it together so there's integration between the pieces and then move to get the granularity because it's so easy to talk broad-brush.

One AC member particularly appreciated considerations like technical science communications, the upcoming rulemaking for the OCS, and also community engagement. No matter what happens on the technical side, nothing is going to really move without strong community engagement.

The depth and breadth of the research was appreciated but it should move forward to something practical. Many times, at the end of a presentation one AC member was thinking "I don't know what to do with that". They were trying to understand how this can inform their policy and the program they are going to develop. At the end, it would be helpful to say how program results will be useful in the real world and how these results could translate into policy.

1. **What should we do with new funding?**

Could a real-world cluster plan be made similar to work in the UK?

Can you expand the machine learning work with that large data set?

A specific case study that is fully integrated and looks at capture, transport, and storage would be instructive. How would we make this particular site work? How many injection wells are we going to need? Are the wells there? What condition are they in? How much money is it going to cost to remediate the facilities so that we can use CCS here to actually have a fully worked up case study. Make it basically a dry run for what a storage developer would do in reality.

GoMCarb is a really interesting case because they have so much data. Can the team share some of the findings from this project to the other countries or other projects?

Is there any integration between capture, transport and storage project that can be worked up as an example? The elephant in the room is the offshore lease in Jefferson County where Talos and now Chevron are pledging to develop, so can the project work with Talos and Chevron to make that a bit more open source, and use that as a learning? Can we make that a case study that the rest of the industry can learn from? Also, if Talos is doing it in that area, then the benefits of GoMCarb could be in doing a project at a distance sufficient to understand a different depositional and structural framework. So going down to the Corpus Christi area might be useful. The oil and gas industry have traditionally drilled the anticlines but deposition is going to be concentrated in the synclines. So, what you find geologically in the anticlines is different from what's going to be the synclines. Therefore, is there enough money to drill a characterization well into a syncline? Can injectivity tests actually start to ground truth some of those resource assessments?

The next thing would be requesting sufficient funding to drill a characterization well and to do extensive characterization and experimentation, but there may already be enough commercial interest that such funding would not be awarded. It's time to integrate with real world engineering and offshore exploration issues. We acknowledge existing wells, but we rarely find a cement bond log for these wells. How much cement was put in these wells such that these wells are really safe and useful? Can they be used for monitoring or are they only a leakage risk? There needs to be an effort at integrating geology at all these different scales with actual real-world production practices and petroleum engineering development issues. You have two different major facies types in this lower middle Miocene which could be very different in terms of reservoir connectivity, and they need to be looked at as possibly separate areas to address in the integration. Important elements were in Harry Hull's work where he defined 16 para-sequences. Are the sandstones in flow communication beyond the data that you have at a

specific well site? Small baffles may be effective at residual trapping along the way. Another highlight was in the Chandelier Sound presentation. We saw some stratal slice work that Dallas Dunlap did, and that was really important. We saw quite a bit of excellent material, certainly in terms of sand, shale, or fluid flow and visualizing pores at a 6 millimeter by 6-millimeter scale. Very excellent and interesting work, but it's time to really dig down into a real-life simulation where you've got realistic unknowns about compartmentalization, the cement status, and individual wells. Can you safely inject? Are many wells only good for observation wells? Are they safe in terms of possible leakage pathways? We really need to begin to understand what has to be invested in, and is this more possible with the interest that the industry now has?

It's probably imperative to collaborate with an operator who's willing to share data on what are the likely issues with wells in actual fields in the potential storage trends. Hopefully not an operator who's abandoned a bunch of wells, but an operator who's been diligent and may have a good data set to work on and then create examples that would realistically illustrate the level of effort needed to ensure safety, integrity and injectability. This would also serve to create a depositional systems-based model of where the CO_2 would go based on the heterogeneity that you can document in those reservoirs.

Coming from the regulatory perspective, we must reassure the public that these projects are safe and environmentally sound. . So, for example, the presentation that Oldenburg did was very easy to understand, very clear. That kind of presentation is useful, in particular answering how potentially worst-case scenarios would be addressed. Such a study would help support the assurance that these projects can be done safely. One AC member suggested that supporting a pilot project in the offshore would help with reassurance, to demonstrate that these projects can be done effectively. Create a permit application. What is difficult is understanding the certainty of what volume and what rate an operator can commit to. Storage resource is more than just pore space, it must include the simple equation of injection rate times number of years the project is committing to that justifies the infrastructure spend. However, GoMCarb should not in any way discount the storage resource; great injectivity into a constrained compartment does not make for a successful project. The AC suggests that the researchers address the cluster concept, with field and aquifer assessment because they have different characteristics. By putting them together you get the high confidence of a field with the higher potential storage resource of a larger aquifer and one de-risks the aquifer while using the field as a swing injector. The project should create a storage development plan and an example permit application. It doesn't matter what the regulations are because they all have the same elements and overall objectives. Then you really start to highlight where the unknowns and issues are that may require some fixes or legislation to help address. One of the presentations referred to onshore wells and the number of legacy wells, and that thinking is important because the key is to get those records out of garages and into digital systems before they are lost or destroyed.

A pilot demonstration project would be excellent. Considering the development of infrastructure, how will cost estimates be impacted by inflation and supply chain issues? Can 45Q be enough now that we have greater inflation? 45Q doesn't scale up with inflation for a number of years and the Committee is curious if there's any work planned on re-examining costs for deployment of large-scale CCS in the region with current supply chain issues and cost increases. How is this going to actually impact deployment? Consider this from an advocacy standpoint. Is any bolstering of regular communication for policymakers planned? One Committee member has received a lot of strange pushback and mixed signals from various stakeholders and policymakers about storage in the region. There are a lot of misconceptions, a lot of uncertainties, and just general lack of knowledge .so it would be very helpful to bolster communications with these groups.

2. Feedback on Tasks

Task 2 Storage Resource

It could be fruitful to perform targeted Machine Learning (ML) to improve certain reservoir simulations especially once their uncertainties are evaluated. Some of the presented reservoir simulations appeared as a black box exercise. So, incorporating more science into reservoir models would be appropriate.

How Alex approached the dry hole evaluation and the forensic way he picked that apart was informative and useful. The Excel sheet that he put together to evaluate that critical pressure would be a really useful tool to be developed a bit more to be either shared externally or developed into a tool like Easitool. It would be informative to use that approach and generate different scenarios.

Some improvements in simulation using ML that may add a form of facies connotation to that effort could be helpful, especially in trying to extrapolate from one area to another. If the project has an example or a pilot in a given set of facies and then be able to go to a different part of the depositional system and expect similar facies, that could be really helpful. For example, there may be multiple fluvial systems in the GoMCarb region. Machine learning is obviously a very powerful tool, but needs another element in that regard as far as the MVA task is concerned. Existing wells need to be looked at a lot more closely because the Committee feels there is going to be a lot of questions about these wells as part of the public dialogue. We heard multiple times that several researchers felt that the existing wells were the most likely leakage pathway, not necessarily fault planes, which in many cases are sealing, so how does all this existing hardware fit into the MVA plan? Consider what answers can be given to those questions since the regulator or the environmental community will ask about that existing infrastructure.

Task 3 Risk and Modelling

For an offshore blowout for risk assessment, is there any assessment on the damage to the marine ecosystem? Of course, the seawater will locally get more acidic, but what will be the ecological outcome? Teaching models to predict CO_2 imbibition or flow through lithologies is really powerful.

Good to see that integration happened between the different strands of risk and modelling.

The project needs to develop and explain the concept of the seep. The Committee wanted to better understand what was said about faulting and the connection with natural seeps and how that didn't necessarily mean, because you have a seep, that you could have leakage through the seep. Regarding ocean acidity, is potential leakage through fault pathways going to damage those communities? Tie in Tasks 2 and 3.

One thing researchers have not mentioned is salt touch down. But in the modelling, take this pore scale work, which was brilliant, into the simulator to create a workflow that allows you to predict what your storage is going to be if you're in a syncline. That's very, important as well if you've got unfixable wells that you must avoid and not have your plume intersect. And you need to have confidence in your injection patterns and locations. That sort of thing was done for fault leakage in the DETECT project recently finished.

One AC member commented that there is a risk in focusing on a percentage of the fracture gradient as being a safe working pressure; rather, each basin, structure, and tectonic regime may have different stresses and a different failure point. Focus on 60 or 70% of the fracture gradient may lead you into trouble because fracture gradient is measuring a different thing than the Mohr-Coulomb failure criteria, which is actually the way that things are more likely to fail. The fracture gradient is tensile, while Mohr-Coulomb failure is in shear mode, at a lower pore pressure.

Task 4 MVA

The presentation by Tony Knap on the extreme variability of the marine environment is significant and how to avoid false positives in this environment is important. The project should address the issue of avoiding false positives.

MVA in shallow marine systems is very site specific. Wave energy and the biofouling issues are significant and it's tempting to say we can’t do it. But there are things that can be done and there needs to be more discussion worldwide with other projects having the exact same problems with MVA. What can be measured? The project has to be really selective about what research is chosen to make it cost effective and useful. The project should focus on the things that are potentially most useful, and there's a lot more work in the MVA sphere that needs to be integrated.

How to map the CO_2 in the reservoir because its different in the saline reservoirs. The AC believes the early stage is really difficult to map. Also, consider how to deal with low pressure and resulting low injectivity because of the

JT cooling effect.

Given the importance of MVA, and how you actually monitor these projects, and given some of the challenges that we heard about, the project may need more cutting-edge problem-solving in this area.

Task 5 Infrastructure

Task 5 is progressing but it's still a little bit unclear as to whether pre-existing infrastructure is an advantage or a liability. Perhaps there should be a legal lens applied here to think through some of the chain of title issues and answer that question: is it going to be worth it to actually reuse any infrastructure?

Investigations should move from generalities to specifics on wells, pipelines, and platform refits. One AC member company tried to reuse a platform and it was "death by 1,000 cuts" and they are now going for a greenfield site.

It might be impactful to consider when doing source sink mapping to develop a case study, or similar, that directly looks at impacted communities and how infrastructure can be built in a way that minimizes negative impacts to those communities.

Knowledge Dissemination

More outreach about community benefits is important. What are the actual community benefits? It would be helpful to have a case study on what those benefits actually are at a community level and have focused community engagement to present these. This is lacking all around for CCS projects, but there's an opportunity here to pair benefits and more active engagement.

The project should look at the Castor offshore subsurface gas storage project as an example of how things can go wrong. A gas storage project near Barcelona was cancelled when it was starting to fill because it created felt seismic events onshore. People were protesting on the beach. The courts shut it down. That teaches us a lot about public outreach, public concerns, and what may happen if an NGO takes a project like Castor and uses it to sensitize a population. There were felt events, then they ended the project. This example will help you understand how you will communicate these risks.

We need communication materials. We need them available when we have public meetings Perhaps there is a way to partner with industry or potential project developers on some of the communication aspects. We're spending so much time just developing the program and the regulations and the policy that it would be significant to try to partner, especially for public meetings or stakeholder meetings, or any kind of outreach.

The Regional Carbon Sequestration Partnerships have developed much material on outreach over the last decade and there is a large volume of available outreach material. Most of it is available on the websites of the individual partnerships and we should make it applicable to the offshore.

Tim Dixon, Katherine Romanak and Rob Finley on behalf of the Advisory Committee, 12 July 2022

7. Presentations, Publications, Patents, etc.

Perhaps the most scientifically impactful results from GoMCarb's research are the following thirteen peer-reviewed publications peer-reviewed papers from GoMCarb-supported research., which resulted from GoMCarb supported research:

Chen and Hosseini (2026)

Ni et al. (2025)

Achyut et al. (2025)

Ubillus, Bakhshian, et al. (2025)

Ubillus, Ni, et al. (2025)

Ni et al. (2024)

Trevino et al. (2024)

Madugula et al. (2024)

A. P. Bump and Hovorka (2024)

Alexander P. Bump and Hovorka (2023)

Atkinson et al. (2024)

Araque-Martinez and Lake (2021)

Zeng et al. (2023)

Tip A. Meckel et al. (2023)

Ni et al. (2023)

Ulfah et al. (2022)

T.A. Meckel et al. (2021)

Krishnamurthy et al. (2022)

Alexander P. Bump et al. (2021)

Curtis M. Oldenburg and Zhang (2022)

Ni and Meckel (2021)

Blackford et al. (2021)

Madugula et al. (2021)

C. M. Oldenburg and Pan (2020)

8. References

Achyut, M., Hailun, N., Seyed Ahmad, M., & Ralf, R. H. (2025). Performance assessment of graph theory towards predicting fluid flow in rocks across multiple spatial scales. *Advances in Water Resources, 204*, 105045. https://www.sciencedirect.com/science/article/pii/S0309170825001599

Araque-Martinez, A. N., & Lake, L. W. (2021). The Effect of Compressibility and Outer Boundaries on Incipient Viscous Fingering. *SPE Reservoir Evaluation & Engineering, 24*(03), 619-638. https://doi.org/10.2118/201310-PA

Atkinson, L., Dankel, D. J., & Romanak, K. D. (2024). The effect of monitoring complexity on stakeholder acceptance of CO2 geological storage projects in the US gulf coast region. *Frontiers in Marine Science, 10*, 17. Article. <Go to ISI>://WOS:001153494600001

Berelson, W. M., McManus, J., Severmann, S., & Rollins, N. (2019). Benthic fluxes from hypoxia-influenced Gulf of Mexico sediments: Impact on bottom water acidification. *Marine chemistry, 209*, 94-106.

Bianchi, T. S., DiMarco, S. F., Cowan Jr, J., Hetland, R. D., Chapman, P., Day, J., & Allison, M. (2010). The science of hypoxia in the Northern Gulf of Mexico: a review. *Science of The Total Environment, 408*(7), 1471-1484.

Blackford, J., Romanak, K., Huvenne, V. A. I., Lichtschlag, A., Strong, J. A., Alendal, G., et al. (2021). Efficient marine environmental characterisation to support monitoring of geological CO2 storage. *International Journal of Greenhouse Gas Control, 109*, 103388. https://www.sciencedirect.com/science/article/pii/S1750583621001407

Bump, A. P., Bakhshian, S., Ni, H., Hovorka, S. D., Olariu, M. I., Dunlap, D., et al. (2023). Composite confining systems: Rethinking geologic seals for permanent CO2 sequestration. *International Journal of Greenhouse Gas Control, 126*, 103908. https://www.sciencedirect.com/science/article/pii/S1750583623000786

Bump, A. P., & Hovorka, S. D. (2023). Minimizing exposure to legacy wells and avoiding conflict between storage projects: Exploring area of review as a screening tool. *International Journal of Greenhouse Gas Control, 129*, 103967. https://www.sciencedirect.com/science/article/pii/S1750583623001378

Bump, A. P., & Hovorka, S. D. (2024). Pressure space: The key subsurface commodity for CCS. *International Journal of Greenhouse Gas Control, 136*, 16. <Go to ISI>://WOS:001287329400001

Bump, A. P., Hovorka, S. D., & Meckel, T. A. (2021). Common risk segment mapping: Streamlining exploration for carbon storage sites, with application to coastal Texas and Louisiana. *International Journal of Greenhouse Gas Control, 111*, 103457. https://www.sciencedirect.com/science/article/pii/S1750583621002097

Chen, J., & Hosseini, S. A. (2026). Optimal CO2 storage management considering safety constraints in multi-stakeholder multi-site GCS projects: A Markov game perspective. *International Journal of Greenhouse Gas Control, 154*, 104682. https://www.sciencedirect.com/science/article/pii/S1750583626001143

Dixon, T., & Romanak, K. D. (2015). Improving monitoring protocols for CO2 geological storage with technical advances in CO2 attribution monitoring. *International Journal of Greenhouse Gas Control, 41*, 29-40. http://www.sciencedirect.com/science/article/pii/S1750583615001929

Dvorkin, J., & Nur, A. (1996). Elasticity of high-porosity sandstones: Theory for two North Sea data sets. *Geophysics, 61*(5), 1363-1370. <Go to ISI>://WOS:A1996VJ95600011

Ganjdanesh, R., & Hosseini, S., A. . (2017). Geologic Carbon Storage Capacity Estimation Using Enhanced Analytical Simulation Tool (EASiTool). *Energy Procedia, 114*, 4690-4696. https://www.sciencedirect.com/science/article/pii/S1876610217317952

Goodman, A., Hakala, A., Bromhal, G., Deel, D., Rodosta, T., Frailey, S., et al. (2011). US DOE methodology for the development of geologic storage potential for carbon dioxide at the national and regional scale. *International Journal of Greenhouse Gas Control, 5*(4), 952-965. <Go to ISI>://WOS:000294700900035

Hetland, R. D., & DiMarco, S. F. (2008). How does the character of oxygen demand control the structure of hypoxia on the Texas–Louisiana continental shelf? *Journal of Marine Systems, 70*(1-2), 49-62.

Jarvis, B. M., Lehrter, J. C., Lowe, L. L., Hagy, J. D., Wan, Y., Murrell, M. C., et al. (2020). Modeling spatiotemporal patterns of ecosystem metabolism and organic carbon dynamics affecting hypoxia on the Louisiana Continental Shelf. *Journal of Geophysical Research: Oceans, 125*(4), e2019JC015630.

Jenkins, C. (2020). The State of the Art in Monitoring and Verification: an update five years on. *International Journal of Greenhouse Gas Control, 100*, 103118.

Jenkins, C., Chadwick, A., & Hovorka, S. D. (2015). The state of the art in monitoring and verification—ten years on. *International Journal of Greenhouse Gas Control, 40*, 312-349.

Krishnamurthy, P. G., DiCarlo, D., & Meckel, T. (2022). Geologic Heterogeneity Controls on Trapping and Migration of CO2. *Geophysical Research Letters, 49*(16), e2022GL099104. https://doi.org/10.1029/2022GL099104

Lehrter, J. C., Beddick, D. L., Devereux, R., Yates, D. F., & Murrell, M. C. (2012). Sediment-water fluxes of dissolved inorganic carbon, O 2, nutrients, and N 2 from the hypoxic region of the Louisiana continental

shelf. *Biogeochemistry, 109*(1), 233-252.

Madugula, A. C. S., Jeffryes, C., Henry, J., Gossage, J., & Benson, T. J. (2024). A simulation-based model studying monoethanolamine and aprotic heterocyclic anion ionic liquid (AHA-IL) mixtures for carbon capture. *Computers & Chemical Engineering, 183*, 108599. https://www.sciencedirect.com/science/article/pii/S0098135424000176

Madugula, A. C. S., Sachde, D., Hovorka, S. D., Meckel, T. A., & Benson, T. J. (2021). Estimation of CO_2 emissions from petroleum refineries based on the total operable capacity for carbon capture applications. *Chemical Engineering Journal Advances, 8*, 100162. https://www.sciencedirect.com/science/article/pii/S2666821121000788

Meckel, T. A., Bump, A. P., Hovorka, S. D., & Trevino, R. H. (2021). Carbon capture, utilization, and storage hub development on the Gulf Coast. *Greenhouse Gases: Science and Technology, n/a*(n/a). https://onlinelibrary.wiley.com/doi/abs/10.1002/ghg.2082

Meckel, T. A., Treviño, R. H., Hovorka, S. D., & Bump, A. P. (2023). Mapping existing wellbore locations to compare technical risks between onshore and offshore CCS activities in Texas. *Greenhouse Gases: Science and Technology, 13*(3), 493-504. https://onlinelibrary.wiley.com/doi/abs/10.1002/ghg.2220

Miller-Way, T., Boland, G. S., Rowe, G. T., & Twilley, R. R. (1994). Sediment oxygen consumption and benthic nutrient fluxes on the Louisiana continental shelf: a methodological comparison. *Estuaries, 17*(4), 809-815.

Morse, J. W., Boland, G., & Rowe, G. T. (1999). Agilled'benthic chamber for extended measurement of sediment-water fluxes. *Marine chemistry, 66*(3-4), 225-230.

Ni, H., Bakhshian, S., & Meckel, T. A. (2023). Effects of grain size and small-scale bedform architecture on CO2 saturation from buoyancy-driven flow. *Nature Scientific Reports, 13*(1), 2474. https://doi.org/10.1038/s41598-023-29360-y

Ni, H., Bump, A. P., & Bakhshian, S. (2024). An experimental investigation on the CO2 storage capacity of the composite confining system. *International Journal of Greenhouse Gas Control, 134*, 104125. https://www.sciencedirect.com/science/article/pii/S1750583624000689

Ni, H., Li, B., Darraj, N., Ren, B., Harris, C., Krishnamurthy, P. G., et al. (2025). The impact of capillary heterogeneity on CO2 flow and trapping across scales. *Earth-Science Reviews, 270*, 105257. https://www.sciencedirect.com/science/article/pii/S0012825225002181

Ni, H., & Meckel, T. A. (2021). Characterizing the Effect of Capillary Heterogeneity on Multiphase Flow Pulsation in an Intermediate-Scale Beadpack Experiment Using Time Series Clustering and Frequency Analysis. *Water Resources Research, 57*(11), e2021WR030876. https://doi.org/10.1029/2021WR030876. https://doi.org/10.1029/2021WR030876

Nunnally, C. C., Quigg, A., DiMarco, S., Chapman, P., & Rowe, G. T. (2014). Benthic–pelagic coupling in the Gulf of Mexico hypoxic area: Sedimentary enhancement of hypoxic conditions and near bottom primary production. *Continental Shelf Research, 85*, 143-152.

Nunnally, C. C., Rowe, G. T., Thornton, D. C., & Quigg, A. (2013). Sedimentary oxygen consumption and nutrient regeneration in the northern Gulf of Mexico hypoxic zone. *Journal of Coastal Research*(63 (10063)), 84-96.

Oldenburg, C. M., & Pan, L. H. (2020). Major CO2 blowouts from offshore wells are strongly attenuated in water deeper than 50 m. *Greenhouse Gases-Science and Technology, 10*(1), 15-31. <Go to ISI>://WOS:000504315300001

Oldenburg, C. M., & Zhang, Y. (2022). Downwind dispersion of CO2 from a major subsea blowout in shallow offshore waters. *Greenhouse Gases: Science and Technology, 12*(2), 321-331. https://onlinelibrary.wiley.com/doi/abs/10.1002/ghg.2144

Omar, A. M., García-Ibáñez, M. I., Schaap, A., Oleynik, A., Esposito, M., Jeansson, E., et al. (2021). Detection and quantification of CO2 seepage in seawater using the stoichiometric Cseep method: Results from a recent subsea CO2 release experiment in the North Sea. *International Journal of Greenhouse Gas Control, 108*, 103310.

Rabalais, N. N., Turner, R., Gupta, B. S., Boesch, D., Chapman, P., & Murrell, M. (2007). Hypoxia in the northern Gulf of Mexico: Does the science support the plan to reduce, mitigate, and control hypoxia? *Estuaries and Coasts, 30*(5), 753-772.

Rabalais, N. N., Turner, R. E., & Scavia, D. (2002). Beyond Science into Policy: Gulf of Mexico Hypoxia and the Mississippi River: Nutrient policy development for the Mississippi River watershed reflects the accumulated scientific evidence that the increase in nitrogen loading is the primary factor in the worsening of hypoxia in the northern Gulf of Mexico. *BioScience, 52*(2), 129-142.

Romanak, K., & Dixon, T. (2022). CO2 storage guidelines and the science of monitoring: Achieving project success under the California Low Carbon Fuel Standard CCS Protocol and other global regulations. *International Journal of Greenhouse Gas Control, 113*, 103523.

Romanak, K. D., Bennett, P. C., Yang, C., & Hovorka, S. (2012). Process-based approach to CO2 leakage detection by vadose zone gas monitoring at geologic CO2 storage sites. *Geophysical Research Letters, 39*(15), L15405. http://dx.doi.org/10.1029/2012GL052426

Rowe, G., & Chapman, P. (2002). Hypoxia in the northern Gulf of Mexico: some nagging questions. *Gulf Mex Sci, 20*, 153-160.

Rowe, G. T. (2001). Seasonal hypoxia in the bottom water off the Mississippi River delta. *Journal of Environmental Quality, 30*(2), 281-290.

Sands, C., Connelly, D., & Blackford, J. (2021). Introduction to the STEMM-CCS special issue. *International Journal of Greenhouse Gas Control, 113*, 103553.

Sun, S., Nishimura, S., Sato, T., & Uchimoto, K. (2020). *Indicator for CO 2 concentration in seawater using DIC and DO.* Paper presented at the Global Oceans 2020: Singapore–US Gulf Coast.

T. Camargo, J., Hamon, F., Mazuyer, A., Meckel, T., Castelletto, N., & White, J. A. (2022, 23-24 Oct 2022). *Deformation Monitoring Feasibility for Offshore Carbon Storage in the Gulf-of-Mexico.* Paper presented at the 16th International Conference on Greenhouse Gas Control Technologies, GHGT-16, Lyon, France.

Trevino, R. H., Hovorka, S. D., Dunlap, D. B., Larson, R. C., Hentz, T. F., Hosseini, S. A., et al. (2024). A phased workflow to define permit-ready locations for large volume CO2 injection and storage. *Greenhouse Gases: Science and Technology, 14*(1), 95-110. https://onlinelibrary.wiley.com/doi/abs/10.1002/ghg.2253 ,eprint = https://onlinelibrary.wiley.com/doi/pdf/10.1002/ghg.2253

Ubillus, J. E., Bakhshian, S., Ni, H., DiCarlo, D., & Meckel, T. (2025). Informing field-scale CO2storage simulations with sandbox experiments: The effect of small-scale heterogeneities. *International Journal of Greenhouse Gas Control, 141*, 104318. https://www.sciencedirect.com/science/article/pii/S1750583625000167

Ubillus, J. E., Ni, H., DiCarlo, D., & Meckel, T. (2025). Experimental Investigation of Buoyant Flow in Realistic Bedforms With Heterogeneous Wettability. *SPE Journal*, 1-11. https://doi.org/10.2118/224402-PA

Uchimoto, K., Nishimura, M., Kita, J., & Xue, Z. (2018). Detecting CO2 leakage at offshore storage sites using the covariance between the partial pressure of CO2 and the saturation of dissolved oxygen in seawater. *International Journal of Greenhouse Gas Control, 72*, 130-137.

Uchimoto, K., Watanabe, Y., & Xue, Z. (2021). Seasonal dependence of false-positives in detection of anomalous pCO2 using the covariance method with dissolved oxygen in monitoring offshore CO2 storage sites. *Marine Pollution Bulletin, 166*, 112238.

Ulfah, M., Hosseini, S., Hovorka, S., Bump, A., Bakhshian, S., & Dunlap, D. (2022). Assessing Impacts on Pressure Stabilization and Leasing Acreage for CO2 Storage Utilizing Oil Migration Concepts. *International Journal of Greenhouse Gas Control, 115*, 103612. https://www.sciencedirect.com/science/article/pii/S1750583622000317

Zeng, H., He, Y., Olariu, M., & Treviño, R. (2023). Machine learning-based inversion for acoustic impedance with large synthetic training data: Workflow and data characterization. *Geophysics, 88*(2), R193-R207. https://doi.org/10.1190/geo2021-0726.1

9. Acknowledgements

The seismic datasets (volumes) were interpreted using Haliburton's Landmark and Schlumberger's Petrel platforms. The software from both platforms was available to the Partnership's Bureau of Economic Geology (BEG) team via the, respective, Haliburton and Schlumberger university grant programs, for which we are sincerely grateful.

The Petra well interpretation software was available to the Partnership's Bureau of Economic Geology (BEG) team via IHS Petra's university grant program. We are most grateful.

We extend our gratitude is to the Computer Modeling Group, Calgary, Canada (CMG) for providing CMG-GEM and associated software.

Appendix A
Fluid Inclusion Stratigraphy Analysis
Well F1970023a-2

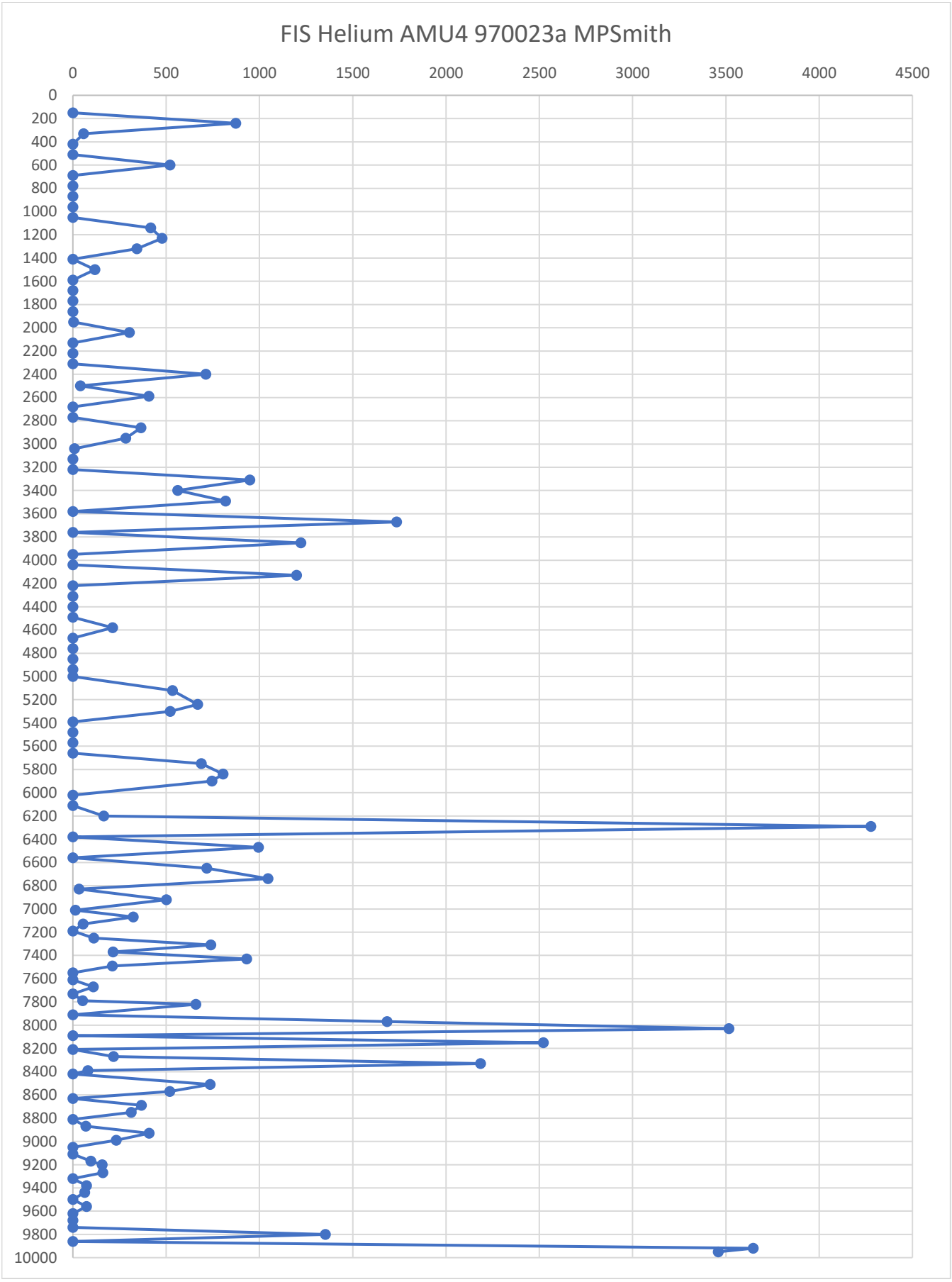
FIS Helium AMU4 970023a MPSmith
0
500
1000
1500
2000
2500
3000
3500
4000
4500
0
200
400
600
800
1000
1200
1400
1600
1800
2000
2200
2400
2600
2800
3000
3200
3400
3600
3800
4000
4200
4400
4600
4800
5000
5200
5400
5600
5800
6000
6200
6400
6600
6800
7000
7200
7400
7600
7800
8000
8200
8400
8600
8800
9000
9200
9400
9600
9800
10000

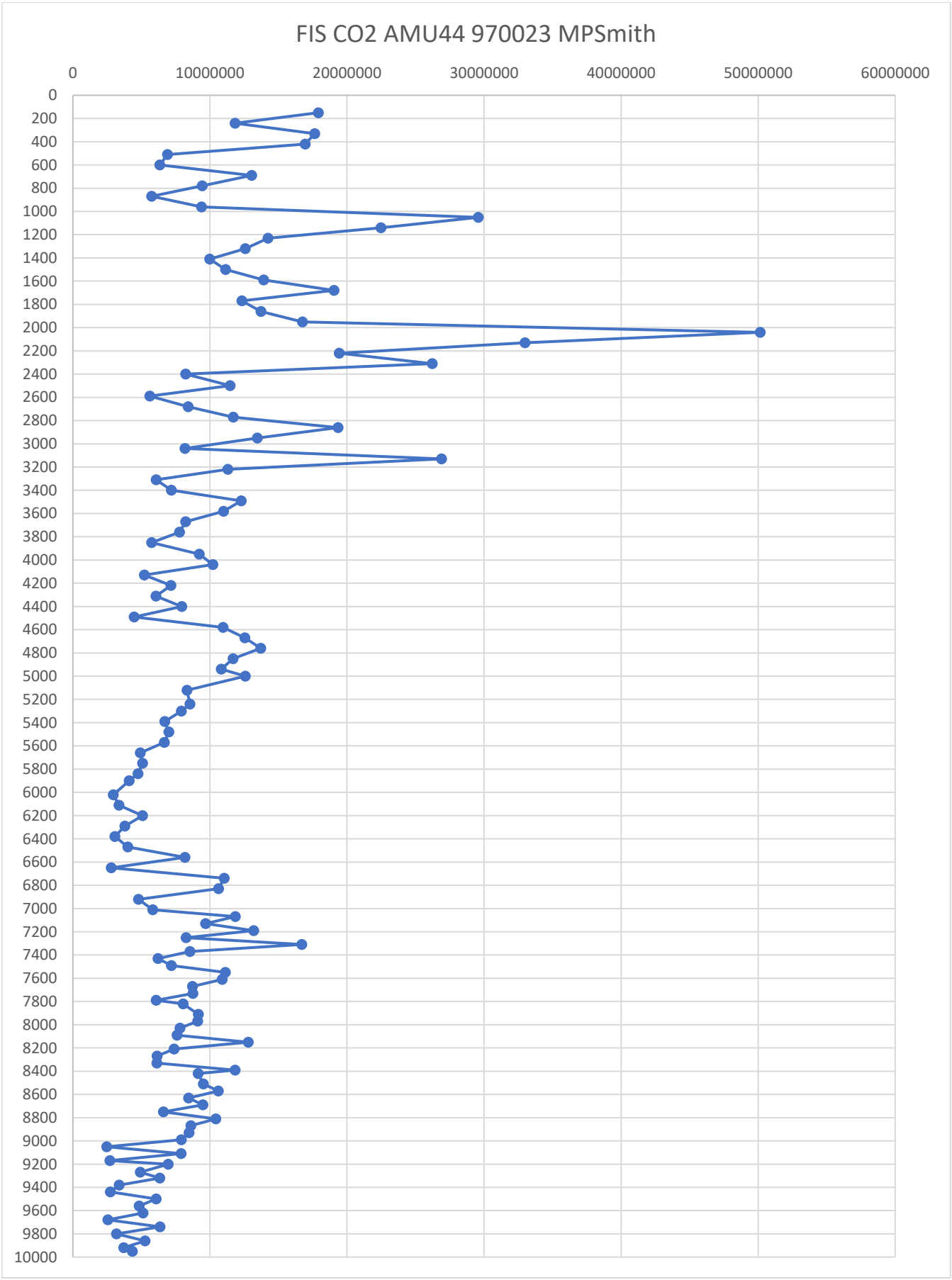
FIS CO2 AMU44 970023 MPSmith
0
10000000
20000000
30000000
40000000
50000000
60000000
0
200
400
600
800
1000
1200
1400
1600
1800
2000
2200
2400
2600
2800
3000
3200
3400
3600
3800
4000
4200
4400
4600
4800
5000
5200
5400
5600
5800
6000
6200
6400
6600
6800
7000
7200
7400
7600
7800
8000
8200
8400
8600
8800
9000
9200
9400
9600
9800
10000

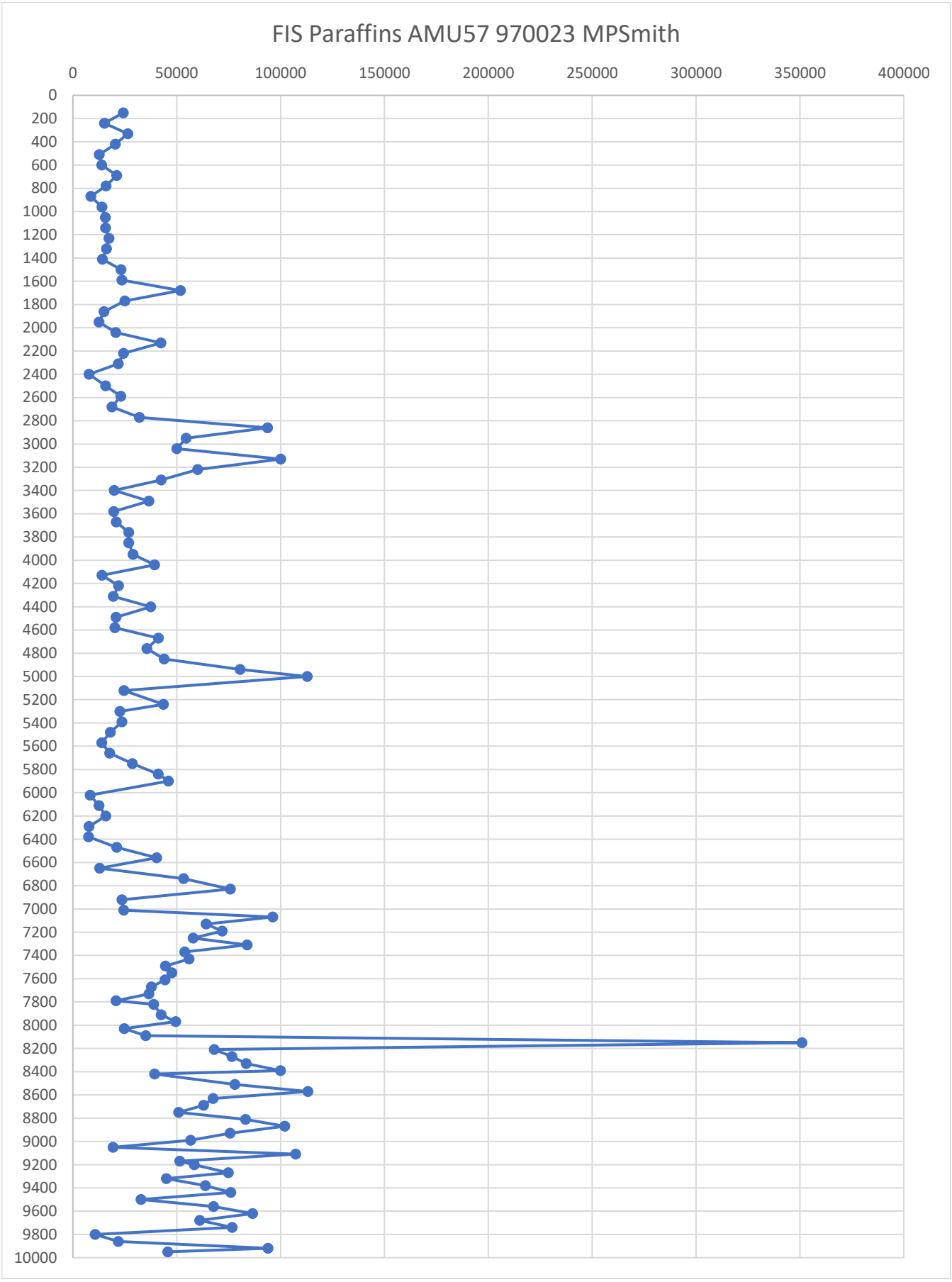
FIS Paraffins AMU57 970023 MPSmith
0
50000
100000
150000
200000
250000
300000
350000
400000
0
200
400
600
800
1000
1200
1400
1600
1800
2000
2200
2400
2600
2800
3000
3200
3400
3600
3800
4000
4200
4400
4600
4800
5000
5200
5400
5600
5800
6000
6200
6400
6600
6800
7000
7200
7400
7600
7800
8000
8200
8400
8600
8800
9000
9200
9400
9600
9800
10000

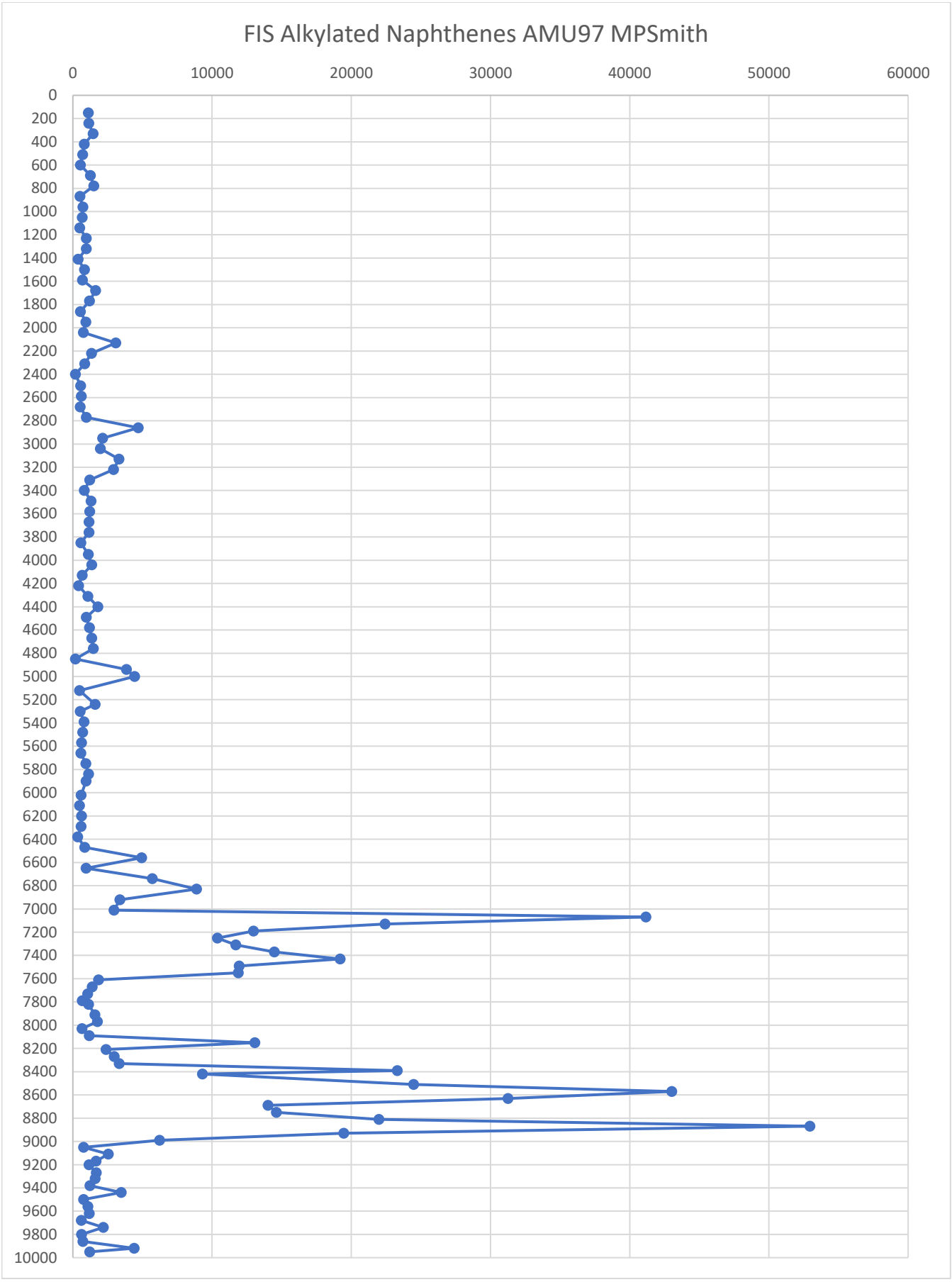
FIS Alkylated Naphthenes AMU97 MPSmith
0
10000
20000
30000
40000
50000
60000
0
200
400
600
800
1000
1200
1400
1600
1800
2000
2200
2400
2600
2800
3000
3200
3400
3600
3800
4000
4200
4400
4600
4800
5000
5200
5400
5600
5800
6000
6200
6400
6600
6800
7000
7200
7400
7600
7800
8000
8200
8400
8600
8800
9000
9200
9400
9600
9800
10000

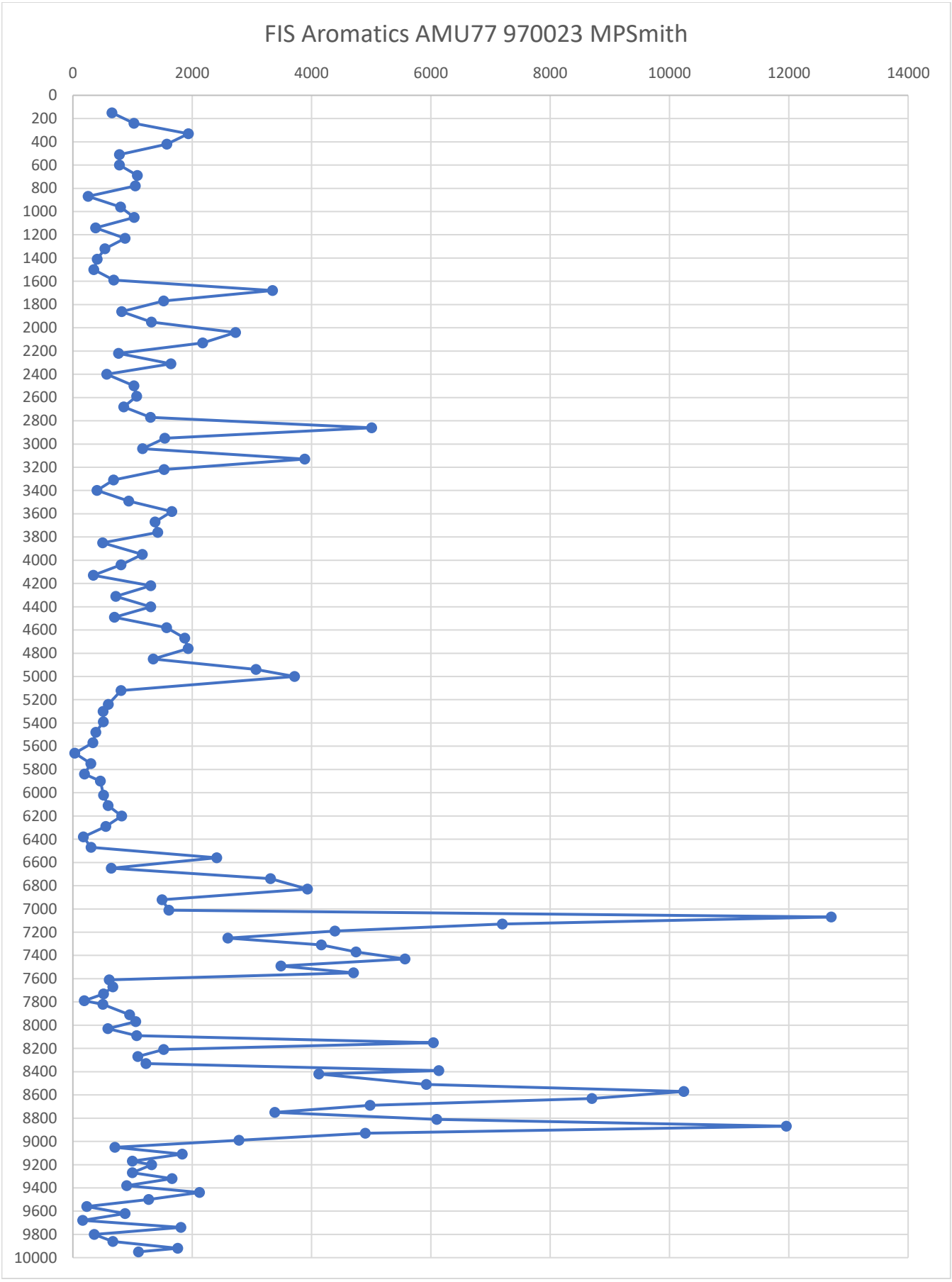
FIS Aromatics AMU77 970023 MPSmith
0
2000
4000
6000
8000
10000
12000
14000
0
200
400
600
800
1000
1200
1400
1600
1800
2000
2200
2400
2600
2800
3000
3200
3400
3600
3800
4000
4200
4400
4600
4800
5000
5200
5400
5600
5800
6000
6200
6400
6600
6800
7000
7200
7400
7600
7800
8000
8200
8400
8600
8800
9000
9200
9400
9600
9800
10000

Appendix B
Fluid Inclusion Stratigraphy Analysis
Well F1970022a-2

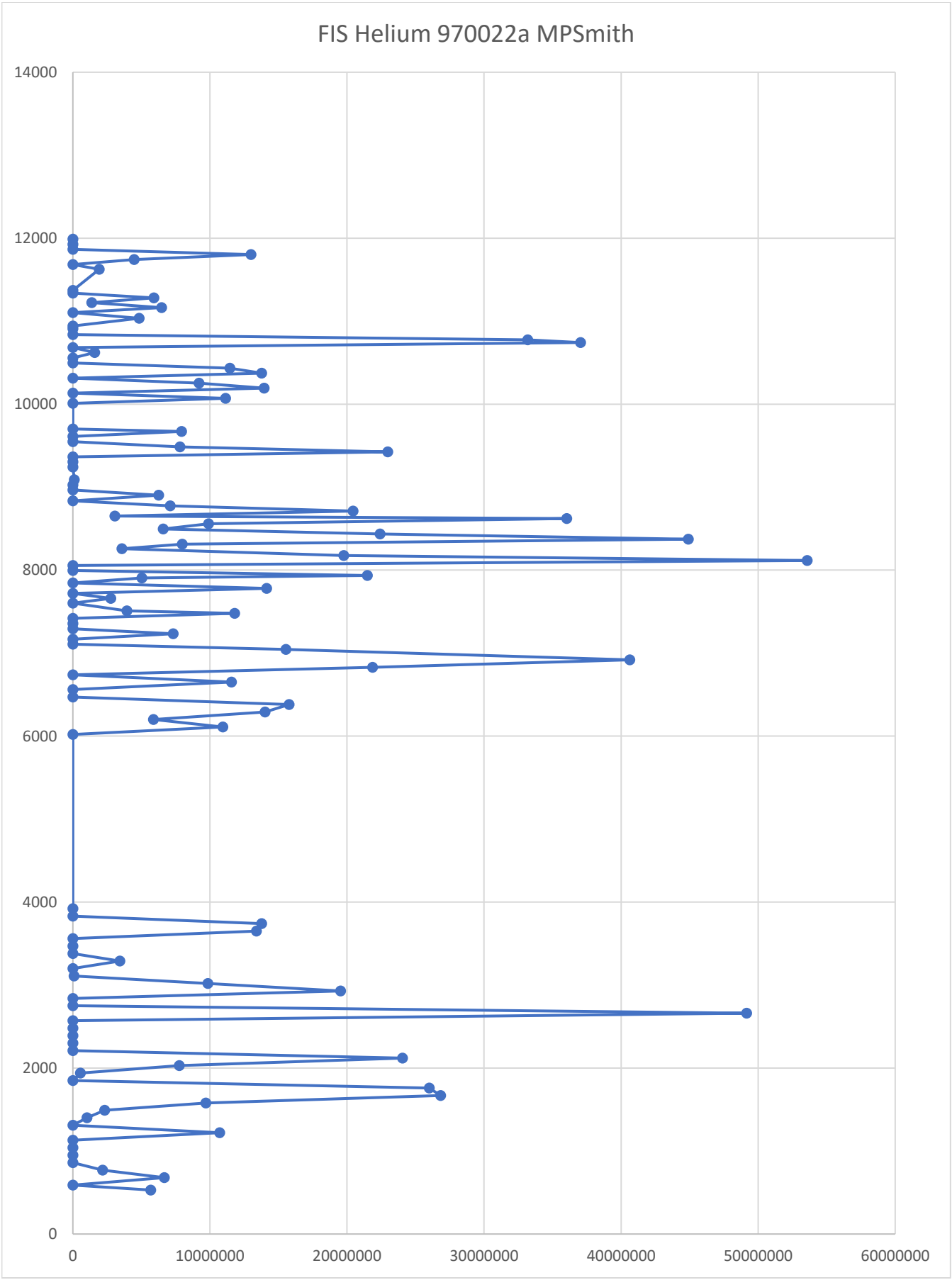
FIS Helium 970022a MPSmith
14000
12000
10000
8000
6000
4000
2000
0
0
10000000
20000000
30000000
40000000
50000000
60000000

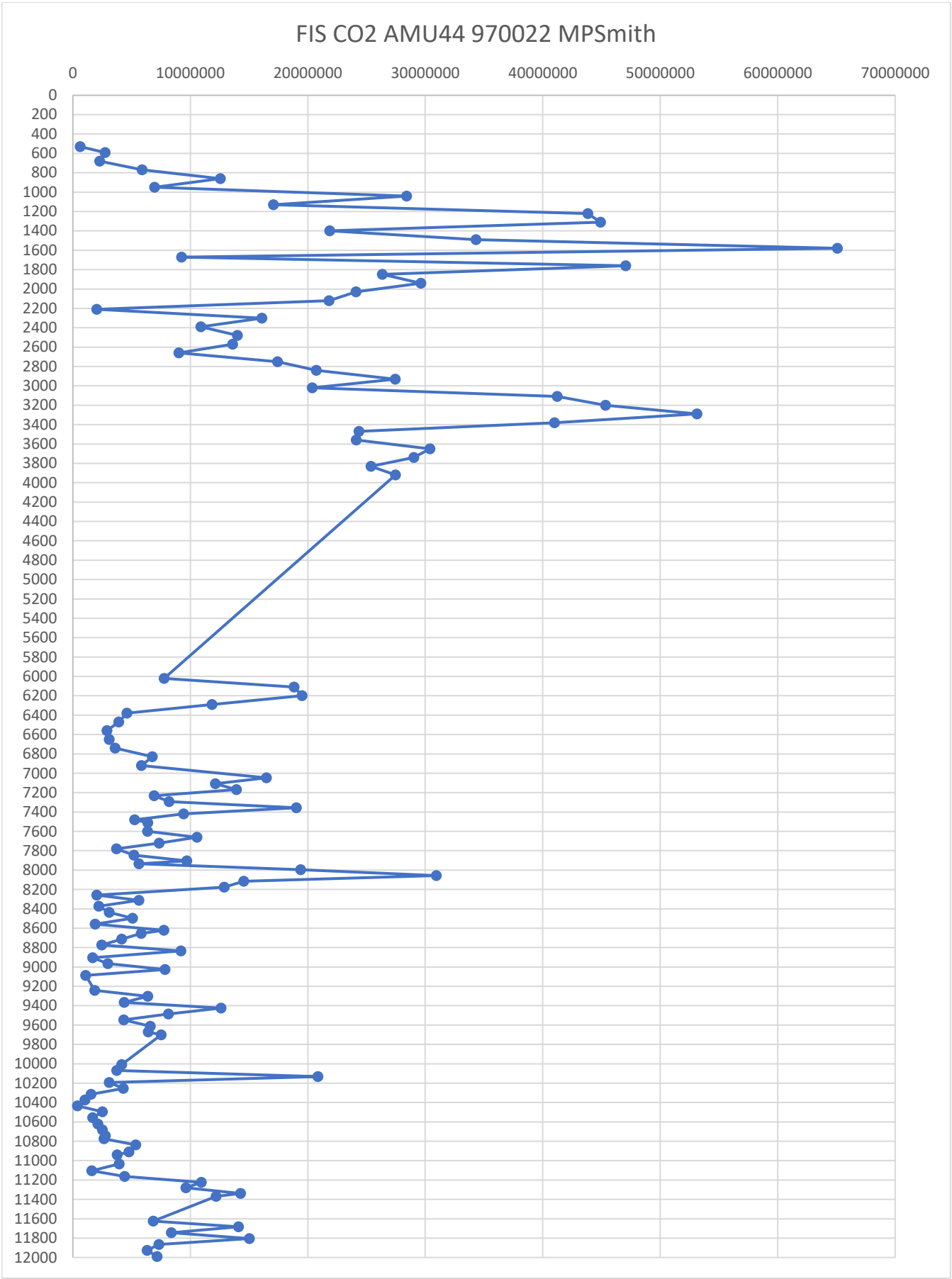
FIS CO2 AMU44 970022 MPSmith
0
10000000
20000000
30000000
40000000
50000000
60000000
70000000
0
200
400
600
800
1000
1200
1400
1600
1800
2000
2200
2400
2600
2800
3000
3200
3400
3600
3800
4000
4200
4400
4600
4800
5000
5200
5400
5600
5800
6000
6200
6400
6600
6800
7000
7200
7400
7600
7800
8000
8200
8400
8600
8800
9000
9200
9400
9600
9800
10000
10200
10400
10600
10800
11000
11200
11400
11600
11800
12000

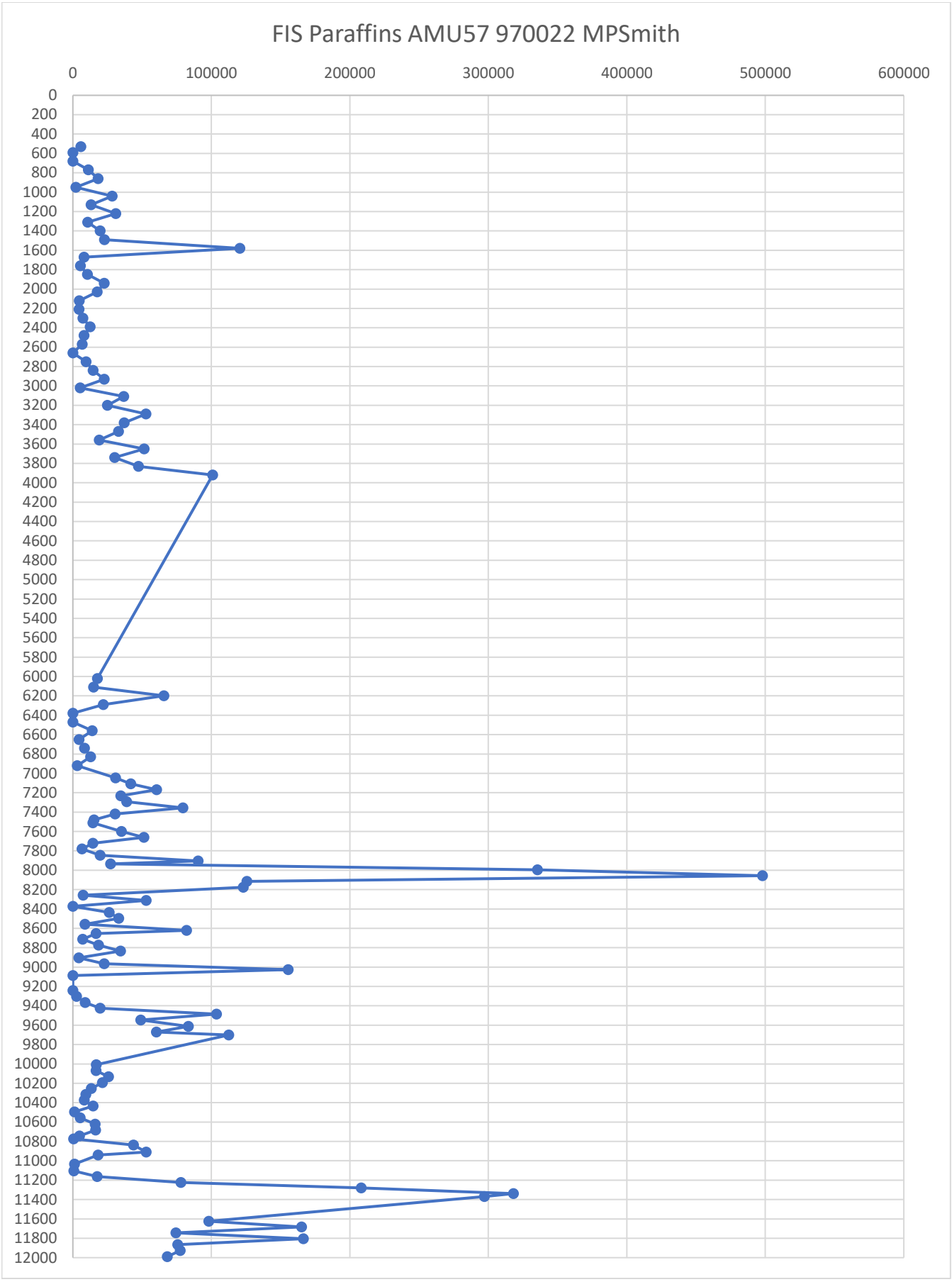
FIS Paraffins AMU57 970022 MPSmith
0
100000
200000
300000
400000
500000
600000
0
200
400
600
800
1000
1200
1400
1600
1800
2000
2200
2400
2600
2800
3000
3200
3400
3600
3800
4000
4200
4400
4600
4800
5000
5200
5400
5600
5800
6000
6200
6400
6600
6800
7000
7200
7400
7600
7800
8000
8200
8400
8600
8800
9000
9200
9400
9600
9800
10000
10200
10400
10600
10800
11000
11200
11400
11600
11800
12000

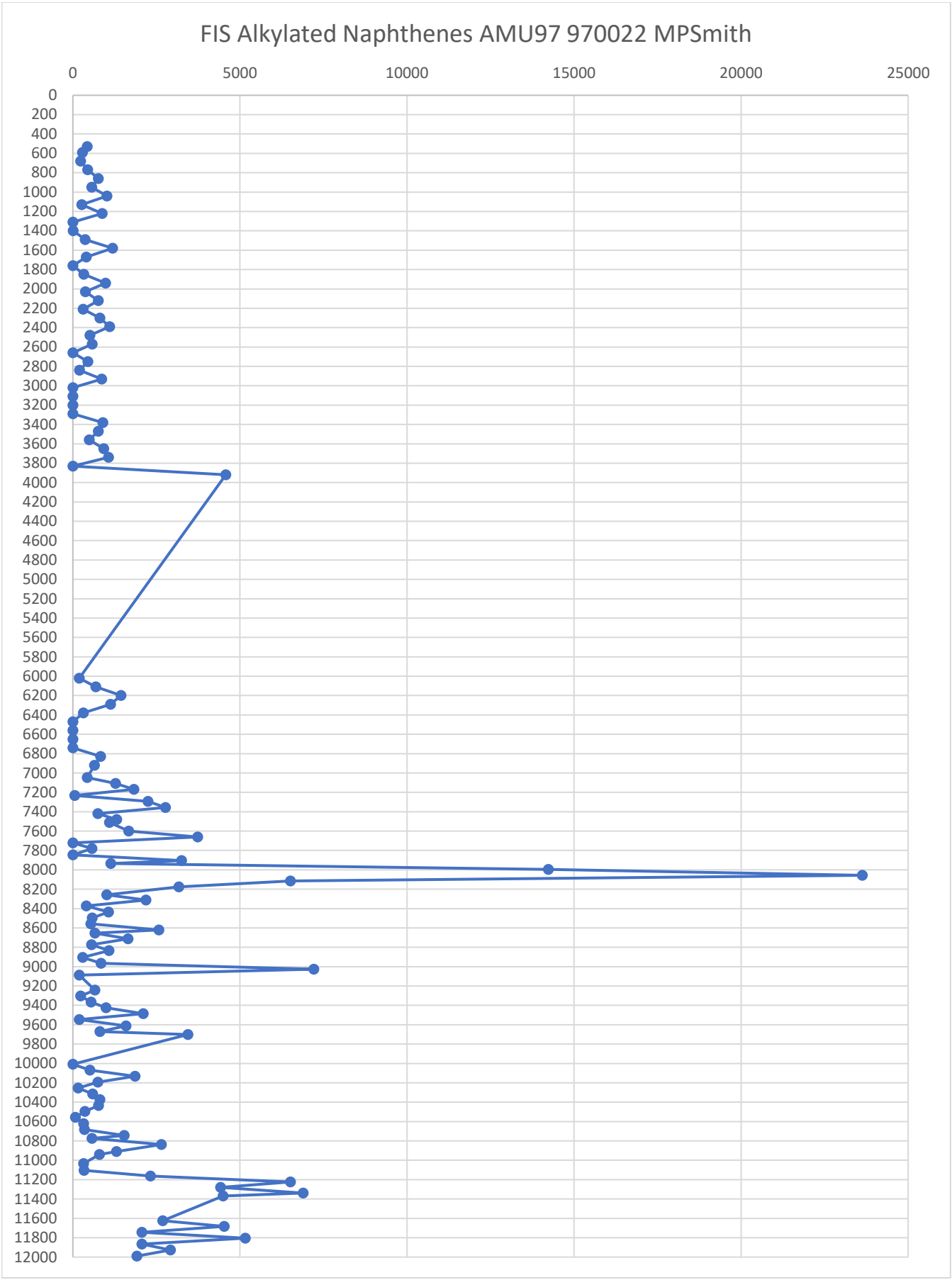
FIS Alkylated Naphthenes AMU97 970022 MPSmith
0
5000
10000
15000
20000
25000
0
200
400
600
800
1000
1200
1400
1600
1800
2000
2200
2400
2600
2800
3000
3200
3400
3600
3800
4000
4200
4400
4600
4800
5000
5200
5400
5600
5800
6000
6200
6400
6600
6800
7000
7200
7400
7600
7800
8000
8200
8400
8600
8800
9000
9200
9400
9600
9800
10000
10200
10400
10600
10800
11000
11200
11400
11600
11800
12000

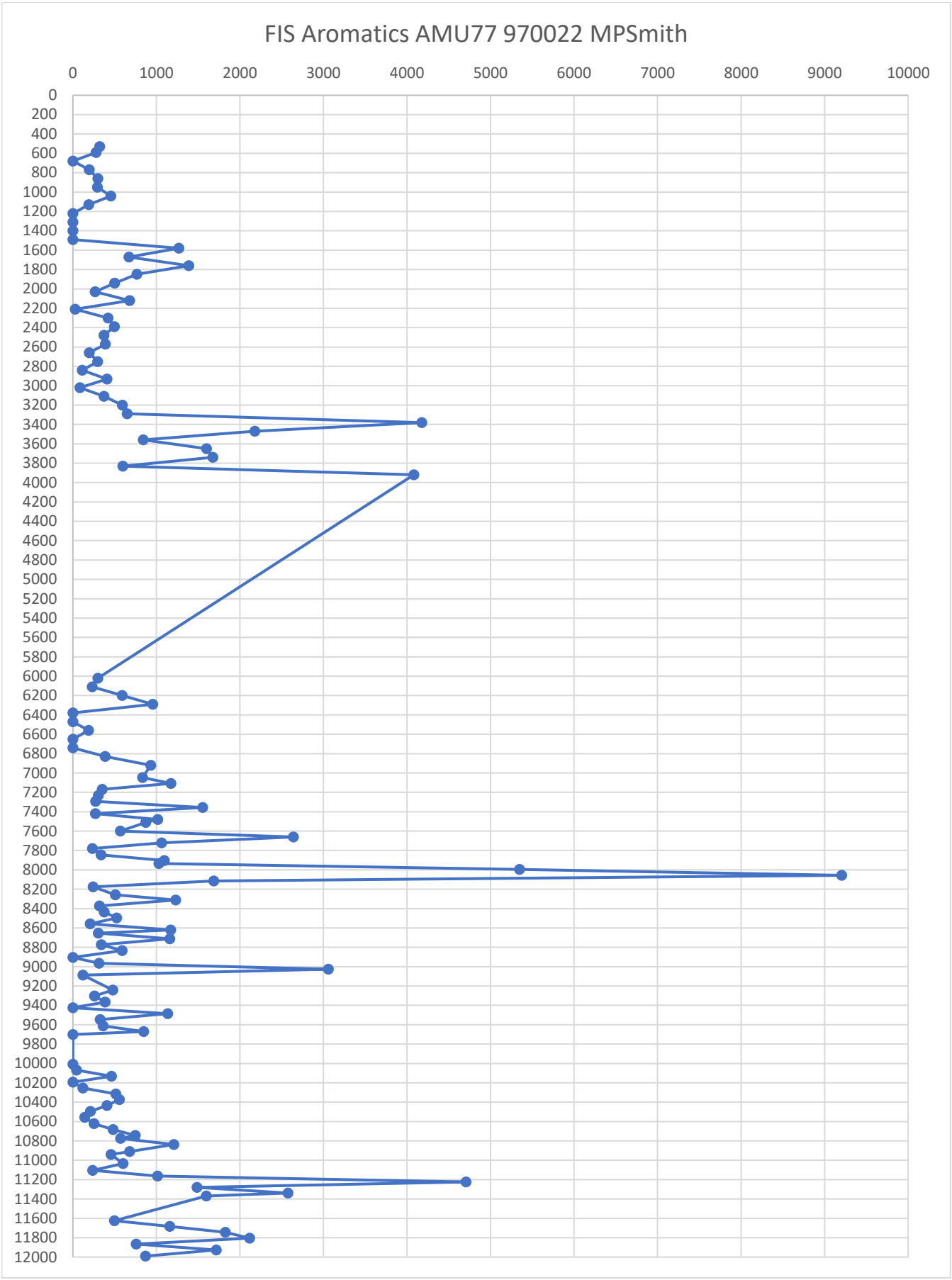
FIS Aromatics AMU77 970022 MPSmith
0
1000
2000
3000
4000
5000
6000
7000
8000
9000
10000
0
200
400
600
800
1000
1200
1400
1600
1800
2000
2200
2400
2600
2800
3000
3200
3400
3600
3800
4000
4200
4400
4600
4800
5000
5200
5400
5600
5800
6000
6200
6400
6600
6800
7000
7200
7400
7600
7800
8000
8200
8400
8600
8800
9000
9200
9400
9600
9800
10000
10200
10400
10600
10800
11000
11200
11400
11600
11800
12000

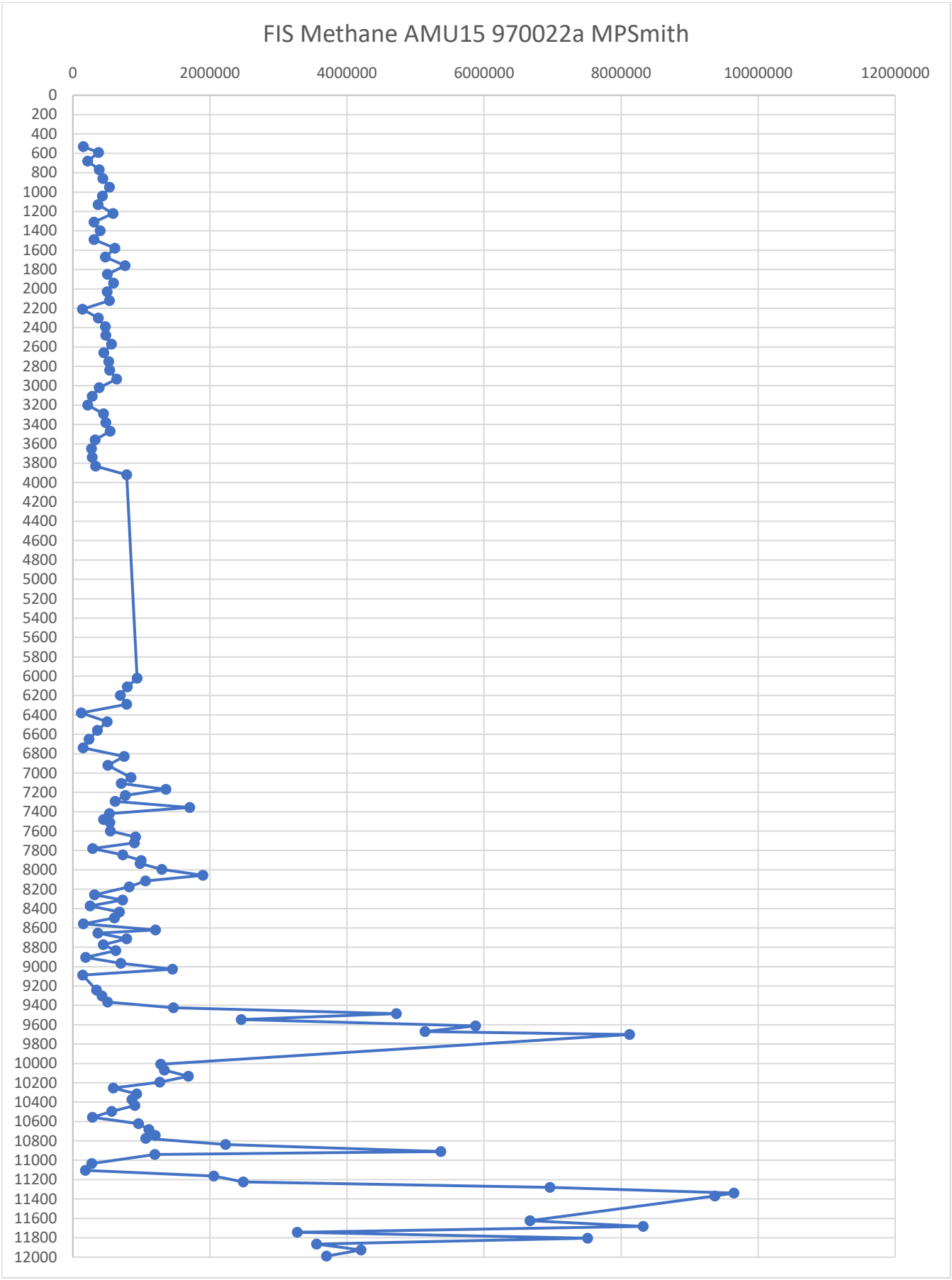
FIS Methane AMU15 970022a MPSmith
0
2000000
4000000
6000000
8000000
10000000
12000000
0
200
400
600
800
1000
1200
1400
1600
1800
2000
2200
2400
2600
2800
3000
3200
3400
3600
3800
4000
4200
4400
4600
4800
5000
5200
5400
5600
5800
6000
6200
6400
6600
6800
7000
7200
7400
7600
7800
8000
8200
8400
8600
8800
9000
9200
9400
9600
9800
10000
10200
10400
10600
10800
11000
11200
11400
11600
11800
12000

Appendix C
Plume Migration and Pressure Evolution Analyses

ENERGY AND EARTH RESOURCES GRADUATE PROGRAM

multidisciplinary studies for interdisciplinary solutions

Plume Migration and Pressure Evolution Analyses for Recommendations in Offshore CO_2 Storage Acreage Leasing Policy

Melianna Ulfah

M.S. in Energy and Earth Resources

Supervisor: Dr. Susan D. Hovorka

TEXAS Geosciences
The University of Texas at Austin
Jackson School of Geosciences

Bureau of Economic Geology

GCCC
GULF COAST CARBON CENTER

Study Area

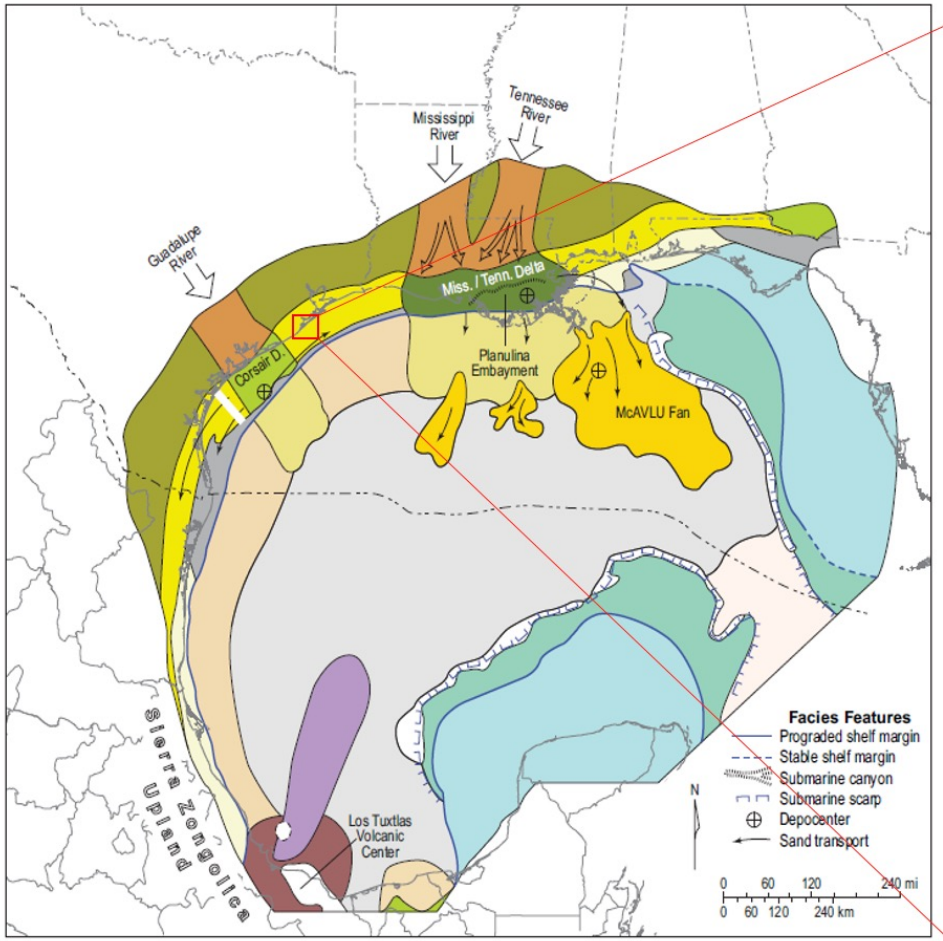

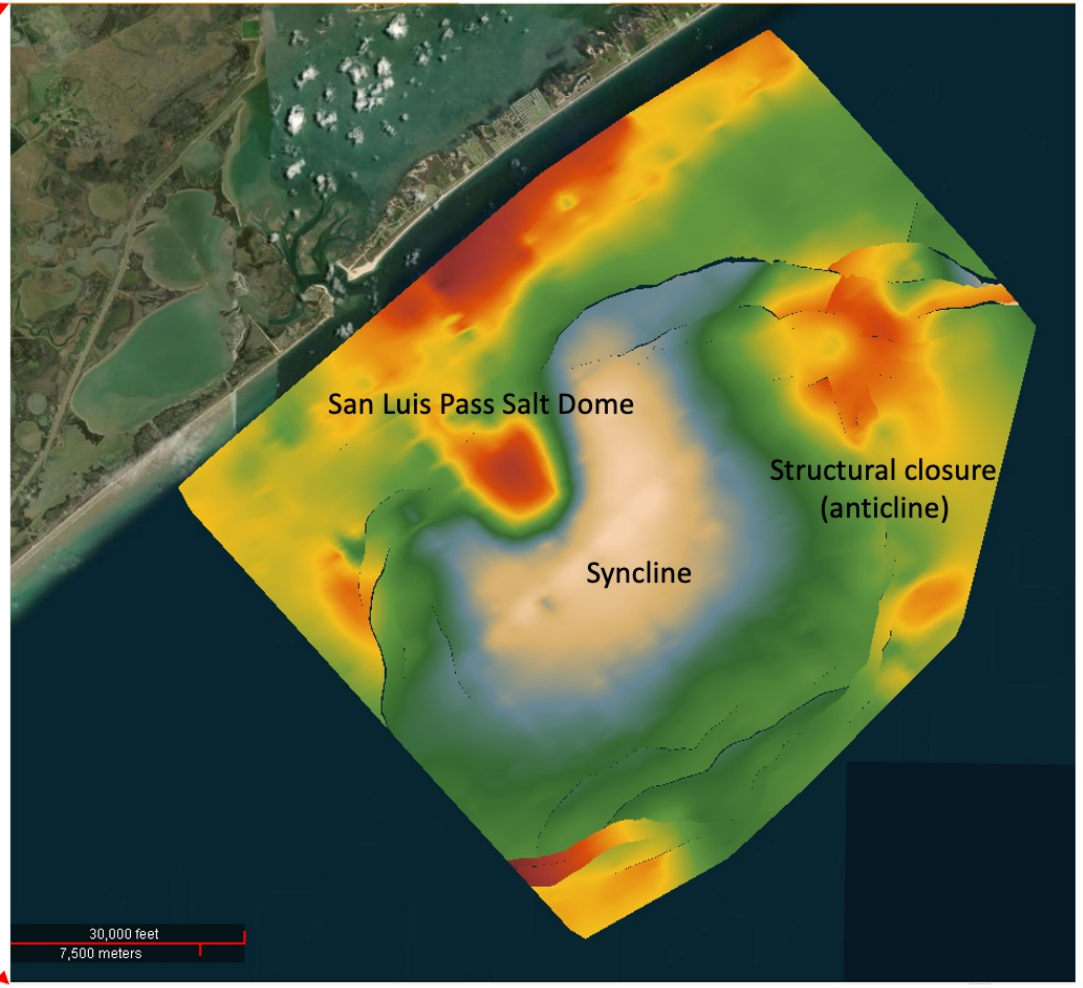

Depth Map top of MFS 6 (top capacity)

General depositional environment: Wave-dominated delta-fed shore zone system

GCCC GULF COAST CARBON CENTER

BUREAU OF ECONOMIC GEOLOGY

TEXAS Geosciences
The University of Texas at Austin
Jackson School of Geosciences

ENERGY AND EARTH RESOURCES GRADUATE PROGRAM
multidisciplinary studies for interdisciplinary solutions

Seismic and Well Log Characterization

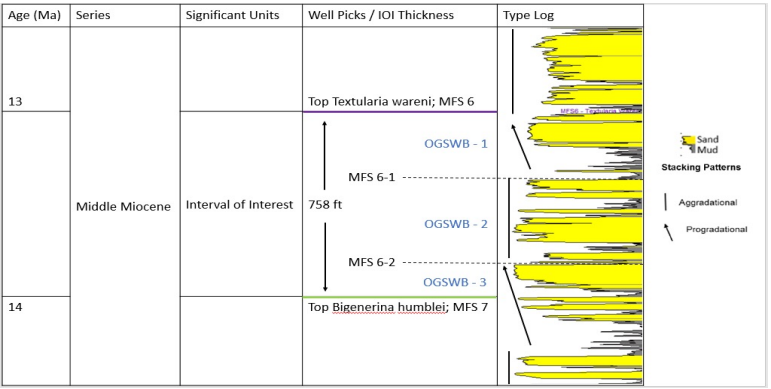

Identifying depositional stacking pattern from SP log data

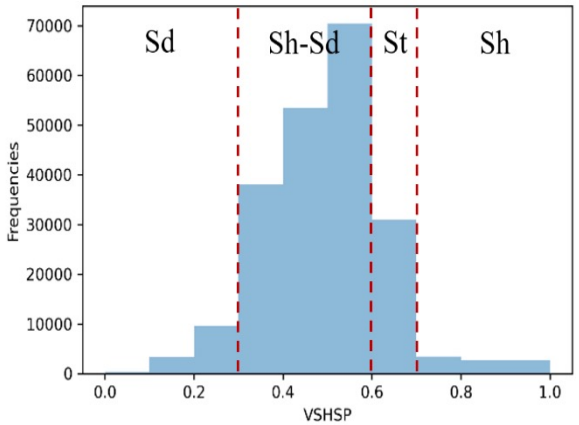

Multiwell histogram analysis for identifying lithofacies

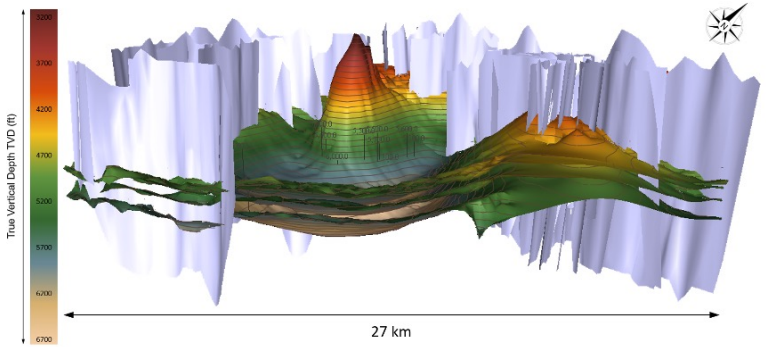

Interpreted Horizon and Fault from 3D Seismic interpretation

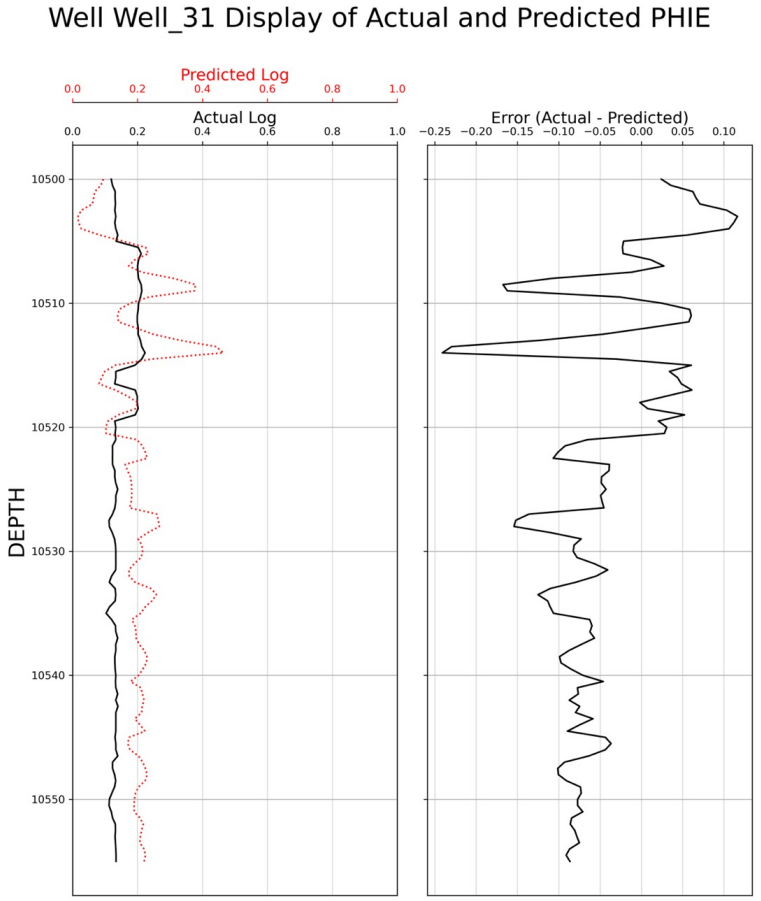

Neural Network Algorithm to predict PHIE from incomplete well data

GCCC GULF COAST CARBON CENTER
BUREAU OF ECONOMIC GEOLOGY
TEXAS Geosciences
The University of Texas at Austin
Jackson School of Geosciences
ENERGY AND EARTH RESOURCES GRADUATE PROGRAM
multidisciplinary studies for interdisciplinary solutions

Geostatistical Modeling

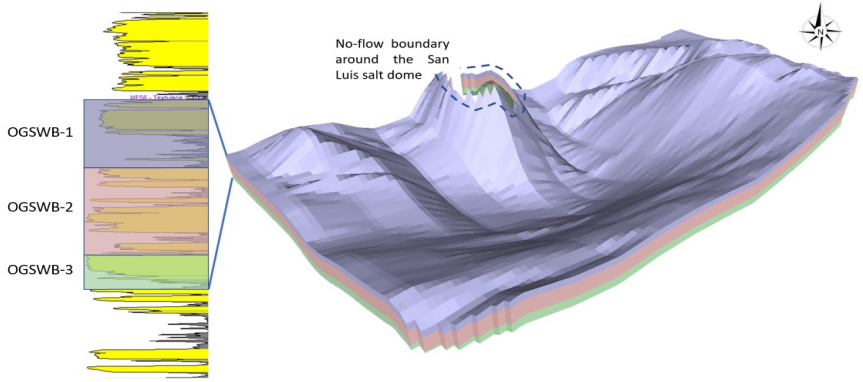

Geocellular Grid
from 3D Seismic interpretation

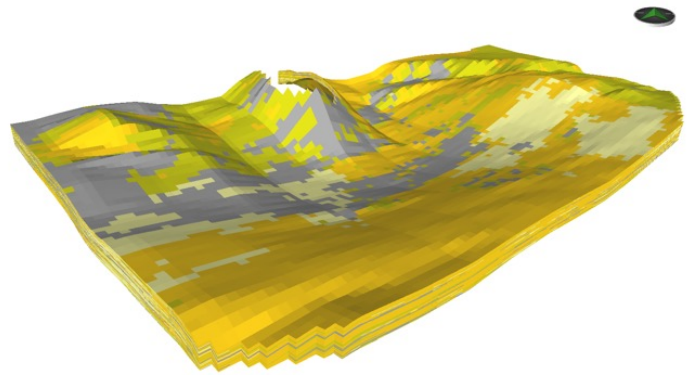

Facies Model

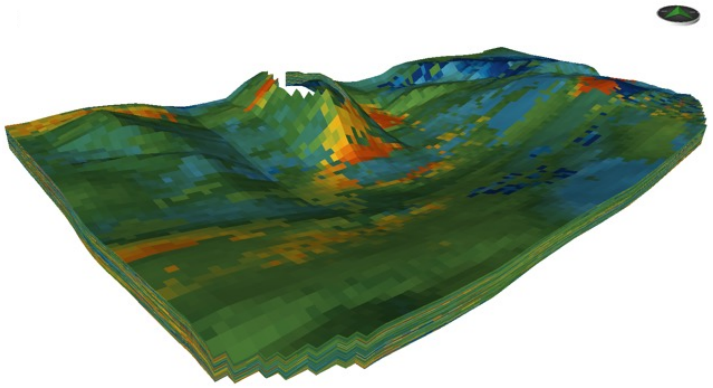

Porosity Model

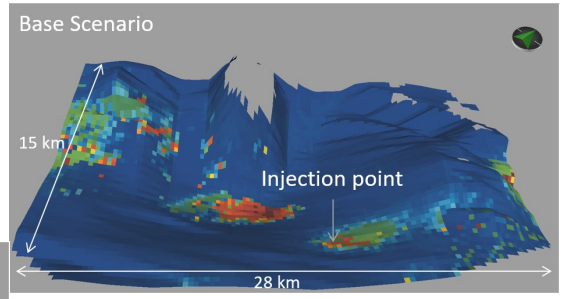

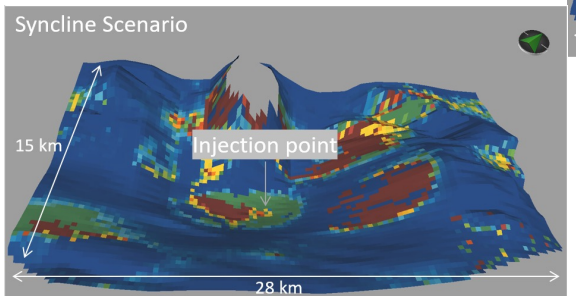

Permeability Model with
two injection scenarios

GCCC GULF COAST CARBON CENTER

BUREAU OF ECONOMIC GEOLOGY

TEXAS Geosciences
The University of Texas at Austin
Jackson School of Geosciences

ENERGY AND EARTH RESOURCES GRADUATE PROGRAM
multidisciplinary studies for interdisciplinary solutions

Base Case Scenario

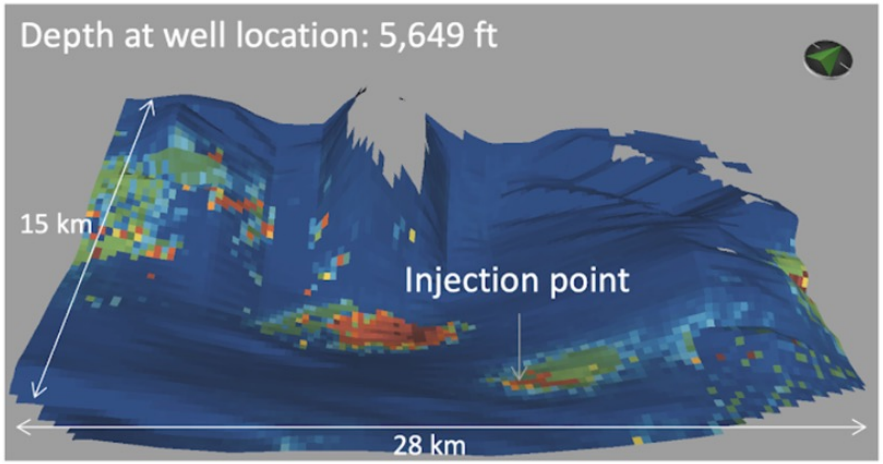

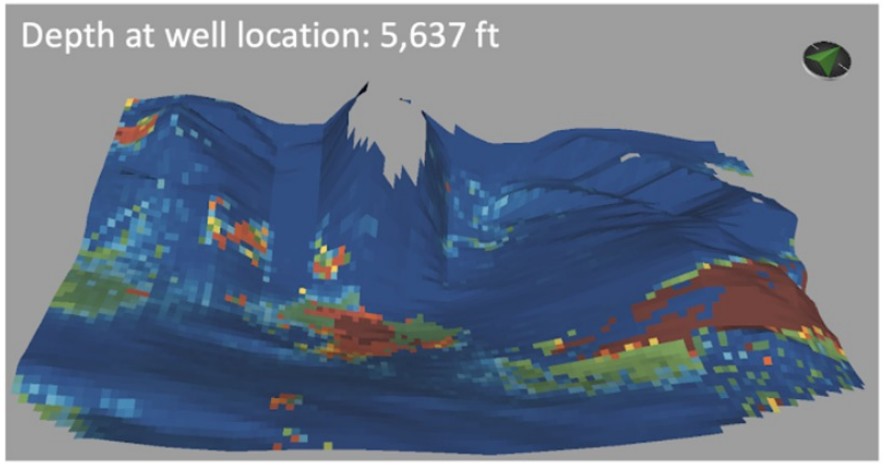

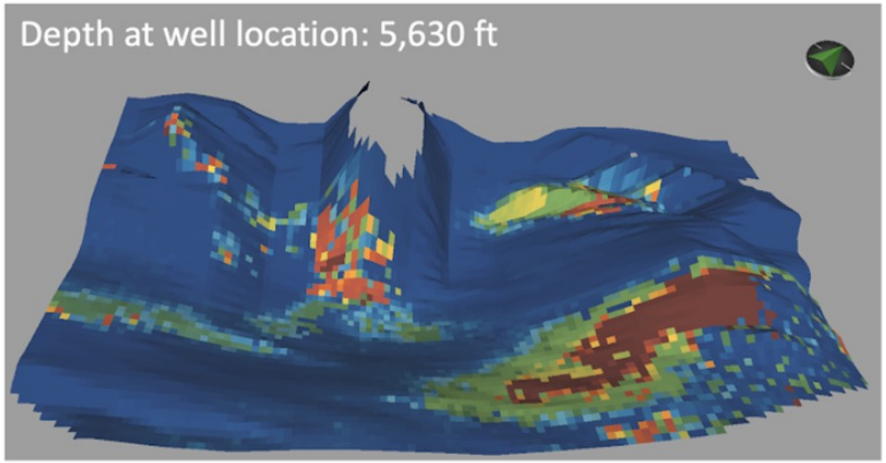

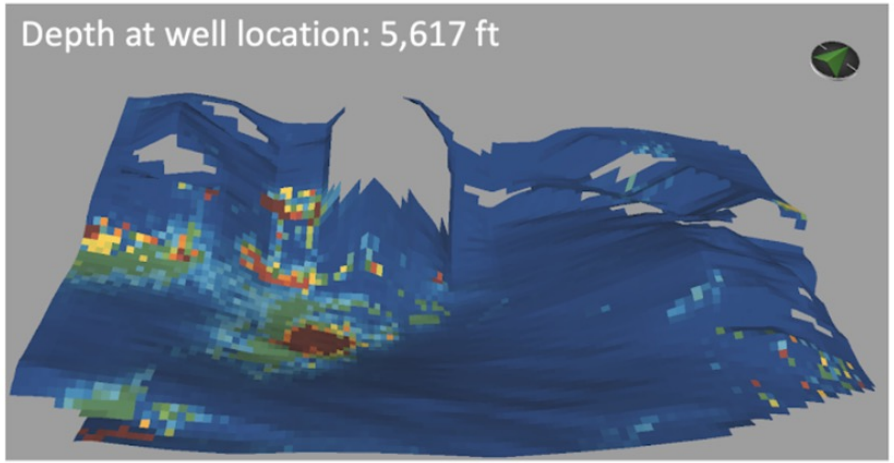

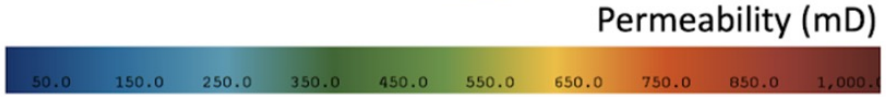

GCCC GULF COAST CARBON CENTER

BUREAU OF ECONOMIC GEOLOGY

TEXAS Geosciences
The University of Texas at Austin
Jackson School of Geosciences

ENERGY AND EARTH RESOURCES GRADUATE PROGRAM
multidisciplinary studies for interdisciplinary solutions

Inject-at-Syncline Scenario

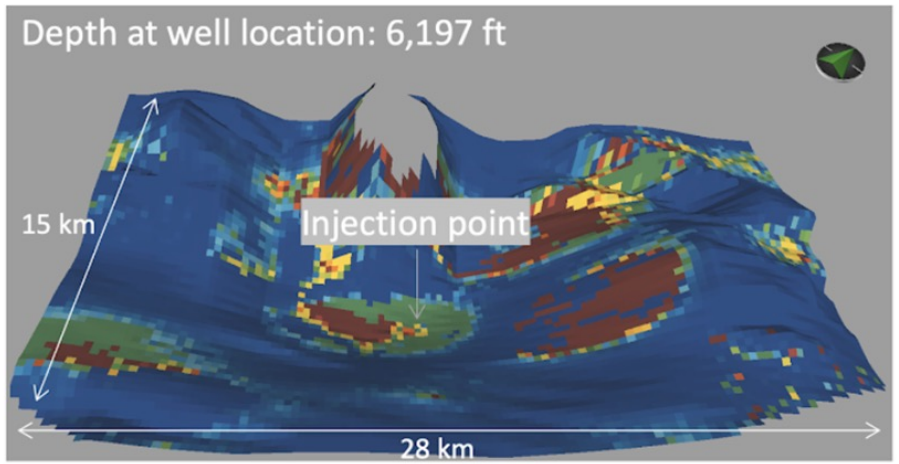

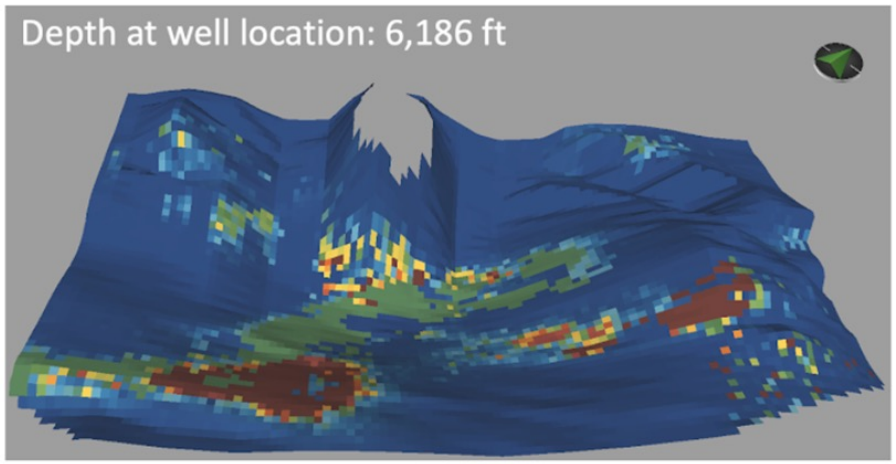

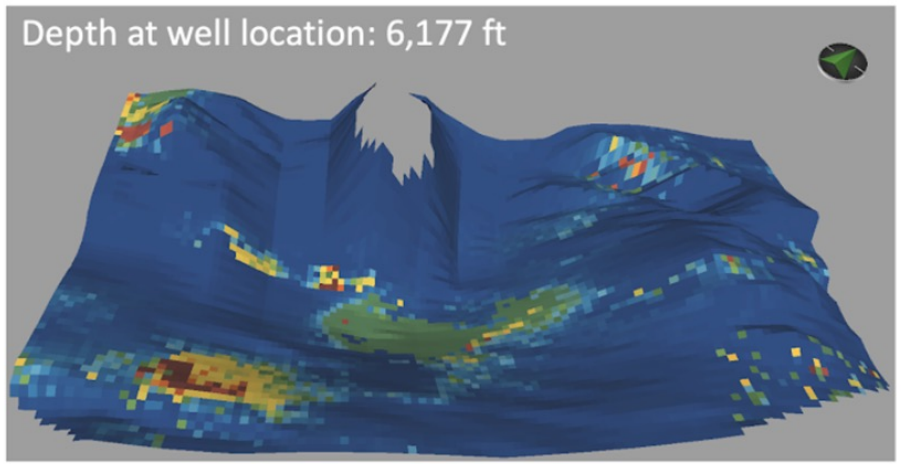

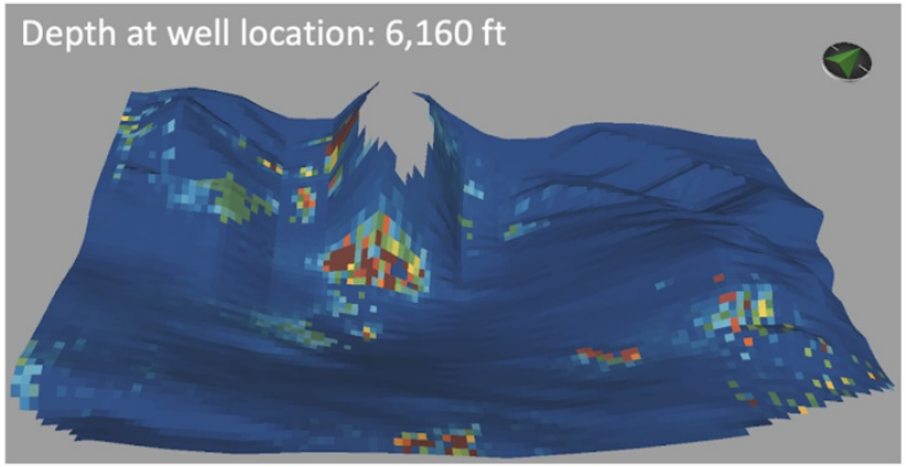

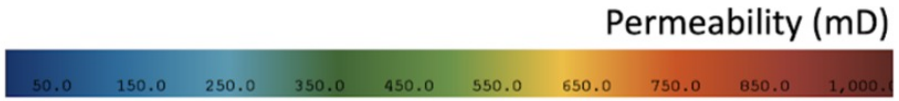

GCCC GULF COAST CARBON CENTER

BUREAU OF ECONOMIC GEOLOGY

TEXAS Geosciences
The University of Texas at Austin
Jackson School of Geosciences

ENERGY AND EARTH RESOURCES GRADUATE PROGRAM
multidisciplinary studies for interdisciplinary solutions

Base Scenario

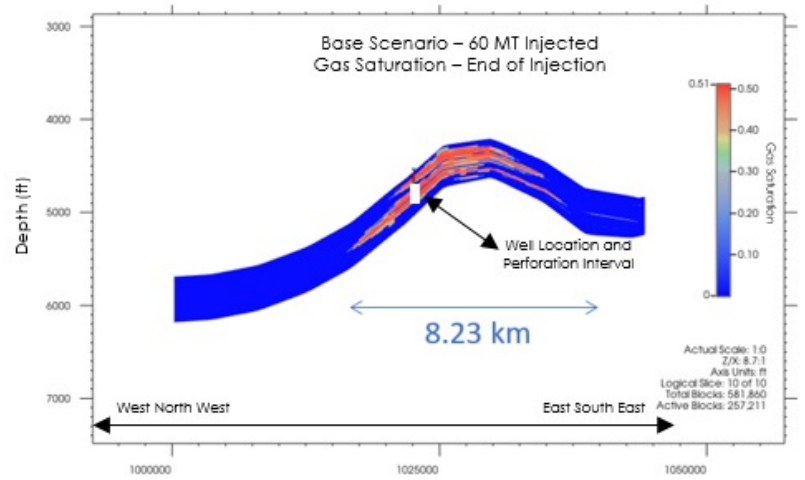

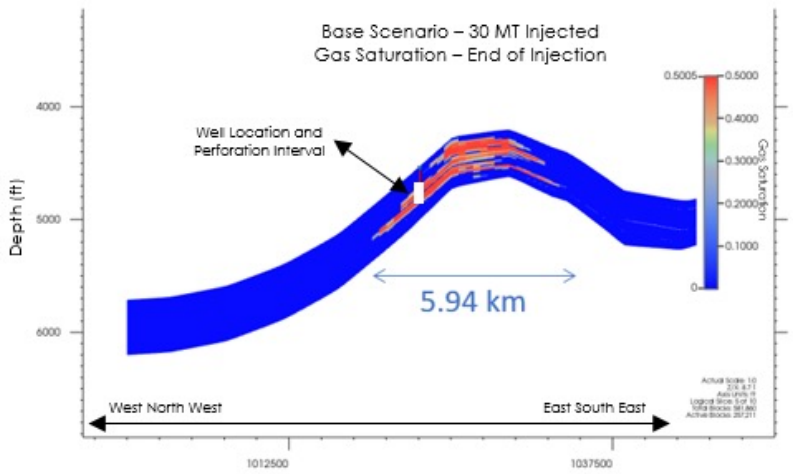

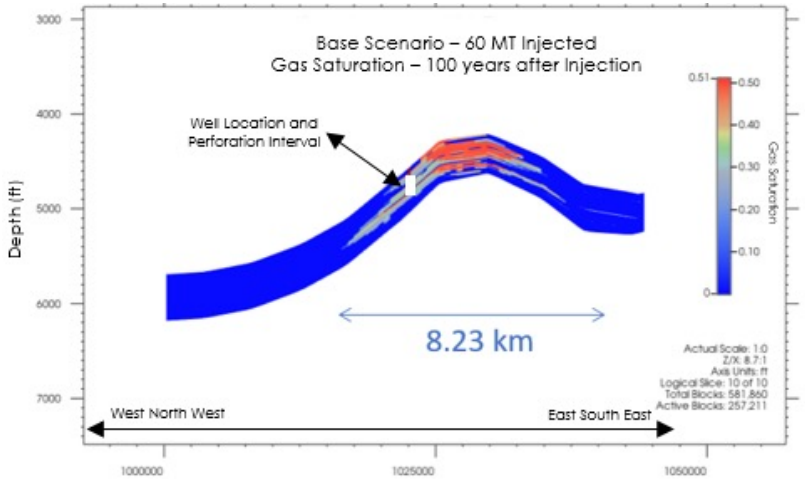

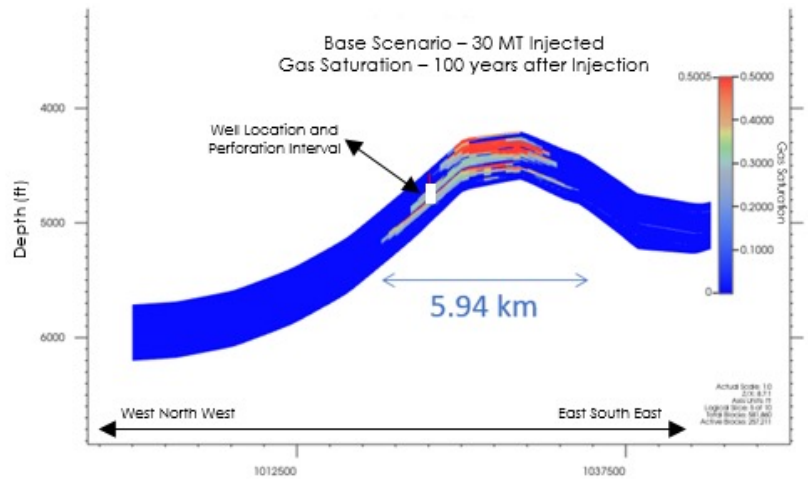

Syncline Scenario

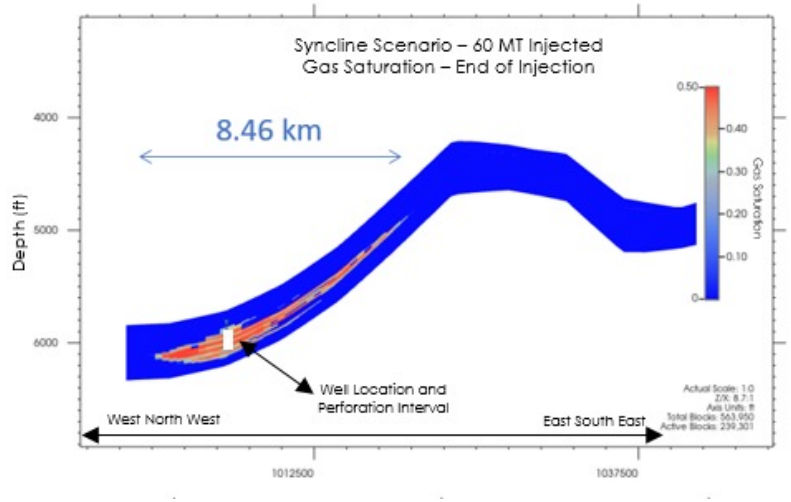

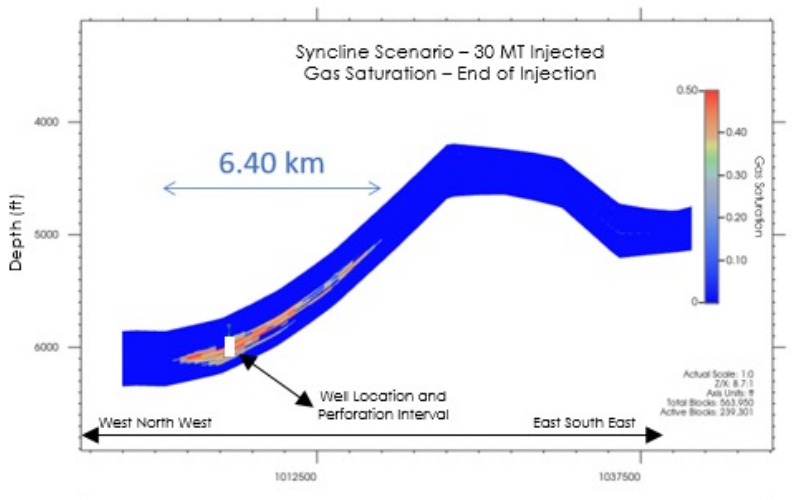

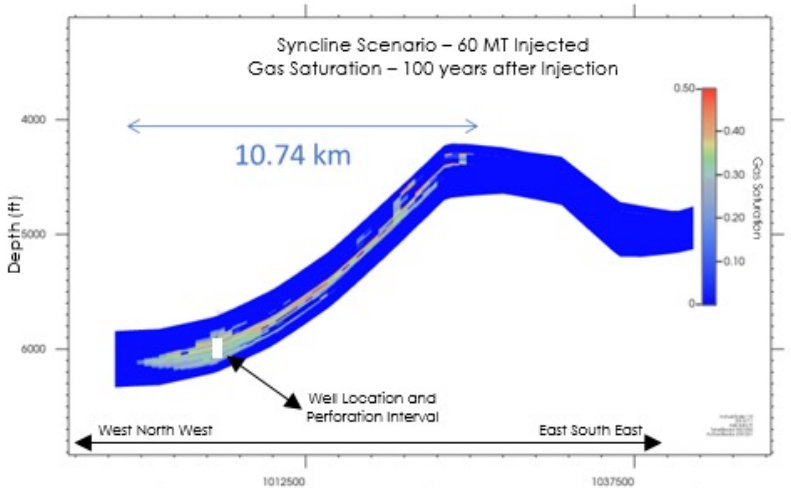

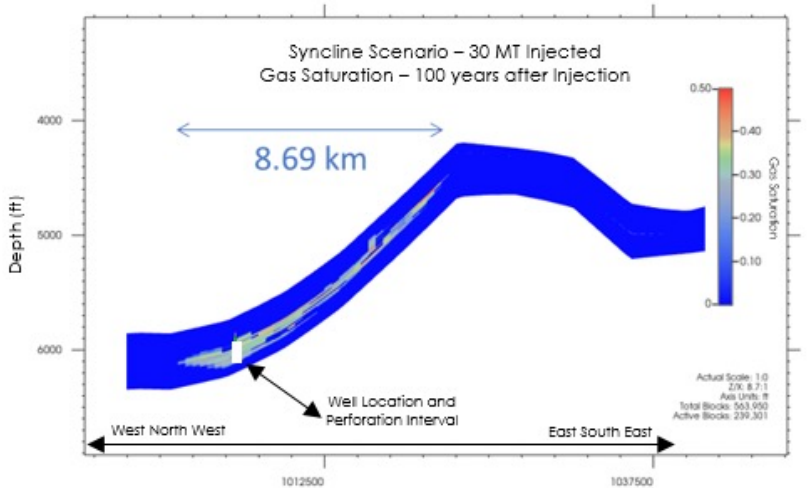

GCCC GULF COAST CARBON CENTER
BUREAU OF ECONOMIC GEOLOGY
TEXAS Geosciences
The University of Texas at Austin
Jackson School of Geosciences
ENERGY AND EARTH RESOURCES GRADUATE PROGRAM
multidisciplinary studies for interdisciplinary solutions

Plume Shape After 30 Years of Continuous Injection

Base Scenario

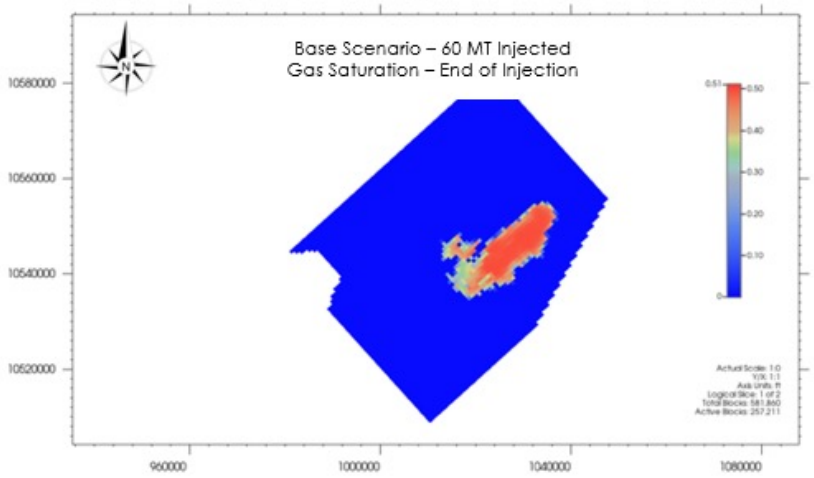

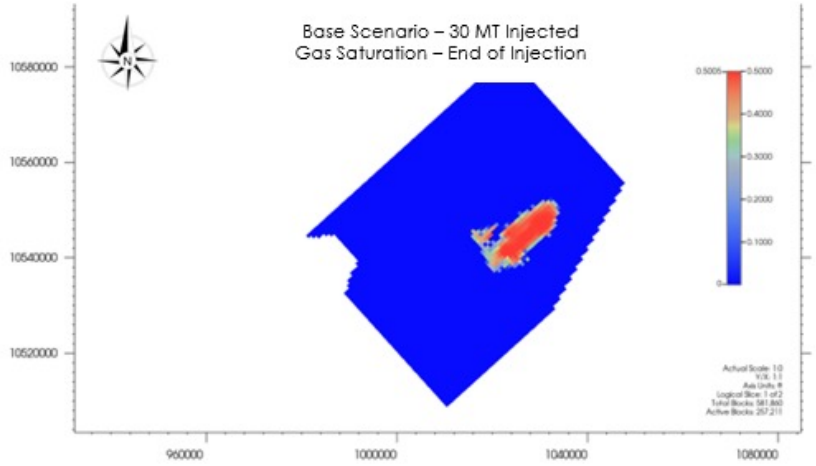

Syncline Scenario

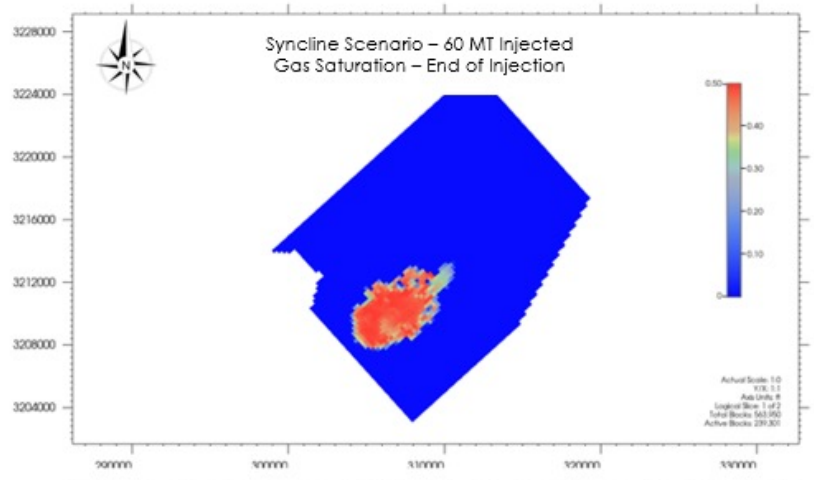

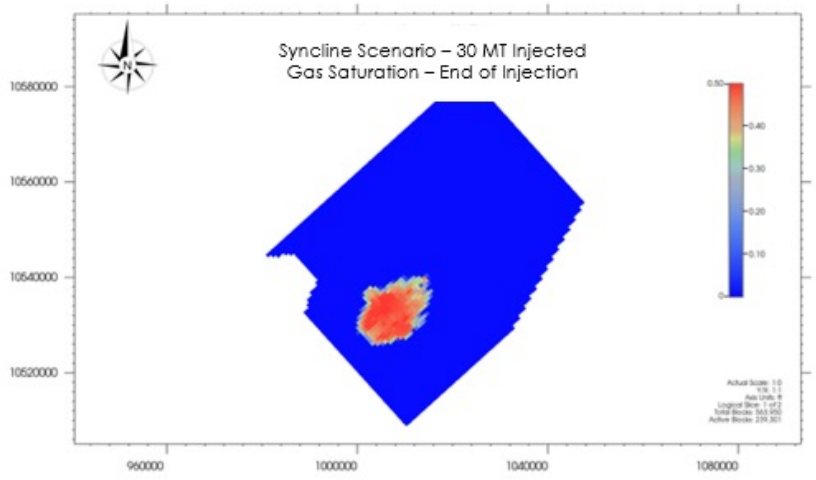

GCCC GULF COAST CARBON CENTER
BUREAU OF ECONOMIC GEOLOGY
TEXAS Geosciences
The University of Texas at Austin
Jackson School of Geosciences
ENERGY AND EARTH RESOURCES GRADUATE PROGRAM
multidisciplinary studies for interdisciplinary solutions

Plume Shape 100 Years After Injection Stops

Base Scenario

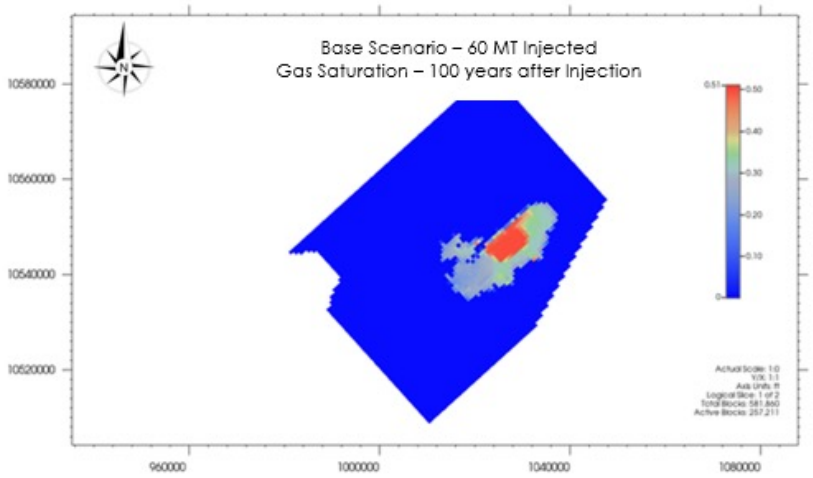

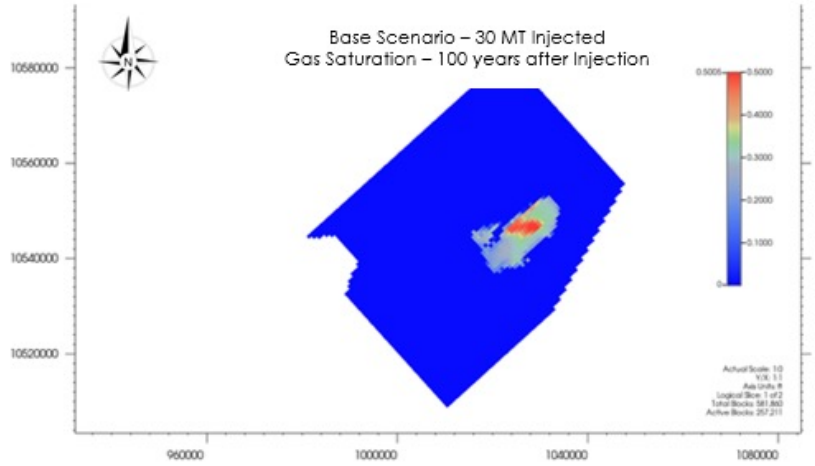

Syncline Scenario

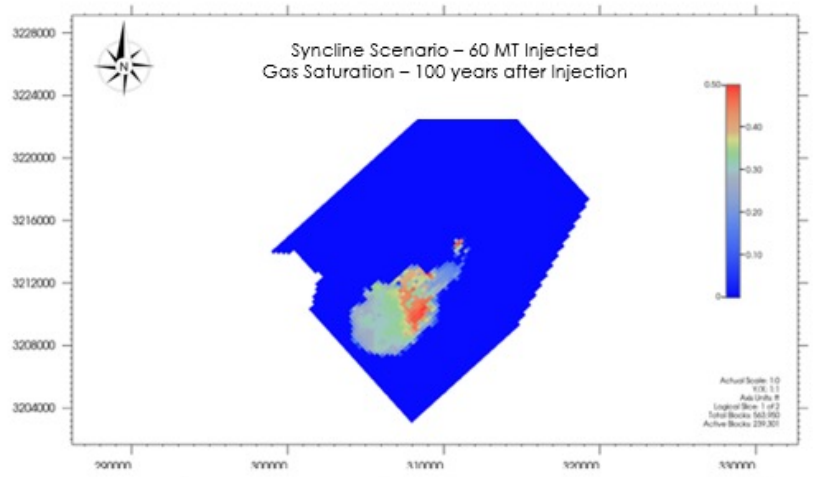

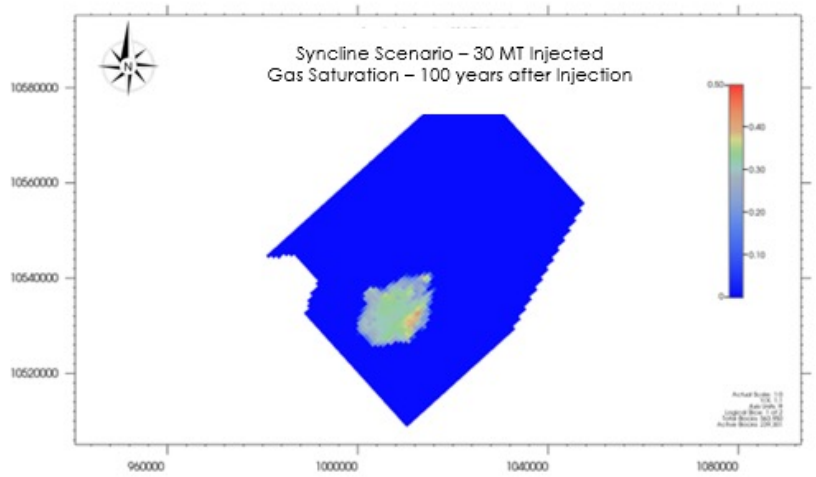

Syncline or Base Case? Let the numbers help you decide…

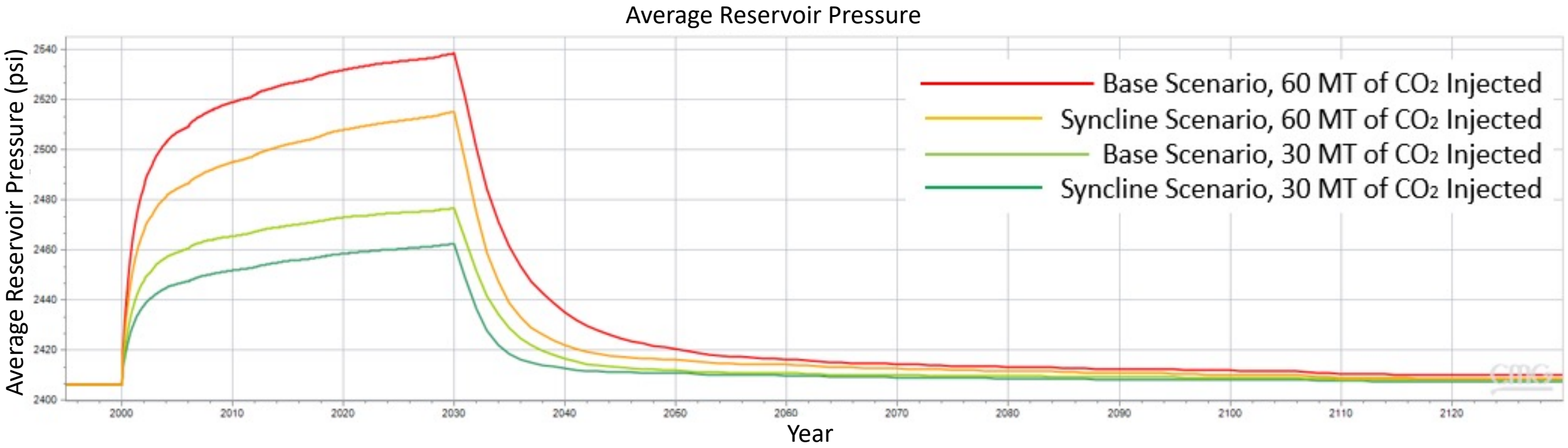

Case	Time of pressure to 2410 psi	Maximum up-dip migration distance	Maximum area contacted by CO_2	Storage/Acreage ratio (million tons/km²)
Syncline scenario – 60 MT	58 years	10.74 km	67.73 km²	0.88
Syncline scenario – 30 MT	20 years	8.69 km	44.84 km²	0.67
Base scenario – 60 MT	77 years	8.23 km	50.27 km²	1.19
Base scenario – 30 MT	25 years	5.94 km	26.81 km²	1.12

What about placing more wells?

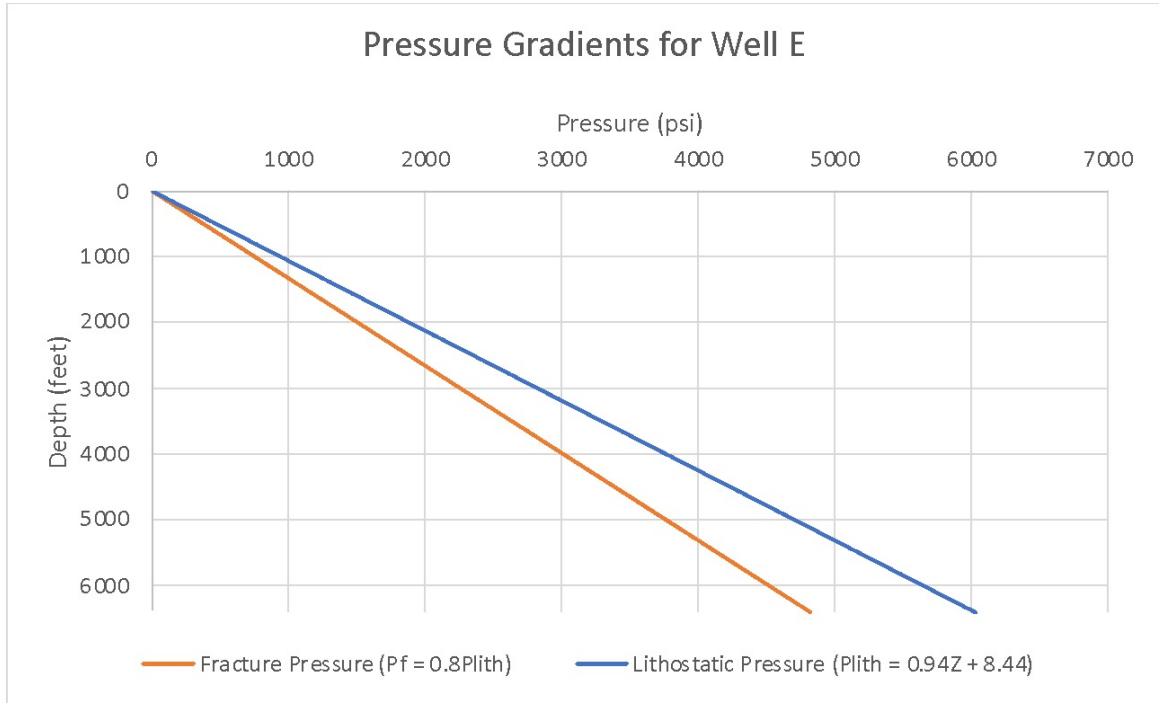

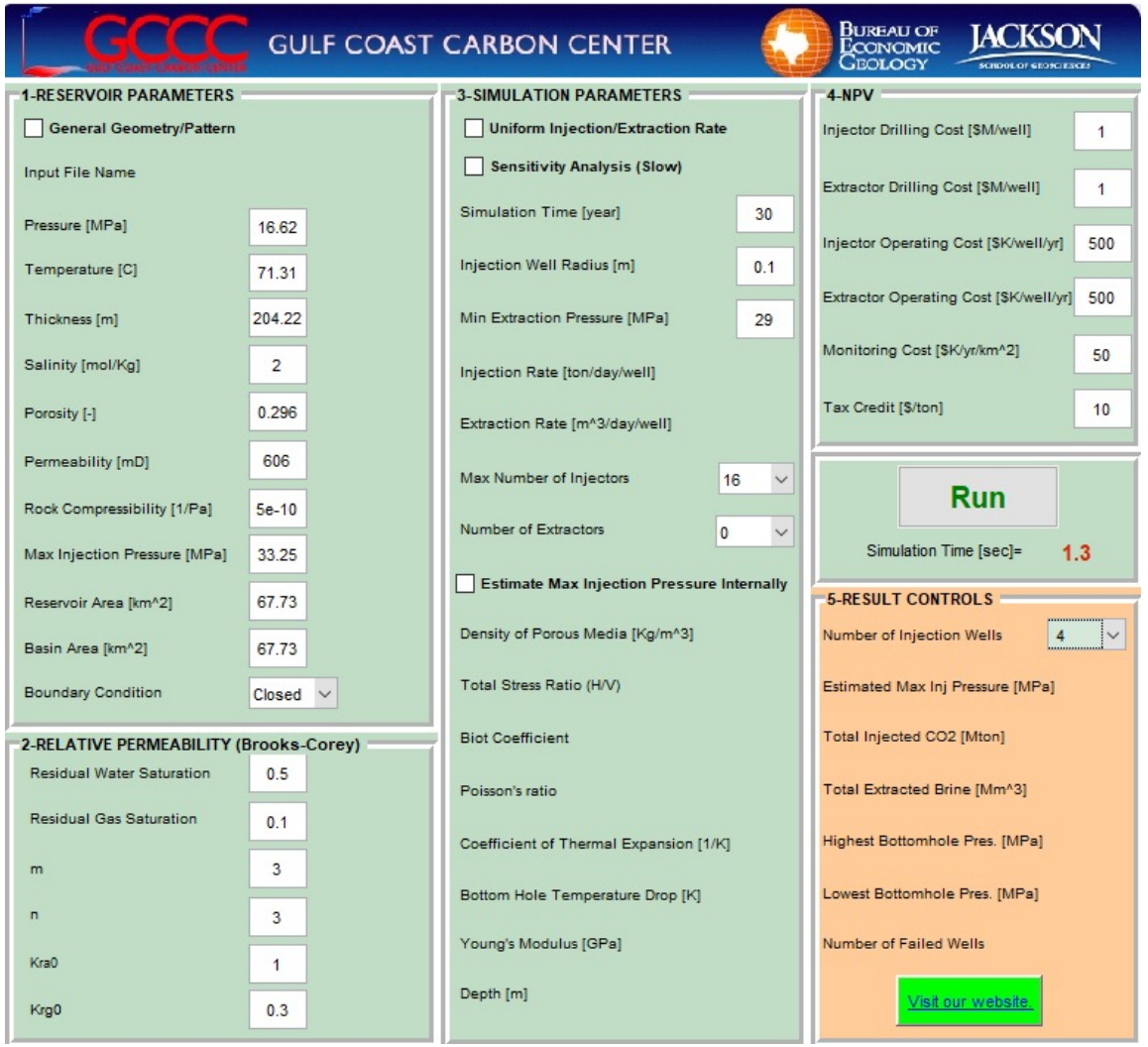

More Wells = Less Injectivity

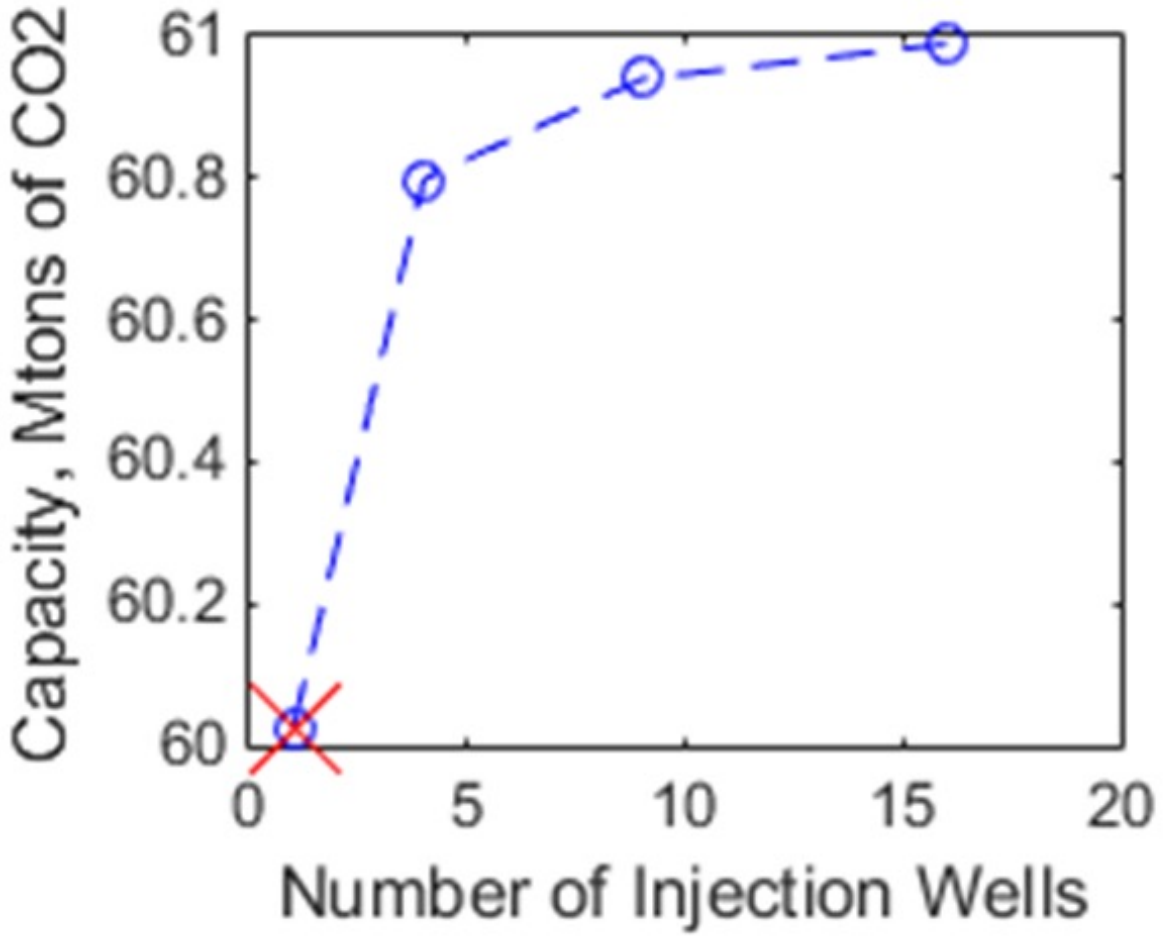

Policy Recommendations

1. Consider the acreage leasing timeline in light of the plume stabilization timeline.

2. Value the acreage differently according to either the stratigraphical heterogeneity or the type of the structural closure.

3. Limit the number of wells for CO_2 storage project operating in one elevated pressure area.

TEXAS Geosciences
The University of Texas at Austin
Jackson School of Geosciences

GCCC
GULF COAST CARBON CENTER

Partnership for carbon capture & offshore geologic storage
GoMCarb

Bureau of Economic Geology

DEPARTMENT OF ENERGY · UNITED STATES OF AMERICA ·

Acknowledgement

Dr. Susan Hovorka

Dr. David Spence

Dr. Seyyed Hosseini

Dr. Alex Bump

ENERGY AND EARTH RESOURCES GRADUATE PROGRAM
multidisciplinary studies for interdisciplinary solutions

Appendix D

Trimeric Well Assessment Memo - 25 March 2022

TRIMERIC CORPORATION

P.O. Box 826
Buda, TX 78610

TO: Ramon Trevino, Susan Hovorka, Tip Meckel, Alex Bump – UT BEG

FROM: Katherine Dombrowski, Darshan Sachde – Trimeric Corporation

DATE: 25 March 2022

SUBJECT: **Existing Well Re-use Assessment for CO_2 Injection for GoMCarb, rev 0**

1 Introduction

The University of Texas at Austin's Bureau of Economic Geology (BEG) is leading the project "Offshore Gulf of Mexico Partnership for Carbon Storage – Resources and Technology Development GOMCarb" under U.S. Department of Energy award DE-FE0031558. Trimeric is a project team member of GoMCarb. The primary objective of the project is to develop an Offshore Carbon Storage Partnership focused on offshore (sub-seafloor) geologic storage in the Gulf of Mexico (GoM). The Partnership combines the capabilities and experience of industry, academia, and government to develop and validate key technologies and best practices to ensure safe, long-term, economically viable carbon storage in offshore environments.

A key component of Trimeric's scope falls under Task 5 – Infrastructure, Operations and Permitting[1]. For Subtask 5.1 – CO_2 Transport and Delivery, the objective is to assess CO_2 transport and delivery options in the GoM. This subtask includes an assessment of the potential to reuse existing oil and gas infrastructure (e.g., pipelines, platforms, and wells) for CO_2 transport and delivery and to identify how this assessment may impact CO_2 storage project development in the GoM. This memorandum will summarize the progress of re-use assessment for existing wells in the GoM.

The structure of this memorandum is as follows (each section heading is hyperlinked for easy navigation):

> **2. Overview of Methodology.** This section describes the use of analog sites HI-10L and HI-24L as the basis for this well assessment study.

[1] Please refer to the Statement of Project Objectives (SOPO) document for details on the full GoMCarb project scope including Task 5.

3. Well Data Sources for this Memorandum. This section describes the types of data obtained from the Railroad Commission's GIS Viewer and from Subscription Databases available to the University of Texas.

4. Wellbore Status. This section explains the wellbore categorizations used by the Railroad Commission, how Trimeric used these data to assign wellbore status, and how wellbore status may affect re-use of wells for CO_2 injection.

5. Well Screening Parameters. This section summarizes the types of well characterization data available from the databases and proposes a methodology for using those data to make preliminary assessments of well re-use potential.

6. Analysis of RRC Data for HI-10L and HI-24L. This section presents the well data gathered for HI-10L and HI-24L and explains the process and effort required to reconcile information between the RRC GIS Viewer and the Subscription Databases.

7. Well Workflow. This section proposes a preliminary workflow to repurpose the well and address integrity of neighboring wells if viable well candidates are identified for repurposing for CO_2 injection.

8. Conclusions

9. Recommendations for Future Investigation

10. Appendix – Well Identification Primer

11. Appendix – Well Queries via RRC Database

12. Appendix – Example Images and Reports

2 Overview of Methodology

The broad approach applied for the well re-use assessment can be summarized as follows:

- Identify well data sources for federal and state waters within the GoMCarb project region
- Develop screening parameters to assess suitability for re-use and to assess well integrity risks. These parameters provide a high-level view of the scale of the opportunity/risk for developing CO_2 storage in a field with existing wells.
- Apply screening criteria to wells in identified analog sites for this project.

To facilitate a more detailed evaluation of specific well re-use candidates, an "analog site" for a CO_2 storage project was utilized. The GoMCarb project team agreed that the High Island Block

10-L[2] (HI-10L) in Texas state waters would serve as the analog site for this study. The HI-10L site is generically representative of locations in the GoM region that would be attractive for capture and storage projects (favorable geology based on initial data, shallow water region, proximity to a high density of CO_2 sources). The analog site provides the requisite specific characteristics and information about a storage site to facilitate a more detailed evaluation of infrastructure while maintaining some generality to allow extrapolation of findings and conclusions across the GoMCarb region. The wells in HI-10L are not active for oil and gas production, so the project team later added High Island Block 24-L (HI-24L) as another "analog site" to include active wells in the study. Active wells were more likely to be newer and have more data available. For this project, searches were performed within these pre-defined blocks; however, these blocks do not correspond to the confines of any single reservoir (i.e., the proposed geological storage field in which HI-10L is located extends beyond HI-10L). The purpose of searching by block was to facilitate data queries that illustrate the type of information that can be obtained for offshore wells.

The following sections in the memorandum summarize the results of the evaluation alongside additional details regarding the methodology.

3 Well Data Sources for this Memorandum

Trimeric initially screened wells in Texas state waters of the Gulf of Mexico by working with well information obtained online from the Texas Railroad Commission (RRC), including a Geographic Information System (GIS) map of oil and gas assets and queries of RRC's databases for these assets. The RRC Oil and Gas Data Queries can be accessed from the following website:

https://www.rrc.state.tx.us/resource-center/research/research-queries/

The Public GIS Viewer can be accessed from the following website:

https://www.rrc.state.tx.us/resource-center/research/gis-viewer/

According to the RRC's website, oil and gas well records for all RRC districts are available for the period 1964 to the present through the Oil and Gas Imaged Records Query[3], as well as through the Public GIS Viewer and the RRC's Oil and Gas Data Queries. Oil and gas records

[2] "Blocks" refer to state-owned and defined offshore/ submerged land tracts. The tracts can be viewed via the Texas Railroad Commission website (https://gis.rrc.texas.gov/GISViewer/) or the Texas General Land Office Website (https://gisweb.glo.texas.gov/glomapjs/index.html

[3] https://www.rrc.state.tx.us/resource-center/research/research-queries/imaged-records/imaged-records-menu/

prior to 1981 are also available on microformat (microfilm, microfiche, unit jackets). The contents of RRC's records include:

- Application to Drill (W-1 and location plat). Applications to Drill submitted to the Commission after May 2005 are in electronic format only and available through the Drilling Permit (Form W-1) Application Query,
- Gas/oil completion reports (G-1/W-2 and attachments),
- Plugging reports (W-3 and attachments),
- P-4's (Producer's Transportation Authority), and
- Miscellaneous (correspondence, back pressure curve, dual completion packets, directional survey, etc.).

Some of these reports are described in Section 11 Appendix – Well Queries via RRC Database and examples are provided in Section 12 Appendix – Example Images and Reports.

Information from the RRC was supplemented with well information from the commercial databases subscribed to by the UT BEG (heretofore referred to as the Subscription Databases for this memorandum). These Subscription Databases included:

- IHS Enerdeq – This subscription database allows for ready access to Scout tickets. Scout tickets are files that summarize the information available on a single well that the operator is willing to share with the public.
- IHS Petra – This subscription database has information for wells in both state and federal waters and allows for users to add their own information to the well records.
- Lexco OWL7 – This subscription database is specific to the Gulf of Mexico; it is populated with information from the Bureau of Ocean Energy Management (BOEM) and Bureau of Safety and Environmental Enforcement (BSEE); therefore, its focus is on federal asset information.

For this evaluation, wells were tracked by primarily API number. An API number is an industry standard established by the American Petroleum Institute. The API is a unique, permanent, 10-digit identifier assigned to each well drilled for oil and gas in the United States. The first two digits are the state code (42 for Texas), the next three digits are the county code (708 for High Island Large Block), and the last five digits form the unique number assigned to identify the wellbore within the county. Section 6.1 provides more detailed information about the locations of HI-10L and HI-24L within Texas's state waters. Texas assigns a unique 10-digit API number for each surface location. All wellbores originating from a single surface location share the same 10-digit API number; therefore, a single 10-digit API number could represent one wellbore or multiple wellbores. The RRC uses the "Well Number" field to track multiple wellbores

associated with a single API number; however, some RRC reports output API numbers without the additional well number field which complicates the assessment of well assets.

Wells were also tracked via the US Well Number (UWI), where available. In 2010, the API transferred custody of well numbering to the Professional Petroleum Data Management (PPDM) Association.[4,5] The PPDM transitioned the well numbering scheme to a 12-digit UWI, which is a revision of the API Well Number. The 12-digit code allows for tracking of individual wellbores associated with a single surface location. To maintain the integrity of well information, the first ten digits of the UWI code correspond to the API number, where possible. The 11th and 12th digits refer to the wellbore code. Adding a 13th and 14th digit to the UWI is optional; there is no official standard for the use of these digits. Some states use 12-digit schemes or 14-digit numbering schemes. Texas continues to use a 10-digit code to capture all wellbores (i.e., no ability to distinguish between wellbores via the Texas identification number). The well data stored by the RRC is based on a 10-digit code, while the well data from the Subscription Databases is based on a 14-digit code.

4 Wellbore Status

For the purposes of this memo, Trimeric attempted to follow the wellbore categorization used by the RRC. The RRC categorizes wells based on their physical status and compliance with regulatory reporting requirements. First, RRC categorizes wells into one of three categories: active, plugged, and inactive wells. Each of these categories has subcategorizations, as shown in Figure 1 and described in the subsection below.

[4] PPDM, Well Identification United States, 2014.

[5] PPDM, US State by State Comparison of Unique Well Identification (UWI) Practices, 2015.

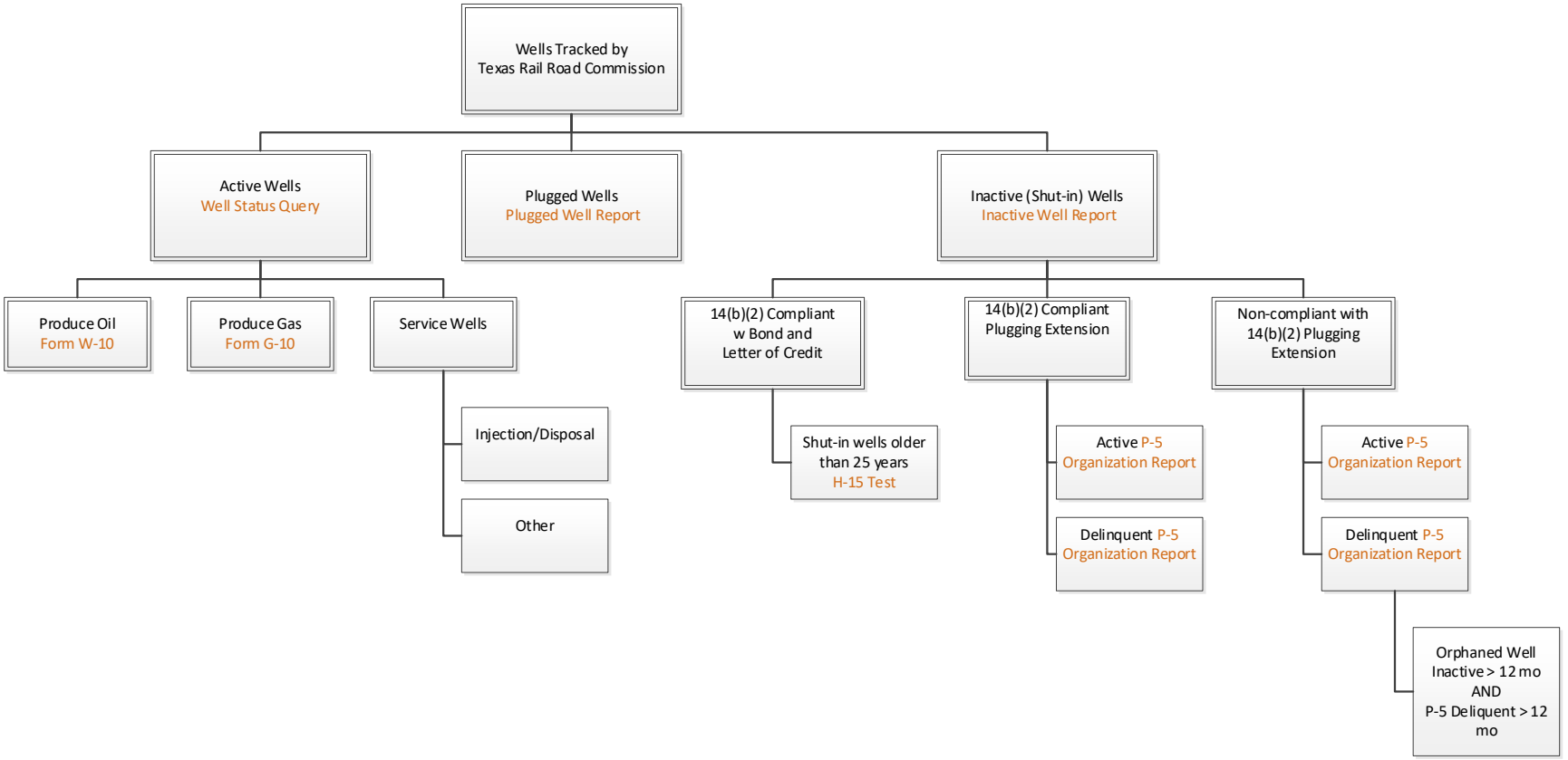

Figure 1. Well Categories used by Texas Railroad Commission (with Associated Reports shown in Orange Text).

4.1 Overview of Texas RRC Wellbore Status Categorization

There are three broad categories of wellbore status tracked by the RRC, each with multiple sub-categories, which then determines the testing and documentation that operators must file with RRC. The three broad categories of **wellbore status** are as follows (see also Figure 1):

- **Active wells:** Active wells are currently producing oil and/or gas or are service wells used for injection or disposal. Oil wells file form W-10, and gas wells file form G-10 on an annual basis.
- **Plugged wells:** Plugged wells have been plugged at strategic locations along the well depth with concrete and/or mechanical bridge plugs. Wells are plugged at end of service life to prevent a pathway for migration of fluids from the hydrocarbon bearing zones to formations with usable water or to surface waters. Plugged well reports (W-3 form) are available via the RRC.
    - **Dry holes** are wells that were drilled but did not produce hydrocarbons. In the GIS Viewer Glossary,[6] RRC defines a dry hole as "a plugged well that never produced oil or gas".[7]
- **Inactive wells:** An inactive well (or shut-in well) is an unplugged well that has been spudded (i.e., well drilling process was started by removing sedimentary material with a drill bit) or has been equipped with cemented casing and that has no reported production or other permitted activity for a period of greater than 12 months. Operators of inactive wells must either restore the well to active operation, plug the well, or obtain RRC approval for a Section 14(b)(2) extension of deadline for plugging.[8] For unplugged wells more than 25 years old, the RRC requires an annual fluid level or hydraulic pressure test for the well via the RRC's H-15 program.[9]

---

[6] https://gis.rrc.texas.gov/GISViewer/GISViewer/docs/publicVeiwerGlossary.pdf

[7] Section 3.14 Plugging of the Texas Administrative Code Title 16, Part 1 indicates that plugging operations for dry holes should commence within one year after drilling ceases, unless a plugging extension is granted. If the plugging extension is granted for a dry well, it is typically classified by RRC as an inactive (or shut-in) well (from site: https://www.law.cornell.edu/regulations/texas/16-Tex-Admin-Code-3-14.) Therefore, it appears that wells listed as "dry holes" in the GIS Viewer are plugged wells; however, outside of the GIS Viewer, the use of the term dry hole does not necessarily imply a plugged well.

[8] To be a 14(b)(2)-compliant well, the plugging extension must be renewed each year. Extensions may be granted by RRC if the operator has a current P-5 Organization Report, the operator has the right to operate the well, and the well is in compliance with RRC rules.

[9] https://rrc.texas.gov/oil-and-gas/compliance-enforcement/h-15-program/

- Inactive wells may be **compliant** or **non-compliant** with respect to Section 14(b)(2) plugging extension.
- **Orphaned wells** are inactive, non-compliant wells that have been inactive a minimum of 12 months and the responsible operator's Organizational Report (P-5) has been delinquent for greater than 12 months.

4.2 Assignment of Wellbore Status Designations and Associated Uncertainties

Trimeric compiled wellbore status statistics for HI-10L and HI-24L for the purpose of illustrating the relative number of wells that are plugged, open, etc. within each leasing block. The compilation of wellbore status statistics was not straightforward, due to inconsistencies in the wells that appeared in the two datasets (as described in Section 6.3) and also due to uncertainties in the reported wellbore status data (as described below). Therefore, the wellbore status categorization statistics presented in this memo should be treated as approximate values and used only for the purposes of evaluating broad trends.

Both the RRC GIS Viewer and UT's Subscription Databases contained various indicators of wellbore status. The RRC GIS database included a field for "wellbore status" that was populated as either PLUG, DRY, OPEN, or was BLANK.

- When the wellbore status was PLUG, the RRC GIS database typically gave a plugging date. This plugging date typically corresponded to the "abandonment date" in the Subscription Database. When wellbore status was PLUG, there was also typically a plugging report in the Subscription Database. The presence of a plugging report in the Subscription Databases was not necessarily evidence of a plugged well; it sometimes was associated with a partially plugged well (as noted in the 'Well Type' or 'Type Well' field in the GIS tool[10]) with no "abandonment date" provided in the Subscription Database.
- When the wellbore status was DRY, this appeared to be an indication of a plugged well. The GIS feature type was also often also listed as 'Dry Hole', which the RRC GIS tool defined as being plugged.[11] For HI-10L, the twelve wells with DRY wellbore status in GIS also had a plugging report in the Subscription Database corroborating a plugged status. For HI-24L, UT could not find plugging reports in the Subscription Database for

[10] The data downloaded from the RRC GIS database includes a "Well_Type" field; sometimes, this field is called "Type_Well" in other GIS reports. Examples of data entered into this "Well Type" or "Type_Well" field include: history, partial plug, no production, producing, temp abandoned, shut in, shut-in-multi-compl, not eligible for allowable. For some wells, this field is blank.

[11] While the RRC GIS tool defines a dry hole as being plugged, the term dry hole does not necessarily imply a plugged well when used more colloquially in text of other RRC reports. For example, in the RRC's Well Plugging Primer, the term dry hole is used in the context of a well that has not produced but may not yet be plugged.

the three wells in GIS with DRY wellbore status; these three wells were older wells for which no ten-digit API number had been assigned in GIS.

- When wellbore status was OPEN, there were several different corresponding 'Type Well' status that could appear in the RRC GIS record:
    - If the 'Type Well' indicated PRODUCING, Trimeric classified the well as an active and producing well for the purpose of this analysis.
    - Sometimes 'Type Well' indicated NO PRODUCTION or TEMP ABANDONED. Wells with either of these classifications could also be classified as ORPHAN and appeared on the RRC's Orphaned Well report. These wells were not orphaned if well had only stopped producing in the last year.
- When the wellbore status was BLANK, there was often no information about the well in RRC GIS, and it often did not have an assigned API number. When the wellbore could be matched to the Subscription Databases, Trimeric used that additional information to classify the wellbore. When the GIS feature type in the viewer was listed as "Dry Hole", but the wellbore status was blank, Trimeric classified the well as plugged, in accordance with the definition of a dry hole in the GIS Viewer glossary.
- For a few wells, Trimeric was unable to interpret the wellbore status from the available data, so Trimeric classified the wellbore status as UKNOWN.

While the RRC uses a defined set of wellbore status categorizations (i.e., open, plugged) in its databases, additional terms that further indicate well status (e.g., shut-in, abandoned, dry, unplugged, dry hole) are also used by the RRC in its publications and within its database records and within the oil and gas industry. Trimeric has observed that these terms are sometimes not used consistently across and within organizations. For example, the use of the term "abandon" or "abandoned" is often inconsistently applied. The term "**abandoned**" is used throughout RRC's Well Plugging Primer[12]; while never formally defined in the document, the term's use suggests that abandoned wells are non-compliant with Section 14(b)(2) and may require plugging by RRC. However, the use of the term "abandon" elsewhere in the industry may have a different connotation. For example, in Schlumberger's Oilfield Glossary[13], the term "plug and abandon" is defined as "to prepare a well to be closed permanently, usually after either logs determine there is insufficient hydrocarbon potential to complete the well, or after production operations have drained the reservoir." Likewise, in interviewing oil and gas industry experts, the term abandoned was used to indicate a plugged well. And in the Subscription Databases, when a well is properly plugged, it has a listed "Abandonment Date". Similarly, Trimeric has observed

[12] "Well Plugging Primer", Published by Well Plugging Section, Oil and Gas Division, Texas Railroad Commission, January 2000.

[13] https://glossary.oilfield.slb.com/

inconsistent application of the term dry hole; the formal definition by RRC indicates a plugged dry hole, while the colloquial use does not necessarily imply the dry hole has been plugged. Therefore, the user may want to seek additional clarification of these wellbore status terms when encountered outside of the RRC database.

4.3 Assessment of Well Status Categories for Reuse in CO_2 Injection and/or Potential CO_2 Leak Risk

Existing wells pose a potential benefit as well as a possible risk to the establishment of an offshore CO_2 storage facility in the shallow waters of the Gulf of Mexico. These wells may have the potential for reuse as the well infrastructure for CO_2 injection; however, neighboring existing wells that are not used for injection could also pose a potential CO_2 leak risk if they are not properly plugged. This section explores the potential to assess reuse and risk using the well status categories available in the GIS database. The discussion in this memorandum is limited to the type of data available within the GIS database and is given in relative comparison terms (older versus newer; plugged versus active, etc.). The discussions in this memorandum does not represent a technical feasibility assessment of well reuse and leakage risks, which is beyond the scope of this work.

Active wells are potential candidates for CO_2 storage via enhanced oil recovery, and/or are future targets for re-purposing for CO_2 injection into a CO_2 storage reservoir (which may or may not be a depleted hydrocarbon reservoir). As the production rate of an active well slows down and revenues decrease, the producer may choose to convert the well to inactive status or to plug the well. From an economic perspective, it would be advantageous economically to transition end-of-life active wells to CO_2 injection to avoid plugging costs. Well records may be more complete and well condition may be better known for these end-of-life active wells than for ones that have sat inactive for some time, and perhaps have changed ownership as the economic viability of the field has waned.

Plugged wells are potential candidates for nearer-term CO_2 storage projects. Plugged wells are reused in onshore projects; the cap is cut off and the concrete plugs are drilled out of the wellbore. Oftentimes the casing is removed from the well during the plugging process. According to Trimeric's interviews with industry experts, re-tapping a plugged well on-shore carries project risk, but it does occur in practice. The risk is larger for re-tapping a plugged well offshore due to the increased expense of working offshore. Trimeric reviewed one report [IEAGHG 2018] that states that "an oil or gas well that has been plugged and abandoned will not be reusable"; however, no reasoning for the assertion was provided. Regardless of whether any individual well can practically be reused for CO_2 injection, it is still important to understand the design and history of the wells within the targeted CO_2 reservoir, as any well within the reservoir poses a potential leak risk.

Plugged wells within a reservoir field pose a potential CO_2 leak risk; the construction materials and well abandonment procedures may not have considered the presence of high concentrations of CO_2. These wells may be susceptible to casing string corrosion and cement plug corrosion.[14] Plugged wells in Texas state waters must follow RRC regulations for the plugging process and should have plugging records available in RRC files. The RRC's W-3 Plugging Record includes information on the amount, type, and location of cement plugs, whether non-drillable material (other than casing) was left in the well and the depth of this material, the casing and tubing record after plugging, the open hole and perforated intervals, whether the well was filled with mud-laden fluid per RRC regulations and the method for applying the mud, and the name and address of the service company that mixed and pumped cement into the well. Plugging reports (form W-3) remain in suspense files; suspense files dated 2000 through present are available in an online imaged records query; suspense files from previous years are on microfilm.[15]

Inactive wells are also potential candidates for nearer-term CO_2 storage projects; however, the uncertainty associated with well integrity increases the longer the well has been inactive. Wells are taken out of service when they are not economic to operate; inactive wells may change ownership multiple times, increasing the potential to lose valuable well information. Inactive wells within the targeted CO_2 reservoir will need to be plugged to close CO_2 leakage pathways.

Orphaned wells, i.e., inactive wells that are non-compliant with their 14(b)(2) plugging extension and are non-compliant with their P-5 Organization Report, may be the riskiest candidates within the CO_2 field. The RRC plugs orphaned wells that pose the highest risks to the integrity of ground and surface waters, at an average cost of $200,000 per offshore well (as reported in the year 2000).[16] The RRC also reports the yearly average per-foot cost for the RRC to plug wells, on a district-by-district basis for 2010 through 2020.[17] District 3 includes the onshore counties around Houston as well as the offshore areas including the High Island Block; the RRC reported value changes significantly from year to year, from $12.13/ft (in FY2013) to $5.22 (in FY2017) back up to $13.93/ft for FY2020.

The uncertainty and cost for RRC to plug 14(b)(2) non-compliant, inactive wells is likely higher than what a typical operator would face when plugging a 14(b)(2) compliant well. The higher

[14] IEAGHG, "Re-Use of Oil & Gas Facilities for CO_2 Transport and Storage", 2018/06, July 2018.

[15] https://www.rrc.state.tx.us/oil-and-gas/research-and-statistics/obtaining-commission-records/oil-and-gas-well-records/

[16] Railroad Commission of Texas, Oil and Gas Division, Well Plugging Section. Well Plugging Primer, January 2000.

[17] https://rrc.texas.gov/oil-and-gas/compliance-enforcement/hb-2259-hb-3134-inactive-well-requirements/cost-calculation/

costs and uncertainty are due to the older age of the wells, insufficient data in the well records to reflect downhole operations, and the frequency with which operators dispose of "junk" down boreholes; this "junk" must be retrieved before plugging wells. For these reasons, RRC reports that the cost of plugging some non-compliant, inactive wells can be ten-fold the average cost. CO_2 reservoirs with orphaned wells will have higher cost uncertainty associated with plugging these wells to secure the reservoir against CO_2 leaks; as such, project budgets will need to include a higher set-aside to address this uncertainty.

5 Well Screening Parameters

Trimeric created a list of well parameters that could be used to preliminarily assess the potential to reuse oil and gas wells for CO_2 injection and to assess the risk/cost that existing wells may pose for CO_2 injection even if they are not re-used. These parameters are suggested based on Trimeric's own experience with CO_2 sequestration projects, Trimeric's interviews with subject matter experts on oil and gas wells, including in the Gulf of Mexico, and with experts on CO_2 injection into the subsurface, either for EOR or storage in saline aquifers, and Trimeric's review of literature.

The screening parameters were organized into three phases, with each subsequent phase representing more effort and/or cost to obtain and evaluate the screening data. The first pass criteria consist of data readily available from databases, including public ones such as housed at RRC and commercial databases that are offered to the public on a subscription basis (such as IHS Enerdeq, IHS Petra, Lexco OWL 7). By readily available data, we mean data that is readily output into digital files and tables and can be subjected to coarse screening criteria to possibly reduce the size of the dataset. The second pass criteria include information that are available in these databases but require additional research beyond top-line numbers or summary statistics to extract the needed information; an example would be data or information that can be found in permits filed with the RRC that requires searching individual permit documents to find the needed information. The third pass criteria may incur more significant acquisition costs because the data likely do not currently exist and will require significant expenditure to measure and/or obtain the data. The rationales for developing the criteria for each phase are discussed below.

These screening criteria represent key data that should be considered when evaluating a reservoir for development for CO_2 injection. In some cases, the criteria represent desired design features for the re-purposing of candidate wells for CO_2 injection. In other cases, the criteria point may provide an indication of the potential for increased costs to develop the reservoir for CO_2 injection, as the integrity of all wells within the injection field must be addressed even if they are

not re-used (i.e., these criteria represent the risk of the presence of the wells in the injection field).

First-pass screening criteria include:

- **Number of wells:** The greater the number of wells in a reservoir, the greater the risk of CO_2 leakage from the reservoir and the greater the upfront cost for ensuring the integrity of existing wells in the reservoir. This parameter may be useful in a relative ranking of potentially viable storage locations.
- **Construction/completion date**: At a minimum, a well re-used for CO_2 injection should be constructed after 1970 to ensure that "modern" well construction methods were used, which should reduce the risk of well integrity problems.[18] Also, older wells in the Gulf of Mexico will not be gravel packed; gravel packing is a practice to help prevent "sanding"[19] of wells. However, public records for a sanded well will just show a cessation of production without a reason, obscuring the potential risk of sanding to the well integrity.[20]
- **Casing diameter:** The casing diameter needs to be wide enough to accommodate the injection tubing string and to accommodate modern tools for well workovers.
- **Wellbore status:** The number of active, plugged, inactive wells with a valid 14(b)(2) extension for plugging, and orphaned wells should be evaluated. All wells, regardless of wellbore status or potential for re-use, will need their wellbore integrity assured; the amount of work involved to assure integrity may be in part a function of the wellbore status. Orphaned wells, which are unplugged, inactive wells with a lapsed 14(b)(2) extension and a lapsed organizational report for the operator, will be at higher risk of having well integrity issues and incomplete well records.
- **Total vertical depth:** The total vertical depth of the well should ideally reach the CO_2 injection zone of interest for re-use candidates. For wells that are not re-use candidates, but within the field, if the total vertical depth indicates they terminate within the CO_2 injection zone, it may represent an increased risk of leakage.

Second-pass screening criteria include:

- **Pressure test results:** Active production wells report stabilized shut-in wellhead pressure (SIWH) and flowing pressure on an annual basis. Disposal wells, fluid injection wells (used for enhanced oil recovery), and gas reservoir storage wells are required (per the Texas RRC) to undergo mechanical integrity tests to demonstrate the absence of

[18] Per 2019 conversation with oil and gas expert, JL.

[19] Sanding refers to the flow of sand with produced fluids (particularly water) from a well and the accumulation of sand in various components of the well. Sanding can lead to erosion and other failures of the well.

[20] Per 2019 conversation with oil and gas expert, JT.

significant leaks in tubing, packer, and casing.[21] These tests include an initial pressure test, an annual test as required by permit, and a five-year pressure test. Plugged wells are automatically excluded from testing. While databases such as IHS Petra have completion reports for most wells, pressure tests are much less available.

- **Cement type:** The cement type must be compatible with CO_2, both for well completion and well plugging. While the CO_2 itself may have very low moisture levels, the storage zone itself may have significant moisture. Therefore, some experts recommend that new wells used for CO_2 injection use CO_2-resistant cement across the whole injection zone.[22]
- **Reputation of organization completing the well and plugging:** Anecdotally, industry experts have indicated that the biggest factor is a well's suitability for reuse will be the quality of the organization completing the well and plugging the well (if well has been plugged and abandoned). CO_2 injection may increase reservoir pressure; when applied to a poorly plugged well, formation fluids may bypass the plugging materials and migrate uphole. According to the National Petroleum Council, most wells are plugged at the lowest cost possible to follow requirements of the regulating agency, as there is no return on investment for plugging activities.[23]
- **Ownership history:** A well with fewer transfers of ownership is more likely to have been operated by owners with sufficient resources to maintain the wells. According to RRC in the year 2000, bay wells have on average six transfers of ownership per well, and "this type of continued transfer of well can and often does result in RRC having to undertake plugging operations because the responsible operators don't have the financial resources to plug the wells".[24]

Third-pass screening criteria include:

- **Review of owner's well records**: If a project proceeds to a negotiation phase with the wells' owners, then the offer will likely be contingent upon review of the owner's well records. According to the experts consulted by Trimeric, these records should be reviewed thoroughly, as they will reveal information that is not available in public documents. For example, the owner's records are more likely to contain information

[21] https://www.rrc.texas.gov/oil-and-gas/publications-and-notices/manuals/injection-disposal-well-manual/summary-of-testing-requirements/general-testing-requirements/

[22] Sacuta, N. et al. "International Energy Agency (IEA) Greenhouse Gas (GHG) Weyburn-Midale CO_2 Monitoring and Storage Project." Final Technical Report for DE-FE0002697. 30 September 2015.

[23] National Petroleum Council, Technology Subgroup of the Operations and Environment Task Group. "Paper #2-25. Plugging and Abandonment of Oil and Gas Wells." Working Document of the NPC North American Resource Development Study, made available 15 September 2011.

[24] Railroad Commission Well Plugging Section. Well Plugging Primer. January 2000.

about problems encountered with a well and whether items were left behind in the well. However, even owner's records are not always complete on these accounts.

- **Well integrity testing:** After studying the owner's well records, the well integrity will need to be verified with testing and measurement. This is a costly operation, so it is only undertaken once the well has cleared all other screening criteria.

6 Analysis of RRC Data for HI-10L and HI-24L

6.1 Locations of HI-10L and HI-24L

The analog sites for this work are HI-10L and HI-24 in the High Island Block in Texas State Waters. The High Island Block is offshore from RRC District 03 (see map in Appendix 12.1), which encompasses the onshore counties around Houston, including the coastal counties of Jefferson, Chamber, Galveston, Brazoria, and Matagorda Counties. The High Island Small Block hugs the Texas coast and is completely within Texas state waters, while the High Island Large Block spans Texas state waters and federal waters; the green line running parallel to the Texas coast in Figure 2 marks the boundary between state and federal waters. The High Island Block is associated with API County Number 708.

The analog sites HI-10L and HI-24L are located within Texas state waters, as shown in Figure 3. Figure 4 shows the pipelines traversing HI-10L and HI-24L.

Figure 2. Map Showing Location of High Island Large Block Relative to the Texas Coast.

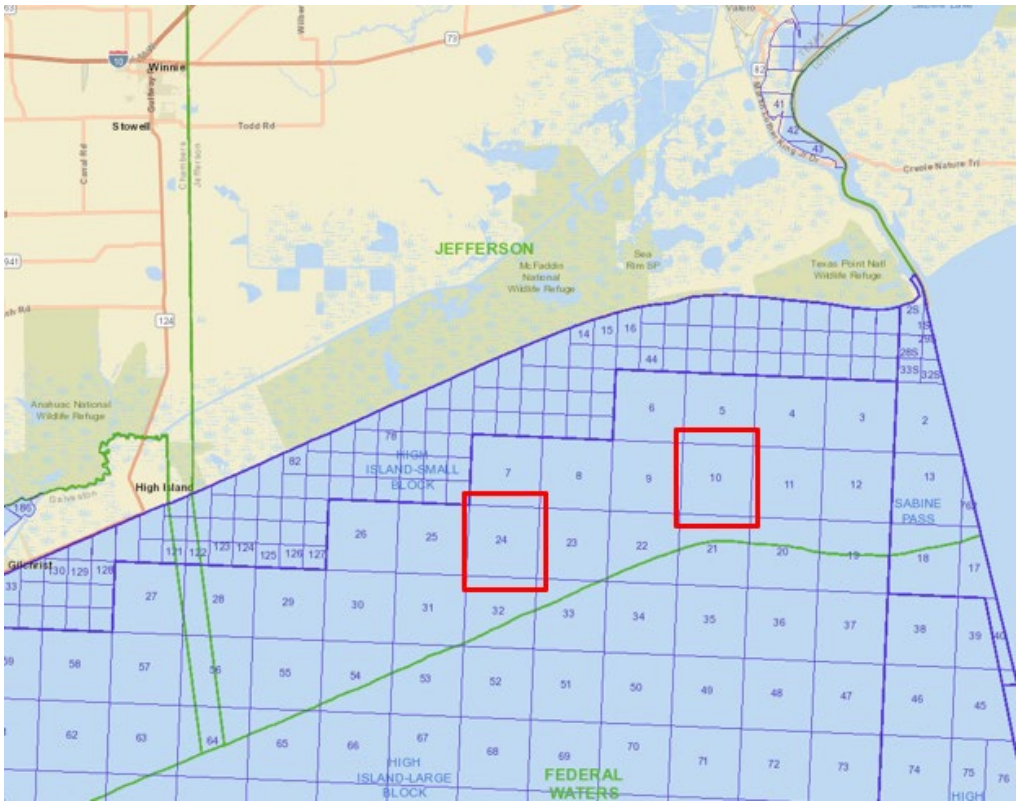

Figure 3. Locations of HI-10L and HI-24L within state waters of High Island Large Block.

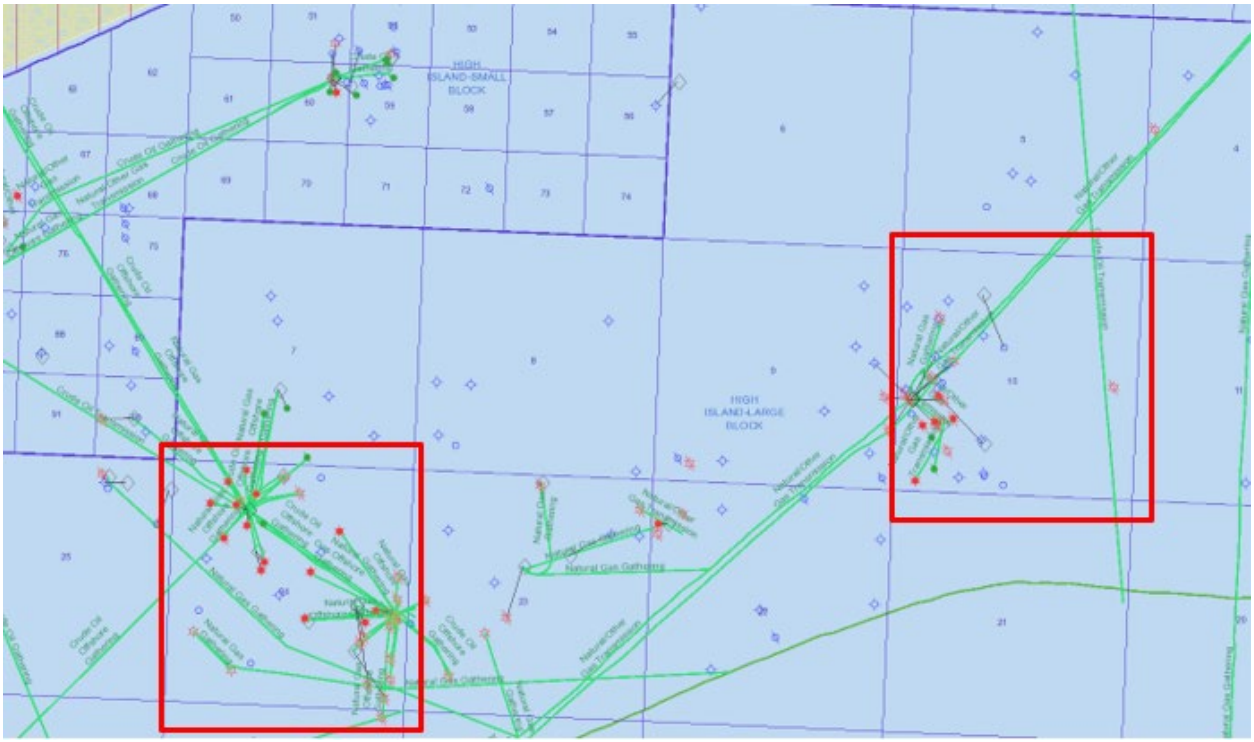

Figure 4. Map Showing Pipelines Crossing through HI-10L and HI-24L.

6.2 Well Features Identified with RRC GIS Tool

The RRC maintains a GIS mapping tool that can be used to identify well features. To see offshore features, the option for Offshore and Bay Tracts must be enabled within the Visibility menu. Figure 5 and Figure 6 show the well features in HI-10L and HI-24L, respectively.

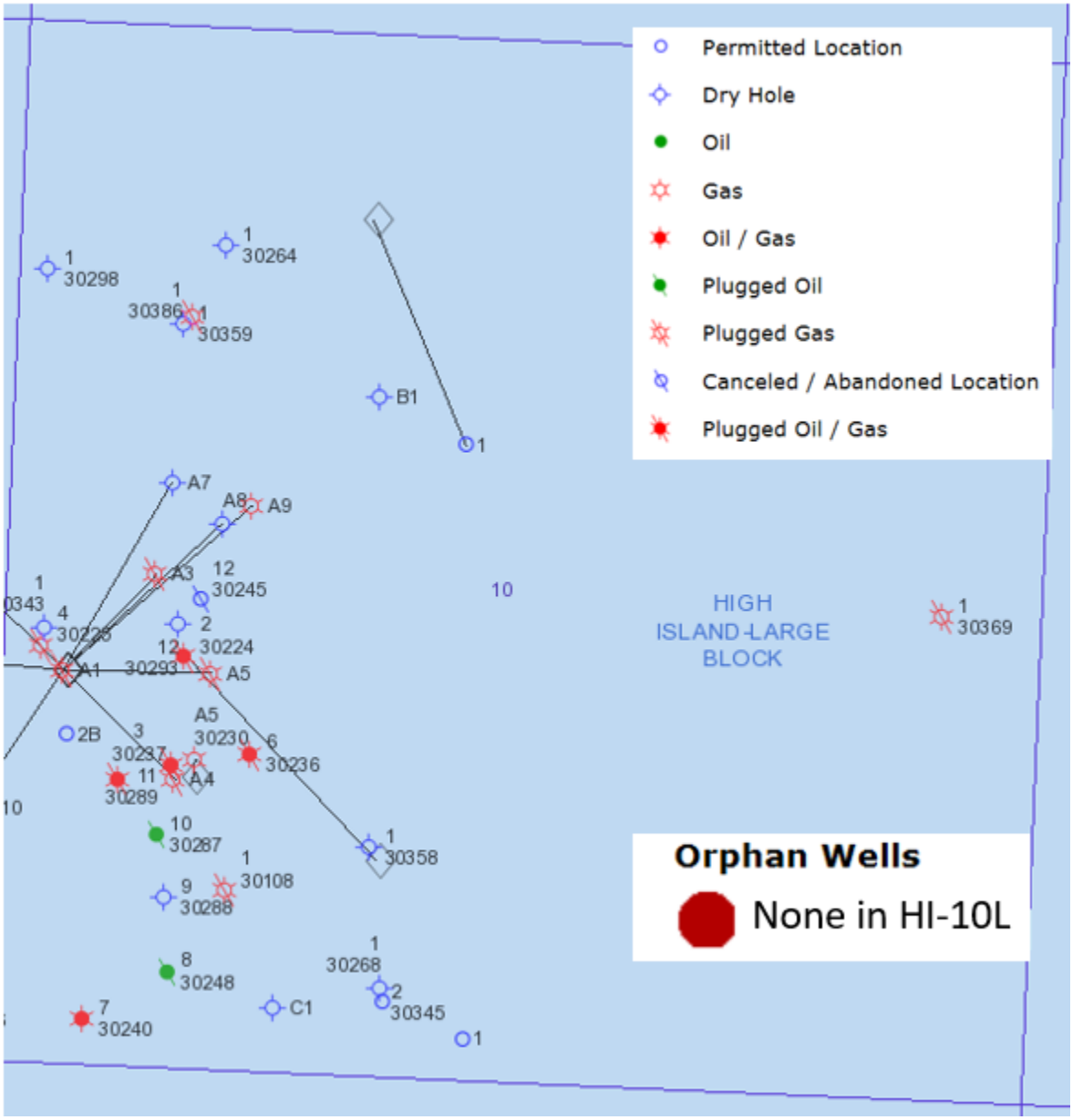

Figure 5. Well Features in HI-10L.

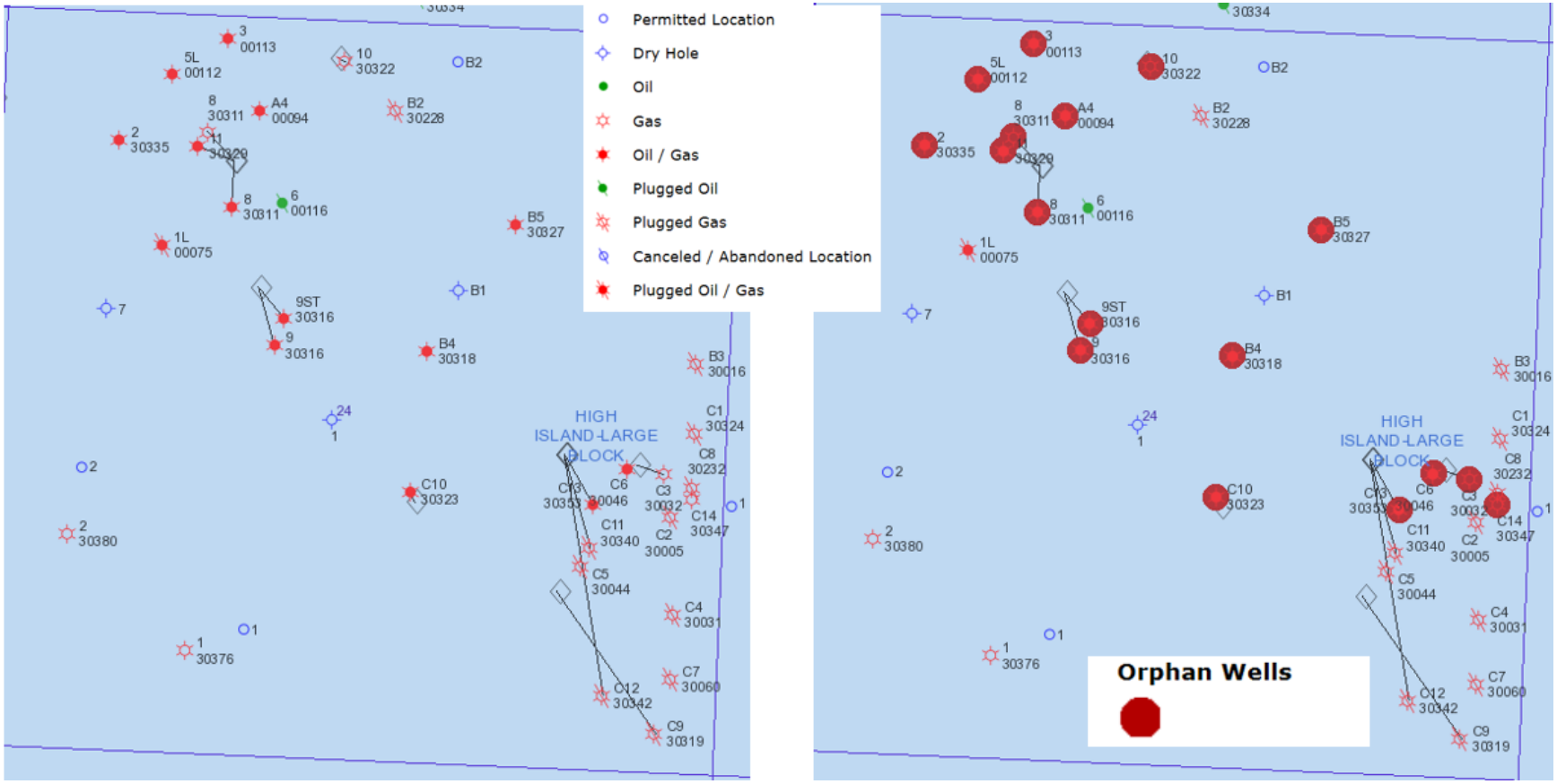

Figure 6. Well Features in HI-24L, with Orphaned Wells Highlighted in Figure on the Right.

Within the GIS viewer, the user can click on a well feature to view the well's attributes, including any scanned documents. The user can also download a csv file with the well attributes within a specified radius of a point on the GIS map; the downloaded file does not include links to the scanned documents.

Example GIS well attributes are shown in Appendices 12.2 through 12.5 for a dry hole, active gas well, plugged well, and orphaned well in HI-24L. The well attributes include the API number, GIS well number, GIS symbol description, and GIS coordinates. Other well attributes available in the GIS database may also include wellbore status (open, plug, partial plug), type of well (producing, temp abandoned, etc), last permit issued, last permit operator, total depth, lease name, and lease ID (five-digit number assigned by RRC to each lease in a field; lease ID is unique within each district). For some wells, scanned records are available for well logs, drilling permits, production data, etc. The readability of the scanned documents ranges from poor to very good.

6.3 Comparison of Well Data from RRC GIS and UT's Commercial Databases

The RRC's GIS database and the Subscription Databases were the two main sources of well information that Trimeric consulted to determine the number and status of wellbores (e.g., open, plugged, orphaned, etc.) in HI-10L and HI-24L. Trimeric's investigation began with the RRC's GIS Viewer database to identify wells in the two leasing blocks. Trimeric then asked UT to query the Subscription Databases to pull additional data for the wells in these leasing blocks, including well, casing, and perforation depths, and test reports (such as plugging records, pressure tests, cement logs, and caliper logs). The query of the Subscription Databases resulted in dozens more wells being identified as associated with these leasing blocks, as compared to the RRC GIS Viewer. Significant effort was required to investigate the apparent mismatch in well datasets between the two databases.

Comparing data between the two datasets was complicated by several factors:

- **The two databases use different well identification numbers.**
    - The RRC uses a 10-digit API number for well identification; therefore, APIs mark only a unique surface location and do not indicate if multiple wellbores are present.
    - The Subscription Database uses the more modern 14-digit UWI number for well identification: the first ten digits should correspond to the API number when possible, the next two digits allow for tracking of multiple wellbores as the same

surface location, and the final two digits are used to store additional information. For many wells in the Subscription Databases the final four digits were all zeros, but some wells had non-zero values in the final four digits, which led to multiple wells in the Subscription Databases corresponding to a single API number in the GIS database.

- **The RRC database did not assign full API numbers to the oldest wells.**
    - The oldest wells (from the 1950s) are referred to by RRC with "API 708" (the county number) and then "Well #", where the # is a one- or two-digit letter/number. These older wells have full 14-digit UWI numbers in the Subscription Databases. For HI-10L and HI-24L, UT used the GIS location of each older well to match the well identifiers between the two datasets.

A well-by-well comparison of the well datasets was further complicated by inconsistencies between the RRC GIS database and UT's commercial databases. Some examples of inconsistencies for HI-10L are described in the following bullets:

- One of the wells in the RRC GIS for HI-10L shows up as API 42606, a value that implies it belongs in county number 606 not the High Island's county number 708. The listed GIS coordinates are within HI-10L; UT used the GIS coordinates to match this well to UWI 42708000100000 in the Subscription Databases.
- Figure 7 shows an example of three wells identified by the Subscription Databases as being associated with HI-10L, but they are physically located outside its borders. The corresponding API numbers for these wells were visible in the RRC GIS Viewer in their respective lease blocks.
- The Subscription Databases identified other UWIs as being associated with HI-10L (e.g., 42708000120000, 42708300270000, 42708300350000, 42708000050000, 42708000110000, 42708000130000), but their corresponding APIs were not found in the RRC GIS Viewer search.[25]

[25] To verify that these wells are indeed located in HI-10L, UT would need to obtain the GIS coordinates for these wells from the Subscription Databases.

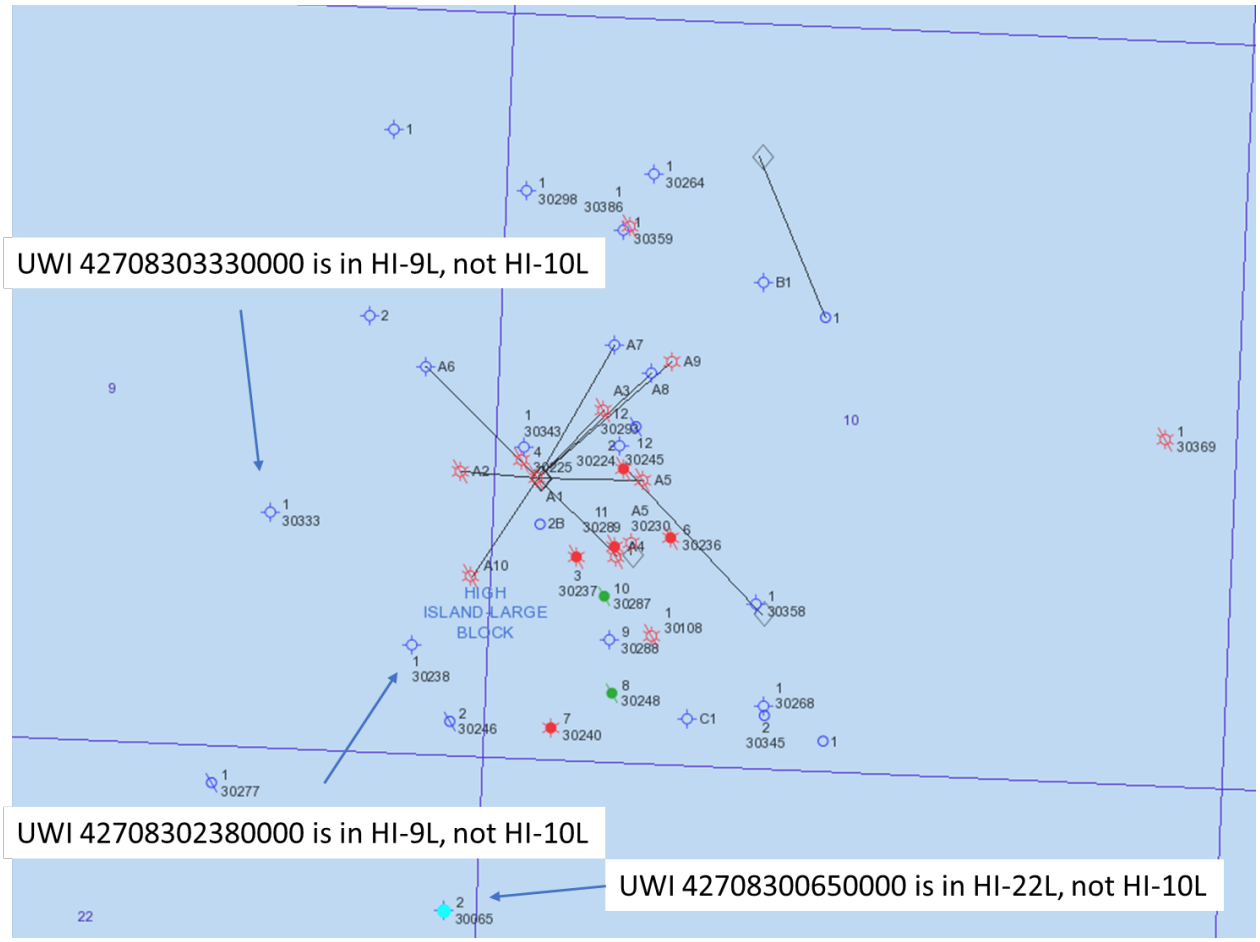

Figure 7. The Subscription Databases tagged several wells as being in HI-10L, but they are physically located outside of the HI-10L boundaries.

Some examples of inconsistencies for HI-24L are described in the following bullets:

- As illustrated in Figure 8, the Subscription Database tagged dozens of wells as being associated with HI-24L (i.e., the grey circles in Figure 8), but many of these wells' locations were not within HI-24L's boundaries (i.e., fell outside the blue boundary of HI-24L). The GIS coordinates of some wells fell in neighboring lease blocks such as HI-7L, HI-23L, HI-25L, HI-32L, as well as lease blocks that were beyond HI-24L's immediate neighbors.
- Some wells appeared to have different ID numbers assigned in the two databases.
    - As shown in Figure 9, UWI 4270800074000 in the Subscription Database is in the same location as well B1 (no API assigned) in the RRC GIS Viewer. Well B1 is an example of a well record with very little information; the data marker in the GIS Viewer indicates it is a dry hole, but the well status field (along with most other fields) is blank.

  - In another example, UWI 42708001110000 in UT's commercial database had nearly the same GIS coordinates (Latitude = 29.52859, Longitude = -94.11081) as API 70830324 (Longitude = 29.5285082; Longitude = -94.1108618) in the RRC database. Other well features, such as the wellbore status and total vertical depth, matched between these well records, indicating these two records are likely the same wellbore.
- Sometimes, a well identified by the Subscription Database fell within the HI-24L boundary but had no apparent corresponding well (based on location) in the RRC GIS viewer, as shown in Figure 10 for UWI 42708000160000.
- When multiple wells were associated with an API number, manual effort was needed to reconcile the data with the Subscription Databases. For example, for API 70830311, the RRC GIS Viewer indicates one surface location and two wells (Number 8 Oil/Gas Well and Number 8 Gas Well). The Subscription Database shows six UWIs associated with this API number. The GIS coordinates are not exact matches between the two databases (though they are fairly close), so other fields were used to match identities: UWI 42708303110000 corresponds to the Number 8 Oil/Gas Well, UWI 42708303110100, 0101, 0102, and 0103 are in the exact same location and correspond to the Number 8 Gas Well, and extension 0104 was "canceled". Figure 11 shows another example of multiple entries for API 70830316.

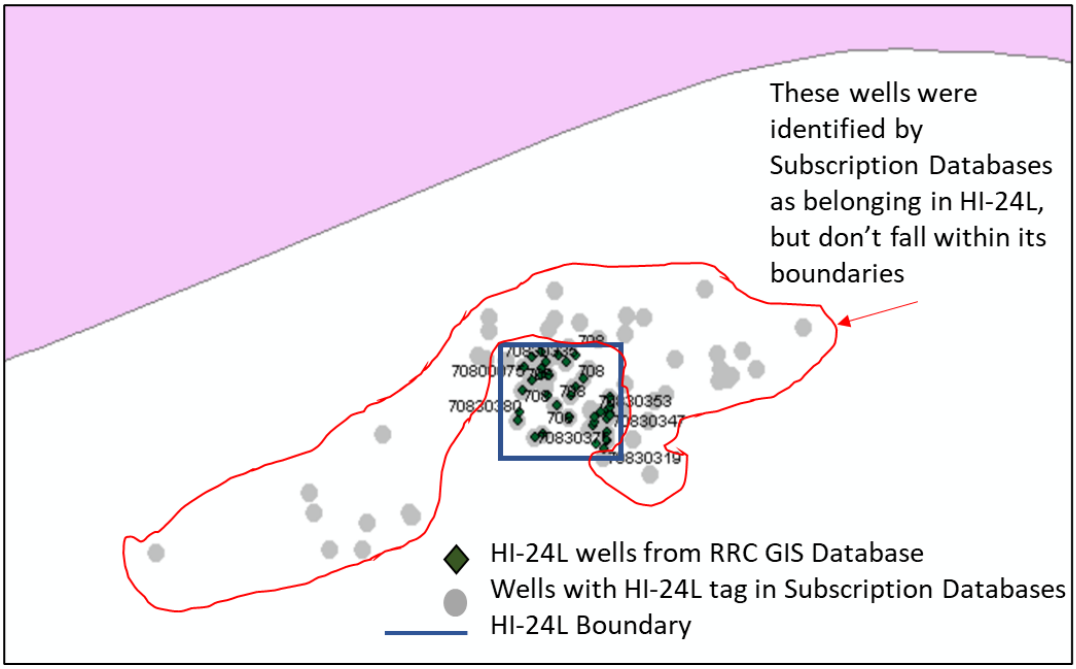

Figure 8. UT's Database tag many wells that are outside HI-24L boundaries as being associated with HI-24L.

RRC GIS Viewer symbol indicates B1 is Dry Hole, but
RRC GIS Database record is empty for Wellbore Status:

API	Well_Number	Symbol_Desc	Lat27	Long27	Lat83	Long83	Wellbore_Status	Last_Permit_Issu	Last_Permit_Operator_Numbe
708	B1	Dry Hole	29.5369361	-94.1269123	29.53716	-94.12709081			

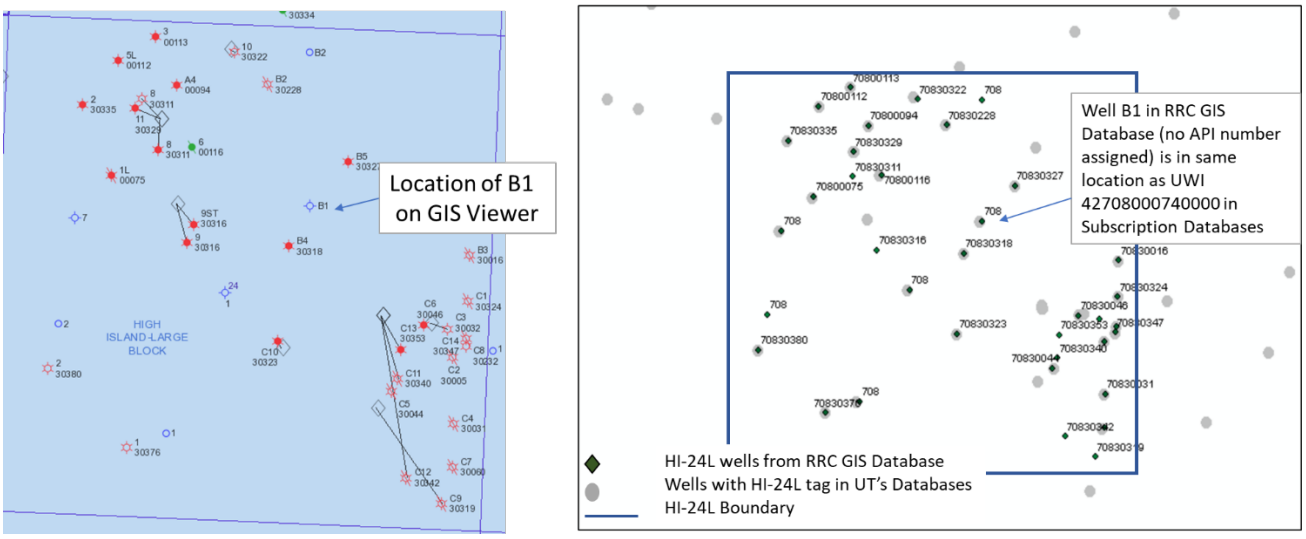

Figure 9. Comparison of Data Available in RRC GIS Viewer for Well B1 in HI-24L and for UWI 42708000740000 in UT's Databases.

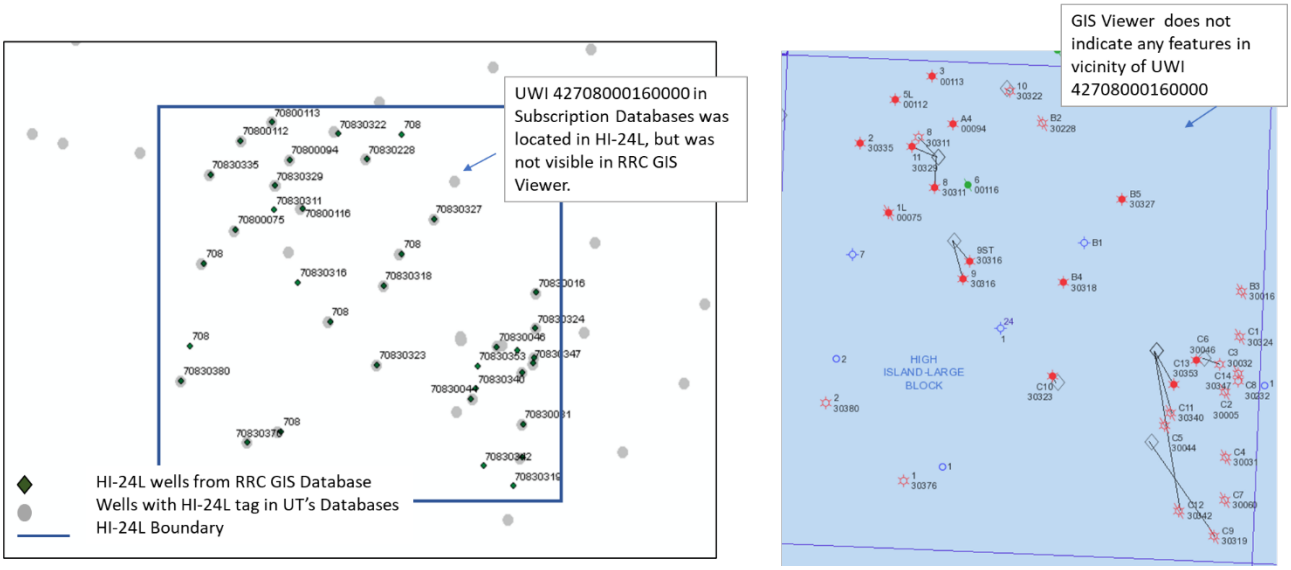

Figure 10. UT's Database identifies some well features within the HI-24L boundaries (e.g., UWI 42708000160000) that have no apparent corresponding well feature in RRC GIS Viewer.

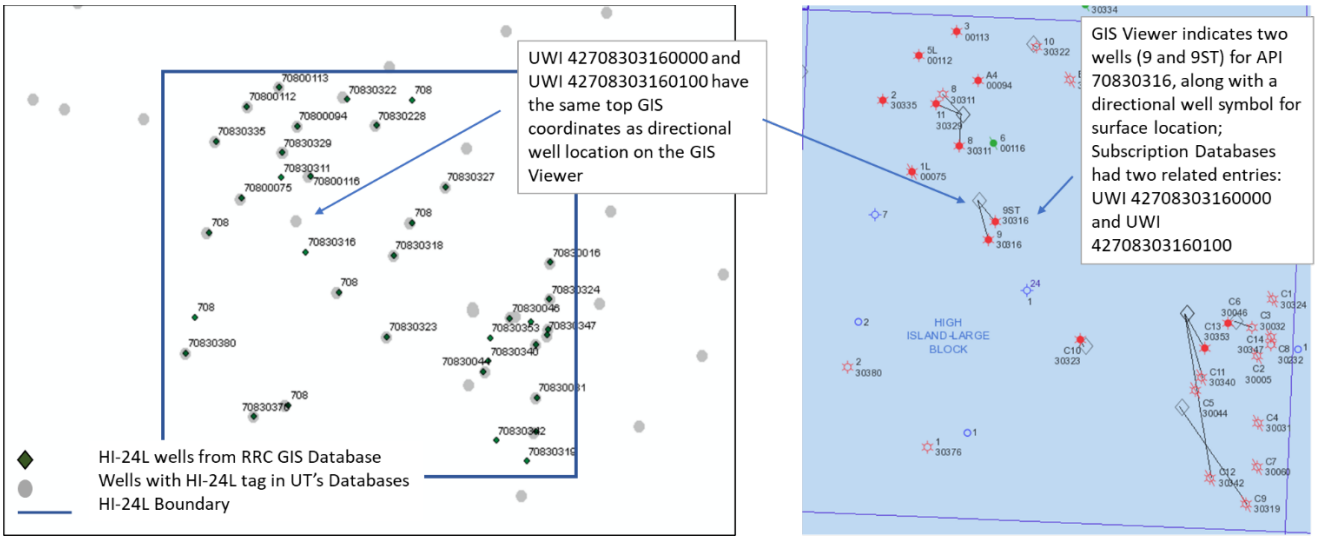

Figure 11. Some UWI records in the Subscription Databases correspond to a Directional Well location in RRC GIS Viewer.

As a result of these inconsistencies in data representation, significant manual effort was expended in reconciling the two datasets, including mapping physical locations of each well and comparing well attributes (such as total vertical depth, completion dates, etc.) to match well data between the databases and quantify the well characteristics in the leasing blocks.

Because the Subscription Databases pulled wells that were outside the leasing blocks, Trimeric conducted the well screening analysis for the wells identified in the RRC GIS Viewer (which were reliably within the leasing block), supplemented with information about these wells that was available in the Subscription Databases. Trimeric did not include the additional wells identified by the Subscription Databases as having a HI-10L or HI-24L tag, if they did not match a HI-10L or HI-24L well in the RRC GIS Viewer database (i.e., while these wells may actually exist within the lease blocks, the inconsistency between the databases led to exclusion from the screening study).

Based on the methodology described above, Trimeric assigned wellbore status to the wells in each of the leasing blocks, as shown in Figure 12 for HI-10L and in Figure 13 for HI-24L. The next section presents the results from a preliminary well screening analysis on the attributes of these wells.

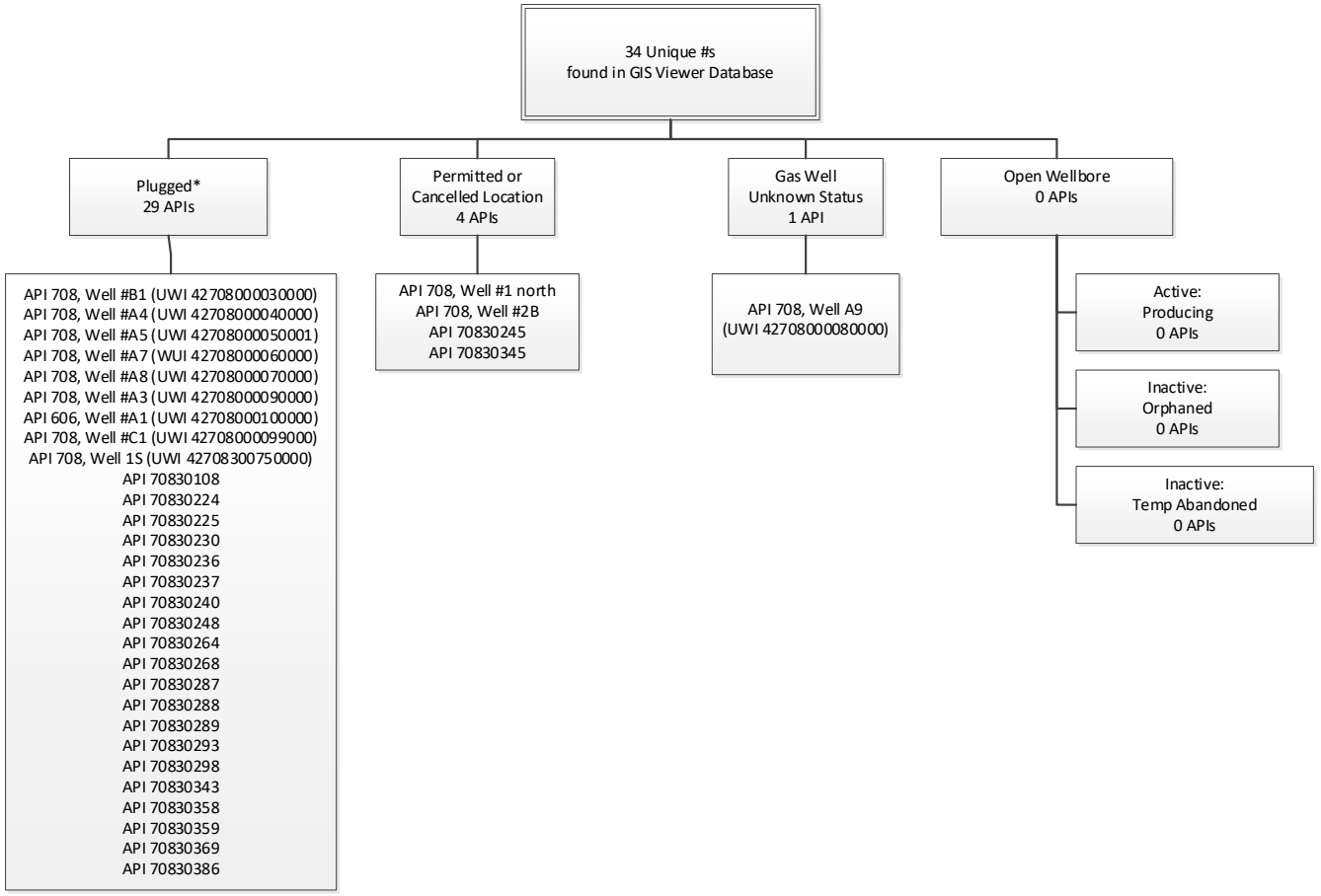

Figure 12. Wellbores Status as Determined from RRC GIS Viewer and Subscription Databases for HI-10L.

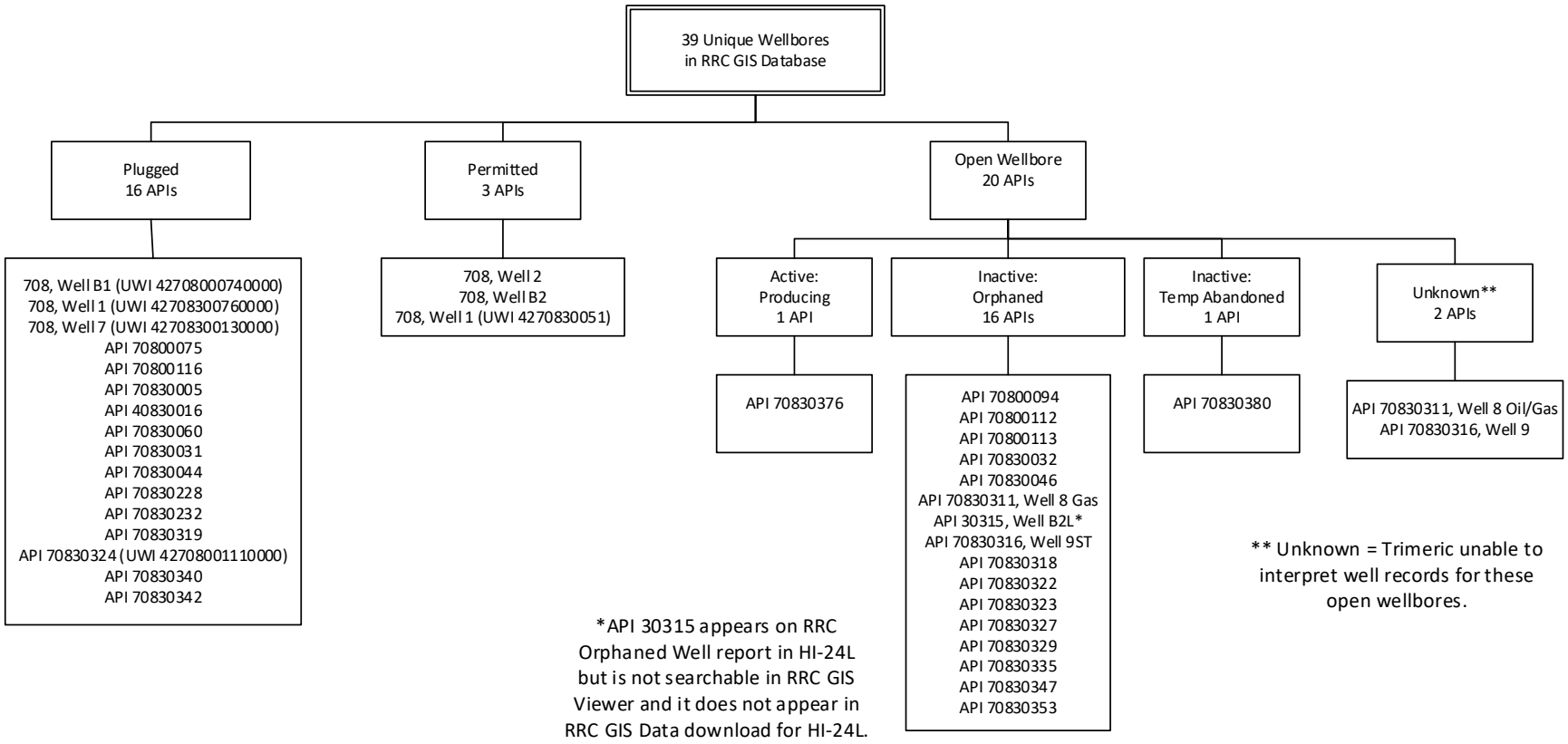

Figure 13. Wellbore Status as Determined from RRC GIS Viewer and Subscription Databases for HI-24L.

6.4 Well Screening Parameters Applied to HI-10L and HI-24L

Section 5 Well Screening Parameters described first-tier screening criteria that could be used to begin the assessment for well reuse/leak risk of a field. These criteria are ones that are readily available and sortable in electronic databases. Table 1 shows the results of applying the criteria to HI-10L and HI-24L for number of wells, wellbore status, well completion data, and availability of reports. These statistics were compiled based on the wells visible in the RRC GIS Viewer, supplemented with data for these wells available in the Subscription Databases; these tallies do not include wells tagged as being associated with the leasing blocks by the Subscription Database if those wells did not fall within the leasing block boundary (see Section 6.3 for further discussion).

Observations include:

- **Wellbore Status for HI-10L.** HI-10L contained 34 UWIs/APIs, of which 4 APIs were for permitted/cancelled wells (i.e., no drilling occurred), leaving 30 drilled wellbores. All but one of these wellbores has been plugged. One wellbore had a status that could not be determined by Trimeric from the databases. There were no currently active, producing wells in HI-10L.
- **Wellbore Status for HI-24L.** HI-24L contained 39 UWIs/APIs, of which 3 APIs were for permitted/cancelled wells (i.e., no drilling occurred), leaving 36 drilled wells. Only 16 of these 36 wells were plugged. The remaining 20 wells had open wellbores, of which only one was actively producing. One open wellbore stopped production in March 2021 and was classified by RRC as temporarily abandoned. Sixteen open wellbores were classified by RRC as orphaned, with inactive time periods ranging from 36 to 260 months. Trimeric could not assess the status of the other two open wellbores; they shared API numbers with orphaned wells but these wellbores were not marked as orphaned by RRC, nor were they marked as producing.
- **Well Completion Dates.** Both HI-10L and HI-24L contain several wells constructed before 1970, indicating older well construction methods. No wells have been constructed in either HI-10L or HI-24L after 2010, so all wells in these leasing blocks are more than twenty years old.
- **Well Reports.** In the Subscription Databases, plugging reports were the most available of the well reports tallied for HI-10L and HI-24L. The presence of a plugging report for a

well does not necessarily indicate that the ultimate disposition of the well is plugged; [26] some orphaned wells had plugging reports in the Subscription Database while some plugged wellbores did not have plugging reports available in the Subscription Database. Cement logs were more available than pressure test reports, which were more common than caliper logs. Only two wells in HI-in HI-24L (API 70830108 and API 7083040) and one well in HI-24L10L (API 70830322) had all four reports available in the Subscription Database. While the Subscription Database may not contain these reports, it is possible that the reports are in the well owner's records.

[26] For example, an API number may have plugging reports available in the Subscriptions database, but also be classified in the GIS tool as "partially plugged" in the 'Well_Type' field and as OPEN in the 'Wellbore_Status' field.

Table 1. Well Screening Parameters Applied to HI-10L and HI-24L.

	HI-10L	HI-24L
Number of UWIs/APIs	34	39
Wellbore status		
Plugged	29	16
Permitted/Cancelled	4	3
Unknown Status	1	2
Active: Producing	0	1
Inactive: Temp Abandoned	0	1
Inactive: Orphan	0	16
Well Completion Date		
< 1970	9	4
1970 – 1979	6	8
1980 – 1989	10	6
1990 – 1999	3	8
2000 – 2010	2	0
Unknown	0	11
# Wells w/ Reports Available in Subscription Database		
Plugging	29	20
Cement Logs	20	21
Pressure Tests	11	21
Caliper Logs	4	2
Plugging & Cement	19	17
Plugging, Cement, & Pressure	10	15
All Four Tests	2	1

7 Well Workflow

EPA Underground Injection Control Well Class VI Program applies to wells used for injection of CO_2 into underground surface rock formation for long-term storage. If an existing well is to be re-permitted as a Class VI well, the well must be demonstrated to be suitable for the application in terms of mechanical integrity, material strength, the material compatibility/corrosion

resistance of the well, and the ability of the well to accommodate testing and workover equipment.

If potentially viable well candidates are identified for repurposing for CO_2 injection, the following work may be needed to repurpose the well and assure the integrity of neighboring wells in the associated reservoir; this list is not intended to be comprehensive.

- **Well integrity will need to be verified.** Wellbore integrity, for both the injection well as well as for other wells within the reservoir, is important for ensuring that injected CO_2 stays within the intended formation. Injection of CO_2 into a depleted reservoir will increase the pressure in the reservoir, putting additional stresses on the wells. The *potential* for leakage could be indicated by factors such as age of well, applicable regulations, the well abandonment method, well completion activities, cement, and well type.[27] Wellbore integrity was evaluated in the Weyburn-Midale field, which had been studied for over a decade as part of CO_2 monitoring and storage projects.[28] The parameters most likely to affect integrity of wells included cementing, debonding between casings and wall rock, and channeling in the cement itself. Even with a records review, a wellbore evaluation would be required to confirm the downhole status, including formation characteristics, casing condition, cement location, and joint locations.
- **Wells may need to be remediated to address integrity problems**. Remediation might be required prior to injection or might be deferred if the CO_2 plume will take time to reach the wellbore of interest; Sacuta (2015) recommends that remedial operations focus on the injection zone only.[29] According to one of the experts Trimeric consulted, virtually any well-integrity issue can be fixed, but it will represent a cost and schedule risk, and well integrity is often worse than the records indicate.[30] It is difficult to anticipate what work will be needed to fix a well-integrity issue before re-entering the well and potential costs may vary substantially from well to well. This cost uncertainty must be accounted for with project cost set-asides.
- **Well casings may need replacement.** It may be possible to recomplete the well within existing casing strings, or the well casings may need replacement. Corrosion resistant stainless steel (typically 13% Cr) may be specified when outer casings are in contact with formation water bearing rocks; carbon steel may be sufficient when water content (and thus carbonic acid formation) is low. Likewise, a cement compatible with CO_2 is needed.

[27] Glazewski, K. "Wellbore Integrity." EERC Presentation to IEAGHG CCS Summer School. 19 July 2016.

[28] Sacuta, N. et al. "International Energy Agency (IEA) Greenhouse Gas (GHG) Weyburn-Midale CO_2 Monitoring and Storage Project." Final Technical Report for DE-FE0002697. 30 September, 2015.

[29] Sacuta, N. et al. "International Energy Agency (IEA) Greenhouse Gas (GHG) Weyburn-Midale CO_2 Monitoring and Storage Project." Final Technical Report for DE-FE0002697. 30 September, 2015.

[30] Per 2019 conversation with oil and gas expert, JL.

- **Well casings and cement will need to be re-perforated**. Perforations will need to be in the desired injection zone, and the perforation length required for CO_2 injection is typically higher than required for oil/gas production. For example, wells in HI-10L had perforation lengths averaging 20 feet and ranging from 3 feet to 200 feet in the hydrocarbon producing zone.
- **New production tubing, well-heads and Christmas trees should be installed** using alloys and pressure ratings compatible with CO_2 service and suitable for injection (not extraction). The well-head should use CO_2-resistant materials, such as for elastomers used in thread seals. Wells constructed for O&G production will likely not have accounted for high CO_2 concentrations in their design; CO_2 leakage pathways may develop in cement plugs and casing strings if they are not designed for CO_2 service.

8 Conclusions

Trimeric conducted a preliminary review of data for the wells located in HI-10L and HI-24L site leasing blocks in the shallow state waters of the Gulf of Mexico to gain an understanding of the quality/type of data available, develop a process to utilize/assess the data, and summarize high-level opportunities and challenges of both re-use and well-integrity risks for CO_2 injection and storage. The primary source of data was Railroad Commission's (RRC's) GIS Viewer and its associated database. Subscription Databases available from UT were used to gather additional data on the wells. The data were used to perform a high-level screening of the wells in the leasing blocks for potential re-use for CO_2 injection and to assess well integrity risks for CO_2 storage. A workflow to re-purpose wells for CO_2 injection and assess the well integrity of other wells in the field was also developed.

There were a number of apparent inconsistencies in the data contained within and between these two data sources, resulting in significant effort to compile the datasets on a well-by-well basis. For example, the Subscription Databases identified dozens of wells tagged to the HI-10L and HI-24L leasing blocks that were not physically located in the leasing block; Trimeric removed these wells from the analysis of the leasing blocks. The databases use different identification systems for the wells (API number in RRC GIS Viewer and UWI number in Subscription Databases), which further complicated the analysis.

The challenges with data inconsistency highlight a key aspect of due diligence that must occur whether wells are being considered for re-use or being assessed a risk for leakage in storage reservoir. Due to these dataset inconsistencies, the statistics compiled by Trimeric have some degree of uncertainty associated with them. As such, the well statistics generated in this report should primarily be used for the purpose of illustrating the types of data available and not as firm quantification of the well status in these leasing blocks.

The evaluation in this report represents a conceptual study rather than the development of a specific CO_2 injection and storage project. Therefore, Trimeric's investigation was purposefully limited to publicly available datasets (whether free or subscription based). For a specific project opportunity that is being shepherded by a project developer, consulting the well owners' records may help address some of the ambiguities in the public records. If uncertainty still exists after reviewing owners' records and engaging experts in the local area, other methods that have been developed in onshore application may be available (e.g., a magnetic geophysical survey of the shallow subsurface of the sea floor could help to identify ferrous metallic anomalies that can be attributed to buried metal objects such as well casings).

Some key characteristics of the well stock in HI-10L and HI-24L leasing blocks can be summarized from the analysis in this report:

- Age Distribution:
    - Each leasing block contains several wells constructed before 1970, when modern well construction methods came into practice, increasing both re-use and well integrity risks. For HI-10L, nine of 30 completed wells were constructed before 1970. For HI-24L, at least four of 37 wells were constructed before 1970; there were eleven other wells for which construction date was not identified.
    - All but two wells were constructed before the year 2000, reflecting the skew of the age distribution towards older wells. This is another high-level measure of the risk associated with wells in these key proxy regions for CO_2 storage in the Gulf of Mexico.
- Well Status:
    - All but one well in HI-10L was plugged; Trimeric was unable to determine the wellbore status for that single well. HI-24L contained one active well and many inactive, unplugged wells.
    - Leasing block HI-24L had 16 of the 25 orphaned wells in the High Island Large Block state waters; these wells all had the same operator. The other orphaned wells were in HI-55L (4 wells) and HI-98L (5 wells); all of these wells had the same operator, but it was a different operator from the orphaned wells in HI-24L.
    - While the large number of unplugged wells in HI-24L could present a possible opportunity for well reuse for CO_2 injection, an orphaned well carries more risk in terms of uncertainties in its physical integrity and associated costs to plug or restore the well.

When looking for data regarding specific wells, well integrity data were difficult to query in the RRC Databases, but well reports (such as plugging reports, cement logs, pressure tests, and

caliper logs) were more readily found in the Subscription Databases. The well reports data also had limitations - many wells that were classified by RRC as plugged did not have associated plugging reports available in the Subscription Databases. Only 3 of the 73 wells in HI-10L and HI-24L had all four report types (plugging reports, cement logs, pressure tests, and caliper logs) available. Any repurposing of wells or assessment of well integrity for leakage prevention will likely require additional investment of time to obtain well records from well owners, and perhaps investment in testing for more current/reliable well integrity data.

Because HI-10L and HI-24L may not be representative of the full GoMCarb study region, broad conclusions about well re-use or well integrity risks cannot be extrapolated beyond these regions.

9 Recommendations for Future Investigation

To better understand the potential for the reuse of (or leakage risk from) wells in the Gulf of Mexico for CO_2 injection, the following investigations may be useful:

- **Perform a "sampling" of representative well datasets across the GoMCarb region**. The project team has discussed the idea of investigating several "transects" along the GoMCarb region of the Gulf of Mexico. A transect in this context refers to a narrow region of offshore waters spanning out perpendicularly from a point on the shoreline to some pre-determined distance from the shore. The transect sampling could extend into federal waters, as the current study has thus far been limited to analog lease blocks in Texas state waters. The purpose of this approach is to analyze several discrete locations along the GoMCarb project region with the goal of evaluating a representative dataset for the GoMCarb region while limiting the amount of well data that must be collected, processed, and evaluated. Even with this sampling approach, the evaluation is expected to be labor-intensive due to the challenges highlighted in this report with well data collection and evaluation.
- **Screen for low-density well regions**. Determine if there are CO_2 reservoirs in GoM shallow waters with lower densities of wells. Such locations may represent an opportunity to assure well integrity with lower risk and/or lower investment.
- **Perform a more detailed assessment of individual wells.** For a well with a robust dataset in the Subscription Databases (e.g., API 70830322 in HI-24L, API 70830108 and API 7083040 in HI-10L), consult a subject matter expert to interpret data regarding potential to reuse well or potential for leak via the well.
- **Use onshore analogs and subject matter experts to refine the offshore well re-use workflow and leverage existing best practices**. Consult a subject matter expert to assess the frequency with which on-shore wells are re-used and discuss the re-use process, so as

to inform the opportunity for offshore reuse. Review proposed workflow from this document with the expert, and develop workflow into a diagram identifying key steps. Provide more quantification of reuse criteria, where possible (e.g., quantify a minimum casing diameter to accommodate well workovers).

- **Develop characteristic cost ranges for well integrity testing and plugging of offshore wells**. Consult a well expert to quantify the range of costs expected to conduct well integrity testing and to plug offshore wells (both 14(b)(2) compliant and non-compliant wells).
- **Consult a well construction expert for specific technical topics, including (but not limited to):**
    - Determine if an existing wellbore that does not reach the CO_2 injection zone of interest will still have potential value for reuse.
    - Review cement log data and compare to cement recommendations for CO_2 resistance.

10 Appendix – Well Identification Primer

The PPDM provided the following diagrams in its publication, Well Identification United States (2014). These diagrams are useful for interpreting the information provided in an API and/or UWI number.

WELL COMPONENT DEFINITIONS

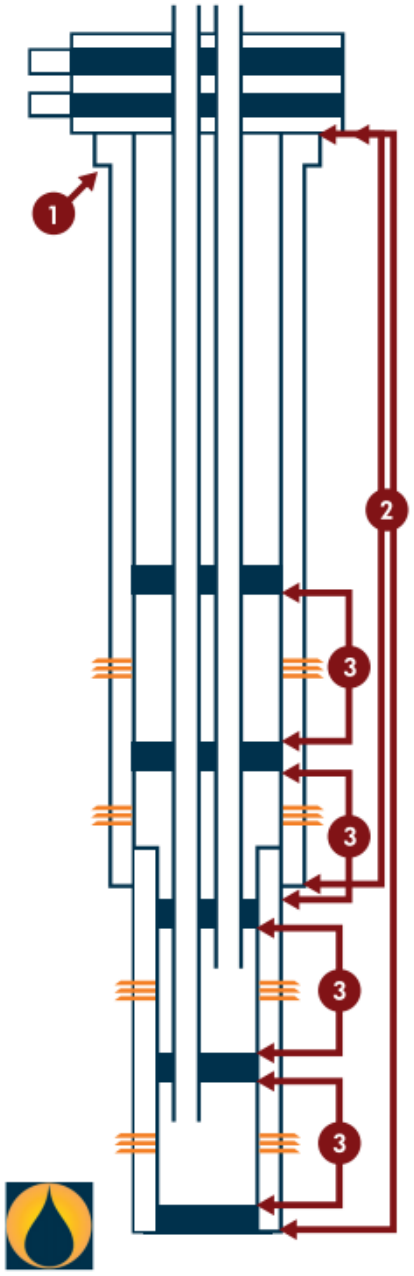

Well
A Well is a proposed or actual drilled hole in the ground designed to exchange (or facilitate the exchange of) fluids between a subsurface reservoir and the surface (or another reservoir), or to enable the detection and measurement of rock properties.

Well Identifiers
An identifier refers to names, numeric or alphanumeric sequences, codes, tags, abbreviations and so on that are maintained or exist in industry, government, vendor, business partner, or proprietary systems, datasets or documents whose purpose is to uniquely identify a single Well or Well component (i.e., Well Origin, Wellbore, Wellbore Completion).

1. **Well Origin (WO)**
   A Well Origin is the location on the surface of the earth or seabed where the drill bit is planned to penetrate or does penetrate the earth to establish or rework a Well.

2. **Wellbore (WB)**
   A Wellbore is a path of drilled footage from the Well Origin (top/start) to a terminating point (bottom/end).

3. **Wellbore Completion (C)**
   A Wellbore Completion is a set of one or more Wellbore Contact Intervals that function as a unit to produce or inject fluids.

WELL IDENTIFIERS USA

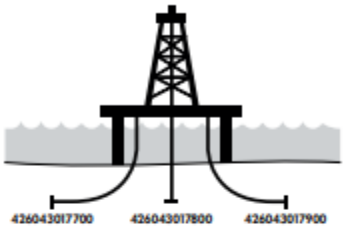

Platform Wells
Wells from an offshore platform. Each is a separate penetration of the earth's seabed. Therefore, each has a different well code (digits 6 – 10). There are three Wells, each with one Wellbore. The drilling order is not implied in the number.

State Code	County Code	Well Code	Wellbore Code
42	604	30177	00
42	604	30178	00
42	604	30179	00

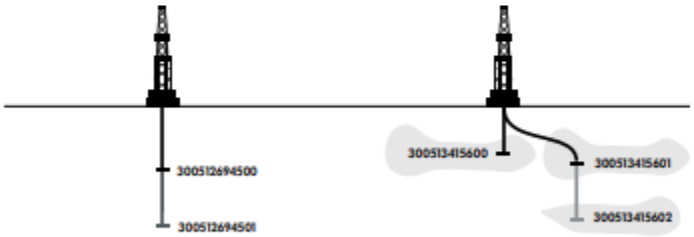

State Code	County Code	Well Code	Wellbore Code
30	051	26945	00
30	051	26945	01

State Code	County Code	Well Code	Wellbore Code
30	051	34156	00
30	051	34156	01
30	051	34156	02

Deepening
Deepening an existing Wellbore creates a new Wellbore, thus requiring a new US Well Identification Number, subject to the definition of deepening set by the Authority. Note that the first 10 digits remain the same.

11 Appendix – Well Queries via RRC Database

The RRC Well Query tools allow the user to query for various well characteristics. The following subsections illustrate the types of data available in these queries by describing the results for HI-10L and HI-24L:

- Wellbore Query
- Well Status Report and Completion Report
- Inactive Well Report
- Orphaned Well Report
- Gas Proration Schedule Query
- Oil Proration Schedule Query

11.1 Wellbore Query

The RRC's wellbore report returns the active and inactive wells based on query inputs from the user. Plugged wells that are no longer monitored by RRC did not appear in the reports for HI-10L or HI-24L. The RRC's wellbore report for County = High Island Large Block returned 48 well entries when the report was run on 27 May 2021, of which 0 were in HI-10L and 26 were in HI-24L (see Appendix 12.6). The RRC's wellbore report may contains multiple wells for the same API; additional information about the completions can be viewed by clicking on each wellbore item in the query. Of the 26 wellbores in HI-24L, 24 wellbores were inactive and two wellbores were active (API 70830376 and API 70830380) at the time the report was run; one of the HI-24L wellbores (API 70830380) later became inactive. Of the 24 inactive wells listed in the wellbore query, there were 16 unique API numbers, which corresponded to the 16 APIs numbers on the orphaned well list. Eight of these APIs had only a single well listed, while the other eight APIs had two wells listed (e.g., B5-L and B5U for API 70830327).

11.2 Well Status Reports and Completion Reports

The RRC's well status report provides the G-10 Gas Well Status Reports for active wells. For Lease ID 230456 (corresponds to API 70830376) and Lease ID 231670 (corresponds to API 70830380), the two most recently active wells in HI-24L, there were 15 G-10 reports, dating back to 2014. Examples of the recent G-10 reports (from 2021) these wells are provided in Appendix 12.7 and Appendix 12.8.

In the Completions Report Query, wells can be queried by Lease ID (among other fields) for G-1 (Gas Well) and W-2 (Oil Well) Reports for Test, Completion, or Recompletion. Report G-1 for formerly active Lease ID 231670 (API 70830380) in HI-24L is shown in Appendix 12.9.

Completion reports were also found for some of the inactive wells in HI-24L; Report W-2 filed in 2012 for inactive Lease ID 26021 (API 70800094) is provided in Appendix 12.10 as an example of an Oil Well W-2 report.

11.3 Inactive Well Report

RRC provides a monthly update of inactive wells in an Inactive Well Aging Report (IWAR). This report includes the first month of inactivity, which is listed as the shut-in date.

The RRC's monthly reports of inactive wells can be accessed at this website:

https://rrc.texas.gov/oil-and-gas/compliance-enforcement/hb-2259-hb-3134-inactive-well-requirements/inactive-well-aging-report-iwar/

RRC also has an Inactive Well Query tool that allows the user to search for inactive wells by operator, district, field, or county. However, these data can only be downloaded if search is restricted to a single operator.

The Inactive Well Report for May 2021 shows 46 inactive wells in the High Island Large Block (API County Number 708), of which 0 inactive wells were located in HI-10L and 24 inactive wells were located in HI-24L. Appendix 12.11 lists the inactive wells from HI-24L to illustrate the data that can be obtained from this report.

11.4 Orphaned Well Report

RRC provides a monthly update of orphaned wells in an Orphan Well Report. This report includes

The RRC's monthly reports of orphaned wells can be accessed at this website:
https://www.rrc.texas.gov/oil-and-gas/research-and-statistics/well-information/orphan-wells-12-months/

RRC also has an Orphan Well Query tool to search orphan wells by well type, district, county, field, operator, and API number.

The Orphan Well Report for May 2021 shows 25 orphaned wells in High Island Large Block (API County Number 708), of which 0 orphaned wells were located in HI-10L and 16 orphaned wells were located in HI24L. Appendix 12.12 lists the orphaned wells from HI-24L to illustrate the data that can be obtained from this report. Each of the 16 API numbers listed was unique; there were no entries for second wells associated with any of these API numbers. However, in the wellbore query report described earlier, eight of the orphaned APIs each have two well

numbers associated with them, making unclear the total number of orphaned wellbores in HI-24L.

11.5 Gas Proration Schedule Query

RRC has a Gas Proration Schedule Query tool that allows the user to query by district. A query for District 03 (which encompasses High Island Large Block) can be downloaded to a spreadsheet and filtered for HI-10L and HI-24L fields. For the report query on 27 May 2021, there were no HI-10L entries in this report, and there were 17 entries for HI-24L (see App 12.13). Two of the HI-24L entries were for active wells (API 70830376 and API 70830380); the other 15 entries were for orphaned wells. Of the 15 orphaned well line items, API 70800112 had two entries (one for Well 5U and one for Well 5L), and API 70830335 had two entries (one for Well2U and one for Well 2L). The remaining entries had one well per API number.

11.6 Oil Proration Schedule Query

RRC has an Oil Proration Schedule Query tool that allows the user to query by county. A query for High Island Large Block can be downloaded to a spreadsheet and filtered for HI-10L and HI-24L fields. For the report query on 28 May 2021, there were no HI-10L entries in this report, and there were 9 entries for HI-24L (see App 12.14). The oil proration report includes fields for Unit/Well Type, which indicates that these 9 wells are either shut in or have no production; all of these wells are on the orphaned well list. Of the 9 wells listed, two wells were associated with API 70830315 (one for B2U and one for B2L); the rest had one well associated with each API.

The report also includes a field for Daily Allowable Oil/Gas which indicates permit violations. Each HI-24L on the oil proration list had a violation listed. One well had a 14B2 extension denied; two wells had delinquent W-10, and six wells had an H-15 violation. The H-15 Program is for testing of older inactive wells; a test notice is sent when the RRC identifies a well that is more than 25 years old that is inactive or has not reported production during the previous twelve-month period.

12 Appendix – Example Images and Reports

Item 1 - O&G District Map from Texas Railroad Commission

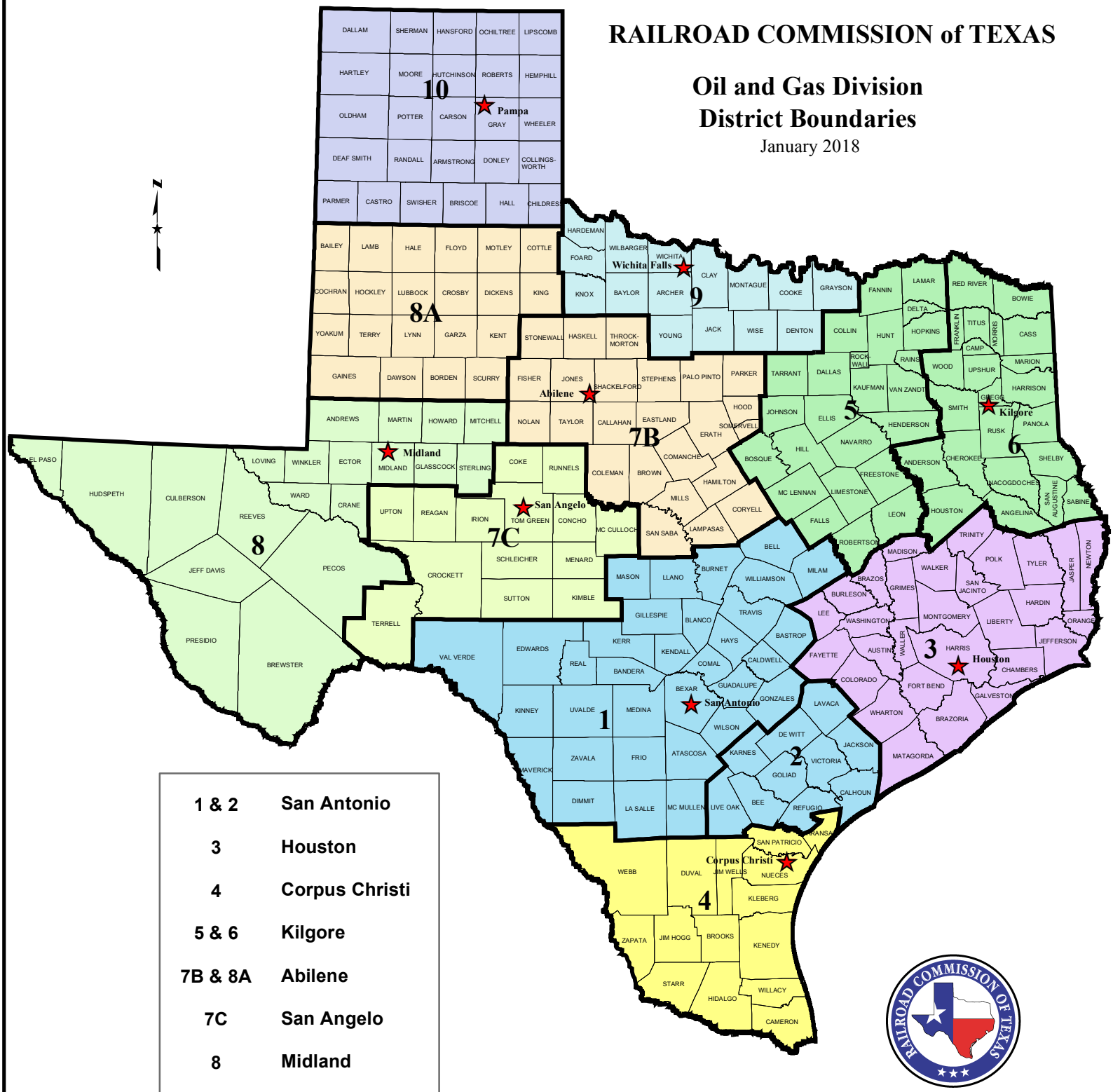

Item 2 – Well Attributes of an Example Dry Well in HI-24L

GIS Identify Results - Well Location Attributes

Number of identify results: 1

Print

Result #1	
API	**708**
GIS WELL NUMBER	7
GIS SYMBOL DESCRIPTION	Dry Hole
GIS LOCATION SOURCE	Commission`s hardcopy map
GIS LAT (NAD27)	29.535831
GIS LONG (NAD27)	-94.150740
GIS LAT (NAD83)	29.536058
GIS LONG (NAD83)	-94.150919

Item 3 – Well Attributes of an Example Active Gas Well in HI-24L

GIS Identify Results - Well Location Attributes

Number of identify results: 1

Print

Result #1		
API	**70830380**	
GIS WELL NUMBER	2	
GIS SYMBOL DESCRIPTION	Gas Well	
GIS LOCATION SOURCE	Coordinates - Operator reported	
GIS LAT (NAD27)	2452294.022638	
GIS LONG (NAD27)	4855552.113189	
GIS LAT (NAD83)	29.522843	
GIS LONG (NAD83)	-94.153627	
Well Logs	Drilling Permits	Disposal Permits

OPERATOR/WELLBORE	
WELLBORE STATUS	OPEN
LAST PERMIT ISSUED	631842
LAST PERMIT OPERATOR NUMBER	895237
LAST PERMIT OPERATOR	WALTER OIL & GAS CORPORATION
LAST PERMIT LEASE NAME	STATE TRACT 24-L N/2 SW/4
TOTAL DEPTH	14146
SURFACE LOCATION	Offshore
ABSTRACT	
SURVEY	
BLOCK	
SECTION	
DISTANCE 1	
DIRECTION 1	
DISTANCE 2	
DIRECTION 2	
Oil/Gas Imaged Records for API:70830380	
COMPLETION RECORD	
PRORATION SCHEDULE	GAS
DISTRICT	03
LEASE/ID	231670
OPERATOR NUMBER	887952
OPERATOR	W&T OFFSHORE, INC.
LEASE NAME	STATE TRACT 24-L N/2 SW/4
FIELD	HIGH ISLAND BLK 24L (LJ)

WELL NUMBER	2
TYPE WELL	PRODUCING
ON SCHEDULE	YES
production data query(pdq)	oil/gas imaged records for lease/id: 231670

Item 4 – Well Attributes of an Example Plugged Well in HI-24L

GIS Identify Results - Well Location Attributes

Number of identify results: 1

Print

Result #1		
API	**70830031**	
GIS WELL NUMBER	C4	
GIS SYMBOL DESCRIPTION	Plugged Gas Well	
GIS LOCATION SOURCE	Commission`s hardcopy map	
GIS LAT (NAD27)	29.517782	
GIS LONG (NAD27)	-94.112303	
GIS LAT (NAD83)	29.518010	
GIS LONG (NAD83)	-94.112481	
Well Logs	Drilling Permits	Disposal Permits

OPERATOR/WELLBORE	
WELLBORE STATUS	PLUG
LAST PERMIT ISSUED	
LAST PERMIT OPERATOR NUMBER	
LAST PERMIT OPERATOR	
LAST PERMIT LEASE NAME	
TOTAL DEPTH	13388
SURFACE LOCATION	Offshore
ABSTRACT	
SURVEY	
BLOCK	
SECTION	
DISTANCE 1	
DIRECTION 1	
DISTANCE 2	
DIRECTION 2	
Oil/Gas Imaged Records for API:70830031	
COMPLETION RECORD	
PRORATION SCHEDULE	GAS
DISTRICT	03
LEASE/ID	049203
OPERATOR NUMBER	029340
OPERATOR	ARCO OIL & GAS CO.
LEASE NAME	STATE LEASE 59456
FIELD	HIGH IS. BLK. 24L (FB-E, IG)

WELL NUMBER	C 4 L
TYPE WELL	HISTORY
ON SCHEDULE	NO
production data query(pdq)	oil/gas imaged records for lease/id: 049203
COMPLETION RECORD	
PRORATION SCHEDULE	GAS
DISTRICT	03
LEASE/ID	049204
OPERATOR NUMBER	029340
OPERATOR	ARCO OIL & GAS CO.
LEASE NAME	STATE LEASE 59456
FIELD	HIGH IS. BLK. 24L (FB-E, HI)
WELL NUMBER	C 4 U
TYPE WELL	HISTORY
ON SCHEDULE	NO
production data query(pdq)	oil/gas imaged records for lease/id: 049204
PLUGGING RECORD	
DATE PLUGGED	08/06/1991
PLUG DEPTH	13338
PLUGGING OPERATOR	
PLUGGED LEASE	

Item 5 – Well Attributes of an Example Orphaned Well in HI-24L

GIS Identify Results - Well Location Attributes

Number of identify results: 1

Print

Result #1		
API	**70830322**	
GIS WELL NUMBER	10	
GIS SYMBOL DESCRIPTION	Gas Well	
GIS LOCATION SOURCE	Coordinates - Operator reported	
GIS LAT (NAD27)	29.550411	
GIS LONG (NAD27)	-94.134604	
GIS LAT (NAD83)	29.550637	
GIS LONG (NAD83)	-94.134783	
Well Logs	Drilling Permits	Disposal Permits

OPERATOR/WELLBORE	
WELLBORE STATUS	OPEN
LAST PERMIT ISSUED	424230
LAST PERMIT OPERATOR NUMBER	883810
LAST PERMIT OPERATOR	VASTAR RESOURCES, INC.
LAST PERMIT LEASE NAME	HIGH ISLAND 24L (SL59455)
TOTAL DEPTH	8100
SURFACE LOCATION	Offshore
ABSTRACT	
SURVEY	HIGH ISLAND AREA, ST. TR. 24L
BLOCK	
SECTION	
DISTANCE 1	7145
DIRECTION 1	W
DISTANCE 2	802
DIRECTION 2	N
Oil/Gas Imaged Records for API:70830322	
COMPLETION RECORD	
PRORATION SCHEDULE	GAS
DISTRICT	03
LEASE/ID	133775
OPERATOR NUMBER	029340
OPERATOR	ARCO OIL & GAS CO.
LEASE NAME	HIGH ISLAND 24L (SL 59455)
FIELD	HIGH IS. BLK. 24L (FB-B, HI)

WELL NUMBER	10
TYPE WELL	HISTORY
ON SCHEDULE	NO
production data query(pdq)	oil/gas imaged records for lease/id: 133775
COMPLETION RECORD	
PRORATION SCHEDULE	GAS
DISTRICT	03
LEASE/ID	140618
OPERATOR NUMBER	029340
OPERATOR	ARCO OIL & GAS CO.
LEASE NAME	HIGH ISLAND 24L (SL 59455)
FIELD	HIGH ISLAND BLK. 24-L (FB-B, HH)
WELL NUMBER	10
TYPE WELL	HISTORY
ON SCHEDULE	NO
production data query(pdq)	oil/gas imaged records for lease/id: 140618
COMPLETION RECORD	
PRORATION SCHEDULE	GAS
DISTRICT	03
LEASE/ID	142347
OPERATOR NUMBER	883810
OPERATOR	VASTAR RESOURCES, INC.
LEASE NAME	HIGH ISLAND 24L (SL 59455)
FIELD	HIGH ISLAND BLK 24L (FB-B, HC)
WELL NUMBER	10
TYPE WELL	HISTORY
ON SCHEDULE	NO
production data query(pdq)	oil/gas imaged records for lease/id: 142347
COMPLETION RECORD	
This well has been classified as an Orphan Well by the RRC. If you are interested in becoming the well operator please use the link below for further instruction. *orphanwelltakeoverprocedure.pdf*	
PRORATION SCHEDULE	GAS
DISTRICT	03
LEASE/ID	150773
OPERATOR NUMBER	430717

OPERATOR	JEFFERSON BLOCK 24 OIL & GAS LLC
LEASE NAME	HIGH ISLAND 24L (SL59455)
FIELD	HIGH IS. BLK. 24L (FB-B, GP)
WELL NUMBER	10
TYPE WELL	TEMP ABANDONED
ON SCHEDULE	YES
production data query(pdq)	oil/gas imaged records for lease/id: 150773

Item 6 – Wellbore Report for High Island Large Block, from 27 May 2021

Wellbore Report, High Island LB county, Y210527

Search Criteria:									
Lease Type: Both									
County: HIGH IS-LB									
Schedule Type: Current									
API No.	District	Lease No.	Lease Name	Well No.	Field Name	Operator Name	County	On Schedule	API Depth
70830385	3	271916	S.T. 23-L N/2 SW/4	1	BLOCK 23-L (LH-0)	ENERGY XXI TEXAS ONSHORE, LLC	HIGH IS-LB	Y	13698
70830385	3	246589	S.T. 23-L N/2 SW/4	1	BLOCK 23L (LH-13)	LLOG EXPLORATION TEXAS, L.P.	HIGH IS-LB	Y	13698
70830385	3	271503	S.T. 23-L N/2 SW/4	1	BLOCK 23L (LH-13)	WALTER OIL & GAS CORPORATION	HIGH IS-LB	Y	13698
70830095	3	73071	STATE TRACT 98-L	1	BLOCK 98-L	SEIRAN E & P COMPANY, LLC	HIGH IS-LB	Y	9440
70830101	3	73070	STATE TRACT 98-L	3	BLOCK 98-L	SEIRAN E & P COMPANY, LLC	HIGH IS-LB	Y	10042
70830283	3	104475	STATE TRACT 98-L	7	BLOCK 98-L	SEIRAN E & P COMPANY, LLC	HIGH IS-LB	Y	9772
70830312	3	125715	STATE TRACT 98-L	8	BLOCK 98-L	SEIRAN E & P COMPANY, LLC	HIGH IS-LB	Y	10068
70830362	3	186724	STATE TRACT 98-L	10	BLOCK 98-L (AMPH B)	SEIRAN E & P COMPANY, LLC	HIGH IS-LB	Y	6597
70830341	3	25327	STATE TRACT 98-L	1	BLOCK 98-L (MA-1)	GULF COAST OPERATIONS, LLC	HIGH IS-LB	Y	10380
70830341	3	25326	STATE TRACT 98-L	1L	BLOCK 98-L (MA-2)	GULF COAST OPERATIONS, LLC	HIGH IS-LB	Y	10380
70830341	3	188834	STATE TRACT 98-L	1U	BLOCK 98-L (MA-4A)	COASTLAND OPERATIONS, LLC	HIGH IS-LB	Y	10380
70830341	3	188835	STATE TRACT 98-L	1L	BLOCK 98-L (SD-A)	COASTLAND OPERATIONS, LLC	HIGH IS-LB	Y	10380
70830032	3	148594	STATE LEASE 59456	C3	HIGH IS BLK.24L(FB-E,GP)	JEFFERSON BLOCK 24 OIL & GAS LLC	HIGH IS-LB	Y	12000
70830046	3	165605	HIGH ISLAND 24L SL 59456	C6	HIGH IS BLK.24L(FB-E,GP)	JEFFERSON BLOCK 24 OIL & GAS LLC	HIGH IS-LB	Y	9150
70830315	3	9726	STATE LEASE 60729	B2U	HIGH IS. BLK. 24L (FB-A, HC)	JEFFERSON BLOCK 24 OIL & GAS LLC	HIGH IS-LB	Y	8476
70830322	3	150773	HIGH ISLAND 24L (SL59455)	10	HIGH IS. BLK. 24L (FB-B, GP)	JEFFERSON BLOCK 24 OIL & GAS LLC	HIGH IS-LB	Y	8100
70800112	3	55960	STATE LEASE 59455	5U	HIGH IS. BLK. 24L (FB-C, GK)	JEFFERSON BLOCK 24 OIL & GAS LLC	HIGH IS-LB	Y	11500
70830311	3	174818	HIGH ISLAND 24L SL 59455	8	HIGH IS. BLK. 24L (FB-C, GK)	JEFFERSON BLOCK 24 OIL & GAS LLC	HIGH IS-LB	Y	8150
70830335	3	138259	STATE LEASE 59455	2-U	HIGH IS. BLK. 24L (FB-C, GK)	JEFFERSON BLOCK 24 OIL & GAS LLC	HIGH IS-LB	Y	9113
70830329	3	9695	STATE LEASE 59455	11U	HIGH IS. BLK. 24L (FB-C, GL)	JEFFERSON BLOCK 24 OIL & GAS LLC	HIGH IS-LB	Y	8740
70800112	3	47122	STATE LEASE 59455	5L	HIGH IS. BLK. 24L (FB-C, HC)	JEFFERSON BLOCK 24 OIL & GAS LLC	HIGH IS-LB	Y	11500
70800113	3	47118	STATE LEASE 59455	3L	HIGH IS. BLK. 24L (FB-C, HC)	JEFFERSON BLOCK 24 OIL & GAS LLC	HIGH IS-LB	Y	8500
70830329	3	138911	S/L 59455, HIGH ISLAND 24L	11-L	HIGH IS. BLK. 24L (FB-C, HC)	JEFFERSON BLOCK 24 OIL & GAS LLC	HIGH IS-LB	Y	8740
70830335	3	47121	STATE LEASE 59455	2L	HIGH IS. BLK. 24L (FB-C, HC)	JEFFERSON BLOCK 24 OIL & GAS LLC	HIGH IS-LB	Y	9113
70830318	3	133033	STATE LEASE 59454	B4	HIGH IS. BLK. 24L (FB-D, HC)	JEFFERSON BLOCK 24 OIL & GAS LLC	HIGH IS-LB	Y	8670
70830327	3	20820	STATE LEASE 59454	B5U	HIGH IS. BLK. 24L (FB-DD, HC)	JEFFERSON BLOCK 24 OIL & GAS LLC	HIGH IS-LB	Y	8956
70830316	3	26154	HIGH ISLAND 24L SL 59455	9ST	HIGH IS. BLK. 24L (FB-DD, HF)	JEFFERSON BLOCK 24 OIL & GAS LLC	HIGH IS-LB	Y	8853
70830327	3	141065	STATE LEASE 59454	B5-L	HIGH IS. BLK. 24L (FB-DD, HF)	JEFFERSON BLOCK 24 OIL & GAS LLC	HIGH IS-LB	Y	8956
70830353	3	23759	HIGH ISLAND 24L SL59456	C13	HIGH IS. BLK. 24L (FB-E, HC)	JEFFERSON BLOCK 24 OIL & GAS LLC	HIGH IS-LB	Y	9344
70830353	3	167568	HIGH ISLAND 24L SL59456	C13	HIGH IS. BLK. 24L (FB-E, HF)	JEFFERSON BLOCK 24 OIL & GAS LLC	HIGH IS-LB	Y	9344
70830347	3	162015	HIGH ISLAND 24L SL 59456	C14	HIGH IS. BLK. 24L (FB-E, IG)	JEFFERSON BLOCK 24 OIL & GAS LLC	HIGH IS-LB	Y	9639
70800094	3	244703	HIGH ISLAND 24-L, N/2, NW/4	A4	HIGH IS. BLK. 24-L (FJ SAND)	JEFFERSON BLOCK 24 OIL & GAS LLC	HIGH IS-LB	Y	9950
70800094	3	26021	HIGH ISLAND 24-L, N/2, NW/4	A4	HIGH IS. BLK. 24L(FB-C, CM-11)	JEFFERSON BLOCK 24 OIL & GAS LLC	HIGH IS-LB	Y	9950
70800113	3	9707	STATE LEASE 59455	3U	HIGH IS. BLK. 24L(FB-C, CM-11)	JEFFERSON BLOCK 24 OIL & GAS LLC	HIGH IS-LB	Y	8500
70830323	3	25415	STATE LEASE 103389	C10	HIGH IS.BLK. 24-L (HD SD)	JEFFERSON BLOCK 24 OIL & GAS LLC	HIGH IS-LB	Y	14320
70830376	3	230456	STATE TRACT 24-L S/2 SW/4	1	HIGH ISLAND BLK 24L (LJ)	W&T OFFSHORE, INC.	HIGH IS-LB	Y	14988
70830380	3	231670	STATE TRACT 24-L N/2 SW/4	2	HIGH ISLAND BLK 24L (LJ)	W&T OFFSHORE, INC.	HIGH IS-LB	Y	14146
70830378	3	249014	MF114921 HI 31-L	1	HIGH ISLAND BLK 30-L (9100)	FIELDWOOD ENERGY OFFSHORE LLC	HIGH IS-LB	Y	10400
70830315	3	20448	STATE LEASE 60729	B2L	HIGH ISLAND BLK. 24-L (FB-A, HF)	JEFFERSON BLOCK 24 OIL & GAS LLC	HIGH IS-LB	Y	8476
70830379	3	251636	MF 106158 HI 31-L	1	HIGH ISLAND BLK. 30 (8700)	FIELDWOOD ENERGY OFFSHORE LLC	HIGH IS-LB	Y	10500
70830379	3	251489	MF106158 HI ST 31-L	1	HIGH ISLAND BLK. 30-L (8985)	FIELDWOOD ENERGY OFFSHORE LLC	HIGH IS-LB	Y	10500
70830389	3	26516	MF114921 HI 31-L	1	HIGH ISLAND BLK. 30-L (8985)	FIELDWOOD ENERGY OFFSHORE LLC	HIGH IS-LB	Y	8956
70830366	3	24635	BLOCK 55-L SW/4	5L	HIGH ISLAND BLK. 55-L (DB-6)	SEIRAN E & P COMPANY, LLC	HIGH IS-LB	Y	8109
70830367	3	204073	BLOCK 55-L SW/4	6L	HIGH ISLAND BLK. 55-L (DB-6)	SEIRAN E & P COMPANY, LLC	HIGH IS-LB	Y	8118
70830366	3	24634	BLOCK 55-L SW/4	5U	HIGH ISLAND BLK.55-L (DISC. B)	SEIRAN E & P COMPANY, LLC	HIGH IS-LB	Y	8109
70830367	3	204070	BLOCK 55-L SW/4	6U	HIGH ISLAND BLK.55-L (DISC. B)	SEIRAN E & P COMPANY, LLC	HIGH IS-LB	Y	8118
70830368	3	207119	BLOCK 55-L SW/4	4	HIGH ISLAND BLK.55-L (DISC. B)	SEIRAN E & P COMPANY, LLC	HIGH IS-LB	Y	8078
70830370	3	208600	BLOCK 56-L S/2, SE/4	1	HIGH ISLAND BLK.55-L (DISC. B-4)	SEIRAN E & P COMPANY, LLC	HIGH IS-LB	Y	8223

Item 7 – Example G-10 Report from Lease ID 230456 in HI-24L

OPERATOR NAME AND ADDRESS including city, state and

W&T OFFSHORE, INC.
ATTN STEVE HAMM
5718 WESTHEIMER ROAD STE 700
HOUSTON,TX,77057

GAS WELL STATUS REPORT

RAILROAD COMMISSION OF TEXAS
Oil and Gas Division
P.O. Box 12967
Austin, TX 78711-2967

Tracking 1639780 Status: Processed

Reason for Filing

[X] Survey [ ] Retest
[ ] Initial Test [ ] Correctio

Operator P-5 Organization 887952

RRC Dist. No. 03

G-

REV.7/95

Test Period: 11/01/2020 through 01/31/2021
Due Date: 02/01/2021
Effective 03/01/2021

FIELD NAME * LEASE NAME	RRC IDENT NO. WELL NO.	DATE TESTED MO/DAY/YR MARK X FOR SHUT-IN WELL	GAS PRODUCED MCF/DAY** GAS SPEC. GRAVITY	CONDENSATE PRODUCED CONDENSATE GRAVITY(API)	WATER PROD (BBL/DAY) X BOTTOMHOLE PREASSURE PSIA	***SIWH PRESSURE PSIA ***FLOWING PRESSURE PSIA
HIGH ISLAND BLK 24L (LJ) STATE TRACT 24-L S/2 SW/4	230456 1	01/04/2021	558 MCF 0.627	0.0 BBL	10 BBL 0	1545 705
			MCF	BBL	BBL	
			MCF	BBL	BBL	
			MCF	BBL	BBL	
			MCF	BBL	BBL	
			MCF	BBL	BBL	
			MCF	BBL	BBL	
			MCF	BBL	BBL	
			MCF	BBL	BBL	
			MCF	BBL	BBL	

CERTIFICATIO I declare under penalties prescribed in Texas Natural Resources Code, Sec.91.143., that I am authorized to make this report, that this report was prepared by me or uder my supervision and direction, and that data and facts stated herin are true, correct, and complete to the best of my knowledge.

Signature: Kathy Mueller, Regulatory Analyst **Title:** Regulatory Analyst **Phone:** (713) 624-7320 **Date:** 02/25/2021

* AN ASTERISK PREPRINTED ON A SURVEY IDENTIFIES WELL SUBJECT TO COMMINGLING TEST REQUIREMENT ** GAS PRODUCTION RATE, IN MCF, IS TO BE REPORTED FULL-WELL STREAM, INCLUDING "X" AN "X" PREPRINTED ON A SURVEY IN THE BOTTOMHOLE PRESSURE BOX INDICATES A BOTTOMHOLE PRESSURE MUST BE REPORTED FOR THE WELL *** PREASSURE FOR THE TEXAS HUGOTON FIELD IS REPORTED IN PSIG

Item 8 – Example G-10 Report from Lease ID 231670 in HI-24L

OPERATOR NAME AND ADDRESS including city, state and

W&T OFFSHORE, INC.
ATTN STEVE HAMM
5718 WESTHEIMER ROAD STE 700
HOUSTON,TX,77057

GAS WELL STATUS REPORT

RAILROAD COMMISSION OF TEXAS
Oil and Gas Division
P.O. Box 12967
Austin, TX 78711-2967

Tracking 1620857 Status: Processed

Reason for Filing

[X] Survey [ ] Retest [ ] Initial Test [ ] Correctio

Operator P-5 Organization 887952

RRC Dist. No. 03

G-

REV.7/95

Test Period: 11/01/2020 through 01/31/2021
Due Date: 02/01/2021
Effective 03/01/2021

FIELD NAME * LEASE NAME	RRC IDENT NO. WELL NO.	DATE TESTED MO/DAY/YR MARK X FOR SHUT-IN WELL	GAS PRODUCED MCF/DAY** GAS SPEC. GRAVITY	CONDENSATE PRODUCED CONDENSATE GRAVITY(API)	WATER PROD (BBL/DAY) X BOTTOMHOLE PREASSURE PSIA	***SIWH PRESSURE PSIA ***FLOWING PRESSURE PSIA
HIGH ISLAND BLK 24L (LJ) STATE TRACT 24-L N/2 SW/4	231670 2	01/17/2021	1733 MCF 0.616	31.0 BBL 50.2	0 BBL	7500 6500
			MCF	BBL	BBL	
			MCF	BBL	BBL	
			MCF	BBL	BBL	
			MCF	BBL	BBL	
			MCF	BBL	BBL	
			MCF	BBL	BBL	
			MCF	BBL	BBL	
			MCF	BBL	BBL	
			MCF	BBL	BBL	

CERTIFICATIO I declare under penalties prescribed in Texas Natural Resources Code, Sec.91.143., that I am authorized to make this report, that this report was prepared by me or uder my supervision and direction, and that data and facts stated herin are true, correct, and complete to the best of my knowledge.

Signature: Kathy Mueller, Regulatory Analyst **Title:** Regulatory Analyst **Phone:** (713) 624-7320 **Date:** 02/01/2021

* AN ASTERISK PREPRINTED ON A SURVEY IDENTIFIES WELL SUBJECT TO COMMINGLING TEST REQUIREMENT ** GAS PRODUCTION RATE, IN MCF, IS TO BE REPORTED FULL-WELL STREAM, INCLUDING "X" AN "X" PREPRINTED ON A SURVEY IN THE BOTTOMHOLE PRESSURE BOX INDICATES A BOTTOMHOLE PRESSURE MUST BE REPORTED FOR THE WELL *** PREASSURE FOR THE TEXAS HUGOTON FIELD IS REPORTED IN PSIG

Item 9 – G-1 Completion Report for Lease ID 231670 in HI-24L

RAILROAD COMMISSION OF TEXAS

Form G-1

1701 N. Congress
P.O. Box 12967
Austin, Texas 78701-2967

Status: Approved
Date: 08/31/2020
Tracking No.: 238195

GAS WELL BACK PRESSURE TEST, COMPLETION OR RECOMPLETION REPORT,

OPERATOR INFORMATION

Operator W&T OFFSHORE, INC. **Operator** 887952
Operator ATTN STEVE HAMM 5718 WESTHEIMER ROAD STE 700 HOUSTON, TX 77057-0000

WELL INFORMATION

API 42-708-30380 **County:** JEFFERSON
Well 2 **RRC District** 03
Lease STATE TRACT 24-L N/2 SW/4 **Field** HIGH ISLAND BLK 24L (LJ)
RRC Gas ID 231670 **Field No.:** 41209975
Location Section: ,Block: , Survey: G.O.M. ST. TR. 24-L, Abstract:

Latitude **Longitud**
This well is 30 **miles in** SW
direction PORT ARTHUR,
which is the nearest town in the

FILING INFORMATION

Purpose of Well Record Only
Type of Other/Recompletion
Well Type: Producing **Completion or Recompletion** 07/10/2020

Type of Permit	Date	Permit No.
Permit to Drill, Plug Back, or	01/18/2007	631842
Rule 37 Exception		
Fluid Injection		
O&G Waste Disposal		
Other:		

COMPLETION INFORMATION

Spud 02/13/2007 **Date of first production after rig** 07/10/2020
Date plug back, deepening, drilling operation 06/28/2020 **Date plug back, deepening, recompletion, drilling operation** 07/10/2020
Number of producing wells on this lease this field (reservoir) including this 1 **Distance to nearest well in lease & reservoir** 0.0
Total number of acres in 720.00 **Elevation** 97 RKB
Total depth TVD 14146 **Total depth MD**
Plug back depth TVD 13661 **Plug back depth MD**
Was directional survey made other inclination (Form W- No **Rotation time within surface casing Is Cementing Affidavit (Form W-15)** No
Recompletion or Yes **Multiple** No
Type(s) of electric or other log(s) None
Electric Log Other Description:
Location of well, relative to nearest lease boundaries of lease on which this well is 654.0 **Feet from the** South **Line and** 1730.2 **Feet from the** West **Line of the** STATE TRACT 24-L N/2 SW/4 **Lease.** **Off Lease:** No

FORMER FIELD (WITH RESERVOIR) & GAS ID OR OIL LEASE NO.

Field & Reservoir	Gas ID or Oil Lease	Well No.	Prior Service Type

G1: N/A

PACKET: N/A

FOR NEW DRILL OR RE-ENTRY, SURFACE CASING DEPTH DETERMINED BY:

GAU Groundwater Protection		**Depth**	0.0	**Date**	01/08/2007
SWR 13 Exception		**Depth**			

GAS MEASUREMENT DATA

Date of **Gas measurement method**

Gas production during test

Was the well preflowed for 48 No

Run No.	Line size	Orif. or Choke Size (in.)	24 hr. Coeff. Orif. Or Choke	Static Pm or Choke (in.)	Diff (hw)	Flow Temp (°F)	Temp. (Ftf)	Gravity (Fg)	Compress (Fpv)	Volume (MCF/day)

N/A

FIELD DATA AND PRESSURE CALCULATIONS

Gravity (dry **Gravity (liquid hydrocarbons) (Deg.**

Gas-Liquid Hydro Ratio (CF/Bbl): **Gravity (mixture):**

Avg. shut in temp. (° **Bottom hole temp. and** **°F@** **FT**

Run	Time of Run (Min.)	Choke Size	Wellhead Pressure	Wellhead Flow Temp (°F)

N/A

CASING RECORD

Ro	Type of Casing	Casing Size (in.)	Hole Size	Setting Depth	Multi - Stage Tool	Multi - Stage Shoe	Cement Class	Cement Amoun	Slurry Volume (cu.	Top of Cement (ft.)	TOC Determined By
1	Surface	20	26	915			A	1960	3654.0	165	Calculation
2	Intermediate	13 3/8	17 1/2	3496			A	2725	4954.0	165	Calculation
3	Intermediate	9 5/8	12 1/4	9880			PREM	2322	3000.0	3000	Calculation

LINER RECORD

Ro	Liner Size	Hole Size (in.)	Liner Top	Liner Bottom	Cement Class	Cement Amoun	Slurry Volume (cu. ft.)	Top of Cement (ft.)	TOC Determined By
1	7 5/8	8 1/2	9642	12950	H	256	320.0	9642	Calculation
2	5 1/2	6 1/2	12753	14146	DENSCRETE	319	287.0	12753	Calculation

TUBING RECORD

Ro	Size (in.)	Depth Size (ft.)	Packer Depth (ft.)/Type
1	3 1/2	13670	13670 / BAKER F1

PRODUCING/INJECTION/DISPOSAL INTERVAL

Ro	Open hole?	From (ft.)	To (ft.)
1	No	L 13475	13540
2	No	L 13619	13625

ACID, FRACTURE, CEMENT SQUEEZE, CAST IRON BRIDGE PLUG, RETAINER, ETC.

Was hydraulic fracturing treatment No

Is well equipped with a downhole actuation sleeve? No

If yes, actuation pressure

Production casing test pressure (PSIG)

Actual maximum pressure (PSIG) during hydraulic fracturing

fracturin

Has the hydraulic fracturing fluid disclosure been

No

Ro	Type of Operation	Amount and Kind of Material Used	Depth Interval (ft.)	
1	Cast Iron Bridge Plug	CIBP AT 13681' WITH 20' CEMENT ON TOP	13661.0	13681.0

FORMATION RECORD

Formations	Encountere	Depth TVD	Depth MD	Is formation isolated?	Remarks
ROB MAYERI	Yes	5960.0		Yes	
SIPH DEBISI	Yes	8730.0		Yes	

Do the producing interval of this well produce H2S with a concentration in excess of 100 ppm No

Is the completion being downhole commingled (SWR No

REMARKS

PLUGBACK AND RECOMPLETE IN SAME FIELD.

RRC REMARKS

PUBLIC COMMENTS:

CASING RECORD :

TUBING RECORD:

PRODUCING/INJECTION/DISPOSAL INTERVAL :

ACID, FRACTURE, CEMENT SQUEEZE, CAST IRON BRIDGE PLUG, RETAINER, ETC. :

GAS MEASUREMENT DATE REMARK:

OPERATOR'S CERTIFICATION			
Printed	Kathy Mueller	**Title**	Regulatory Analyst
Telephone	(713) 624-7320	**Date**	08/21/2020

Item 10 – W-2 Completion Report for Lease ID 26021 in HI-24L

RAILROAD COMMISSION OF TEXAS

Form W-2

1701 N. Congress
P.O. Box 12967
Austin, Texas 78701-2967

Status: Approved
Date: 02/22/2013
Tracking No.: 54014

OIL WELL POTENTIAL TEST, COMPLETION OR RECOMPLETION REPORT,

OPERATOR INFORMATION

Operator JEFFERSON BLOCK 24 OIL & GAS LLC **Operator** 430717
Operator 4820 HOLLY TREE DR DALLAS, TX 75287-0000

WELL INFORMATION

API 42-708-00094 **County:** JEFFERSON
Well No.: A 4 **RRC District** 03
Lease HIGH ISLAND 24-L, N/2, NW/4 **Field** HIGH IS. BLK. 24L(FB-C, CM-11)
RRC Lease 26021 **Field No.:** 41209120
Location Section: ,Block: , Survey: G.O.M. HIGH ISLAND 24-L, Abstract:

Latitude **Longitud**
This well is **miles in a**
direction from 16 MILES SOUTHEAST OF HIGH ISLAND,
which is the nearest town in the

FILING INFORMATION

Purpose of Initial Potential
Type of Plug Back
Well Type: Producing **Completion or Recompletion** 08/20/2012

Type of Permit	Date	Permit No.
Permit to Drill, Plug Back, or	09/11/2012	747421
Rule 37 Exception		
Fluid Injection		
O&G Waste Disposal		
Other:		

COMPLETION INFORMATION

Spud **Date of first production after rig** 08/20/2012
Date plug back, deepening, drilling operation 08/19/2012 **Date plug back, deepening, recompletion, drilling operation** 08/20/2012
Number of producing wells on this lease this field (reservoir) including this 1 **Distance to nearest well in lease & reservoir** 0.0
Total number of acres in 720.00 **Elevation** 0 GL
Total depth TVD 9950 **Total depth MD**
Plug back depth TVD 6505 **Plug back depth MD**
Was directional survey made other inclination (Form W- No **Rotation time within surface casing Is Cementing Affidavit (Form W-15)** No
Recompletion or No **Multiple** No
Type(s) of electric or other log(s) None
Electric Log Other Description:

Location of well, relative to nearest lease of lease on which this well is 2006.0 **Feet from the** North **Line and** 5495.0 **Feet from the** West **Line of the** HIGH ISLAND 24-L, N/2, NW/4 **Lease.** **Off Lease :** No

FORMER FIELD (WITH RESERVOIR) & GAS ID OR OIL LEASE NO.

	Field & Reservoir	Gas ID or Oil Lease	Well No.	Prior Service Type
W2:	N/A			

PACKET	HIGH IS. BLK. 24-L (FJ SAND)	244703	A 4

FOR NEW DRILL OR RE-ENTRY, SURFACE CASING DEPTH DETERMINED BY:

GAU Groundwater Protection Determination	**Depth**	**Date**	04/24/2007
SWR 13 Exception	**Depth**		

INITIAL POTENTIAL TEST DATA FOR NEW COMPLETION OR RECOMPLETION

Date of	08/28/2012	**Production**	Gas Lift
Number of hours	24	**Choke**	
Was swab used during this	No	**Oil produced prior to**	0.00

PRODUCTION DURING TEST PERIOD:

Oil	116.00	**Gas**	784
Gas - Oil	6758	**Flowing Tubing**	330.00
Water	2347		

CALCULATED 24-HOUR RATE

Oil	116.0	**Gas**	784
Oil Gravity - API - 60.:	36.0	**Casing**	810.00
Water	2347		

CASING RECORD

Ro	Type of Casing	Casing Size (in.)	Hole Size	Setting Depth	Multi - Stage Tool	Multi - Stage Shoe	Cement Class	Cement Amoun	Slurry Volume (cu.	Top of Cement (ft.)	TOC Determined By
1		20	26	627			A	1250	0.0	0	
2		10 3/4	15	2542			H	1700	2615.0	0	
3		7 5/8	9 7/8	9950			H	740	799.0	5020	

LINER RECORD

Ro	Liner Size	Hole Size	Liner Top	Liner Bottom	Cement Class	Cement Amoun	Slurry Volume (cu.	Top of Cement (ft.)	TOC Determined

N/A

TUBING RECORD

Ro	Size (in.)	Depth Size (ft.)	Packer Depth (ft.)/Type
1	2 7/8	5554	5554 /

PRODUCING/INJECTION/DISPOSAL INTERVAL

Ro	Open hole?	From (ft.)	To (ft.)
1	No	L 5728	5750.0
2	No	L 5768	5778.0

ACID, FRACTURE, CEMENT SQUEEZE, CAST IRON BRIDGE PLUG, RETAINER, ETC.

Was hydraulic fracturing treatment No

Is well equipped with a downhole sleeve? No

If yes, actuation pressure

Production casing test pressure (PSIG)

Actual maximum pressure (PSIG) during hydraulic fracturing

fracturin

Has the hydraulic fracturing fluid disclosure been

No

Ro	Type of Operation	Amount and Kind of Material Used	Depth Interval (ft.)	
1		CLOSED SLIDING SLEEVE @ 6462	6480	6502
2		OPENED SLIDING SLEEVE @ 5716, SET 7 5/8 RETRIEVABLE PKR @ 5788	5728	5778

FORMATION RECORD

Formations	Encountere	Depth TVD	Depth MD	Is formation	Remarks
NA		0.0			
NA		0.0			
NA		0.0			

Do the producing interval of this well produce H2S with a concentration in excess of 100 ppm No

Is the completion being downhole commingled No

REMARKS

WELL WAS ORIGINALLY DRILLED IN THE SIXTIES; NO FORMATION RECORD AVAIL. ALL INFORMATION PROVIDED BY OPERATOR. MARY ANN ZABOROWSKI

RRC REMARKS

PUBLIC COMMENTS:

CASING RECORD :

NO USABLE QUALITY WATER AT THIS LOCATION.

TUBING RECORD:

PRODUCING/INJECTION/DISPOSAL INTERVAL :

ACID, FRACTURE, CEMENT SQUEEZE, CAST IRON BRIDGE PLUG, RETAINER, ETC. :

POTENTIAL TEST DATA:

OPERATOR'S CERTIFICATION			
Printed	Mary Ann Zaborowski	**Title:**	Regulatory Manager
Telephone	(281) 698-8555	**Date**	01/21/2013

Item 11 – Inactive Well List for HI-24L as of 08 May 2021

Inactive Well List, TX RRC, Y210508, filtered for HI-24L

Operator Number	Operator Name	API County Number	API Unique Number	County Name	O/G Code	District Code	Lease Number
430717	JEFFERSON BLOCK 24 OIL & GAS LLC	708	94	HIGH IS-LB	G	03	244703
430717	JEFFERSON BLOCK 24 OIL & GAS LLC	708	94	HIGH IS-LB	O	03	26021
430717	JEFFERSON BLOCK 24 OIL & GAS LLC	708	112	HIGH IS-LB	G	03	55960
430717	JEFFERSON BLOCK 24 OIL & GAS LLC	708	112	HIGH IS-LB	G	03	47122
430717	JEFFERSON BLOCK 24 OIL & GAS LLC	708	113	HIGH IS-LB	O	03	9707
430717	JEFFERSON BLOCK 24 OIL & GAS LLC	708	113	HIGH IS-LB	G	03	47118
430717	JEFFERSON BLOCK 24 OIL & GAS LLC	708	30032	HIGH IS-LB	G	03	148594
430717	JEFFERSON BLOCK 24 OIL & GAS LLC	708	30046	HIGH IS-LB	G	03	165605
430717	JEFFERSON BLOCK 24 OIL & GAS LLC	708	30311	HIGH IS-LB	G	03	174818
430717	JEFFERSON BLOCK 24 OIL & GAS LLC	708	30315	HIGH IS-LB	O	03	9726
430717	JEFFERSON BLOCK 24 OIL & GAS LLC	708	30315	HIGH IS-LB	O	03	20448
430717	JEFFERSON BLOCK 24 OIL & GAS LLC	708	30316	HIGH IS-LB	O	03	26154
430717	JEFFERSON BLOCK 24 OIL & GAS LLC	708	30318	HIGH IS-LB	G	03	133033
430717	JEFFERSON BLOCK 24 OIL & GAS LLC	708	30322	HIGH IS-LB	G	03	150773
430717	JEFFERSON BLOCK 24 OIL & GAS LLC	708	30323	HIGH IS-LB	O	03	25415
430717	JEFFERSON BLOCK 24 OIL & GAS LLC	708	30327	HIGH IS-LB	O	03	20820
430717	JEFFERSON BLOCK 24 OIL & GAS LLC	708	30327	HIGH IS-LB	G	03	141065
430717	JEFFERSON BLOCK 24 OIL & GAS LLC	708	30329	HIGH IS-LB	O	03	9695
430717	JEFFERSON BLOCK 24 OIL & GAS LLC	708	30329	HIGH IS-LB	G	03	138911
430717	JEFFERSON BLOCK 24 OIL & GAS LLC	708	30335	HIGH IS-LB	G	03	138259
430717	JEFFERSON BLOCK 24 OIL & GAS LLC	708	30335	HIGH IS-LB	G	03	47121
430717	JEFFERSON BLOCK 24 OIL & GAS LLC	708	30347	HIGH IS-LB	G	03	162015
430717	JEFFERSON BLOCK 24 OIL & GAS LLC	708	30353	HIGH IS-LB	O	03	23759
430717	JEFFERSON BLOCK 24 OIL & GAS LLC	708	30353	HIGH IS-LB	G	03	167568

Inactive Well List, TX RRC, Y210508, filtered for HI-24L

API County Number	API Unique Number	Well Number	Oil Unit Number	Lease Name	Field Number
708	94	A 4		HIGH ISLAND 24-L, N/2, NW/4	41142500
708	94	A 4		HIGH ISLAND 24-L, N/2, NW/4	41209120
708	112	5 U		STATE LEASE 59455	41209155
708	112	5 L		STATE LEASE 59455	41209200
708	113	3 U		STATE LEASE 59455	41209120
708	113	3 L		STATE LEASE 59455	41209200
708	30032	C 3		STATE LEASE 59456	41209505
708	30046	C 6		HIGH ISLAND 24L SL 59456	41209505
708	30311	8		HIGH ISLAND 24L SL 59455	41209155
708	30315	B 2 U		STATE LEASE 60729	41209040
708	30315	B 2L		STATE LEASE 60729	41209045
708	30316	9ST		HIGH ISLAND 24L SL 59455	41209491
708	30318	B 4		STATE LEASE 59454	41209360
708	30322	10		HIGH ISLAND 24L (SL59455)	41209058
708	30323	C 10		STATE LEASE 103389	41142600
708	30327	B 5U		STATE LEASE 59454	41209490
708	30327	B 5-L		STATE LEASE 59454	41209491
708	30329	11 U		STATE LEASE 59455	41209160
708	30329	11-L		S/L 59455, HIGH ISLAND 24L	41209200
708	30335	2-U		STATE LEASE 59455	41209155
708	30335	2 L		STATE LEASE 59455	41209200
708	30347	C 14		HIGH ISLAND 24L SL 59456	41209680
708	30353	C 13		HIGH ISLAND 24L SL59456	41209520
708	30353	C 13		HIGH ISLAND 24L SL59456	41209600

Inactive Well List, TX RRC, Y210508, filtered for HI-24L

API County Number	API Unique Number	Field Name	Water/Land Code	API Depth	Shut In Date	P5 Renewal Month	P5 Renewal Year
708	94	HIGH IS. BLK. 24-L (FJ SAND)	O	9950	201609	2	2022
708	94	HIGH IS. BLK. 24L(FB-C, CM-11)	O	9950	201609	2	2022
708	112	HIGH IS. BLK. 24L (FB-C, GK)	O	11500	201607	2	2022
708	112	HIGH IS. BLK. 24L (FB-C, HC)	O	11500	201607	2	2022
708	113	HIGH IS. BLK. 24L(FB-C, CM-11)	O	8500	200203	2	2022
708	113	HIGH IS. BLK. 24L (FB-C, HC)	O	8500	200203	2	2022
708	30032	HIGH IS BLK.24L(FB-E,GP)	O	12000	199801	2	2022
708	30046	HIGH IS BLK.24L(FB-E,GP)	O	9150	199901	2	2022
708	30311	HIGH IS. BLK. 24L (FB-C, GK)	O	8150	199901	2	2022
708	30315	HIGH IS. BLK. 24L (FB-A, HC)	O	8476	201609	2	2022
708	30315	HIGH ISLAND BLK. 24-L (FB-A, HF)	O	8476	201609	2	2022
708	30316	HIGH IS. BLK. 24L (FB-DD, HF)	O	8853	201609	2	2022
708	30318	HIGH IS. BLK. 24L (FB-D, HC)	O	8670	201508	2	2022
708	30322	HIGH IS. BLK. 24L (FB-B, GP)	O	8100	199801	2	2022
708	30323	HIGH IS.BLK. 24-L (HD SD)	O	14320	201511	2	2022
708	30327	HIGH IS. BLK. 24L (FB-DD, HC)	O	8956	201609	2	2022
708	30327	HIGH IS. BLK. 24L (FB-DD, HF)	O	8956	201609	2	2022
708	30329	HIGH IS. BLK. 24L (FB-C, GL)	O	8740	201607	2	2022
708	30329	HIGH IS. BLK. 24L (FB-C, HC)	O	8740	201607	2	2022
708	30335	HIGH IS. BLK. 24L (FB-C, GK)	O	9113	199806	2	2022
708	30335	HIGH IS. BLK. 24L (FB-C, HC)	O	9113	199806	2	2022
708	30347	HIGH IS. BLK. 24L (FB-E, IG)	O	9639	200205	2	2022
708	30353	HIGH IS. BLK. 24L (FB-E, HC)	O	9344	201609	2	2022
708	30353	HIGH IS. BLK. 24L (FB-E, HF)	O	9344	201609	2	2022

Inactive Well List, TX RRC, Y210508, filtered for HI-24L

API County Number	API Unique Number	P5 Originating Status	Current 5 Yr Inactive	Current 10 Yr Inactive	Aged 5 Year Inactive	Aged 10 Year Inactive	Current Inactive Years	Current Inactive Months	Aged Inactive Years
708	94	D			Y		4	8	5
708	94	D			Y		4	8	5
708	112	D			Y		4	10	5
708	112	D			Y		4	10	5
708	113	D		Y		Y	19	2	19
708	113	D		Y		Y	19	2	19
708	30032	D		Y		Y	23	4	24
708	30046	D		Y		Y	22	4	23
708	30311	D		Y		Y	22	4	23
708	30315	D			Y		4	8	5
708	30315	D			Y		4	8	5
708	30316	D			Y		4	8	5
708	30318	D	Y		Y		5	9	6
708	30322	D		Y		Y	23	4	24
708	30323	D	Y		Y		5	6	6
708	30327	D			Y		4	8	5
708	30327	D			Y		4	8	5
708	30329	D			Y		4	10	5
708	30329	D			Y		4	10	5
708	30335	D		Y		Y	22	11	23
708	30335	D		Y		Y	22	11	23
708	30347	D		Y		Y	19	0	19
708	30353	D			Y		4	8	5
708	30353	D			Y		4	8	5

Inactive Well List, TX RRC, Y210508, filtered for HI-24L

API County Number	API Unique Number	Aged Inactive Months	Extension Status						
708	94	5	D						X
708	94	5	D						X
708	112	7	D						X
708	112	7	D						X
708	113	11	D						X
708	113	11	D						X
708	30032	1	D						X
708	30046	1	D						X
708	30311	1	D						X
708	30315	5	D						X
708	30315	5	D						X
708	30316	5	D						X
708	30318	6	D						X
708	30322	1	D						X
708	30323	3	D						X
708	30327	5	D						X
708	30327	5	D						X
708	30329	7	D						X
708	30329	7	D						X
708	30335	8	D						X
708	30335	8	D						X
708	30347	9	D						
708	30353	5	D						
708	30353	5	D						

Inactive Well List, TX RRC, Y210508, filtered for HI-24L

API County Number	API Unique Number	Extension Denial Data							
708	94	O				R			
708	94	O				R			
708	112	O				R			
708	112	O				R			
708	113	O				R			
708	113	O				R			
708	30032	O				R			
708	30046	O				R			
708	30311	O				R			
708	30315	O				R			
708	30315	O				R			
708	30316	O				R			
708	30318	O				R			
708	30322	O				R			
708	30323	O				R			
708	30327	O				R			
708	30327	O				R			
708	30329	O				R			
708	30329	O				R			
708	30335	O				R			
708	30335	O				R			
708	30347	O				R			
708	30353	O				R			
708	30353	O				R			

Inactive Well List, TX RRC, Y210508, filtered for HI-24L

API County Number	API Unique Number	Cost Calculation	Well Plugged	Compliance Due Date	Original Completion Date	5 Yr. Phase-In	
708	94	0	N	0	19690617		
708	94	0	N	0	19690617		
708	112	0	N	0	19690430		
708	112	0	N	0	19690430		
708	113	0	N	0	19690121		
708	113	0	N	0	19690121		
708	30032	0	N	0	19851130		
708	30046	0	N	0	19700704		
708	30311	0	N	0	19870324		
708	30315	0	N	0	19890127		
708	30315	0	N	0	19890127		
708	30316	0	N	0	19890126		
708	30318	0	N	0	19890224		
708	30322	0	N	0	19891201		
708	30323	0	N	0	19900419		
708	30327	0	N	0	19900826		
708	30327	0	N	0	19900826		
708	30329	0	N	0	19900929		
708	30329	0	N	0	19900929		
708	30335	0	N	0	19690716		
708	30335	0	N	0	19690716		
708	30347	0	N	0	19961123		
708	30353	0	N	0	19970303		
708	30353	0	N	0	19970303		

Item 12 – Orphan Well List for HI-24L as of 21 May 2021

Orphan Well List, TX RRC, Y210521, filtered for HI-24L

District	API Number	OFCU Well Priority	Status	Operator Name	Operator Number
03	70800094			JEFFERSON BLOCK 24 OIL & GAS LLC	430717
03	70800112			JEFFERSON BLOCK 24 OIL & GAS LLC	430717
03	70800113			JEFFERSON BLOCK 24 OIL & GAS LLC	430717
03	70830032			JEFFERSON BLOCK 24 OIL & GAS LLC	430717
03	70830046			JEFFERSON BLOCK 24 OIL & GAS LLC	430717
03	70830311			JEFFERSON BLOCK 24 OIL & GAS LLC	430717
03	70830315			JEFFERSON BLOCK 24 OIL & GAS LLC	430717
03	70830316			JEFFERSON BLOCK 24 OIL & GAS LLC	430717
03	70830318			JEFFERSON BLOCK 24 OIL & GAS LLC	430717
03	70830322			JEFFERSON BLOCK 24 OIL & GAS LLC	430717
03	70830323			JEFFERSON BLOCK 24 OIL & GAS LLC	430717
03	70830327			JEFFERSON BLOCK 24 OIL & GAS LLC	430717
03	70830329			JEFFERSON BLOCK 24 OIL & GAS LLC	430717
03	70830335			JEFFERSON BLOCK 24 OIL & GAS LLC	430717
03	70830347			JEFFERSON BLOCK 24 OIL & GAS LLC	430717
03	70830353			JEFFERSON BLOCK 24 OIL & GAS LLC	430717

Orphan Well List, TX RRC, Y210521, filtered for HI-24L

API Number	Lease Name	Lease Number	Well Number	BONDED_DEPTH
70800094	HIGH ISLAND 24-L, N/2, NW/4	26021	A 4	9950
70800112	STATE LEASE 59455	047122	5 L	11500
70800113	STATE LEASE 59455	09707	3 U	8500
70830032	STATE LEASE 59456	148594	C 3	12000
70830046	HIGH ISLAND 24L SL 59456	165605	C 6	9150
70830311	HIGH ISLAND 24L SL 59455	174818	8	8150
70830315	STATE LEASE 60729	20448	B 2L	8476
70830316	HIGH ISLAND 24L SL 59455	26154	9ST	8853
70830318	STATE LEASE 59454	133033	B 4	8670
70830322	HIGH ISLAND 24L (SL59455)	150773	10	8100
70830323	STATE LEASE 103389	25415	C 10	14320
70830327	STATE LEASE 59454	20820	B 5U	8956
70830329	S/L 59455, HIGH ISLAND 24L	138911	11-L	8740
70830335	STATE LEASE 59455	047121	2 L	9113
70830347	HIGH ISLAND 24L SL 59456	162015	C 14	9639
70830353	HIGH ISLAND 24L SL59456	23759	C 13	9344

Orphan Well List, TX RRC, Y210521, filtered for HI-24L

API Number	Field Name	County	SFP Code	ICE Inspection Date
70800094	HIGH IS. BLK. 24L(FB-C, CM-11)	HIGH IS-LB		5/1/2017
70800112	HIGH IS. BLK. 24L (FB-C, HC)	HIGH IS-LB		5/1/2017
70800113	HIGH IS. BLK. 24L(FB-C, CM-11)	HIGH IS-LB		5/1/2017
70830032	HIGH IS BLK.24L(FB-E,GP)	HIGH IS-LB		5/1/2017
70830046	HIGH IS BLK.24L(FB-E,GP)	HIGH IS-LB		5/1/2017
70830311	HIGH IS. BLK. 24L (FB-C, GK)	HIGH IS-LB		5/1/2017
70830315	HIGH ISLAND BLK. 24-L (FB-A, HF)	HIGH IS-LB		5/1/2017
70830316	HIGH IS. BLK. 24L (FB-DD, HF)	HIGH IS-LB		5/1/2017
70830318	HIGH IS. BLK. 24L (FB-D, HC)	HIGH IS-LB		5/1/2017
70830322	HIGH IS. BLK. 24L (FB-B, GP)	HIGH IS-LB		5/1/2017
70830323	HIGH IS.BLK. 24-L (HD SD)	HIGH IS-LB		5/1/2017
70830327	HIGH IS. BLK. 24L (FB-DD, HC)	HIGH IS-LB		5/1/2017
70830329	HIGH IS. BLK. 24L (FB-C, HC)	HIGH IS-LB		5/1/2017
70830335	HIGH IS. BLK. 24L (FB-C, HC)	HIGH IS-LB		5/1/2017
70830347	HIGH IS. BLK. 24L (FB-E, IG)	HIGH IS-LB		5/1/2017
70830353	HIGH IS. BLK. 24L (FB-E, HC)	HIGH IS-LB		5/1/2017

Orphan Well List, TX RRC, Y210521, filtered for HI-24L

API Number	ICE Last Inspection ID	SB639-Enf	SB639-R15	Operator Months Delinquent
70800094	215979	Enf		44
70800112	215984	Enf		44
70800113	215986	Enf		44
70830032	213965	Enf		44
70830046	213966	Enf		44
70830311	215970	Enf		44
70830315	215992	Enf		44
70830316	213974	Enf		44
70830318	213975	Enf		44
70830322	215987	Enf		44
70830323	213970	Enf		44
70830327	215969	Enf		44
70830329	215972	Enf		44
70830335	215975	Enf		44
70830347	213964	Enf		44
70830353	213969	Enf		44

Item 13 – Gas Proration Schedule for HI-24L as of 27 May 2021

Gas Proration Schedule, TX RRC, Y210527, filtered for HI-24L

Search Criteria:												
District: 03												
API No.	District	Lease No.	Lease Name	Well No.	Field No.	Field Name	Field Type	Operator No.	Operator Name	Acres	Deliv. (MCF)	Allowable
70800094	3	244703	HIGH ISLAND 24-L, N/2, NW/4	A 4	41142500	HIGH IS. BLK. 24-L (FJ SAND)		430717	JEFFERSON BLOCK 24 OIL & GAS LLC	0	0	0 K
70800112	3	55960	STATE LEASE 59455	5 U	41209155	HIGH IS. BLK. 24L (FB-C, GK)		430717	JEFFERSON BLOCK 24 OIL & GAS LLC	0	0	0 J
70800112	3	47122	STATE LEASE 59455	5 L	41209200	HIGH IS. BLK. 24L (FB-C, HC)		430717	JEFFERSON BLOCK 24 OIL & GAS LLC	80	0	0 K
70800113	3	47118	STATE LEASE 59455	3 L	41209200	HIGH IS. BLK. 24L (FB-C, HC)		430717	JEFFERSON BLOCK 24 OIL & GAS LLC	80	0	0 K
70830032	3	148594	STATE LEASE 59456	C 3	41209505	HIGH IS BLK.24L(FB-E,GP)		430717	JEFFERSON BLOCK 24 OIL & GAS LLC	0	0	0 K
70830046	3	165605	HIGH ISLAND 24L SL 59456	C 6	41209505	HIGH IS BLK.24L(FB-E,GP)		430717	JEFFERSON BLOCK 24 OIL & GAS LLC	0	0	0 K
70830311	3	174818	HIGH ISLAND 24L SL 59455	8	41209155	HIGH IS. BLK. 24L (FB-C, GK)		430717	JEFFERSON BLOCK 24 OIL & GAS LLC	0	0	0 K
70830318	3	133033	STATE LEASE 59454	B 4	41209360	HIGH IS. BLK. 24L (FB-D, HC)		430717	JEFFERSON BLOCK 24 OIL & GAS LLC	80	0	0 K
70830322	3	150773	HIGH ISLAND 24L (SL59455)	10	41209058	HIGH IS. BLK. 24L (FB-B, GP)		430717	JEFFERSON BLOCK 24 OIL & GAS LLC	0	0	0 K
70830327	3	141065	STATE LEASE 59454	B 5-L	41209491	HIGH IS. BLK. 24L (FB-DD, HF)		430717	JEFFERSON BLOCK 24 OIL & GAS LLC	0	0	0 K
70830329	3	138911	S/L 59455, HIGH ISLAND 24L	11-L	41209200	HIGH IS. BLK. 24L (FB-C, HC)		430717	JEFFERSON BLOCK 24 OIL & GAS LLC	80	0	0 K
70830335	3	138259	STATE LEASE 59455	2-U	41209155	HIGH IS. BLK. 24L (FB-C, GK)		430717	JEFFERSON BLOCK 24 OIL & GAS LLC	0	0	0 J
70830335	3	47121	STATE LEASE 59455	2 L	41209200	HIGH IS. BLK. 24L (FB-C, HC)		430717	JEFFERSON BLOCK 24 OIL & GAS LLC	80	0	0 K
70830347	3	162015	HIGH ISLAND 24L SL 59456	C 14	41209680	HIGH IS. BLK. 24L (FB-E, IG)		430717	JEFFERSON BLOCK 24 OIL & GAS LLC	80	0	0 K
70830353	3	167568	HIGH ISLAND 24L SL59456	C 13	41209600	HIGH IS. BLK. 24L (FB-E, HF)		430717	JEFFERSON BLOCK 24 OIL & GAS LLC	80	0	0 K
70830376	3	230456	STATE TRACT 24-L S/2 SW/4	1	41209975	HIGH ISLAND BLK 24L (LJ)		887952	W&T OFFSHORE, INC.	0	558	540 X
70830380	3	231670	STATE TRACT 24-L N/2 SW/4	2	41209975	HIGH ISLAND BLK 24L (LJ)		887952	W&T OFFSHORE, INC.	0	1733	46590 X

Item 14 – Oil Proration Schedule for HI-24L as of 28 May 2021

Oil Proration Schedule, TX RRC, Y210528, High Island, filtered for HI-24L

Search Criteria:						
County: HIGH IS-LB						
API No.	District	Lease No.	Lease Name	Well No.	Field No	Field Name
70830315	3	9726	STATE LEASE 60729	B 2 U	41209040	HIGH IS. BLK. 24L (FB-A, HC)
70830329	3	9695	STATE LEASE 59455	11 U	41209160	HIGH IS. BLK. 24L (FB-C, GL)
70830327	3	20820	STATE LEASE 59454	B 5U	41209490	HIGH IS. BLK. 24L (FB-DD, HC)
70830316	3	26154	HIGH ISLAND 24L SL 59455	9ST	41209491	HIGH IS. BLK. 24L (FB-DD, HF)
70830353	3	23759	HIGH ISLAND 24L SL59456	C 13	41209520	HIGH IS. BLK. 24L (FB-E, HC)
70800094	3	26021	HIGH ISLAND 24-L, N/2, NW/4	A 4	41209120	HIGH IS. BLK. 24L(FB-C, CM-11)
70800113	3	9707	STATE LEASE 59455	3 U	41209120	HIGH IS. BLK. 24L(FB-C, CM-11)
70830323	3	25415	STATE LEASE 103389	C 10	41142600	HIGH IS.BLK. 24-L (HD SD)
70830315	3	20448	STATE LEASE 60729	B 2L	41209045	HIGH ISLAND BLK. 24-L (FB-A, HF)

Oil Proration Schedule, TX RRC, Y210528, High Island, filtered for HI-24L

Search Criteria:							
County: HIGH IS-LB							
API No.	District	Lease No.	Field Type	Operator No.	Operator Name	Unit No.	Potential (BBL)
70830315	3	9726	REGULAR	430717	JEFFERSON BLOCK 24 OIL & GAS LLC		0
70830329	3	9695	REGULAR	430717	JEFFERSON BLOCK 24 OIL & GAS LLC		0
70830327	3	20820	REGULAR	430717	JEFFERSON BLOCK 24 OIL & GAS LLC		0
70830316	3	26154	REGULAR	430717	JEFFERSON BLOCK 24 OIL & GAS LLC		0
70830353	3	23759	REGULAR	430717	JEFFERSON BLOCK 24 OIL & GAS LLC		0
70800094	3	26021	REGULAR	430717	JEFFERSON BLOCK 24 OIL & GAS LLC		0
70800113	3	9707	REGULAR	430717	JEFFERSON BLOCK 24 OIL & GAS LLC		0
70830323	3	25415	REGULAR	430717	JEFFERSON BLOCK 24 OIL & GAS LLC		0
70830315	3	20448	REGULAR	430717	JEFFERSON BLOCK 24 OIL & GAS LLC		0

Oil Proration Schedule, TX RRC, Y210528, High Island, filtered for HI-24L

Search Criteria:						
County: HIGH IS-LB						
API No.	District	Lease No.	Gas/Oil Ratio	Acres	Daily Allowable - Oil / Gas	Unit or Well Type
70830315	3	9726	0	80	DELINQUENT W-10	SHUT IN
70830329	3	9695	0	80	DELINQUENT W-10	SHUT IN
70830327	3	20820	26785	0	* H-15 VIOLATION *	NO PRODUCTION
70830316	3	26154	1563	0	* H-15 VIOLATION *	NO PRODUCTION
70830353	3	23759	53947	0	14B2 EXT DENIED	NO PRODUCTION
70800094	3	26021	2077	80	* H-15 VIOLATION *	NO PRODUCTION
70800113	3	9707	0	80	* H-15 VIOLATION *	SHUT IN
70830323	3	25415	25102	0	* H-15 VIOLATION *	NO PRODUCTION
70830315	3	20448	1008	0	* H-15 VIOLATION *	NO PRODUCTION

Appendix E

Trimeric - Wellbore Status and Spud Dates

Wellbore Status and Spud Date (*as of spring, 2023*)

Table C.1. Well Tallies for Galveston Area Federal Database, by Wellbore Status and Spud Date

	Galveston							
Number of UWIs/APIs	778	**Spud Date**						
Wellbore status		< 1970	1970 – 1979	1980 – 1989	1990 – 1999	2000 – 2009	2010-2022	Unknown
Sidetrack/Bypass	110	10	21	16	36	16	11	0
Cancelled	2	0	0	0	0	0	0	2
Completed	20	0	2	0	4	5	9	0
Permanently Abandoned	639	174	79	170	164	49	3	0
Temporarily Abandoned	6	0	3	0	1	2	0	0
Drilling Active	0	0	0	0	0	0	0	0
Approved Sidetrack	1	0	0	0	0	0	0	0

Table A.2. Well Tallies for High Island Area Federal Database, by Wellbore Status and Spud Date

	High Island							
Number of UWIs/APIs	3881	**Spud Date**						
Wellbore status		< 1970	1970 – 1979	1980 – 1989	1990 – 1999	2000 – 2009	2010 – 2022	Unknown
Sidetrack/Bypass	1000	12	250	286	272	170	10	0
Cancelled	108	0	0	0	0	0	0	108
Completed	186	0	23	47	54	53	9	0
Permanently Abandoned	2434	101	830	691	479	318	15	0
Temporarily Abandoned	153	1	37	50	39	21	5	0
Drilling Active	0	0	0	0	0	0	0	0
Approved Sidetrack	0	0	0	0	0	0	0	0

Table A.3. Well Tallies for East Breaks Area Federal Database, by Wellbore Status and Spud Date

	East Breaks							
Number of UWIs/APIs	433	**Spud Date**						
Wellbore status		< 1970	1970 – 1979	1980 – 1989	1990 – 1999	2000 – 2009	2010 – 2022	Unknown
Sidetrack/Bypass	158	0	1	71	37	47	2	0
Cancelled	12	0	0	0	0	0	0	12
Completed	53	0	0	27	8	18	0	0
Permanently Abandoned	186	0	21	52	38	72	3	0
Temporarily Abandoned	23	0	0	20	1	1	1	0
Drilling Active	1	0	0	0	0	0	1	0

Table A.4. Well Tallies for Garden Banks Area Federal Database, by Wellbore Status and Spud Date

	Garden Banks							
Number of UWIs/APIs	802	**Spud Date**						
Wellbore status		< 1970	1970 – 1979	1980 – 1989	1990 – 1999	2000 – 2009	2010 – 2022	Unknown
Sidetrack/Bypass	378	0	1	47	109	186	35	0
Cancelled	6	0	0	0	0	3	1	2
Completed	62	0	0	0	12	31	19	0
Permanently Abandoned	318	0	8	63	137	96	14	0
Temporarily Abandoned	38	0	0	1	26	7	4	0

Table A.5. Well Tallies for Keathley Canyon Area Federal Database, by Wellbore Status and Spud Date

	Keathley Canyon							
Number of UWIs/APIs	129	**Spud Date**						
Wellbore status		< 1970	1970 – 1979	1980 – 1989	1990 – 1999	2000 – 2009	2010– 2022	Unknown
Sidetrack/Bypass	56	0	0	0	0	13	43	0
Cancelled	7	0	0	0	0	0	0	7
Completed	17	0	0	0	0	1	16	0
Permanently Abandoned	42	0	0	0	1	13	28	0
Temporarily Abandoned	6	0	0	0	0	2	4	0
Drilling Active	1	0	0	0	0	0	1	0
Approved Sidetrack	0	0	0	0	0	0	0	0

Appendix F

Aker - CO_2 Storage Offshore Facilities Evaluation

GoMCarb CO_2 Storage – BP2 Offshore Facilities Evaluation

Rev. 01

Table of Contents

List of Figures

List of Tables

1 Executive Summary

Aker Solutions is committed to developing projects and sustainable technologies that contribute to the development of low carbon solutions. This vision for the future of the energy business, and decades of experience make Aker Solution a key partner in complex CCS projects. Norther Lights, executed in collaboration with Equinor in Norway, is an example of our ambitions goals. Aker Solutions is also part of the LINCCS project that aims to promote collaboration between partners to identify and develop solutions across the entire CCS value chain. This valuable experience is brought to the GOMCarb project.

In Budget Period 2, Aker Solutions builds on the information provided in previous work /1/ and offers new insights on field operational requirements and applicable technologies. The study explores philosophies and design criteria based on best industry practices. This approach takes into consideration the early nature of the project and offers a broad understanding of the impact that uncertain design factors can have on the recommendations (Appendix A).

As for the basis of the design, the study considers that a CO_2 capture plant will be located onshore whereas injection will take place offshore. The base case describes an onshore/offshore pipeline servicing 5 injection wells located in shallow water in High Island 24-L (HI 24L). The study compares different field topologies and concludes that for the given well count and top hole locations, a daisy chain configuration is an efficient solution.

The discussion on subsea systems and topside injection facilities is common in shallow waters of the Gulf of Mexico. The offshore wells are initially recommended to be developed as shallow water platforms with dry trees. This is mainly defined by the OPEX cost for subsea equipment, the potential for high marine growth and risk for ocean users.

The proposal includes a control system with an onshore control station and an umbilical connecting the offshore wells. An all-electric system with communication on power cables is recommended as a cost effective solution.

Budget and schedule estimates are updated in BP2 for both dry and subsea options along with a technology readiness assessment.

As further design data is consolidated, the report concludes with a summary of future work and additional tasks necessary to increase the level of confidence in the recommended solutions.

Aker Solutions is proud of being part of this work in collaboration with the other consortium partners that will surely drive the future development of CCS in the Gulf of Mexico.

2 Introduction

2.1 Background

Gulf of Mexico Partnership for Offshore Carbon Storage (GoMCarb) aims to ensure the safe, long term, and economically viable offshore storage of carbon in the Gulf of Mexico region. GoMCarb and a concurrent partnership led by SECARB focuses on assessing offshore geologic carbon storage beneath the Gulf of Mexico. Although, the offshore region provides unique challenges to carbon storage, it also provides unique opportunities.

The GoMCarb partnership compiles data and expertise in the region, integrating academic research institutions, government entities, and industry affiliates to address knowledge gaps, regulatory issues, infrastructure requirements, and geologic and engineering technical challenges associated with storing CO_2. Deep underground offshore geologic reservoirs offer the most practical, cost-effective, and low-risk storage options for reducing CO_2 emissions and promoting commercial development in the region. While Carbon Capture and Storage (CCS) has been researched for almost two decades, only recently have the opportunities and advantages of offshore storage beneath the seafloor of the Gulf of Mexico been identified.

The states bordering the Gulf of Mexico (Texas, Louisiana, Mississippi, Alabama, and Florida) emit a large proportion of total U.S. CO_2 emissions from industrial sources, at the same time the surrounding offshore geology provides some of the greatest potential for CO_2 storage. As one of the most explored subsurface geologic basins in the world (for oil and natural gas), the Gulf of Mexico (GOM) is data-rich and well-understood with large storage resources and high-quality seals. The GOM offshore basin is one of the largest volume regional geologic sinks in the United States for large-scale CCS activities.

The lessons learned in the Gulf of Mexico can be applied to other offshore areas nationally, enabling major reductions in national emissions. The integration of capture, transport, and permanent geologic storage is crucial to further develop offshore storage options.

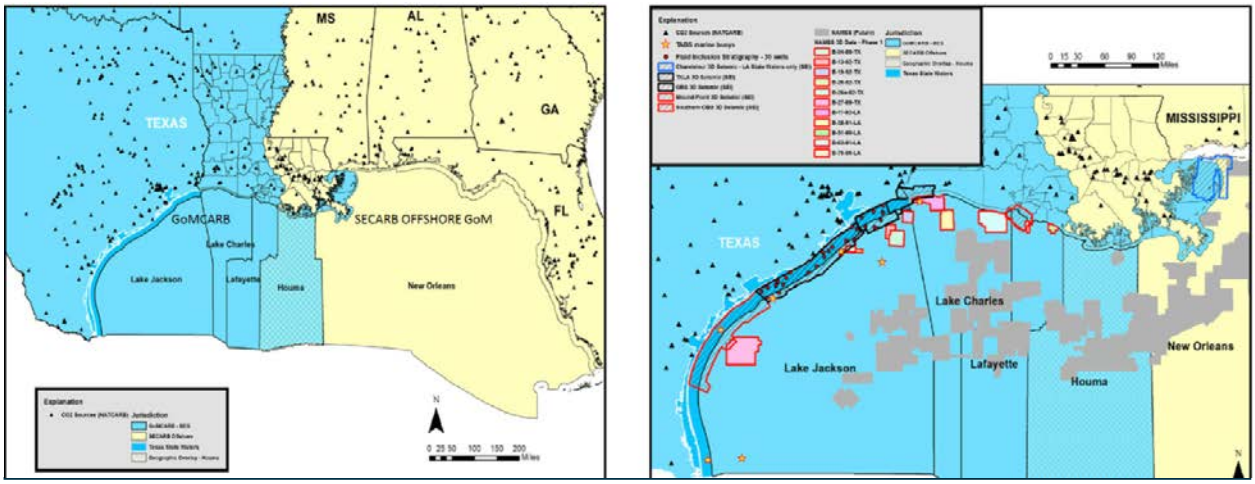

Figure 2-1. Northern GOM Map Showing Primary Geographic Region of Interest

2.2 Objective

Aker Solutions has defined the following objectives for Budget Period 2:

- To thoroughly examine development options and recommend an efficient field architecture.
- To update and develop design basis and philosophies to ensure effective and safe operations.
- To evaluate subsea and dry injection tree options for shallow water in the Gulf of Mexico and recommend the most appropriate alternative.
- To propose a safe, robust, and technically advanced design for the main equipment and components required for the project.
- To assess the technical maturity of the proposed solutions and identify any perceived technology gaps that may require further attention.
- To re-evaluate costs and equipment lead times based on the new design proposals.

2.3 Scope of Work

Aker Solutions is one of the principal peers assigned to contribute to Task 5-Infrastructure. The general scope of Task 5 is to identify options for offshore CO_2 transport and delivery, assess logistics, risks and regulations in the Gulf region, and evaluate the feasibility of decommissioning and re-purposing existing infrastructure to facilitate offshore CO_2 storage.

Aker Solutions' scope of work for the project is to provide detailed descriptions of suitable offshore systems and solutions. It is understood that other consortium members will be responsible for describing reservoir and well completion, monitoring, onshore facilities, onshore to offshore pipeline network, existing infrastructure, and corresponding costs, as applicable.

2.4 Assumptions & Clarifications

Aker Solutions made a number of assumptions in the course of this study work:

- Five wells are assumed as the base case (configuration presented in Figure 3-1). Additional wells can be added at a later stage if necessary.
- High Island 24-L (HI 24L) is used as representative site. The site is assumed to have similar characteristics as a potential future project.
- The wells are located in 60ft water depth and approximately 2.3km apart. The impact of changes in this design parameter is discussed throughout the document.
- Aker Solutions has assumed a set of design criteria/boundaries to assess feasibility, development conditions, limitations and opportunities. Main field development and operating assumptions are included in Section 3.
- 1 MTA per injection well is considered as basis for injection.
- CO_2 source and quality are not currently defined. It is considered that there is an onshore CO_2 capture plant with the required equipment to compresses CO_2 for transport in dense phase.
- Currently there are no facilities on site, and this is considered a green field development. Re-using of neighboring infrastructure is not considered at this stage.

2.5 Team Composition

The Aker Solutions execution team consisted of a multidisciplinary and experienced group with personnel from: Front End, Flow Assurance, Offshore Facilities, Subsea, Power and Controls. The different groups were located in the USA and Norway.

2.6 Battery Limits

Aker Solutions has considered the following battery limits.

CO_2 Processing Plant and Compression Station

CO_2 capture and required compression equipment are not within the scope of this document.

Pipeline/In-Line Structures/Jumpers

The scope of Aker Solutions starts at the connection flange between the tree and the jumper spool. Onshore/offshore pipeline(s), inline structures and jumpers are usually included in the SURF package and therefore excluded from this work.

Chemical Injection

While the document has outlined typical chemical injection requirements, detailed definition of chemical injection skids and similar onshore facilities are not part of the study scope.

On-Shore Control Room

Aker Solutions' scope includes the Control Room equipment located at shore-crossing except the chemical injection skids and hook up to other facilities (power, water, communications). Buildings are excluded from this scope of work as well as control equipment at other locations and integration with other control systems.

Offshore Injection Equipment

The scope of work includes offshore equipment related to well access, platforms, XMT, distribution and interconnection systems. However, wellhead and sub-surface equipment are not considered part of the study scope.

Power/Controls Umbilical

Power and controls umbilical and required terminations, distribution equipment and connections to the well are included in the scope.

3 Basis for Design

Aker Solutions has develop a basis for design based on the limited information available at this stage. The purpose of the following sections is to provide preliminary data to support initial flow assurance studies and, consequently, system design. A detailed design basis will need to be stablished when more data becomes available.

3.1 Design Parameters

3.1.1 Site Characteristics and CO_2 Storage

The GoMCarb development is initially based on a 5-wells CO_2 injection system located above the aquifer formation in High Island 24-L (HI 24L). The injection wells are situated in the sand layers close to the bottom of the reservoir and are expected to inject a total of 1 MTA/well of CO_2. It is anticipated that all wells required to achieve the injection targets will be managed within one injection system. However, contingency and flexibility should be added for future expansion.

CO_2 migration in the aquifer formation over the field's life has yet to be confirmed. Currently, the well spacing is set at 2.3km, but this will need to be verified in future phases. The need and location of potential monitoring wells will also need to be evaluated in future work.

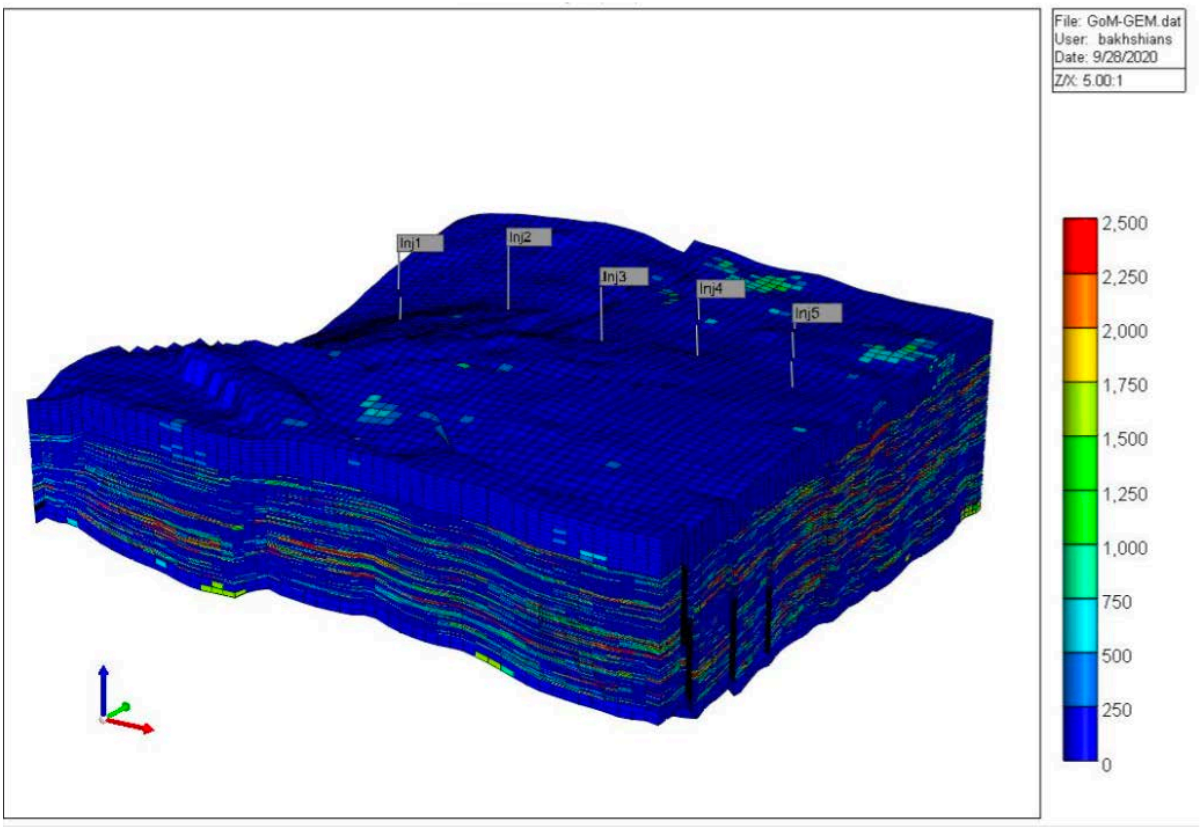

Figure 3-1. Formation and Well Locations

3.1.2 CO_2 Composition

It is recommended that CO_2 is transported and injected in the supercritical state. It is assumed that the system is sized to ensure correct pressure profiles, and the reservoir pressure is sufficiently high to secure liquid phase conditions at the wellhead for all operational scenarios and flowrates.

The flow stream should aim to achieve 99% CO_2 purity. High levels of impurities, such as N_2 and CH_4, should be avoided, as they can cause:

- A two-phase operating region under certain injection scenarios.
- A reduction in available operating envelope for single-phase transport.
- An increase in required pipeline wall thickness to meet the running ductile fracture criteria due to the increase in saturation pressure.
- A reduction in CO_2 storage capacity due to reductions of CO_2 density.

Free water in the CO_2 stream should be avoided.

3.1.3 Water Depth

Water depth at injection site is assumed to be 60ft.

3.1.4 Operating Life

The operating life for the field development is 30 years. If well(s) may potentially serve as reservoir monitoring wells beyond the injection service life, equipment design considerations should be made to extend the service life of the specific asset.

3.1.5 Design Pressure

The design pressure will be determined as part of flow assurance analyses and based on the observed operating pressures, governing design codes and recommendations. Initially, it is expected that the operating pressure will be in the range of 150-300 bara. Therefore, it is recommended to consider offshore equipment design pressure of 345 bar/5,000 psi.

3.1.6 Design Temperature

No active heating of the pipeline or insulation is currently being considered for the study case. The CO_2 temperature will decline in the offshore pipeline, and the normal operating temperature will be close to sea water temperature (in the range of 10°C to 15°C in this water depth).

During transient events involving depressurization, lower temperatures than the normal operating temperatures may occur. Flow assurance studies will be necessary to confirm operational scenarios and equipment design temperature.

3.1.7 Soil Conditions

In order to carry out the conceptual and detailed design of the structural foundations, it is necessary to have site-specific soil conditions. However, at present, these conditions have not been defined. Therefore, typical soil conditions for the area can be used for this study.

3.2 Design Philosophies and Functional Requirements

Generic functional requirements for an injection system have been identified for the purpose of this study. Field specific functional requirements will be developed once reservoir simulations are performed, injection targets are determined, drilling strategies are clarified, well locations are defined and flow assurance analyses are concluded. The functional requirements proposed in this section are based on present engineering experience and knowledge from ongoing and planned offshore CO_2 injection systems.

3.2.1 Systems Availability

The equipment and control system will be designed to optimize reliability and availability with minimum maintenance and intervention. Recommendations for operating the equipment will be included in operation manuals during detailed engineering.

3.2.2 Control System Philosophy

Onshore control of the offshore injection system is stablished as the base case option. Specific functional requirements for the controls system will be developed in future phases.

An all-electric system approach has been considered the base case as discussed in Section 8.1.

3.2.3 Barrier Philosophy

The barrier philosophy for the system is intended to ensure safe operation and control of unwanted releases to the environment. As base case, the well barrier set-up shall be in accordance with Norsok D-010 for CO_2 injection well design, including trees. This approach is based on the following considerations:

- The loss of containment of a CO_2 well/reservoir is of a high criticality level due to large CO_2 spill to the environment, which can potentially lead to significant economic and environmental consequences (including the potential loss of equipment/infrastructure).
- A CO_2 well may potentially be exposed to a hydrocarbon reservoir.
- Existing CO_2 injection wells are planned with a well construction equivalent to a well utilized for hydrocarbons production.

The system shall be designed with a minimum of two barriers towards the environment at all intervention access points, where one of the two barriers can be a passive barrier element. In a temporary condition, such as change-out of equipment during intervention, a single barrier

between active flowline and environment is acceptable, provided that the single barrier has been verified ahead of disconnecting the second (passive) barrier.

Periodic well barrier verification is traditionally performed by pressure testing, either as an in-flow test with pressure from reservoir and pressure evacuation from the opposite side or as a pressure test by creating the required differential pressure across the barrier by use of MEG/MeOH. Testing is performed at certain intervals, with more frequent testing in the early service life of the well. This testing philosophy will need to be aligned with regulatory requirements.

It is presently assumed that CO_2 injection wells will require conventional DHSV as the primary well barrier. With regards to other types of barriers in the upper well completion, the following alternatives can be considered:

- Plug; glass type and/or mechanical type
- Tubing isolation valve(s)

3.2.4 Annulus Monitoring and Pressure Management

Annulus pressure management is an essential aspect of well integrity management. Generally, annulus pressure must be maintained and monitored at the desired levels. In CO_2 injection wells, the annulus pressure may drop in the start-up phase as the annulus cools from CO_2 flow. This may cause the liquid level in the annulus to fall below the readable pressure gauge at the XMT while injecting. One traditional way of managing this challenge is to top up the annulus with MEG/MeOH to achieve a positive pressure that can be monitored by the XMT annulus PTT sensors. In the opposite operational scenario (well heating up after a well shut-in), pressure is bled down through the umbilical service line. Other methods of managing and monitoring annulus pressure can be explored:

- Accepting low pressure conditions in the annulus with the absence of direct pressure reading and relying on pressure readings from the downhole pressure gauges.
- Introducing an inert gas into the annulus as a passive pressure compensator, which could potentially allow autonomous control of the annulus pressure without the need for direct actions.

For CO_2 injection wells, annulus pressure management by service line may need to be accommodated either as a primary function or as a contingency function. As the response time for acting upon any event on annulus pressure may be short, either as a primary or as a secondary method, valve actuation needs to be maintained by remote operations and any MEG/MeOH service should be supplied via permanent umbilical facilities.

Alternative ways of depressurizing CO_2 are proposed to potentially avoid implementing an umbilical line for bleed off (service line):

- Bleed off to dedicated ROV skid with an accumulator bank, assuming test activity is supported by intervention.
- Bleed off to sea. However, regulatory requirements and physical behavior of depressurizing liquid/dense phase to sea need further investigation.

A service access system should be implemented in the tree system to allow access to the injection and annulus bores for the following purposes:

- To conduct contingency chemical or other washout fluid treatment in well/reservoir.
- For hydrate remediation purposes.
- To carry out well circulation operations as required.

As a preliminary guidance, the service access system in the tree should have a minimum bore size of 2” ID.

3.2.5 Pigging Philosophy

For the offshore injection system, it is considered that inspection and operational pigging will be required during the operating life of the field. It is recommended to have a system designed for one-way pipeline pigging after installation along with pigging facilities for the pipeline (i.e. pig receivers/launchers).

The following pigging operations should be considered during the design of the flowline system:

- Pipeline pigging during pipeline installation and RFO (Ready For Operation) activities.
- Pipeline inspection pigging at regular intervals.
- Operational pigging as a contingency to remove pipeline debris and liquid.

3.2.6 Material Selection Philosophy

When selecting materials for offshore systems that transport CO_2, the main philosophy is to minimize full life-cycle costs, ensure the intended production design life and maintain the fabrication schedule. It is crucial to select suitable materials that are compatible with specific CO_2 properties and composition.

If H_2S is present in the aquifer, equipment in contact with injection and aquifer fluids should be designed, as minimum, as Class EE according to API 17D.

For CO_2 injection systems, special considerations should be made regarding the interaction of polymers and CO_2 as polymers can be damaged or degraded over time. It is generally recommended to avoid the use of polymers with CO_2 in vapor phase. The absorption rate in polymers increases when CO_2 is in supercritical phase. Currently, there is a lack of empirical tests evaluating the performance of polymers and CO_2 in supercritical phase, therefore it is recommended to avoid the use of polymers also in these conditions and use metal-to-metal seals as both primary and secondary seals.

For dense phase CO_2, metal-to-metal seals are recommended as primary barrier. Secondary barriers can be of polymeric material such as PEEK, PTFE or FFKM. If other materials are selected, testing may be necessary.

3.2.7 Chemical Injection Philosophy

It is considered that intermittent chemical injection will be required at the XMT and downhole. The equipment will be designed to allow MEG/MeOH injection for preservation and barrier testing. Other chemical injection requirements may be identified as once the operating philosophy is developed.

Any chemicals required to preserve the pipeline upstream of the shore crossing will be injected at CO_2 terminal. It should be possible to inject chemicals at ILTs and other locations from intervention vessels or via subsea ROV skid.

Wax, asphaltene, scale, or sand are not expected.

3.2.8 Protection Philosophy

Permanently installed equipment will be protected. The design criteria for equipment protection from dropped object loads are dependent on the impact energy, location and frequency with which lifting operation will be performed.

Where significant dropped object potential exists, impact protection criteria for equipment should be based on the risks associated with potential dropped objects.

It is considered that all subsea equipment will require to be fishing-friendly. The system should have a dropped object protection, covering the XT, distribution equipment and umbilical interface.

Ship collision requirements related to shallow water structures should be considered as part of the design.

3.2.9 Inspection, Maintenance, and Repair (IMR) Philosophy

All components will be designed for the project's target availability, operability, and maintainability requirements and, where possible, without the need for regular planned intervention maintenance over the field life. Items that are prone to failure, should be designed for replacement as required.

Well intervention with wireline and coil tubing must be possible.

3.2.10 Tie-In Philosophy

Diver flanges are considered for tie-in of main equipment to pipeline.

3.2.11 Subsea Operations

Both ROV and diver operations are considered possible for the field. As general principle, it is recommended to design equipment functions for either ROV or diver operations to avoid a mix of interfaces and tools.

3.2.12 HSSE Philosophy

The overall goal is to minimize harm to people, environment and asset in all project phases. The ALARP principle should be applied to all concept evaluations to ensure risks are kept as low as reasonably possible.

The system is designed considering that the CO_2 onshore terminal will maintain the required safety functions to protect the offshore system from over-pressurization.

In the event of well shutdown initiated by host facilities via power cut, well barrier valves in well and tree will close.

3.2.13 Operational Safety Philosophy

CO_2 is toxic to humans at certain concentrations and exposure durations. Accidental releases may also form dry ice and expose personnel and piping/equipment to very low temperatures in the vicinity of the sublimation temperature (- 78.5°C).

CO_2 is also a heavy gas causing slow dispersion in air during accidents. It tends to form clouds at ground level and dispersion is influenced by terrain topology.

Operational risks may also include salt precipitation, acidized formation water and CO_2 hydrate.

Operational safety requires further investigation including:

- Defining major accident hazards.
- Mapping relevant safety barriers (gas detection, segment isolation, depressurization system, escape, safe area, etc.).
- Investigating the consequences of potential major accidents.
- Proposing risk-reducing measures where appropriate.

3.2.14 Flow Management

Injection Choke

A remotely operated choke valve is required for flow control of each well. The choke and controls system should enable automatic regulation of the injection pressure, which is crucial for optimizing the injection rate and ensuring that the CO_2 remains in a dense phase.

While the expected wear on the choke valve is low under CO_2 service and flowing conditions, it should still be independently retrievable to ensure timely maintenance and prevent any potential disruptions in the injection process. To establish the required choke Cv range, flow assurance analyses should be performed to determine the appropriate range for optimal operation.

Flow metering

Virtual metering is suggested as the base case, but physical single-phase flowmeters, such as Venturi-type meters, may also be considered.

3.2.15 Well Design and Intervention Philosophy

There is a current need for agreed and common industry practices related to the design of CO_2 injection wells. This includes qualification of well barrier elements, testing for medium to long term integrity and low temperatures. A CO_2 resistant design includes considerations related to CO_2 resistant cement, casing, tubing, packers and other exposed downhole and surface equipment. A common industry practice is also needed concerning plug and abandonment of CO_2 injection wells.

Well completion configurations are determined based on geological and reservoir characteristics through the drilling program. A slim well casing program with 5” and 7” tubing options is considered the base case for this study.

An 18 3/4" size connector with a rig BOP interface is recommended for the well, as these systems are qualified for a wide range of applications in the Gulf of Mexico. Alternatively, lighter 13 5/8" systems can be considered, although the tubing size may limit the number of downhole lines that can be run through the tubing hanger.

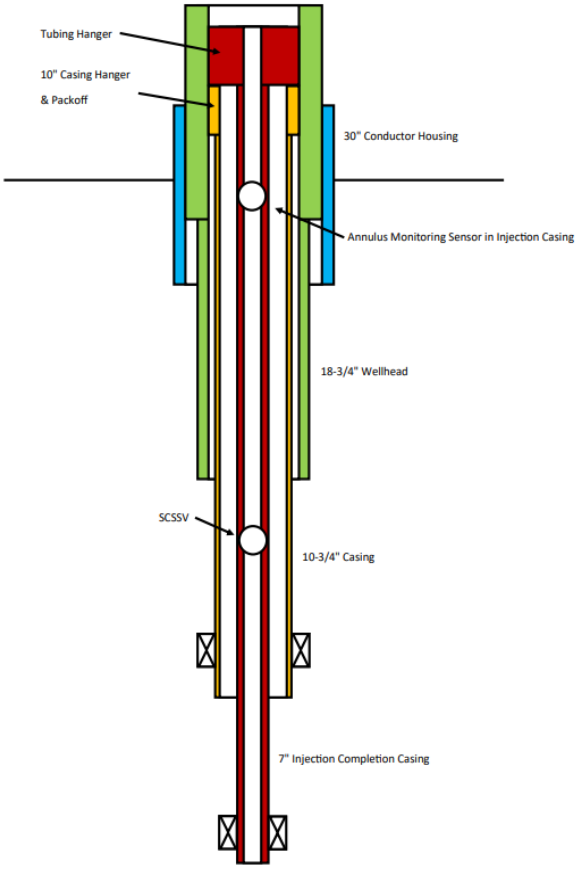

Figure 3-2. Well Architecture - Example

A jack-up/barge drilling rig is assumed to be used for drilling and completion, as a water depth of 60ft is too shallow for a semi-submersible or other drill rig designs. The well(s) will be designed for possible intervention with coiled tubing, wireline and slick line. Installation and retrieval of subsea components, including the XMT, are planned to be performed by RLWI or IMR vessel.

Heavy workover operations are not anticipated but the designs should allow this type of intervention.

3.2.16 Downhole Functionality

The following downhole functionalities are assumed.

Function	Type	No. feed through lines	Comment
SCSSV	Electric	1	Pending on vendor selection
Fibre optic	FO	1	DAS or DTS
Smart Completion	Electric	1	
Chemical Injection	Hydrualic	1	ID to be determined

Table 3-1. Downhole Functions

3.2.17 Instrumentation and Monitoring

The required instrumentation and monitoring equipment will be defined as part of the operating philosophy to ensure safe operation of the system.

Well monitoring is essential. The offshore injection XMTs will be equipped with downhole fiber optic and downhole gauges for monitoring of the aquifer formation.

A leak detection system is required for detection of potential CO_2 /2/. A BAT assessment, supported by system evaluations and analyses, will determine the appropriate leak detection technology. Subsea, active and passive acoustic leak technologies are potential candidates. Alternatively, or complementary, leakage detection based on mass balance monitoring system may be considered. In this case, leak detection is based on the correspondence between onshore measured CO_2 flow, pressure and temperature compared to offshore measured flow, pressure and temperature at the injection well.

Monitoring of CO_2 injection, acquisition and interpretation of various kinds of well and reservoir data are important for control during the injection period and beyond /3/. Monitoring data can be acquired in the injection and observation well(s) by means of instrumentation and by surface measurements (see Section 8.6).

3.2.18 Constructability and Installability

The main equipment should be designed to be easily installable and retrievable. Weight, installation methodology, and intervention should be carefully considered to allow conventional installation vessels to perform offshore operations.

3.2.19 Reuse of Existing Facilities

The reuse of existing oil and gas networks/facilities is an option, but this will require thorough integrity assessments to determine the remaining equipment life. For the purpose of this study, reuse of existing facilities is not considered.

3.2.20 ALARP Principle

Aker Solutions has applied the ALARP (As Low As Reasonably Possible) principle to all designs and operations. The ALARP principle is commonly used in engineering and process safety to reduce risks to the lowest possible level, taking into account technical feasibility and economic viability. The overall ALARP process is based on three steps: 1) Identification of the potential risk improvement; 2) Evaluations and recommendations; 3) Recording and approval.

Additional risk reductions should continue in future phases in the form of HAZIDs and HAZOPs. These studies help to identify potential hazards and risks associated with the project, assess their potential impact, and recommend measures to mitigate them.

3.2.21 BAT Principle and Technology Maturity Evaluation

The CO_2 injection and transport builds on technologies deployed for the O&G industry /4/. The BAT principle is critical in selecting the most appropriate technology to ensure safe and efficient operations, this includes the selection of equipment that is mature and has been qualified for use. In addition, new technologies that may be better adapted to the unique requirements of CO_2 will be developed in the medium term.

Aker Solutions has investigated, as part of the study, different options available on the market to propose the best possible solutions. Technology maturity and qualification status have been key drivers in the selection and design of the equipment. Future work will be required to optimize the concepts and propose technologies that may be better adapted to CO_2 transport and injection.

4 Design Codes and Norms

In general, the majority of design norms and codes for CO_2 transportation and injection derive from the O&G industry. Some specialized codes and standards have been developed to address CO_2 capture, transportation, and geological storage, such as the ISO 279xx series. DNV has also published recommended practices for CO_2 transportation in pipelines. Yet, the design of offshore equipment still relies heavily on existing O&G standards, which have been updated to include a CO_2 injection component.

The following is an indicative list of codes, recommended practices and standards that are commonly applied to CO_2 transport and offshore injection systems.

Design Code	Title	Revision
49 CFR § 195	Transportation of hazardous liquids by pipeline	2022
ASME B31.4	Pipeline Transportation Systems for Liquids and Slurries	2019
ASME B31.8	Gas Transmission and Distribution Piping Systems	2020
ISO 13623	Petroleum and natural gas industries — Pipeline transportation systems	2017
ISO 27913	Carbon dioxide capture, transportation and geological storage — Pipeline transportation systems	2016
DNV-ST-F101	Submarine pipeline systems	2021
DNV-RP-F104	Design and operation of carbon dioxide pipelines	2021
ISO 13628 Series	Petroleum and natural gas industries — Design and operation of subsea production systems	
ISO 10423/API 6A	Petroleum and natural gas industries — Drilling and production equipment — Wellhead and tree equipment	2022
ISO 15156	Petroleum and natural gas industries — Materials for use in H_2S-containing environments in oil and gas production	2020
API RP 555	Process Analysers	
API STD 521	Pressure-relieving and Depressuring Systems, Sixth Edition	
ASME B31.3	Process Piping	
ASME BPVC.VIII-2	ASME Boiler and Pressure Vessel Code Division 2 Alternative Rules	2021
TEMA	Tubular Exchanger Manufacturing Association	10th Edition
API STD 520 Part I	Sizing, Selection, and Installation of Pressure-Relieving Devices in Refineries; Part I - Sizing and Selection	
API STD 520 Part II	Sizing, Selection, and Installation of Pressure-relieving Devices Part II-Installation - 6th Edition	
API RP 551	Process Measurement Instrumentation	
IEC 60534	Industrial Process Control Valves	
ISO 5167	Fluid Measurement with Orifice Plates, Nozzles and Venturi Tubes Inserted in Circular cross-section Conduits Running Full	
API 17F	Standard for Subsea Production Control Systems	4th Edition
DNV-RP-F109	On-bottom stability design of submarine pipelines, cables and umbilicals	2021
DNV – CO_2 Wells	Guideline for risk management of existing wells at CO2 geological storage sites	2011

Table 4-1. Applicable Standards

5 Concept of Operations

The concept of operations, design parameters and philosophies form the basis for the field architecture. The following considerations are made:

- CO_2 is transported from the onshore plant to offshore wells in a single pipeline with enough pressure in the fluid to be injected in the desired conditions.
- The CO_2 is kept in single phase (super critical condition, dense phase) in all operating conditions.
- The pipeline is considered to be 10.75” OD – 0.6” WT and allows pigging from onshore facility to pipeline end.
- The injection rate is 1 MTA/well. CO_2 is supplied without free water. Hydrate formation in pipeline systems is not considered as a credible risk during normal operation. However, hydrate remediation and contingency measures should be identified.
- Any chemical required to maintain pipeline integrity will be injected at the onshore location.
- 5off offshore wells are identified, located 3-10 miles off the Texas Gulf coast, and 2.3km apart.
- Wells are drilled vertically, and an injection tree is placed on top of the well. A jack-up rig is required for drilling and intervention operations.
- A control room is located onshore, and a control umbilical services the offshore wells.
- Flow into single well is regulated by a remotely operated choke at each well location.

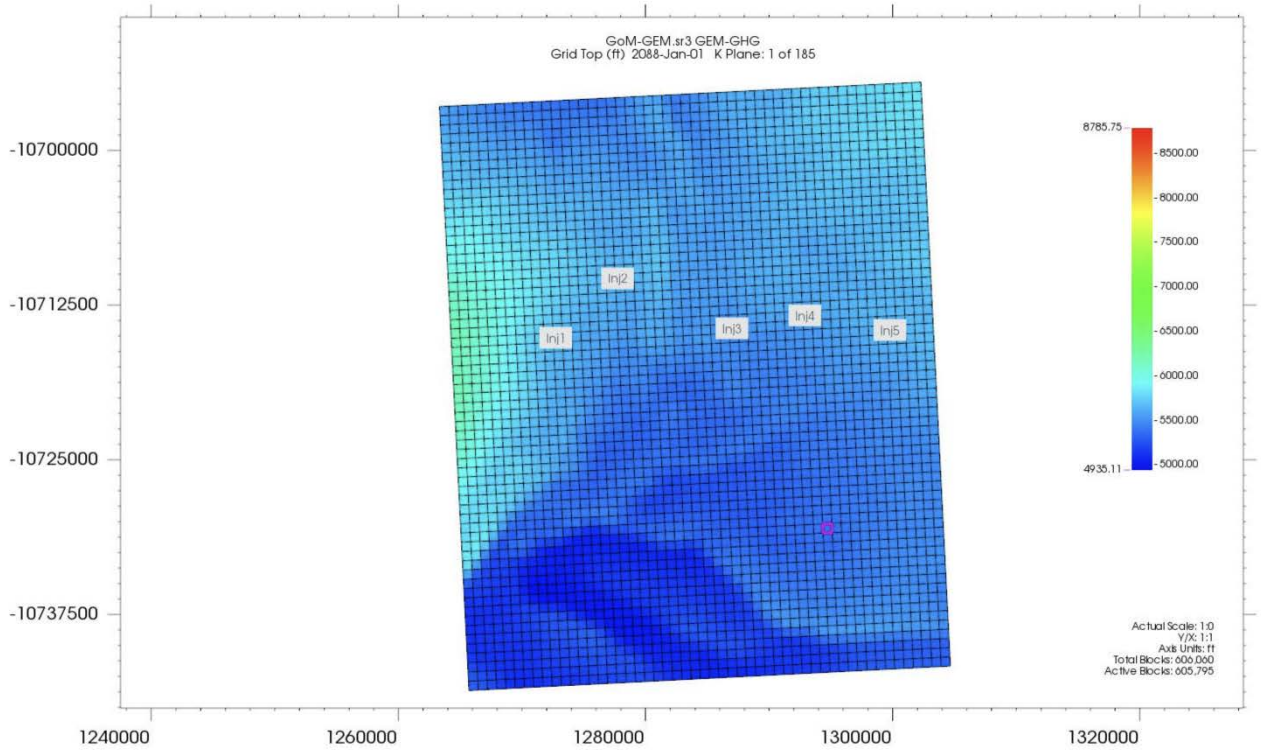

Figure 5-1. Preliminary Well Locations (as Provided to Aker Solutions)

- Consolidation of CO_2 metering will be performed at the onshore facilities and virtual flow metering is used to manage flow to each well.
- Pressure and temperature conditions are measured at the well and downhole locations.
- MEG/MeOH can be injected into the system via the control umbilical or by means of hot stabs strategically located on structures and injection trees.
- Annulus pressure management is maintained by de-pressurization and top-up from service/chemical line in the umbilical.
- At system shutdown, injection can remain in its pressurized condition for long durations.
- All well barrier elements shall be verified periodically by measures developed for an all-electric CO_2 subsea injection system.
- Tie-in and start-up of new wells will be performed without shutting down the injection pipeline system. Provisions shall be made in the flowline facilities to allow pre-commissioning of the future pipeline facility without disturbing the operating pipeline.

6 Field Development

The architecture of the system should enable the seamless transportation and distribution from the onshore CO_2 storage and processing facility. The offshore field architecture can only be finalized once the following is stablished: reservoir targets, drilling strategy, trajectories and well locations. This section presents concepts and recommendations for a generic system design and main building blocks. The aim is to provide a basis for further refinement once a higher level of certainty is attained in future phases.

6.1 Field Development Options

6.1.1 Daisy Chain

A daisy chain configuration is a common layout, where the wells are connected to a main pipeline that mirrors the position of the wells. For this topology to be effective, the location of the wells should allow the pipeline to be laid without sharp turns or complex installation corridors. In the base case of five wells in a relatively straight line, this configuration is considered feasible.

To connect the wells to the main pipeline, short-length spools and inline tees (ILTs) are commonly used. Alternatively, a flow base can be incorporated into the well trees. The main pipeline usually terminates in a pipeline end termination (PLET), which can serve as an expansion hub if additional wells are added in the future. Pig receiving facilities are typically connected to the PLET to facilitate regular maintenance operations.

This is a simple and effective field architecture for satellite wells that minimizes the number of required structures. However, if the well locations are spread in a non-linear pattern, this configuration tends to result in longer pipeline lengths, and other field architectures that include collection and distribution hubs may be more suitable.

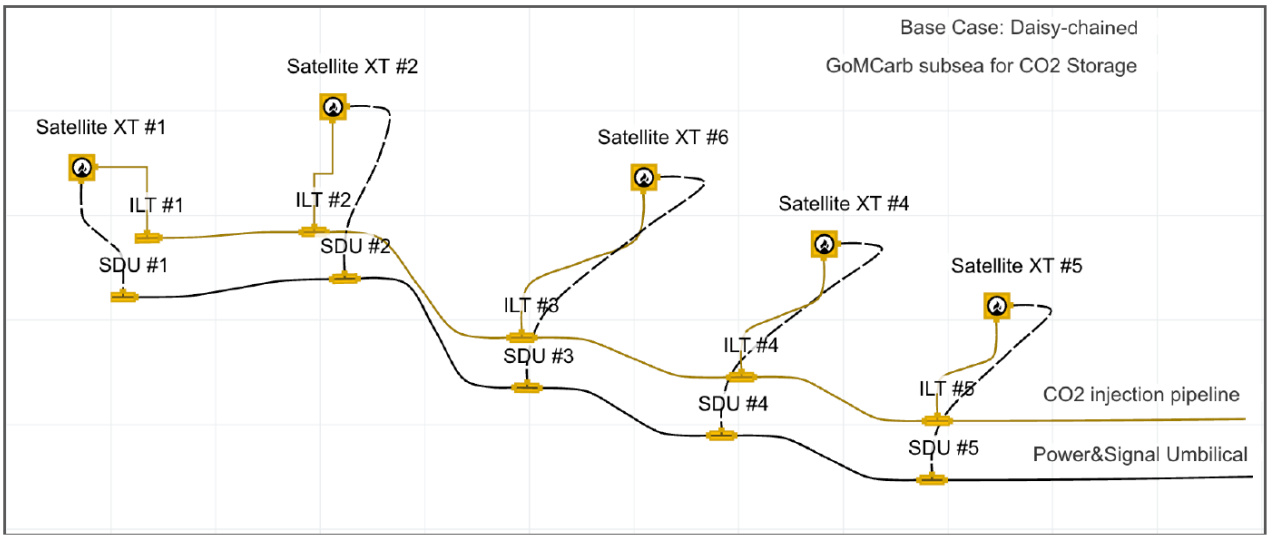

Figure 6-1. Daisy Chain Configuration

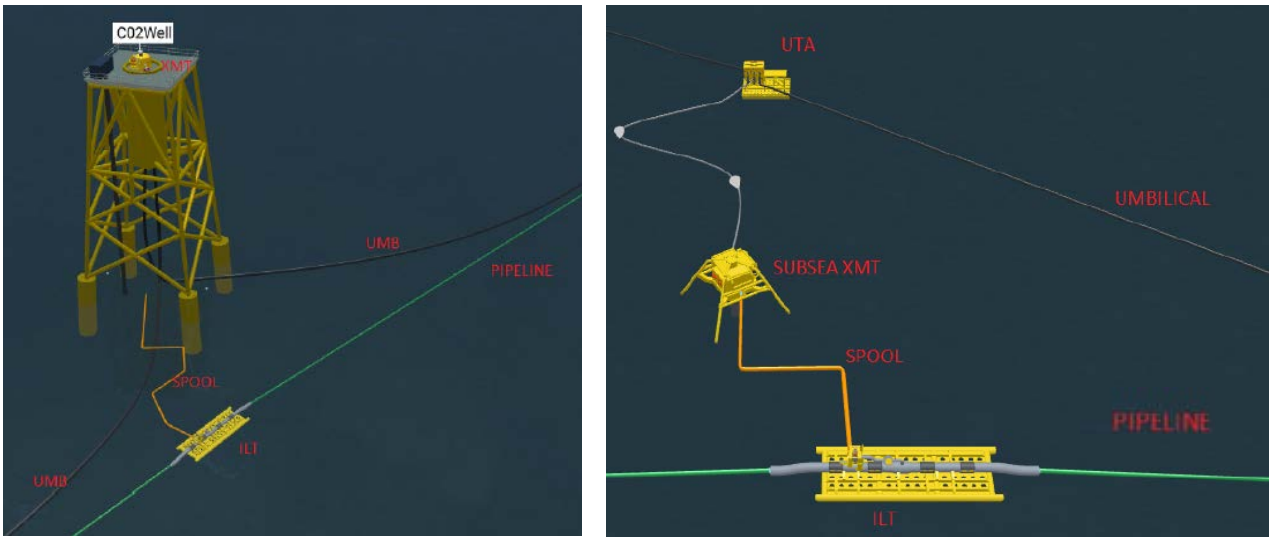

Figure 6-2. Details of XMT Connection to Pipeline a) Dry Tree b) Subsea Tree

6.1.2 Satellite Wells with Distribution Hub

In this field architecture, additional structures are installed in the vicinity of the wells to act as distribution hubs. The main injection pipeline is connected to these manifold structures, and branch-length pipelines, usually of smaller diameter, connect the injection wells to the manifolds. The manifold structures are typically equipped with functionalities related to distribution, flow management, metering, and chemical injection.

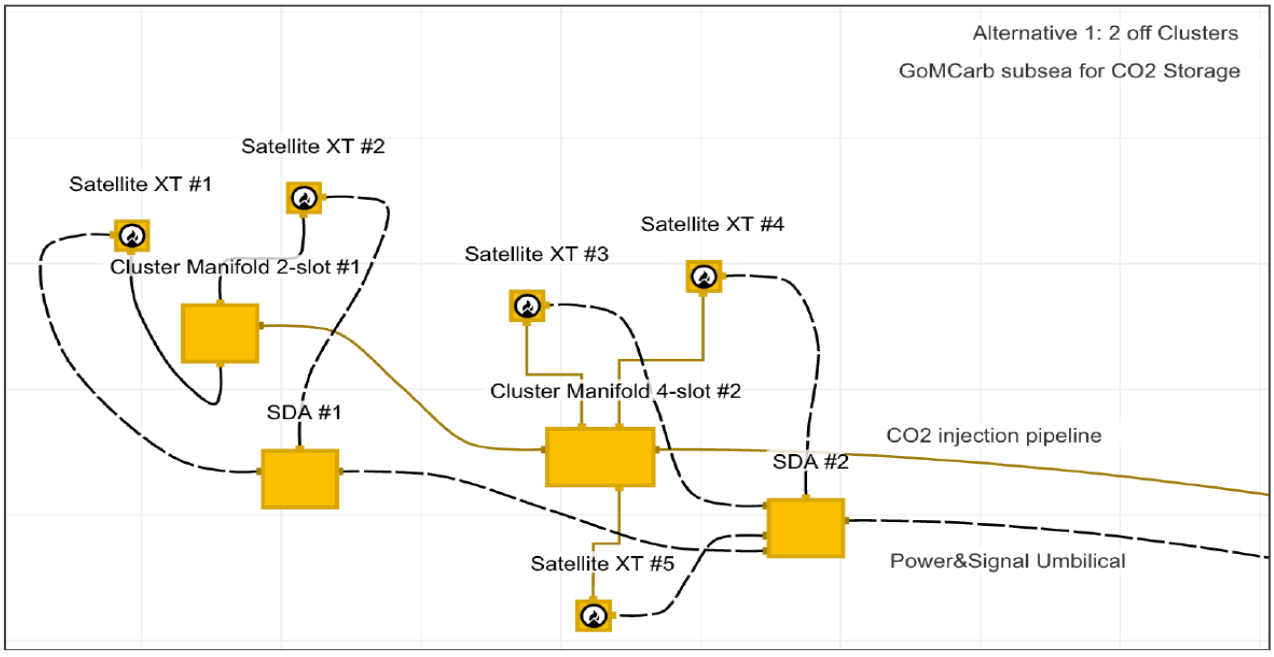

Figure 6-3. Satellite Wells with Distribution Manifold

If vessel transport or offshore offloading facilities are involved, this configuration can offer advantages and additional flexibility in directing the flow (See Section 6.3 - Other Forms of Transportation).

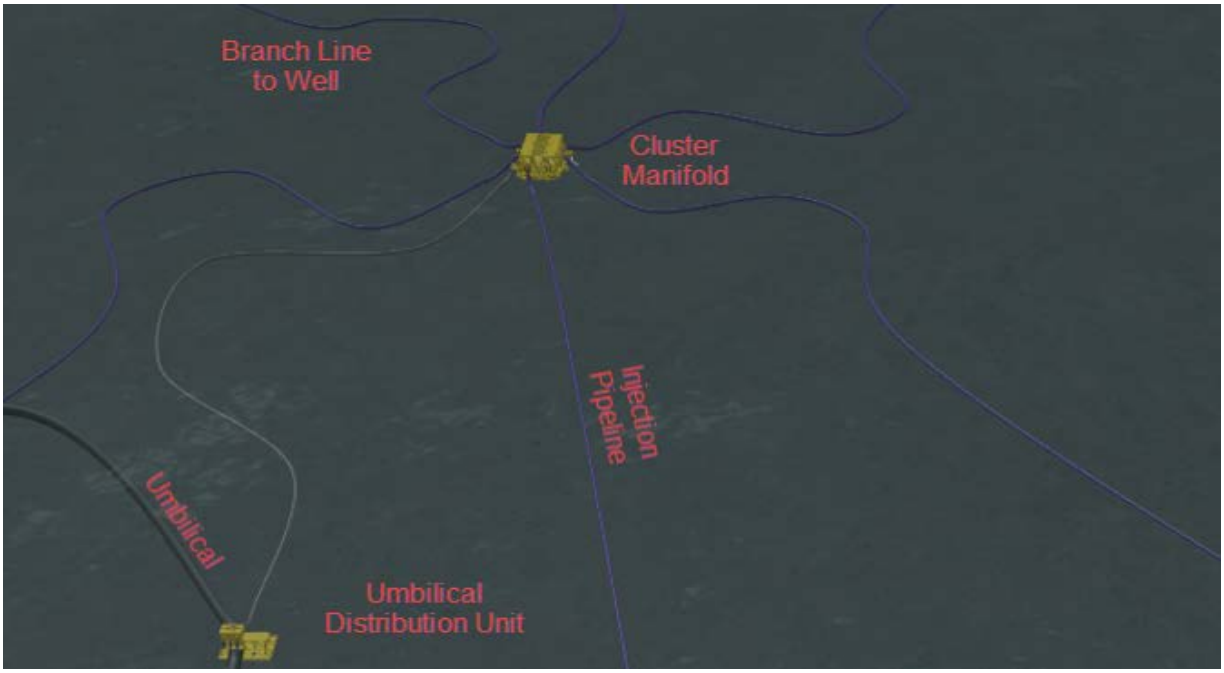

Figure 6-4. Details of Distribution Manifold in a Satellite Well Configuration

6.2 Field Layout Recommendations

Based on Aker Solutions' experience in developing CO_2 offshore injection systems, several key factors should be considered in selecting the field layout:

- To minimize drilling complexity and associated costs, it is recommended to select a flexible architecture for well top-hole locations, ideally promoting short horizontal step-outs, which has the potential for lowest DRILLEX. Considering the required well spacing, this eliminates template configurations and indicates satellite wells are better suited for this development.
- On-shore and offshore pipelines tend to be the largest contributor to CAPEX. This varies with pipe diameter, WT and routing. In general, pipeline optimizations should be prioritized.
- Considering the low number of initial wells, it is advisable to keep a low CAPEX and reduce the number of additional structures. To accommodate varying field development schedules, drilling and equipment installation, a flexible field architecture is preferred.

In the context of this study, well location and spacing are the key factors defining the field topology. A daisy chain configuration is recommended as it offers the simplest layout in terms of equipment requirements, installation, and pre-commissioning operations. Additionally, the daisy chain configuration presents the shortest cumulative pipeline lengths and lowest number of in-line structures, making it a cost-effective option.

If future tie-backs are identified, the satellite option can be a good candidate as it offers more flexibility to expand the offshore system and possibilities to reduce the internal diameter of branch pipelines, leading to cost savings.

Hybrid architectures are also possible and should be re-evaluated once the final well locations are determined.

6.3 Additional Considerations

Well Locations

The selection of the number and location of wells is crucial in defining an effective field architecture. This involves a thorough understanding of the formation and drilling requirements. Further work will be necessary in future phases once these parameters are better defined.

Monitoring and Bleed-Off Wells

Monitoring wells may be necessary to track CO_2 migration in the formation. These wells are typically located on the outskirts of the field to monitor CO_2 migration outside pre-established formation boundaries, especially in near shore developments where CO_2 migration may impact water reservoirs used for human consumption. Monitoring wells are usually not connected to the injection pipeline.

In addition, depending on the geologic conditions, bleed-off wells may be necessary to bleed off excess water.

Area Congestion

The area initially selected for the location of the CO_2 injection wells is highly trafficked and congested with numerous existing platforms, subsea wells, ship lanes, pipelines and umbilicals. Optimal field layouts may not be possible, and existing infrastructure must be taken into account to minimize crossings and reduce the risk of ship collisions.

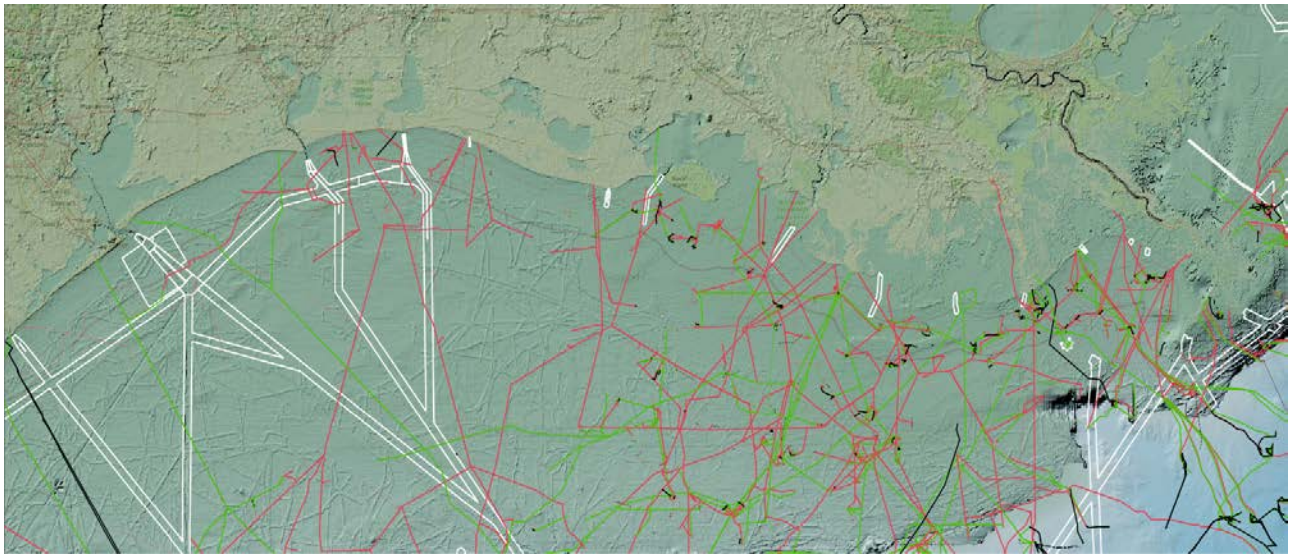

Figure 6-5. Infrastructure and Shipping Fairways (BOEM)

Other Forms of Transportation

The CO_2 transportation methodology highly depends on source of CO_2 and step-outs. While the base case for this study involves transportation from shore via pipeline, other transportation methods may be feasible. For instance, vessels can transport CO_2 to an offshore facility connected to the subsea distribution system. This facility can encompass all the necessary functions to manage the offloading process, as well as compression equipment to inject CO_2 into the pipeline within the required operating envelope.

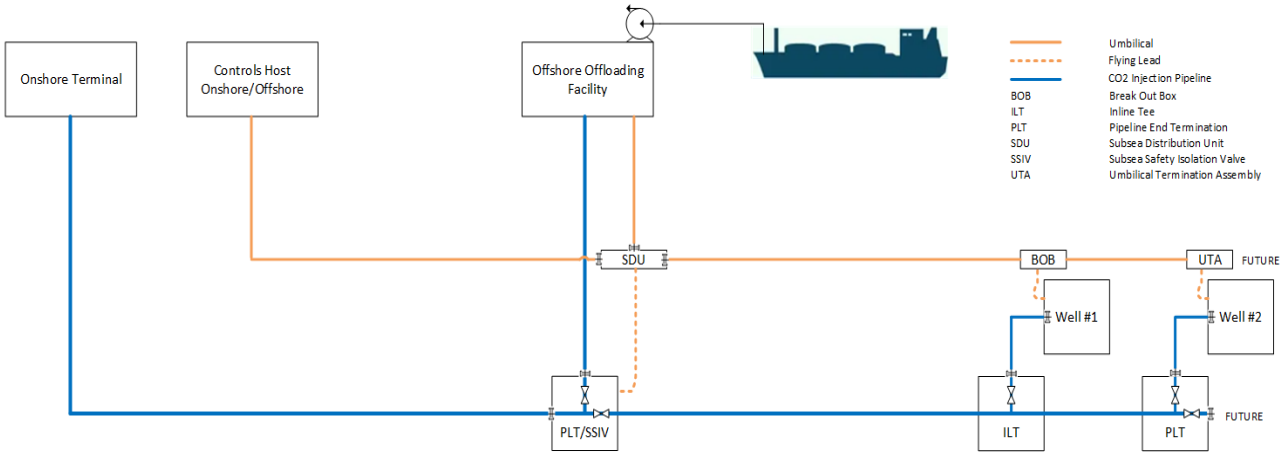

Figure 6-6. Offshore CO_2 Offloading Facility - Example

7 Offshore Injection System

Aker Solution has conducted as part of the study work in BP2 a comparison between subsea and topside injection tree options. This chapter offers an overview of the two tree designs and presents additional information to aid in the selection of the most suitable tree solution for the project.

7.1 Subsea Injection Tree System

The subsea injection tree is located on the seabed and connected to the main pipeline by means of spools. The tree is powered and controlled via the umbilical and flying leads that provide electric power, signals and chemicals.

Horizontal and vertical trees can be used for the application. Final tree selection will need to be performed on the basis of well design and drilling strategies. For the purpose of conceptual work, it is recommended to use a vertical tree system as the base case.

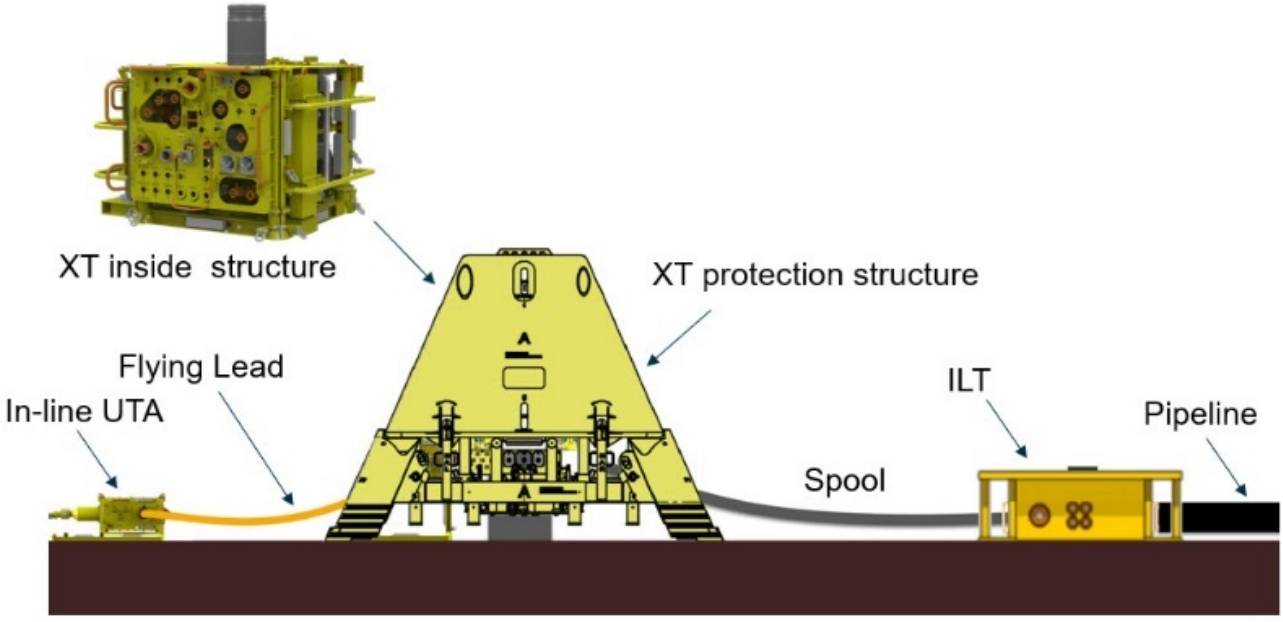

Figure 7-1. Subsea Injection XMT

7.1.1 Overview

The subsea XMT system comprises valves and sensors that enable the safe and controlled injection of CO_2 in the reservoir formation. At this early stage, the specifications for the XMT are not yet defined, and the XMT functionalities outlined in this report are based on Aker Solutions' experience from other CCS projects (Northern Lights and LINCCS). The recommended design parameters for the subsea tree are described in Table 7-1.

Product	Parameter	Value
All-Electric Vertical XMT 	Type	Vertical w/ concentric monobore
	Main bore	5" (7” bore is possible)
	Annulus	2"
	Design Pressure	5 Ksi or 10 Ksi (Depending on application)
	Design Temperature	-18 to 121˚ C
	Flow meter	Virtual
	Choke Type	Retrievable Choke Insert
	Feed-through	Electric, Fiber, Hydraulic
	BOP/Wellhead Interface	18 3/4”
	Tie-in Connection	Diver Flange

Table 7-1. Subsea XMT - Design Parameters

Wellhead System

Generally, an 18 3/4" wellhead system (and XMTs) are qualified for a wide range of applications in the Gulf of Mexico. Lighter 13 5/8" system can be a viable alternative to consider, however tubing sizes may limit the number of downhole lines that can be run through the tubing hanger.

Protection Structure

Based on the selected XMT type and vendor, various overtrawlable protection structures are available. To minimize both the initial hardware cost and installation expense, it is advisable to opt for a simple structure that is either integrated into the XMT or attached to the conductor.

Downhole Safety Valve

Control of downhole devices (i.e. SCSSV) is assumed to be electrically actuated. There are several vendors currently developing electric actuated SCSSVs, and it is likely to be field proven by the time the GOMCarb project is executed. Additionally, a subsea HPU can be locally installed if the downhole valve requires hydraulic actuation.

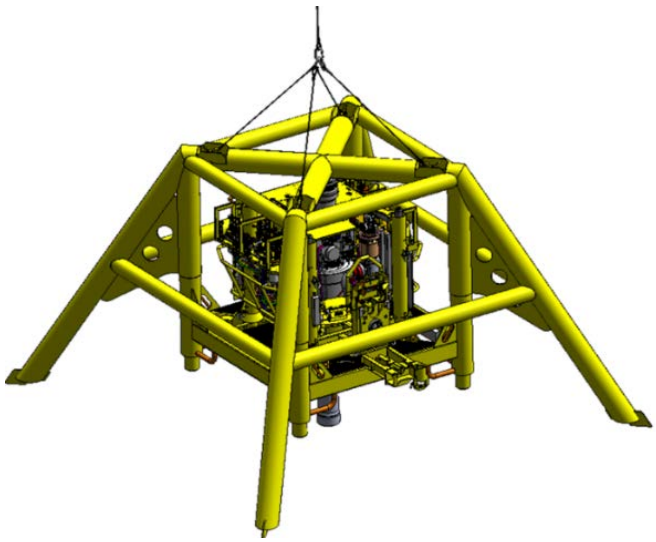

Figure 7-2. Subsea Tree with Overtrawlable Structure

7.1.2 All-Electric Tree Architecture

The All-Electric system architecture is based on a distributed controls topology with logic and energy storage located directly on the valve.

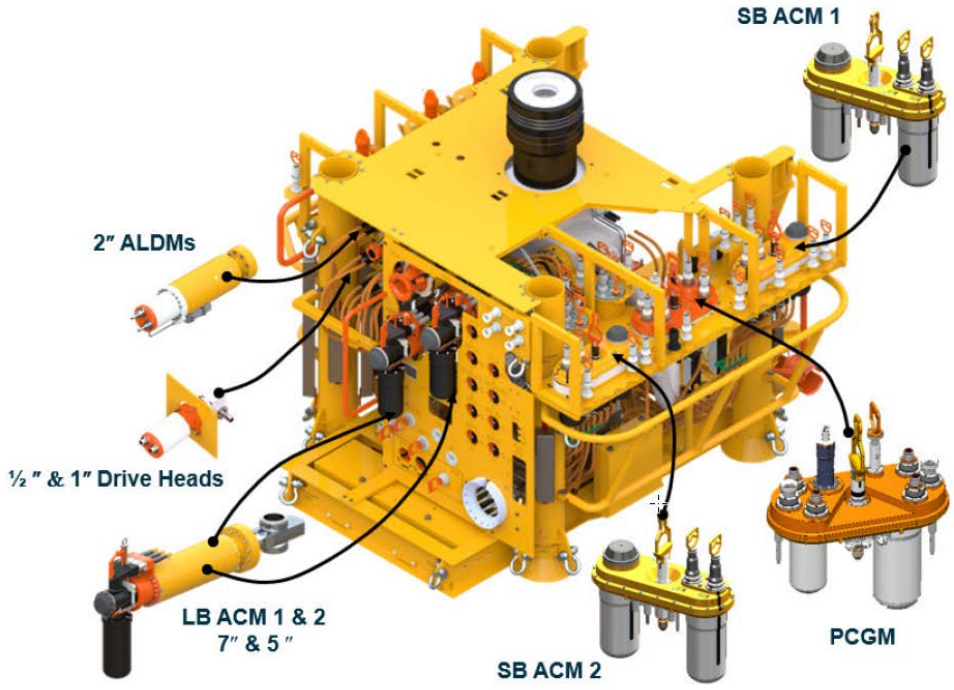

Figure 7-3. All-Electric Tree Architecture

The primary interface towards the rest of the system is the Power and Communication Gateway Module (PCGM). The PCGM is encapsulated in an ROV retrievable canister and provides a variety of interfaces for connection and communication towards the onshore control equipment, the Actuator Control Modules (ACM) and other external subsea devices.

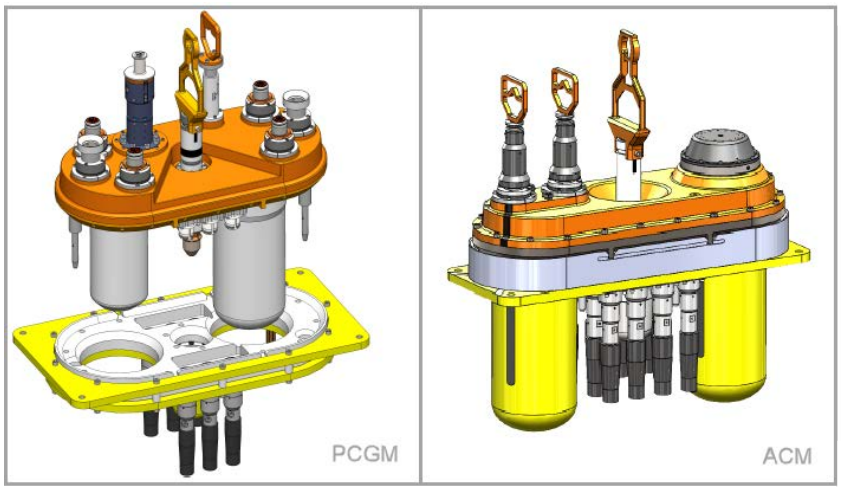

Figure 7-4. PCGM and ACM

Valve actuation is achieved by permanently installed drive-heads that are connected to ACMs by EFLs. The ACM is ROV retrievable and mounted on the XMT. On loss of power, the PCGM will stop operating, however, the ACMs have battery backup that allows control and monitoring of critical instruments and shutdown valves.

Additionally, an EL-Drive can be deployed on chokes and isolation valves to increase the level of electric actuation.

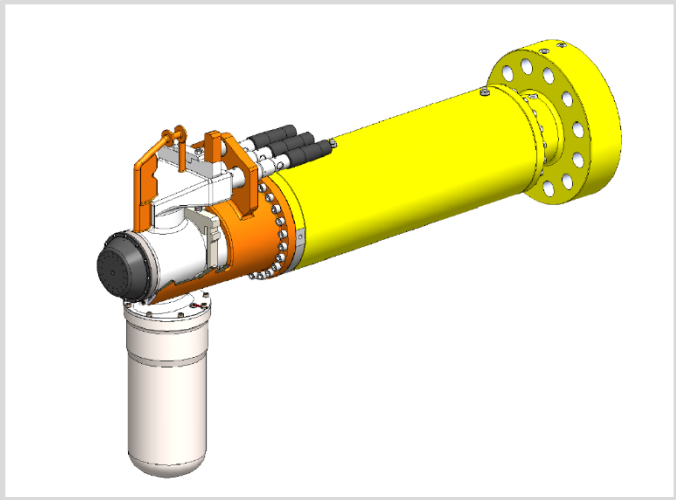

Figure 7-5. ACM Mounted on Actuator

Figure 7-6. EL-Drive

7.1.3 Valve Layout

Aker Solutions has been optimizing and standardizing tree functionalities as depicted in Figure 7-7. This proposed valve layout is based on Aker Solutions' experience and involvement in other projects and should be re-evaluated once tree requirements are defined.

The XMT design features a retrievable choke insert with and EL-Drive and a diver flange. All valves are electrically actuated by the remote control system, except the ASV which is only used during installation/intervention and is hydraulically operated. The all-electric approach simplifies the tree layout by reducing weight and footprint.

Instrumentation on the XMT is simplified for CO_2 injection and virtual metering is recommended to increase tree standardization and simplicity.

The feed-through system in the XMT and the Tubing Hanger enables both electric and optical signals. In the Tubing Hanger, Aker Solutions uses an Annulus Isolation Valve (AIV) that can be opened and closed using an ROV. This saves operational time when installing and retrieving the XMT as there is no need for setting a mechanical TH plug in the annulus.

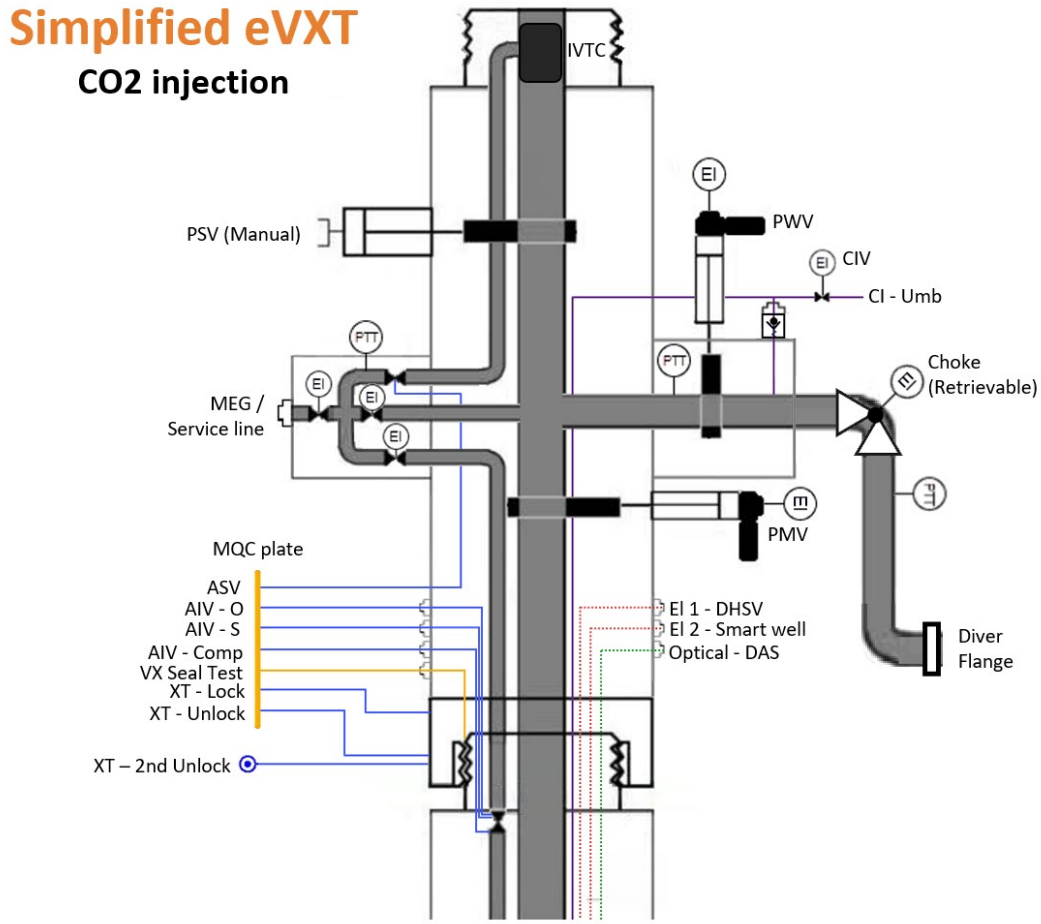

Figure 7-7. XMT Valve Layout (Conceptual)

7.1.4 Other Considerations

The design of most CO_2 injection subsea trees is based on those used in the O&G industry. It is expected that future efforts simplify these systems and bring the unit cost down. Future CO_2 injection trees are likely to resemble “injection heads” and perform the same functions as conventional trees but in a simplified manner e.g. by reducing the number of barrier valves and external interfaces. These simplifications are currently not meeting present codes and regulations that will need to be modified to accommodate requirements specifically applicable to CO_2 injection wells. Until then, CO_2 injection tree design will continue to follow the legacy framework from O&G.

7.2 Dry Injection Tree

7.2.1 Overview

The dry tree concept for CO_2 injection consists of a remotely operated unmanned platform connected to the injection pipeline and controlled via the umbilical. The CO_2 injection platform comprises three main components: 1. Deck and topside equipment; 2. Monopile (submerged substructure that supports the topside); 3. Pile penetrating the soil. The well conductor is located inside the monopile that acts as a caisson. The umbilical J-tube and injection riser are located outside of the monopile, fixed with supports and terminated on the platform deck.

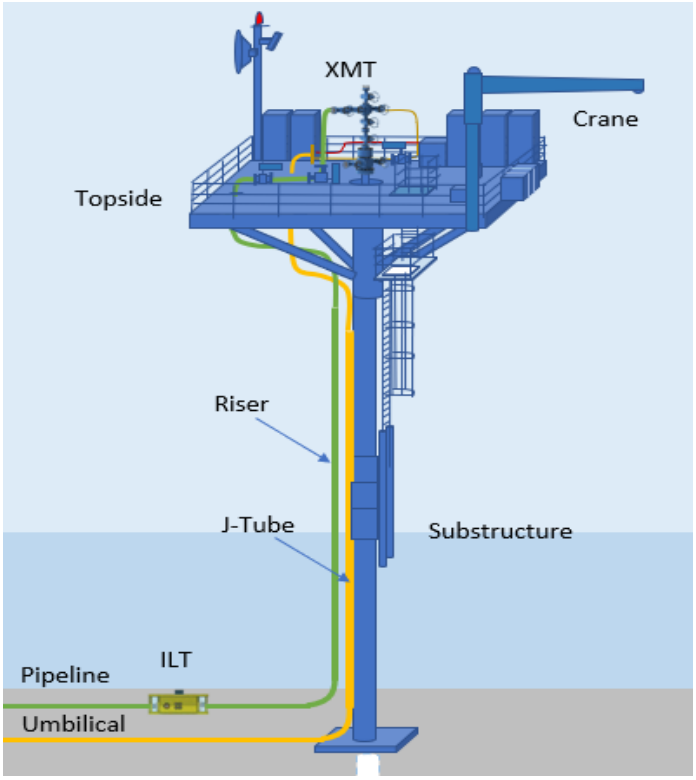

Figure 7-8. Single Wellhead Platform Concept Design

The unmanned CO_2 injection platform is equipped with:

- Topside facilities including well slot for CO_2 injection and surface XMT with 5" main bore (7" XMT can also be installed if required). All-electric and hydraulic XMT options are possible.
- Isolation Valve located on main deck.
- Provisions for MEG injection during valve testing, well clean-up and start-up.
- 1 off 6" ID rigid CO_2 risers with flanged connector on seabed.
- 1 off 3,5" ID Kill Fluid connection for jack-up rig.
- 1 off 10" ID J-tube for umbilical.
- Crane.
- Access point from a fast mobilization boat (service vessel).

In this dry tree alternative, the possibility of remote operations, low maintenance requirements and high uptime provide safe and environmentally friendly field operations. Platform maintenance visits are expected once a year and helideck, lifeboat and shelter are not necessary.

7.2.2 Topside Design

The injection platform is designed to accommodate a single dry CO_2 injection tree with the same basic functionalities as a subsea tree (Figure 7-9). Other process equipment is also located topside and includes all required well barriers and operational safety valves. The safety design philosophy is based on minimum equipment and functionalities while focusing on high quality of materials and components to ensure robustness of the design.

CO_2 is supplied to the platform via a riser connected to the ILT and pipeline, a XV valve located on the main deck acts as main barrier to the pipeline system. The dry XMT is equipped with a remotely operated choke valve for flow control management. Pressure and temperature transmitters are located upstream and downstream of the choke to further monitor flowing conditions. A number of pressure and temperature transmitters can also be included to monitor the annulus and downhole operations.

The dry XMT can be supplied as a hydraulic or electric tree system, with the electrical tree option being the base case for the study due to its reduced maintenance, lower environmental impact (discharge), and easier and more predictable operation. The dry XMT also features electric, hydraulic and optical downhole functions.

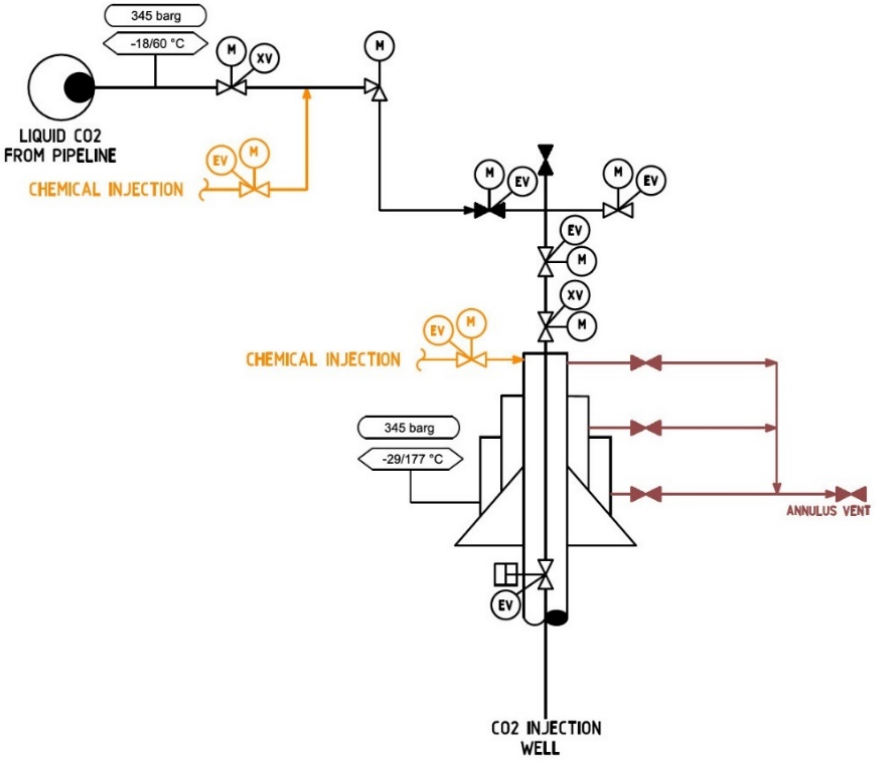

Figure 7-9. Dry Tree Flow Schematic - Example

The control umbilical is connected to the topside control panel to provide power and signal to the XMT. The system is designed for remote control, monitoring and safe start-up/shut-down from the on-shore control room.

MEG injection is also provided through the umbilical and can be used for water displacement, valve testing and pressure balancing prior to maintenance.

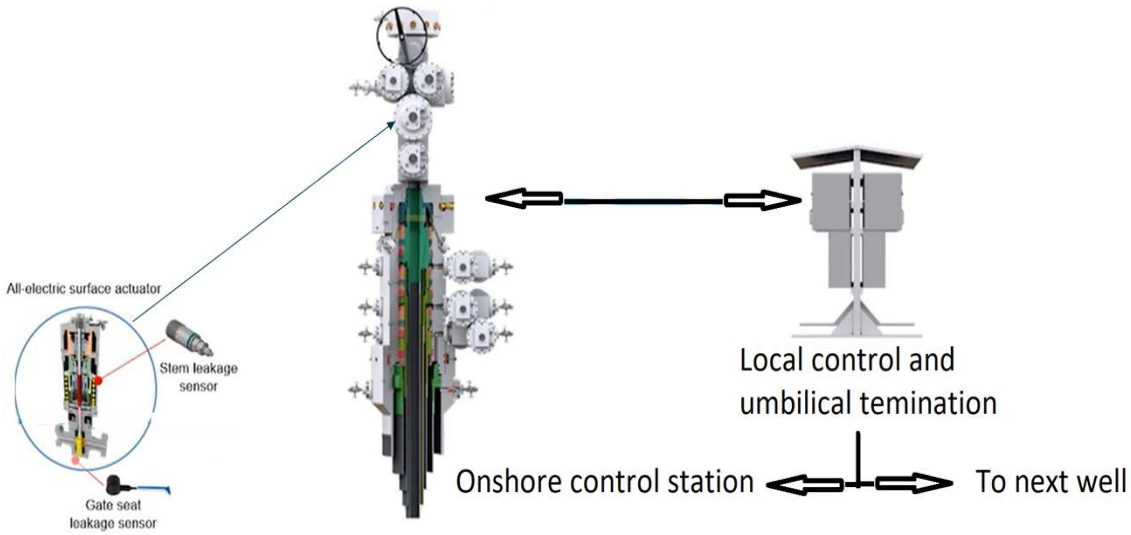

Figure 7-10. Electric Dry Tree System - Example (Courtesy of Schlumberger)

To reduce topside facilities, it is considered that fresh water, hot water, compressed air and nitrogen will be provided either through the jack-up rig during well intervention or lifted onboard from a service vessel during maintenance. Alternatively, provisions for a hose reel station at deck for connection to a service vessel can be made.

The topside design is independent of the substructure and presents opportunities for standardization and cost reduction.

7.2.3 Substructure Design

The selection of a suitable substructure is a critical design decision, which largely depends on the prevailing soil conditions, water depth, and topside design. With increasing water depth, the complexity and cost of the substructure also increase.

To facilitate the selection process, Aker Solutions has conducted an evaluation of the typical soil conditions, bathymetry, and metaocean data in the area of interest. Based on this analysis, a pre-selection of potential substructure designs is depicted in Figure 7-11.

Free Standing Caisson | Braced Caisson | Tripod

Criteria	Free Std. Caisson	Braced Caisson	Tripod	4 Legged
Water Depth (m)	**Up to 20m**	**10m - 60m**	10m – 80m	20m -150m
Nos. of Conductor	1 to 2	1 to 2	> 2	> 2
Max Topside Weight	Up to 150MT	Up to 300MT	Up to 700MT	Up to 2000MT
Boat Landing	Low Impact (Surfer landing)	Low Impact (Small Boat landing)	Standard (Standard boat landing)	Standard (Standard boat landing)
Ship Collisions	Restricted	Restricted	Restricted	DNVGL-RP-C204
Foundation	1 Caisson	1 Caisson 2 Piles	3 Piles	4-8 Piles

Figure 7-11. Evaluation of Substructure Designs

In principle, the free standing caisson substructure is deemed an appropriate solution for the water depth considered in the study (60ft). This substructure design offers adequate protection for the conductor within the monopile structure, which also minimizes drag forces.

The impact of increasing water depth can be seen in Figure 7-12. In deeper waters, Aker Solutions recommends investigating the use of bracing. This would incur additional costs but it would allow for standardization of the topside and main caisson substructure, with the main changes seen only in the additional bracing supports.

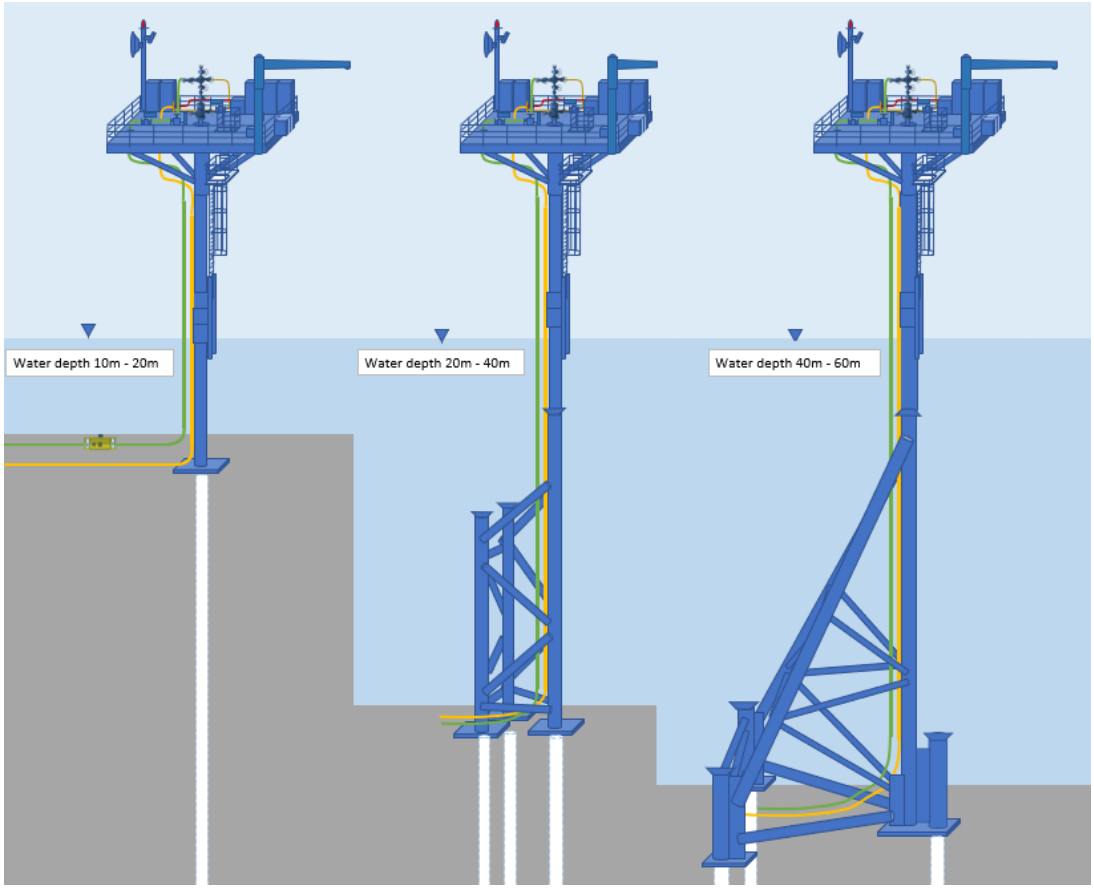

Figure 7-12. Substructure Bracing for Extended Water Depth

7.3 Injection System Evaluation and Discussion

As part of this study, dry and wet XMT system options are evaluated based on the design information currently available. Water depth is considered the main driver in this selection, thus the discussion includes potential sensitivities to evaluate the impact of different water depths.

CAPEX Considerations

The main cost elements for dry and wet XMT systems are described in Table 7-2.

Description	Items Included
Wet XMT System	• Protection structure • Subsea XT incl. control modules • UTA & Flying Leads
Dry XMT System	• Complete platform, incl. piles • Dry XMT, incl. control unit • Extra support for the platform for waters beyond 60ft

Table 7-2. Dry vs Wet XMT - Cost Elements

The cost for the wet XMT system is independent of the water depth, whereas the dry XT system cost is impacted by increasing water depth (driven by the complexity of the platform structure). As a general guideline, the deeper the field location the higher the structure cost.

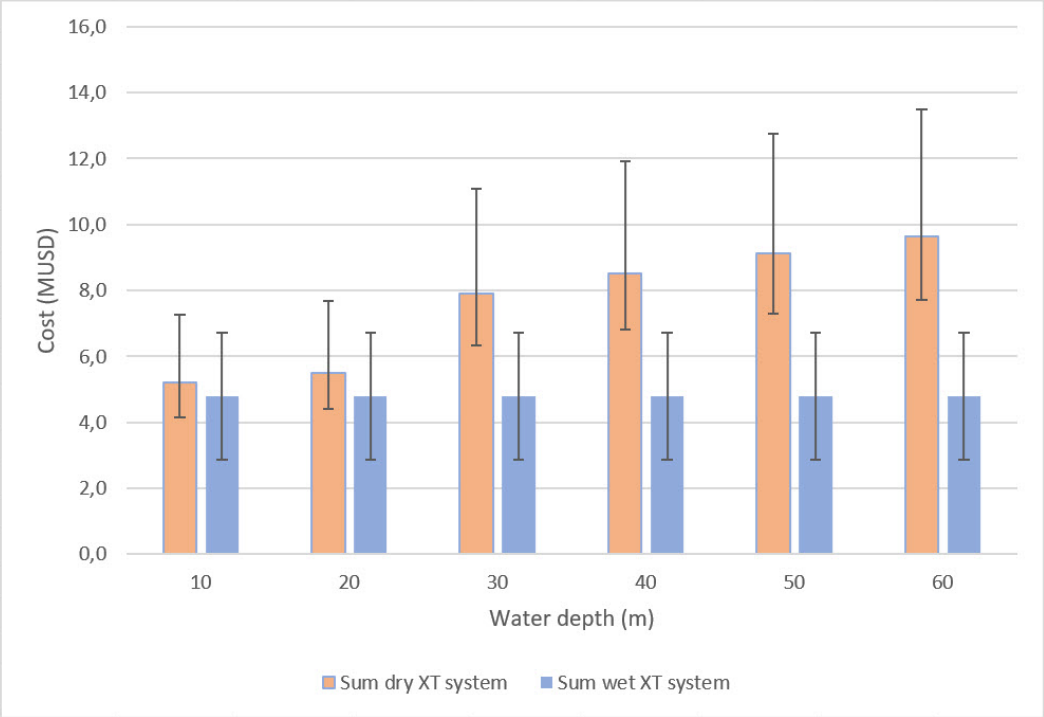

Figure 7-13. Cost Comparison for Wet & Dry XMT Systems in Different Water Depths

Drilling Operations

At this stage, it is assumed that vertical drilling for both options is performed in a similar fashion and is not considered a differentiation factor.

Installation methods

The installation time for the wet and dry XMT systems is estimated to be similar. For the dry tree solution, platform installation is initially estimated to take 2-3 days using a jack-up rig and 3-4 days using a crane vessel. The installation of the subsea XMT and running of the HP riser are estimated to take approximately 2-4 days.

There are optimizations to the sequence of operations and equipment used during installation for both options, but at this stage, it is deemed that installation time and complexity are similar.

Intervention Considerations

Both wet and dry XMT systems require a jack-up rig to perform light and heavy intervention. However, the main difference is that wet XMT systems require a high pressure and workover riser to be used to form a safe conduit to the subsea XMT.

Intervention operations on a dry tree are relatively simple, as a jack-up rig/barge can be used. The pressure control equipment can be connected directly on top of the dry XMT offering reductions of installation time compared to a subsea XMT system. Moreover, it is also possible to have a larger topside crane to cater for wireline operations and avoid the use of a jack-up rig (coiled tubing operations would still require a jack-up rig).This option would greatly decrease the intervention cost but it would have an impact on the platform CAPEX.

For a subsea XMT systems, a jack-up rig/barge will be required for intervention. A high pressure riser is required to be run and installed on the XMT with a topside BOP. To maintain two barriers, a workover riser is run inside the HP riser that lands and latches on the XMT hub. The pressure control equipment for the intervention system is mounted topside above the BOP. Running the HP riser and the workover riser is estimated to take about 30-40 hours in 60m water depth. Additional equipment will also be needed. These factors make the intervention campaigns for the wet XMT more complex and costly compared to a dry XT system.

Maintenance

Maintenance and repair operations on a dry XMT are significantly simpler than those required on a subsea XMT. It is worth noting that subsea XMTs are also designed to overcome this drawback by incorporating redundant and highly reliable components and materials. Critical components are also designed to be retrievable subsea with minimum downtime.

One particular challenge in the warm and shallow waters of the Gulf of Mexico is marine growth and mineral deposits, which can adversely affect subsea equipment. Aker Solutions has experienced marine fouling in water depths up to 100m. This is a clear advantage for dry XMT solutions as subsea equipment would require additional maintenance (probably once every 1-2 years). Antifouling coatings have been used to decrease the adhesion force between surfaces and organisms, this can decrease marine fouling but not prevent it. There are different aspects (region, temperature, fouling pressure, etc) to consider when evaluating anti-fouling coatings, copper content and release rates. If toxicity is a concern, there are options for biocide-free antifouling coatings (usually silicone based), these coatings have shown similar performance to copper based coatings in certain cases. Adding a soft layer, for example a tarpaulin or a net around the subsea equipment, may mitigate the action of marine fouling. This will need to be studied in more detailed in further work.

For the life of field, it is considered that potential maintenance and repair cost for subsea equipment is generally higher. Periodic visual inspections of the subsea equipment must be carried out in accordance with specific maintenance philosophies.

In general, it is concluded that dry tree solutions present clear advantages over wet trees in this category.

Collisions and Area Congestion

While offshore platforms may be more intrusive in areas of high vessel traffic and fishing activities, using subsea equipment in shallow waters poses a significant risk due to tidal cycles. The illustration in Figure 7-14 shows a stack-up for a conventional subsea tree. High and low tides,

seasonal water level changes and weather events can have a significant impact on whether subsea equipment can be used in shallow waters without becoming a potential hazard for vessel traffic and other ocean users.

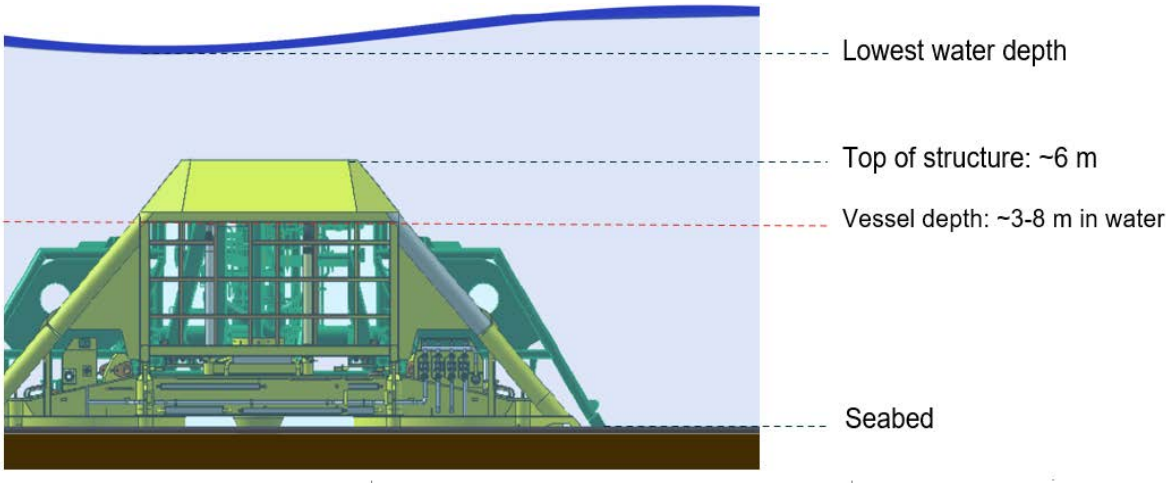

Figure 7-14. Subsea XMT Stack-Up

7.4 Recommendations

Aker Solutions has performed an evaluation of wet and dry tree solutions based on the data available and concluded that water depth is a key factor in determining the correct injection system. For water depths of 60ft and below, both options present a comparable CAPEX and main differences are related to intervention, maintenance, simplicity of operations, and risk to equipment and other ocean users in ultra-shallow waters. In principle, dry tree solutions present benefits in these categories.

In the future, it is important to monitor simplifications of subsea trees for CO_2 injection as they become “injection heads” and may provide significant CAPEX improvements and simplification of operations for shallow water use. The reduction in CAPEX for subsea injection trees is critical to overcome other perceived disadvantages.

8 Control System

The control system architecture is based on onshore control from the control room, where all required equipment and chemical skids are located, with an umbilical servicing the offshore wells. It is assumed that the control station will be remotely connected to the CO_2 capture facility where compression equipment feeding the pipeline is present.

The location of the control facilities plays a significant role in determining the step-out distances to the injection wells, which defines the control system architecture, power, and signal distribution. In this study, it is recommended to locate the control facility near the shore crossing.

8.1 All-Electric vs Electro-Hydraulic Control System

The offshore equipment can be controlled based on an all-electric architecture or a more conventional electro-hydraulic system. In simple terms, the main difference between the two proposals is valve actuation. An all-electric system uses electric actuators, whereas a hydraulic system requires hydraulic fluid to operate the valves. Electro-hydraulic systems have been the de-facto technology for the majority of O&G developments in the past decade. This system requires an HPU and tubes in the umbilical to supply control fluid to the offshore equipment. As step outs and water depth increase, this type of system can become more cumbersome, and additional equipment such as accumulator banks or subsea HPUs may be required. CAPEX cost is highly dictated by the number and size of tubes/conduits required in the umbilical. Additionally, OPEX cost, mainly related to the use of control fluid, can be high in open-loop control systems.

As an alternative, an all-electric system relies on electric power cores in the umbilical to actuate the offshore equipment. There is a low OPEX cost related to this type of systems and they offer high reliability and predictable operations. The main disadvantage has been the higher cost and lower maturity of electric actuators. This has changed in recent years with O&G vendors investing in development programs and standardizing all-electric platforms that promote simplifications.

It is envisioned that the all-electric technology will make systems intrinsically safer, more reliable, more environmentally friendly and more cost competitive while providing higher performance. Aker Solutions decided to present an all-electric system in the GOMCarb project as the base case, building on the experience from Northern Lights. This assessment should be revised once well locations and tree functionalities are identified, and tree type and vendor are selected. The use of traditional electro-hydraulic systems is still a feasible option, should further evaluation indicate this is a solution aligned with project objectives.

Enhanced Operations and Monitoring	• Electric motors maintain high level of efficiency and full torque capability at any water depth, unlike hydraulic systems that must overcome hydrostatic pressure. • Continuous reporting of valve position provides real-time process status updates. Local batteries on actuators serve as fail-safe-close safety functions and enable valve profiling during shutdown conditions. • Critical instrument pressure and temperature readings can be logged during shutdowns, even when the power is off.
Maintenance and Testing	• Well barrier actuators are periodically tested electrically and mechanically with minimum impact on production. This enables smarter intervention philosophies and reduces intervention time and frequency.
Performance	• Key resources are decentralized to each valve by deploying a distributed control topology. • Valves have their own energy source (battery) and rotary drive module (motor, gear box and brake) allowing for higher level of independent valve control. Well isolation can be achieved by running several electrical actuators simultaneously, closing large bore valves and small bore valves in parallel. • Choke valves may be closed earlier in a shutdown sequence reducing wear to secondary barrier elements. Chokes might also be operated in parallel. • New shutdown sequences can be enabled to improve the start-up process. Equalization of injection Wing Valve, for example, might be faster in a well where the injection Choke Valve was closed first. • Elimination of charge-up times which are typically long for hydraulic systems, especially in longer step-outs.
Simplifications and Cost Reduction	• An all-electric system eliminates the cost of hydraulic fluid with the added benefits of eliminating discharges to sea. • Onshore HPU is not required reducing: cost, CO_2 footprint, and human exposure to noise, vibration and hydraulic-pressure. • Electric umbilicals tend to have a smaller cross-section, allowing longer continuous lengths to be manufactured and spooled. Overall weight is reduced, facilitating the use of a smaller umbilical installation vessel. • The all-electric platform enables cost competitive, spring-less XMT systems based on smart electric actuators. This eliminates larger controls equipment (SCM) and small bore tubing on the XMT.

Table 8-1. Advantages of All-Electric Systems

8.2 Onshore Equipment

The main control equipment will be located in the control station near the shore-crossing and can be operated remotely e.g. by the control system at CO_2 capture facility. The main onshore equipment is described below.

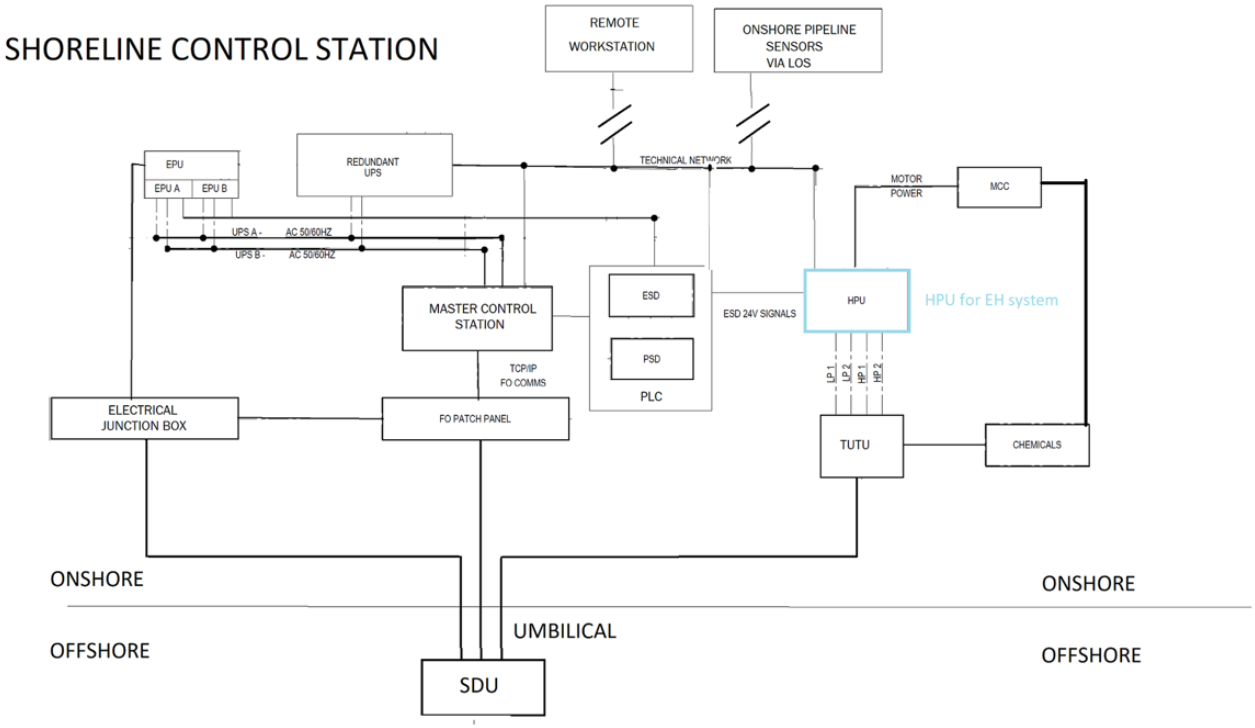

Figure 8-1. Control System On-shore Architecture

Master Control Station (MCS)

The Master Control Station (MCS) serves as the central control and monitoring hub for the injection system equipment and electrical power unit. It features a single rack design with dual redundant industrial PCs that operate on a hot standby basis, ensuring there is no single point of failure. Additionally, an internal PLC operates as a watchdog system to monitor the rack's functions.

The MCS offers a Graphical User Interface (GUI) that provides trending, logging, reporting, and alarm capabilities. This GUI can be mirrored on a remote operator workstation in a different location. The MCS is configured in a master/slave arrangement where it can either be in complete control as the Master or controlled as a node of another control system in Slave mode.

To ensure optimal functioning, the MCS must be installed in an enclosed non-hazardous environment with HVAC facilities within a controlled maximum ambient temperature.

Electrical Power Unit (EPU)

The Electrical Power Unit (EPU) is responsible for providing controlled power supply to the control system power network. It consists of two segregated channels, EPU A and B, to prevent single points of failure and facilitate maintenance operations. Each EPU includes relays and contactors on the input power lines, controlled by the ESD system. Due to the low power requirements of the controls equipment for the injection system, it is possible to fit the components of EPU A and EPU B into a single cabinet.

Figure 8-2. MCS

Figure 8-3. EPU

ESD/PSD Nodes

The ESD/PSD system interfaces with the CO_2 capture facility and the injection system to ensure a reliable connection for ESD and PSD shutdowns. The ESD signals are hardwired to the UPS unit, allowing for an emergency shutdown of the injection system. The PSD signals are broadcasted to the MCS and executed as a discrete sequence of command events between MCS, CO_2 capture facility equipment, and compression unit.

ESD/PSD actions will be further developed at subsequent phases of the project in the form of standard Cause and Effect diagrams in conjunction with the CO_2 capture equipment control system.

Chemical Injection Unit

The Chemical Injection Unit (CIU) is used to provide MEG for well operations and barrier testing. The pump is sized based on flow assurance studies to deliver MEG at the adequate pressure and flow rate.

Umbilical Termination

The control umbilical is terminated onshore and connected to the control equipment. A number of electric, fiber optic and hydraulic junction boxes bring the required services to the umbilical termination for further distribution to the offshore system.

8.3 Offshore Equipment

The main offshore control equipment is located on the injection trees and described in Section 7.1 and 7.2. An all-electric approach is followed for the purpose of this study (see Section 8.1).

The offshore trees are equipped with electric actuators and sensors/instruments that are controlled and monitored by the onshore equipment. The trees include an electric downhole safety valve, it is advisable to confirm requirements with downhole safety valve vendors.

Virtual flow-metering is the preferred solution for flow monitoring and management.

8.4 Power and Communications

The proposed control system has low complexity with relatively short step-outs, limited offshore instrumentation and lack of bandwidth demanding equipment. To reduce umbilical and distribution cost, Aker Solutions recommends a combined power and signal system (comms superimposed on the power lines). Other alternatives that can be explored if design parameters change include:

- Fiber optics allow for wide bandwidth fast communications; the umbilical includes fiber optic communication for DAS and any unallocated fibers could be used for comms to either the control system or individual equipment added later.
- Segregated communication and power is possible by adding discrete copper lines in the umbilical. This allows fast communication while presenting lower cost than fiber communication.
- In particular for dry trees, radio frequencies are available by utilizing Tampnets 4G/5G network or via LOS RF transmission back to the shoreline control station.

Either low voltage AC or DC could be utilized in the system. As step-outs are short, AC voltage is considered for the base case. In the event that there are future field expansion requirements and step-outs increase, a DC system should be re-evaluated. Figure 8-4 offers details of the differing power requirements over differing distances. Further work is required to establish a power and signal analyses to verify system feasibility.

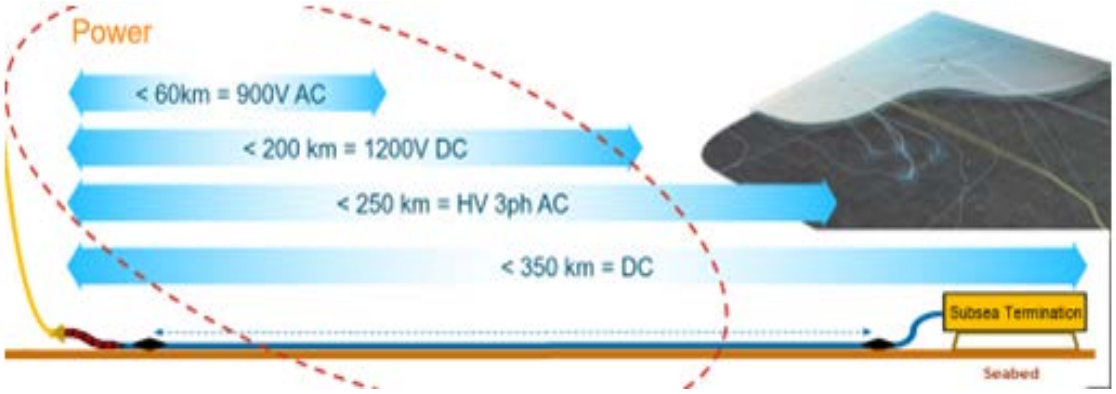

Figure 8-4. Power System and Recommended Distances

8.5 Downhole Fiber Optic Sensing

Aker Solutions has seen in recent studies the addition of downhole fiber optic sensing. This system is available from several vendors for temperature (DTS, Distributed Temperature Sensing) and acoustics (DAS, Distributed Acoustic Sensing). The optical fiber will typically run from the well all the way to the onshore facility where the interrogator unit is commonly located. The injection control system is transparent and simply provides the facilities to transfer the fiber-optic signals from downhole to the interrogator unit. This type of systems typically consists of:

- A downhole sensing fiber (often specially modified for enhanced response)
- Protective encapsulation of the downhole fiber (for enhanced lifetime)
- Wellhead/Tubing Hanger feed-through
- OFL with possibly an optical circulator
- Fiber lines in the umbilical
- Interrogator unit

For the sake of discussion, Aker solutions has included fiber optic lines in the umbilical and all offshore trees are equipped with facilities for a DAS system.

8.6 Leakage Monitoring Strategies

Leak monitoring is a topic that is currently being debated in the industry with scattered descriptions and recommendations. CO_2 leaks in onshore pipelines and offshore systems could pose risks to:

- Residents in populated areas.
- Personnel working on platforms and other parts of the system.
- Water column and seabed resources.
- Sub-surface resources.

/4/ raises an interesting point and currently it is difficult to determine what volume or rate of CO_2 leakage is considered significant. In general, leak avoidance and detection techniques rely on: 1) Design robust system to avoid leaks, commonly done by selecting the right barrier philosophy and materials for the design life; 2) Be able to detect potential leaks if they occur by using specific instrumentation; 3) Be able to control and minimize leaks, usually done by segmenting the system and using valves to reduce or isolate leaks. In this context, there are several techniques that can be used to detect CO_2 leaks and this should be further evaluated using ALARP and BAT principles. For the purpose of the study, Aker Solutions recommends evaluating different solutions:

For Pipeline Monitoring and Leak Control

- Virtual monitoring of pipelines by using existing pressure sensors and metering instruments.
- Segmentation and compartmentalization of the pipeline by using isolation valves.

For Injection Tree Monitoring

- Use of existing pressure sensors to identify potential leaks.
- Acoustic sensors for subsea well monitoring and detection of CO_2 bubbles in the water column.
- CO_2 infrared sensors for detection subsea.
- CO_2 sniffers for onshore and topside facilities.

/3/ includes further information on various surface measurement techniques that can be applied to leak characterization. 4-D seismic has proven most successful on the industry-scale offshore projects of Sleipner and Snøhvit, yielding the geometry of the CO_2 plume with high resolution, while gravimetry has given complementary information on CO_2 in-situ density and dissolution rates in the formation water. Onshore, surface elevation and microseismic data have proven valuable for monitoring injection and storage, and these techniques can be extended to offshore applications.

Cost is an important aspect of a monitoring program, subsurface and surface conditions that vary from site to site make a tailor-made plan necessary for each case. Equipment reliability and a system of documentation which works over a time-span of generations are vital for a successful monitoring program.

8.7 Umbilical Construction

The umbilical runs from the shore control room to the offshore wells and includes MEG line, power and fiber optic cores. In dry tree systems, the umbilical is terminated topside in a control panel with direct connection to the dry XMT (Figure 7-10). For subsea trees, the umbilical is terminated in a UTA and flying leads bring power, signal and MEG to the subsea XMT (Figure 7-1).

Power, signal and hydraulic analyses are required to determine the specific umbilical line sizes. Figure 8-5 offers a reference case of a simple umbilical cross section. Umbilical optimizations, specially reduction or elimination of hydraulic and chemical injection tubing, should be analyzed. In this context, it is also interesting to study local power generation and chemical storage at well locations (mostly applicable to dry tree concepts).

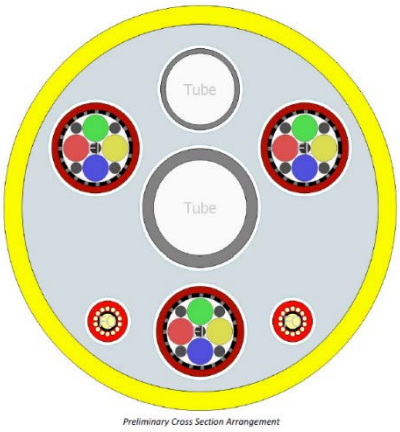

	QTY	Design Pressure	Size
FO	2		24 fibers
EL	3	-	16mm2
MEG/MeOH	1	345bar	1"
Spare HYD	1	345bar	3/4"

Figure 8-5. Preliminary Umbilical Cross-Section

9 Technology Readiness

Technology Readiness Level (TRL) is an important indicator of technical maturity and is closely linked to a specific set of operating parameters and environmental conditions. Any changes in the operating regime or environment can affect the TRL, leading to a downgrade for more demanding conditions or an upgrade for less demanding ones.

Eight TRLs have been defined /5/ ranging from 0, corresponding to an unproven idea, to 7, which represents proven technology that is already installed and operating in the relevant conditions. Technologies categorized as $4 \leq TRL \leq 7$ can be considered as qualified for a defined range of operating conditions. New or modified technology can be classified as $0 \leq TRL < 4$, and further qualification work is needed to achieve the required technical maturity for a defined application.

Aker Solutions has evaluated the technical maturity of main system components and summarized the findings in Table 9-1. As indicated in /4/, the majority of technologies used in CO_2 transport derive from the O&G industry. Thus, the majority of building blocks present a high TRL. Future optimizations, simplification and developments driven by cost reductions are expected, this may lower the TRL for some components but no significant step-changes are expected in the near future.

The lowest TRL is for subsea all-electric XMTs that are currently in development with future installation being plan in the next few years. Subsea hydraulic XMT are at a higher TRL and can be a feasible alternative if this is considered a technical risk.

Technology	Description	TRL	Remarks
Controls	MCS	7	
	EPU	7	
Dry Electric XMT	Surface electric actuators	5	Surface actuators from Schlumberger. 2 1/16" to 6 3/8".
Subsea Electric XMT	eVXT assy	3	Aker Solutions eVXT: Planned for a system test in Q1 2023 which will take the eVXT to TRL 5.
	Electric actuated valves	4	
	Electrical Control modules	3	Modular control system that sits on the XT for controlling electric valves.
Tie-in Connectors	Diver Flanges	7	
Umbilical and Distribution	Umbilical	7	
	UTA	7	
	Flying Leads	7	
Platform	Free-Standing Caisson	7	

Table 9-1. Main Equipment - Technology Readiness

10 Project Estimates

10.1 Cost Estimates

Aker Solution provides Class 4 (+/-40%) price estimates in Table 10-1 and Table 10-2 according to AACE International Recommended Practice No. 18R-97 and aligned with internal costing protocols. The current non-binding prices are based on key assumptions described below. It is recommended to see also Section 2.6 to understand the system battery limits.

- Costing estimates are based on historical data and past experience.
- The estimates do not take into account current challenges in supply chain, market conditions and other world events that may disrupt the execution of the work.
- The estimate excludes taxes and duties such as VAT, import duties, investment tax, etc.
- Engineering and project management costs are not included. Project Management can be considered as up to 15% of the offshore equipment cost.
- Equipment transportation and equipment storage are excluded.
- Installation, hook-up, commissioning costs and support are not part of the estimates.
- Only control modules in the control room are included. Buildings and other facilities are excluded.
- Chemical tanks and skids are not included.
- The foundation system has been included in the estimations, but further work is required to analyze soil conditions.
- Umbilical length is considered to be 15km. Reels or reel logistics are excluded.
- PLRs are excluded.
- The DAS system is considered optional and provided by a 3rd party vendor. FO lines in the umbilical and OFLs are included.
- Pipeline, in-line structures and jumper spools are considered part of the SURF scope.
- No connections, hubs termination heads, etc, are included only diver flanges.
- Pressure flanges, valves or stabs, test, installation or protection caps are excluded.
- Wellheads for both wet and dry tree options are excluded. Sub-surface equipment is not included in the estimates. The Tubing Hanger is included.
- Other exclusions
    - Test, transportation, handling and installation equipment/tooling.
    - Capital, manufacturing, test, installation and operations spares.
    - Offshore operations, drilling and installation.
    - Operational, intervention and abandonment costs or other services.
    - Qualification, verification testing and SITs.
    - Consumables.

Item	Description	Qty	Price (MUSD)
Onshore Control Station	Control Modules	NA	0.6
Wellhead Platform	Platform including All Electric Dry Tree	5	45.5
Umbilical	Umbilical & Distribution Equipment	NA	5.4
		TOTAL	51.5

Table 10-1. Price Estimates - Dry Tree Option

Item	Description	Qty	Price (MUSD)
Onshore Control Station	Control Modules	NA	0.6
Subsea XMT*	Subsea All Electric Tree with Cover	5	33.5
Umbilical	Umbilical & Distribution Equipment	NA	7.4
		TOTAL	41.5

Table 10-2. Price Estimates - Subsea Tree Option

*Subsea XMT price based on current versions of CO_2 Injection Tree. Further cost reductions are foreseen in coming years with concepts evolving towards low profile injection heads and simplified completion.

10.2 Equipment Lead Times

Aker Solutions has provided in Table 10-3 lead times for main equipment based on previous project estimates. It is assumed that the majority of the engineering work will be performed during pre-FEED and FEED phases requiring only a short engineering phase during project execution. The lead times presented are indicative only and consider duration of fabrication, assembly and testing of the equipment. Further refinement will be required in future phases.

Item	Description	Qty	Lead Time
Subsea XMT	Subsea All Electric Tree with Protection Structure	5	18-20 months
Platforms with Dry XMT	Platform including All-Electric Dry Tree.	5	12 months
Umbilical	Umbilical & Distribution	1	15 months
Onshore Controls	Onshore Controls	1	18 months

Table 10-3. Indicative Project Lead Times

11 Recommendations for Future Work

Suggestions and recommendations for further work have been included in different sections of the report. The next natural step would be to perform more detailed studies to verify the feasibility of the proposed concepts and increase certainty while identifying optimization and simplification opportunities. The following additional activities are recommended in future study phases.

System Engineering, Process & Flow Assurance

- Update and develop design basis.
- Optimization of field layout and hardware selection based on location and distance between wells, plans for future expansion, maximum step-out distance, system sizing, etc.
- Define material compatibility analysis based on field specific injection fluid.
- Verify well operations to validate virtual metering and choke size for operations.
- Investigate alternatives for tree valve testing and chemical injection needs.
- Develop process safety philosophy.

Offshore Injection System

- Continue the evaluation of dry and wet trees considering field location and water depth.
- Define tree functional requirements and develop tree concepts.
- Design of foundation system according to actual soil condition data.

Control System

- Develop overall control and operating philosophy.
- Perform hydraulic, power and signal analyses to verify equipment sizing.
- Develop umbilical cross-section and evaluate umbilical-less system for dry tree alternatives.
- Define interfaces to remote control systems.
- Evaluate and select of a monitoring and leak detection strategy.

Cost and Schedule

- Produce updated cost and schedule estimates to increase execution certainty.

12 References

/1/ GoMCarb Subsea for CO2 Storage BP1

/2/ 49 CFR 195 – Transportation of Hazardous Liquids by Pipeline

/3/ NPD CO_2 storage ATLAS Norwegian continental shelf

/4/ BOEM 2018-004 Best Management Practices for Offshore Transportation and Sub-Seabed Geologic Storage of Carbon Dioxide

/5/ API 17N - Recommended Practice for Subsea Production System Reliability and Technical Risk Management, 2nd Edition

13 Abbreviations

ACM/AECM	Actuator Electronic Control Module
ALARP	As Low As Reasonably Possible
AIV	Annulus Isolation Valve
API	American Petroleum Institute
ASV	Annulus Valve
BAT	Best Available Technology
BOEM	Bureau of Ocean Energy Management
BOP	Blowout Preventer
CAPEX	Capital Expenditure
CCS	Carbon Capture Storage
CFD	Code of Federal Regulations
CIU	Chemical Injection Unit
CT	Coiled Tubing
DAS	Distributed Acoustic Sensor
DHS/DHSV	Downhole Safety (Valve)
DNV	Det Norske Veritas
DTS	Distributed Temperature Sensor
EFL	Electric Flying Lead
EH	Electro-Hydraulic
Elec	Electric
EPU	Electric Power Unit
ESD	Emergency Shutdown
FEED	Front End Engineering Design
FO	Fiber Optic
GOM	Gulf of Mexico
GUI	Graphic User Interface
HAZID	Hazard Identification
HAZOP	Hazard and Operability Study
HFL	Hydraulic Flying Leads
HP	High Pressure
HPU	Hydraulic Power Unit
HSSE	Health, Safety, Security, Environment
HVAC	Heating, Ventilation and Air Conditioning
Hyd	Hydraulic
ID	Inner Diameter
IGS	Integrated Guide Base Structure

ILT	In-line Tee
IMR	Inspection, Maintenance, Repair
ISO	International Standard Organization
LP	Low Pressure
MCS	Master Control Station
MEG	Monoethylene Glycol
O&G	Oil and Gas
OD	Outer Diameter
OFL	Optical Flying Lead
OPEX	Operational Expenditure
PCGM/PCGEM	Power and Communications Gateway Electronic Module
PLC	Programmable Logic Controller
PLEM	Pipeline End Manifold
PLET	Pipeline End Termination
PLR	Pig Launcher Receiver
PMV	Production Master Valve
PSD	Process Shut Down
PTT	Pressure Temperature Transducer
PWV	Production Wing Valve
RFO	Ready for Operation
RLWI	Riserless Light Well Intervention
ROV	Remote Operated Vehicle
SCM	Subsea Control Module
SCSSV	Surface Controlled Sub Surface Valve
SDA/SDU	Subsea Distribution Assembly Unit
SIT	System Integrity Test
SURF	Subsea Umbilicals, Risers and Flowlines
TH	Tubing Hanger
TRL	Technology Readiness Level
TUTU	Topside Umbilical Termination Unit
UPS	Uninterrupted Power Supply
UTA	Umbilical Termination Unit
VAT	Value Added Tax
WT	Wall Thickness
XMT/XT	Christmas Tree
XV	Isolation Valve

14 Appendix A – Sensitivities Evaluation

Step Changes in Cost/Technology			
Variable Cost Component	**Basis for Requirement & Related Field Characteristics**	**Equipment Impacted by Change**	**Rough Equipment Changes by Module**
Changes in Water Depth	Site selection is not defined and changes in water depth will impact the screening of subsea and dry trees. In general, in shallow waters up to 60ft, a dry tree on a structure with a caisson design and braising presents an overall lower CAPEX+OPEX cost.	Changes in water depth do not affect the design of subsea equipment that in many cases has been qualified for deep waters. Selection of shallow water structures will be significantly impacted by water depth. Simpler structures (braised caisson) can be used in shallow waters up to 60ft. Deeper waters requires more complex and costly structures such as 4 leg structures or jackets. If the structure's cost increases, the high CAPEX may offset the lower OPEX.	For water depths between 20-60ft, dry trees seem the better option. It also offers opportunities to simplify the umbilical and control equipment. For deeper waters, the subsea tree has certain advantages in terms of initial investment cost that may justify this solution.
Additional Wells	The number of wells and location has a direct impact on • Field architecture • Pipeline Design • Control System Architecture • Umbilical The impact will be more severe with increasing number of wells. Monitoring wells may also be required. These wells aren't usually connected to the main CO_2 distribution pipeline but required power and communications.	Depending on locations and number of wells, a daisy chain configuration may no longer be valid. Large number of wells located in clusters will probably dictate a hybrid solution. Pipeline cost will be affected. It may be beneficial to reduce pipeline size for remote well locations and include distribution centers. Umbilical and distribution equipment will also be impacted. The impact will be less severe in an all-electric system. Power transmission and communications philosophy can also be affected.	Pipeline size may increase to add the new wells. Distribution hubs may be required depending on well locations. This will increase overall SURF and SPS cost. Power and signal analyses will be required to determine the impact on the control system and umbilical. Potentially, the number of power quads may increase and fiber optic communication can become more relevant. Higher number of wells will also mean additional umbilical length and more distribution equipment.

Step Out Change	Changes to the site location due to reservoir conditions will lead to changes in step-outs and water depth. Area congestion can also push the wells to be located further away from shore in order to simplify pipeline routing, avoid crossings or hazards from/to other ocean users. In general, increasing the step out will have a direct impact on: • Pipeline • Umbilical • Control Architecture Flow assurance considerations will need to be re-evaluated.	Power transmission is directly impacted by long step-outs. This may lead to an increasing number of umbilical quads or a change in the power transmission system, use of transformers, etc. Communications may also be affected and use of fiber optic can become more relevant as step outs increase. Hydraulic systems and chemical distribution are more severely impacted by this change as hydraulic tubes will need to be re-sized and higher pressures may be required to overcome additional losses. On the other hand, systems closer to shore can benefit from direct hydraulic control. In extreme cases, pipeline redesign and intermediate compression should be considered.	Power transmission may require additional and larger power cables and the use of transformers should be studied. A DC system can be interesting if the step-out is beyond 200km. Communications can also be impacted and fiber optics may be required. Depending on the control architecture this change may lead to additional subsea modules. Umbilical length and total cost will be affected. In general, longer distances translate to bigger tube diameters, and larger power cables.
Power & Signal system **Controls Topology**	Low voltage power system is suitable for the studied cases and no additional offshore transformers would be required. If the step-out increases significantly, this will need to be re-evaluated. The main design factors are the offshore consumers (usually low duty low demand valves) and step-out. The current proposal considers comms on power cables. Changing to a fully segregated power system would increase number of cables. Adding instrumentation that demands high bandwidth, such as multiphase meters, can impact the communication methodology and fiber optic communication may be needed.	The equipment impacted will be: • Topside and subsea trees • Umbilical and distribution • Onshore and offshore control equipment In an all-electric system, additional instrumentation requiring other communication methodologies will have limited impact on the control system architecture compared to an electro-hydraulic topology.	Shifting to DC or FO is currently not considered necessary. Significant changes to the number of wells and step-out need to happen before these systems become relevant. A change from all-electric to a hydraulic system will require a change of the topside and subsea tree. It is expected an increase in footprint and larger valve actuators. The umbilical will also be impacted with changes to the number of quads and distribution equipment.

Tree Functionalities	Current CO_2 injection trees follow similar design requirements as O&G trees. Number of barrier elements and control equipment should be investigated further. All electric systems present a better platform to allow for simplification and minimizing tree size. If hydraulic functions are required, the tree, umbilical and control system will be impacted potentially leading to higher cost. Defining downhole functions is key to have a sounded well construction philosophy. Reducing number of lines could lead to slimmer system and bigger downhole tubbing while still using qualified solutions.	If number of barriers is reduced, the tree will have a significant cost reduction and become an “injection head” with minimal instrumentation. With reduction on number downhole functions 13 5/8” system may be possible	Considering the majority of trees are based on more stringent requirements from O&G, changes will in general lead to simplifications and cost reductions
Umbilical	Umbilical cost dependents on: • Number of lines and services • Length • Water depth • Metocean conditions The umbilical is terminated at the shoreline facility and connected to the offshore wells. This is considered to be a static umbilical. Umbilical connection to subsea trees is done by flying leads and depend on number of wells and services provided (hydraulic, fiber optic, electric). Other components such as bend restrictors, buoyancy elements, and others need to be identified as part of the analysis work.	The length and number of services define the main cost elements in the umbilical. If number of wells and step outs increase, the umbilical cost will also increase. The cross section could be affected, specially hydraulic tubes may grow in diameter. Hydraulic tubes are the main contributors to cost. It is recommended to verify if chemical injection can be achieved by other means rather than via the umbilical.	In case of dry trees, there are options for local power generation using solar panels and chemical skids with a small HPU. Communication could also be achieved wirelessly. For dry trees an umbilical-less system could be envisioned. For subsea trees, reduction or elimination of tubes would be the most cost effective alternative.